Abstract Volume
19th Swiss Geoscience Meeting

Online, 19 + 20 November 2021

Climate, Resources and Environment: conflicts, synergies & compromises

scnat
akademie der naturwissenschaften
académie des sciences naturelles
swiss academy of sciences
accademia di scienze naturali

UNIVERSITÉ DE GENÈVE
FACULTÉ DES SCIENCES
Section des sciences de la Terre et de l'environnement

Cover Photo: le Jet d›eau de Genève. credit, Pierre Dèzes, SCNAT

19th Swiss Geoscience Meeting, 2021

Table of contents

Abstracts

1	Structural Geology, Tectonics and Geodynamics	2
2	Mineralogy, Petrology, Geochemistry	70
3	Stable and radiogenic isotope geochemistry	116
4+5	Environmental Biogeochemistry of Trace Elements & Natural Organic Matter, Trace Metals and Nanoparticle Biogeochemistry	146
6	Palaeontology	172
7	Stratigraphy and Sedimentology: processes and deposits through time	200
8	Seismic Hazard and Risk in Switzerland: From Science to Mitigation	230
9	Deep geothermal energy, CO_2-storage and exploration of the subsurface	248
10	Scientific Drilling is Going Strong, Scientific Drilling Matters!	294
11	Quaternary environments: landscapes, climate, ecosystems and human activity during the past 2.6 million years	324
13	Geomorphology	350
14	Hydrology and Hydrogeology	370
15	Limnology in Switzerland	400
16	Cryospheric Sciences	428
17	Atmospheric Composition and Biosphere-Atmosphere Interactions	464
18	Tackling the Climate Crisis: Interdisciplinary Perspectives on Climate Change Education and Communication	488
19	Geoscience and Geoinformation, Earth Observation and Remote Sensing – Combined Symposium	496
20	Scalability, transferability and transformative potential of global change research in mountains	522
21	Human Geographies: Materials, Natures, Politics	526
22	Human Geographies: Bodies, Cultures, Societies	542
23	Human Geographies: Cities, Regions, Economies	552

Organisation

Host Institution

Section of Earth and Environmental Sciences at the University of Geneva

Patronnage

Platform Geosciences of the Swiss Academy of Sciences SCNAT

Local Organizing Committee

Vera Slaveykova
Silvia Omodeo Salé
Sandrine Le Houedec
Matteo Lupi
Kalin Kouzmanov
Jöel Ruch
Jean-Luc Loizeau
Luca Guglielmetti
Luca Caricchi
Andrea Moscariello (President)

Coordination

Pierre Dèzes

Participating Societies and Organisations

Commission for the Swiss Journal of Palaeontology

Forum Landscape, Alps, Parks (FOLAP)

Interdisciplinary Centre for Mountain Research

International Union of Geodesy and Geophysics, Swiss Committee (IUGG)

International Union of Geological Sciences, Swiss Committee (IUGS)

Mountain Research Initiative

Schweizerischen Gesellschaft für Erdbebeningenieurwesen und Baudynamik (SGEB)

Swiss Association of Geographers (ASG)

Swiss Association for Geographic Education (VGDch)

Swiss Commission for Phenology and Seasonality (CPS)

Swiss Commission for Remote Sensing (SCRS)

Swiss Commission on Atmospheric Chemistry and Physics (ACP)

Swiss Committee for Stratigraphy (Platform Geosciences/SCNAT)

SWISS DRILLING

Swiss Geodetic Commission (SGC)
Swiss Geological Society (SGG/SGS)
Swiss Geological Survey (swisstopo)
Swiss Geomorphological Society (SGGm/SSGm)
Swiss Geophysical Commission (SGPK)
Swiss Geothermal Society
Swiss Hydrogeological Society (SGH)
Swiss Hydrological Commission (CHy)
Swiss Paleontological Society (SPG/SPS, Swiss Geological Society)
Swiss Snow, Ice and Permafrost Society (SIP)
Swiss Society for Hydrology and Limnology (SGHL/SSHL)
Swiss Society for Quaternary Research (CH-QUAT)
Swiss Society of Mineralogy and Petrology (SMPG/SSMP, Swiss Geological Society)
Swiss Tectonics Studies Group (Swiss Geological Society)

01. Structural Geology, Tectonics and Geodynamics

Sandra Borderie, Paul Tackley, Jonas Ruh

Swiss Tectonics Studies Group of the Swiss Geological Society

TALKS:

1.1 Akker I.V., Herwegh M., Berger A., Aschwanden L., Mazurek M., Madritsch H.: Microscale deformation and related mineralization in the Opalinus Clay of central northern Switzerland

1.2 Alkhimenkov Y., Utkin I., Khakimova L., Alvizuri C., Quintal B., Podladchikov Y.: Spontaneous earthquake nucleation in elasto-plastic media

1.3 Balázs A., Faccenna C., Gerya T., Ueda K., Funiciello F.: The Dynamics of Forearc – Back-arc basins: Numerical Models and Observations from the Mediterranean

1.4 Bilau A., Bienveignant D., Rolland Y., Schwartz S., Godeau N., Guihou A., Deschamps P., Boschetti L., Mangenot X., Brigaud B., Dumont T.: Thin-skin subalpine tectonic chronology constrained by U-Pb calcite on faults mirrors and fractured pebbles.

1.5 Gerya T., Stern R.J., Pellissier L., Stemmler D., Balazs A., Gray T., Rogger Y., Van Agtmaal L., Tackley P.: Biogeodynamics: influence of plate tectonics on life evolution and biodiversity

1.6 Grujic D., Rolfe O., Negrini M., Prior D.: Spatial and temporal interplay between viscous and brittle deformational processes in a continental megathrust: case study across the Main Central Thrust in the Himalaya

1.7 Gunatilake T., Miller S.A.: Spatio-temporal complexity of aftershocks in the Apennines controlled by permeability dynamics and decarbonization

1.8 Hauvette L., Sommaruga A., Borderie S., Mosar J., Meyer M.: New tectonic map in the Geneva Basin, combination of surface and sub-surface data (Switzerland and France)

1.9 Marro A., Sommaruga A., Hauvette L., Borderie S., Schori M., Mosar J.: Tectonics of the Western Internal Jura Fold-and-Thrust Belt: from the Geneva Basin (Switzerland) to La Bienne Valley (France). Mapping and forward modelling.

1.10 Panza E., Ruch J.: Interaction of faulting and magma propagation in oblique extensional settings (North Volcanic Zone, Iceland) using UAV-based structural data

1.11 Radaideh O., Sommaruga A., Mosar J: Tectonic paleostress and tectonic geomorphology in the close vicinity of the Pontarlier strike-slip fault system (Swiss and French Jura fold and- thrust belt)

1.12 Rast M., Galli A., Ruh J., Madonna C., Guillong M.: Geology along the Bedretto tunnel: kinematic and geochronologic constraints on the evolution of the Gotthard Massif (Central Alps)

1.13 Rime V., Foubert A., Atnafu B., Kidane T.: New geological mapping of the Afar depression: from review towards the understanding of basin dynamics during active rifting

1.14 Roger M., de Leeuw J., van der Beek P., Husson L.: Diachronous evolution of the Carpathians belt and foreland, from low-T thermochronology inversion and isopach maps analysis.

1.15 Ruch J., Bufféral S., Panza E., Mannini S., Óskarsson B., Gies N., Alvizuri C., Hjartardóttir A.R.: Oblique rifting event during the 2021 Reykjanes seismo-tectonic and volcanic crisis (SW Iceland).

1.16 Truttmann S., Diehl T., Herwegh M.: Probabilistic 3D Fault Network Models of Seismogenic Faults: Case Studies from the Northern Valais

1.17 Yan J., Ballmer M., Waszek L., Tauzin B., Tackley P.J.: Seismic-geodynamic constraints on compositional heterogeneity near the 660-km discontinuity

1.18 Zwaan F., Schreurs G.: CT-scanned analog models of lithospheric-scale rifting

POSTERS:

P 1.1 Alhamad M., Bruna P., Bertotti G., Moscariello A., Eruteya O., Welch M., Oldfield S.: Fracture Network Prediction in the Geneva Basin: A Geothermal Case Study

P 1.2 Borderie S., Mosar J., Hauvette L., Marro A., Sommaruga A., Meyer M.: Stress in the Geneva Basin and adjacent Jura fold-and-thrust belt (Switzerland and France), insights from numerical modelling

P 1.3 de Leeuw A., Vincent S.J., Matoshko A., Matoshko A., Stoica M., Nicoara I.: Geodynamic evolution of the East Carpathian Foreland Basin since the Middle Miocene: Implications for sediment supply to the Black Sea and Dacian Basin

P 1.4 Diehl T., Herwegh M., Schmid S., Nibourel L.: Present-day deformation of the Aar Massif: New insights from three recent ML4 strike-slip earthquakes

P 1.5 Fabbri S.C., Mair D., Schmid T., Piccoli F.: Automated lineament detection using Tensor Voting: A case study from the Swiss Alps (Grimselpass & Zermatt, Switzerland)

P 1.6 Frings K.A., von Hagke C., Dunkl I., Luijendijk E., Madritsch H.: Using the spread in apatite (U-Th)/He single grain ages to constrain the thermal history of the Northern Swiss Molasse Basin

P 1.7 Gray T., Tackley P., Gerya T., Stern R.J.: The Neoproterozoic transition to modern plate tectonics and complex life: A global scale numerical modelling approach

P 1.8 Halter W.R., Macherel E., Duretz T., Schmalholz S.M.: Numerical modelling of strain localization by anisotropy generation during viscous deformation

P 1.9 Hufford L.J., Tokle L., Behr W.M.: Experimental investigation of glaucophane rheology through general shear deformation experiments

P 1.10 Wang L., Wu R., Li Y., Selvadurai P., Madonna C., Lei Q.: Microcrack-driven Emergence of Stress Relaxation in Granitic Rock: Laboratory Observation and Numerical Simulation

P 1.11 Liu M., Gerya T.: Surplus melt induces the dynamic LAB near the mid-ocean ridge

P 1.12 Macherel E., Podladchikov Y., Räss L., Schmalholz S.M.: GPU-based pseudo-transient finite difference solution for 3-D gravity- and shear-driven power-law viscous flow

P 1.13 Mannini S., Ruch J., Hollingsworth J, Swanson D.S., Johanson I.: Giant Volcano Flank Motion Imaged by Historical Air Photos Correlation during the M7.7 Kalapana Earthquake (1975), Big Island, Hawaii

P 1.14 Marguin V., Simpson G.: Influence of fluids on the earthquake cycle based on numerical modeling

P 1.15 Musso Piantelli F., Mair D., Herwegh M., Berger A., Kurmann E., Wiederkehr M., Schlunegger F., Möri A., Baumberger R.: 4D reconstruction of a Fold and thrust belt: the case of the asymmetric Doldenhorn nappe-Aar Massif system (Central Swiss Alps)

P 1.16 Nevskaya N., Zhan W., Stünitz H., Berger A., Herwegh M.: Brittle-viscous transition in fine-grained granitoid fault rocks – deforming natural rock samples in the Griggs Rig apparatus

P 1.17 Perret M., Gasparrini M., Teles V., Mondino F., Guglielmetti L., Omodeo Salé S., Moscariello A.: Fracture network characterization associated with the transpressive Vuache fault, a possible outcrop analogue of the Geneva Basin geothermal system.

P 1.18 Ruh J.B., Tokle L., Behr W.M.: Numerical Modelling of Grain Size Evolution in Granitoid Shear Zones

P 1.19 Scarponi M., Hetényi G., IvreaArray Team: New constraints on the Ivrea Geophysical Body at intra-crustal scales (Western Alps, Europe): a combination of gravimetry, passive seismology and rock's physical properties

P 1.20 Schmid T., Schreurs G., Adam J.: Styles of fault growth influencing rift propagation in rotational rift settings: Insights from crustal scale analogue models

P 1.21 Tokle L., Braden Z., Cisneros M., Behr W.M.: Structural Mapping of the Eclogite Zone, Tauern Window: Implications on the rheology of the subduction zone interface

P 1.22 Turlin F., Moritz R., Keskin S., Utku Sönmez S., Ulyanov A.: Variscan granitoid in the Eastern Pontides, NE Turkey, records a 2.0 Ga history of Gondwana-derived terranes

P 1.23 Ursprung A., Borderie S., Sommaruga A., Mosar J.: A geological profile and kinematically balanced cross-section through the Mont Tendre and Mont Risoux

P 1.24 Van Agtmaal L., Balazs A., May D., Gerya T.: From the India-Eurasia corner collision to lateral extrusion: results from 3D coupled numerical models

P 1.25 Verard C., Ragon C., Kasparian J., Brunetti M.: The PANALESIS model and its applications to the Permian – Triassic climate oscillations

P 1.26 Zhan W., Nevskaya N., Niemeijer A., Berger A., Spiers C.J., Herwegh M.: The effect of temperature on the frictional behavior of simulated ultrafine-grained granitoid gouge: an experimental investigation using a Ring Shear Apparatus

P 1.27 Zwaan F., Chenin P., Erratt D., Manatschal G., Schreurs G.: Interaction between mantle and crustal weaknesses during rifting: insights from laboratory experiments

P 1.28 Zwaan F., Rosenau M., Maestrelli D.: The influence of initial salt basin geometry on salt tectonics: insights from laboratory experiments

1.1
Microscale deformation and related mineralization in the Opalinus Clay of central northern Switzerland

Ismay Vénice Akker[1], Marco Herwegh[1], Alfons Berger[1], Lukas Aschwanden[1], Martin Mazurek[1], Herfried Madritsch[2]

[1] *Institute of Geological Sciences, University of Bern, Bern, Switzerland (ismay.akker@geo.unibe.ch)*
[2] *Swiss National Cooperative for the Disposal of Radioactive Waste (Nagra), Wettingen, Switzerland*

The thick regionally undeformed main section of Opalinus Clay of central northern Switzerland (between Olten and Schaffhausen) is foreseen to host the Swiss deep geological repository for radioactive waste. Currently, Nagra conducts a deep drilling campaign across three potential siting regions. We are performing a combined microstructural and geochemical study on drill core samples of the argillaceous Opalinus Clay host rock in order to better understand its deformation during tectonic processes in the geological past. Core samples are investigated by low and high-resolution optical light microscopy together with scanning electron microscopy (SEM) in combination with energy-dispersive X-ray spectroscopy (EDX).

Deformation structures observed across the Opalinus Clay structures vary between the different localities/drill sites. The samples from the easternmost localities near the Middle Miocene Bodensee-Hegau Graben are typically affected by normal faults, and mm to cm-scale shear zones in the matrix. Many of these deformation structures include secondary mineral precipitates, mostly calcite and celestite. Typical macroscopic deformation features in the cores from the more westerly localities close to the Jura fold-and-thrust belt include: different generations of thrust faults, either with or without syn-kinematic slickensides on the surfaces. Typically, fibrous veins occur parallel to such thrust faults. The microstructural characterization allows for detecting relative timing relationships, as is the case in Fig. 1. Here a fibrous calcite vein is crosscut by a parallel thrust fault with syn-kinematic slickenside. This timing relationship is connected with a change of trace elements in the calcite. These measurements show clear differences in Fe, Mg and Mn in the calcite, which reflect chemical differences of these two mineralization events (Fig. 1).

By combining the in-situ microstructures including overprinting relationships with the in-situ micro-chemistry we yield relative timing of fracturing and faulting events. This is best documented by differences in mineralization of new mineral phases. Regarding these coupled deformation-mineralization events in the Opalinus Clay, the first results of our study do imply regionally differences likely related to a varying intensity of certain tectonic events across the investigation area.

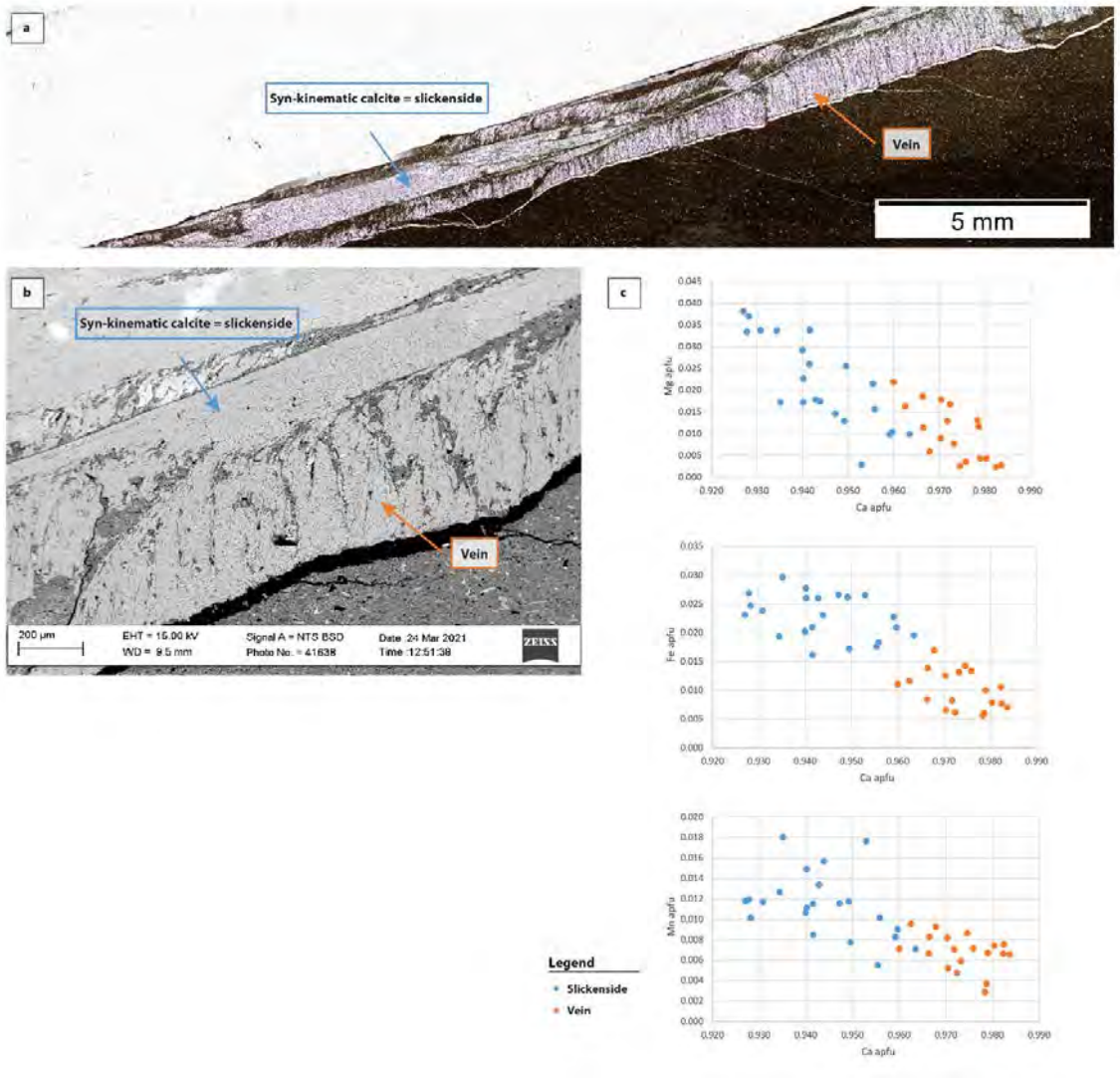

Figure 1. Examplary Opalinus Clay sample showing a fibrous vein, which is crosscut by syn-kinematic calcite (slickenside). a) Light microscopic image of crosscutting relationship. b) SEM backscatter image of crosscutting relationship and c) EDX measurements of calcite in vein material compared to slickenside show two distinct groups in the major element chemistry (Mg, Fe and Mn).

1.2
Spontaneous earthquake nucleation in elasto-plastic media

Yury Alkhimenkov[1,2], Ivan Utkin[2], Lyudmila Khakimova[1,2], Celso Alvizuri[1], Beatriz Quintal [1], Yury Podladchikov[1,2]

[1] *Institute of Earth Sciences & Swiss Geocomputing Centre, University of Lausanne, Lausanne, Switzerland (yury.alkhimenkov@unil.ch)*
[2] *Faculty of Mechanics and Mathematics, Moscow State University, Moscow, Russia*

Earthquakes are seismic events that are caused in the Earth's subsurface either by natural processes (e.g. tectonic activity) or by anthropogenic activities (e.g. fluid injection). A lot of research has been done to resolve the mechanism of seismic triggering events, but the physics behind the earthquake nucleation is still poorly understood. The limitations in knowledge are associated with (i) oversimplified physics in analytical models and numerical simulations, which only describe a subset of the seismic cycle's features, (ii) mainly one- or two-dimensional modeling studies bounded by the lack of computing power, (iii) lack of fully coupled physical models resolving thermo-hydro-mechanical interactions. All these limitations result in little predictive power of the current models.

We propose a new mechanism of earthquake nucleation (Figure 1). We consider an elasto-plastic rheology, where the plasticity is implemented using a pressure-dependent Coulomb yield theory. So far in 2D, we apply a pure shear boundary condition and slowly increase shear stress in the simulation. At some point, the stress reaches the Coulomb yield surface and then local strain localizations start to develop (Minakov and Yarushina, 2021) resulting in fractal shear bands (Figure 1b). The evolution of the strain localizations is spontaneous and cannot be rigorously predicted. Per one load increment, only a local new strain localisation appears which results in stress drop (Figure 1c). This new strain localisation can be visible in the anti-symmetric displacement field (Figure 1a), which corresponds to the initial condition for the earthquake nucleation. This triggering mechanism is similar to a particular double-couple (DC) moment tensor source, typically observed in real earthquakes. Real earthquakes may also include more complicated processes with non-DC components which can be analysed with seismic full moment tensors (e.g., Alvizuri et al., 2018). Our new numerical algorithm simulates the quasi-static loading and wave propagation mechanics simultaneously and can be further extended to capture a more complex rheology. Furthermore, follow up studies will be performed in 3D.

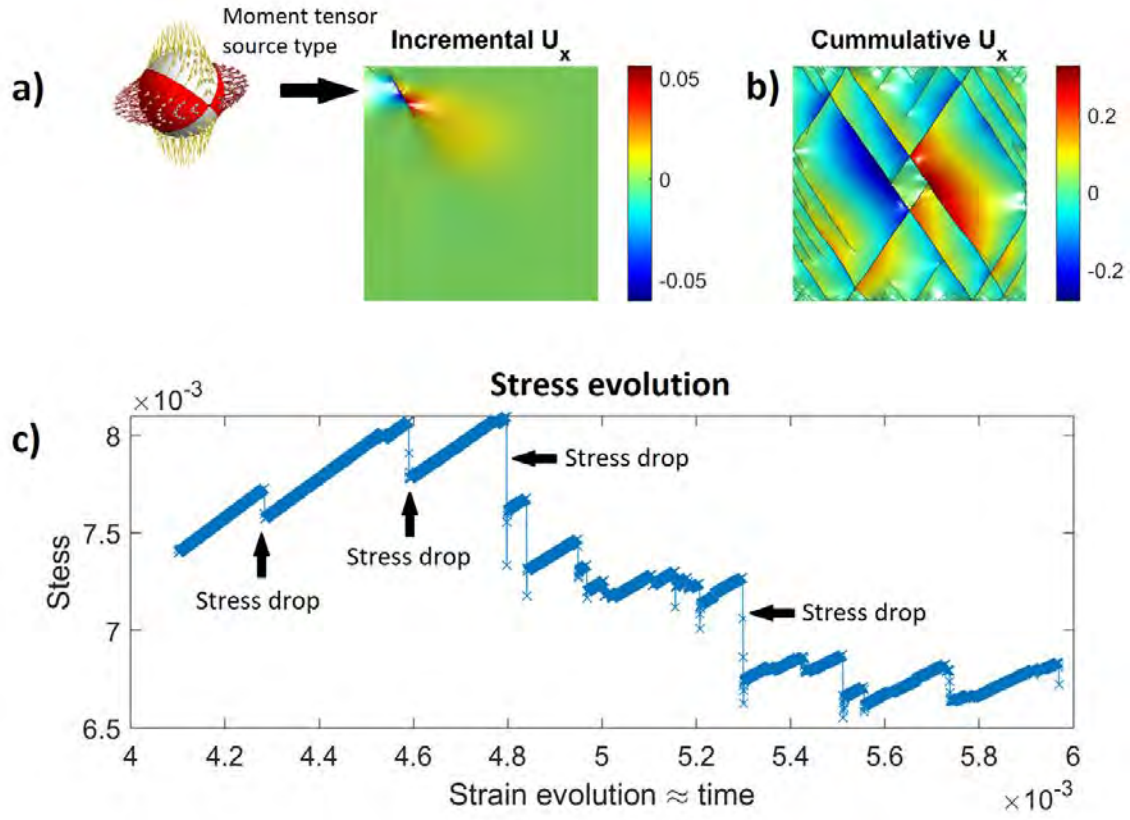

Figure 1. Conceptual model of spontaneous earthquake nucleation. Panel (a) illustrates the displacement field corresponding to a stress drop; this displacement field represents the focal mechanism. Panel (b) illustrates the fractal strain localisation pattern of the displacement field developed during the cumulative evolution of the strain field. Panel (c) shows the stress evolution in the model with time. The inset in panel (a) represents the moment tensor source. All quantities are dimensionless.

REFERENCES

Minakov, A. and Yarushina, V., 2021. Elastoplastic source model for microseismicity and acoustic emission. Geophysical Journal International, 227(1), pp.33-53.

Alvizuri, C., Silwal, V., Krischer, L. and Tape, C., 2018. Estimation of full moment tensors, including uncertainties, for nuclear explosions, volcanic events, and earthquakes. Journal of Geophysical Research: Solid Earth, 123(6), pp.5099-5119.

1.3
The Dynamics of Forearc – Back-arc basins: Numerical Models and Observations from the Mediterranean

Attila Balázs[1], Claudio Faccenna[2,3], Taras Gerya[1], Kosuke Ueda[1], Francesca Funiciello[2]

[1] ETH Zürich, Department of Earth Sciences, Zürich, Switzerland (attila.balazs@erdw.ethz.ch)
[2] Università Roma Tre, Department of Sciences, Rome, Italy
[3] University of Texas at Austin, Department of Geology, Austin, USA

The evolution of oceanic and continental subduction zones is linked to the rise and demise of forearc and back-arc sedimentary basins in the overriding plate. Subsidence and uplift rates of these distinct basins are controlled by variations in plate convergence and subduction velocities and determined by the rheological and thermal structure of the lithosphere. In this study we conducted a series of high-resolution 2D numerical models of oceanic subduction and subsequent continental collision. The numerical code I2ELVIS handles elasto-visco-plastic rheologies and involves erosion, sedimentation, and hydration processes. Accommodation space and sedimentary basins are formed on top of the accretionary wedge creating piggy-back or wedge-top forearc basins, while retro-forearc basins are formed on the overriding continental plate in a wide syncline structure overlying the subduction interface at ca. 200 km distance from the accretionary wedge between a forearc high and the volcanic arc. Forced subduction initiation and initial overriding plate compression results in a flexural proto-forearc basin its syn-kinematic sedimentary age can constrain the age of subduction initiation.

Higher subsidence rates are recorded in the syncline structure of the retro-forearc basin when the slab dip angle is higher and the subduction interface is stronger and before the slab reaches the 660 km discontinuity. This implies the importance of the trench suction force as the main driver for the up to 3-4 km negative residual topographic signals. Extensional back-arc basins are either formed along inherited crustal or lithospheric weak zones at large distance from the arc region or are created above the hydrated mantle wedge originating from arc rifting. Back-arc subsidence is primarily governed by crustal and lithospheric thinning controlled by slab roll-back. During mature free-fall subduction and the climax of slab roll-back the forearc high subsides beneath sea-level and the locus of the forearc depocenter migrates trench-ward reflected by upper plate tilting. Onset of collision and continental subduction is linked to the rapid uplift of the forearc basins; however, the back-arc region records ongoing extension during soft collision. Finally, during hard collision the forearc and back-arc basins are ultimately affected by compression. Our results are compared with the evolution of the Mediterranean and we classify the Western and Eastern Alboran, Paola and Tyrrhenian, Transylvanian and Pannonian Basins to be genetically similar forearc – back-arc basins, respectively.

1.4
Thin-skin subalpine tectonic chronology constrained by U-Pb calcite on faults mirrors and fractured pebbles.

Antonin Bilau[1,2], Dorian Bienveignant[2], Yann Rolland[1,2], Stéphane Schwartz[2], Nicolas Godeau[3], Abel Guihou[3], Pierre Deschamps[3], Louise Boschetti[1,2], Xavier Mangenot[4], Benjamin Brigaud[5], Thierry Dumont[2].

1 EDYTEM - Université Savoie Mont Blanc - 5 Bd de la Mer Caspienne, 73370 Le-Bourget-du-Lac, France. (antonin.bilau@univ-smb.fr)
2 ISTerre - Université Grenoble Alpes - 1381 Rue de la Piscine, 38610 Gières, France.
3 CEREGE - Aix-Marseille Université - Technopôle de l'Arbois-Méditerranée, BP80, 13545 Aix-en-Provence, France.
4 CALTECH - Geological and Planetary Sciences - 1200 E California Blvd, Pasadena, CA 91125, USA.
5 Université Paris-Saclay – CNRS - GEOPS - Rue du Belvédère Bâtiment 504, 91400, Orsay, France.

Along orogenic systems two main tectonic styles occur, thick-skin tectonics involving crystalline basements and thin-skin tectonics involving only superficial sedimentary and a flat decoupling layer (e.g., Phillipe et al., 1998). In the Western Alps, thick-skin tectonics allows exhumation of External Crystalline Massifs (Pelvoux, Belledonne Mont Blanc…) while further West, foreland basin undergoes thin-skin tectonics associated to the developement of folds and thrusts. This study focuses on Vercors and Chartreuse subalpine massifs deformation history. These massifs are structured by frontal thrusts which transport the folded Jurassic/Cretaceous sedimentary cover over the Miocene molassic basins. Until now, the initiation of the deformation sequence is only estimated by relative cross-cutting relationships of molasse sediments using deposition ages, obtained by Sr isotopic ratios on bioclasts. These ages range between 21.3±0.3 Ma and 12.7±1.5 (Kalifi et al., 2021). To bring new direct constraints on the deformation ages, in-situ U-Pb on calcite were applied on fault mirrors and on fractured pebbles in the underthrusted molasse.

We obtained 14 calcite crystallization ages related to the activity of at least 3 main thrusts. The oldest recorded ages are of ~15 Ma (4 ages), only obtained at Saint-Nizier-du-Moucherotte on the highest and most internal thrust (eastern Vercors Massif), *Fig. 1*. Clumped isotope Δ_{47} on a fractured pebble gives a temperature of 149°C and $\delta^{18}O_{fluid}$ of 13,9‰ (SMOW). This temperature is interpreted as a minimum circulation depth at which the fluid is in thermal equilibrium with the host-rock. This 1st thrust results from a deep underthrusting of 4-6 km depending on the applied geotherm, in agreement with previous vitrinite and raman estimates (e.g., Bellahsen et al., 2014).

South-eastern Chartreuse thrust shows younger initial ages of 12.3±0.5 Ma. The second major thrust system to the north-west is dated at 12.2±0.7 Ma and 12.7±0.2 Ma at Rencurel (Vercors) and 13.8±1.8 Ma at Châtelard (Chartreuse), which is in agreement with an in-sequence propagation of the thrust belt from 15 to 12 Ma. Δ_{47} measured on fault plane breccia from Rencurel gives temperature about 100°C cooler (crystallization temperature of 54°C) compared to Saint-Nizier-du-Moucherotte molasse, with $\delta^{18}O_{fluid}$ of 5,1‰ (SMOW). This lower temperature can easily be explained by the Miocene basin thickness and shallow underthrusting at a depth of around 2 km. Younger ages from 9.5±0.9 Ma to 2.1±1.8 Ma are observed in a fairly evenly distributed way in all the thrusts, which is in agreement with a diffuse reactivation of the thrust stack in an 'hors-sequence' mode. Fault planes, slickensides and fractured pebble displacement analysis allow the reconstruction of the paleostress tensors using TectonicsFP and a Numerical method for Dynamic Analysis (NDA) (Spang 1972) and P-B-T (Marrett & Allmendinger, 1990). It has been done on 5 dated locations which are all coherent to a N110°E compressive axis.

Over 26 analyses, a mean value of 1.24‰ $\delta^{13}C_{cal.\ VPDB}$ (except 2 lower values of -7,43‰ and -9.22‰) and a mean value of -6.72‰ $\delta^{18}O_{cal.\ VPDB}$ are recorded in our samples. This signature is close to the one of the host-rock and can be attributed to a meteoric derived fluid more or less evolved during circulation in the basin and following equilibration with host-rocks during underthrusting.
In addition to bringing fault activation timing constraints on subalpine massifs thin-skin structuration, this study combines techniques that can be coupled to dating methods to infer calcite crystallization environment and provide a detailed comprehension of the tectonic evolution of the frontal part of the western alpine foreland.

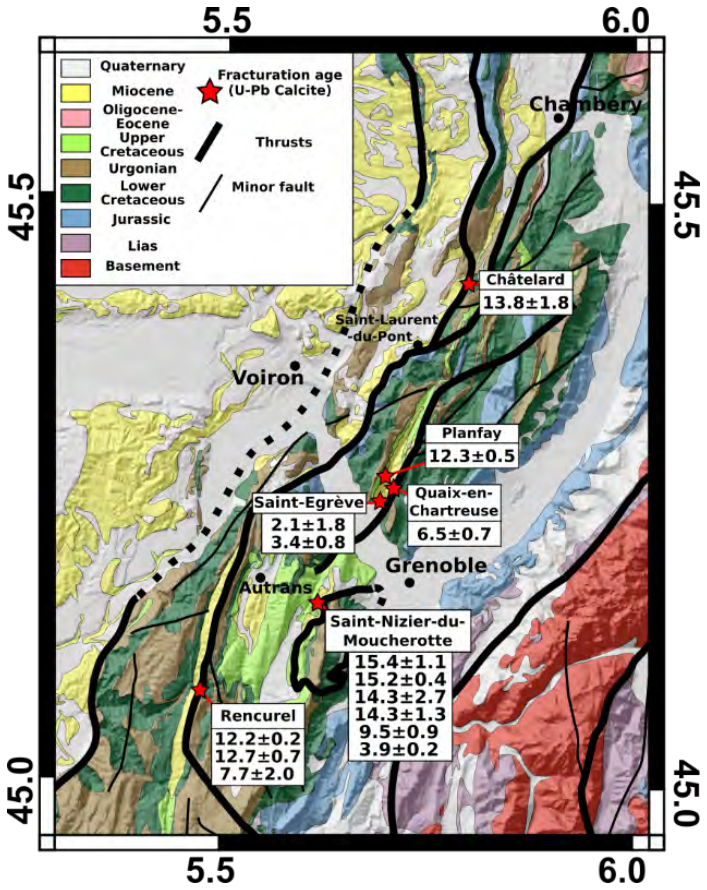

Figure 1. Geological map of subalpine massif (Vercors/Chartreuse) with fracturation ages (ages are in Ma with 2σ error).

REFERENCES

Bellahsen, N., Mouthereau, F., Boutoux, A., Bellanger, M., Lacombe, O., Jolivet, L., et Rolland, Y. 2014: Collision kinematics in the western external Alps, Tectonics, 33, 1055–1088.

Kalifi, A., Leloup, P. H., Sorrel, P., Galy, A., Demory, F., Spina, V., ... & Rubino, J. L. 2021: Chronology of thrust propagation from an updated tectono-sedimentary framework of the Miocene molasse (western Alps). Solid Earth Discussions, 1-68.

Marrett, R. A. & Allmendinger, R. W. 1990: Kinematic analysis of fault-slip data, Journal of Structural Geology, 12(8), 973-986.

Philippe, Y., Deville, E. and Mascle, A. 1998: Thin skinned inversion tectonics at oblique basin margins: example of the western Vercors and Chartreuse Subalpine massifs (SE France), Geological Society, London, Special Publications, 134, 239-26.

Spang, J.H. 1972: Numerical Method for Dynamic Analysis of Calcite Twin Lamellae, Geological Society America Bulletin, 83, 467-472.

1.5

Biogeodynamics: influence of plate tectonics on life evolution and biodiversity

Gerya, T.1., Stern, R.J.2, Pellissier, L.3, Stemmler, D.1, Balazs, A.1, Gray, T.1, Rogger, Y.1, Van Agtmaal, L.1, Tackley, P.1

1 Institute of Geophysics, Dept. of Earth sciences, ETH, Sonneggstrasse 5, 8092 Zurich, Switzerland
2 Geosciences Department, University of Texas at Dallas, USA
3 Department of Environmental Systems Science, ETH Zurich, Switzerland

Earth's geodynamic evolution is intimately coupled to the evolution of its atmosphere, oceans, landscape and life and we aim to understand this coupling better through the emerging transdisciplinary field of biogeodynamics. Firstly, life is sustained by a critical set of elements contained within rock, ocean and atmosphere reservoirs and cycled between Earth's surface and interior via various tectonic, magmatic and surface processes. Second, plate tectonic processes such as redistributing continents, growing mountain ranges, forming land bridges, and opening and closing of oceans and marine gateways provide environmental pressures that isolate and stimulate populations to adapt and evolve; recombining these features further stimulates evolution. Modern plate tectonics - established sometime before the Cambrian explosion - is often viewed as a strong promoter of biological evolution. Compared to single lid tectonic styles, plate tectonics better creates and destroys continental and continental shelf habitats, supplies nutrients, modulates climate, and exerts continuous moderate environmental pressures that drive evolution.

Importantly, long timescales of biological evolution estimated from analysis of DNA changes and fossils are comparable to those of major geodynamic cycles such as the Supercontinent Cycle and the Wilson Cycle. Therefore, computational biogeodynamics (i.e., coupled modeling of Earth's interior, atmosphere, ocean, sea-level, climate, landscape and life evolution) stands as one of the frontier research tasks in geodynamics, ecology and evolution as well as related disciplines. Here, we propose the development and employment of both regional- and global-scale 3D high-resolution bio-geodynamical modeling toolkits, coupling (i) available global and regional magmatic-thermomechanical models of geodynamic processes, (ii) landscape evolution models, (iii) simulations of long-term atmospheric, ocean and climate change and (iv) spatially-explicit models of species speciation, evolution and extinction. We show preliminary results suggesting critical roles of plate tectonic motions and mantle plume-lithosphere interactions on life evolution and spatial-temporal biodiversity distribution. The implications for exploring exoplanets are obvious.

1.6
Spatial and temporal interplay between viscous and brittle deformational processes in a continental megathrust: case study across the Main Central Thrust in the Himalaya

Djordje Grujic[1], Olivia Rolfe[1], Marianne Negrini[2], David Prior[2]

1 Department of Earth and Environmental Sciences, Dalhousie University, 1459 Oxford street, Halifax, Canada (dgrujic@dal.ca)
2 Department of Geology, University of Otago, 360 Leith Street, Dunedin 9016, New Zealand

Continuum of stress, strength, slip and creep in the subduction zone plate interfaces is realized by various mechanisms of stress loading the seismogenic zone of a megathrust by creep in its deeper, ductile part. Most of the understanding of these interactions was acquired through seismological and theoretical studies.
We investigate such megathrust system across a range of observation scales and approaches, including field observations, microanalyses, innovative thermochronology, and numerical modelling (Grujic et al. 2020). The outcrops of the main Himalayan structures expose a sequence from ductile shear zones to brittle faults. As all these structures merge into the Himalayan basal décollement, the Main Himalayan thrust, it can be safely assumed that the rocks now at the surface were within the MHT at the time of their deformation. Himalayan thrusts therefore collectively crosscut many lithologies and have operated over broad ranges of pressure, temperature, and strain rates. From north to south, from older to younger, the sequence of outcrops of mylonite, ultramylonites, cataclasites, to fault gouge represent distinct zones into which deformation has localized.
Microstructural and textural analyses of quartz mylonites from the Main Central thrust allow identification of switches of deformation mechanisms caused by reductions in pressure and temperature during exhumation, and they provide quantitative constraints on stress history. At some localities there is an evolution of samples experiencing shifts to higher stress deformation that may be a result of interaction between end-member mechanisms where viscous flow cannot accommodate all the imposed displacement, which leads to “semi-brittle” deformation. Alternatively, the pulses of high stress associated with earthquakes might also be involved in generating bimodal populations of dynamically recrystallized grains. At other localities, however, there is an evolution of samples experiencing switches to lower stress deformation. The latter microstructures may be results coeval decrease of strain rate and temperature. These two contrasting deformation histories should be a focus of our future studies of megathrust systems.

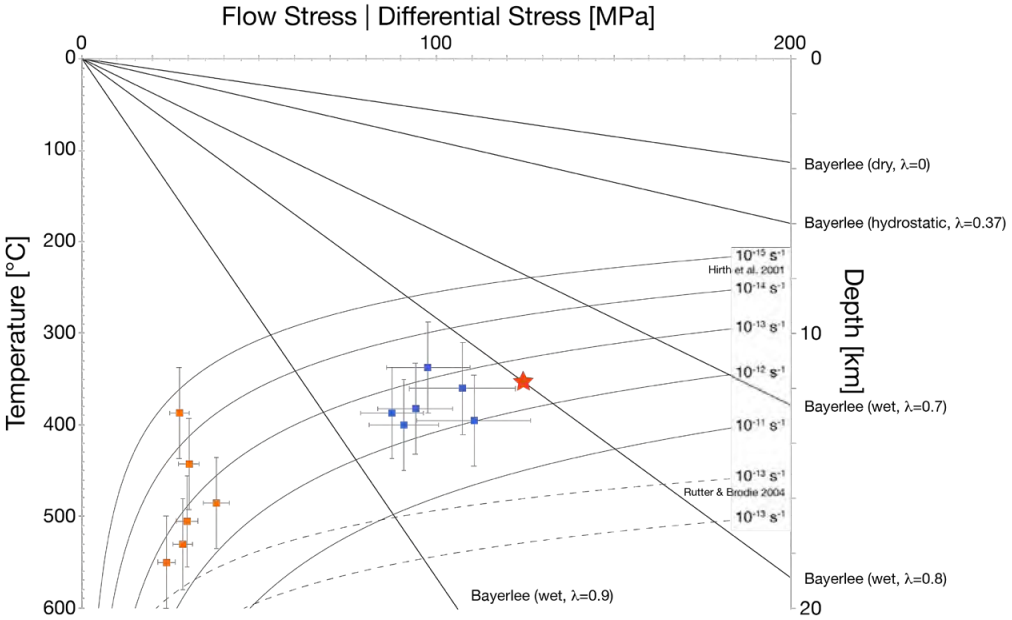

Figure 1. Strength profile of the shear zone. The temperature scale is for the ductile part and the depth scale is for the brittle part. There is no unique or steady geothermal gradient for an active megathrust. Orange symbols: flow stresses at corresponding peak deformation temperatures. The temperature gradient across the shear zone is inverted, therefore, the data points are from top (bottom of the figure) to bottom of the shear zone (up in in the figure). Blue symbols: flow stresses derived from the small, dynamically recrystallised grains and inferred deformation temperatures. Red star: most likely stresses at the brittle ductile transition. Depth of it was determined from the geometry of the shear zone and from the modelled thermal field (Grujic et al. 2020). Straight lines are the strength profiles in thrust regime for different coefficients of fluid pressure. The λ=0.8 was determined from the geometric analysis of the current Himalayan foreland fold-and-thrust belt.

REFERENCES

Grujic, D., Ashley, K. T., Coble, M. A., Coutand, I., Kellett, D. A., Larson, K. P., Whipp Jr, D. M., Gao, M., and Whynot, N. 2020: Deformational temperatures across the Lesser Himalayan Sequence in eastern Bhutan and their implications for the deformation history of the Main Central Thrust. Tectonics 39, 4, e2019TC005914, https://doi.org/10.1029/2019TC005914

1.7
Spatio-temporal complexity of aftershocks in the Apennines controlled by permeability dynamics and decarbonization

Thanushika Gunatilake* & Stephen A. Miller

Center for Hydrogeology and Geothermics (CHYN)University of Neuchâtel, Neuchâtel, 2000, Switzerland (thanushika.gunatilake@unine.ch)

In 2016, a series of large normal-fault earthquakes in the Apennines filled the seismic gap between the 1997 Colfiorito earthquake and the 2009 L'Aquila earthquakes. These earthquakes, known as the Amatrice-Visso-Norcia sequence (AVN), triggered hundreds of thousands of aftershocks in the first year, extending over 60 km along strike. The Colfiorito and L'Aquila aftershocks showed a significant high fluid-pressure (CO2) component in their genesis, and in this work, we show that the AVN sequence is also driven by high-pressure fluids. We propose that the AVN sequence is driven by both deeply-derived fluids and high pressure fluids internally generated by thermal decomposition. Using a non-linear diffusion model that captures permeability dynamics in the crust combined with a source term to account for thermal decomposition, we show excellent agreement between model and observations along nine profiles spanning the entire sequence. Excellent agreement is found for all profiles between modelled and observed cumulative number of aftershocks, despite the dramatic differences between the nine profiles. Excellent agreement is also found in spatial comparisons between the calculated fluid pressure and the hypocenters of about 35,000 well-located aftershocks. These results provide convincing evidence that aftershocks in the Apennines are predominantly fluid-driven, and we also propose that this model can capture any non-Omori type aftershock behavior.

1.8
New tectonic map in the Geneva Basin, combination of surface and sub-surface data (Switzerland and France)

Louis Hauvette[1,2], Anna Sommaruga[1], Sandra Borderie[1], Jon Mosar[1] & Michel Meyer[3]

[1] *Unit of Earth Sciences, Geosciences Department, University of Fribourg, Chemin du Musée 6, CH-1700 Fribourg (louis.hauvette@unifr.ch)*
[2] *Geneva Geo Energy (GGE), Rue des vieux grenadiers 8, CH-1205 Genève*
[3] *Services Industriels de Genève (SIG), Chemin Château-Bloch 2, CH-1219 Le Lignon*

The Northern Alpine foreland is divided into two domains: the Molasse Basin and the Jura fold-and-thrust belt (FTB), both transported towards NW. These domains are detached from the mechanical basement above a *décollement* in the Triassic evaporites. Thrusts, folds and strike-slip faults are the major structures developing in the detached Mesozoic and Cenozoic sedimentary cover of the area. The Geneva Basin, in western Switzerland, is part of the Plateau Molasse within the Molasse Basin and is limited to the NW by the Jura FTB and to the SE by the Subalpine Molasse. The 2020 Geothermal project of the Canton Geneva has provided an incentive to re-assess the subsurface geology of this area and its ties to the geology expressed at the surface.

The first objective was to build a tectonic map of the Greater Geneva Basin. The main input for this task is the interpretation of vintages since 1960' and recently acquired 2D seismic data (2018) combined with well data, that all represent the most valuable source of geological information of the subsurface. However, this data set also contains its limitations, including its resolution, and especially the high uncertainty related to the correlation of fault indications in between 2D seismic profiles. Therefore, it was crucial to develop a consistent methodology that tries in a first step to extract the maximum of useful results from the 2D seismic interpretation, and in a second step to constrain these results at best with available surface information. Subsequently we combined and implemented all information and interpretations on a common map, in order to build a final tectonic map. Fault indications from two seismic horizons, near Base Cenozoic (nBCen) and near Top Dogger (nTDo), are projected into the map with the adequate symbols of the type of fault interpreted. Major dip change lines and fold axis observed on seismic sections are also displayed as coloured points on map (intersection points between the dip change lines and fold axis (both sticks on seismic sections) with the following horizons, nBCen and nTDo) and thus define dip domains that help discriminate structural domains. This information is combined with bedding strike and dip changes on the surface map to devise axial surface traces and fault traces (supposed and observed). We further used a tectonic geomorphology approach (including lineament) to constrain our tectonic map.

It was thus possible to identify several major structures:

- strike-slip faults mainly oriented NW-SE and E-W, which reach into the Jura FTB.
- E-W fault corridors of about 10 km long and 500m large have been identified in the Meyrin area. This E-W structural direction is supported also by several geomorphological lineaments crossing the whole southern Geneva Basin and which are interpreted to reflect main tectonic structures.
- anticlines and synclines with a general NE-SW orientation, perpendicular to the general compressional direction. The folds may have a modest lateral extent and are frequently intersected by the subvertical fault corridors.
- close to the Humilly-2 well, a distinct fault has been interpreted as a NE-SW extensional synsedimentary growth fault with possible salt flow. This structure appears to have been compressionally reactivated.

The Vuache Fault Zone with its slightly distinct orientation form a different structural boundary, as shown by the transpressional lateral ramp geometries in the hanginwall.

The final tectonic map along with a catalogue of the seismic sections interpreted (pdf), and a compilation of subsurface depth maps (resulting from seismic interpretation), may bring a complete new structural review of the Geneva Basin.

1.9
Tectonics of the Western Internal Jura Fold-and-Thrust Belt: from the Geneva Basin (Switzerland) to La Bienne Valley (France). Mapping and forward modelling.

Adeline Marro[1], Anna Sommaruga[1], Louis Hauvette[1], Sandra Borderie[1], Marc Schori[1], Jon Mosar[1]

[1] *Earth Sciences Unit, Department of Geosciences, University of Fribourg, Chemin du Musée 6, 1700 Fribourg (adeline.marro@unifr.ch)*

Numerous geological studies have investigated for decades the Western part of the Jura Fold-and-Thrust Belt (FTB) to the NW of the Geneva Basin. However, since the beginning of the "GEothermie2020" project, new data such as stratigraphic harmonization, seismicity measurements, log data from drill holes, and seismic interpretations, have provided new, and more detailed knowledge about regional tectonics. In this context we re-assessed the structural geology of the Western Jura FTB in the frame of a Master thesis which focuses on the Internal part of the Western Jura FTB, between the Crêt de la Neige anticline, the Crêt au Merle summit and La Bienne valley. A forward model along a valid and balanced cross-section of the study area provides new insight on the kinematic evolution.

In a first step, a cross-section has been constructed using seismic interpretations (Hauvette, in prep.), original field measurements and a harmonized geological map based on a stratigraphic compilation from the literature. Based on these seismic depth-converted lines and the elevation model of the Pre-Mesozoic basement of Schori (2021), the depth of the near base Mesozoic horizon has been well constrained. Thus, we can show, that top basement under the Jura domain is dipping 1.3° to the SE, whereas under the Geneva Basin it is dipping between 2.7°-3.3° to the SE. The change in angle located under the SE flank of the Crêt de la Neige anticline is considered to be linked to a preexisting Paleozoic normal fault with a supposed offset of 180 meters.

Based on our initial cross-section and our refined depth of the near base Mesozoic horizon, we develop a new kinematic model of the Western Internal Jura by using the forward modelling technique implemented in the software Move 2020.1 from Petroleum Experts. The kinematic forward modelling applies fault-bend folds, trishear and fault-parallel flow algorithms. The results yield a total shortening of 23.6 km for the Western Internal Jura. Our forward model shows a thin-skinned style and forward stepping deformation. The forward stepping sequence is accompanied by minor back-stepping thrust sequences. The sequence is the result of a iterative approach to fit the best possible sequence of deformation to our initial cross section (surface data and seismic horizon data). Thus, imbricate fault-bend folding can explain the high southern slope of the Crêt de la Neige and the Crêt au Merle anticlines. The first deformation is attributed to the thrusting of the Crêt de la Neige anticline (shortening of 4.8 km) followed by the Crêt Chalam thrust and its imbrications (shortening of 6,4 km), then, the Tacon thrust (shortening of 8.4 km) and the Bienne thrust (shortening of 3.4 km). Based on seismic interpretations, duplexes have been constructed in the Keuper evaporites (shortening 600 meters). In addition to the primary décollement level situated at the base of the Keuper evaporites, three other detachments levels have been used to explain the structurally and topographically elevated position of the Valserine syncline, the Crêt au Merle anticline, the Pesse syncline, and the valley south of the Tacon river. These detachment levels are found in the marly layers of the Aalenian "faciès de transition" units, the Oxfordian "Couches d'Effingen-Geissberg" members and the Berriasian Goldberg formation. Using such a multiple thrust horizon approach avoids having to introduce thick evaporitic duplexes in the Keuper units, high basement horst or inverted Permo-Carboniferous graben structures.

Due to the modelling limitations, in a final step, the forward model has been slightly modified in some areas to better comply with the surface data. According to the seismic interpretations, reverse faults inducing a fold, simplified duplexes and a suspected Permo-Carboniferous graben has been added manually in the Geneva Basin. The final result is a kinematically viable cross-section of the Western Internal Jura, from the Geneva Basin to La Bienne valley, with deep structures validated by forward modelling (figure 1).

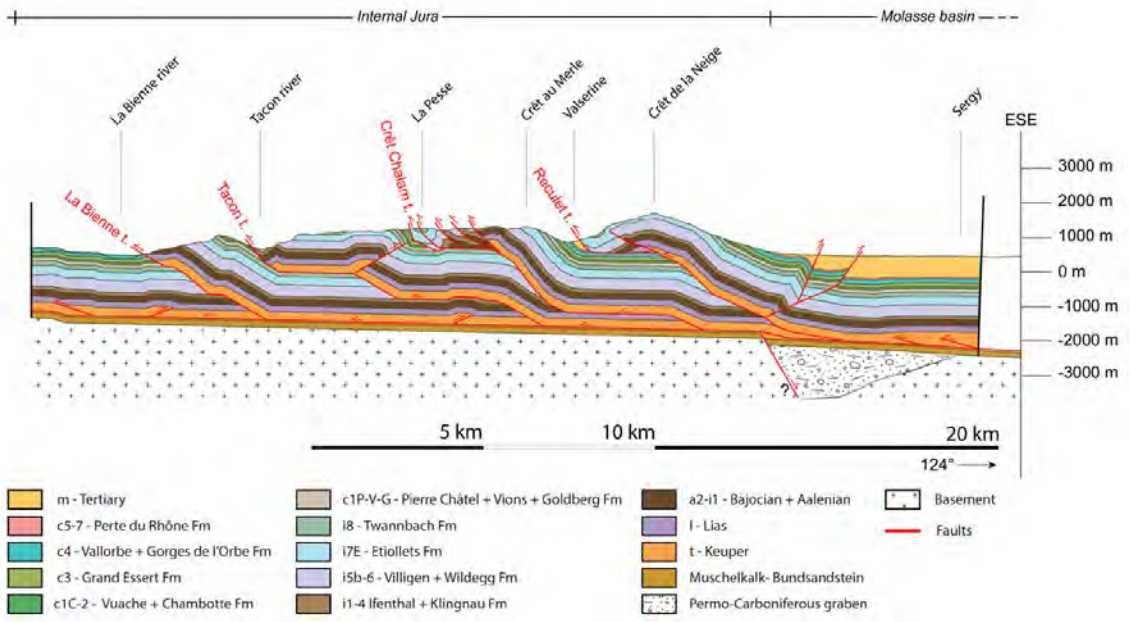

Figure 1. Final balanced cross-section between the Geneva Basin and La Bienne Valley. This section is the final result of the forward model modified in some sectors to respect the near-surface structures. In the Geneva Basin, reverse faults inducing a fold and simplified duplexes have been added manually. Based on seismic data, a suspected Permo-carboniferous graben is presented under the Molasse basin.

REFERENCES

Hauvette, L. (in prep): Seismic interpretation of the Greater Geneva Basin: Tectonics between the Mt Salève and the Jura "Haute-Chaîne" (France and Switzerland). PhD thesis. University of Fribourg.

Schori, M. (2021): The Development of the Jura Fold-and-Thrust Belt: pre-existing Basement Structures and the Formation of Ramps. PhD thesis, submitted June 2021. University of Fribourg.

1.10
Interaction of faulting and magma propagation in oblique extensional settings (North Volcanic Zone, Iceland) using UAV-based structural data

Elisabetta Panza[1], Joël Ruch[1]

[1] *Department of Earth Sciences, University of Geneva, Rue des Maraîchers 13, 1205 Genève (elisabetta.panza@unige.ch)*

Understanding how magma propagates in the crust and eventually where it will erupt is one of the key challenges in volcanology. Most models assume that magma propagates in a homogeneous crust, without accounting for inherited structures. However, in volcano-tectonically active systems, inherited structures are common.

In this study, we analyse the role of inherited crustal structures and their reactivation on the propagation of magma in extensional tectonic environments.

Being a rift lying on top of a mantle plume, Iceland hosts several volcano-tectonic events related to the extension of the Mid-Atlantic Ridge, which is here exceptionally exposed above sea level. It is, therefore, a perfect location to observe the interplay between extensional tectonics structures and magmatic processes. In historical time we identified 15 main volcano-tectonic events that released over days or weeks the tectonic strain deficit accumulated over several decades or centuries. The crustal opening associated with dike emplacement during volcano-tectonic events is of the same order of magnitude of the strain deficit accumulated since the previous event in the same area, as shown, for example, by Holuhraun events in 1797 and in 2014-2015. Thus, timing and location of such events suggest a cyclic nature of strain loading and release, expressed as a steady ~2cm/yr average extension rate in the far-field and as discrete, often metrical stepwise opening in the near-field.

We focus on the North Volcanic Zone, which is one of the most active rift branches of Iceland and we selected three zones, delimited by Fjallagjá graben to the North and the Holuhraun to the South. In these segments, as seen from satellite images, structures progressively bend from an almost N-S orientation to a rather NE-SW one, while the strain field of the rift stays the same throughout, with a constant extension vector's azimuth of ~104°. To test a potential opening obliquity, we performed extensive UAV surveys, covering ~32 km2 with 46 flights. We obtained ~3 cm/px DEMs and ~2 cm/px orthomosaics, which are the base of the following near-field morphological and structural analysis, looking at fractures, topography effects, and kinematic indicators. The processed imagery revealed typical structures related to volcano-tectonic processes, such as monoclines, open fractures, nested grabens, and exposed a graben with intrusions oblique to the graben shoulders.

Specific attention is paid to obliquity between various sets of structures and volcanic morphologies, especially considering the progressively evolving geometry relation of the structures with the current opening vector along the rift segment. In fact, > 70% of rifts on Earth are oblique and inherited structures are not necessarily always perfectly oriented with the current opening direction.

Results show that eruptive fissures and volcanic morphologies are on average parallel to the main axis of the current rift extension, but ~10°-20° consistently oblique to the enclosing graben shoulders.
The integration of UAV high-resolution mapping widened the availability of near-field structural datasets, through which we aim at unveiling fundamental processes of magma transport in the crust.

1.11
Tectonic paleostress and tectonic geomorphology in the close vicinity of the Pontarlier strike-slip fault system (Swiss and French Jura fold and- thrust belt)

Omar M. A. Radaideh[1], Anna Sommaruga[1] and Jon Mosar[1]

[1] Département de Géosciences, Université de Fribourg, Chemin du Musée 6, 1700 Fribourg, Suisse (Omar_M_Sabbah@yahoo.com; jon.mosar@unifr.ch)

This work focuses particularly on the combined tecto-geomorphic and paleostress studies to decipher the style and orientations of tectonic stress fields and to detect their signatures in the present-day fluvial landscape in the northern Alpine Foreland. Two adjacent study areas across the northern Alpine Foreland, the westernmost part of Switzerland and the region of Pontarlier strike-slip fault system in the Swiss and French Jura fold-and-thrust belt, were respectively selected for the detailed tecto-geomorphic and paleostress analyses.

Using high resolution digital elevation model, the diverse geomorphic responses of fluvial landscapes to tectonic deformations were highlighted in the westernmost part of Switzerland on the basis of a combined analysis of hypsometric curves and integrals, transverse topographic symmetry index, and channel length-gradient index. This strategy was additionally supported by analysis of topographic-swath profiles and geophysical and sub/surface geological data. The obtained results not only show clear indications of the importance role of tectonics in the landscape development, which can't be explained as being the results of variation in lithology and/or climate, but also provide convincing evidence of Cenozoic reactivation of some buried Mesozoic faults in the relatively deep subsurface.The presence of sharp convex upward hypsometric curve with high hypsometric integral value, a noticeable drainage migration/deflection, and steep channel gradients with prominent knickpoints, which almost coincide in space with sudden variations in the depth of the subsurface geologic layers and in the geophysical properties, manifest the role of tectonic activity in the development of present-day landscapes in the westernmost part of Switzerland.

The paleostress analysis of new heterogeneous fault-slip datasets, together with new chronological field observations, through using the P-B-T-axes and Right Dihedral methods, have allowed reconstruction of successive tectonic events under which brittle deformations occurred in the region of Pontarlier strike-slip fault system. These events, which are well correlated with those recognized in the other parts of European Platform, composed of a sequence, from oldest to youngest, of N-S-trending strike-slip, NW-SE-trending extensional, NW-SE-trending compressional, and ~NW-SE-trending strike-slip stress deformations. They occurred prior to, during and after the onset of Jura folding and thrusting, and related to convergence and subsequent collision between the Adriatic microplate and Eurasia plate since Early Cenozoic times. The latest tectonic deformation event, derived from this study, shows similar stress style and direction to the present-day stress field given by the inversions of earthquake focal mechanisms.

1.12
Geology along the Bedretto tunnel: kinematic and geochronologic constraints on the evolution of the Gotthard Massif (Central Alps)

Markus Rast[1], Andrea Galli[2], Jonas B. Ruh[1], Claudio Madonna[1], Marcel Guillong[2]

[1] Geological Institute, ETH Zürich, Zürich, Switzerland (markus.rast@erdw.ethz.ch)
[2] Institute of Geochemistry and Petrology, ETH Zürich, Zürich, Switzerland

The unlined Bedretto tunnel crosses large parts of the crystalline zone of the Gotthard massif (Central Alps), which offers the possibility to study late-Variscan plutonic rocks (Rotondo granite) and parts of their Caledonian (poly-) metamorphic host rocks (Tremola and Prato series). The Rotondo granite consists to a large part of an equigranular, fine-grained granite (Labhart, 2005). However, the Bedretto tunnel also revealed exposures of a porphyritic granite, showing that the Rotondo granite is not homogeneous. Some parts of the Rotondo granite exhibit a weak foliation and ductile deformation is localized along discrete granitic ductile shear zones (G-DSZ) or quartz-biotite-rich ductile shear zones (QB-DSZ).
This study presents structural data mapped along the Bedretto tunnel, with emphasis on ductile deformation features in the Rotondo granite. Further constraints derived from microstructural and U-Pb geochronological evidence lead to the following insights:

(1) Both, G-DSZ and QB-DSZ dip generally steeply towards north and are related to top-to-south reverse shearing. Features of dynamic recrystallization suggest that ductile deformation in the Rotondo granite may have occurred at or below Alpine peak temperature conditions of ca. 475 – 500 °C (Bousquet et al., 2012), which was reached after the Gotthard massif was thrusted onto the Aar massif (’D2 stage’, e.g. Herwegh et al., 2017). Therefore, the ductile deformation in the Rotondo granite is probably related to southward-verging backthrusting of the Gotthard massif that took place after the ‘D2 stage’. However, a pre-Alpine deformation event cannot be excluded based on the present data.

(2) Zircons from two varieties of Rotondo granite show overlapping $^{206}Pb/^{238}U$ age ranges of 285 − 319 Ma (equigranular granite) and 280 − 335 Ma (porphyritic granite), which indicate that both varieties are part of the same late-Variscan magmatic event. The $^{206}Pb/^{238}U$ age data of the present study are consistent with the commonly accepted intrusion age of the Rotondo granite of 294 ± 1.1 Ma (Sergeev et al., 1995).

(3) A significant number of zircons from a QB-DSZ are older than the upper boundary of the granite age range (i.e. > 335 Ma), which is not the case for zircons extracted from the granite samples. Therefore, the parent material of the QB-DSZ must be older than the Rotondo granite. This in turn means that the QB-DSZ are not sheared lamprophyres as previously thought (e.g. Lützenkirchen and Loew), but basement rock inclusions within the granite (sheared xenoliths).

REFERENCES

Bousquet, R., Oberhänsli, R., Schmid, S. M., Berger, A., Wiederkehr, M., Robert, C., Möller, A., Rosenberg, C., Zeilinger, G., Molli, G., and Koller, F. (2012). Metamorphic framework of the Alps (1:1’000’000). Commission for the Geological Map of the World, Paris.

Herwegh, M., Berger, A., Baumberger, R., Wehrens, P., and Kissling, E. (2017). Large-Scale Crustal-Block-Extrusion During Late Alpine Collision. Scientific Reports, 7(1):1–10.

Labhart, T. P. (2005). Erläuterungen zum Geologischen Atlas der Schweiz 1:25000, Val Bedretto, Atlasblatt 68. Bundesamt für Wasser und Geologie, Bern-Ittigen.

Lützenkirchen, V. and Loew, S. (2011). Late Alpine brittle faulting in the Rotondo granite (Switzerland): Deformation mechanisms and fault evolution. Swiss Journal of Geosciences, 104(1):31–54.

Sergeev, S. A., Meier, M., and Steiger, R. H. (1995). Improving the resolution of single-grain U/Pb dating by use of zircon extracted from feldspar: Application to the Variscan magmatic cycle in the central Alps. Earth and Planetary Science Letters, 134(1-2):37–51.

1.13
New geological mapping of the Afar depression: from review towards the understanding of basin dynamics during active rifting

Valentin Rime[1], Anneleen Foubert[1], Balemwal Atnafu[2], Tesfaye Kidane[3]

1 Department of Geosciences, University of Fibourg, Ch. Du Musée 6, 1700 Fribourg (valentin.rime@unifr.ch)
2 School of Earth Sciences, Addis Ababa University, Addis Ababa, Ethiopia
3 School of Agricultural, Earth and Environmental Sciences, University of Kwazulu-Natal, Westville Campus, Durban, South Africa

Geological mapping has been used since the early days of geosciences to understand the processes that shaped our planet. Geological mapping is a keystone in the interpretation of geological observations and forms the base for any advanced geo-analytical work.

The Afar Depression forms a triple junction between three rift systems: the Red Sea Rift, the Gulf of Aden Rift and the Main Ethiopian Rift which is part of the East African Rift System. Important mapping efforts in the area during the 60s and 70s provided very valuable input for the understanding of the local geology but also for the development of global tectonic, volcanological and sedimentary concepts in active rift zones. This study presents the compilation of a new geological map of the Afar depression. It is the first one of its kind in the sense that it covers the complete Afar depression and includes the full sedimentary and magmatic cover for the complete Phanerozoic. This map is based on extensive literature research, remote sensing (multispectral satellite imagery and DEM) and fieldwork. It shows the complexity of the system with the interaction of multiple tectonic plates, blocks, rift segments, sedimentary basins and volcanic areas that evolve through time and space. This integrative geological map covering the full Afar depression allows the better understanding of the evolution of continental breakup and will help in the better comprehension of rift processes and passive margin development worldwide.

1.14
Diachronous evolution of the Carpathians belt and foreland, from low-T thermochronology inversion and isopach maps analysis.

Marion Roger[1], Arjan de Leeuw[1], Peter van der Beek[2], Laurent Husson[1,3]

1 ISTerre, Institut des Sciences de la Terre, Université Grenoble Alpes, 1381 rue de la Piscine, 38 058 Grenoble cedex 9, France (marion.roger@univ-grenoble-alpes.fr)
2 Institut für Geowissenschaften, Universität Potsdam, Karl-Liebknecht-Str. 24-25 Haus 27, 14476 Potsdam-Golm, Germany
3 CNRS, ISTerre, Institut des Sciences de la Terre, 1381 rue de la Piscine, 38 058 Grenoble cedex 9, France

Mountain belt tectonic evolution is frequently diachronous along strike either because of oblique convergence or because of non-straight continental margins. This has direct implications for the exhumation dynamics of the belt, lateral frontal thrust propagation and exhumation rate heterogeneity along the collision front. It also impacts upon the creation of relief and orogenic precipitation, and thus erosion. If the collision evolves diachronously along the mountain chain the same may be true for the foreland basin, including the flexural behaviour of the underlying crust and filling of the basins by the sedimentary system (e.g., the Pyrenees, Anatolia-Zagros, Taiwan, New-Zealand). Even though it is well established that there is a direct relationship between wedge exhumation and erosion-sedimentation processes in adjacent basins (Sinclair and Allen, 1992; Willett et al., 1993), both phenomena are rarely studied in tandem (but see Morris et al., 1998; Curry et al., 2019, 2021). This might be the case because it needs a significant amount of data from both the basin and the mountain belt, as well as a multidisciplinary approach.

We use the Carpathians as a case study for a diachronously evolving collision belt. There is a good number of published low-temperature thermochronology data throughout the belt (~300 data for AFT, ZFT, AHe and ZHe thermochronometers; Sanders et al., 1999; Leever et al., 2006; Mazzoli et al., 2010; Merten et al., 2010; Andreucci et al., 2013, 2015; Castelluccio et al., 2016; Nakapelyukh et al., 2018)up to 4 km of erosiontook placeovertheactivelydeformingorogen,andthee rosionpatternsformsa mirroredimageof the subsurfacdeeformingwedge.Theerosionproductsaredepositedin flankingmolassebasinswhich subsidecdontemporaneousdluyeto thegrowingtopographiwc eightof thewedge.Deformationof thewedgewaspresumablyactivefrom theearlyto lateMiocene,butapatiteFT agesbetween14 and9 Ma andtracklengthmodelingpredictanaccelerationof erosionrates(0.5-0.3 mm/yr, and ample information on the stratigraphy of the foreland basin (Oszczypko, 2006; Leever et al., 2006; Matoshko et al., 2016; de Leeuw et al., 2020Jagiellonian University, Institute of Geological Sciences, Oleandry 2a, PL-30-063 Kraków, Poland, e-mail: nestor@geos.ing.uj.edu.pl. (received: June 23, 2005; accepted: February 2, 2006 and references therein). We calculated an exhumation model for the whole West and East Carpathians using the Pecube program (Braun et al., 2012)the PECUBE code has been under continuous development as its use became wider and addressed different tectonic–geomorphic problems. This paper describes several major recent improvements in the code, including its integration with an inverse-modeling package based on the Neighborhood Algorithm, the incorporation of fault-controlled kinematics, several different ways to address topographic and drainage change through time, the ability to predict subsurface (tunnel or borehole. It iterates through thousands of exhumation scenarios and uses Bayesian statistics to select the parameters which best fit the compiled thermochronology data. This shows how exhumation rates change per nappe and per region over time, which translates into eroded sediment volumes across the belt from the Oligocene onward. On the basin side, a 3D model was built with more than a hundred geological cross-sections, seismic sections, geological maps and 600 field observations (de Leeuw et al., 2020), which we used to construct isopach maps for important stratigraphic intervals. These reveal the pattern of depocenter migration along the foreland.

As a result, we obtain combined maps of exhumation of the Carpathians belt and sedimentation in the basin. These are providing new insights into the relation between wedge construction and generation and accommodation of sediment fluxes which is clearly diachronous from NW to SE, in line with Neogene volcanism, lateral frontal thrust propagation and axial sediment transport in the foreland basin. (Seghedi et al., 2019; Nemčok et al., 2006; de Leeuw et al., 2020)(ii

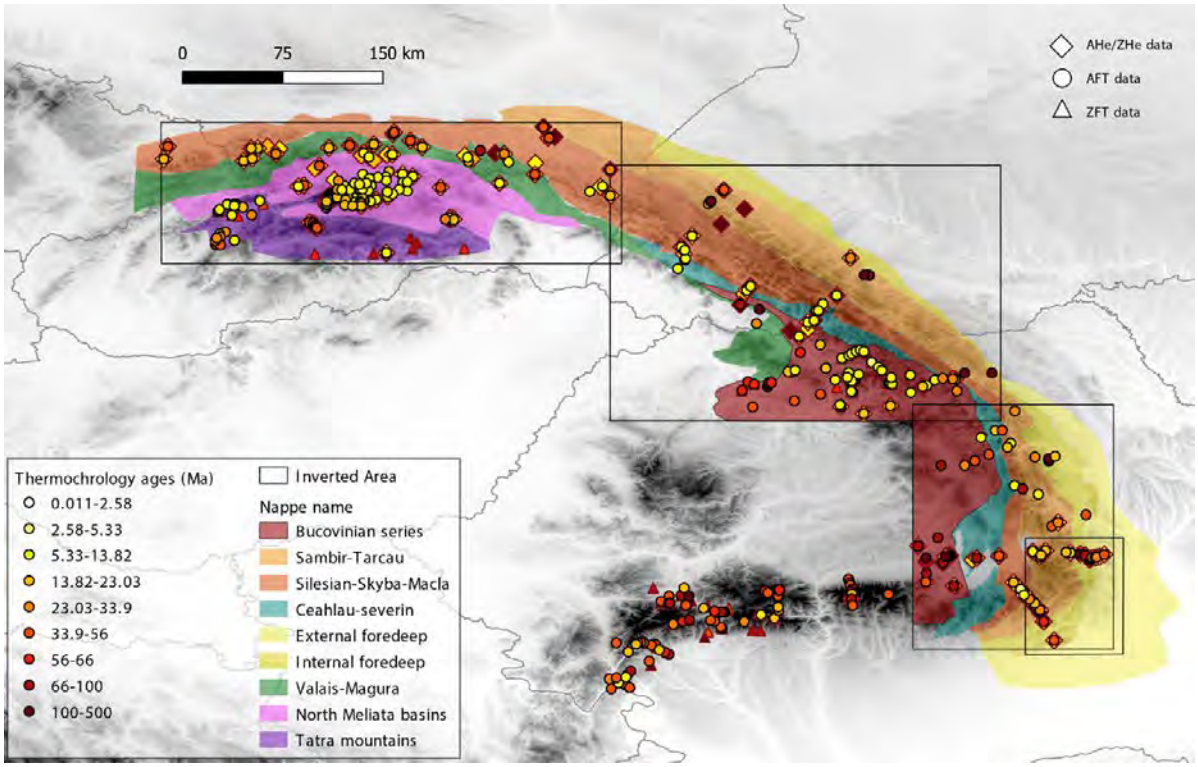

Figure 1. Carpathians Belt low-temperature thermochronology database (compilation from published articles), comprising AFT, ZFT, AHe and ZHe thermochronmeters. Colored block represent the different tectonics dommain as identified in Schmid et al., 2008. The grey rectangles shows the surface areas where the inversions were mades.

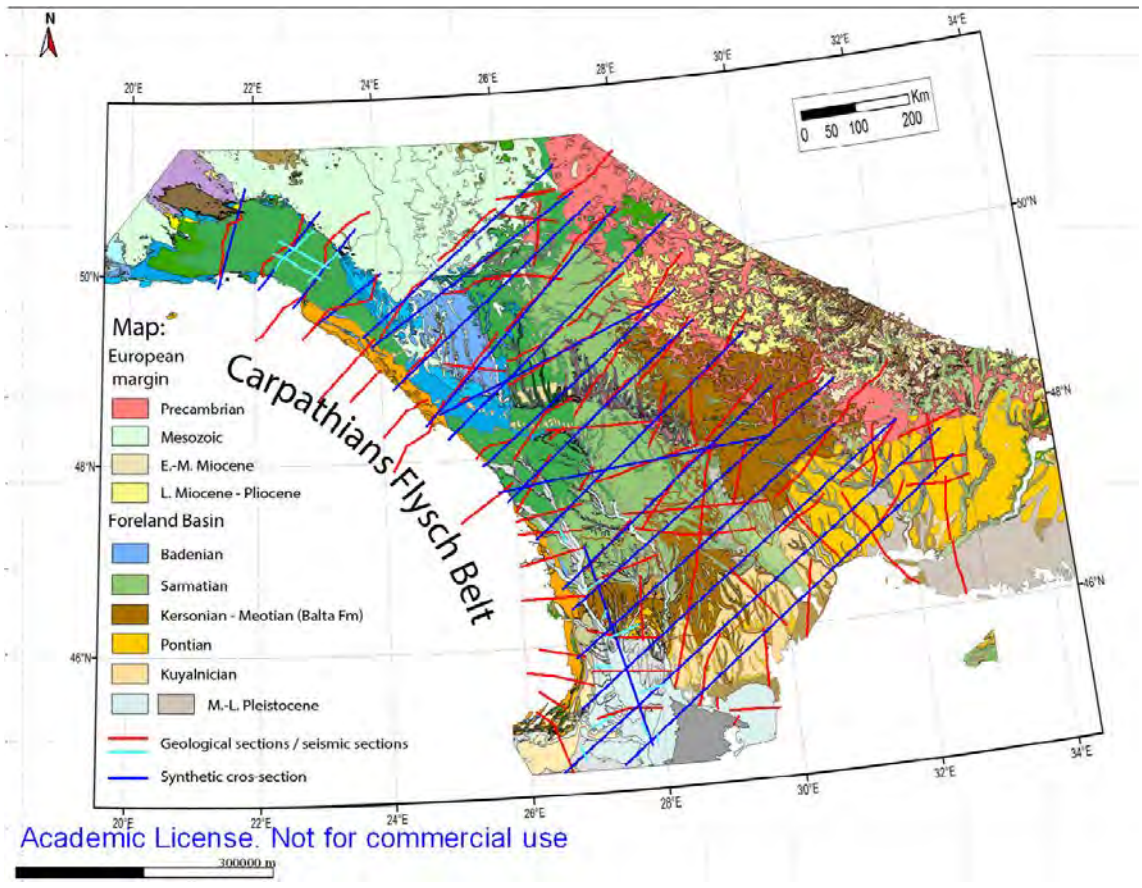

Figure 2. Carpathians Foreland Basin 3D model on the MOVE (PetEx) software, Color code is for the different sediment from the Miocene. The geological and seismic cross-sections (respectively in red and light blue) allow us to built synthetic cross-section across the basin (dark blue sections).

REFERENCES

Andreucci, B., Castelluccio, A., Jankowski, L., Mazzoli, S., Szaniawski, R., and Zattin, M.: Burial and exhumation history of the Polish Outer Carpathians: Discriminating the role of thrusting and post-thrusting extension, Tectonophysics, 608, 866–883, https://doi.org/10.1016/j.tecto.2013.07.030, 2013.

Andreucci, B., Castelluccio, A., Corrado, S., Jankowski, L., Mazzoli, S., Szaniawski, R., and Zattin, M.: Interplay between the thermal evolution of an orogenic wedge and its retro-wedge basin: An example from the Ukrainian Carpathians, Geological Society of America Bulletin, 127, 410–427, https://doi.org/10.1130/B31067.1, 2015.

Braun, J., van der Beek, P., Valla, P., Robert, X., Herman, F., Glotzbach, C., Pedersen, V., Perry, C., Simon-Labric, T., and Prigent, C.: Quantifying rates of landscape evolution and tectonic processes by thermochronology and numerical modeling of crustal heat transport using PECUBE, Tectonophysics, 524–525, 1–28, https://doi.org/10.1016/j.tecto.2011.12.035, 2012.

Castelluccio, A., Mazzoli, S., Andreucci, B., Jankowski, L., Szaniawski, R., and Zattin, M.: Building and exhumation of the Western Carpathians: New constraints from sequentially restored, balanced cross sections integrated with low-temperature thermochronometry: WESTERN CARPATHIANS TECTONIC EVOLUTION, Tectonics, 35, 2698–2733, https://doi.org/10.1002/2016TC004190, 2016.

Curry, M. E., van der Beek, P., Huismans, R. S., Wolf, S. G., and Muñoz, J.-A.: Evolving paleotopography and lithospheric flexure of the Pyrenean Orogen from 3D flexural modeling and basin analysis, Earth and Planetary Science Letters, 515, 26–37, https://doi.org/10.1016/j.epsl.2019.03.009, 2019.

Curry, M. E., Beek, P. van der, Huismans, R. S., Wolf, S. G., Fillon, C., and Muñoz, J.-A.: Spatio-temporal patterns of Pyrenean exhumation revealed by inverse thermo-kinematic modeling of a large thermochronologic data set, 49, 738–742, https://doi.org/10.1130/G48687.1, 2021.

de Leeuw, A., Vincent, S. J., Matoshko, A., Matoshko, A., Stoica, M., and Nicoara, I.: Late Miocene sediment delivery from the axial drainage systemof the East Carpathian foreland basin to the Black Sea, https://doi.org/10.1130/G47318.1, 2020.

Leever, K. A., Matenco, L., Bertotti, G., Cloetingh, S., and Drijkoningen, G. G.: Late orogenic vertical movements in the Carpathian Bend Zone - seismic constraints on the transition zone from orogen to foredeep: Late orogenic vertical movements in the Carpathian Bend Zone, 18, 521–545, https://doi.org/10.1111/j.1365-2117.2006.00306.x, 2006.

Matoshko, A., Matoshko, A., de Leeuw, A., and Stoica, M.: Facies analysis of the Balta Formation: Evidence for a large late Miocene fluvio-deltaic system in the East Carpathian Foreland, Sedimentary Geology, 343, 165–189, https://doi.org/10.1016/j.sedgeo.2016.08.004, 2016.

Mazzoli, S., Jankowski, L., Szaniawski, R., and Zattin, M.: Low-T thermochronometric evidence for post-thrusting (<11 Ma) exhumation in the Western Outer Carpathians, Poland, Comptes Rendus Geoscience, 342, 162–169, https://doi.org/10.1016/j.crte.2009.11.001, 2010.

Merten, S., Matenco, L., Foeken, J. P. T., Stuart, F. M., and Andriessen, P. A. M.: From nappe stacking to out-of-sequence postcollisional deformations: Cretaceous to Quaternary exhumation history of the SE Carpathians assessed by low-temperature thermochronology: EXHUMATION HISTORY OF THE SE CARPATHIANS, Tectonics, 29, https://doi.org/10.1029/2009TC002550, 2010.

Morris, Sinclair, and Yell: Exhumation of the Pyrenean orogen: implications for sediment discharge, Basin Research, 10, 69–85, https://doi.org/10.1046/j.1365-2117.1998.00053.x, 1998.

Nakapelyukh, M., Bubniak, I., Bubniak, A., Jonckheere, R., and Ratschbacher, L.: Cenozoic structural evolution, thermal history, and erosion of the Ukrainian Carpathians fold-thrust belt, Tectonophysics, 722, 197–209, https://doi.org/10.1016/j.tecto.2017.11.009, 2018.

Nemčok, M., Pogácsás, G., and Pospíšil, L.: Activity Timing of the Main Tectonic Systems in the Carpathian–Pannonian Region in Relation to the Rollback Destruction of the Lithosphere, in: The Carpathians and Their Foreland: Geology and Hydrocarbon Researces: AAPG Memoir 84, edited by: Golonka, J. and Picha, F. J., The American Association of Petroleum Geologists, Tulsa, Oklahoma, U.S.A., 743–766, https://doi.org/10.1306/985627M843083, 2006.

Oszczypko, N.: Late Jurassic-Miocene evolution of the Outer Carpathian fold-and-thrust belt and its foredeep basin (Western Carpathians, Poland), 25, 2006.

Sanders, C. A. E., Andriessen, P. A. M., and Cloetingh, S. A. P. L.: Life cycle of the East Carpathian orogen: Erosion history of a doubly vergent critical wedge assessed by fission track thermochronology, J. Geophys. Res., 104, 29095–29112, https://doi.org/10.1029/1998JB900046, 1999.

Schmid, S. M., Bernoulli, D., Fügenschuh, B., Matenco, L., Schefer, S., Schuster, R., Tischler, M., and Ustaszewski, K.: The Alpine-Carpathian-Dinaridic orogenic system: correlation and evolution of tectonic units, Swiss J. Geosci., 101, 139–183, https://doi.org/10.1007/s00015-008-1247-3, 2008.

Seghedi, I., Besutiu, L., Mirea, V., Zlagnean, L., Popa, R.-G., Szakács, A., Atanasiu, L., Pomeran, M., and Vişan, M.: Tectono-magmatic characteristics of post-collisional magmatism: Case study East Carpathians, Călimani-Gurghiu-Harghita volcanic range, Physics of the Earth and Planetary Interiors, 293, 106270, https://doi.org/10.1016/j.pepi.2019.106270, 2019.

Sinclair, H. D. and Allen, P. A.: Vertical versus horizontal motions in the Alpine orogenic wedge: stratigraphic response in the foreland basin, Basin Research, 4, 215–232, https://doi.org/10.1111/j.1365-2117.1992.tb00046.x, 1992.

Willett, S., Beaumont, C., and Fullsack, P.: Mechanical model for the tectonics of doubly vergent compressional orogens, 5, 1993.

1.15
Oblique rifting event during the 2021 Reykjanes seismo-tectonic and volcanic crisis (SW Iceland).

Joël Ruch[1], Simon Bufféral[1,2], Elisabetta Panza[1], Stefano Mannini[1], Birgir Óskarsson[3], Nils Gies[3], Celso Alvizuri[4], Ásta Rut Hjartardóttir[5]

[1] Department of Earth Sciences, University of Geneva (joel.ruch@unige.ch)
[2] Institut de Physique du Globe de Paris, France
[3] Icelandic Institute of Natural History, Reykjavik, Iceland
[4] Institute of Earth Sciences, University of Lausanne
[5] Institute of Earth Sciences, University of Iceland, Reykjavik, Iceland

The Reykjanes Peninsula has been affected by a seismo-tectonic crisis that started with a strong seismic swarm the 24 February 2021. This activity has been followed by a volcanic eruption the 19 March, the first after ~800 years of quiescence in this region. The Reykjanes Peninsula is a highly oblique rift zone and separates the American from the Eurasian tectonic plates. The Peninsula hosts four overlapping rifts and connects to the Mid Atlantic Ridge to the South East and to the South Icelandic Seismic Zone to the West. The structural relation between the plate boundary (oriented N070), the volcanic alignments (N040) and the ground ruptures related to large M_w5 magnitude earthquakes (N175) is still poorly understood. The 2021 crisis gives us a unique opportunity to better understand how these different structures relate and interact together from depth up to the surface.

The seismic swarm occurred between the 20 February 2021 and the 20 March with 550 earthquakes with magnitudes larger than three and six events with M_w>5<5.7. Hypocentres highlighted a 10 km long segment oriented NE-SW with lateral excursions of seismic activity to the SW reaching the town of Grindavik, located seven kilometres away. Radar satellite images (InSAR) showed a 50 cm subsidence overprinted on the seismicity segment, with two uplift lobes at its periphery, indicating that a dike was intruding the area. The seismicity shut down 48 to 24 hours prior the eruption that is since then aseismic.

We have been collecting extensive structural data and mapped the entire fracture field that developed during the crisis. These structures that are nowadays gone, whether recovered by lava flows of the growing volcano or weathered by rain and wind when located on sand plains, are unique testimony of the interaction between magma intrusions and regional tectonics. Field observations show widespread ground cracks affecting the intrusion area with left-stepping en-echelon metrical segments separated by centimetric push up ridges indicating right lateral strike-slip faulting. To get the full picture of the fracture field, we used a fixed-wing drone and mapped most of the ground ruptures over an area of ~30 km^2. We then processed high-resolution (<5 cm) orthophotos and DEM and found two main NS oriented fracture zones of 3 to 4 kilometres-long made of en-echelon structures with very limited extensional cracks, even in the vicinity of the eruption site. These two main structures correspond to the location of three earthquakes of M_w>5. We then used optical image correlation technique analysing air photos acquired before and after the three earthquakes of M_w5.7 (24 February), M_w5.0 and M_w5.6 (7 and 14 March, respectively). Results show a clear NS oriented shear direction (right lateral motion) of up to 10 cm with few cm of opening, in good agreement with focal mechanisms that show strike-slip faulting. The strucutral data collected in the field and with the drone integrated with seismicity, InSAR and optical image correlation suggest an overall bookshelf geometry broken up by a dike intrusion.

1.16
Probabilistic 3D Fault Network Models of Seismogenic Faults: Case Studies from the Northern Valais

Sandro Truttmann[1], Tobias Diehl[2], Marco Herwegh[1]

[1] *Institute of Geological Sciences, University of Bern, Baltzerstrasse 1&3, CH-3012 Bern (sandro.truttmann@geo.unibe.ch)*
[2] *Swiss Seismological Service SED, ETH Zürich, Sonneggstrasse 5, CH-8092 Zürich*

In regions with minor crustal deformation and distributed weak to moderate seismic activity, such as the Swiss Alps, identification of seismogenic faults at the surface is rather challenging, often even not possible. However, more profound information about the abundance, geometric properties and kinematics of seismogenic faults is required to improve the seismotectonic characterization and the assessment of seismic hazard in such regions.

Within the project SeismoTeCH, we aim to obtain knowledge on abundance and properties of active seismogenic faults in Switzerland. In this study, we develop a Python algorithm that uses high-precision, relatively relocated earthquake hypocenters to derive full-scale probabilistic 3D fault network models at depth. We apply the algorithm to the events of two relocated seismic sequences in the northern Valais in the proximity of the Rawil depression, close to the villages of St. Leonard and Anzère. For both earthquake sequences, we image subvertical, approximately E-W striking fault systems with dextral strike-slip movements and compressional stepover faults at unprecedented spatial resolution. Using the local stress field derived from the focal mechanisms of the respective sequence, we are able to quantify the stress states and kinematics of the seismogenic faults and gain insights into the propagation of the seismicity across the stepovers.

The increasing number of recorded events and continuous advances in earthquake relocation procedures will provide new datasets on which our method can be applied. This will enable the detection and characterisation of further sub-surface seismogenic fault systems without relying on the scarce and often unreliable surface information. In future work, we also aim to apply the algorithm to regional-scale, relatively relocated earthquake catalogs to detect further active fault systems in an automated way.

1.17
Seismic-geodynamic constraints on compositional heterogeneity near the 660-km discontinuity

Jun Yan[1], Maxim Ballmer[2,1], Lauren Waszek[3], Benoit Tauzin[4] & Paul Tackley[1]

[1] Institute of Geophysics, ETH Zurich, Sonneggstrasse 5, CH-8092 Zurich (jun.yan@erdw.ethz.ch)
[2] University College London, Department of Earth Sciences, London, WC1E 6BS, UK
[3] James Cook University, Physical Sciences, Douglas, QLD 4811, Australia
[4] Université de Lyon, UCBL, ENSL, CNRS, LGL-TPE, Villeurbanne, France

One of the main features of plate tectonics is the recycling of subducting slabs into the deep mantle, which may result in multi-scale thermal and compositional heterogeneity. Both geochemical and seismological observations suggest that Earth's mantle is heterogeneous on small as well as large scales. The detailed thermochemical structure, however, remain poorly understood due to the complexity of the plate-mantle system, and the mainly indirect observations. To test the compositionally layered mantle hypothesis, here we perform a joint analysis of self-consistent global geodynamic models and the global-scale dataset of S660S waves reflecting off the 660-km discontinuity. Thermodynamic modeling and synthetic seismic analysis show that compositionally layered and compositionally non-layered mantle models have distinct distributions of reflection coefficients at 660-km discontinuity. The compositionally layered model features with a large number of small reflection coefficients at ~600-km depth, which can be contribute to the subducted mid-ocean ridge basalt segregates from subducted harzburgite to accumulate in the mantle transition zone (MTZ). Our observed global distribution of reflection coefficients at ~660 km depth is more consistent with compositionally layered mantle as predicted in the thermochemical model. The results of our joint seismic-geodynamic constraints provide a better understanding of the nature, formation and distribution of compositional heterogeneity near the 660-km discontinuity of MTZ.

1.18
CT-scanned analog models of lithospheric-scale rifting

Frank Zwaan[1], Guido Schreurs[1]

[1] *University of Bern, Institute of Geological Sciences, Baltzerstrasse 1+3 Bern, Switzerland (frank.zwaan@geo.unibe.ch)*

Analogue modeling studies of rifting routinely focus on the crustal part of the lithosphere, and often the isostatic effects that are related to the thinning of the lithosphere are ignored. Some modelers included the whole lithosphere in their models by having it float on top of a heavy fluid simulating the sub-lithospheric mantle (e.g. Brun & Beslier 1996). Such lithospheric-scale models have provided highly useful insights into rift evolution. However, monitoring internal model deformation is a major challenge, since surface observations often do not provide direct clues on deformation deep down in the model. We therefore present a new set of lithospheric-scale models of orthogonal and oblique rifting, completed in an X-ray CT-scanner.

The models involved a typical 4-layer lithosphere, with brittle sand layers representing the competent upper crust and upper lithospheric mantel, and viscous layers representing the ductile lower crust and lower lithospheric mantle (Fig. 1a). This 4-layer lithosphere was built up within a rectangular frame able to accommodate both orthogonal and oblique extension. This frame itself was placed within a basin of glucose syrup layer simulating the uppermost part of the sub-lithospheric mantle (i.e. the asthenosphere). When stretching the model lithosphere, deformation was accompanied by syrup flow into the space below the model lithosphere (Fig. 1). A “seed” (a ridge of viscous material [ø ca. 1 cm]) was inserted at the base of the upper mantle to localize deformation (Fig. 1a). Model evolution was closely monitored through high-resolution time-lapse photography and CT-scanning at 15 min intervals.

Early on in Model 1 (orthogonal extension), the seed localized normal faulting in the upper mantle layer (Fig. 1a-b). This deformation was then transferred into the upper crustal layer via low-angle shear zones in the viscous lower crust, generating dual grabens and a general topographic depression in between (Figs. 1b, c). The left-hand one of these grabens was dominant and as extension progressed, a right-lateral shear zone cutting through the whole lithosphere developed (Fig. 1d). Meanwhile, the stretching and thinning of the lithosphere split the upper mantle layer, and the lower mantle (and especially the asthenosphere) rose up, bringing the former in contact with the lower crust.

Model 2 reveals that 45˚ oblique extension also led to deformation in the strong upper lithospheric mantle layer, but did not cause the same localization of deformation on the surface as in Model 1 (Fig. 1a, e). Instead, only a general topographic depression developed, where upper crustal faulting only occurred at the model boundaries, even after > 3 h of extension (Fig. 1e). Hence we increased the extension velocity and thus the coupling between the upper lithospheric mantle and upper crustal layers (due to the strain-rate dependent rheology of the viscous lower crustal layer). As a result, faulting started localizing in the upper crustal layer (Fig. 1f), forming two bands of en echelon grabens on both sides of the mantle weakness (Fig. 1g).
These first model results show that both the novel modeling machine and the set-up function well, especially since the general (orthogonal extension model) results are similar to those of e.g. Brun & Beslier (1996). Yet our new CT-scans provide the first-ever direct insights into the internal deformation of a complete lithospheric-scale rifting model. Future particle image velocitmetry (PIV) analysis of these CT data will provide quantitative insights into internal deformation in such models. Furthermore, our second model suggests that oblique extension leads to less efficient localization of deformation, as higher extension rates are required to induce faulting in the upper crust. This result seems to contradict the proposal by Brune et al. (2012) that oblique rifting promotes break-up.

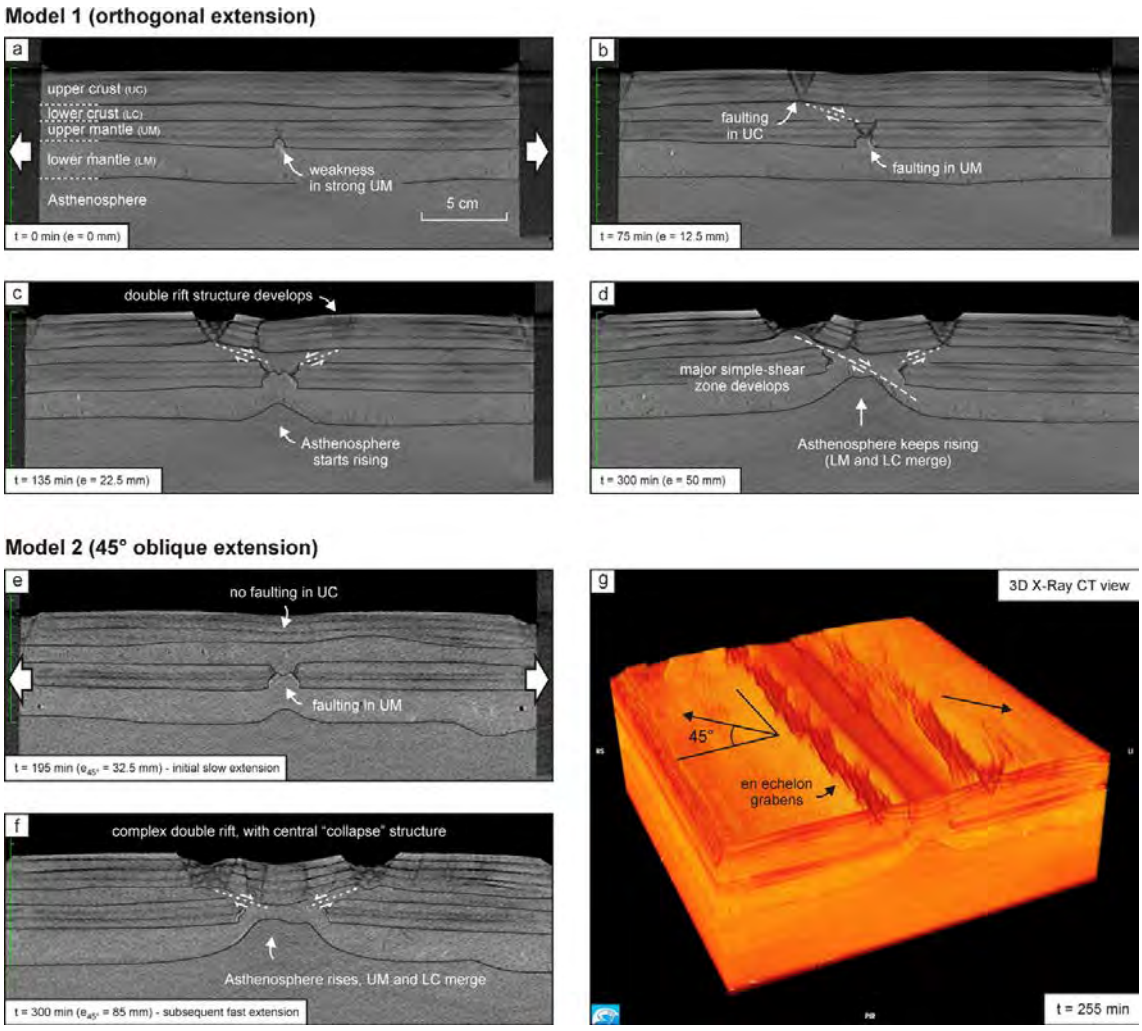

Figure 1. (a-d) CT sections of Model 1 (orthogonal extension, 10 mm/h over 5 h). (e-f) CT sections of Model 2 (45˚ oblique extension), with a first slow extension phase and a second fast extension phase (e) end of phase 1 (10 mm/h for 195 min), (f) end of phase 2 (30 mm/h for 1:45 h). (g) 3D CT view of Model 2 at t = 255 min.

REFERENCES

Brune, S., Popov, A.A., & Sobolev, S.V. 2012. Journal of Geophysical Research. https://doi.org/10.1029/2011JB008860

Brun, J.P., & Beslier, M.O. 1996. Earth and Planetary Science Letters. V142, 161-173. https://doi.org/10.1016/0012-821X(96)00080-5

P 1.1
Fracture Network Prediction in the Geneva Basin: A Geothermal Case Study

Mahmood A. Alhamad[1], Pierre-Olivier Bruna[1], Giovanni Bertotti[1], Andrea Moscariello[2], Ovie Eruteya[2], Michael Welch[3], Simon Oldfield[3]

[1] Department of Geoscience and Engineering, Delft University of Technology, Delft, The Netherlands
[2] University of Geneva, Department of Earth Sciences, Rue des Maraichers 13, CH-1205 Geneva, Switzerland
[3] *Danish Hydrocarbon Research and Technology Centre (DHRTC), Danmarks Tekniske Universitet, Elektrovej Bygning 375, 2800 Kgs Lyngby, Denmark*

Exploration activity of geothermal energy resources is being carried in Geneva Basin in the framework of the 'GEothermie2020' to cover the cold/heat water production and electricity demand of both domestic and industrial sectors. In Geneva Basin, the fracture networks in the Lower Cretaceous carbonate aquifer are proven to provide enough permeability to the geothermal system. The aim of this study is to improve the knowledge of the subsurface for the ongoing geothermal exploration effort by predicting the geometry of the subsurface fracture network. A Discrete Fracture Network (DFN) was generated by integrating the available seismic and well data. The DFN modelling approach is using a novel workflow that is based on a geomechanical forward simulation approach (4D).

The dataset includes two 2D seismic lines and a range of log data from GEo-01 well. The seismic data were used to generate 3D fault and stratigraphic models providing a structural framework for fracture network simulation. The well data which include interpreted fractures from borehole image (BHI) log and a range of classical well logs (e.g., GR, density, sonic) allowed to characterise locally the fracture network and retrieve geomechanical data. The GR and the derived Young's modulus logs were used to mechanically partition the Lower Cretaceous interval where a variation in the rock's stiffness between different stratigraphic formations was observed. Information about paleo-tectonic stress were derived from the fracture data which were used to prepare the model inputs. In the well, the fractures have fairly constant orientation along the Lower Cretaceous interval. The geometric characterisation of the fractures indicated that they were formed under normal stress tectonic regime which relates to the subsidence history prior to Alpine shortening. More specifically, for each of the considered stratigraphic formations, different directions of the fractures were observed. This observation could be explained by the variation in rock's stiffness between different stratigraphic formations.

Two techniques were used to model the subsurface fracture network: i) a paleo-tectonic stress inversion and ii) fracture network forward modelling (4D). The paleo-tectonic stress inversion tool estimates the paleostress and recovers the distribution of the stress and strain tensors. The fracture network forward modelling simulates the fracture nucleation, propagation, and interaction through time. The modelled DFN honours the fractures geometry at the well location. Away from the well, the model is constrained by the subsurface fault geometry and by far-field tectonic stress. Technically, the modelled DFN consists of stacked series of 2 metres thick layers acting as individual mechanical units (e.g., the model is producing layer-bound fracture network). One of the main limitations of this approach is that it cannot consider multiple tectonic regimes to simulate the fracture network. In addition, this approach requires large computational power. Unlike the stochastic method, the adapted geomechanical method considers important underlying mechanical and tectonic constrains. Different methods have their own advantages; hybrid approaches that assimilate the advantages of different methods should be investigated.

REFERENCES

Maerten, L., Maerten, F., Lejri, M., and Gillespie, P. (2016). Geomechanical paleostress inversion using fracture data. Journal of structural Geology, 89:197-213.

Moscariello, A. (2019). Exploring for geo-energy resources in the Geneva Basin (western Switzerland): opportunities and challenges. Swiss Bulletin fur angewandte Geologie, 24(2):105-124.

Welch, M. J., Luthje, M., and Glad, A. C. (2019). Influence of fracture nucleation and propagation rates on fracture geometry: insights from geomechanical modelling. Petroleum Geoscience, 25(4):470-489.

P 1.2
Stress in the Geneva Basin and adjacent Jura fold-and-thrust belt (Switzerland and France), insights from numerical modelling

Sandra Borderie[1], Jon Mosar[1], Louis Hauvette[1,2], Adeline Marro[1], Anna Sommaruga[1] and Michel Meyer[3]

[1] *Earth Sciences Unit, Department of Geosciences, University of Fribourg, Chemin du Musée 6, CH-1700 Fribourg (sandra.borderie@unifr.ch)*
[2] *Geneva Geo Energy (GGE), Rue des vieux grenadiers 8, CH-1205 Genève*
[3] *Services Industriels de Genève (SIG), Chemin Château-Bloch 2, CH-1219 Le Lignon*

The Northern Alpine foreland is divided into two domains: the Molasse Basin and the Jura fold-and-thrust belt (FTB). The Mesozoic and Cenozoic sedimentary cover of this area is deformed by thrust-related folds and strike-slip faults. The main structures root in a basal Triassic *décollement*. The Geneva Basin, located in western Switzerland, is part of the Plateau Molasse (belonging to the Molasse Basin), and is limited to the NW by the Jura FTB, to the SW by the Vuache fault, and to the SE by the Mont Salève ramp related anticline and the Subalpine Molasse.

If current seismicity indicates that the Geneva Basin is tectonically active, few data regarding the state of stress in the area are currently available. The goal of this study is to densify the knowledge of the state of stress in the Geneva Basin and in the adjacent Jura FTB, by using numerical modelling.

The first part of the study is a regional study. In a 2D section, we study the impact of the friction along the basal *décollement*, on the localisation of deformation and on the associated stress field. Results indicate that depending on the friction, deformation will localise at the rear of the Mont Salève, in the Geneva Basin or at the frontal part of the Jura FTB (Figure 1). In the range of frictions where deformation localises in the Geneva Basin, the distribution of stress varies. Differential stress is higher and more localised for higher basal frictions.

The second part of the study is more local. The prototype section is based on seismic interpretation of a seismic surveys in the Geneva Basin. We study the impact of friction along the inherited faults on incipient deformation. Results indicate that a decrease in the fault's friction allows forwards propagation of deformation and allows reactivation of inherited faults. If the friction in the faults is too low, deformation will localise at the first inherited fault (i.e. the Salève thrust in this case study). The stress fields vary depending on the localisation of deformation. Stress magnitudes are lower and more distributed when all faults have the same friction. The more deformation is localised on a structure, the more stress concentration is observed.
These results allow to better constrain the mechanical context of these sections and to populate this part of the Northern Alpine foreland with stress data.

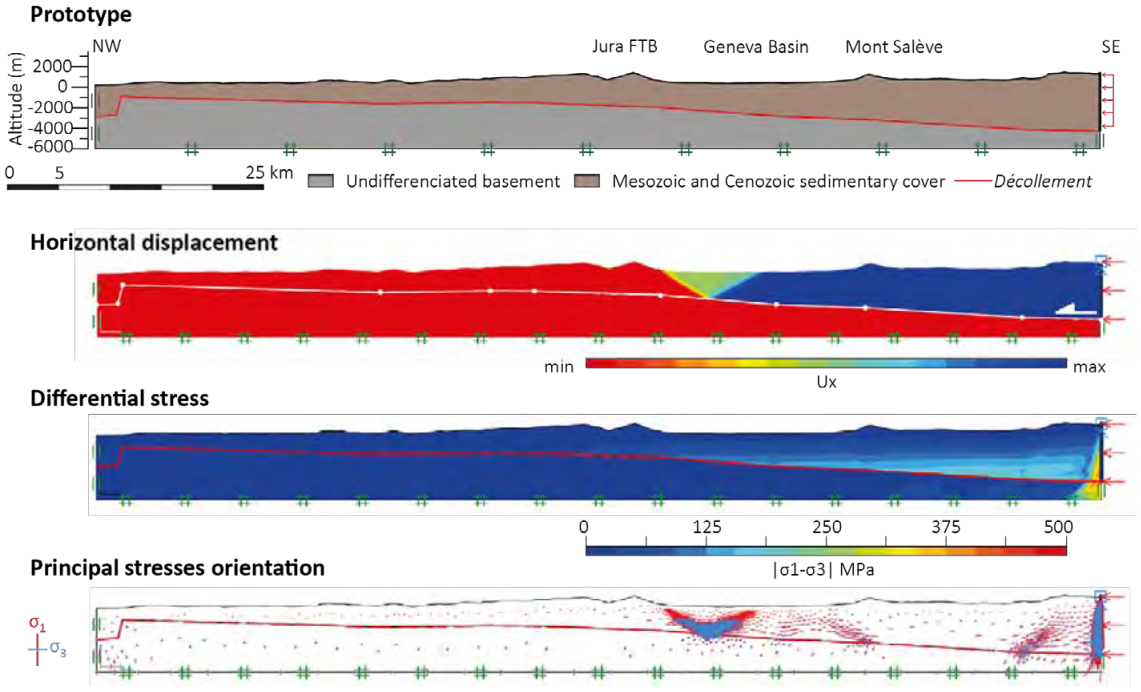

Figure 1: Example of results for the regional scale study, for a friction along the basal *décollement* of 5°. In this condition, the deformation is located in the Geneva Basin, before the first thrust of the Jura FTB.

P 1.3
Geodynamic evolution of the East Carpathian Foreland Basin since the Middle Miocene: Implications for sediment supply to the Black Sea and Dacian Basin

Arjan de Leeuw[1], Stephen J. Vincent[2], Anton Matoshko[3], Andrei Matoshko[3], Marius Stoica[4], Igor Nicoara[5]

[1] *Institut des Sciences de la Terre (ISTerre), Université Grenoble Alpes, CS40700, 38058 Grenoble Cedex 9, France (arjan.de-leeuw@univ-grenoble-alpes.fr)*
[2] *CASP, West Building, Madingley Rise, Madingley Road, Cambridge, CB3 0UD, UK*
[3] *1/25 Draizera Street, 02217, Kyiv, Ukraine*
[4] *Faculty of Geology and Geophysics, University of Bucharest, Bălcescu Boulevard 1, 010041 Bucharest, Romania*
[5] *Institute of Geology and Seismology, 60/3 Gheorghe Asachi Street, Chişinău MD-2028, Republic of Moldova*

The Carpathian orogen is part of the Alpine-Himalayan collision zone and formed as the result of the collision of the Tisza-Dacia and ALCAPA mega-units with the European southern margin, following a protracted phase of subduction, slab roll-back and accretionary wedge formation. The foreland basin of the East Carpathians is 800 km long and stretches out across Poland, Ukraine, Moldova and Romania. We use the results of our intensive field research to unravel the sedimentary architecture of this basin and reveal how it responded to the final phases of foreland vergent thrusting, continental collision and subsequent slab detachment. We discuss the asymmetry in the basins evolution and eventual inversion and relate this to the diachronous evolution of the Carpathian orogen. We also address the impact of changing subsidence patterns and base-level changes on connectivity with the Central and Eastern Paratethys, important for faunal exchange and patterns of endemism. We finally show that continental collision led to the establishment of a Late Miocene NW-SE prograding axial drainage system in the foreland supplying abundant sediment to the NW Black Sea, thus triggering large-scale shelf edge progradation.

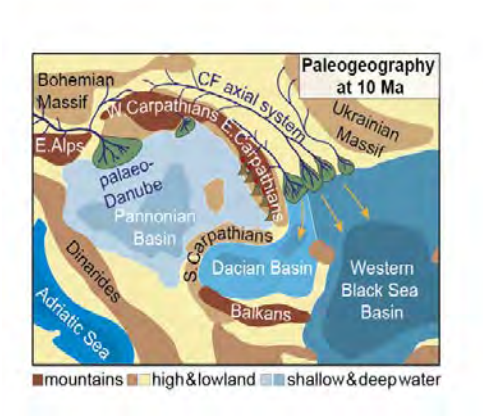

Figure 1. Schematic paleogeography of southeast Europe 10 m.y. ago based on de Leeuw et al. (2020) and Magyar et al. (2019, and references therein). CF—Carpathian foreland.

REFERENCES

de Leeuw, A., et al., 2020, Late Miocene sediment delivery from the axial drainage system of the East Carpathian foreland basin to the Black Sea: Geology, v. 48 (8), p. 761–765.

Magyar, I., Krezsek, C., and Tari, G., 2019, Clinoforms as paleogeographic tools: Development of the Danube catchment above the deep Paratethyan basins in central and southeast Europe: Basin Research, v. 32 (2), p. 320-331.

P 1.4
Present-day deformation of the Aar Massif: New insights from three recent M_L4 strike-slip earthquakes

Tobias Diehl[1], Marco Herwegh[2], Stefan Schmid[3], Lukas Nibourel[4]

[1] Swiss Seismological Service, ETH Zurich, 8092, Switzerland (tobias.diehl@sed.ethz.ch)
[2] Institute of Geological Sciences, University of Bern, Switzerland
[3] Institute of Geophysics, ETH Zurich, 8092, Switzerland
[4] Georesources Switzerland Group, ETH Zurich, 8092, Switzerland

Since 2017, three strike-slip earthquakes of local magnitudes $M_L \geq 4.0$ occurred within the central and eastern parts of the Aar Massif. Focal mechanisms of main- and aftershocks as well as high-precision relative hypocentre relocations of these events provide new insights in the present-day deformation processes and active faults of this external massif. The largest of these earthquakes was the M_L4.6 Urnerboden earthquake of March 2017. The main rupture was previously associated with an NNW-SSE striking sinistral strike-slip fault.

In contrast, the Elm/Steinibach earthquake sequence of 2020, which locates only about 16 km west of the Urnerboden source region, is clearly related to an ENE-WSW striking dextral fault. This remarkable sequence initiated with a first peak in seismic activity in May 2020 and culminated in an M_L4.3 earthquake on October 25th. The Swiss Seismological Service located more than 340 earthquakes associated with this sequence in 2020, 15 of them with $M_L \geq 2.5$. Reliable first-motion focal mechanisms could be calculated for 10 earthquakes. For the mainshock and the largest aftershock (M_L3.9), full moment-tensor solutions were derived from waveform inversion. The relocated hypocentres image two main fault segments. The eastern one, mainly active during the first peak in May, extends over about 1 km and is oriented approximately E-W. The western segment strikes ENE-WSW and extends over a length of about 2 km. The M_L4.3 mainshock locates within a bending zone, separating the two fault segments. The relatively low double-couple component of its moment tensor (64%) suggests possible volumetric changes caused by geometric complexities, e.g. by a rupture across a non-planar, bended or segmented fault plane.

The third strike-slip earthquake analysed in detail is the M_L4.0 event of July 2021, which located about 5 km NW of the Furkapass. A first-motion focal mechanism as well as a full moment tensor were computed for the mainshock. Aftershock activity in this sequence, however, was low and preliminary relative relocations cannot conclusively distinguish between an NNE-SSW striking sinistral and a WNW-ESE striking dextral fault plain.

Finally, we complemented the data provided by these M4 sequences by additional, smaller-sized earthquake to map orientation and kinematics of seismogenic structures as well as principal stress axes within the Aar Massif. Our results suggest that present-day brittle deformation within the massif is dominated by strike-slip faulting accommodated by fault systems of different orientations. To better understand the existence of this strike-slip regime in a region characterized by maximum change in uplift rates, we consider additional geological and geodetic data as well as a new tomographic model, which provides new constraints on the subsurface structure of the Aar Massif.

P 1.5
Automated lineament detection using Tensor Voting: A case study from the Swiss Alps (Grimselpass & Zermatt, Switzerland)

Stefano C. Fabbri[1], David Mair[2], Timothy Schmid[2], Francesca Piccoli[2]

[1] Institute of Geological Sciences, Oeschger Centre of Climate Change Research, University of Bern, Baltzerstr. 1+3, CH-3012 Bern, (stefano.fabbri@geo.unibe.ch)
[2] Institute of Geological Sciences, University of Bern, Baltzerstr. 1+3, CH-3012 Bern

The extraction of straight linear topographic features (lineaments) from satellite images, e.g. Digital Elevation Models (DEM) derived from Light Detection and Ranging (LiDAR) images, is a common instrument to identify overall, ideally fault-based, trends of tectonic elements (e.g. Smith and Pain, 2009). The importance and the fundamental concept of using lineaments as a tool to disclose the hidden architecture of the underlying basement finds applications in a wide spectrum of disciplines from structural tectonics to petrological field-surveys. Lineaments can be of composite nature and may stem from drainage lines, crest of ridges, shore lines, tectonic features (faults, joints, foliations, shear zones) and stratigraphic boundaries (Hobbs, 1912).

There are several potential pitfalls to be considered upon the identification of lineaments, especially when performed manually. Potential biases are related to i) the scale, ii) the illumination azimuth on the image and iii) the operator performing the picking (Schreiber et al., 2015), all having significant impacts on the outcome of the lineament identification process. This generally causes poor reproducibility because these three factors affect the number, length and orientation of the lineaments.

However, computerized automated lineament detection removes the major bias of subjectivity introduced by different operators almost entirely, overall yields higher lineament densities and picks are more uniformly distributed and quantitatively more accurate (Vaz et al., 2012). Furthermore, reproducibility is ensured since the outcome solely depends on a set of chosen parameters, and not the interpreter's eye. In this study, we apply an edge detection algorithm to binary images (derived from digital elevation models and outcrop pictures at various scales) and forward them to a tensor voting algorithm, which is a non-iterative method that calculates a tensor field for every element. The tensors were then decomposed to stick and ball components and form basis tensors. For each of the tensors, a preferred orientation was derived to create the most coherent features.

We applied the algorithm to digital elevation models (swissALTI3D, swisstopo) of kilometer-scale from the Grimsel area (Switzerland) and compare the automated lineament picks of the algorithm with handpicked lineaments of the area. Furthermore, we used field pictures of meter-scale from various outcrops at "Trockener Steg" (Zermatt, Switzerland) as input for the algorithm, and present the automated structural interpretation of outcrop pictures and evaluate its relevance for tectonic and structural analysis. We present here first results of the fully automated lineament detection algorithm and review its performance, advantages and drawbacks, in particular when comparing it to human-performed lineament picks and structural interpretations.

REFERENCES

Hobbs, W. H., 1912, Earth features and their meaning; an introduction to geology for the student and the general reader, New York, Macmillan.

Scheiber, T., Fredin, O., Viola, G., Jarna, A., Gasser, D., and Łapińska-Viola, R., (2015) Manual extraction of bedrock lineaments from high-resolution LiDAR data: methodological bias and human perception. GFF, 137(4), p. 362-372.

Smith, M., and Pain, C., (2009) Applications of remote sensing in geomorphology. Progress in Physical Geography, 33(4), p. 568-582.

Vaz, D. A., Di Achille, G., Barata, M. T., and Alves, E. I., (2012) Tectonic lineament mapping of the Thaumasia Plateau, Mars: Comparing results from photointerpretation and a semi-automatic approach. Computers & Geosciences, 48), p. 162-172.

P 1.6
Using the spread in apatite (U-Th)/He single grain ages to constrain the thermal history of the Northern Swiss Molasse Basin

Kevin A. Frings[1], Christoph von Hagke[2], István Dunkl[3], Elco Luijendijk[4], Herfried Madritsch[5]

[1] Geological Institute, RWTH Aachen University, Wüllnerstrasse 2, D-52062 Aachen (frings@geol.rwth-aachen.de)
[2] Department of Geology, Salzburg University PLUS, Hellbrunnerstr. 34, 5020 Salzburg
[3] Geoscience Center, Department of Sedimentology and Environmental Geology, University of Göttingen, Goldschmidtstrasse 3, D-37077 Göttingen
[4] Bundesgesellschaft für Endlagerung, Eschenstraße 55, 31224 Peine, Germany
[5] Nagra, Hardstrasse 73, CH-5430 Wettingen, Switzerland

We use (U-Th)/He thermochronology on detrital apatite grains (AHe) to constrain the magnitude and long-term rates of exhumation of the northern Swiss Molasse Basin. Previous (mostly fission track) studies showed seemingly contradicting age patterns and resulting exhumation estimates (e.g., Mazurek et al., 2006; Cederbom et al., 2011). We hypothesize that this is because the sediments of the Molasse basin derived from different units in the Alps, as well as the Black Forest (Berger et al., 2005; Kuhlemann & Kempf, 2002). Consequently, the Molasse samples contain different populations originating from different source formations having different pre-Molasse temperature histories. Grains from successions below the Molasse Basin deposits (sandstones of Rotliegend and Buntsandstein sediments) possibly experienced additional heating and cooling events predating the formation of the Molasse Basin. As a result of the inherited thermal history, the grains do not resemble a single thermochronometer, but represent different thermochronometers, possibly sensitive to different closure temperatures. This variability of single grain ages can be exploited by dating a large number of grains distributed to a dense set of sampling intervals and performing statistical analysis on their age distribution and chemical parameters. Additionally, we focus on AHe thermochronology as it is sensitive to lower temperatures compared to fission track dating and is thus more suitable to cover the temperature history of the young and shallow Molasse samples.

A recently drilled Nagra borehole Bülach-1 provided the opportunity to carry out an intensive sampling along a 1370 m vertical section of the Molasse Basin. We divided the Molasse section (upper 500 m) into seven sampling intervals of which we dated in sum 45 grains from cutting samples. In comparison, previous studies used around 20 grains for fission track dating in only one or two intervals for the Molasse section (e.g., Mazurek et al., 2006; Cederbom et al., 2011).The drill cores of the successions below the Molasse sediments contain Buntsandstein and Rotliegend sandstones at the bottom 75 meters of the well. We divided these into three intervals, one represents the Buntsandstein and two the Rotliegend sediments. We dated in sum over 60 grains from these intervals.

The ages of the Molasse grains show a spread from 4 Ma to 30 Ma, while most of the grains have younger AHe ages compared to their depositional age. The Buntsandstein and Rotliegend grains show a spread in ages from 2 Ma to 80 Ma. First results from the age destribution indicate that at least two different populations can be identified according to their initial ages and mineral chemistry within the Molasse sample set. The Buntsandstein and Rotliegend sample sets contain up to four different age populations. First estimates on the closure temperatures of the single thermochronometers based on helium concentration (following Shuster et al., 2006) vary between below 60 °C and over 80 °C, which consistently results in a first exhumation estimate of roughly 1050 to 1550 meters. Timing of exhumation is so far less well constrained. First results yield an exhumation phase starting at 12 to 13 Ma, with an end at 4 to 5 Ma.

This study reconciles previously seemingly conflicting estimates of exhumation estimates, and emphasizes the importance to separate different thermochronometers that coexist within a sample set. We show that dating a large number of single grains from a given sample offers the opportunity to statistically separate and characterize such different AHe thermochronometers.

REFERENCES

Berger, J.-P., Reichenbacher, B., Becker, D., Grimm, M., Grimm, K., Picot, L., Storni, A., Pirkenseer, C., Derer, C., Schaefer, A. 2005: Paleogeography of the Upper Rhine Graben (URG) and Swiss Molasse Basin (SMB) from Eocene to Pliocene, Int. J. Earth. Sci. (Geol. Rundsch.), 94, 697-710.

Cederbom, C.E., van der Beek, P., Schlunegger, F., Sinclair, H.D.,& Oncken, O. 2011: Rapid extensive erosion of the North Alpine foreland basin at 5-4 Ma, Basin Res., 23, 528-550.

Kuhlemann, J., & Kempf, O. 2002: Post-Eocene evolution of the North Alpine Foreland Basin and its response to Alpine tectonics, Sediment. Geol., 152, 45-78.

Mazurek, M., Hurlford, A.J., & Leu, W. 2006: Unravelling the multi-stage burial history of the Swiss Molasse basin: integration of apatite fission track, vitrinite reflectance and biomarker isomerisation analysis, Basin Res., 18, 27-50.

Shuster, D.L., Flowers, R.M.,& Farley, K.A. 2006: The influence of natural radiation damage on helium diffusion kinetics in apatite, Earth and Planet. Sci. Let., 249, 148-161.

P 1.7
The Neoproterozoic transition to modern plate tectonics and complex life: A global scale numerical modelling approach

Timothy Gray[1], Paul Tackley[1], Taras Gerya[1], Robert J. Stern[2]

[1] *Institute of Geophysics, ETH Zürich, Sonneggstrasse 5, 8092 Zürich, Switzerland (timothy.gray@erdw.ethz.ch)*
[2] *Geosciences Department, University of Texas at Dallas, Richardson, TX 75083-0688, USA*

The modern episode of plate tectonics is increasingly considered to have begun in the Neoproterozoic following a period of reduced activity known as the 'boring billion' (Sobolev and Brown, 2019; Stern, 2007) when Earth may have been in a less dynamic single lid mode (Stern, 2007). The Neoproterozoic was also a period of radical change in other Earth systems – higher oxygen levels, the Cryogenian glaciations, and finally the emergence and rapid diversification of multicellular life in the Cambrian explosion. The study of the Neoproterozoic transition to modern plate tectonics is therefore central to the emerging multidisciplinary field of Biogeodynamics, the study of coupling between geodynamic processes, atmosphere, ocean, landscape, climate and the evolution of life (Gerya et al. 2020).

The origins of modern plate tectonics on Earth have typically been ascribed to the secular cooling of the mantle enabling local episodes of unstable subduction to become more widespread and stable (Bercovici and Ricard, 2014). Sobolev and Brown (2019) argue that major erosion and sedimentation events, such as the Cryogenian glaciations, were important controls on Earth's tectonic style. The presence of hydrated sediments in active subduction zones enhances their stability through lubrication, thus the Cryogenian glaciations may have reactivated the dormant plate tectonics of the 'boring billion' (Stern, 2007).

The transition to modern plate tectonics is necessarily a global problem operating on a timescale of hundreds of millions of years needed to develop/activate the global plate mosaic (Bercovici and Ricard, 2014). To model the transition numerically, we propose to combine global 3D models of mantle convection with free surface using StagYY (Tackley, 2008) with a simplified model of erosion and sedimentation, and a parameterised description of margin strength which may be modified by subduction zone lubrication and sediment loading. The aim is to determine through modelling the conditions and timescales required to activate a plate tectonic regime from a single lid (Stern, 2007). The results of these global models, particularly models of global topographic evolution, may also be used in conjunction with climate models and models of biological evolution to investigate the ability of different global tectonic regimes to sustain and diversify complex life.

REFERENCES

Sobolev, S. and Brown, M. (2019): *Surface erosion events controlled the evolution of plate tectonics on Earth,* Nature

Stern, R. J (2007): *When and how did plate tectonics begin? Theoretical and empirical considerations,* Chinese Science Bulletin

Gerya, T et al. (2020): *Bio-geodynamics of the Earth: State of the art and future directions,* EGU2020

Bercovici, D. and Ricard, Y. (2014): *Plate tectonics, damage and inheritance,* Nature

Tackley, P. J. (2008): *Modelling compressible mantle convection with large viscosity contrasts in a three-dimensional spherical shell using the yin-yang grid,* Physics of the Earth and Planetary Interiors

P 1.8
Numerical modelling of anisotropy generation during viscous deformation

William R. Halter[1], Emilie Macherel[1], Thibault Duretz[1,2], Stefan M. Schmalholz[1]

[1] ISTE, Université de Lausanne, Géopolis, CH-1015 Lausanne (william.halter@unil.ch)
[2] Univ Rennes, CNRS, Géosciences Rennes, UMR 6118, F-35000 Rennes

In a deforming lithosphere, localization and softening mechanisms are important for subduction initiation or the generation of tectonic nappes during orogeny. Many localization mechanisms have been proposed as being important during the viscous, creeping, deformation of the lithosphere, such as thermal softening, grain size reduction, reaction-induced softening or anisotropy development. However, which localization mechanism is the controlling one and under which deformation conditions is still contentious. In this contribution, we focus on strain localization in viscous material due to the generation of anisotropy, for example due to the development of a foliation. We numerically model the generation and evolution of anisotropy during two-dimensional viscous deformation in order to quantify the impact of anisotropy development on strain localization and on the effective softening. We use a pseudo-transient finite difference (PTFD) method for the numerical solution. We calculate the finite strain ellipse during viscous deformation. The aspect ratio of the finite strain ellipse serves as proxy for the magnitude of anisotropy, which determines the ratio of normal to tangential viscosity. To track the orientation of the anisotropy during deformation, we apply the so-called director method. We will present results of our numerical simulations and discuss their application to natural shear zones.

P 1.9
Experimental investigation of glaucophane rheology through general shear deformation experiments

Hufford, L.J., Tokle, L., and Behr, W.M.

Structural Geology and Tectonics Group, Geological Institute, Department of Earth Sciences, ETH Zurich, Sonneggstrasse 5, 8092, Zürich, Switzerland
(lonnie.hufford@erdw.ethz.ch)

Based on the rock record, glaucophane is a major constituent mineral associated with subducted mafic oceanic crust at blueschist metamorphic facies. Ductile-viscous deformation of glaucophane has been documented in natural blueschists, however, no experimental study has characterized the specific deformation mechanisms that occur in glaucophane. We conduct a suite of general shear deformation experiments in the Griggs apparatus to investigate deformation mechanisms and microstructures of deformed glaucophane over a range of experimental conditions. Experimental samples consist of glaucophane powder separated from natural samples originating from Syros Island, Greece with a grain size of 63-355 μm. Both constant-rate and strain-rate stepping experiments were conducted at 700° and 750°C at a confining pressure of 1 GPa with strain rates ranging from ~$3x10^{-6}$/s to ~$8x10^{-5}$/s. At 1 GPa and 700°C, the microstructure of the constant-rate experiment shows interconnected, recrystallized grains (~10 μm) and porphyroclasts with undulose extinction consistent with bulging dynamic recrystallization. At 1 GPa and 750°C, the microstructure of the constant-rate experiment displays minor amounts of recrystallized grains and subgrain development, where the majority of grains display exsolution textures. Strain-rate stepping experiments at 1 GPa and 700° and 750°C were also completed. A stress exponent of 3.3 was calculated for the 700°C experiment and a stress exponent of 1.5 was calculated for the 750°C experiment; however, the microstructures for both samples exhibit both brittle and ductile deformation mechanisms. Additional constant-rate experiments will be conducted at higher pressures and various strain-rates to assess glaucophane deformation mechanisms and microstructures.

P 1.10
Microcrack-driven Emergence of Stress Relaxation in Granitic Rock: Laboratory Observation and Numerical Simulation

Liang Wang, Rui Wu, Ying Li, Paul Selvadurai, Claudio Madonna, Qinghua Lei*

Department of Earth Sciences, ETH Zürich, Sonneggstrasse 5, CH-8092 Zürich (qinghua.lei@erdw.ethz.ch)*

Understanding the time-dependent deformation and degradation behaviour of brittle rocks is crucial for unravelling the mechanisms and predicting the occurrence of catastrophic failure of geological formations in nature. Phenomena associated with the temporal weakening of rock strength has been extensively studied in the past using creep or stress relaxation tests performed in the laboratory. These studies have revealed three deformational regimes (i.e. primary, secondary, and tertiary stages) in the time domain as a result of microcracking processes. While macroscopic failure of rock may be captured by continuum models that incorporate local weakening behaviors related to microcrack evolution (Main, 2000), there is still no existing model that can quantitatively and physically link evolving microcrack characteristics/dynamics to the formation of system-sized failures (Brantut et al., 2013). To better characterise the microcrack-driven mechanism, we study the progressive failure during relaxation of Herrnholz granitic rock subjected to uniaxial compression in laboratory settings to constrain our numerical research. We develop a micromechanical model that mechanistically captures the emergence of macroscopic failure as a result of the spatio-temporal evolution of microcrack populations. We constrain the numerical model using microscopy-based characteirsation of microcrack patterns and subsequently validate the model using laboratory results of stress relaxation as well as associated acoustic emissions. We further use the model to study the mechanisms underpinning the observed seismic and aseismic deformations in rock samples. Preliminary results show that microcrack characteristics and their evolution strongly affect the formation of the macroscopic rupture plane and, in turn, the bulk response of rock specimens prior to failure. The validated/calibrated numerical model is expected to be useful for identifying possible precursors to catastrophic failure in brittle rocks with important implications for understanding and predicting extreme events in natural systems such as great earthquakes, volcanic eruptions, and rapid landslides.

REFERENCES

Brantut, N., Heap, M.J., Meredith, P.G., Baud, P., 2013: Time-dependent cracking and brittle creep in crustal rocks: A review. Journal of Structural Geology, 52, 17–43.

Main, I.G., 2000: A damage mechanics model for power-law creep and earthquake aftershock and foreshock sequences. Geophysical Journal International, 142, 151–161.

P 1.11
Surplus melt induces the dynamic LAB near the mid-ocean ridge

Mingqi Liu*, Taras Gerya

Department of Earth Sciences, ETH Zurich, Sonneggstrasse 5, CH-8092 Zurich (mingqi.liu@erdw.ethz.ch)*

Recently, geophysical observation through Sp receiver functions and MT imaging showed that the tectonic plate thickness undulates with age and lithosphere-asthenosphere boundary (LAB) is sharp discontinuities near the equatorial Mid-Atlantic ridge, which is not consistent with a purely thermal model. Several mechanisms have been proposed to explain the discrepancy: (1) Rayleigh wave anisotropy; (2) near solidus temperature; (3) mantle oxidation; (4) elastically accommodated grain boundary sliding; or (5) partial melt in the mantle. However, it still remains elusive. Here, we explore the formation mechanism of the sharp LAB discontinuities as well as the influence in plate tectonics through 3D self-consistent magmatic-thermomechanical numerical models. Numerical modelling results show that the sharp LAB discontinuities occur in two different configurations: (1) peeling melt is far from the mid-ocean ridge with persisting over several million years; (2) melt rises from depth and ponds beneath the plate, finally forming the new mid-ocean ridge. Both these two configurations are closely related to ridge jumps and transform faults. Ridge jumps will peel melt from the mid-ocean ridge and transform faults can induce the abnormal melt generation. In addition, localized melt leads to the small-scale convection beneath the plate and decreases the drag resistance at the base of the lithosphere.

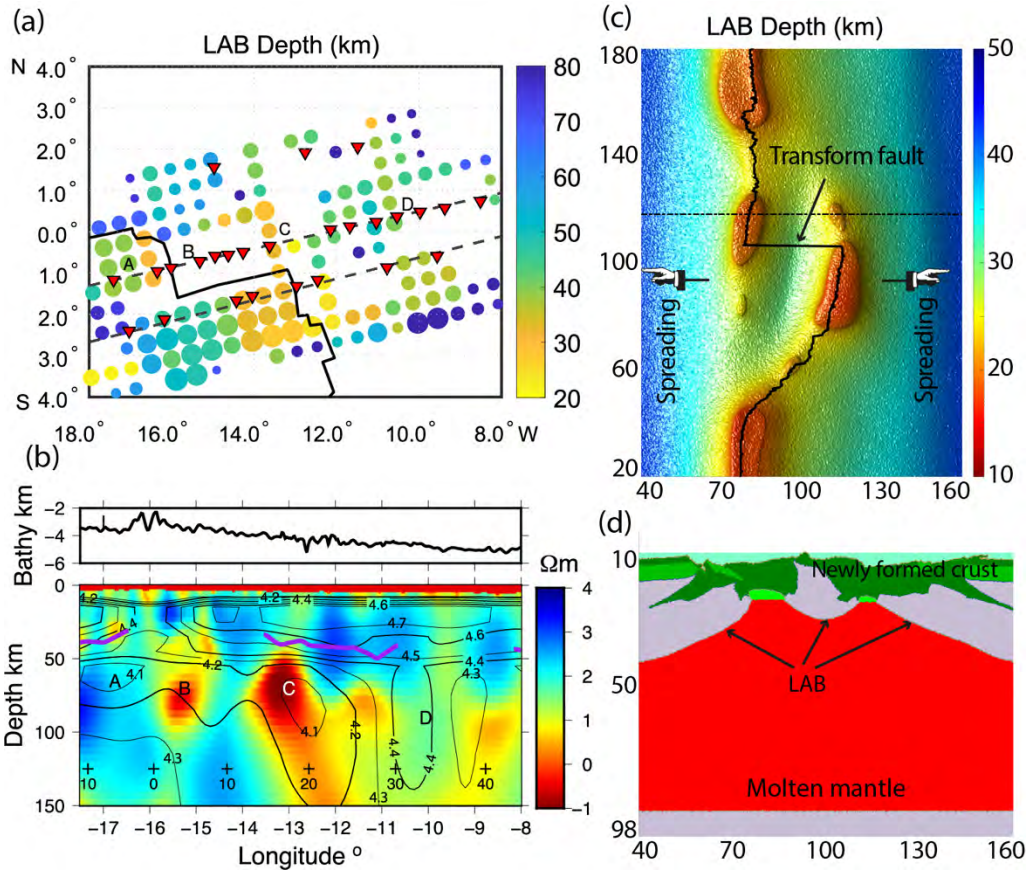

Figure 1: Comparison between observation and numerical modelling. Observation near the equatorial Mid-Atlantic Ridge (Rychert et al., 2021): (a) Map view of LAB depth from Sp receiver function; (b) Shear-wave velocity and resistivity along the dashed black line in (a). Numerical modeling: (c) Map view of LAB depth; (d) Composition along the dashed black line in (c). Thick black lines in (a, b) marks mid-ocean ridges.

REFERENCES

Rychert, C. A., Tharimena, S., Harmon, N., et al. (2021). A dynamic lithosphere–asthenosphere boundary near the equatorial Mid-Atlantic Ridge. Earth and Planetary Science Letters, 566, 116949.

P 1.12
GPU-based pseudo-transient finite difference solution for 3-D gravity- and shear-driven power-law viscous flow

Emilie Macherel[1], Yuri Podladchikov[1], Ludovic Räss[2,3], Stefan M. Schmalholz[1]

[1] University *of* Lausanne, ISTE, Lausanne, Switzerland (emilie.macherel@unil.ch)
[2] *Laboratory of Hydraulics, Hydrology and Glaciology (VAW), ETH Zurich, Switzerland*
[3] *Swiss Federal Institute for Forest, Snow and Landscape Research (WSL), Birmensdorf, Switzerland*

Power-law viscous flow accurately describes the first-order features of long-term lithosphere deformation. The stresses resulting from a deforming lithosphere control processes such as metamorphic reactions, decompression melting, subduction initiation or earthquakes. Calculating these stresses in a three-dimensional (3-D), geometrically and mechanically heterogeneous lithosphere requires high-resolution and high-performance computing.

Here, we present numerical simulations of 3-D power-law viscous flow. We apply the pseudo-transient finite difference (PTFD) method, which enables efficient simulations of high-resolution 3-D deformation processes by implementing an iterative implicit solution strategy of the governing equations. The main challenges for the PTFD method are to guarantee convergence, minimize the required iteration count and speed-up the iterations. We implemented the PTFD algorithm using the Julia language (julialang.org) to enable optimal parallel execution on multiple CPUs and GPUs using the ParallelStencil.jl module (https://github.com/omlins/ParallelStencil.jl). ParallelStencil.jl enables execution on multi-threaded CPUs and Nvidia GPUs using a single switch.

We present PTFD simulations of mechanically heterogeneous, incompressible 3-D power-law viscous flow under gravity in cartesian coordinates. The heterogeneity is described by a spherical inclusion that is weaker and less dense than the surrounding material. The viscous flow is described by a linear combination of a linear viscous and a power-law viscous flow law, representing diffusion and dislocation creep, respectively. The iterative solution strategy builds upon pseudo-viscoelastic behavior to minimize iteration count by exploiting the fundamental characteristics of viscoelastic wave propagation. We performed systematic numerical simulations to investigate the impact of (i) buoyancy versus shear forces and (ii) linear versus power-law viscous flow on the vertical velocity of the spherical inclusion under bulk strike-slip shearing. We report the systematic results using the controlling dimensionless numbers and compare the numerical results with analytical predictions for buoyancy-driven flow of inclusions in a power-law matrix. We also aim to unveil preliminary results for 3-D cylindrical configurations and to discuss potential applications of our simulations to plutons associated with strike-slip shear zones.

P 1.13
Giant Volcano Flank Motion Imaged by Historical Air Photos Correlation during the M7.7 Kalapana Earthquake (1975), Big Island, Hawaii

Stefano Mannini[1], Joël Ruch[1], James Hollingsworth[2], Donald A. Swanson[3], Ingrid Johanson[3]

[1] Department of Earth Sciences, University of Geneva, Rue des Maraîchers 13, 1205, Geneva, Switzerland
[2] ISTerre Université Grenoble Alpes, UMR 5275 CNRS, 1381 Rue de la Piscine, 38610 Gières, France
[3] U.S. Geological Survey - Hawaiian Volcano Observatory, 1266 Kamehameha Ave., Hilo, HI 96720, United States of America

Volcanic islands are often subject to flank instability being a combination of magma intrusions along rift zones and gravitational spreading. The Kīlauea is one of the most active volcano on Earth and its south flank show recurrent flank acceleration related to large earthquakes and magma intrusions. Kīlauea is made of a central caldera flanked by the East and Southwest Rift Zones, the Koa'e and the Hilina fault systems and a deep subhorizontal detachment, all being part of the volcano flank instability. During the last two centuries, six major earthquakes (6<M<7.7) have occurred on the south flank of the volcano (1823, M7; 1868, M7.9; 1954, M6.5; 1975, M7.7; 1989, M6.1; 2018 M6.9), generating in some cases large flank motion, supporting a cyclic behavior of the flank instability and related volcano-tectonic processes (Swanson et al., 1976).

Here we focus on the M7.7 Kalapana earthquake that occurred on 29 November 1975. It triggered a large co-seismic ground displacement of several meters all over the south flank of the Kilauea volcano and a tsunami has been damaging the Big Island coasts (Tilling et al., 1976). The identification and quantification of the entire co-seismic rupture and the faults that have been reactivated during the event remained poorly studied and is the focus of our study.

Using optical imagery correlation technique, we analyzed the displacement that occurred during the 1975 earthquake. We used 26 and 22 photos as pre-event (October 1974 and July 1975, respectively) and 7 and 44 for the post-event time period (December 1976 and March 1977, respectively). Results show metrical horizontal displacement (north-south direction) along a 25 km long East West sector of the Kīlauea south flank (Figure 1). We show for the first time displacement maps covering the entire 1975 earthquake fault rupture and highlight the reactivation of Hilina and Holei Pali during the earthquake with up to eight and three meters of offset, respectively, in good agreement with localized EDM measurements (Lipman et al., 1985). Several other secondary faults have been activated close to the shore and their extension were previously unnoticed. Episodic flank motions on volcanic islands are rare events and this work contributes to the overall comprehension of volcano flank instability elsewhere.

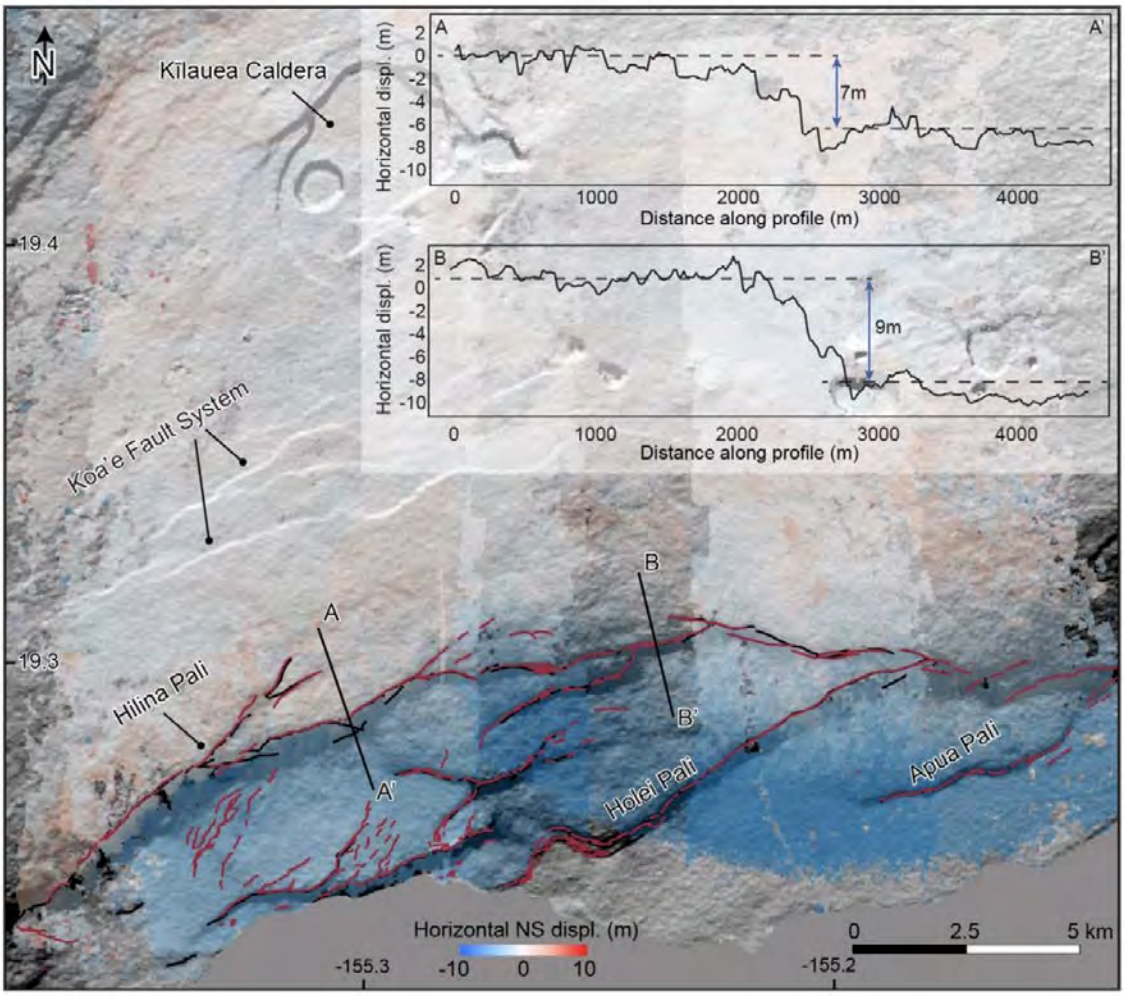

Figure 1. Displacement map of the Hilina fault (south flank of the Kilauea volcano, Hawaii) triggered by the M7.7 Kalapana earthquake in 1975 overlaid on a 30m DEM. Profiles (A-A') and (B-B') show horizontal displacement in the North South direction; blue indicates southward motion. The red lines are the faults mapped using the displacement map.

REFERENCES

Lipman, P.W., Lockwood, J.P., Okamura, R.T., Swanson, D.A., Yamashita, K.M., 1985: Ground deformation associated with the 1975 magnitude-7.2 earthquake and resulting changes in activity of Kīlauea Volcano, Hawai'i. U. S. Geol. Surv. Prof. Pap. 1276, 45 pp.

Swanson, D. A., Duffield, W. A., and Fiske, R. S., 1976: Displacement of the south flank of Kīlauea Volcano: The result of forceful intrusion of magma into the rift zones: U.S. Geol. Survey Prof. Paper 963, 39 p.

Tilling, R. L, Koyanagi, R. Y., Lipman, P. W., Lockwood, J. P.,Moore, J. G., and Swanson, D. A., 1976: Earthquake and related catastrophic events, island of Hawaii, November 29, 1975: a preliminary report: U.S. Geological Survey Circular 740, 33

P 1.14
Influence of fluids on the earthquake cycle based on numerical modeling

Valentin MARGUIN*, Guy SIMPSON

Department of Earth Sciences, University of Geneva, Rue des Maraîchers 13, Geneva, Switzerland.
(valentin.marguin@unige.ch)*

The strength and sliding behavior of faults in the upper crust is largely controlled by friction and the effective stress, which is itself modulated by the fluid pressure (Sibson, 1990). However, while many studies have investigated the role of friction on the earthquake cycle (Marone, C.,1998), relatively little effort has gone into understanding effects linked to dynamic changes in fluid pressure (see however Zhu et al, 2020). Here, we explore coupled interactions between slow tectonic loading and fluid pressure generation during the interseismic period with rapid sliding and elastic stress transfer during earthquakes on a plane strain thrust fault in two dimensions. Our models incorporate rate- and state-dependent friction along with dramatic changes in the fault permeability during sliding. Preliminary results show that elevated fluid pressures near the base of the seismogenic layer provides a means for faults to slip at shear stress levels that are well below those required for static sliding. In these modes, earthquakes are nucleated where fluid pressures are locally high. Ruptures are then propagated as slip pulses onto stronger parts of the fault facilitated by dramatic coseismic weakening (Di Toro et al., 2004). Overall, ruptures in the presence of fluids are slow relative to ruptures in dry crust (as also found by Passelègue et al, 2020). These results might eventually enable one to distinguish ‘tectonic earthquakes’ from earthquakes that are driven by variations in fluid pressure.

REFERENCES

Marone, C. (1998). The effect of loading rate on static friction and the rate of fault healing during the earthquake cycle. Nature, 391(6662), 69–72.

Zhu, W., Allison, K. L., Dunham, E. M., & Yang, Y. (2020). Fault Valving and Pore Pressure Evolution in Simulations of Earthquake Sequences and Aseismic Slip. 1–16.

Sibson, R. H. (1992). Implications of fault-valve behaviour for rupture nucleation and recurrence. Tectonophysics, 211(1–4), 283–293.

Di Toro, G., Goldsby, D. L., & Tullis, T. E. (2004). Friction falls towards zero in quartz rock as slip velocity approaches seismic rates. Nature, 427(6973), 436–439.

Passelègue, F. X., Almakari, M., Dublanchet, P., Barras, F., Fortin, J., & Violay, M. (2020). Initial effective stress controls the nature of earthquakes. Nature Communications, 11(1), 1–8.

P 1.15
4D reconstruction of a Fold and thrust belt: the case of the asymmetric Doldenhorn nappe-Aar Massif system (Central Swiss Alps)

Ferdinando Musso Piantelli[1], David Mair[1], Marco Herwegh[1], Alfons Berger[1], Eva Kurmann[2], Michael Wiederkehr[2], Fritz Schlunegger[1], Andreas Möri[2] and Roland Baumberger[2]

[1] *Institute of Geological Sciences University of Bern, Baltzerstrasse 1+3, 3012 Bern, Switzerland*
[2] *Federal Office of Topography swisstopo, Seftigenstrasse 264, 3084 Bern, Switzerland*

In most orogenic systems, Fold and Thrust Belts (FTBs) represent essential major tectonic deformation style in mid- to upper crustal levels. Identifying the factors that control their development is therefore fundamental to understand the long- and short-term dynamics of mountain building processes. Often FTBs evolve from inversion of passive continental margins. Their three-dimensional architecture consists of a combination of discontinuous fault systems and geometrical asymmetries (Lymer et al. 2019) leading to significant along-strike variations. During basin inversion by compressional tectonics, such structures are inherited as a fingerprint of the former margin architecture and subsequent deformation style. Yet, little is known about the lateral along strike structural variations and their role in inversion tectonics. The so far frequently applied cross-sectional visualization approach of a FTB is insufficient to resolve and outline the 3D complexity of a belt in its entirety. Alternatively, the integration of three-dimensional modelling and restoration techniques provides crucial and necessary information for characterizing the 3D structural disposition of a FTB, allowing the reconstruction of fault network and the detection of inconsistences in structural interpretations.

Based on (i) a detailed digital geo-tectonic map, (ii) 3D structural model of the current tectonic situation and (iii) sequential retro-deformation, this work elaborates the 4D evolution of the central Helvetic part of the former European passive continental margin. It focus in particular on the Doldenhorn Nappe (DN) and the underlying western Aar massif (external Central Alps, Switzerland). The DN is one of the lowermost units of the Helvetic nappe system that exhibits distinct 3-D structural features such as lateral variation of the geometry and deformation style (Herwegh and Pfiffner 2005). To examine the impact of such parameters on the evolution of a FTB, we built a 4D geological reconstruction of the DN during the last Alpine cycle (30 to 0 Ma). The DN as a natural laboratory, allows to: (i) illustrate the former 3D morphology and variability of parts of the European passive continental margin (Fig. 1); (ii) show the effect of along-strike variations during basin inversion in the framework of continent-continent collision; and (iii) provide insights, which aid in tightening the structural geology and the analogue-numerical modelling for an improved understanding of the evolution of FTBs.

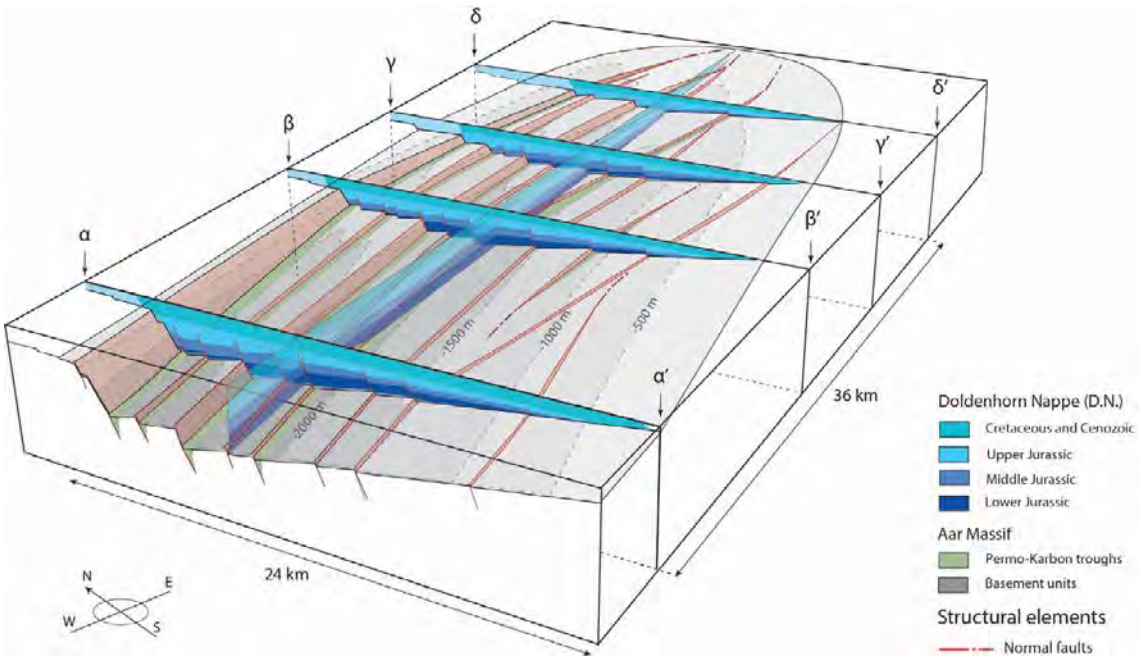

Figure 1. 3D reconstruction of the Doldenhorn basin (sediment infill constrained by stratigraphic data) and underlying basement (grey) of the western Aar Massif (30 Ma). The basin is framed by a large-scale half graben that becomes progressively shallower and less extended towards the east and the south.

REFERENCES

Herwegh, M., & Pfiffner, O. A. (2005). Tectono-metamorphic evolution of a nappe stack: A case study of the Swiss Alps. Tectonophysics, 404, 55–76.

Lymer, G., Cresswell, D. J., Reston, T. J., Bull, J. M., Sawyer, D. S., Morgan, J. K., Stevenson, C., Causer, A., Minshull, T. A., Shillington D. J. (2019). 3D development of detachment faulting during continental breakup. Earth and Planetary Science Letters, 515, 90-99

P 1.16
Brittle-viscous transition in fine-grained granitoid fault rocks – deforming natural rock samples in the Griggs Rig apparatus

Natalia Nevskaya[1], Weijia Zhan[1], Holger Stünitz[2,3], Alfons Berger[1], Marco Herwegh[1]

[1] Geologisches Institut, University of Bern, Baltzerstrasse 1+3, CH-3012 Bern (natalia.nevskaya@geo.unibe.ch)
[2] *Department of Geology, Tromsø University, Dramsveien 201, 9037 Tromsø, Norway*
[3] *Institut des Sciences de la Terre d›Orléans (ISTO), Université d›Orléans, 1A rue de la Férollerie, 45100 Orléans, France*

For Earth's mid- to upper crustal rheology, the physico-chemical properties of the two most abundant minerals quartz and feldspar commonly are used in numerical models. In a simple two-phase rheological model, quartz will represent the weakest and feldspar the strongest end member phase. However, field studies on granitoid shear zones reveal that the highest strain is localized strongly in shear zones consisting of ultrafine-grained polymineralic mixtures of quartz, feldspars, mica and epidote, showing a weaker rheology than any of the end member minerals. Yet, the effective rheology of these ultrafine-grained polymineralic tectonites is unknown.

In this study, we try to fill the knowledge gap by deforming solid, fine-grained, natural rock samples in a Griggs Rig apparatus. The starting material is an ultramylonite from the Central Aar Granite (Aar Massif, Central Alps). It consists of quartz, albite, K-feldspar, dark mica, and epidote of 150 - 15 µm grain size. In the first experimental series at 650°C, 12kbar confining pressure, and constant strain rate, we modified the total strain (5 to 25%), and water content (0.2%wt or no added water) in pure shear experiments. From evaluating the mechanical data and performing detailed microstructural analysis, we conclude: 1) a strong localization of the deformation in a narrow, fracture-initiated shear zone with grain sizes in nanometre scale; 2) a 10 to 100 µm wide viscous deformation zone around the aforementioned zone 1 with elongated grains and minor grain size reduction (grain size on the µm scale); 3) reactions to produce omphacite.

The Zone 1 is 15-75 µm wide, but accommodates the major amount of deformation. This zone is oriented at a 30° to 40° angle to the compression direction of the experiment and represents a very strong strain localisation independent of the orientation of pre-existing strong anisotropies of the foliated mylonite.

The mechanical data shows that these mylonites are weaker than granites with comparable composition but larger grain size. In comparison to literature data they are also weaker than pure end member quartz and feldspar experiments – fitting well with the observations made in nature. The initialization of the localized shear zone may be related to fracturing, whereas the main strain is accommodated by viscous processes inside the extremely fine grained layer. Future experiments and detailed microstructural analysis of these layers will give further insights in the deformation mechanisms of such polymineralic systems. The available observations (see above, point 1-3) already demonstrate the importance of interaction between fracturing, reaction weakening and viscous deformation in the fine-grained aggregates, a process suite which is not active in nearly mono-mineralic experiments (i.e. quartz or feldspar).

P 1.17
Fracture network characterization associated with the transpressive Vuache fault, a possible outcrop analogue of the Geneva Basin geothermal system.

Marc Perret [1,3], Marta Gasparrini [1,2], Vanessa Teles [1], Fiammetta Mondino [4], Luca Guglielmetti [3], Silvia Omodeo Salé [3], Andrea Moscariello [3]

[1] *IFP Energies nouvelles, 1 et 4 avenue de Bois-Préau 92852 Rueil-Malmaison Cedex – France (marc.perret@ifpen.fr)*
[2] *University of Milan, Earth Sciences Department, Via Mangiagalli 34, 20131 Milan, Italy*
[3] *Département des Sciences de la Terre et de l'Environnement, Université de Genève, 13 Rue des Maraîchers 1205 Genève, Switzerland*
[4] *Geneva Earth Resources, Rue Jean Jaquet, 10 1201 Genève, Switzerland*

In the context of energy transition and increased interest towards greener energy sources, such as geothermal energy, sedimentary basins appear as the next targets to develop. The reconstruction of paleo-fluid flow in fractures may contribute to predict the occurrence of cementation at the reservoir scale. Outcrop analogues of potential subsurface reservoirs constitute excellent opportunities to analyze paleo-fluid properties (i.e. temperature, composition, pressure, timing), origins and pathways, and provide constraints to predict the present-day cementation conditions of the reservoirs in the subsurface. Exhumed analogues, such as the Salève or Vuache mountains (France) reveal the presence of paleo-circulation of fluids through cemented fractures. The joint characterization of fossil geothermal systems and existing ones, combined with numerical modelling, is an innovative and promising approach to improve the determination and prediction of reservoir parameters.

The Vuache fault is an important structure in the Geneva Basin (western termination of the Swiss Molasse Basin; Figure 1A) tectonic framework. Despite numerous studies having contributed to constrain its geometry and extension, illustrate the fault segmentation at depth and its role in the accommodation of alpine tectonic movements, the fracture pattern of carbonate formations constituting the massif remain poorly constrained.

This study focuses on the Mont Vuache where scanline analyses allowed to determine reservoir fracture mode and intensity. On-field structural analyses revealed the complex structural framework of the Vuache Fault crossing the basin and passing along the Mont Vuache. Petrographic characterization of vein cements (by optical microscopy and cathodoluminescence) was performed on mineralized fractures (veins) sampled in outcrops. Plugs and hand specimens were prepared as polished thin sections for petrographic purposes.

A selection of three representative outcrops were studied along the Vuache Mountain. Sinistral and dextral strike-slip faults were recorded along the profile and sense of movement was deciphered thanks to slickensides. Several fracture sets were identified in the Upper Jurassic and Lower Cretaceous limestones. The main fracture sets showed orientations striking E-W, N-S, NW-SE and associated with minor NE-SW sets (Figure 1B). The fractures comprised mostly joints and calcite-filled veins (Figure 1C) interpreted as tension fractures, typical of I (opening) mode. Fracture intensity was lower in Jurassic rocks compared to Cretaceous outcrops. A conceptual model comprising Riedel fractures and fault reactivations is used to explain the development of fractures in the Vuache fault zone. Riedel shears striking NW-SE and antithetic R' faults, oriented WNW-ESE, have been reported crossing the main strike-slip fault plane.

Hand specimens and plugs were recovered from all studied carbonate formations along scanlines. Petrographic analyses of calcite veins show a rather significant variation in the textures of the mineralized veins. The veins are composed of "blocky" and "elongated blocky" calcite, often showing crack-seal texture (Figure 1D). This texture consists in several generations of calcite cements interpreted as a succession of fracture opening and sealing events. In fact, this corresponds to several episodes of fault reactivation leading to fluid circulation and calcite precipitation.

This study represents an important contribution aimed at characterizing the fracture and paleo-fluid circulation in the Geneva Basin highlighting in particular the complexity of structures in the Vuache fossil geothermal system as a potential analogue of similar structure buried in the basin.

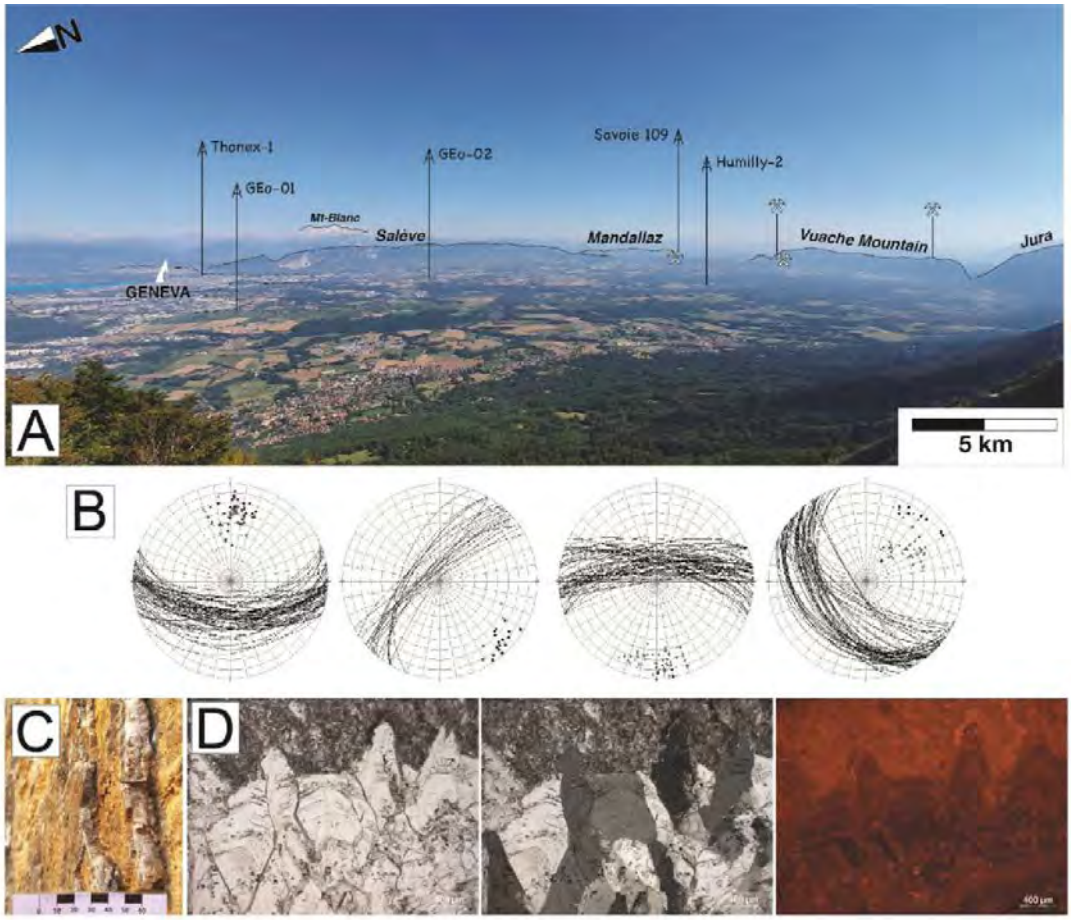

Figure 1. A. Panoramic view of the Geneva Basin and surrounding massifs. Well and outcrop locations are projected on the photograph. B. Polar diagrams (Lower hemisphere) of main fracture sets. C. Calcite crack-seal veins. D. Calcite crystals with elongated blocky habitus (PPL; CPL; CL).

P 1.18
Numerical Modelling of Grain Size Evolution in Granitoid Shear Zones

Jonas B. Ruh[1], Leif Tokle[1], Whitney M. Behr[1]

[1] *Geologisches Institut, Departement Erdwissenschaften, ETH Zürich, Sonneggsrasse 5, CH-8092 Zürich (jonas.ruh@erdw.ethz.ch)*

Localization of strain during deformation of crustal rocks to form narrow shear zones requires a certain amount of weakening. Bulk weakening of a deforming shear zone may for example result from geometric reorgaization of strong and weak phases, from increased deformation-related fluid flow, or from local temperature increase due to shear heating. A further weakening effect mainly occurring during the infancy of shear zones is work-related grain size reduction and the activation of grain size-dependent diffusion creep.

To test the importance of grain size reduction for mechanical weakening of granitoid crustal shear zones, a numerical model of initially undeformed granitoid texture was set up and sheared to a total shear strain of 10. The numerical finite difference code solves for the conservation of momentum (Stokes) and mass with a visco-elasto-plastic rheology. The model domain measures 5x5 cm and the initial distribution of quartz, plagioclase, and biotite is designed after an image of the Rotondo granite (Figure 1). Top and bottom velocities describe simple shear while the left and right prescribe periodic boundaries.

For both quartz and plagioclase (anorthite), flow laws for dislocation and grain size-dependent diffusion creep are implemented and act parallelely. Grain size evolution is implemented in form of the paleowattmeter (Austin & Evans, 2007) with mineral-specific grain growth laws. The right panel in figure 1 shows the necessary grain sizes for quartz and plagioclase to switch to diffusion creep diominated deformation for the applied bulk strain rate.

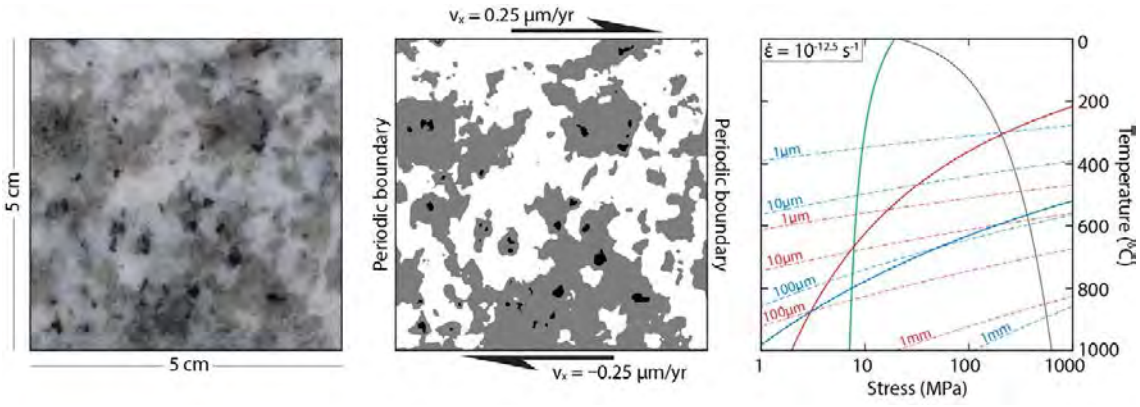

Figure 1. Numerical setup and applied flow laws. Left: 5x5 cm image of a hand specimen from the Rotondo granite. Center: Simplified tecture (ImageJ) with quartz (grey), plagioclase (white), and biotite (black). Right: Strength profiles of quartz (red), anorthite (blue), and single-crystal biotite (green). Full lines: Dislocation creep, dashed lines: diffusion creep.

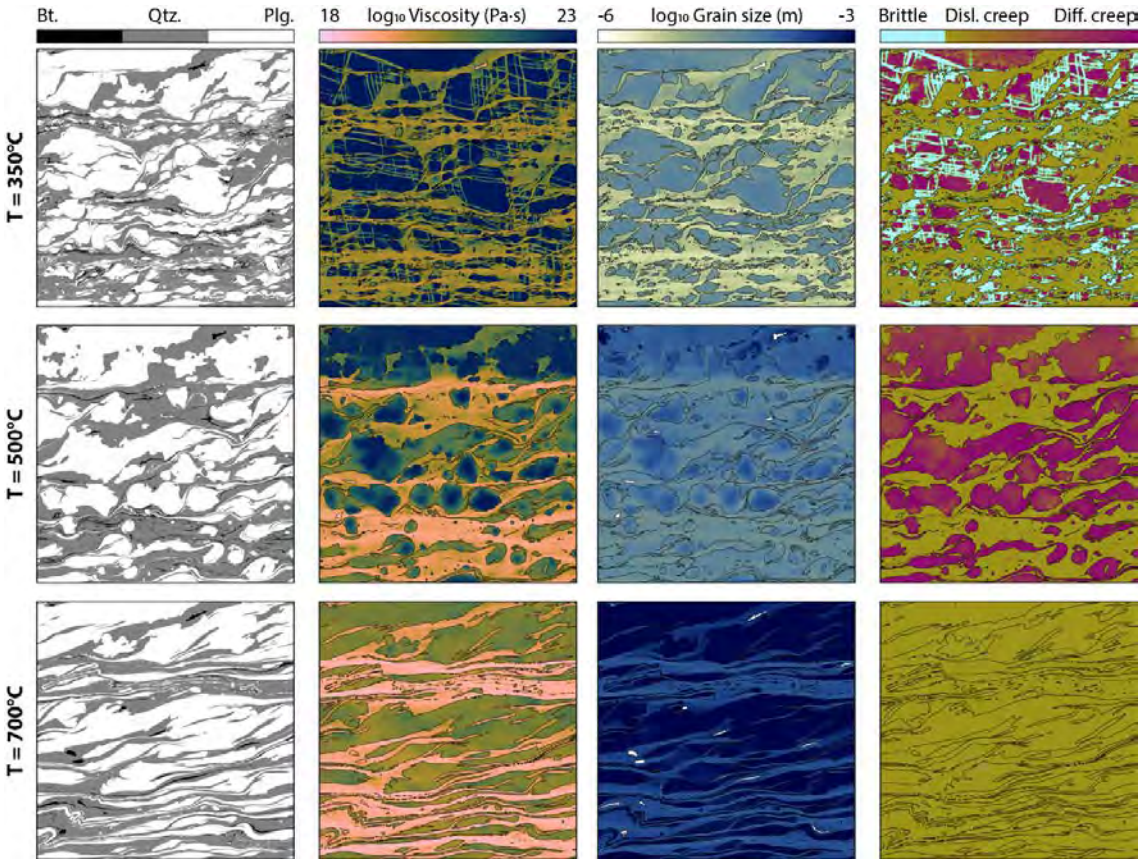

Figure 2. Composition (left), viscosity (second left), grain size (second right), and deformation mechanism (right) of numerical experiments after a shear strain of 10.

Results illustrate the variable textural evolution of shear zones at different temperatures (Figure 2). Quartz deforms dominantly under dislocation creep, which is grain size independent. Therefore, no grain size-related weakening is imposed in the quartz rheology. Plagioclase behaves brittle at lw temperatures and dominantly under diffusion creep at intermediate temperatures, which implies a mechanical weakening related to grain size reduction. At higher temperatures, plagioclase switches to dislocation creep as the dominant deformation mechanism, which invokes constant stress at constant strain rates.

The presented numerical study underlines the importance of grain size-related weakening of crustal shear zones, but only at intermediate temperatures above the brittle-ductile transition (400–450°C) and below the activation of dislocation creep in plagioclase (~650°C).

REFERENCES

Austin, N. J. & Evans, B. 2007: Paleowattmeters: A scaling relation for dynamically recrystallized grain size, Geology, 35 (4), 343-346.

P 1.19
New constraints on the Ivrea Geophysical Body at intra-crustal scales (Western Alps, Europe): a combination of gravimetry, passive seismology and rock's physical properties

Matteo Scarponi[1], György Hetényi[1], the IvreaArray Team

[1]*Institute of Earth Sciences, University of Lausanne, Lausanne, Switzerland (matteo.scarponi@unil.ch)*

We have collected and analysed new seismic and gravity data, to investigate intra-crustal geophysical anomalies. Across the target area of the Ivrea-Verbano Zone, the newly collected geophysical data provided a final coverage of unprecedented resolution compared to previous studies, bridging the resolution-gap between lithospheric geophysical investigations and sub-km-scale surface geological observations, which affected the interpretation of numerous previous studies in the Alpine domain. We collected 207 new relative gravity data points across the Ivrea- Verbano zone, to investigate the density crustal structure of the well-known Ivrea geophysical body (IGB), both at a higher resolution than before and in a novel way. In fact, we processed the gravity data to obtain the Bouguer gravity anomaly field, whose pronounced positive peak well represents the subsurface dense anomalous structure, and we defined the Niggli correction: a density-dependent gravity correction which accounts for the effect of the observed surface density variations in the area, associated with the lower to middle crustal outcrops of the Ivrea-Verbano zone. The Niggli correction extends the surface geological observations from surface to sea level and its magnitude can reach up to 30mGal. Modelling the Niggli gravity anomaly considers the surface density information provided by previous geological studies, and therefore allows to address the crustal density structure of the Ivrea geophysical body more properly. We modelled the body as a single, 3D density-contrast interface beneath the Ivrea-Verbano zone: the model presents an optimal density contrast of 400 $kg \cdot m^{-3}$ with respect to the background crustal structure and it supports the presence of a dense body located very close to the surface, as shallow as 0 to 2 km below the sea level. Further sensitivity tests suggest a plausible density contrast range of 300 to 500 $kg \cdot m^{-3}$ and a spatially sharp density gradient (< 4 km), with the relatively denser model presenting a narrower and slightly deeper interface with respect to the lighter one. The interpretation of these results, in light of the geological knowledge of the area, allowed also to distinguish among possible candidate rocks for the Ivrea geophysical body composition. Considering a natural increase of densities with depth, which is a reasonable assumption for the continental crust, and the metamorphic grade of the area, which presents high temperature metamorphism in the southern Alps (to which the body structurally belongs) and high-pressure metamorphism in the western Alps, felsic and high-pressure metamorphic rocks (eclogites) were excluded as main composing rocks of the Ivrea geophysical body. Instead, mafic or ultramafic plutonic rocks are the most likely components for the lithology of the body. In addition to the gravity data collected in the Ivrea-Verbano zone, we installed and maintained a network of 10 broadband seismic stations (IvreaArray, https://doi.org/10.5281/zenodo.1038209) in collaboration with colleagues from the INGV and the Czech Academy of Sciences. This array operated for 2 years and 3 months, from June 2017 to September 2019. The 10 seismic stations were installed along a West-East linear profile along Val Sesia, at 5 km inter-station spacing, starting few kilometres West of the Insubric Line, and crossing the Ivrea-Verbano zone until the Eastern side of Lago Maggiore, naturally connecting the profile to a permanent station. We used and processed the new seismic and gravity data to refine and further constrain a 2D cross-section of the IGB along the Val Sesia profile. To do this, we modelled the Ivrea body as a single and common density and shear-wave velocity contrast interface, whose initial geometry was based on the structure of the recent 3D density model. We designed, implemented and ran an algorithm which executes a performance-driven random walk in the model space (i.e., the ensemble of all the possible Ivrea body models), to preferentially explore the better fitting areas of the 9D parameter space defining the model. Processing the collected gravity data together with the new seismic data as migrated P-to-S converted waves lead to new constraints on the IGB structure. A shallow and relatively sharp interface is resolved over at least 20 km horizontal distance in the western part of the seismic profile (between 8.11°E and 8.43°E). The inversion results present two main groups of well-fitting model geometries, presenting different characteristics for the shallowest portion the Ivrea body: a flat and gently eastward-dipping interface between 3 and 7 km depth, and a structure with a local peak reaching as shallow as 1-3 km depth, beneath the three westernmost stations (8.11° E and 8.25°E). While both groups of models agree with a western boundary associated with the steeply westward-dipping Insubric Line, the latter is more consistent with the well-known lower crustal rock complex outcropping at the western edge of the Ivrea-Verbano Zone. The retrieved IGB velocity and density contrasts relative to the surroundings are in general good agreement with the physical properties of the rock samples collected in the area and analysed in earlier studies. The results span a rather broad range of acceptable shear-wave velocity contrasts (0.5 to 1.2 $km \cdot s^{-1}$), providing slightly higher velocities than those from field samples and/or trends in the literature. In terms of density, a reasonably narrow range of better-fitting density contrasts of 200 to 400 $kg \cdot m^{-3}$ is found, in agreement with the results from the earlier 3D Ivrea body modelling, which favoured a density contrast of 400 $kg \cdot m^{-3}$, and also in agreement with earlier gravity studies in the literature. We further analysed the amplitude and the frequency content of a stack of high-quality P-to- S converted waves (receiver functions), to constrain the sharpness of the vertical velocity gradient associated with the shallow IGB discontinuity. By comparing the stack with synthetics for different maximum frequency contents, we found thicknesses of 0.8 km to 0.4 km as reasonable higher and lower limits for the shallow

velocity-gradient associated with the top of the Ivrea body discontinuity near its shallower structural position. The presented studies provide novel geophysical knowledge on the intra-crustal structure associated with the IGB, with promising results for the foreseen continental drilling project DIVE: Drilling the Ivrea-Verbano zonE (Pistone et al. 2017), aiming at investigating the physics, the chemistry and the evolution of the very exposed outcrops in the Ivrea-Verbano Zone and the structures just beneath.

REFERENCES

Pistone M, Müntener O, Ziberna L, Hetényi G, and Zanetti A 2017: Report on the ICDP workshop DIVE (Drilling the Ivrea–Verbano zonE). Scientific Drilling, 23:47–56.

P 1.20
Styles of fault growth influencing rift propagation in rotational rift settings: Insights from crustal scale analogue models

Timothy Schmid[1], Guido Schreurs[1], Jürgen Adam[2]

[1] Institute of Geological Sciences, University of Bern, Baltzerstrasse 1, CH-3012 Bern (timothy.schmid@geo.unibe.ch)
[2] Department of Earth Sciences, Royal Holloway University of London, Egham, United Kingdom

We present new results and findings from an analogue modelling series with a divergence velocity gradient to simulate continental rifting in rotational systems on a crustal scale. Our analogue model set up consists of a simplified two-layer mechanical system simulating an upper brittle and a lower ductile crust (respectively quartz sand and PDMS-corundum sand mixture). A rod of ductile material ("seed"), placed on top of the viscous layer acts as a structural weakness at the base of the brittle layer, and ensures localized rifting. The applied divergence velocity gradient causes rotational rifting and propagating deformation towards a rotation axis.

We investigate and quantify the effect of such a rift-axis parallel extension gradient on fault growth and rift propagation. For the quantitative analysis, we apply 3D Stereo Digital Image Correlation, a technique which combines 3D surface topography and respective 3D displacement fields from time-series stereo images (e.g., Adam et al., 2005). In combination with X-Ray computed tomography, we gain a comprehensive understanding of deformation evolution in analogue models of rotational rifting.

Spatiotemporal high resolution analyses of our models reveals insights into the 3D deformation structures of rotational rifting and depicts rift propagation based on fault growth according to a hybrid fault growth model (Rotevatn et al., 2019). Such hybrid fault growth is characterized by an early stage of rapid fault lengthening due to fault segment linkage and infrequent strain accumulation (i.e., displacement). The first stage is followed by an extended stage of dominant strain accumulation accompanied by minor fault lengthening. Early fault linkage occurs bidirectionally enabling high rift tip propagation rates, which rapidly drop after switching to linear unidirectional fault growth oriented towards the rotation axis.

When rift tip propagation rates are high, strain accumulation shows partitioning between competing conjugate normal faults with fault activity switching repeatedly from one segment of a normal fault to a segment on the oppositely dipping normal fault. When rift tip propagation rates slow down (i.e., after an early lengthening stage), active faulting migrates from the rift boundary faults inwards to intra-rift normal faults. These processes occur stepwise along the rift axis as a function of bulk strain and applied strain rates resulting in a characteristic deformation pattern where different fault generations are simultaneously active.

Results from this analogue modelling study show that elements of conceptual fault growth models, formulated under orthogonal extension, also apply to rift settings under rotational extension and significantly determine rift propagation and narrowing of faulting activity. Early stages of bidirectional lengthening and strain accumulation may be difficult to resolve in nature where often time constraints on fault activity are rather poor. Furthermore, our results highlight the importance of the rift-axis parallel, time-dependent evolution of fault segments for the understanding of the tectonic history in rotational rift settings.

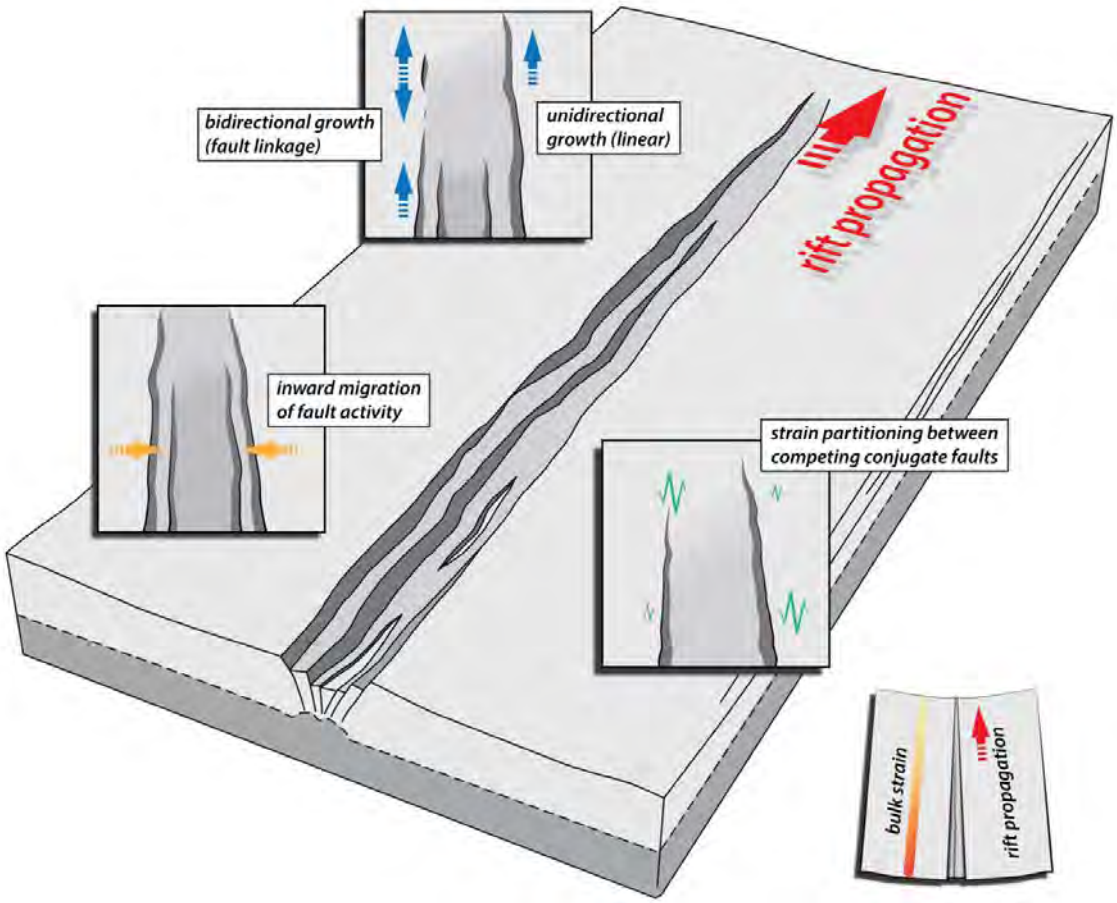

Figure 1: Sketch showing the key mechanism of rift propagation in our analogue models due to a pivoting motion about a rotation axis. Deformation processes occur stepwise as a function of increasing bulk strain with increasing distance with respect to the rotation axis.

REFERENCES

Adam, J., Urai, J., Wieneke, B., Oncken, O., Pfeiffer, K., Kukowski, N., Lohrmann, J., Hoth, S., Van Der Zee, W., Schmatz, J. (2005). Shear localization and strain distribution during tectonic faulting - New insights from granular-flow experiments and high-resolution optical image correlation techniques. Journal of Structural Geology 27, 283–301.

Rotevatn, A., Jackson, C.A.-L., Tvedt, A. B., Bell, R. E., Blækkan, I., 2019. How do normal faults grow? Journal of Structural Geology 125, 174-184.

P 1.21
Structural Mapping of the Eclogite Zone, Tauern Window: Implications on the rheology of the subduction zone interface

Tokle, L., Braden, Z., Cisneros, M[1], and Behr, W.M.

Structural Geology and Tectonics Group, Geological Institute, Department of Earth Sciences, ETH Zurich, Sonneggstrasse 5, 8092, Zürich, Switzerland (leif.tokle@erdw.ethz.ch)

The subduction zone interface is a shear zone of varying thickness defining the boundary between the subducting plate and the overriding plate. An important constraint on the rheology of the subduction zone interface is the amount of sediment that is deposited on the down going plate and the rheological contrast between the metasedimentary and metabasic rocks at various temperature and pressure conditions. To address this, we conducted field work in the Eclogite Zone in the Tauern Window, Austria to assess the rheological contrast between deformed metasedimentary and metabasic rocks at eclogite facies. The Eclogite Zone is ideal to study the rheology of the subduction zone interface because it has been shown previously that the metasedimentary and metabasic rocks were subducted and exhumed to the surface as a single structural unit to eclogite facies where the metabasic rocks still show microstructural relationships from peak metamorphic conditions. Using various field techniques we are creating 2-D and 3-D structural maps around Eissee, which encompasses the largest structural cross-section of the Eclogite zone, to understand the structural relationships between the metasedimentary and metabasic units. In addition, we have conducted quartz-in-garnet inclusion barometry in both metasedimentary and metabasic rocks as well as graphite thermometry to compare with previous thermal and barometric techiques. Finally, we are analyzing eclogite boudin size, shape, and host mineralogy to assess the rheological contrast between the metasediments and metabasic rocks.

P 1.22
Variscan granitoid in the Eastern Pontides, NE Turkey, records a 2.0 Ga history of Gondwana-derived terranes

François Turlin[1], Robert Moritz[1], Serdar Keskin[2], Şafak Utku Sönmez[1], Alexey Ulyanov[3]

[1] *Department of Earth Sciences, University of Geneva, Rue des Maraîchers 13, 1205 Geneva (francois.turlin@unige.ch)*
[2] *General Directorate of Mineral Research and Exploration (MTA), Eastern Black Sea District Office, TR-61010 Trabzon, Turkey*
[3] *Institute of Earth Sciences, University of Lausanne, Lausanne, Switzerland*

The Eastern Pontides in NE Turkey are part of the Alpine Orogeny. They formed by accretion of a Gondwana-derived terrane to the Eurasian margin and subsequently underwent orogenic events associated with the closure of Paleotethys and Neotethys oceans. Relics of Gondwana's inheritance within the Eastern Pontides are rare. The oldest records of the pre-Alpine evolution are Carboniferous granitoids (~309-323 Ma, this study and unpublished U-Pb zircon ages) that crop out in the central part of the belt as a concordant "boutonnière" of Variscan plutons. Among these Carboniferous plutons, the Artvin granitoid is one of the best preserved and most exposed examples (Fig. 1). It is in contact in the northeast and southwest with Jurassic detrital sedimentary sequences of the Berta Formation; its northwestern and southeastern margins are obliterated by normal faults that probably also facilitated its exhumation during the successive thermal relaxation/ orogenic collapses of that belt.

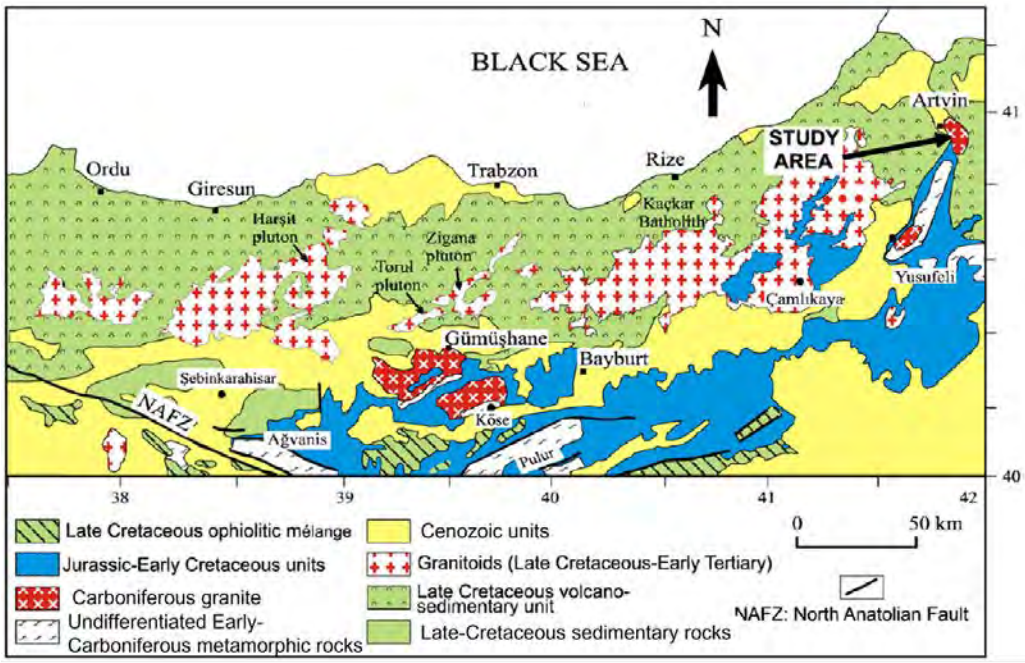

Figure 1. Simplified geological map of the Eastern Pontides showing the location of the Carboniferous granitoids and of the Artvin granitoid (modified after Dokuz et al., 2010).

The Artvin granitoid is composed of several granitic phases. Here, we present new LA-ICP-MS U-Pb zircon dates for these phases. The first phase is a leucogranite dated at 324.4 ± 0.6 Ma; inherited zircon cores as old as ca. 2.4 Ga are frequent in it. The second phase of leucogranite hosts xenoliths of partially molten micaschist and felsic intrusive rocks. The granitic matrix is dated at 323.7 ± 0.8 Ma with abundant inheritance as old as ca. 1.9 Ga. The main volume of the Artvin granitoid consists of a leucogranite dated at 320.6 ± 0.6 Ma. It is crosscut by mafic dykes and sills, and by micro-leucogranite dykes. The latter has been dated at 315.4 ± 0.7 Ma, based on one representative example.

Accordingly, the different granitic phases of the Artvin granitoid cover a range of crystallization ages, pointing to a dynamic emplacement of the pluton during the Variscan Orogeny. This pluton represents a perfect natural laboratory to investigate the Variscan history of the Eastern Pontides. Moreover, the zircon crystals record a ~2.0 Ga inheritance. Coupling whole-rock geochemistry, Hf-O isotopic compositions and trace elements in zircon to the available U-Pb dates will allow us to reconstruct the evolution of a Gondwana crustal segment of the Eastern Pontides since the Early-Paleoproterozoic.

REFERENCE

Dokuz, A., Karsli, O., Chen, B., & Uysal, I. 2010: Sources and petrogenesis of Jurassic granitoids in the Yusufeli area, Northeastern Turkey: Implications for pre- and post-collisional lithospheric thinning of the eastern Pontides, Tectonophysics, 480, 259–279

P 1.23
A geological profile and kinematically balanced cross-section through the Mont Tendre and Mont Risoux

Anina Ursprung[1], Sandra Borderie[1], Anna Sommaruga[1], Jon Mosar[1]

[1] *Unit of Earth Sciences, Department of Geosciences, Univesity of Fribourg, Chemin du Musée 6, CH-1700 Fribourg (anina.ursprung@unifr.ch)*

The study area of this Master thesis is located in the Internal Jura Mountains (Haute Chaîne), in the area from the Mont Tendre, Vallée de Joux and the Mont Risoux in the Canton of Vaud (Switzerland) to the Vallée de la Saine in the Jura department (France).
The aims are to investigate the local surface and subsurface geology and to comprehend the geometry of the geological structures in order to better understand the formation of the Jura folds and associated thrusts on a regional scale. These objectives are accomplished by constructing a geological profile and by forward modelling of a kinematically balanced cross-section using the program MOVE (Midland Valley).

The construction of the geological profile is achieved by the compilation of the following data sources: the study of the geological maps (Aubert, 1941; Aubert, 1963; Falconnier, 1951) and original new fieldwork which helped to gain a better understanding of the outcropping geology. Dip data were collected along the cross-section in order to obtain a dense data network needed for the construction of the geological profile. Available subsurface data include the Risoux-1 deep well which lies 2.3 km to the west from the cross-section. Its description (Winnock, 1961) includes multiple repetitions of several Mesozoic layers and is therefore an important, yet intricate, data source which pictures the geological architecture of the subsurface. Additionally, existing interpretation of the seismic lines (Shell Switzerland 1972 – 1974, 1976) give another essential insight into geological construction of the Jura Mountains. This interpretation (Sommaruga, 1997) helps to define the near top horizon depths of the Mesozoic layers. Moreover, the base of the Mesozoic layers and therefore the lower boundary of the geological profile is defined by the digital surface model of the top pre-Mesozoic basement (Schori, 2021). The comparison and compilation of these data sources determine the local stratigraphic column. Lastly, the modelling of the kinematically balanced cross-section permits to propose a chronology of the thrust development leading to the formation of the Jura Mountains.

Our preliminary results (Figure 1) propose that the main regional thrust runs through the broad Risoux anticline towards the foreland. It is rooted in the basal décollement and only reaches the surface in the syncline of the Vallée de la Saine some 10km farther north. This main thrust is responsible for a particularly long displacement and the doubling of the Mesozoic cover. The hanging wall of the Risoux anticline is composed of a fishtail structure and also of a pop-up structure which explain the multiple and proven thrusts passing through the Risoux-1 deep well as well as the repeated doubling of the Mesozoic cover. The other major structure, the Mont Tendre anticline, also shows a thrust towards the foreland which reaches the surface in the syncline of the Vallée de Joux. The steep southeastern limb of the anticline is caused by the several backthrusts rooted in the main thrust towards the hinterland.
It is however important to underline that this work is still in progress to resolve inconsistancies such as the excess length of the Dogger and Liassic below the Mont Risoux anticline. These problems will be adressed by a kinematically balanced cross-section construction.

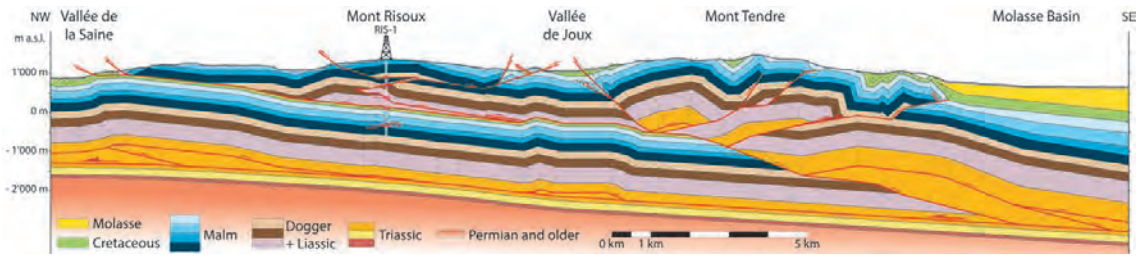

Figure 1. Non-balanced geological profile through the Internal Jura.

REFERENCES

Aubert, D. 1941 : CN 1221 Vallée de Joux. Atlas géologique de la Suisse 1:25'000. Commission géologique de la Soc. Helv. des sciences naturelles, number 17.

Aubert, D. 1963 : CN 1202 Orbe. Atlas géologique de la Suisse 1:25'000, Organe de la Soc. Helv. des sciences naturelles, number 42.

Falconnier, A. 1951 : CN 1241 Les Plats-Marchairuz-La Cure-Arzier-Gimel. Atlas géologique de la Suisse 1:25'000,

Commission géologique Suisse Organe de la Soc. Helv. des sciences naturelles, number 25.

Schori M. 2021 (in review): The Development of the Jura Fold-and-Thrust Belt: pre-existing Basement Structures and the Formation of Ramps. Doctoral Thesis, Unit of Earth Sciences, Department of Geosciences, Faculty of Science, University of Fribourg, p. 75 – 89.

Sommaruga A. 1997 : Geology of the central Jura and the Molasse basin: New insight into an evaporite-base foreland fold and thrust belt. Mémoires de la Société Neuchâteloise de Sciences Naturelles, 12: 176 pp.

Winnock, E. 1961: Résultats géologiques du forage Risoux 1. Bull. Ver. Schweizer. Petrol.-Geol. Un. -Ing. 28 (74), p. 17 – 26.

P 1.24
From the India-Eurasia corner collision to lateral extrusion: results from 3D coupled numerical models

Luuk van Agtmaal[1], Attila Balazs[1], Dave May[2], Taras Gerya[1]

[1] *Institute of Geophysics, ETH Zürich, Sonneggstrasse 5, CH-8092 Zürich (luuk.vanagtmaal@erdw.ethz.ch)*
[2] *University of California San Diego, Scripps Institution of Oceanography, La Jolla, CA, USA*

Plate tectonics, surface processes and climatic variations shape and drive the formation of orogens. Oceanic and continental subduction, and subsequent collision, all shape surface topography over time. Surface processes, erosion and sediment re-distribution change the stress and temperature field within the lithosphere. In turn, these determine the style of deformation the resulting topographic fingerprints. The India-Eurasia collision zone provides an ideal natural example where these interactions can be studied. To this aim, we use a 3D coupled numerical modelling approach. The study area encompasses the area around the eastern corner of this collisional zone, where GPS measurement data show significant east-south-eastward extrusion of continental crust (Figure 1). We use large-scale regional, lithospheric-scale models. The models use non-Newtonian, visco-plastic rheologies and account for diffusion-advection-based erosion and sedimentation. The northward indentation (push) of India is combined with laterally varying velocity boundary conditions, applied to the south-eastern and eastern boundaries of the model domain, to see how this affects the topographic signature. These experiments were conducted using the thermo-mechanical code I3ELVIS (Gerya and Yuen, 2007) coupled to the FDSPM surface processes code, based on diffusion-advection (Munch et al., 2017). The results of the experiments will yield new insights about the processes involved in this complex natural example of continental corner collision.

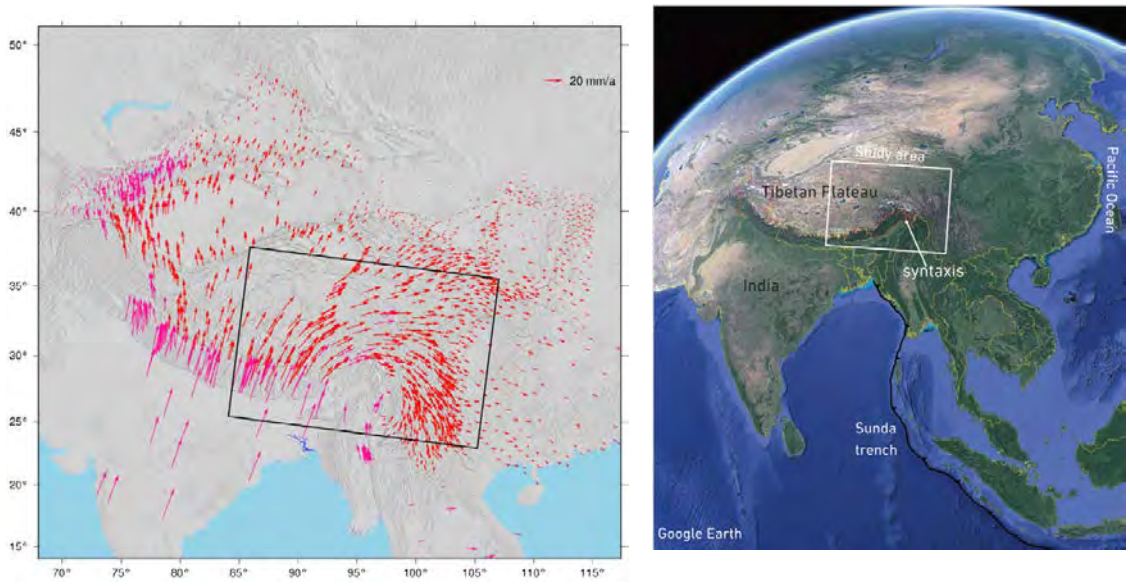

Figure 1. Left panel: Location of the study area in the GPS solutions of Wang et al., (2017) showing significant clockwise rotations in the crustal deformation pattern. Right panel: Zoomed-out view of the study area within the Eas-Asian tectonic setting.

REFERENCES

Gerya, T. V., & Yuen, D. A. (2007). Robust characteristics method for modelling multiphase visco-elasto-plastic thermo-mechanical problems. Physics of the Earth and Planetary Interiors, 163(1-4), 83-105.

Munch, J., Ueda, K., Burg, J. P., May, D., & Gerya, T. (2017, April). 3D Numerical modelling of topography development associated with curved subduction zones. In EGU General Assembly Conference Abstracts (p. 12975).

Wang, W., Qiao, X., Yang, S., & Wang, D. (2017). Present-day velocity field and block kinematics of Tibetan Plateau from GPS measurements. Geophysical Journal International, 208(2), 1088-1102.

P 1.25
The Panalesis model and its applications to the Permian – Triassic climate oscillations

by Christian Vérard*, Charline Ragon, Jérôme Kasparian and Maura Brunetti

* *christian.verard@unige.ch*

A global plate tectonic model is a model that contains tectonic plates, with given shapes (on a spherical surface) and given forces and tectonic context at their boundaries. From one time slice to the next, the inheritance of those shapes and the geodynamics at those plate boundaries must be taken into account and implemented in accordance with geological records in space and time. The Panalesis model is such a model and reconstructs not only continental areas but also oceanic realm from 888 Ma (Tonian) to present-day.

Once a version of the plate tectonic model is complete, it can be converted into palæo-DEM (digital elevation model) covering 100% of the Earth's surface. Palæo-DEM can then be used to run other models, in particular palæo-climate models like the MITgcm.

Here are examples on possible steady states found in climate simulations at the Permian – Triassic Boundary (*ca*. 250 Ma) and how they compare with palæo-biome interpretation derived from fossil plants. This work shows how tectonic – climate interaction can be better understood in deep time and how it can be used in the future for retro-feedback in an integrated approach of palæogeography determination.

P 1.26
The effect of temperature on the frictional behavior of simulated ultrafine-grained granitoid gouge: an experimental investigation using a Ring Shear Apparatus

Weijia Zhan[1], Natalia Nevskaya[1], André Niemeijer[2], Alfons Berger[1], Chris Spiers[2], Marco Herwegh[1]

[1] Institute of Geological Sciences, University of Bern, Baltzerstrasse 1+3, CH-3012 Bern (weijia.zhan@geo.unibe.ch)
[2] Faculty of Geosciences, HPT Laboratory, Utrecht University, Princetonlaan 4, 3584 CB Utrecht, Netherlands

In the continental crust, exhumed shear zones frequently show widespread ultrafine-grained fault rocks of predominantly granitoid compositions, often accompanied with cyclical earthquake activity in upper to middle crustal levels (e.g., Wehrens et al. 2016; Herwegh et al., 2020; Scholz, 1998). The switch between fast seismic slip and slow interseismic activities suggests that there is a variation of the fault rock friction stability during sliding. Temperature is considered to play a key role in controlling the frictional stability of fault rocks and thus the nucleation of earthquakes. However, the frictional behavior of ultrafine-grained granitoid fault rocks and the influence of temperature on the frictional stability of granitoid shear zones are still not well understood.

We investigate the frictional behavior of a simulated fault gouge under hydrothermal conditions using a Ring Shear Apparatus. Simulated fault gouges were derived from natural granitoid ultramylonites collected from a shear zone at the NAGRA Grimsel Test Site (Central Swiss Alps). Powdered starting material has a mean grain size of ~55 µm. The first series of velocity stepping experiments were carried out at temperatures of 27, 100, 200, 300, 400, 500 and 600°C to determine the velocity dependence of friction. In the framework of rate-and-state friction, a velocity-strengthening system is frictionally stable, whereas a velocity-weakening system is frictionally unstable. The second experimental series were conducted at constant strain rate with temperatures of 200, 450 and 650°C, under an effective normal stress of 100 MPa and a sliding velocity of 1 µm/s.

We document that the friction of wet simulated ultrafine-grained granitoid gouge remains relatively constant at friction coefficients µ≈0.75 at lower temperature up to 450°C, but it rapidly decreases to µ ≈0.5 at 650°C. This pronounced change suggests that temperature has little effect on friction at low temperature, but it affects rheology at higher temperature, probably by incorporating viscous deformation processes. The microstructures of gouge deformed under wet-hot conditions show underdeveloped Riedel shear fractures, minor grain-size reduction (except for the formation of sliding-parallel shear zones next to the gouge-piston interface) compared with gouge sheared at cold conditions. In addition, two transitions from velocity strengthening to velocity weakening and the reverse occur at temperatures of T≈100°C and T≈400°C, respectively.

Frictional instability between temperatures of 100-400°C is characterized with abundant unstable sliding and regular stick-slips. In terms of crustal faulting, these data indicates a seismogenic window that possibly limits the depth distribution of earthquakes on faults in granitoid shear zones.

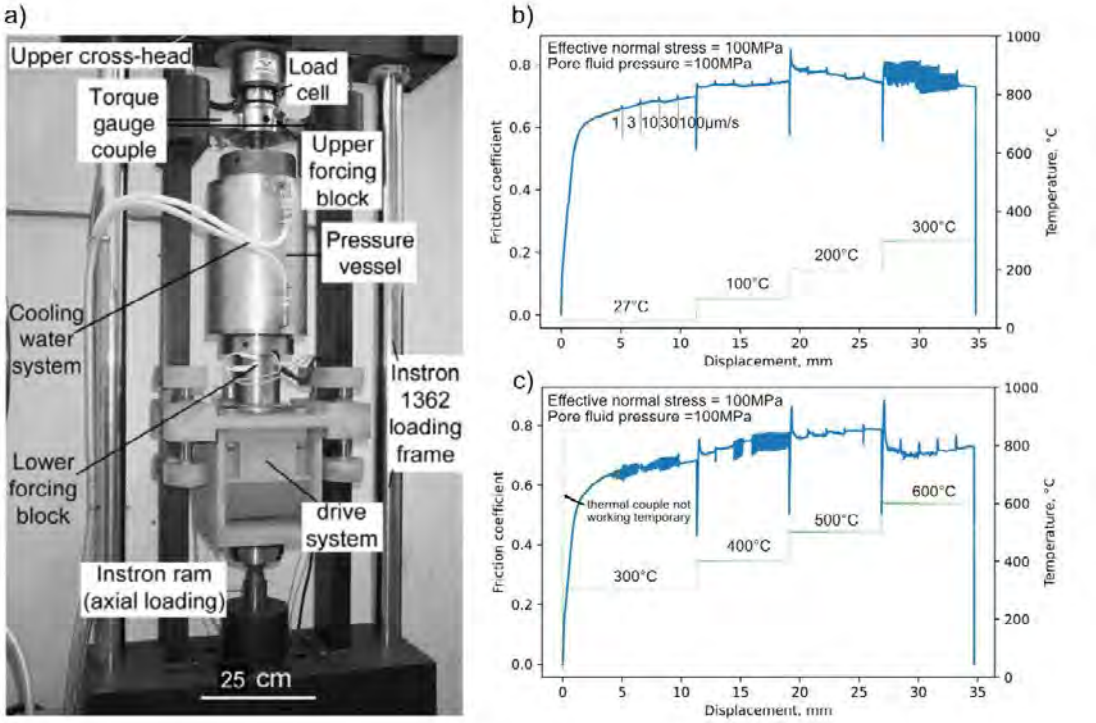

Figure 1. a) Photograph of the Ring Shear Apparatus used (Niemeijer et al., 2008). Plots of friction as a function of displacement for velocity stepping experiments at b) temperatures of 27, 100, 200 and 300°C and at c) temperatures of 300, 400, 500, 600°C.

REFERENCES

Wehrens, P. C., Berger, A., Peters, M., Spillmann, T., Herwegh, M. 2016: Deformation at the frictional-viscous transition: Evidence for cycles of fluid-assisted embrittlement and ductile deformation in the granitoid crust, Tectonophysics, 693, 66-84.

Herwegh, M., Berger, A., Glotzbach, C., Wangenheim, C., Mock, S., Wejrens, P., Baumberger, R., Egli, D., & Kissling, E. 2020: Late stages of continent-continent collision: timing, kinematic evolution, and exhumation of the Northern rim (Aar Massif) of the Alps, Earth-Science Review, 200, 102959.

Scholz, C. H. 1998: Earthquakes and friction laws, Nature, 391, 37-42.

Niemeijer, A., Spiers, C. J., & Peach, C. 2008: Frictional behaviour of simulated quartz fault gouges under hydrothermal conditions: Results from ultra-high strain rotary shear experiments, Tectonophysics, 460, 288-303.

P 1.27
Interaction between mantle and crustal weaknesses during rifting: insights from laboratory experiments

Frank Zwaan[1], Pauline Chenin[2], Duncan Erratt[2], Gianreto Manatschal[2], Guido Schreurs[1]

[1] *University of Bern, IfG, Baltzerstrasse 1, 3012 Bern, CH (frank.zwaan@geo.unibe.ch)*
[2] *Univ. Strasbourg, CNRS, ENGEES, ITES UMR 7063, 5 r. Descartes, 67084, France*

During rifting, deformation often localizes along weaknesses originating from previous tectonic phases, and weaknesses in the strong upper crust or upper mantle are expected to particularly affect rift evolution. When simulating the influence of such weaknesses in analogue or numerical models, modellers often focus on either crustal or mantle heterogeneities. By contrast, here we present results from 3D analogue models to test the combined effect and relative impact of (differently oriented) mantle and crustal weaknesses on rift systems.

Our model set-up involves a rigid base plate fixed to a mobile sidewall (Fig. 1). When this sidewall moves outward, the edge of the base plate creates a “velocity discontinuity” (VD) acting as a shear zone in the strong upper mantle. The VD is either parallel to the model axis, or 30˚ oblique. On top of this base plate, a viscous layer represents the ductile lower crust, overlain by a sand cover simulating the brittle upper crust. Crustal weaknesses were included by adding “seeds” (i.e. smal ridges of viscous material at the base of the sand layer), or by pre-cutting the sand. We applied different crustal weakness orientations too.

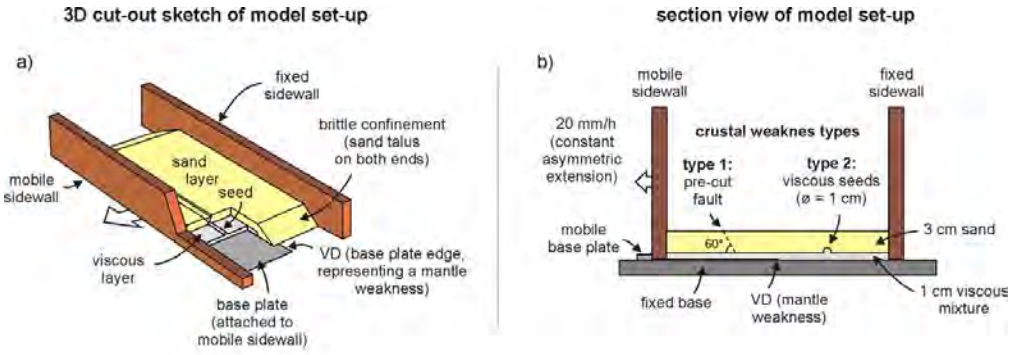

Figure 1. Model set-up. (a) 3D sketch of general set-up. VD: velocity discontinuity representing a weakness in the upper mantle. (b) Section view depicting model layering and crustal weaknesses. From Zwaan et al. (2021)

Without weaknesses in the model crust, a model axis-parallel VD forms a rift basin along the model axis (Fig. 2a, b), and an oblique VD creates a series of en echelon grabens (Fig. 2c). Adding crustal weaknesses strongly affects rift structures: reactivated pre-cut faults partially overprint and segment the VD-induced rift zone (Fig. 2d, e), which is even more pronounced in models with viscous seeds. The orientation of the weaknesses with respect to both the regional divergence direction and each other has an important effect on their subsequent (re-) activation (Fig. 2d–k). Both the VD and modelled crustal weaknesses are most active when oriented orthogonally to the regional divergence direction, the ideal setting for normal fault development (Fig. 2d-j). In case a VD or crustal weakness is oriented obliquely to the regional divergence direction, it is less likely to be activated. Yet when the VD and the crustal weaknesses are parallel, both effectively localize deformation, even when both are oblique to the divergence direction (Fig. 2j). Furthermore, increasing the divergence rate causes enhanced coupling between the VD and the overlying materials, overprinting the dominant seed-controlled structures (compare Fig. 2i and Fig. 2k).

We thus find that the orientation and relative strength of weaknesses in the mantle and crust, as well as divergence rates control subsequent rift structures. These structures can be complex due to the interplay of the above factors, and importantly, all form in the same divergence setting, without the need to invoke multiphase rifting and changing rift kinematics. These results provide a strong incentive to reassess the tectonic interpretation of various natural examples.

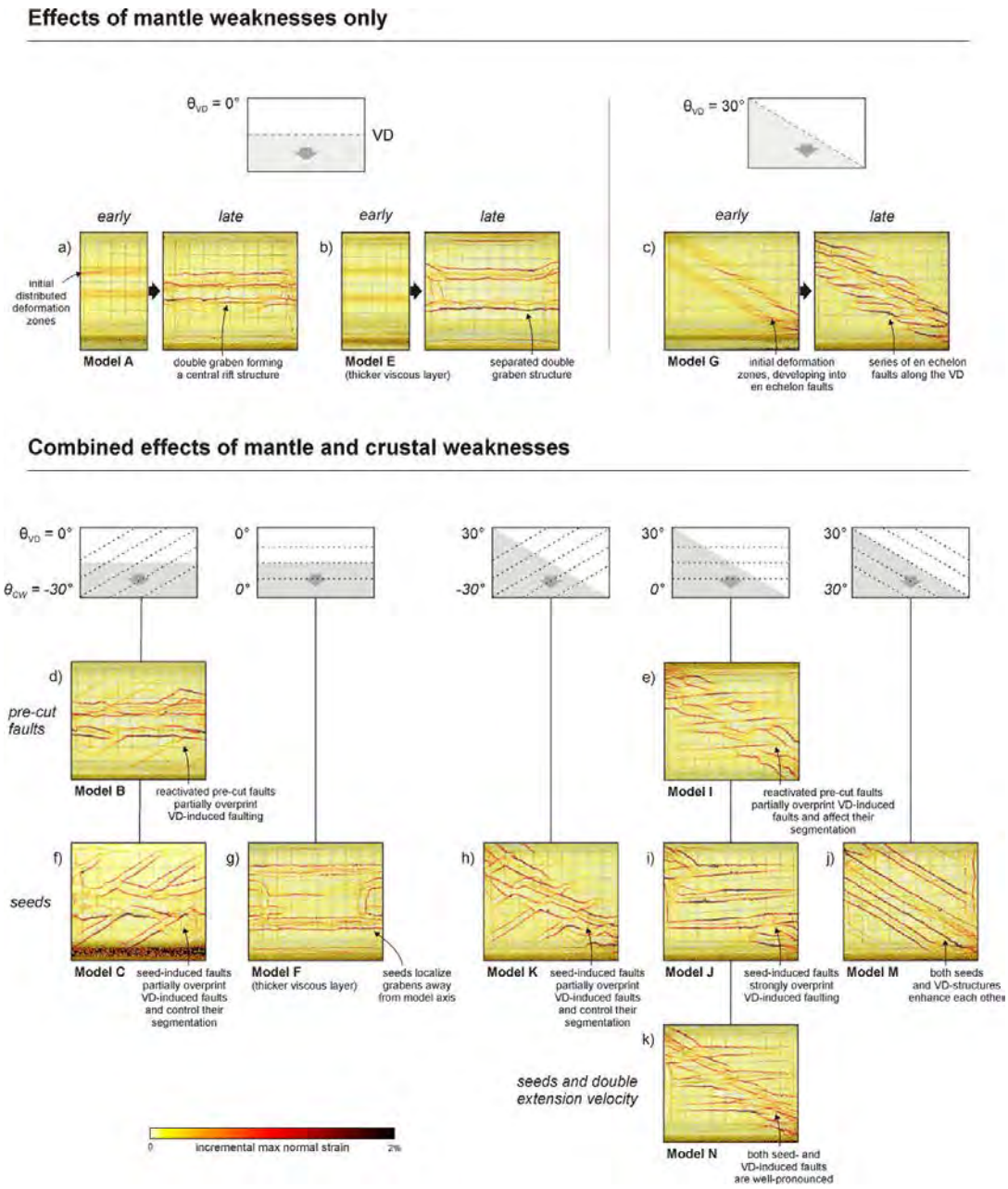

Figure 2. Summary of model results (PIV-derived strain maps). θ_{VD} and θ_{CW}: angle of VD and simulated crustal weaknesses. From Zwaan et al. (2021).

REFERENCES

Zwaan, F., et al. (2021): Solid Earth. https://doi.org/10.5194/se-12-1473-2021

P 1.28
The influence of initial salt basin geometry on salt tectonics: insights from laboratory experiments

Frank Zwaan[1,2,3], Matthias Rosenau[4], Daniele Maestrelli[5]

[1] *Université de Rennes 1, 35042 Rennes cedex, France (frank. zwaan@geo.unibe.ch)*
[2] *Università degli Studi di Firenze, Via G. La Pira 4, 50121 Florence, Italy*
[3] *Universität Bern, Baltzerstrasse 1+3, 3012 Bern, Switzerland*
[4] *Helmholtz-Zentrum Potsdam - GFZ, Telegrafenberg 14473, Potsdam, Germany*
[5] *Consiglio Nazionale delle Richerche, Via G. La Pira 4, 50121 Florence, Italy*

As a rifted margin starts tilting due to thermal subsidence, evaporitic bodies can become unstable, initiating gravity-driven salt tectonics. Our understanding of such processes has greatly benefitted from tectonic modelling efforts, yet a topic that has gotten limited attention so far is the influence of large-scale salt basin geometry on subsequent salt tectonics. The aim of this work is therefore to systematically test how salt basin geometry (initial salt basin depocenter location, i.e. where salt is thickest, as well as mean salt thickness) influence salt tectonic systems by means of analogue experiments. A total of 35 experiments were analyzed qualitatively using top view photography, and quantitatively via Particle Image Velocimetry (PIV) and 3D photogrammetry (Structure-from-Motion, SfM) to obtain their surface displacement and topographic evolution (Fig. 1).

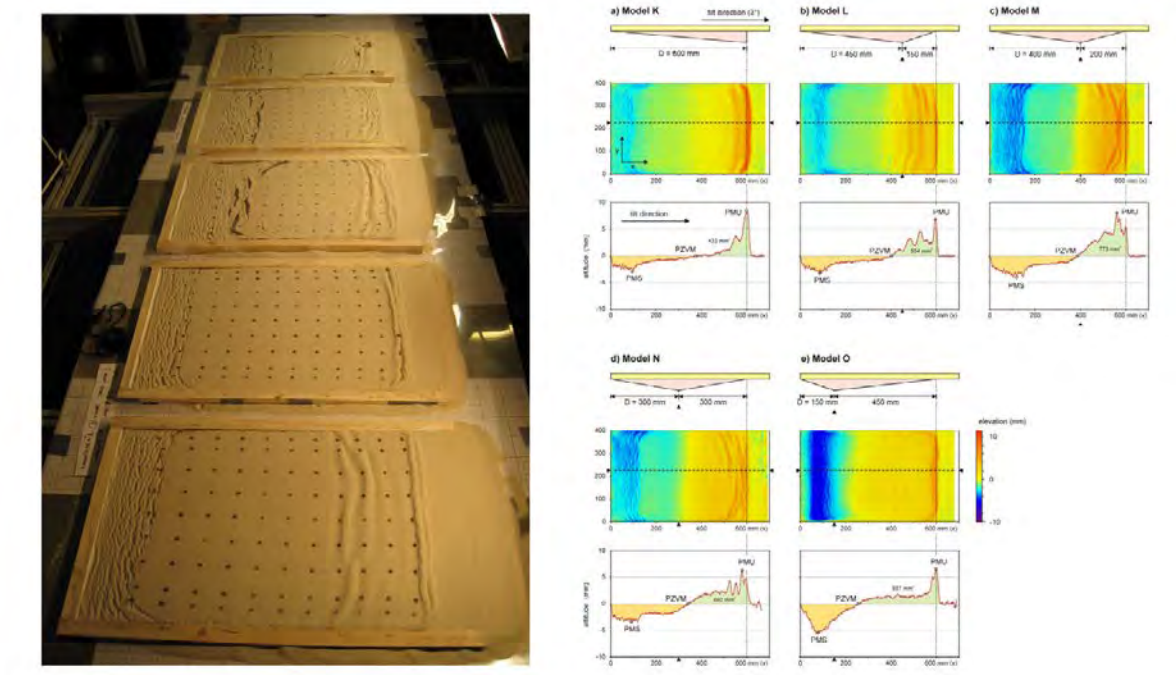

Figure 1. Left: example of a model run. Image © Frank Zwaan. Right: example of topography analysis on models K-O. From Zwaan et al. (2021).

Our model results show that the degree of (instantaneous) margin basin tilt, followed by the mean salt thickness are dominant factors controlling deformation, as enhancing basin tilt and/or mean salt thickness promotes deformation. Focusing on experiments with constant basin tilt and mean salt thickness to filter out these dominant factors, we find that the initial salt depocenter location has various effects on the distribution and expression of tectonic domains (Fig. 2). Most importantly, a more upslope depocenter leads to increased downslope displacement of material, and more subsidence (localized accommodation space generation) in the upslope domain when compared to a setting involving a depocenter situated farther downslope (Fig. 2). A significant factor in these differences is the basal drag associated with locally thinner salt layers. When comparing our results with natural examples, we find a fair correlation expressed in the links between salt depocenter location and post-salt depositional patterns: the subsidence distribution due to the specific salt depocenter location creates accommodation space for subsequent sedimentation. These correlations are applicable when interpreting the early stages of salt tectonics, when sedimentary loading has not become dominant yet.

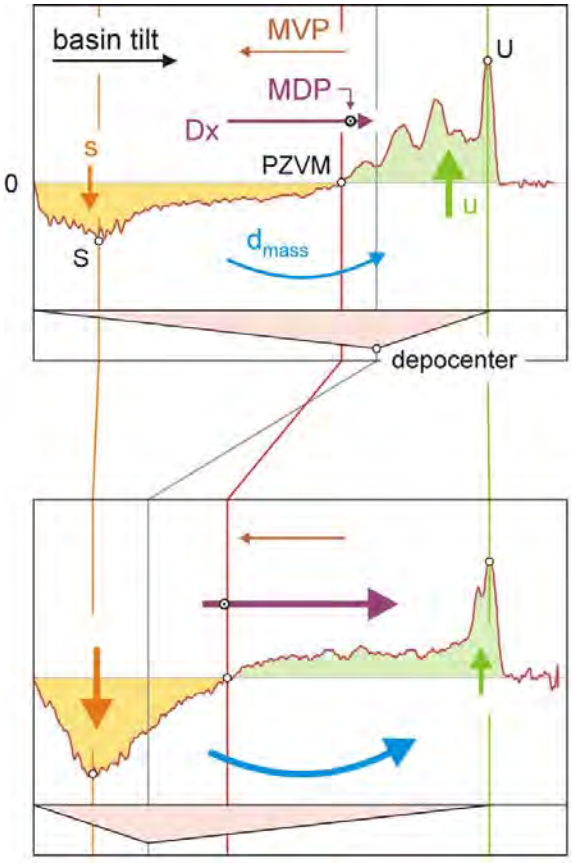

downslope salt basin depocenter:

- PZVM upslope from depocenter
- moderate subsidence (s)
- very high uplift (u)
- low horizontal displacement (Dx)
- MDP relatively downslope
- MVP generally migrates upslope over time
- moderate mass displacement (d_{mass})

upslope salt basin depocenter:

- PZVM downslope from depocenter
- very high subsidence (s)
- high uplift (u)
- high horizontal displacement (Dx)
- MDP relatively upslope
- MVP generally migrates upslope over time
- high mass displacement (d_{mass})
- stable point of max. vertical motion (S, U) compared to downslope depocenter models

Figure 2. Summary of model results: impact of initial basin geometry on deformation and topography in salt tectonic systems. MDP: maximum displacement point (location of maximum cumulative displacement), MVP: maximum velocity point (location of maximum incremental displacement) PZVM: point of zero vertical motion. From Zwaan et al. (2021).

REFERENCES

Zwaan, F., Rosenau, M., & Maestrelli, D. 2021: How initial basin geometry influences gravity-driven salt tectonics: Insights from laboratory experiments, Mar. Petrol. Geol. https://doi.org/10.1016/j.marpetgeo.2021.105195

02. Mineralogy, Petrology, Geochemistry

Francesca Piccoli, Florence Begue, Julien Allaz

Swiss Society of Mineralogy and Petrology (SSMP)

TALKS:

2.1 Aluç A., Moritz R., Kuşcu I., Ulianov A., Karcı M.: Geology, Geochemistry, and Mineralogy of Porphyry-Epithermal Systems at the Kirazlı District, Biga Peninsula, NW Turkey

2.2 Castellanos Melendez M.P., Dilles J., Chelle-Michou C.: A high-precision petrochronology look Into the Yerington batholith, Nevada, USA: Perspectives on the lifetime of magmatic-hydrothermal systems

2.3 Colon D., Schaltegger U., Seligman A., Bindeman I.: Contrasting hot and cold rhyolitic caldera volcanism predating the Columbia River Flood Basalts, northwest USA

2.4 Hakim K., Tian M., Bower D.J, Heng K.: Seafloor Weathering on Oceanworlds

2.5 Higgins O., Sheldrake T., Caricchi L.: A data-driven approach to quantify the thermal-chemical architecture of arc volcanoes

2.6 Keller F., Guillong M., Popa R.-G., Bachmann O.: In-situ inclusion-bearing ilmenite $^{230}Th/^{238}U$ geochronology of quaternary volcanic deposits by laser ablation inductively coupled plasma-mass spectrometry (LA-ICP-MS)

2.7 Klein B., Jagoutz O., Rezeau H.: Rapid construction of continental arc crust during a high magma flux event: the Bear Valley Intrusive Suite, Sierra Nevada, CA, USA

2.8 Liu J.H., Lanari P., Li Z., Wu C.M.: Two types of metagabbros to study the meaning of garnet-dominant corona textures in metagabbro

2.9 Pedemonte G., Kouzmanov K., Bergoeing J.-P., Stefanova E., Spangenberg J., Kingsley T., Bourassa Y.: Trace element and S-isotope geochemistry of sphalerite in the distal Zn-Pb(-Ag) skarn deposit of Santander, Central Peru

2.10 Simian L., Allaz J., Fonseca Teixeira L.M., Bachmann O., Chelle-Michou C.: Petrology, mineralogy, and dating of granites in Northern Pikes Peak batholith, Colorado (USA)

2.11 Tagliaferri A., Schenker F.L., Schmalholz S.M., Ulianov A.: LA-ICP-MS U-Pb dating on zircons from the Lepontine Dome (Central European Alps)

2.12 Tamblyn R., Hand M., Morrissey L., Phillips G., Anczkiewicz R., Zack T.: The petrological reocrd of eclogite polymetamorphism in an oceanic subduction channel

2.13 Vieira Duarte J., Pettke T., Piccoli F., Hermann J.: Evolution of oxide-silicate geochemistry and systematics during subduction of hydrous ultramafic rocks (Central Alps, Switzerland)

2.14 Virmond A.L., Wotzlaw J.-F., Chelle-Michou C.: Zircon petrochronology of behemothian porphyry copper systems

2.15 Wang H.A.O., Grolimund D., Franz L., Mathys D., Schultz-Güttler R., Krzemnicki M.S.: Analysis of Sheet-like Inclusion in Cu-bearing Tourmaline from Brazil

2.16 Wolf R.C., Diamond L.W., Belgrano T.M., Pettke T.: Source rocks and leaching processes for metals in mafic VMS deposits: Semail ophiolite, Oman

2.17 Wotzlaw J.F., Bastian L., Guillong M., Forni F., Laurent O., Neukampf J., Sulpizio R., Chelle-Michou C., Bachmann O.: Garnet petrochronology reveals the lifetime and dynamics of phonolitic magma chambers at Somma-Vesuvius

2.18 Zhang Q.W.L., Lanari P., Li Z.M.G., Wu C.M.: The discovery of retrograde eclogite in the Dunhuang Orogenic Belt, northwestern China

POSTERS:

P 2.1 Amrein A., Baumgartner L.P., Robyr M.: Metamorphic gradient in the Nufenenpass area

P 2.2 Antoine C., Spikings R., Miletic Doric D., Marsh J.S., Gaynor S.P., Schaltegger U.: Tracking Disturbances in the ^{40}Ar-^{39}Ar Isotopic System in Plagioclase Crystals of the Karoo Flood Basalts

P 2.3 Degen S., Allaz J., Krzemnicki M.S., Franz L., Reusser R.: Characterisation of gem-quality spessartine-bearing metapelites from the northern Kaoko Belt, Namibia

P 2.4 Dominguez H., Lanari P., Riel N.: Transport and impact of aqueous fluids in subduction settings: insight from coupling two-phase modelling and oxygen isotopes.

P 2.5 Espinel Pachón I.M., de Haller A., Kouzmanov K.,Tollan P., Spangenberg J.: Mineralizing fluids in the Catalina Huanca carbonate-replacement Zn-Pb-Ag deposit, southern Peru.

P 2.6 Fonseca Teixeira L.M., Bachmann O., Allaz J.: Magmatic to hydrothermal conditions in the transition from an A-type granite to a pegmatite in the Pikes Peak Batholith

P 2.7 Grocolas T., Toussaint A., Müntener O., Jossevel C.: Low pressure crystal accumulation and melt segregation within the Western Adamello tonalite (Italy)

P 2.8 Jorgenson C., Higgins O., Petrelli M., Begue F., Caricchi L.: A novel thermobarometer: how to use machine learning to discover the secrets of volcanoes

P 2.9 Lüder M., Hermann J., Reynes J., Tamblyn R.: A new method to measure water in randomly oriented rutile grains

P 2.10 Markmann T., Lanari P.: Metamorphic reactions as soft or hard triggers for fluid flows?

P 2.11 Musu A., Caricchi L., Perugini D., Corsaro R.A., Vetere F., Petrelli M.: Growth and analysis of experimentally zoned crystals: the competition between crystal growth and elements diffusion

P 2.12 Peverelli V., Berger A., Mulch A., Pettke T., Piccoli F., Herwegh M.: Pre-Alpine hydrothermal activity in the Aar Massif granitoids

P 2.13 Piccoli F., Rubatto D., Hermann J., Vitale Brovarone A.: Dating fluid release and deformation in the ultramafic oceanic lithosphere using perovskite and titanite

P 2.14 Pierre S., Monecke T., Gysi A.P., Diamond L.W.: Submarine hydrothermal vent fluid compositions reflect global tectonic petrogenesis

P 2.15 Reynes J., Hermann J., Lanari P., Bovay T.: OH incorporation and retention in high pressure garnet from the Zermatt ophiolite

P 2.16 Sonmez S.U., Moritz R., Lavoie J., Golay T., Gialli S., Turlin F., Popkhadze N., Natsvlishvili M., Aydın Ü., Keskin S., Spangenberg J.: Diversity of Late Cretaceous epithermal systems of the Georgian Bolnisi and Turkish Artvin Districts: Products of a single ore-forming system during final Neotethyan subduction

P 2.17 Sun Y., Schmitt A.K., Pappalardo L., Russo M.: Quantification of excess ^{231}Pa in late Quaternary igneous baddeleyite

2.1
Geology, Geochemistry, and Mineralogy of Porphyry-Epithermal Systems at the Kirazlı District, Biga Peninsula, NW Turkey

Ali Aluç[1, 2], Robert Moritz[1], Ilkay Kuşcu[2], Alexey Ulianov[3], Mehtap Karcı[4]

[1] University of Geneva, Earth Sciences, Rue des Maraîchers 13, CH-1205, Genève, Switzerland (ali.aluc@etu.unige.ch)
[2] Muğla Sıtkı Koçman University, Kötekli, Menteşe, TR-48000 Muğla, Turkey
[3] Institute of Earth Sciences, University of Lausanne, Lausanne, Switzerland
[4] Dogu Biga Madencilik subsidiary of Alamos Gold INC., Etili, Çan, TR-17400 Çanakkale, Turkey

The Kirazlı district is located at the center of the Biga Peninsula, which hosts numerous high-(HS), low- and intermediate-sulfidation epithermal Au–Ag±Cu, porphyry Au–Cu–Mo, and base-metal skarn deposits and prospects at the north-western tip of the Anatolian plate. The district contains a high sulfidation (HS) epithermal Au-Ag deposit (0.33 Mt at 0.71 Au; Cormier et al., 2017)) and a porphyry Cu-Mo occurrence. The district includes five target zones, namely: Kirazlı Main, Çatalkaya, Kale, Rock Pile, and Iri. The NNW-SSE trending HS orebody lies beneath the Kirazlı main zone, and the porphyry Cu-Mo mineralization at Kale has been intersected by drilling. The epithermal mineralization is hosted by a volcanic-volcaniclastic sequence consisting mainly of a basaltic andesite lava flow and lithic/crystal tuff cropping out as irregular bodies at Kirazlı main and Çatalkaya. These units are locally silicified and brecciated. An undifferentiated intrusive rock hosts the porphyry mineralization and is highly deformed by conjugate fault systems.

The whole-rock geochemistry together with geochronology revealed that the enrichment in LILE and depletion in HFSE are the common features of three distinct high-K calc-alkaline magmatic suits, which are intermediate intrusions (41.7 – 40.3 Ma), plagioclase-phyric andesite (37.6 – 38.7 Ma), and basaltic andesite and pyroclastic rocks (33.0 – 31.4). Based on the REE, multi-element, and tectonic discrimination diagrams, we conclude that the generation and emplacement of the volcanic and plutonic rocks at the Kirazlı district derived from a metasomatized mantle affected by AFC processes and/or crustal contamination in a volcanic arc environment.

The host lithological units in the Kirazlı district have been affected by pervasive hydrothermal alteration. A mineral-based alteration map shows that Kirazlı Main has a proximal to distal zoned alteration pattern, including silicification, alunite-, dickite- and more regional kaolinite-rich alteration assemblages, and subsidiary montmorillonite., Pyrophyllite- and sericite-rich alteration zones are more prominent towards the Çatalkaya and Kale zones, at topographically lower elevations. They document a transition from epithermal to porphyry environments. The whole-rock K/Ar age of quartz-alunite alteration in Kirazlı Main zone is 30.7 ± 1.5 Ma (Yigit 2012).

The Cu-Mo mineralization occurs as dissemination and porphyry-type veins in potassic alteration overprinted by sericite-chlorite and younger argillic alterations in the Kale zone. Reopening of the porphyry veins promotes the precipitation of the base metal-rich phase. Late molybdenite event cross-cut earlier phases and occurs as dissemination and quartz-pyrite-molybdenite veins. The late Au-Ag mineralization is observed as disseminations, small veins, and veinlets within argillaceous and silicified (mainly vuggy and massive) host rocks and hydrothermal breccia in the HS environment.

REFERENCES

Cormier, A., Jutras, M., Welhener, H., Minard, T., Chiaramello, P., & Cremeens, J. 2017a. NI 43-101 Technical Report Feasibility Study Technical Report on the Kirazlı Project, Çanakkale Province, Turkey. Prepared for Alamos Gold INC.

Yigit, O., 2012. A prospective sector in the Tethyan Metallogenic Belt: Geology and geochronology of mineral deposits in the Biga Peninsula, NW Turkey. Ore Geol Rev. 46, 118-148. doi: 10.1016/j.oregeorev.2011.09.015

2.2
A high-precision petrochronology look Into the Yerington batholith, Nevada, USA: Perspectives on the lifetime of magmatic-hydrothermal systems

Maria Paula Castellanos Melendez[1], John Dilles[2], Cyril Chelle-Michou[1]

[1] Department of Earth Sciences, ETH Zürich, 8092 Zürich, Switzerland (maria.castellanos@erdw.ethz.ch)
[2] College of Earth, Ocean and Atmospheric Sciences, Oregon State University, Corvallis, Oregon 97331, USA

Calc-alkaline arc magmatism above convergent plate boundaries not only characterize the bulk of the continental crust, but are also related to porphyry copper deposits, the main copper source for our society. However, the formation of such deposits is not common and the processes that lead to it and that control their sizes are not entirely known. The Yerington batholith, Nevada, USA, hosts several porphyry copper deposits associated to calc-alkaline Jurassic magmatism. In contrast to most other porphyry copper deposits, its unique exposure caused by Cenozoic tilting of an upper-crustal section from the plutonic bodies to the volcanic equivalents, provides an ideal setting to study the magmatic roots of these deposits. High-precision zircon and titanite petrochronology (ID-TIMS U-Pb geochronology and LA-ICPMS trace element geochemistry) sheds light on the magmatic evolution of the composite batholith and the extraction of porphyritic dikes that resulted in copper mineralization. Our results show a continuous geochemical and geochronological evolution that extends over 2 Ma, doubling the previously defined lifetime of the magmatic-hydrothermal system (Dilles and Wright, 1988). The overlap between the youngest zircon dates In the McLeod Hill quartz-monzodiorite and the oldest zircon dates In the Bear quartz-monzonite, opens the possibility for coeval crystallization along a transitional Interface between the two units. Similarly, the significant overlap between the zircon dates In the Bear quartz-monzonite and the Luhr Hill granite, could Indicate contemporaneity. Geochemically, the youngest zircons in the porphyritic dikes are characterized by the most evolved signatures, supporting the Idea that they were extracted from the most evolved pockets of melt towards the end of the magmatic evolution. Such continuity In the Yerington batholith zircon record could Imply a different thermal evolution for the Jurassic magmatism, questioning the previously Interpreted significant hiatuses between each plutonic body (Schöpa et al., 2017). High-precision titanite petrochronology supports these observations, showing continuously and overlapping younger dates from the oldest plutons towards the younger porphyry stocks. Initial zircon analyses confirm the presence of coeval volcanism and plutonism during the first stages of the evolution of the Yerington batholith. However, the consequence of related volcanic activity on porphyry copper deposit formation Is yet to be established. With highly precise geochronology and In-situ geochemistry of accessory phases we aim to help unraveling the lifetime of a magmatic-hydrothermal system, the different time factors that could play a role in the formation of porphyry copper deposits and the impact that volcanic activity could have on their development, size and metal endowment.

REFERENCES

John H. Dilles, James E. Wright; The chronology of early Mesozoic arc magmatism in the Yerington district of western Nevada and its regional implications. GSA Bulletin 1988;; 100 (5): 644–652. doi: https://doi.org/10.1130/0016-7606(1988)100<0644:TCOEMA>2.3.CO;2.

Anne Schöpa, Catherine Annen, John H. Dilles, R. Stephen J. Sparks, Jon D. Blundy; Magma Emplacement Rates and Porphyry Copper Deposits: Thermal Modeling of the Yerington Batholith, Nevada. Economic Geology 2017;; 112 (7): 1653–1672. doi: https://doi.org/10.5382/econgeo.2017.4525.

2.3
Contrasting hot and cold rhyolitic caldera volcanism predating the Columbia River Flood Basalts, northwest USA

Dylan Colón[1], Urs Schaltegger[1], Angela Seligman[2], Ilya Bindeman[3]

[1] *University of Geneva, 1204 Genève, Switzerland*
[2] *North Dakota Department of Environmental Quality, 58501 Bismark, USA*
[3] *University of Oregon, 97402 Eugene, USA*

Rhyolitic magmatism encompasses a diverse range of both eruptive styles and magmatic compositional trends, the origins of which can be difficult to parse considering the possible different inputs of different mantle and crustal sources. We present the case of the ~40 Ma Wildcat Mountain Caldera and the ~30 Ma Crooked River Caldera, two adjacent but compositionally distinct silicic eruptive systems in an intraplate environment between 60 km and 80 km east of the Cascades subduction arc in the northwest USA. They erupted during the relatively quiescent period between the accretion of the Siletzia oceanic terrane at ~50 Ma and the eruption of the Columbia River Basalts at 17-16 Ma. The Wildcat Mountain system is calc-alkaline and appears to be typical of large volume tuffs in arcs worldwide, with abundant phenocrysts and a “normal” mantle-like isotopic composition. By contrast, the much larger Crooked River volcanic center is tholeiitic, generally crystal-poor, and is also host to rare low-$\delta^{18}O$ rhyolites (Seligman et al., 2014). This unusual feature is also present in the Yellowstone hotspot track to the east and is indicative of magma formation by the melting of shallow, hydrothermally altered rocks.

To investigate the sources of these different magmatic lineages, we obtained new high-precision zircon U-Pb ages and trace element compositions obtained by CA-ID-TIMS and laser ablation ICP-MS respectively for samples from both localities. So far, we find evidence of time-progressive fractional crystallization at Wildcat Mountain, but no clear correlation between ages and zircon compositions at Crooked River. Most strikingly, Ti-in-zircon temperatures indicate near-solidus crystallization temperatures for the Wildcat Mountain Tuff but temperatures of 950-1100°C for various Crooked River units. Crooked River zircon also are very depleted in trace elements relative to those from Wildcat Mountain and have significantly smaller Eu anomalies.

As these magmatic systems occupy nearly identical accreted crustal terrains, we suggest that the differences in the behavior of these systems can be traced to the mantle. Thermal models suggest that a much greater basalt flux into the crust allowed the magmas of the Crooked River system to melt shallow crust prior to eruption, imparting them with diverse δ18O values, analogous to the production of low-$\delta^{18}O$ rhyolites at Yellowstone in the Pleistocene. By contrast, less mantle melting below the Wildcat Mountain center produced a more “classical” cool crystal-rich magma that did not assimilate significant quantities of country rock. We agree with previous suggestions that the high mantle melting rates necessary to produce the Crooked River magmas could be the result of the interaction between delaminating lithosphere and a mantle plume, whereas the Wildcat Mountain magmas may have been formed by delamination without additional heat from a plume.

REFERENCES

Seligman, A.N., Bindeman, I.N., McClaughry, J., Stern, R.A. & Fisher, C., 2014: The earliest low and high δ18O caldera-forming eruptions of the Yellowstone plume: Implications for the 30–40 Ma Oregon calderas and speculations on plume-triggered delaminations. Frontiers in Earth Science, 2, 34.

2.4
Seafloor Weathering on Oceanworlds

Kaustubh Hakim[1], Meng Tian[1], Dan J. Bower[1], Kevin Heng[1]

[1] *University of Bern, Center for Space and Habitability, Gesellschaftsstrasse 6, CH-3012 Bern (kaustubh.hakim@unibe.ch)*

Silicate weathering draws down CO_2 from the atmosphere for eventual burial and long-term storage in the planetary interior. This process is thought to provide an essential negative feedback to the carbonate-silicate cycle to maintain temperate climates on Earth. By implementing chemical thermodynamics and kinetics, we model seafloor silicate weathering and carbonate precipitation on planets covered with oceans (oceanworlds). We test different seafloor lithologies to understand the role of carbonate-forming divalent cations in controlling the efficiency of carbonate-silicate cycle on temperate exoplanets. We find that carbonate precipitation efficiency determines the removal of CO_2 from the ocean-atmosphere system. Depending on the outgassing rate of CO_2 and silicate lithology, the intensity of carbonate removal changes. We also quantify the critical depth of oceans beyond which the carbonate-silicate cycle breaks down.

2.5
A data-driven approach to quantify the thermal-chemical architecture of arc volcanoes

Oliver Higgins[1], Tom Sheldrake[1], Luca Caricchi[1]

[1] *Department of Earth Sciences, University of Geneva, Rue de Maraîchaire 13, CH-1205 Genève, oliver.higgins@unige.ch*

Trans-crustal magmatic systems are thermal-chemical reactors controlled by the pressure (P), temperature (T), melt composition (SiO_2), and water content (H_2O) of the melts within. Assessing these parameters is notoriously difficult yet vital for our understanding of volcanic processes and the risks they pose. Here we employ a data-driven approach to quantify the thermal and chemical (P-T-SiO_2-H_2O) structure of the crust beneath an arc volcano. We apply machine learning thermometers, barometers, chemometers and hygrometers to amphibole and clinopyroxene crystals erupted from the Mount Liamuiga stratovolcano on Saint Kitts (Lesser Antilles). We show that both water-undersaturated and water-saturated magmas interact with a vertically extensive mush over millennial timescales, which chemically and thermally buffers melt composition and temperature, in agreement with the concept of reactive transport. Discrete magma ascent (P- SiO_2-H_2O) paths are responsible for melt-chemical bimodality, also reflected by contrasting eruptive dynamics. Together these observations quantify critical processes in arc-volcanic magma systems that may also govern transitional eruptive behaviour.

2.6
In-situ inclusion-bearing ilmenite $^{230}Th/^{238}U$ geochronology of quaternary volcanic deposits by laser ablation inductively coupled plasma-mass spectrometry (LA-ICP-MS)

Franziska Keller[1], Marcel Guillong[1], Răzvan-Gabriel Popa[1], Olivier Bachmann[1]

[1] *Institute for Geochemistry and Petrology, ETH Zürich, Sonneggstrasse 5, CH-8092 Zürich (franziska.keller@erdw.ethz.ch)*

Better determining the frequency of volcanic eruptions in the Quaternary is fundamental for hazards assessment. Volcanic deposits from this time period are often exceptionally well preserved and hence can provide valuable information about the dynamics of active volcanic systems. The available age constraints on quaternary deposits are usually based on $\delta^{18}O$ isotopic stratigraphy or on applying absolute dating techniques such as ^{14}C dating of charcoal fragments in the deposits, ^{230}Th - ^{238}U disequilibrium dating on zircon crystals, or $^{40}Ar/^{39}Ar$ dating of K-bearing phases. However, many volcanic units, particularly in highly active subduction zones, are too old for ^{14}C and/or lack zircons and K-bearing phases, impeding precise age determinations. ^{230}Th - ^{238}U disequilibrium dating of ilmenites (containing inclusions of apatite and melt) by laser ablation inductively coupled plasma-mass spectrometry (LA-ICP-MS) offers a promising new approach for such systems, due to the ubiquity of inclusion-rich ilmenites in volcanic units, and the time-efficiency of the technique. This contribution presents details and challenges on the method and reports ages obtained on samples from the Aso-4 caldera-forming eruption (Kyushu, Japan; $^{40}Ar/^{39}Ar$ age = 86.4 ± 1.1 ka from Albert et al., 2019). Two independent measurement series yield ages of 89 ± 10 ka (2σ) and 81 ± 15 ka (2σ), respectively, coinciding well with the $^{40}Ar/^{39}Ar$ ages reported in the literature. Pooling of the measurement series improves the statistical error, reporting an age of 83.6 ± 8 ka (2σ). These initial data demonstrate the applicability and reproducibility of this new approach to date young volcanic deposits, on which other techniques cannot be performed.

REFERENCES

Albert, P. G., Smith, V. C., Suzuki, T., McLean, D., Tomlinson, E. L., Miyabuchi, Y., ... & Nakagawa, T. 2019: Geochemical characterisation of the Late Quaternary widespread Japanese tephrostratigraphic markers and correlations to the Lake Suigetsu sedimentary archive (SG06 core), Quaternary Geochronology, 52, 103-131.ha

2.7
Rapid construction of continental arc crust during a high magma flux event: the Bear Valley Intrusive Suite, Sierra Nevada, CA, USA

Benjamin Klein[1,2], Oliver Jagoutz[2], Hervé Rezeau[2]

[1] Institute of Earth Sciences, University of Lausanne, CH-1015 Lausanne (benjaminzachary.klein@unil.ch)
[2] Department of Earth, Atmosphere and Environmental Sciences, Massachusetts Institute of Technology, Cambridge MA, 02139

The Bear Valley Intrusive Suite (BVIS), located in the southernmost Sierra Nevada Batholith (California, USA) exposes a structurally continuous transcrustal magma system spanning emplacement pressures from 3-10 kbars and consisting of lower-crustal gabbros and volumetrically extensive middle- and upper-crustal tonalites. Using high-precision chemical abrasion–isotope dilution–thermal ionization mass spectrometry U-Pb geochronology, we have shown that the bulk of this ca. 100 Ma magmatic system crystallized within 1.39 ± 0.06 million years and that its construction required extremely high magmatic fluxes (~250 km^3/km/m.y.).

Due to this rapid construction, the BVIS represents an unparalleled snapshot of magmatic processes within continental arc crust. In this talk we present field observations combined with whole rock geochemistry to document a fundamental dichotomy within the BVIS. The lower crust of the BVIS is dominantly composed of mafic cumulates that range from hornblende norite to hornblendite, and that preserve originally shallow to horizontal magmatic fabrics. Petrographic observations and mineral compositions suggest that multiple distinct crystallization sequences are recorded by the different varieties of cumulates, and that these crystallization sequences were produced by coexisting parental melts with distinct compositions and H_2O contents. In contrast, the middle and upper crust of the BVIS is dominantly composed of comparatively homogeneous voluminous tonalites with steep fabrics.

These observations collectively provide strong constraints on the magmatic construction of the BVIS. We use the observed dichotomous geochemical stratigraphy, combined with amphibole-plagioclase thermometry to show that melts cooled from temperatures >1050 °C to <900 °C during lower crustal fractionation, and that the shallower felsic tonalites were emplaced dominantly at temperatures <850°C. Additionally, we argue that during this lower crustal fractionation and cooling, relatively dry and wet parental mafic magmas mixed in the lower crust to form magmas with low to intermediate H_2O-contents that are the dominant parental melts to the BVIS tonalites. This model explains a number of the observations within the BVIS such as the distinct mafic cumulate populations including distinctive orthopyroxene-dominated norites, the homogeneous middle and shallow crustal tonalites that are apparently the complement to the heterogenous lower crust, and the difference between the differentiation trends recorded in the BVIS and those documented by experimental studies conducted on hydrous magmas at lower crustal pressures.

2.8
Two types of metagabbros to study the meaning of garnet-dominant corona textures in metagabbro

Jiahui Liu[1,2], Pierre Lanari[2], Zhen Li[1], Chunming Wu[1]

[1] *College of Earth and Planetary Sciences, University of Chinese Academy of Sciences, 100049 Beijing, China (liujiahui16@mails.ucas.ac.cn)*
[2] *Institute of Geological Sciences, University of Bern, Bern, Switzerland*

Corona textures commonly develop as non-equilibrium textures and are usually thought to be associated either with iso-thermal decompression (ITD) or iso-baric cooling (IBC). Corona related to ITD are represented by plagioclase/cordierite + Fe-Mg minerals, possbily indicating unroofing or exhumation process after collision or subduction; whereas corona related to IBC are marked by garnet ± Fe-Mg minerals ± quartz, possibly suggesting extension settings accompanied by magmatic accretion. Recently, however, some studies have suggested that garnet-dominant corona textures could also be developed in partial-transformed metagabbro, which were interpreted as the transitional prograde stage in gabbro-to-granulite/eclogite transformation rather than IBC.

Two types of metagabbros were found in neighboring outcrops (20 m) in the Fuping area, Trans-North China Orogen. Type A metagabbro was totally transformed into granulite, where garnet porphyroblast is rimmed by a corona of plagioclase+clinopyroxne+orthopyroxne+quartz. Type B metagabbro was partially transformed into granulite, showing magmatic relics of clinopyroxene + plagioclase, as well as newly grown metamorphic minerals of amphibole+plagioclase+quartz, the corona of garnet+plagioclase was grown between the pyroxene/amphibole and plagioclase. Geothermobarometry and Phase equilibria modeling show that the Type A metagabbro underwent a clockwise *P–T* path from 0.77 GPa/730 °C (prograde stage), to 1.02 GPa/760 °C (peak stage), and finally to 0.63 GPa/825 °C (retrograde stage). Major and trace element compositions suggest that these two types of metagabbros could share the same origin with a signature of IAB (island arc basalt)-like. Zircon SIMS U-Pb dating yield an age of 1840 ± 15 Ma for Type A metagabbro, and 1837 ± 16 Ma for Type B metagabbro.

These two types of metagabbros display different corona textures of plagioclase-dominant and garnet-dominant, respectively. However, they underwent metamorphism together and therefore could record similar *P–T–t* paths. We propose that type B metagabbro was metamorphosed under insufficient fluid conditions so that metamorphic mineral assemblages are hard to reach an equilibrium state. These results show that garnet-dominant corona textures can be developed in partial-transformed metagabbro due to non-equilibria prograde transformations, rather than during IBC. More work will be further focused on the role of fluid, to understand the effects of fluid activity and reaction dynamics during metamorphism.

This work was supported by the National Natural Science Foundation of China (41890832), Chinese Academy of Sciences (QYZDJ-SSW-DQC036), and the State Scholarship Fund of China Scholarship Council.

2.9
Trace element and S-isotope geochemistry of sphalerite in the distal Zn-Pb(-Ag) skarn deposit of Santander, Central Peru

Giovanni Pedemonte[1], Kalin Kouzmanov[1], Jean-Paul Bergoeing[1], Elitsa Stefanova[2], Jorge Spangenberg[3], Tim Kingsley[4], Yan Bourassa[4]

[1] Department of Earth Sciences, University of Geneva, 1205 Geneva, Switzerland
[2] Geological Institute, Bulgarian Academy of Sciences, 1113 Sofia, Bulgaria
[3] Institute of Earth Sciences, University of Lausanne, 1015 Lausanne, Switzerland
[4] Trevalli Mining Corp., Vancouver, BC, Canada

The Santander deposit, located in the central Andes of Peru, is a polymetallic deposit of distal skarn and carbonate replacement type, which is hosted by Upper Cretaceous carbonate rocks, sharing similar characteristics with other deposits hosted in the same metallogenic belt, such as the Huanzalá, Pachapaqui, Raura, Chungar, and Antamina, among others. Mineralisation at Santander occurs under strong structural control, dominated by regional faults and folds (Cobbing, 1973; Jacay, 2011).

In the present study, several analytical methods (electron microprobe, laser-ablation ICP-MS and sulphur isotope geochemistry) have been employed to characterise the chemistry of sphalerite from four mineralised centres in the Santander deposit, including the Magistrales mine, the former Santander Pipe mine, and the Blato and Puajanca prospects, allowing to identify two generations clearly distinguishable by their petrographic and geochemical characteristics. Early sphalerite generation is Fe-rich (29.02-8.58 mol% FeS) and is associated with a low-sulphidation mineralisation, while late sphalerite is Fe-poor (10.85-1.60 mol% FeS) and associated with an intermediate-sulphidation assemblage (Bergoeing, 2020). The use and combination of high-resolution analytical techniques to complement the petrographic study (such as optical and SEM cathodoluminescence, BSE imaging and QEMSCAN quantitative mineralogy) allow a detailed analysis of the paragenetic sequence by revealing cross-cutting relationships and internal zoning of the sphalerite. LA-ICP-MS analysis shows that the core of the sphalerite has a higher content of Cu, while the rims, usually formed by the second sphalerite generation, has a contrasting composition, with enrichment in Sn, Ga, and Ag without notably modifying the Fe content, but with a much higher value for Mn compared to the core.

An exhaustive Principal Component Analysis was carried out to understand the behaviour of the main clusters of elements (PC1=[Cu, Ag, In], PC2=[Zn, Cd, Fe], PC3=[Ga, Sn, As, Mn] and PC4=[Ge, Se, Co]), with a marked positive correlation between the elements of PC4 and PC1 - PC3, and an inverse correlation between these and the elements of PC2. A review of the main mineral substitution mechanisms and element incorporation factors in the sphalerite is proposed. Due to the absence of micro- and nano-inclusions of sulphosalts, tellurides, and selenides, it is possible that elements such the Ag, Se and Te are incorporated into the sphalerite structure through various substitution mechanisms (e.g., Cook et al., 2009; Ye et al., 2011; Belissont et al., 2014). The incorporation of Sn and In in the sphalerite structure follows the substitution mechanism $3Zn^{2+}$ -> In^{3+} + Sn^{3+} + [V]. Sulphur isotope analyses allow a preliminary evaluation of the source of sulphur involved in the mineralisation of the Santander deposit. The general variability of the $\delta^{34}S$(VCDT) values for the sulphides of the Santander deposit covers a range from 1.1 ‰ to 6.0 ‰., strongly indicates a magmatic-hydrothermal source. The geothermometer proposed by Frenzel et al. (2016) relating Fe, Ga, Ge, In and Mn contents in sphalerite indicates similar temperatures of formation for the two generations of sphalerite (335-270°). These data provide new constraints on the temperature and redox dynamics as well as the fluid evolution of the magmatic-hydrothermal system at the origin of the Santander deposit.

This study was logistically and economically supported by the Trevali Mining Corp (Vancouver, Canada), and research grants from Peru (PRONABEC) and Switzerland (SNF grant 200021_165752).

REFERENCES

Belissont, R., Boiron, M. C., Luais, B., & Cathelineau, M. (2014). LA-ICP-MS analyses of minor and trace elements and bulk Ge isotopes in zoned Ge-rich sphalerites from the Noailhac–Saint-Salvy deposit (France): Insights into incorporation mechanisms and ore deposition processes. Geochimica et Cosmochimica Acta, 126, 518-540.

Bergoeing, J.-P. (2020) Distal Zn-Pb(-Ag) skarn mineralization at Santander, Central Peru. MSc Thesis, Université de Lausanne.

Cobbing, E. J. (1973) IMGEMMET BOLETIN NO. A26: Geología de los cuadrángulos de Barranca, Ámbar, Oyón, Huacho, Huaral y Canta 22-h, 22-i, 22-j, 23-h, 23-i, 23-j. In: Ingemmet Reports. https://repositorio.ingemmet.gob.pe/handle/20.500.12544/144

Cook, N. J., Ciobanu, C. L., Pring, A., Skinner, W., Shimizu, M., Danyushevsky, L., Saini-Eidukat, B., & Melcher, F. (2009) Trace and minor elements in sphalerite: A LA-ICP-MS study, Geochimica et Cosmochimica Acta, Volume 73, Issue 16,

Pages 4761-4791

Frenzel, M., Hirsch, T., & Gutzmer, J. (2016). Gallium, germanium, indium, and other trace and minor elements in sphalerite as a function of deposit type - A meta-analysis. Ore Geology Reviews, 76, 52-78.

Jacay, J. (2011) Observaciones sobre la estratigrafía y estilo tectónico de la mina Santander. Trevali Mining Corp. Internal Report

Ye, L., Cook, N. J., Ciobanu, C. L., Yuping, L., Qian, Z., Tiegeng, L., Wei, G., Yulong, Y. & Danyushevskiy, L. (2011). Trace and minor elements in sphalerite from base metal deposits in South China: A LA-ICP-MS study. Ore Geology Reviews, 39(4), 188-217.

2.10
Petrology, mineralogy, and dating of granites in Northern Pikes Peak batholith, Colorado (USA)

Lucas Simian1 ; Julien Allaz ; Ludmila Maria Fonseca Teixeira ; Olivier Bachmann ; Cyril Chelle-Michou

Institute of Geochemistry and Petrology, ETH Zürich, Clausiusstrasse 25, CH-8091 Zürich (lsimian@student.ethz.ch)

The Pikes Peak batholith, in Colorado (USA), is a classical anorogenic (A-type) granite intruding around 1.08 Ga (Smith, 1999). Its northern part is well-known for its high concentration of REE-rich pegmatites (Simmons & Heinrich, 1980). The elliptical shape of the pegmatites is unusual compared to the more classical dike-shaped pegmatites. Many think they have a magmatic origin and are the last stage of the fractional crystallization/differentiation process (i.e.: London, 2020). Thus, the study of the associated granitic rocks plays a central role in the understanding of pegmatite formation. In this study, the textural and compositional heterogeneity across the Buffalo intrusive center is investigated, along with the age of these granites. Results show that mineralogical and compositional variations occur between samples. Rapakivi, myrmekite and amphibole alteration suggest the participation of a compositionally different magma refill and late potassic alteration. The occurrence of fluorite also suggests that fluorine content of the granite is important. Fluorine is a flux element and likely plays an important role in lowering the crystallization temperature of rock. It is hypothesized that fluorine plays a major role in the segregation and crystallization of the pegmatites, which is supposed to occur well below the granitic solidus (Fonseca Teixeira et al., 2021). In order to better assess this possible under-solidus temperature, the temperature range of the granite is investigated by two-feldspar thermometry. This study proposes a new methodology based on elemental mapping (Donovan et al., 2021), resulting from the improvement of the Electron Microprobe technology. It yields more meaningful temperature estimate from magmatic rocks mostly based on interpretation and numerical treatment of elemental maps (temperature range: 600-750°C) (Fig. 2). Its application goes beyond pegmatite thermometry and could be extended to other study fields. Finally, the granite is studied by LA-ICP-MS U/Pb dating to better constrain the age context in which the Pikes Peak pegmatites crystallized. The past geochronology analyses in the area were mostly based on K/Ar dating. This study intends to give a better age estimate, before being further refined by TIMS analyses in future works. The results (1.06 to 1.08 Ga) correspond to the age already published (between 1.06 and 1.09 Ga), though a noticable difference between samples (Fig.1).

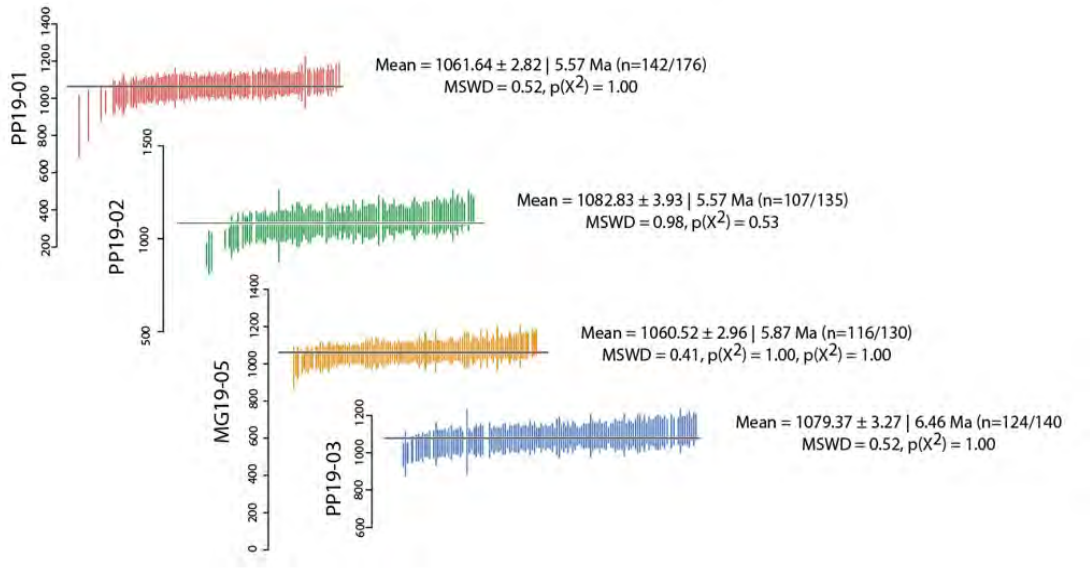

Fig. 1 :Summary of the U-Pb geochronology.

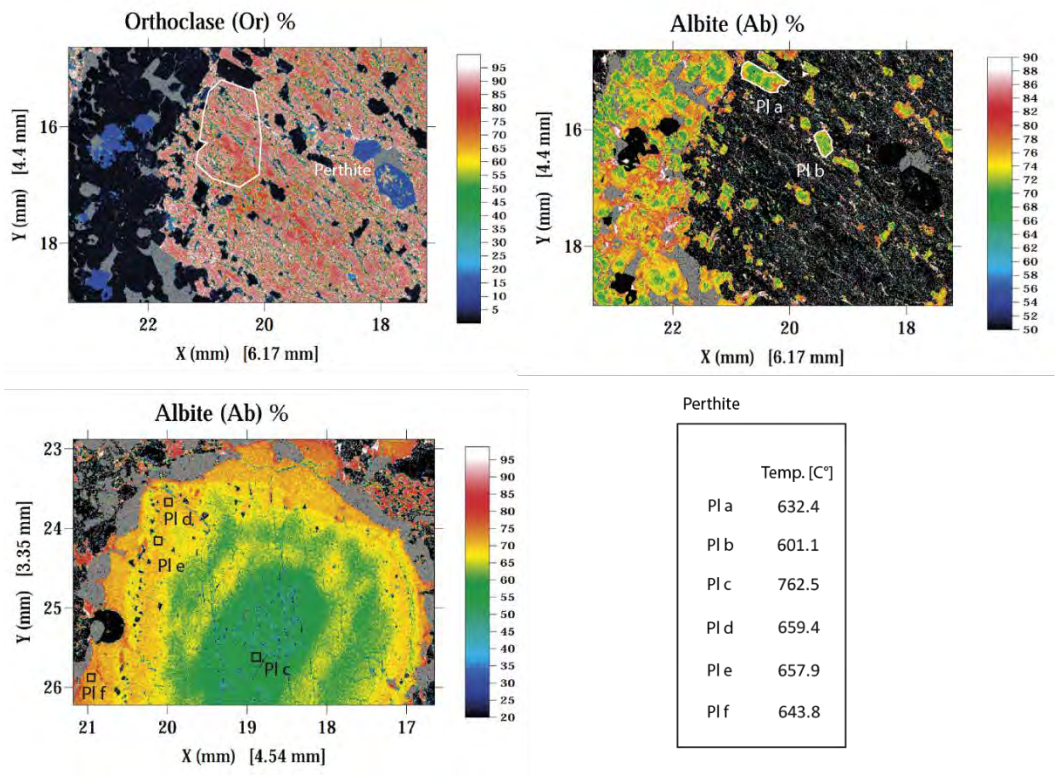

Fig. 2 : Example of the elemental maps used to estimate the crystallization temperature of feldspar in the MG19-05 granite. Thermodynamic parameters of Elkins and Grove(1990).

REFERENCES

Donovan, J. J., Allaz, J. M., Handt, A. Von Der, Seward, G. G. E., & Neill, O. (2021). Quantitative WDS Compositional Mapping Using the Electron Microprobe. American Mineralogist. https://doi.org/10.2138/am-2021-7739

Fonseca Teixeira, L. M., Bachmann, O, Allaz, J. (2021): Magmatic to hydrothermal conditions in the transition from an A-type granite to a pegmatite in the Pikes Peak Batholith, This conference.

London, D. (2020). Pegmatites. Reference Module in Earth Systems and Environmental Sciences, 2008, 1–12. https://doi.org/10.1016/b978-0-12-409548-9.12489-3

Simmons, W. B., & Heinrich, E. W. (1980). Rare-Earth pegmatites of the South Platte District, Colorado. Colorado Geological Survey, Resource Series 11, 138 pp.

Smith, D. R. (1999). A review of the Pikes Peak batholith, Front Range, central Colorado: A “type example” of A-type granitic magmatism. Rocky Mountain Geology, 34(2), 289–312. https://doi.org/10.2113/34.2.289

2.11
LA-ICP-MS U-Pb dating on zircons from the Lepontine Dome (Central European Alps)

Alessia Tagliaferri[1,2], Filippo Luca Schenker[1], Stefan Markus Schmalholz[2], Alexey Ulianov[2]

[1] University of Applied Sciences and Arts of Southern Switzerland (SUPSI), Institute of Earth Sciences, Dipartimento ambiente costruzioni e design, CH-6850 Mendrisio, Switzerland (alessia.tagliaferri@supsi.ch)
[2] University of Lausanne (UNIL), Institute of Earth Sciences (ISTE), Bâtiment Géopolis, Quartier UNIL-Mouline, CH-1015 Lausanne, Switzerland (alessia.tagliaferri@unil.ch)

The Lepontine Dome (Central Alps, Ticino, Switzerland) is a structural dome belonging to the Penninic domain of the European Alps. It is formed by crystalline basement nappes characterized by a strong amphibolite facies imprint. The related Barrovian isograde locally dissect the tectonic nappe contacts. These nappes show an extremely pervasive mineral and stretching lineation (NW-SE directed) suggesting non-coaxial deformation during shearing at peak temperature metamorphic conditions.

In the studied area, the Simano nappe is formed by metagranitoids and by minor paragneisses. The Cima Lunga/Adula nappe above is made of metasediments, mainly quartz-rich gneiss intercalated with amphibolite-gneiss, peridotitic lenses and, locally, calcschist and/or marble. The alternation of lithotypes is mostly parallel to the nappe boundaries and usually constant over their whole, kilometer-scale, length. A progressive change in gneiss texture marks the transition between the Simano and Cima Lunga/Adula nappes: the more stretched texture is evidence for a strain increase from the bottom to the top of the sequence, accompanied by a change in the constituent lithotypes.

Finally, migmatitic leucogneisses have been found at the tectonic contacts between these nappes, indicating syn-tectonic top-to-the foreland deformation accompanied by partial melting. Locally the foliation of these rocks is crosscut by aplitic and pegmatitic dikes. In order to define the temporal duration of melting, U-Pb zircon dating with LA-ICP-MS (Laser Ablation Inductively-Coupled Plasma Mass Spectrometry) has been performed on leucosomes of migmatite, paragneiss, meta-arenite and post-tectonic aplitic and pegmatitic dikes. A 20 μm laser spot permitted to date the thin metamophic rims associated with migmatization.
The results show two main groups of ages centering at ca. 31 and 22 Ma. The latter group presumably dates the intrusion of the post-tectonic dikes. The distribution of ages in samples collected at different structural levels permitted to distinguish the metamorphic events that affected these rock units, and their relationships with the more southern migmatites belonging to the Southern Steep Belt.

2.12
The petrological reocrd of eclogite polymetamorphism in an oceanic subduction channel

Renée Tamblyn[1,2], Martin Hand[2], Laura Morrissey[3], Glen Phillips[4], Robert Anczkiewicz[5], Thomas Zack[6]

[1] *Institut für Geologie, Universtität Bern, Baltzerstrasse 1 + 3, Bern, 3012 (renee.tamblyn@geo.unibe.ch)*
[2] *Department of Earth Sciences, the University of Adelaide, Adelaide, 5005*
[3] *School of Natural and Built Environments, The University of South Australia, 5000, Australia*
[4] *Geological Survey of New South Wales, Maitland, 2320, Australia*
[5] *Institute of Geological Sciences, Polish Academy of Sciences, Kraków, Poland*
[6] *Department of Earth Sciences, The University of Gothenburg, 405 30, Sweden*

Translating burial and exhumation histories from the petrological and geochronological evolution of high-pressure mineral assemblages in subduction channels is key to understanding subduction channel processes. Convective return flow, either serpentinite or sediment hosted, has been suggested as a potential mechanism to retrieve deeply buried rocks and exhume them to the surface (Shreve and Cloos, 1986; Gerya et al., 2002). Numerical modelling predicts that during this convective flow, fragments of oceanic crust can be cycled within a serpentinite-filled subduction channel, experiencing multiple burial cycles (Gerya et al., 2002).

Geochronological and petrological evidence for such cycling during subduction is preserved in a lawsonite-eclogite from serpentinite mélange in the Southern New England Orogen, in eastern Australia. Lu–Hf garnet and lawsonite, U–Pb zircon, U–Pb titanite and Ar–Ar and Rb–Sr phengite geochronology, supported by phase equilibria modelling and garnet zonating patterns, suggests two cycles of burial that accompanied more than 1000 km of subducting slab rollback. Lu–Hf garnet and lawsonite and U–Pb zircon ages constrain the first burial event to ca. 500–490 Ma. This initial subduction of the eclogite formed Lu- and Mn-rich garnet cores, porphyroblastic lawsonite and micro zircons at P–T conditions of at least 2.3 GPa and 550 °C. Partial exhumation to ca. 1.9 GPa and 500 degrees is recorded by approximately 11 vol% garnet dissolution. Reburial of the eclogite resulted in renewed growth of new garnet, and prograde-zoned phengite and recrystallization of titanite at P–T conditions of 2.7 kbar and 590 °C. U–Pb titanite, phengite Rb-Sr and Ar-Ar ages record the recrystallization of these minerals during this second event at ca. 460 Ma. This was then followed by a second exhumation event, where chlorite and glaucophane partially replaced garnet and omphacite respectively, and garnet rims were again reabsorbed, at approximately 2.0 GPa and 500 °C. These conditions fall along a cold approximate geotherm of 7 °C/km, supported by the presence of pristine lawsonite. Partial exhumation and reburial occurred over ca. 30 Ma over an approximate pressure and temperature fluctuation of 1.2 GPa and 140 °C, providing some estimation on the rates of subduction channel material cycling.

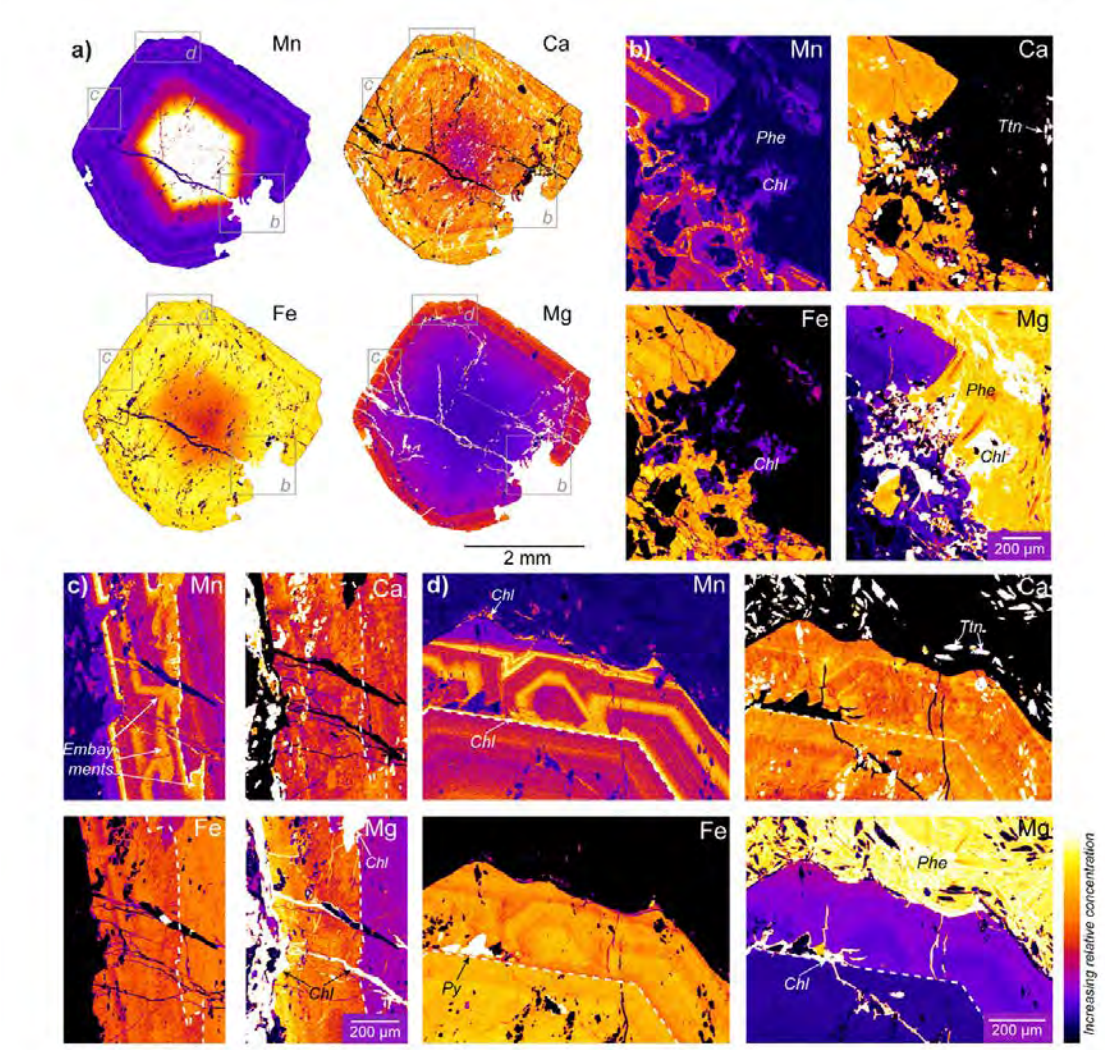

Figure 1. EPMA maps of garnet and surrounding matrix from the eclogite, showing compositional features of two-stage garnet growth. The boundary between garnet from burial 1 and burial 2 is shown as a white dotted line.

REFERENCES

Gerya, T. V, Stöckhert, B., & Perchuk, A. L. (2002). Exhumation of high-pressure metamorphic rocks in a subduction channel: A numerical simulation.

Shreve, R. L., & Cloos, M. (1986). Dynamics of sediment subduction, melange formation, and prism accretion. Journal of Geophysical Research: Solid Earth, 91(B10), 10229–10245.

2.13
Evolution of oxide-silicate geochemistry and systematics during subduction of hydrous ultramafic rocks (Central Alps, Switzerland)

Joana Vieira Duarte[1], Thomas Pettke[1], Francesca Piccoli[1], Jörg Hermann[1]

[1] *Institute of Geological Sciences, University of Bern, Baltzerstrasse 1, CH-3012 Bern (joana.vieira@geo.unibe.ch)*

The stability of magnetite and other oxide minerals in ultramafic rocks plays a major role in controlling redox state and redox budget of the fluids liberated upon progressive dehydration reactions as well as of the residual rocks during subduction. Magnetite recrystallization and production in equilibrium with prograde silicates is observed to occur up to and including the antigorite-out reaction in serpentinized peridotites from Cerro del Almirez (Vieira Duarte et al., 2021). However, the fate of the oxide phases at even higher P-T conditions has remained ill-constrained.

Here we present a comprehensive petrological and geochemical study of oxide – silicate mineral assemblages from selected ultramafic bodies (Val Cama, Alpe Albion, Alpe Arami, Càpoli, and Cima di Gagnone) from the Central Alps, Switzerland. All bodies reached peak metamorphism above the antigorite-out reaction, at different P-T conditions spanning from ca. 650 to 850°C and from 1 to 3 GPa.

Our results show:

(1) A clear trend in spinel group mineral type and composition, with a decrease in magnetite component (Fe^{3+}) and an increase in chromite and spinel components (Cr^{3+} and Al^{3+}) with increasing metamorphic grade (Figure 1, grey arrow), as also suggested by modelling results of Piccoli et al. (2019);

(2) Highly oxidizing conditions at the hematite-magnetite buffer were found in only one chlorite-peridotite sample, where hematite and magnetite occur as inclusions in metamorphic olivine and orthopyroxene produced at the antigorite dehydration reaction.

(3) A correlation between the silicate Mg# (87-96 in olivine) and the oxide modes (ca. 0.5-3.5 vol.%) in the chlorite-peridotites, interpreted to reflect variable extents of oxidation upon initial ocean-floor serpentinization (compare Bretscher et al., 2018). In garnet-peridotites or pyroxenites, such trends are not clear, thus suggesting that other factors such as the magmatic history of the protoliths prior to serpentinisation and/or metasomatism during the subduction cycle including retrograde overprint can be variably prominent.

We conclude that, except for the rare occurene of hematite and magnetite beyond antigorite-dehydration, the prograde evolution of oxides in ultramafic lithologies generaly tends toward an increase of the spinel component, thus lowering the rock buffered $f(O_2)$. Consequently, processes other than highly oxidised slab additions to the sources of arc magmas may also be relevant for producing the relatively oxidized nature of calcalkaline magmatism.

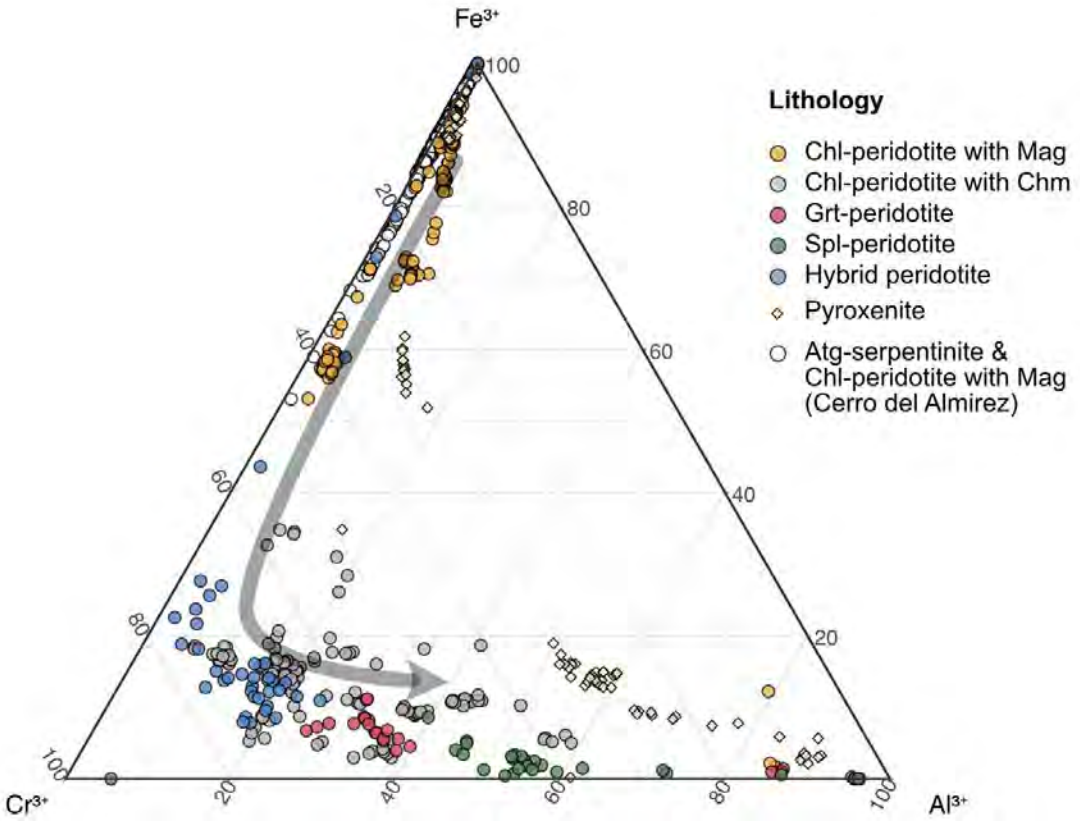

Figure 1. Oxide mineral trends for chlorite-peridotites and garnet-peridotites (circles) and pyroxenite (diamonds). The grey arrow displays the prograde metamorphic evolution of oxide major element composition.

REFERENCES

Bretscher, A., Hermann, J. & Pettke, T. (2018) The influence of oceanic oxidation on serpentinite dehydration during subduction. Earth and Planetary Science Letters 499, 173-184, https://doi.org/10.1016/j.epsl.2018.07.017.

Piccoli, F., Hermann, J., Pettke, T., Connolly, J. A. D., Kempf, E. D. & Vieira Duarte, J. F. 2019: Subducting serpentinites release reduced, not oxidized, aqueous fluids, Scientific Reports, 9, 19573, https://doi.org/10.1038/s41598-019-55944-8.

Vieira Duarte, J. F., Piccoli, F., Pettke, T., & Hermann, J. 2021: Textural and geochemical evidence for magnetite production across antigorite breakdown during subduction, Journal of Petrology, egab053, https://doi.org/10.1093/petrology/egab053.

2.14
Zircon Petrochronology of behemothian porphyry copper systems

Adrianna L. Virmond[1], Jörn-Frederik Wotzlaw[1], Cyril Chelle-Michou[1]

[1] *Department of Earth Sciences, ETH Zürich, Clausiusstrasse 25, 8092 Zürich (adrianna.virmond@erdw.ethz.ch)*

The Chuquicamata District comprises one of the world's biggest copper resources with more than 130 Mt of Cu and a mining history of over a century. The district hosts several deposits (Chuquicamata, Radomiro Tomic, Ministro Hales, Toki Cluster) of varying metal contents, making it ideal to investigate the processes that control the size of porphyry copper deposits. The Chuquicamata Intrusive Complex occurs as a megadike composed of three lithologies. The main and most abundant is the *Este* granodiorite (Ossandón et al, 2001); the *Oeste* porphyry presents finer groundmass and similar composition and mineralogy (Ossandón et al, 2001) and the *Banco* monzogranite is finer grained and more porphyritic than the Este porphyry (Ossandón et al, 2001). Previous geochronology suggests that a protracted magmatic history resulted in at least two superimposed hydrothermal events, contributing to the formation of this outsized deposit (Ballard et al, 2001). The previously reported SHRIMP and LA-ICPMS zircon dates also claim to resolve a 1 Ma gap between emplacement of the Este and the other two porphyries (Oeste and Banco, Ballard et al, 2001), but dates on individual grains overlap for a timespan of almost six million years. New high-precision zircon petrochronology results (U-Pb CA-TIMS geochronology in tandem with LA-ICPMS trace element analysis) confirm a protracted period of zircon crystallization (~1 Ma) within the Este porphyry and resolve an age gap of at least 500 ka between the Este and Banco porphyries. Zircon trace element compositions and Ti-in-zircon temperatures are similar for all porphyries in the Chuquicamata Intrusive Complex, despite the age difference. These observations point to a similar source and a protracted thermal history for the source pluton, which might have been necessary to maintain the hydrothermal activity and ultimately form the ore deposit. High-precision zircon petrochronology provides the necessary accuracy and precision to help unravel what controls the formation of behemothian porphyry deposits.

REFERENCES

Ballard, J. R., Palin, J. M., Williams, I. S., Campbell, I. H., & Faunes A., A. 2001: Two ages of porphyry intrusion resolved for the super-giant Chuquicamata copper deposit of northern Chile by ELA-ICP-MS and SHRIMP. Geology, 29(5), 383–386.

Ossandón C., G., Freraut C., R., Gustafson, L. B., Lindsay, D. D., & Zentilli, M. 2001: Geology of the Chuquicamata Mine: A Progress Report, Economic Geology, 96(2), 249–270.

2.15
Analysis of Sheet-like Inclusion in Cu-bearing Tourmaline from Brazil

Hao A.O. Wang[1], Daniel Grolimund[2], Leander Franz[3], Daniel Mathys[4], Rainer Schultz-Güttler[5], Michael S. Krzemnicki[1]

[1] *Swiss Gemmological Institute SSEF, Basel (hao.wang@ssef.ch)*
[2] *MicroXAS Beamline, Swiss Light Source, Paul Scherrer Institute*
[3] *Dept. of Environmental Sciences, Mineralogy and Petrology, Universität Basel*
[4] *Nano Imaging Lab, Swiss Nanoscience Institute, Universität Basel*
[5] *Institute of Geosciences, University of São Paulo, Brazil*

Cu-bearing tourmaline is one of the most sought-after tourmaline species, due to its rarity and impressive neon-blue color. The first Cu-bearing tourmalines were found in zoned and highly fractionated granitic pegmatites in Paraíba state in northeastern Brazil, therefore they are often called 'Paraíba Tourmaline'. Since then, Cu-bearing tourmaline has been discovered also in Mozambique and Nigeria.

For this study, we focused on a green Cu-bearing tourmaline specimen from Paraíba, which contains a specific type of thin sheet-like inclusions (Figure 1). This rarely-seen type of inclusion has been described so far only in few reports (Fritsch et al. 1990, Brandstätter & Niedermayr 1994, Hartley 2018), suggesting these inclusions to be native Cu and tenorite (CuO) formed by epigenetic exsolution (Koivula et al. 1992).

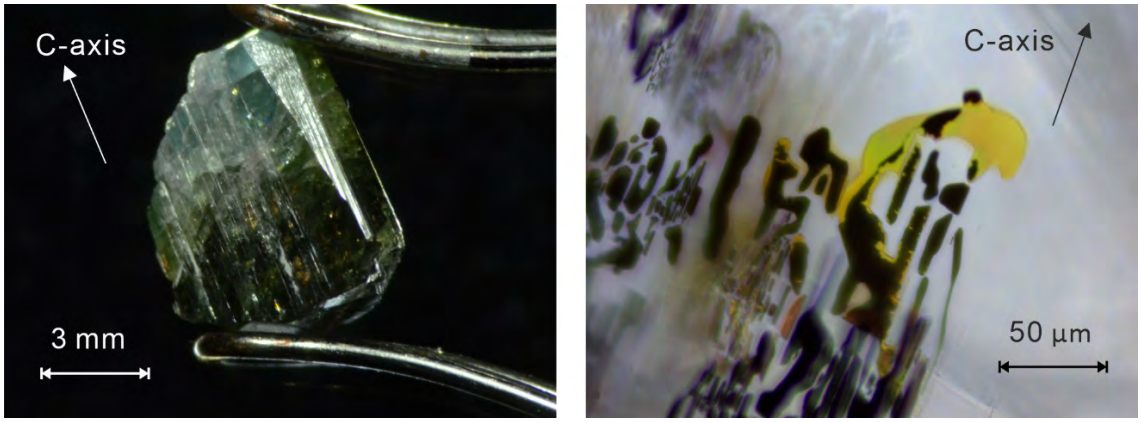

Figure 1. Left: Cu-bearing tourmaline from Brazil containing a specific type of highly reflective inclusion. Crystal width is about 5 mm. Right: Microphoto of the thin sheet-like inclusion in transmission light, revealing that the highly reflective inclusion consists of two clearly separated phases (black and yellow).

In our specimen, these thin sheet-like inclusions are oriented in planes parallel to the C-axis of the host tourmaline and also extend preferentially along its C-axis. By cutting carefully the selected specimen to expose a cross-section of such an inclusion, we were able to further analyze it by using a focused ion beam (FIB) coupled to an SEM system. The sheet-like inclusion is estimated to be about 150 nm in thickness (Figure 2 left). A chemical profile across the inclusion (SEM-EDS) shows an elevated Cu signal, while no local increase of S is observed (Figure 2 right). In contrast to Brandstätter & Niedermayr (1994), we see in our sample no obvious decrease of Cu in the tourmaline host on each side of the thin sheet-like inclusion.

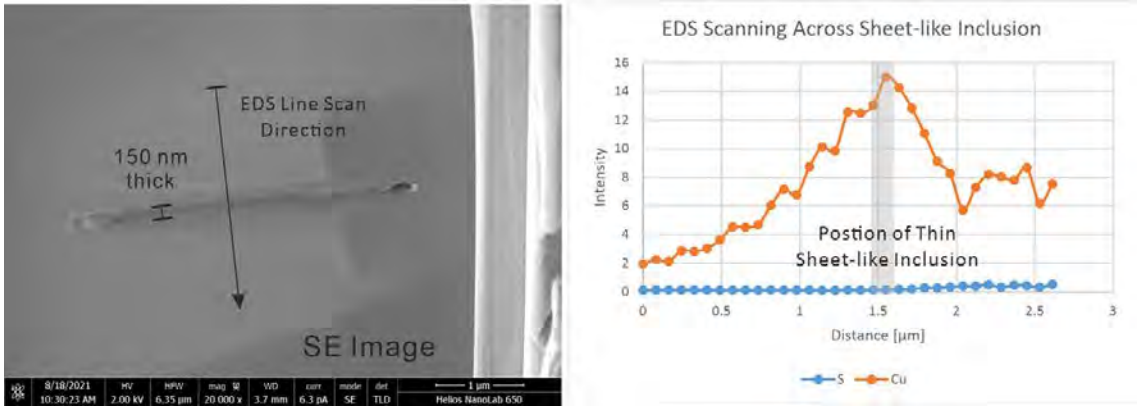

Figure 2. Left: Secondary electron image of the sheet-like inclusion, with a thickness about 150 nm. Right: EDS scan crossing the sheet-like inclusion. The Cu signal is highest at the position of the inclusion, while S remains low.

In the sheet-like inclusion region, micro FTIR detected small changes in the absorption peak positions in the range of around 3000-4000 cm^{-1} (attributed to OH vibrations), when compared to FTIR spectra in the adjacent tourmaline host material. Using Raman spectroscopy, we found a broad band centered at around 2200 cm^{-1} Raman shift with a weak modulation on top of the broad band.

Based on our preliminary data, an unambiguous identification of this Cu-containing thin sheet inclusion is not yet possible. However, our results show no evidence to support the suggested hypothesis that these inclusions form due to epigenetic exsolution from the Cu-bearing tourmaline host.

Consequently, more analytical data is required, specifically to better understand the nature and formation of these inclusions. As an outlook, we plan to analyze this sample further by Synchrotron Radiation X-ray absorption spectroscopy (XAS). Spatially resolved XAS measurements may allow us to detail the Cu oxidation state in these sheet-like inclusions, respectively may provide crucial information on the oxidation conditions during the formation of Cu-bearing tourmaline in these zoned and fractionated pegmatites in Paraíba, Brazil.

REFERENCES

Brandstätter, F., & Niedermayr G. 1994: Copper and Tenorite Inclusions in Cuprian-Elbaite Tourmaline from Paraiba, Brazil, Gems & Gemology, 30, 178–183.

Fritsch, E., Shigley J.E., Rossman G.R., Mercer M.E., Muhlmeister S.M., & Moon M. 1990: Gem-Quality Cuprian-Elbaite Tourmalines From São José Da Batalha, Paraíba, Brazil, Gems & Gemology, 26, 189–205.

Hartley, A., 2018: Native Copper Inclusions in a Cu-bearing Tourmaline, Journal of Gemmology, 36, 203.

Koivula, J.I., Kammerling R.C., & Fritsch E., 1992: Tourmaline with Distinctive Inclusions, Gems & Gemology, 28, 204.

2.16
Source rocks and leaching processes for metals in mafic VMS deposits: Semail ophiolite, Oman

Robin C. Wolf[1], Larryn W. Diamond[1], Thomas M. Belgrano[2], Thomas Pettke[1]

[1] Institute of Geological Sciences, University of Bern, Balzerstrasse 3, CH-3012 Bern (robin.wolf@geo.unibe.ch)
[2] School of Ocean and Earth Science, National Oceanography Centre Southampton, University of Southampton, European Way, Southampton SO14 3ZH UK

Volcanogenic massive sulfide (VMS) deposits are valuable sources of Zn, Cu, Pb, Ag, Au, and other metals. Research since the 1960s has addressed the sources of metals in deposits hosted by mafic rocks in ophiolites, Archean greenstone belts and in-situ oceanic crust. Proposed sources include basalts hydrothermally altered to spilite and epidosite, and influxing magmatic volatiles. Epidosites have been favoured owing to their location along the deep upflow path of fluid convection cells and to their depletion in Cu and Zn (e.g. Jowitt et al., 2012). However, field observations by Gilgen et al. (2016) have demonstrated a mismatch in timing between epidosites and VMS deposits in the Semail ophiolite. Spilitization along the downwelling path has also been proposed to liberate VMS metals, as suggested by the strong Cu depletions in spilitized dykes of the Troodos ophiolite, similar to the depletions in the epidosites, although with less Zn depleted in the spilites (Jowitt et al., 2012). Identification of the source rocks is important for understanding VMS formation and element transfers between the ocean and oceanic crustal rocks, and has significant implications for exploration. However, over 50 years later, the identities of the source rocks and source fluids are still debated.

Our ongoing study aims to determine the source rocks for VMS metals and the mineralogical controls on leaching of VMS metals, by analysing representative stratigraphic transects across the crust of the Semail ophiolite, Oman. We use optical microscopy, Raman spectroscopy, scanning electron microscopy, electron microprobe analysis, X-ray diffraction, and metal-sensitive LA-ICP-MS analysis of whole-rock nano-powder pellets (using the method of Peters and Pettke, 2016) to correlate changes in mineralogy, geochemistry and concentrations of VMS metals across each transect.

Samples along a transect near the Safwa VMS deposit were collected from the base of the Sheeted Dyke Complex (SDC) up to the post-volcanic pelagic sediments that cap the ophiolite (Fig 1). The basal extrusive unit, Geotimes, is comagmatic with the SDC and comprises basalts, basaltic andesites and andesites of MORB-type affinity; it is overlain by post-axial 'Tholeiitic Alley' island-arc tholeiite series lavas, which are in turn overlain by 'Boninitic Alley' boninite series lavas (Belgrano et al., 2019). Fig. 1 shows that Cu concentrations are variable in all units, with a marked increase in the highest values upsection from Geotimes into Tholeiitic Alley lavas. The Zn values are similarly scattered, but with an increase in maximum values with depth at the same unit boundary. In principle, this distribution of metals can be attributed to three factors: a) initial magma (protolith) composition, related to magmatic processes; b) variations in intensity of hydrothermal alteration, where secondary mineral assemblages may control liberation of metals; and c) hydrothermal additions of metals, e.g., as secondary sulfide minerals (observed occasionally in our samples). The Semail ophiolite is famous for its intensity of alteration, which may account for the greater variability in Cu and Zn values compared to less altered, in-situ oceanic crust (Fig 1). We are currently analysing the metal contents of rare pristine volcanic glasses from the ophiolite in order to unravel the roles of the three metal-controlling factors listed above.

REFERENCES

Belgrano, T. M., Diamond, L. W., Vogt, Y., Biedermann, A. R., Gilgen, S. A., and Al-Tobi, K.: A revised map of volcanic units in the Oman ophiolite: insights into the architecture of an oceanic proto-arc volcanic sequence, Solid Earth, 10, 1181–1217.

Gilgen S. A., Diamond L. W. and Mercolli I. (2016) Sub-seafloor epidosite alteration: timing, depth and stratigraphic distribution in the Semail ophiolite, Oman. Lithos, 260, 191–210.

Huang, J., Liu, S.-A., Gao, Y., Xiao, Y., and Chen, S. (2016), Copper and zinc isotope systematics of altered oceanic crust at IODP Site 1256 in the eastern equatorial Pacific, *J. Geophys. Res. Solid Earth*, 121, 7086– 7100.

Jowitt, S. M., Jenkin, G. R. T., Coogan L. A., and Naden, J. (2012) Quantifying the release of base metals from source rocks for volcanogenic massive sulphide deposits: effects of protolith composition and alteration mineralogy. Journal of Geochemical Exploration, 118, 47–59.

Peters D. and Pettke T. (2016) Evaluation of Major to Ultra Trace Element Bulk Rock Chemical Analysis of Nanoparticulate Pressed Powder Pellets by LA-ICP-MS. Geostandards and Geoanalytical Research.

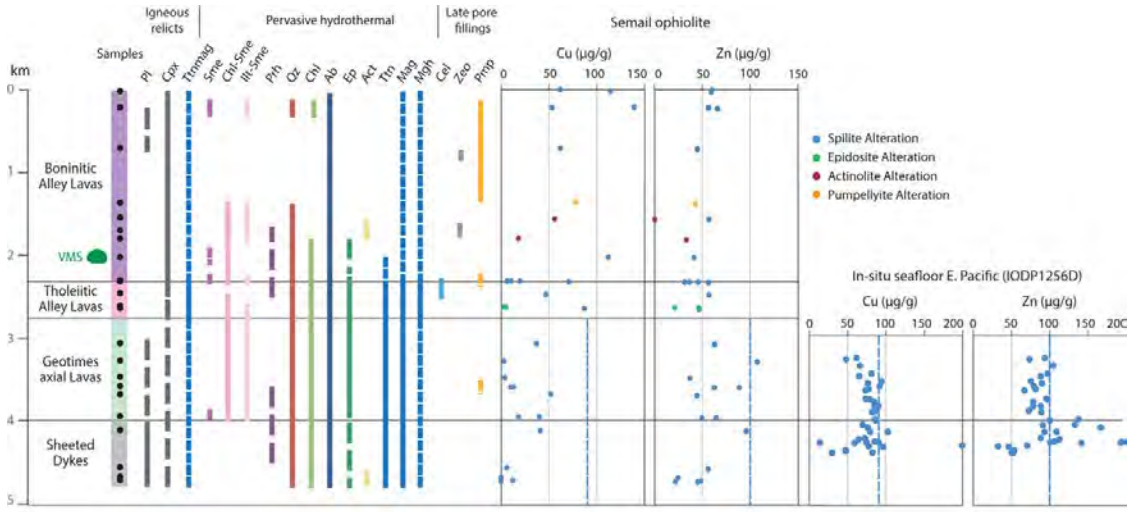

Figure 1. Depth Profile through Safwa Transect, Semail Ophiolite (km scale indicates depth below post-volcanic pelagic sediments). Left panel: volcanostratigraphy and distribution of relict igneous and secondary hydrothermal minerals. Continuous lines = ubiquitous, dashed = locally present. Ttnmag = Titanomagnetite. Opaque minerals from Belgrano et al. (2019). Right panels: Cu and Zn values for Safwa transect (this study) and IODP drill hole 1256D (East Pacific; Huang et al., 2016). Scale is depth (km) below seafloor. Dashed vertical lines = MORB median Cu and Zn contents.

2.17
Garnet petrochronology reveals the lifetime and dynamics of phonolitic magma chambers at Somma-Vesuvius

Jörn-Frederik Wotzlaw[1], Lena Bastian[1], Marcel Guillong[1], Francesca Forni[2], Oscar Laurent[3], Julia Neukampf[4], Roberto Sulpizio[5], Cyril Chelle-Michou[1], Olivier Bachmann[1]

[1] Institute of Geochemistry and Petrology, ETH Zürich, Clausiusstrasse 25, Zürich, Switzerland (joern.wotzlaw@erdw.ethz.ch)
[2] Department of Earth Sciences, Università degli Studi di Milano, Milano, Italy
[3] CNRS, Géosciences Environnement Toulouse, Observatoire Midi-Pyrénées, Toulouse, France
[4] Centre de Recherches Pétrographiques et Géochimiques, Vandœuvre-lès-Nancy, France
[5] Dipartimento di Scienze della Terra e Geoambientali, University of Bari, Bari, Italy

Vesuvius is one of the most iconic active volcanoes on Earth. Historic and archaeological records document numerous hazardous eruptions with thousands of fatalities. Today, more than one-million people live around Vesuvius and are threatened by future volcanic activity. Petrologic and geochemical studies of eruptive products provide important insights into the evolution of the eruption-feeding magma reservoir prior to eruption. Here we quantify the duration of shallow crustal storage and track the evolution of phonolitic magmas prior to major explosive eruptions of Vesuvius employing in-situ uranium-thorium dating of garnet phenocrysts in tandem with detailed geochemical and textural characterization. Garnet uranium-thorium dates provide evidence for progressively shorter pre-eruption storage times throughout the lifetime of the volcano, decreasing from ~5,000 years for the pre-historic Mercato and Avellino eruptions to approximately 1,000 years for the historic AD 79 Pompeii and AD 472 Pollena eruptions. These decreasing residence times mirror the progressively shorter repose intervals between eruptions implying that distinct phonolite magma batches were present throughout most of the volcano's evolution thereby controlling the eruption dynamics by preventing the ascent of mafic magmas from longer-lived and deeper reservoirs. Frequent lower-energy eruptions during the recent history sample this deeper reservoir and suggest that future Plinian eruptions are unlikely without centuries of volcanic quiescence. Crystal residence times from other volcanoes reveal that discrete long-lived deep-seated reservoirs and transient upper-crustal magma chambers are common features of sub-volcanic plumbing systems.

2.18
The discovery of retrograde eclogite in the Dunhuang Orogenic Belt, northwestern China

Qian W.L. Zhang[1,2], Pierre Lanari[2], Zhen M.G. Li, Chun-Ming Wu[1]

[1] *College of Earth and Planetary Sciences, University of Chinese Academy of Sciences, Beijing, China (zhangqian162@mails.ucas.ac.cn)*
[2] *Institute of Geological Sciences, University of Bern, Bern, Switzerland*

As one of the most characteristic products of subduction zones, eclogite offers important clues for unraveling the subduction-exhumation history of an orogen. However, eclogitic assemblages are often easily retrogressed with varying degrees due to late amphibolite to granulite facies metamorphism and/or strong interaction with fluids during exhumation. Retrograde reactions are commonly represented by the replacement of omphacite and garnet by clinopyroxene + plagioclase + amphibole ± quartz forming symplectite and/or corona. The developement of retrogression textures can prevent us from identifying and accurately constraining the conditions of eclogite-facies metamorphism.

The Paleozoic Dunhuang Orogenic Belt (DOB) occupies a particular tectonic location surrounding by the Paleo-Asia Ocean tectonic domain, including the Tianshan, Beishan, and Alxa Tectonic Belts to the north, by the Tethys Ocean tectonic domain including the North Qilian, North Qaidam, and Altyn Orogens to the south, which records widespread Paleozoic subduction-accretionary processes. Since the first discovery of Devonian eclogite (highest X_{Jd} in omphacite is ~0.38) in the Hongliuxia area in southern DOB (Wang et al., 2017), no other eclogite was reported in this area. Instead, metamafic rocks exhibit retrograde textures, especially symplectite consisting of clinopyroxene + plagioclase + amphibole ± quartz. We used quantitative compositional mapping by electron probe micro-analysis for estimating the composition of the former omphacite which could had reached X_{Jd} values of ~0.40. This result is consistent with modeled X_{Jd} values at the pressure-peak *P–T* condition of ~2.12 GPa and 680 °C, typical eclogite-facies metamorphism, constrained by the intersection of Ca and Mg isopleths of garnet.

The discovery of this first retrogressed eclogite sample in the Dunhuang Orogenic Belt further confirms that large scale eclogite-facies conditions associated to subduction were possibly reached in this area. It also shows that we should be cautious when recovering peak *P–T* conditions of strongly retrogressed samples. More detailed studies will focus on fluid-participant retrograde reactions, which could provide important clues for tracing the fluid-rock interaction of high-pressure metamorphic rocks during exhumation.

This work was supported by the National Natural Science Foundation of China (41730215) and the State Scholarship Fund of China Scholarship Council.

REFERENCE

Wang, H. Y. C., Chen, H. X., Zhang, Q. W. L., Shi, M. Y., Yan, Q. R., Hou, Q. L., Zhang, Q., Kusky, T., & Wu, C. M. (2017): Tectonic mélange records the Silurian–Devonian subduction-metamorphic process of the southern Dunhuang terrane, southernmost Central Asian Orogenic Belt. Geology, 45(5), 427-430.

P 2.1
Metamorphic gradient in the Nufenenpass area

Anja Amrein[1], Lukas Baumgartner[1], Martin Robyr[1]

[1] *Institute of Earth Sciences, University of Lausanne, 1015 Lausanne, Switzerland*

Past studies have proposed either a ductily shortened (Klapper and Bucher, 1987) metamorphic gradient, or a jump in metamorphic conditions (Kamber, 1993) in the para-autochtonous sediments of the Gotthard. We set out to test these hypothesis using quartz in garnet inclusion barometry (QUIG, Bonazzi et al., 2019), along with Raman graphite thermometry (GRT, Beyssac et al., 2002), and more traditional phase petrology (PP).

The detailed mapping and structural studies in the Nufenenpass – Cornopass – Griessee – Längstaffel area confirmed in a large part the stratigraphic and structural observations reported in Liszkay-Nagy (1965). The current structure is dominated by variably steep to flat laying fold structures with ENE to WSW strike. In general, the southern limbs of the anticlines are strongly thinned or locally thrusted. We focused the metamorphic studies on the graphite bearing Liassic units of the garnet schists (PP; GRT and QUIG) and Knotenschiefers (PP).

Temperature of ten samples gives homogenous values within its error over the entire investigated area of 511-550°C. QUIG pressure estimates give values of 7.2 kbar in most of the area, but show a significant increase towards the *Corno imbricate zone* (~9.2 kbar). Since no T-variations are observed, maximum temperature is assumed to be achieved after maximum pressure once the units were juxtaposed, which is in agreement with the post-deformational growth of most of the garnet. Sigma garnet clasts and increased pressure conditions measured were obtained for the *Corno imbricate zone*, documenting garnet growth during juxtaposition with the rest of the Nufenen zone. Fluid compositions reveal that they were water rich.

REFERENCES

Beyssac, O., Goffé, B., Chopin, C., & Rouzaud, J. N. (2002). Raman spectra of carbonaceous material in metasediments : A new geothermometer. Journal of Metamorphic Geology, 20(9), 859871. https://doi.org/10.1046/j.1525-1314.2002.00408.x

Bonazzi, M., Tumiati, S., Thomas, J. B., Angel, R. J., & Alvaro, M. (2019). Assessment of the reliability of elastic geobarometry with quartz inclusions. Lithos, 350351, 105201. https://doi.org/10.1016/j.lithos.2019.105201

Kamber, B. S. (1993). Regional metamorphism and uplift along the southern margin of the Gotthard massif : Results from the Nufenenpass area. https://doi.org/10.5169/SEALS-55572

Klaper, E. M., & Bucher-Nurminen, K. (1987). Alpine metamorphism of pelitic schists in the Nufenen Pass area, Lepontine Alps. Journal of Metamorphic Geology, 5(2), 175195. https://doi.org/10.1111/j.1525-1314.1987.tb00378.x

Liszkay-Nagy, M. (1965). Geologie der Sedimentbedeckung des südwestlichen Gotthard-Massivs im Oberwallis. https://doi.org/10.5169/SEALS-163285

P 2.2
Tracking Disturbances in the ^{40}Ar-^{39}Ar Isotopic System in Plagioclase Crystals of the Karoo Flood Basalts

Antoine C., Spikings R., Miletic Doric D., Marsh J.S., Gaynor S.P., Schaltegger U.:

Uni Genève

High precision dating of Large Igneous Provinces (LIP) is useful to understand their link to environmental changes (Courtillot and Renne, 2003), and to provide insights into their geodynamic setting (Encarnación et al., 1996). The Drakensberg continental flood basalts (CFB) of South Africa and Lesotho are part of the Karoo LIP in which the paucity of zircon or baddeleyite renders it difficult to match the sub-permil age precision and accuracy of high-precision U/Pb CA-ID-TIMS age determinations. Previous attempts to date the Karoo lavas using the ^{40}Ar-^{39}Ar method failed to yield sufficient precision and accuracy to resolve the sequential stacking of different basalt units or to give a reasonable emplacement age relative to the intrusive complex. We test the hypothesis that previous, inconsistent ^{40}Ar-^{39}Ar dates of plagioclase were a consequence of degassing of primary, metasomatic and alteration phases (mainly zeolites with subordinate sericite and carbonate) within crystals that were invisible under a binocular microscope in the separates. The lavas are mainly tholeiitic basalts that host two distinct sizes of plagioclase. The larger crystals (250-400 µm) are more altered and fractured than the smaller grains and thus their primary Ar isotopic reservoirs are more likely to have been modified. We present ^{40}Ar-^{39}Ar data from i) leached groundmass, ii) untreated plagioclase that hosts visible alteration phases, iii) untreated plagioclase that is devoid of visible alteration phases (2 grain size aliquots), and iv) leached plagioclase that is devoid of visible alteration phases (2 grain size aliquots). The results of this study may enhance the effectiveness of the ^{40}Ar-^{39}Ar dating technique to accurately constrain the crystallization ages of altered mafic lavas in LIPs. Ar isotope data were collected using a multi-collector Argus VI mass spectrometer by step heating to permit identification of different gas reservoirs in the sample through isochemical dating. The two distinct size fractions yield distinguishable dates that do not overlap, and thus $^{40}Ar/^{39}Ar$ analysis of a bulk plagioclase concentrate would yield an average date. Furthermore, leaching has the effect of enhancing recoil effects on the smaller sized plagioclase (<150 µm), adding another artifact to the already biased dates. Our results suggest that previous ^{40}Ar-^{39}Ar analyses of carefully selected plagioclase separates (Jourdan et al., 2007a; Moulin et al., 2011, 2017) that are not consistent with their high emplacement rate are influenced by post-crystallization open-system modification, and thus do not accurately record the time of crystallization.

P 2.3
Characterisation of gem-quality spessartine-bearing metapelites from the northern Kaoko Belt, Namibia

Sarah Degen[1], Julien Allaz[1], Michael S. Krzemnicki[2,3], Leander Franz[2], Eric Reusser[1]

[1] *Institute of Geochemistry and Petrology, ETH Zürich, Clausiusstrasse 25, CH-8092 Zürich (sadegen@ethz.ch)*
[2] *Institute of Mineralogy and Petrography, University of Basel, Bernoullistrasse 32, CH-4056 Basel*
[3] *Swiss Gemmological Institute SSEF, Aeschengraben 26, CH-4051 Basel*

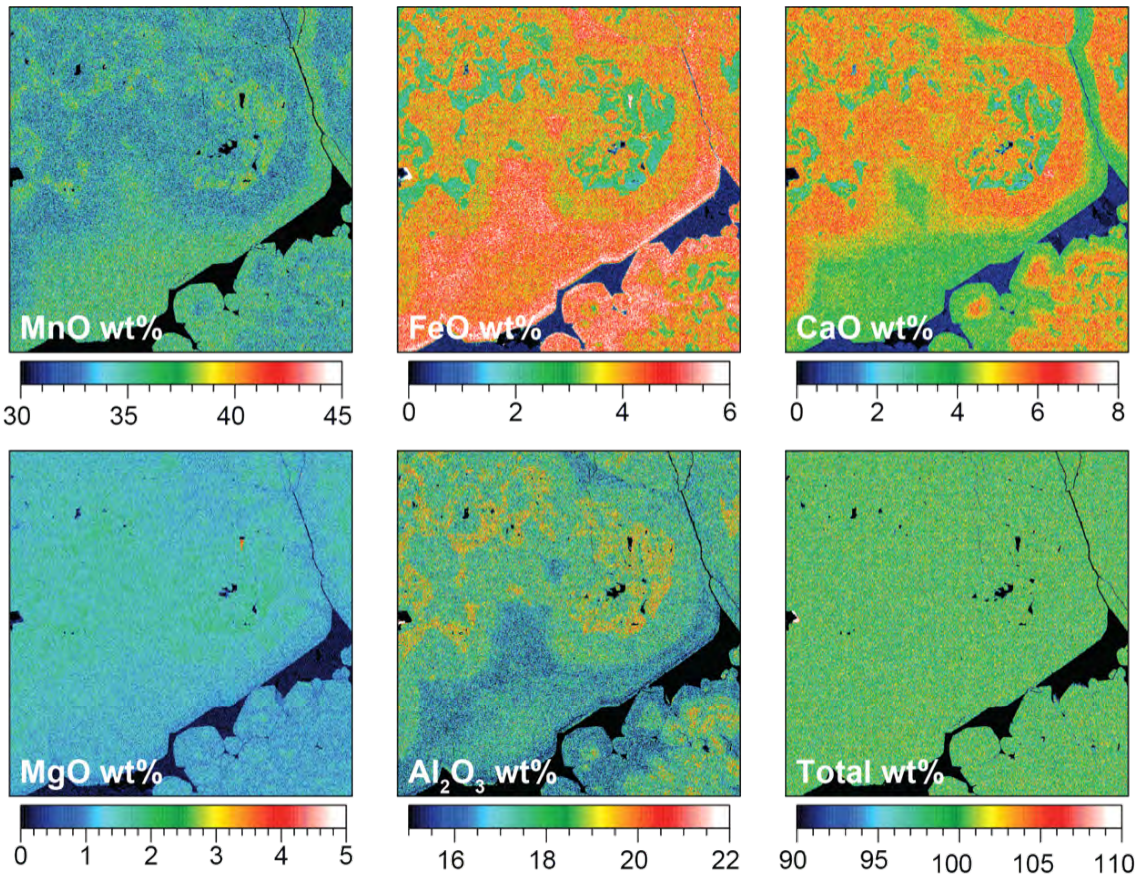

Figure 1. Quantitative element maps in weight-% oxide components for the centre of garnet 1 in sample H1. Field of view is 1.2 x 1.2 mm. Analytical conditions were 15 keV, 50 nA, 40 ms dwell time, 2 µm/px.

Biotite-rich quartzites originating from the conjunction of Kunene River and Marienfluss as well as biotite schists from the Hartmann Mountains (Namibia) host up to cm-sized, mostly euhedral gem-quality spessartine crystals. Garnet compositions from 5 samples were investigated by means of quantitative electron microprobe element maps (Donovan et al., 2021; Fig. 1) and point analyses. The prevailing type of garnet is a spessartine (70-93%), pyrope (4-14%), andradite (0-12%), calderite (0-11%, $Fe_3^{2+}Mn_2^{3+}[SiO_4]_3$) solid solution with the occasional presence of up to 2.6 mole-% blythite ($Mn_3^{2+}Mn_2^{3+}[SiO_4]_3$). The crystals display a predominantly prograde zoning that has to a minor extend been affected by diffusional re-equilibration. Trace element analyes revealed an enrichment in HREE+Y, mostly peaking between the core and the rim. This zonation does not align with the concentration variations that have been observed in case of major elements and it is interpreted to be a consequence of temporally limited availability of REEs, potentially related to the breakdown of a REE-bearing phase after the onset of spessartine growth.

The prevalence of mostly ferric iron in combination with some of the Mn being present in its trivalent state indicates high levels of oxygen fugacity during mineral growth. The protolith of this remarkable mineral assemblage including abundant baryte is interpreted to consist of Mn-rich pelagic sediments that were deposited during the spreading of the Khomas Ocean, as previously described by Bühn et al. (1992). This involved a transport of metals, that were accumulated due to exhalative activity, from deeper levels via upwelling, ultimately leading to a differential precipitation above the redox interface. Application of the Ti-in-biotite thermometer by Wu & Chen (2014) indicates an amphibolite-grade overprint at temperatures between 590 and 655 ± 65 °C and pressures at 0.7-0.8 GPa (pressure conditions according to data by Foster et al., 2009). The metamorphic event responsible for this overprint is associated with the Neoproterozoic to Cambrian Damara Orogeny and is assumed to have taken place between 580 and 550 Ma ago.

The described spessartine garnets can be distinguished from gem-quality spessartines originating from other localities based on their chemical composition on a major element as well as trace element scale. Due to the scarcity of available quantitative information from previously published literature on the mineral chemistry of gem-quality spessartine, especially trace elements, the dataset was limited. The Mg-to-Mn ratio of Namibian spessartine is rather unique and provides a distinction from the majority of other deposits. Furthermore, chondrite normalised REE+Y plots reveal clearly different patterns in comparison to deposits from other countries.

REFERENCES

Bühn, B., Sanistreet, I.G., Okrusch, M. 1992: Late Proterozoic outer shelf manganese and iron deposits at Otjosondu (Namibia) related to the Damaran oceanic opening, Economic Geology, Vol. 87, pp 1393–1411.

Donovan, J. J., Allaz, J. M., von der Handt, A., Seward, G. G. E., Neill O., Goemann, K., Chouinard, J., & Carpenter, P. 2021: Quantitative Compositional Mapping Using the Electron Microprobe, American Mineralogist, in press.

Foster, D.A., Goscombe, B.D & Gray, D.R. 2009: Rapid exhumation of deep crust in an obliquely convergent orogen: The Kaoko Belt of the Damara Orogen, Tectonics, Vol. 28, No 4.

Wu, C.M. & Chen, H.X. 2014: Revised Ti-in-biotite geothermometer for ilmenite- or rutile-bearing crustal metapelites, Science Bullletin (2015), Vol. 60, No. 1, pp 116-121.

P 2.4
Transport and impact of aqueous fluids in subduction settings: insight from coupling two-phase modelling and oxygen isotopes.

Hugo Dominguez[1], Pierre Lanari[1], Nicolas Riel[2]

[1] *Institute of Geological Sciences, University of Bern, 3012 Bern, Switzerland*
[2] *Institute of Geosciences, Johannes Gutenberg University Mainz, J.-J.-Becher-Weg 21, D-55128, Mainz, Germany*

Dehydration reactions occurring during prograde metamorphism generate large amounts of aqueous fluids that ascend through the Earth›s interior. Interactions between these fluids and the surrounding rocks play a major role in element transfer, in particular in subduction zones where fluids participate in the hydration of the mantle wedge, effectively lowering its solidus temperature. Although the processes of aqueous fluids generation are well understood, it remains challenging to track fluid-pathways, leading to a lack of constraints and quantitative data on fluid sources and on the evolution of fluid composition. In particular, the rates at which such events occur, and the mechanisms for fluid transport are still subject to debate.

Oxygen isotopes are sensitive to fluid rock interaction processes and can provide insights on these questions. Recently, an oxygen isotope fractionation model was developed to better quantify the conditions of fluid-rock interaction (Vho et al. 2019). The fractionation model, based on internally consistent thermodynamics data, can be used to determine fluid sources and was applied to simulate mantle wedge hydration.

In this study, we present a preliminary 2D dynamic numerical model simulating two-phase flow channelling due to decompaction weakening in a visco-elastic matrix. The model is coupled with thermodynamics and oxygen isotope simulations to investigate serpentinization mechanism of the mantle wedge. Starting from realistic values of oxygen isotope ratios for the subducting slab and the mantle wedge, chemical interaction and transport of oxygen isotopes is induced by the ascent of an aqueous fluid in the mantle. The goal is to bring new constraints on the timescale and on the geometry of fluid-pathways required to reach isotope ratios observed on serpentinites produced in this type of settings.

This project has received funding from the European Research Council (ERC) under the European Union's Horizon 2020 research and innovation programme (grant agreement No 850530).

REFERENCES

Vho, A., Lanari, P., Rubatto, D. (2019). An internally-consistent database for oxygen isotope fractionation between minerals. Journal of Petrology, 60, 2101–2129.

P 2.5
Mineralizing fluids in the Catalina Huanca carbonate-replacement Zn-Pb-Ag deposit, southern Peru.

Espinel Pachón Iván Mateo[1], de Haller Antoine[1], Kouzmanov Kalin[1] ,Tollan Peter[2], Spangenberg Jorge[3]

[1] Department of Earth Sciences, University of Geneva, Rue des Maraîchers 13, CH-1205 Genève.
[2] Institute of Geochemistry and Petrology, ETH Zürich, 8092 Zürich, Switzerland
[3] Institute of Earth Sciences, University of Lausanne, 1015 Lausanne, Switzerland.

Catalina Huanca is a medium-sized carbonate-replacement (Zn-Pb-Ag) deposit in the Andean Cordillera of southern Peru. The Catalina Huanca mineralization is located at the base of a major Tertiary eastward thrust and consists of veins and replacement bodies. It is controlled by a NE trending horsetail fault structure cutting foreland Tertiary red beds (previously attributed to the Permo-Triassic Mitú Group; Davila et al., 2012) and the overthrusted Pucara Group limestones. Red beds consists of debris-flow horizons grading to sorted sandstones/conglomerates to the west. Clasts consist of sedimentary and igneous rocks, including Pucara limestone. Igneous rocks spatially associated with the mineralization include rhyolitic and trachytic dikes, and ignimbrite beds in the Tertiary red-beds. Rhyolite are apparently pre-ore, but trachytic dikes may be genetically related to the mineralization.

The mineralization consists of veins and carbonate-replacement bodies hosted by the overthrusted Pucara limestones and the red beds unit. The deposit was formed during four mineralization stages grading from low- to high-sulfidation mineral associations: (1) High-temperature skarn minerals ending with mushketovite precipitation; (2) Early polymetallic stage: quartz-pyrite-sericite with trace pyrrhotite, followed by dark Fe-rich sphalerite with chalcopyrite disease; (3) Late polymetallic stage: fluorite, followed by Fe-poor sphalerite-tennantite-tetrahedrite-pyrite-chalcopyrite-quartz and late high-sulfidation veinlets with galena-enargite; (4) Carbonate stage: consists of siderite-rhodochrosite-kaolinite crosscut by late carbonates (calcite-dolomite).

A detailed microthermometric and laser ablation-inductively coupled plasma-mass spectrometry (LA-ICP-MS) study on fluid inclusions in gangue and ore minerals (using near-infrared microscopy) was performed for the early and late polymetallic stages in five different ore bodies: Mariela, Melissa, Silvia, Principal and Amanda 3 Techo. The fluid inclusions studied are two-phase (L+V), with homogenization temperatures between 220° and 350°C and salinities ranging from 2 to 16 wt% NaCl equiv. Boiling evidence can be found in secondary fluid inclusion assemblages hosted in fluorite. Sulfur isotopes, together with the temperature of formation of the analyzed sphalerite allow to calculate the isotopic composition of H_2S in equilibrium with the sphalerite.

The ratios and concentrations of Cl, Br, Na, K, and Ca agree with a magmatic origin of the fluids. Element concentrations of Na, K, B, Li, Cs and Ba plotted versus Cl show two trends corresponding to two successive events (Fig. 1 for Cl, Na, K, Ca). The first trend show nearly constant concentrations and corresponds to fluids from the early higher temperature polymetallic stage present in Mariela, which probably resulted from the boiling of an acidic, metal-rich, magmatic fluid that interacted with carbonate rocks. The second trend shows a progressive decreaze of fluid salinity and temperature during the precipitation of early and late polymetallic stages in Amanda 3 Techo, Melissa and Principal. This second trend suggests dilution by low-salinity fluids, either meteoric water or magmatic vapor condensate. The second option is more probable as it would explain the increased B/Cl ratio compared to the first high-T fluids (Fig.2) , B being preferentially partitioned into the vapor phase (Reyes et al. 1993).

The fluid inclusion compositions and the paragenetic sequence are consistent with pH buffering by carbonate rocks and temperature being the main parameters controlling ore precipitation. Magmatic fluids were apparently the primary source of the Catalina Huanca ore deposit.

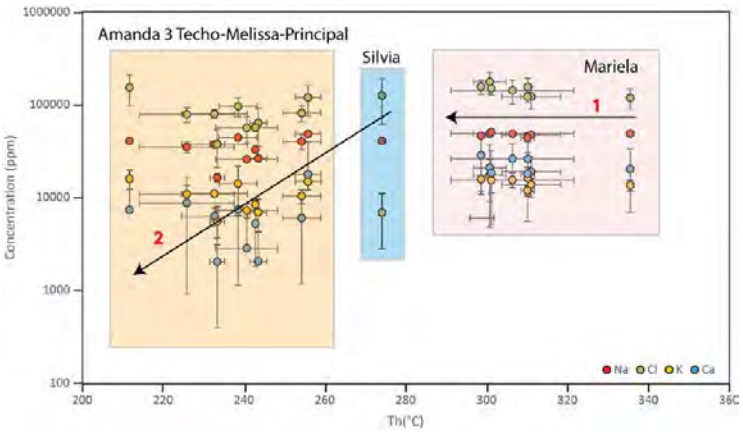

Figure 1. Na, Cl, K, and Ca concentrations vs homogenization temperatures (Th) of primary fluid inclusions in quartz and sphalerite from the early pollymetallic stage and sphalerite from the late pollymetallic stage Errors bars represent 1 σ standard deviation of each fluid inclusion assemblage.

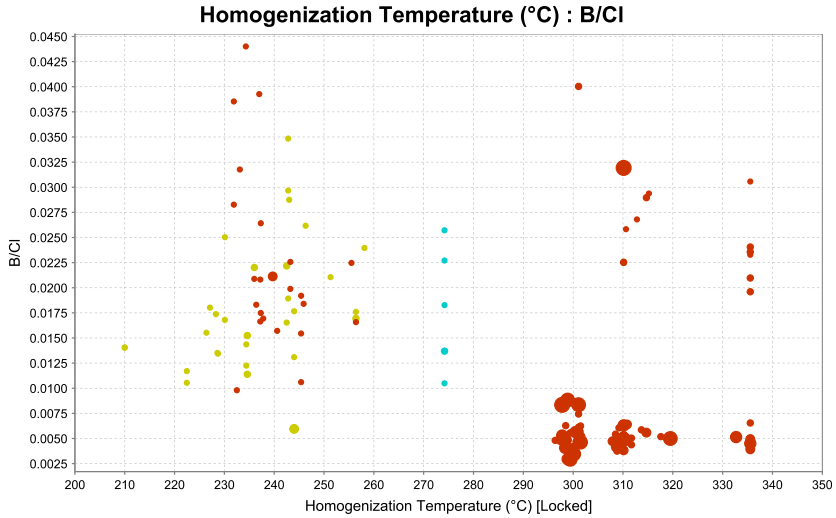

Figure 2. B/Cl ratio vs homogenization temperature (Th) of primary fluid inclusions from early Fe-rich sphalerite (red), late Fe-poor sphalerite (beige), and late quartz (cyan). Symbol size reflects the Cl content. 1= Mariela 2= Amanda 3 Techo, Melissa and Principal.

REFERENCES

Dávila D, Oldham L, Enriquez A, Lopez D (2012) Exploration for Zn-Pb-Ag (Cu-Au) sulfide deposits in Pucara limestone and Mitu conglomerate. Catalina Huanca Mine-Ayacucho-Peru. In: Integrated Exploration and Ore Deposits, SEG-2012, September 23-26Lima, Peru pp 1–2.

Reyes, A.G., Giggenbach, W.F., Saleras, J.R.M., Salonga, N.D., and Vergara, M.C., 1993, Petrology and geochemistry of Alto Peak, a vapor-cored hydrothermal system, Leyte Province, Philippines. Geothermics, v. 22, pp. 479-519

P 2.6
Magmatic to hydrothermal conditions in the transition from an A-type granite to a pegmatite in the Pikes Peak Batholith

Ludmila Maria Fonseca Teixeira[1], Olivier Bachmann[1], Julien Allaz[1]

[1] *Institut für Geochemie und Petrologie, ETH Zürich, Clausiusstrasse 25, CH-8092 Zürich (ludmila.fonseca@erdw.ethz.ch)*

During magma crystallisation, volatile elements are typically incompatible, and progressively increase in the melt to the point of exsolving a magmatic volatile phase (MVP), dominated by H2O. Due to the presence of flux elements (e.g. F, Cl, Li, C), such a MVP can dissolve a significant fraction of “granitic” elements (Si, Al, Na, K), and may be at the origin of pegmatites, potentially representing the link between magmatic and hydrothermal environments. This contribution focuses on an A-type granite, the Pikes Peak Batholith (Colorado, USA) and one of its associated pegmatites, the Wellington Lake Pegmatite. We obtained detailed textural and mineral chemistry data on both lithologies, to assess how and when, in the evolution of the magma, mineral precipitation switches from hydrous silicate melt to fluxed MVP (corresponding to the transition from magmatic to hydrothermal conditions). Crystallisation temperatures obtained for quartz and two-feldspars in the granite samples range from typical magmatic temperatures (~700-800°C) to conditions that are significantly below the H2O-saturated haplogranitic solidus (~500-550°C). The lowest temperatures estimated from the granite samples correspond to outer rims of crystals, small interstitial grains, and fluid inclusion-filled fractures within quartz crystals. The observation of euhedral fluorite crystals indicates high F content in the system and suggests the presence of a highly fluxed MVP at the origin of the low temperature precipitation of quartz and feldspars. In the pegmatite samples, crystallisation temperatures begin at ~660°C for the border zone (“graphic granite”), while the last stages of crystallisation (in the core) occurred at much colder conditions, below 400°C (based on fluid inclusion and Ti-in-quartz thermometry). The border facies of the pegmatite appears concomitant with the last increments of crystallisation in the granite magma, and likely precipitated from a highly fluxed MVP expelled from the nearly fully-crystallized granitic mush. As cooling and crystallisation proceeded in the pegmatite, the MVP became increasingly stripped of most of its granitic components, leading to the precipitation of the clearly hydrothermal quartz core.

P 2.7
Low pressure crystal accumulation and melt segregation within the Western Adamello tonalite (Italy)

Thomas Grocolas[1], Aurore Toussaint[1], Othmar Müntener[1], Christophe Jossevel[1]

[1] *Institute of Earth Sciences, University of Lausanne, CH-1015 Lausanne, Switzerland (thomas.grocolas@unil.ch)*

Our understanding of the nature of the volcanic–plutonic connection within the upper continental crust is limited by the scarcity of outcrops exhibiting clear relationships between a crystal mush in contact with its volcanic counterpart. This limitation hampers our ability to place quantitative constraints on conceptual models which include melt extraction from a shallow crystal mush, and a deeper origin for the intermediate to felsic melts. One way to better characterize the volcanic–plutonic relationship would be to quantify the amount and rates of melt segregation within a crystallizing plutonic body, and to compare these volumes and rates with recent silicic eruptions. Here we investigate the processes of interstitial melt segregation in the calc-alkaline Western Adamello pluton. The Western Adamello tonalite (WAT) is part of the southern Alps and represents an intrusive body emplaced at 2.5 kbar in ~1.2 Myr (Floess 2013; Schaltegger et al. 2019). The WAT exhibits a coarse-grained, equigranular texture and is composed of hornblende partially replaced by biotite, plagioclase, quartz, epidote, titanite, apatite, magnetite, and zircon. K-feldspar is late and occurs as an interstitial phase with quartz. Several types of igneous structures are found, comprising: (i) zoned felsic dikes crosscutting the main tonalite and often containing aplite rims and a pegmatitic core, garnet-bearing dikes represent <5 vol.% of the dikes; (ii) segregations of quartz- and plagioclase-rich domains (0.1 to >10 m) forming schlieren-shaped bodies, which represents *in situ* melt segregations; and (iii) hornblende and biotite accumulations with interstitial plagioclase and quartz. The felsic rocks are spatially associated with hornblende- and biotite-rich zones. Hornblende, biotite, and plagioclase from the tonalite and the hornblende- and biotite-rich rocks have the same range of mineral compositions. We interpret this connection as deformation-driven crystal–melt segregation within the host tonalite. In addition, we show, through phase relationships and major element modeling, that the reaction involving hornblende and biotite follows a peritectic relationship of the form hornblende ± plagioclase + $melt_1$ = biotite ± quartz + $melt_2$. Furthermore, the occurrence of $melt_1$ implies that interstitial melts start to segregate before the partial transformation of hornblende. After determining that some tonalites kept a liquid composition, we quantitatively modeled the crystal–melt segregation process and showed that the host tonalite lost 0 to 70 vol.% of interstitial melt, constraining the maximum efficiency of crystal–melt segregation to 70 % in the Western Adamello. This process, besides crystallization and peritectic reactions, drives the final differentiation of the WAT.

REFERENCES

Floess, D. 2013: Contact metamorphism and emplacement of the Western Adamello tonalite. PhD thesis, University of Lausanne.

Schaltegger, U. et al. 2019: Zircon petrochronology and $^{40}Ar/^{39}Ar$ thermochronology of the Adamello intrusive suite, N. Italy: Monitoring the growth and decay of an incrementally assembled magmatic system. J. Petrol. 60(4), 701–722.

P 2.8
A novel thermobarometer: how to use machine learning to discover the secrets of volcanoes

Corin Jorgenson[1], Oliver Higgins[1], Maurizio Petrelli[2], Florence Begue[1], Luca Caricchi[1]

[1] *Department of Earth Sciences, University of Geneva, Rue de Maraîchaire 13, CH-1205 Genève, (corin.jorgenson@etu.unige.ch)*
[2] *Department of Physics and Geology, University of Perugia, Perugia*

Mineral chemistry offers a unique perspective of the evolution of a volcanic system. Thermobarometry is one such avenue for interrogating the distribution of pressure and temperature of magma storage in magmatic plumbing systems. Developments in random forest based machine learning allows for a data-driven approach to clinopyroxene thermobarometry (Higgins et al., 2021; Petrelli et al., 2020). Here we present an explanation of our optimized random forest clinopyroxene thermobarometer using the R freeware package “extraTrees”. We present a worked example and compare our results with those of existing thermobarometers. We find our model gives standard error estimates comparable to classical thermobarometers (4.4 kbar and 76.0 °C) but can be used for a wider range of magma compositions than classical equation-based thermobarometers (Masotta et al., 2013; Putirka, 2008). Additionally, uncertainty of pressure and temperature estimates is provided for single analyses and can be significantly lower than the standard error estimate. We present two comprehensive R scripts for users to apply the random forest methodology to natural datasets. The first script permits modification and filtering of the model calibration dataset. The second script contains pre-structured models in which users can rapidly input their data to recover pressure and temperature estimates. These scripts are open source and can be accessed at https://github.com/corinjorgenson/RandomForest-cpx-thermobarometer.

REFERENCES

Higgins, O., Sheldrake, T., & Caricchi, L. (2021). Machine learning thermobarometry and chemometry using amphibole and clinopyroxene : a window into the roots of an arc volcano (Mount Liamuiga , Saint Kitts). *EarthArXiv*.

Masotta, M., Mollo, S., Freda, C., Gaeta, M., & Moore, G. (2013). Clinopyroxene–liquid thermometers and barometers specific to alkaline differentiated magmas. *Contributions to Mineralogy and Petrology*, *166*(6), 1545–1561. https://doi.org/10.1007/s00410-013-0927-9

Petrelli, M., Caricchi, L., & Perugini, D. (2020). Machine Learning Thermo - Barometry : Application to Clinopyroxene - Bearing Magmas Journal of Geophysical Research : Solid Earth. *Journal of Geophysical Research: Solid Earth*, *125*. https://doi.org/10.1029/2020JB020130

Putirka, K. D. (2008). Thermometers and barometers for volcanic systems. *Reviews in Mineralogy and Geochemistry*, *69*, 61–120. https://doi.org/10.2138/rmg.2008.69.3

P 2.9
A new method to measure water in randomly oriented rutile grains

Mona Lüder, Jörg Hermann, Julien Reynes, Renee Tamblyn

Institut für Geologie, University of Bern, Baltzerstrasse 1+3, CH-3012 Bern (mona.lueder@geo.unibe.ch)

Rutile is a common accessory mineral occurring at a range of metamorphic grades, in high pressure (>0.8 GPa) rocks such as lawsonite blueschists and eclogites, but can also be found in granulites and upper amphibolite facies rocks. Recently, it has been increasingly used for U-Pb age determinations (e.g. Zack & Kooijman 2017) and Zr-in-Rutile thermometry (e.g. Zack et al. 2004). Several studies show the affinity of rutile to substitute pentavalent (e.g. Nb^{5+} and Ta^{5+}) and trivalent (e.g. Fe^{3+}, Al^{3+}, Cr^{3+}) cations for Ti^{4+}, with the potential of charge balance between penta- and trivalent cations. The effect of H^+ on this substitution mechanisms as possible charge balance for trivalent cations has been widely neglected so far, although studies suggest that rutile can incorporate high amounts of H^+, with measured water contents up to several 1000 ppm.

Early work on water incorporation into rutile has shown that IR absorption is highly anisotropic with virtually no absorption parallel to the crystallographic c-axis and maximum absorption perpendicular to the crystallographic c-axis (e.g. Soffer 1961). Thus, most studies so far were using oriented single grain rutiles to directly measure total absorption, a rather time expensive method. Studies on randomly oriented grains have mainly been performed on other anisotropic minerals, using statistical approaches to calculate total absorption, which resulted in high uncertainties. Hence, the first step to quantify water in rutile is the development of a method to measure IR spectra on randomly oriented grains without high uncertainties. This will allow the analysis of rutile grains in-situ, and therefore the ability to target rutile grains in different textural domains of metamorphic and igneous rock samples, removing the current necessity of mineral separation and orientation.

As rutile is commonly fine grained (<100 µm), conventional mechanic determinations for sample thickness are often not applicable on separated grains. Here we present a new approach to measure water in randomly oriented rutiles. We use oriented cuts of large rutiles and crushed grains of the same samples to show how polarized IR light in varying polarization angles can be used to optain total absorption with much lower uncertainty compared to statistical methods. As sample thickness is needed for calculations of the water content, we present a new calibration using Ti-O overtones to calculate sample thickness from measured FTIR spectra. This calibration is based on statistical measurements of oriented cut samples in varying thickness. Based on those two new methods, water measurements in rutile is more applicable to a variety of different samples.

H^+ incorporation into rutile is proposed to be linked to substitution of trivalent cations onto Ti^{4+}-sites, creating a charge deficit, which would be balanced by H^+ on interstitial positions. Several studies on experimentally doped rutiles have shown trace element-dependant variations of OH-bond positions in FTIR spectra, but very limited work has been done to verify those on natural samples. We analysed the OH-bond positions of natural rutiles from Mg-rich whiteschists of the Dora Maira complex and thus present the first data on Mg-related OH-bond positions of natural rutiles. From our data, we propose an exchange mechanism of $Mg^{2+} + 2H^+$ for one Ti^{4+}. The spectra show a distinct double peak at 3280 cm^{-1} and 3325 cm^{-1}, where the second peak has an absorbance four times as strong. The peak at 3280 cm^{-1} relates to the 'pure rutile' OH-bond position reported in literature, while the second peak is comparable to peaks reported in Mg-doped synthetic rutiles (e.g. Bromiley & Hilairet 2005). Additionally, the Mg-related peak shows a distinct left shoulder, that partially can be characterised as a distinct third peak at around 3340 cm^{-1}. Thus, Mg-linked substitution seems to be the main mechanism for H^+ incorporation in the Dora Maira rutiles, as can be expected from the high Mg-whole rock composition of the Dora Maira whiteschists. Similar studies on samples with high contents of different trace elements (e.g. Fe^{2+}, Fe^{3+}, Cr, Al) in rutiles are necessary to be able to qualify the H^+ incorporation mechanism in un-known samples.

REFERENCES

Bromiley, G.D. & Hilairet, N., 2005: Hydrogen and minor element incorporation in synthetic rutile. Mineral. Mag., 69:345-358.

Soffer, B. H., 1961: Studies of the Optical and Infrared Absorption Spectra of Rutile Single Crystals. J. Chem. Phys., 35: 940-945.

Zack, T., Moraes, R., Kronz, A., 2004: Temperature dependence of Zr in rutile: empirical calibration of a rutile thermometer. Contrib. to Mineral. Petrol. 148: 471-488.

Zack, T. & Kooijman, E., 2017: Petrology and Geochronology of Rutile. Rev. Mineral. Geochem. 83, 443–467.

P 2.10
Metamorphic reactions as soft or hard triggers for fluid flows?

Thorsten Andreas Markmann[1], Pierre Lanari[1]

[1] *Institute of Geological Sciences, University of Bern, Baltzerstrasse, CH-3012 Bern (thorsten.markmann@geo.unibe.ch)*

Migration of aqueous fluids within the crust and interactions with surrounding rocks are fundamental processes on Earth especially in subduction zones. Tracking fluid pathways remains challenging, but has gained attention in recent years. Blueschist and eclogite facies metamorphic rocks have proven to be excellent recorders of fluid-rock interaction processes, as changes in oxygen isotopes in zoned garnet reveal fluctuations in fluid $\delta^{18}O$ composition. Recently, lawsonite breakdown was identified as a possible trigger for pervasive fluid flux linked to rock volume changes (Bovay et al., 2021). The created open-system behaviour is fundamental for subduction zone dynamics, while mineral assemblages may have a greater effect.

In this study, we present a petrological model simulating rock dehydration and fluid extraction at equilibrium via metamorphic reactions along typical subduction *P–T–t* gradients. For several rock types (e.g. metasediment, metabasalt, ultramafics) the model uses Gibb's minimizations coupled with fluid extraction steps and oxygen isotope fractionation. It shows that changes in mineral assemblages and mineral modes can be important for creating (momentary?) fluid-filled porosity as rocks being subducted. For example, the lawsonite out and garnet in reaction for a subducted metasediment at 550 °C and 2.4 GPa can easily reach one volume percent of fluid-filled porosity accompanying a change in density of ~20 kg/m^3. This model is intended to serve as a theoretical basis for the interpretation of fluid fluxes derived from $\delta^{18}O$ measurements in metamorphic minerals (garnet, white mica).

This project has received funding from the European Research Council (ERC) under the European Union's Horizon 2020 research and innovation programme (grant agreement No 850530).

REFERENCES

Bovay, T., Rubatto, D. & Lanari, P. 2021: Pervasive fluid-rock interaction in subducted oceanic crust revealed by oxygen isotope zoning in garnet, Contrib Mineral Petrol, 176, 55.

P 2.11
Growth and analysis of experimentally zoned crystals: the competition between crystal growth and elements diffusion

Alessandro Musu[1], Luca Caricchi[1], Diego Perugini[2], Rosa Anna Corsaro[3], Francesco Vetere[2], Maurizio Petrelli[2]

[1] Department of Earth Sciences, University of Geneva, Rue des Maraîchers 13, CH-1205 Geneva, Switzerland
[2] Department of Physics and Geology, University of Perugia, Piazza dell'Università, 1, 06123 Perugia, Italy
[3] Istituto Nazionale di Geofisica e Vulcanologia, Osservatorio Etneo-Sezione di Catania, Catania, Italy

Magma reservoirs reflect areas of wide physico-chemical variation of magma properties and are directly associated with volcanic activity and the release of the magmatic fluids, responsible for the development of ore deposits (Charlier et al., 2006; Caricchi and Blundy 2015; Cashman et al., 2017). Understanding the processes operating at inaccessible depths is crucial for interpreting monitoring signals and for developing quantitative models to forecast volcanic activity. Minerals witness the evolution of physico-chemical conditions within magma reservoirs over time and record changes in intensive parameters as chemical signals which we see as zoning (Cashman & Blundy 2013, Cheng et al 2017, Probst et al., 2018, Caricchi et al., 2020; Weber et al., 2020).

However, the competition between crystal growth rate and element diffusion in the melt phase can be also responsible for the chemical zoning of minerals, complicating the interpretation of chemical zoning patterns. To extricate this complexity chemically zoned minerals are synthetically grown under controlled conditions at the Petro-Volcanology Research Group of the University of Perugia.

Tephra from 2002-03 Mt. Etna eruption has been used as starting material. The zonation in minerals is controlled inside a high-temperature furnace by oscillating the temperature under three different conditions: static, using a controlled deformation gradient (concentric cylinder apparatus), and using a chaotic mixing regime (Chaotic Magma Mixing Device). We collect major and trace elements distribution maps on a large number of crystals using Electron Probe Micro Analyzer and Laser Ablation Inductively Coupled Plasma Mass Spectrometry. The data are analysed using a series of custom-built machine learning algorithms to disentangle zoning related to thermodynamic variation in the crystal growth conditions from the effects of the competition between diffusion and growth. Backscattered Electron images of the sample are also analysed for Crystal Size Distribution using a Radom Cut correction. The aim of this project is to provide experiments and quantitative tools that will help decipher the chemical signals buried in natural magmatic minerals.

REFERENCES

Caricchi, L., & Blundy, J. (2015). Experimental petrology of monotonous intermediate magmas. Geological Society, London, Special Publications, 422(1), 105-130.

Caricchi, L., Petrelli, M., Bali, E., Sheldrake, T., Pioli, L., & Simpson, G. (2020). A data driven approach to investigate the chemical variability of clinopyroxenes from the 2014–2015 Holuhraun–Bárdarbunga eruption (Iceland). Frontiers in Earth Science, 8, 18.

Cashman, K., & Blundy, J. (2013). Petrological cannibalism: the chemical and textural consequences of incremental magma body growth. Contributions to Minerv alogy and Petrology, 166(3), 703-729.

Cashman, K. V., Sparks, R. S. J., & Blundy, J. D. (2017). Vertically extensive and unstable magmatic systems: a unified view of igneous processes. Science, 355(6331), eaag3055.

Charlier, B., Duchesne, J. C., & Vander Auwera, J. (2006). Magma chamber processes in the Tellnes ilmenite deposit (Rogaland Anorthosite Province, SW Norway) and the formation of Fe–Ti ores in massif-type anorthosites. Chemical Geology, 234(3-4), 264-290.

Cheng, L., Costa, F., & Carniel, R. (2017). Unraveling the presence of multiple plagioclase populations and identification of representative two-dimensional sections using a statistical and numerical approach. American Mineralogist, 102(9), 1894-1905.

Probst, L. C., Sheldrake, T. E., Gander, M. J., Wallace, G., Simpson, G., & Caricchi, L. (2018). A cross correlation method for chemical profiles in minerals, with an application to zircons of the Kilgore Tuff (USA). Contributions to Mineralogy and Petrology, 173(3), 23.

Weber, G., Caricchi, L., Arce, J. L., & Schmitt, A. K. (2020). Determining the current size and state of subvolcanic magma reservoirs. Nature Communications, 11(1), 1-14.

P 2.12
Pre-Alpine hydrothermal activity in the Aar Massif granitoids

Veronica Peverelli[1], Alfons Berger[1], Andreas Mulch[2], Thomas Pettke[1], Francesca Piccoli[1] & Marco Herwegh[1]

[1] Institut für Geologie, University of Bern, Baltzerstrasse 1+3, CH-3012 Bern (veronica.peverelli@geo.unibe.ch)
[2] Senckenberg Biodiversity and Climate Research Centre, Frankfurt, Germany

The Aar Massif is a mid-crustal basement section of the European plate that was heavily deformed during the Alpine orogeny. This deformation produced numerous ductile shear zones, which consist mainly of fine-grained polymineralic (ultra)mylonites deforming by viscous granular flow. Both the granitic protoliths and the shear zones themselves show hydration reactions with respect to a primary granitic composition, whose main expression is widespread alteration of feldspars. So far, the relative timing of such a hydration event (i.e. pre-, syn- or post-deformation) was not clear, and neither was the absolute timing. This piece of information, however, is crucial in order to learn whether Alpine strain localization was initiated in an already mechanically weakened hydrated middle crust, or if hydration was mediated by shear zone formation and is therefore a consequence of Alpine strain localization.

Here we present new evidence for a Pre-Alpine hydrothermal event in the Grimsel Granodiorite and Central Aar Granite of the Aar Massif. Epidote U–Pb geochronology by LA-ICP-MS of the numerous epidote-bearing veins crosscutting these granitoids highlights two main veining episodes: (1) ca. 275 Ma (Permian) with initial $^{207}Pb/^{206}Pb$ ratios of 0.8293–0.8321 and (2) ca. 19–17 Ma (Alpine) with initial $^{207}Pb/^{206}Pb$ ratios of 0.7963–0.7998. The initial Pb isotopic composition of all epidote samples is more radiogenic than that of the bulk host rock at the respective times of vein formation. Bulk hydrogen isotopic measurements of epidote separates by temperature conversion elemental analyzer (TC/EA) of two Permian epidote samples yielded a δD_{ep} of -76 ‰ and -59 ‰ respectively. Unlike the former sample, the latter displays unambiguous textural evidence for fluid–mineral interaction. In addition, it has a similar δD_{ep} value to those measured in Alpine epidote (-55–58 ‰) and in one saussuritic feldspar from the host rock (-51 ‰). This suggests that the bulk hydrogen isotopic signature of some Permian epidote samples was overprinted upon interaction with the Alpine fluids.

The disequilibrium of epidote initial Pb isotopic ratios with the bulk country rock suggests an external origin for all epidote-forming fluids. Hydrogen isotopic signatures of epidote indicate a meteoric component in the Permian fluids, and a metamorphic one in the Alpine ones. The occurrence of Permian hydrothermal activity in the Aar Massif granitoids implies a pre-Alpine pervasive alteration of the Aar Massif granitoid rocks. Alpine deformation may have exploited the stored Permian fluids, and shear zones may have nucleated on hydrothermally determined heterogeneities such as soft altered feldspars and epidote veins. Further fluid infiltration during the Alpine exhumation history of the Aar Massif may have occurred along the dense shear zone network.

P 2.13
Dating fluid release and deformation in the ultramafic oceanic lithosphere using perovskite and titanite

Francesca Piccoli[1], Daniela Rubatto[1], Jörg Hermann[1], Alberto Vitale Brovarone[2]

[1] *Institute of Geological Sciences, Universität Bern, Bern, Switzerland (francesca.piccoli@geo.unibe.ch)*
[2] *Dipartimento di Scienze Biologiche, Geologiche e Ambientali (BiGeA), Alma Mater Studiorum Universit. di Bologna, Bologna, Italy*

Dating dehydration reactions in ultramafic rocks such as serpentinites is notoriously difficult because of the lack of suitable minerals for geochronology. The study of rodingite blackwalls within the serpentinized mantle can potentially bring insights on the timing of dehydration reaction of the country rock. We found that perovskite ($CaTiO_3$) and titanite ($CaTiSiO_5$) can form during hydration of rodingite dykes and the formation of the blackwalls. Therefore, dating these minerals might open new avenues to investigate the timing of fluid-rock interaction and deformation during metamorphism. We present preliminary results of in situ U-Pb dating and trace element analysis by LA-ICP-MS on perovskite and titanite in rodingite blackwalls and perovskite in ophicarbonates from different metamorphic terranes. Titanite U-Pb dating in samples from the Zermatt-Saas unit (Switzerland) returned an age of 45.0 0.8 Ma, consistent with dehydration of the serpentinite and formation of the blackwall at high-pressure conditions. Perovskite in blackwalls have very low U content (ppb) and could not be dated. However, perovskite in ophicarbonates have higher U, ranging from tens to few hundreds of ppm, and are a potential candidate for geochronology of ultramafic lithologies. Perovskite in the two investigated localities Sasso Moro (Malenco unit, Italy) and Balangero (Lanzo Massif, Italy) yield an age of 51.54 0.44 Ma and 49.6 3.8 Ma, respectively. These ages are in line with other constraints on the age of metamorphism in each locality. Moreover, perovskite in blackwalls and in ophicarbonates have different trace element composition suggesting important inheritance from the protolith. The results have implications for U mobility in metamorphic fluids and dating of metamorphic mafic-ultramafic rocks.

P 2.14
Submarine hydrothermal vent fluid compositions reflect global tectonic petrogenesis

Samuel Pierre[1], Thomas Monecke[2], Alexander P. Gysi[3,4] and Larryn W. Diamond[1]

[1] *Rock-Water Interaction Group, Institute of Geological Sciences, University of Bern, Baltzerstrasse 3, 3012 Bern, Switzerland*
(samuel.pierre@geo.unibe.ch)
[2] *Center for Mineral Resources Science, Department of Geology and Geological Engineering, Colorado School of Mines, 1516 Illinois Street, Golden, CO 80401, USA*
[3] *New Mexico Bureau of Geology and Mineral Resources, New Mexico Institute of Mining and Technology, 801 Leroy Place, Socorro, NM 87801, USA*
[4] *Department of Earth and Environmental Science, New Mexico Institute of Mining and Technology, 801 Leroy Place, Socorro, NM 87801, USA*

Submarine hydrothermal vents are the seafloor expression of convection systems that drive seawater circulation through the brittle lithosphere. Over four decades of seafloor research has shown that vent fluid compositions are surprisingly diverse, but the fundamental controls on this variability remain poorly defined. As seawater composition is globally constant, processes such as liquid–vapor separation, degree of water–rock interation and host-rock composition have been proposed. We use a thermodynamic model of fluid-rock interaction to show that the major element chemistry of some 244 vent fluids across the world›s oceans correlate directly with the compositions of the igneous host rocks through which they circulate. Since host-rock composition reflects igneous petrogenesis, this correlation implies a first-order control of geodynamic settings vent fluid compositions. Hydrothermal fluids are uniformly depleted in Mg and enriched in K relative to seawater in all igneous environments while they are exclusively enriched in Ca and in Na in basaltic and in peridotite environments respectively. Considerations of in-situ pH indicate that seawater–rock interaction processes dominate the chemistry of mid-ocean ridge hydrothermal systems, while magmatic volatile admixing is necessary to account for the acidity of hydrothermal fluids encountered in arc-related settings. These findings have implications for estimates of the geochemical mass balance between the oceans and oceanic crust. They also constitute a fundamental basis to interpret the compositional variability of fossil hydrothermal systems in the geologic record, which bears directly on genetic models used by the mineral industry to guide exploration for volcanogenic massive sulfide deposits.

P 2.15
OH incorporation and retention in high pressure garnet from the Zermatt ophiolite

Julien Reynes[1], Jörg Hermann[1], Pierre Lanari[1], Thomas Bovay[1,2]

[1] *Institute of Geological Sciences, University of Bern, Baltzerstrasse 3, Bern, CH-3012 Switzerland (julien.reynes@geo.unibe.ch)*
[2] *Institute of Earth Sciences, University of Lausanne, UNIL-Mouline, Géopolis building, CH-1015 Lausanne*

Garnet is a common mineral in high-pressure metamorphic rocks and grow after breakdown reactions of hydrous phases in the subducted slab. A small quantity of water in the form of OH groups can be incorporated into the garnet structure and therefore bring water to the deep mantle. The Zermatt ophiolite (Switzerland) shows a large variety of garnet bearing rocks that experienced a burrial to ~80 km depth (550 °C and 2.3 GPa) (Angiboust et al. 2009). The garnets feature different solid solutions: grossular-andradite-uvarovite in serpentinites and rodingites, grossular-pyrope-almandine-spessartine in mafic eclogites and meta-sediments. A combination of Fourier transform Infrared spectroscopy (FTIR) and EPMA (Electron microprobe micro-analyser) was used to measure maps ans profiles of OH and major elements in these various garnets. This combination method enables to 1) quantify the OH contents in various garnets 2) study the effects of major-minor elements composition on OH incorporation 3) investigate the spatial repartition of OH in zoned garnets and the retention during their metamorphic history 4) discuss the incorporation mechanisms of OH based on correlation with chemistry and retentivity to diffusive processes.

The capacity for OH incorporation into garnet is governed by its composition. Andradite-rich (400-5000 ppm H_2O) and grossular-rich garnets (200-1800 ppm H_2O) contain at least one order of magnitude more OH than almandine-rich garnet (< 120 ppm H_2O). Ca and Ti appears to be the main drivers for OH incorporation and produces distinct absorption bands that are characteristic of multiple nano-scaled OH-environments.

Microscale analyses profiles and maps reveal the preservation of OH zoning linked with growth zoning of the garnets and do not show any sign of reequilibration due to diffusive processes. Based on these observations and the use of 2D diffusion modelling, H diffusion rates in these rocks are suggested to be as low as $\log(D[m^2.s^{-1}])=-24.5$ at 540 °C.

The garnets of main garnet-bearing rock types of the Saas-Zermatt ophiolite were measured for OH and enable a mass balance model of H_2O to be calculated. The computation suggests that ~3,360 kg H_2O/km (section of oceanic crust)/year can be transported by garnet beyond 80 km depth by the subducting slab and contribute to the deep-Earth water cycle during the Eocene subduction of the Piemont-Ligurian ocean.

REFERENCES

Angiboust, S., Agard, P., Jolivet, L. & Beyssac, O. (2009). The Zermatt-Saas ophiolite: the largest (60-km wide) and deepest (c. 70–80 km) continuous slice of oceanic lithosphere detached from a subduction zone? Terra Nova, 21, 3, 171-180

P 2.16
Diversity of Late Cretaceous epithermal systems of the Georgian Bolnisi and Turkish Artvin Districts: Products of a single ore-forming system during final Neotethyan subduction

Şafak Utku Sönmez[1], Robert Moritz[1], Jonathan Lavoie[1], Titouan Golay[1], Stefano Gialli[1], François Turlin[1], Nino Popkhadze[2], Malkhaz Natsvlishvili[3], Ümit Aydın[4], Serdar Keskin[4], Jorge Spangenberg[5]

[1] *Department of Earth Sciences, University of Geneva, Rue des Maraîchers 13, 1205 Geneva, Switzerland* (*safak.soenmez@unige.ch*)
[2] *Al. Janelidze Institute of Geology, Iv.Javakhishvili Tbilisi State University, Georgia*
[3] *Rich Metals Group, Tbilisi, Georgia*
[4] *General Directorate of Mineral Research and Exploration of Turkey, Department of Mineral Research and Exploration, Ankara 06520, Turkey*
[5] *Institute of Earth Sciences, University of Lausanne, 1015 Lausanne, Switzerland*

This study focuses on Late Cretaceous epithermal systems of the Central Tethyan Metallogenic Belt belonging to both the Eastern Pontides, Turkey and the Lesser Caucasus, Georgia, which are associated with similar geodynamic settings. In this contribution, we compare the host rock, alteration, ore style, and ore mineral characteristics of four of the main prospects and deposits of this prolific belt, namely: Yanikli in the Turkish Artvin District, and the Beqtakari, Sakdrisi, and Madneuli deposits of the Georgian Bolnisi District.

The deposits and prospects of the Bolnisi and Artvin Districts are hosted by Late Cretaceous (89.8 to 83.6Ma and 83.4 to 81.4Ma, respectively) volcanic and volcaniclastic suites, that are the results of bimodal magmatism along the Eurasian margin during the wanning stages of the subduction of the northern branch of the Neotethys. The composition of the volcanic rocks is predominantly rhyolitic to dacitic, with subsidiary intermediate to mafic compositions in each district. There are two dominant generations of dykes in Yanıklı, Artvin. The first dyke generation is NE-oriented, whereas the second one is NW-oriented. Likewise, NE-oriented dykes also crop out in the Bolnisi District.

The main alteration zones include in the Bolnisi and Artvin Districts: argillic alteration (Yanıklı, Beqtakari, Sakdrisi), propylitic alteration (Yanıklı, Beqtakari, Sakdrisi and Madneuli), phyllic alteration (Yanıklı, Sakdrisi, Madneuli), and intense silicification (Beqtakari). The predominant alteration minerals include chlorite, sericite and kaolinite group minerals. Adularia has been identified by XRD in Beqtakari and Sakdrisi. Dickite has been determined in Yanıklı and Sakdrisi. Anhydrite (Yanıklı, Beqtakari) and barite (Yanıklı, Beqtakari, Sakdrisi, Madneuli) were also identified in different alteration zones within both districts.

Two mineralization stages occur in Yanıklı. A first-generation Cu-rich metal assemblage is associated with a predominantly propylitic altered polymictic breccia, and includes subsidiary Pb and Zn. A second generation Zn- and Pb-rich metal assemblage is predominantly hosted by a sericitic altered polymictic breccia, and also contains Au and weak Cu concentrations. In Sakdrisi (32Mt @ 0.57g/t Au, 0.1% Cu), our studies were mainly focused on the Sak-IV and Sak-V open pits. The Sak-IV open pit consists of a deep stockwork of multistage banded Au-Cu-bearing quartz-carbonate veins. The mineralization at the Sak-V open pit is occupied by a deep red gossan-like zone, mainly exploited for gold, whereas the bottom part of the pit is occupied by a strongly chloritized zone crosscut by a stockwork of quartz-poor massive chalcopyrite and pyrite veins. In Madneuli, two different ore types have been identified. A sub-vertical stockwork part (56Mt @ 0.22g/t Au and 0.39% Cu) consists of mainly pyrite, chalcopyrite, and sphalerite with rare enargite, as well as quartz and abundant barite as main gangue minerals in the western flank of the open pit. The second ore type consists of a sub-vertical pyrite-chlorite-hematite-telluride±chalcopyrite gold vein system in the eastern flank of the open pit. Beqtakari (9.4Mt @ 2.93g/t, 33.23g/t Ag, 1.44% Zn, and 0.66% Pb) consists of two different mineralization zones which are an outcropping Au-rich zone and a Au-Ag-Zn-Pb±Cu zone at depth. Ag is nearly absent, except at Beqtkari, where higher grades were reported.

Microthermometric fluid inclusions studies have been conducted in Beqtakari and Sakdrisi. The homogenization temperatures of sphalerite range between 229 to 294°C with salinities between 3.1 to 3.9% NaCl eq. in Beqtakari, and 278 to 273°C with salinities between 5.9 to 6.2 wt% NaCl eq. in Sakdrisi. The sulfur isotope compositions ($\delta^{34}S$) of sulfide minerals from Yanıklı match with those of the Bolnisi District deposits. The $\delta^{34}S$ values of anhydrite samples from Yanıklı and barite samples from Beqtakari partly overlap with the sulfur isotope composition of late Cretaceous seawater sulfate.

Considering the fact that the lithology, alteration and mineralization characteristics of each deposit and prospect of the Bolnisi and the Artvin Districts share similar characteristics, we conclude that they can be interpreted as belonging to the same regional Late Cretaceous ore-forming event. Further studies are needed to understand if they were produced by similar ore-forming fluids derived from similar sources.

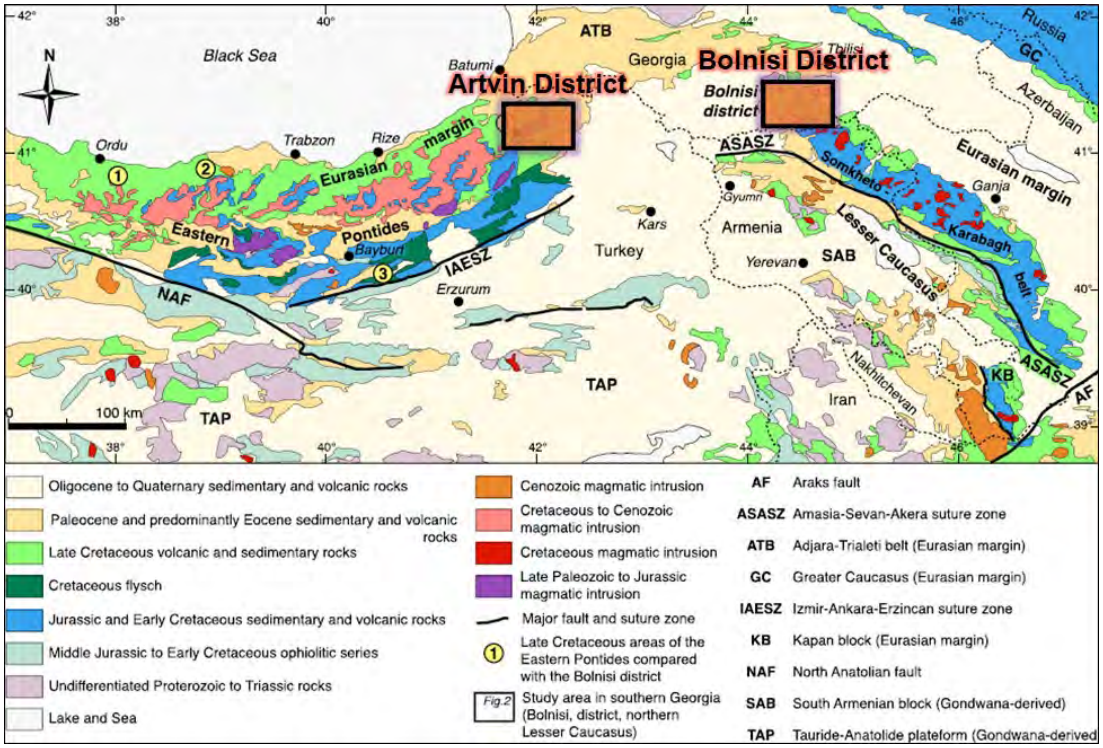

Figure 1. Setting of the Bolnisi and Artvin Districts and regional geology.

P 2.17
Quantification of excess ^{231}Pa in late Quaternary igneous baddeleyite

Yi Sun[1,3], Axel K. Schmitt[1], Lucia Pappalardo[2], Massimo Russo[2]

[1] Institute of Earth Sciences, Heidelberg University, Im Neuenheimer Feld 236, D-69120 Heidelberg, Germany
[2] Istituto Nazionale di Geofisica e Vulcanologia, sezione di Napoli - Osservatorio Vesuviano, via Diocleziano 328, 80124 Naples, Italy
[3] Present address: Institute of Geochemistry and Petrology, ETH Zürich, Clausiusstrasse 25, CH-8092 Zürich, Switzerland (yi.sun@erdw.ethz.ch)

Initial excess protactinium (^{231}Pa) is a frequently suspected source of discordance in baddeleyite (ZrO_2) geochronology, which limits accurate U/Pb dating, but such excesses have never been directly demonstrated. In this study, Pa incorporation in late Holocene baddeleyite from Somma-Vesuvius (Campanian Volcanic Province, central Italy) and Laacher See (East Eifel Volcanic Field, western Germany) was quantified by U-Th-Pa measurements using a large-geometry ion microprobe. Baddeleyite crystals isolated from subvolcanic syenites have average U concentrations of ~200 ppm and are largely stoichiometric with minor abundances of Nb, Hf, Ti, and Fe up to a few weight percent. Measured (^{231}Pa)/(^{235}U) activity ratios are significantly above the secular equilibrium value of unity and range from 3.4(8) to 14.9(2.6) in Vesuvius baddeleyite and from 3.6(9) to 8.9(1.4) in Laacher See baddeleyite (values within parentheses represent uncertainties in the last significant figures reported as 1σ throughout the text). Crystallization ages of 5.12(56) ka (Vesuvius; MSWD = 0.96, n = 12) and 15.6(2.0) ka (Laacher See; MSWD = 0.91, n = 10) were obtained from (^{230}Th)/(^{238}U) disequilibria for the same crystals, which are close to the respective eruption ages. Applying a corresponding age correction indicates average initial (^{231}Pa)/(^{235}U)$_0$ of 8.8(1.0) (Vesuvius) and 7.9(5) (Laacher See). For reasonable melt activities, model baddeleyite-melt distribution coefficients of D_{Pa}/D_U = 5.8(2) and 4.1(2) are obtained for Vesuvius and Laacher See, respectively. Speciation-dependent (Pa^{4+} vs. Pa^{5+}) partitioning coefficients (D values) from crystal lattice strain models for tetra- and pentavalent proxy ions significantly exceed D_{Pa}/D_U inferred from direct analysis of ^{231}Pa for Pa^{5+}. This is consistent with predominantly reduced Pa^{4+} in the melt, for which D values similar to U^{4+} are expected. Contrary to common assumptions, baddeleyite-crystallizing melts from Vesuvius and Laacher See appear to be dominated by Pa^{4+} rather than Pa^{5+}. An initial disequilibrium correction for baddeleyite geochronology using $D_{Pa}/D_U = 5 \pm 1$ is recommended for oxidized phonolitic melt compositions.

REFERENCES

Sun, Y., Schmitt, A. K., Pappalardo, L., & Russo, M. 2020: Quantification of excess ^{231}Pa in late Quaternary igneous baddeleyite. American Mineralogist: Journal of Earth and Planetary Materials, 105(12), 1830- 1840.

03. Stable and radiogenic isotope geochemistry

Afifé El Korh, Nicolas Greber, Andres Rüggeberg

Swiss Society of Mineralogy and Petrology (SSMP)

TALKS:

3.1 Adams A., Baumgartner L.P., Vennemann T., Daval D., Bernard S., Cisneros-Lazaro D., Baronnet A., Grauby O., Guo J., Stolarski J., Meibom A.: Biogenic Carbonate Paleotemperature Records Biased by Grain Boundary Diffusion

3.2 Ahmad Q., Wille M., Rosca C., Labidi J., König S.: Anoxic conditions of Proterozoic deep oceans: Evidence from recycled sediments in plume-influenced MORBs.

3.3 Anand A., Kruttasch P.M., Mezger K.: ^{53}Mn-^{53}Cr chronological and ε54Cr-Δ17O geneological constrains on Erg Chech 002 parent body: source of the oldest andesite in the Solar System

3.4 Chatterjee S., Pandey Om P., Mezger K., Schmitt M K., Kooijman E.: Strontium isotope analyses of matrix apatite and apatite incluions in zircon constrain the evolution of the Paleoarchean Singhbhum Craton

3.5 Clarkson M.O., Hennekam R., Sweere T.C., Andersen M.B., Reichart G.-J., Vance D.: How to identify seafloor anoxia using carbonate U isotopes, despite oxidative diagenesis

3.6 Damanik A., Wille M., Ahmad Q., Grosjean M., Cahyarini S.Y., Vogel H.: Source-to-sink molybdenum (Mo) variability in the ultramafic bedrock-dominated catchment of Lake Towuti, Indonesia

3.7 de Souza G.F., Vance D., Sieber M., Conway T.M., Little S.H.: Re-assessing the influence of particle-hosted sulphide formation on the marine cadmium cycle

3.8 Decraene M.-N., Marin-Carbonne J., Thomazo C., Bouvier A.-S., Brayard A., Olivier N.: Heavy Fe isotope signatures in micropyrites at the Smithian-Spathian boundary (Early Triassic)

3.9 Fleischmann S., Chatterjee A., McManus J., Iyer S.D., Vance D.: The oceanic budget of nickel: new concentration and isotope data from Mn-rich pelagic sediments

3.10 Gaynor S.P., Svensen H.H., Polteau S., Schaltegger U.: Local Melt Contamination and Global Climate Impacts: Geochronology of Karoo LIP Sills in Organic-Rich Shales

3.11 Janssen D.J., Rickli J., Wille M., Hassler C.S., Vogel H., Jaccard S.L.: Chromium cycling in euxinic basins: Implications for the δ^{53}Cr paleoredox proxy from a modern system (Lake Cadagno, Ticino, Switzerland).

3.12 Kruttasch P.M., Anand A., Mezger K.: Temporal and spatial constraints on the ureilite-forming region inferred from Cr isotopes

3.13 Pohlner J.E., El Korh A., Chiaradia M., McCammon C., Rubatto D., Klemd R., Grobéty B.: Inter-mineral iron and oxygen isotope fractionation in eclogites of the Münchberg Massif (Germany)

3.14 Saintilan N.J., Neff C., Delessert S., Sossi P.A., Tollan P.M., Guillong M., Hattendorf B., Allaz J.M., Petitgirard S., Ariztegui D., Farsang S., Chelle-Michou C., Günther D.: Robustness of the bornite (Cu_5FeS_4) rhenium-osmium (^{187}Re–^{187}Os) geochronometer for the quantification of geological and hydrothermal processes – Constraints from microscale spatial distribution and mineralogical residency of rhenium

3.15 Senger M.H., Schaltegger U., Rebeun N., Beukes N.: New high-precision U-Pb zircon CA-ID-TIMS ages on the Paleoproterozoic Makganyene Formation, Griqualand West Basin, South Africa.

3.16 Shalev N., Bontognali T.R.R., Vance D.: Sabkha dolomite as an archive for the magnesium isotope composition of seawater

3.17 Storck J.-C., Greber N.D., Pettke T., Müntener O.: Molybdenum and titanium isotopic data of arc derived differentiates and cumulates

3.18 Vilela N., Vogel H., Greber N.D.: Titanium isotopes in detrital sediments: A reliable proxy for the protoliths composition?

3.19 Zakharov D., Zozulya D., Rubatto D., Colón D.: Neoarchean Continental Exposure and Hydrological Cycle Recorded in a 2.67 Ga Magmatic-Hydrothermal System from Kola Craton, Russia

POSTERS:

P 3.1 Blaser P., Pöppelmeier F., Kaboth-Bahr S., Gutjahr M., Frank M., Waelbroeck C., Jaccard S., Lippold J.: Last Glacial Maximum Atlantic water mass provenance from a multi proxy compilation

P 3.2 de Carvalho C.F.M., Pati S.G.: Accuracy of stable oxygen isotope measurements from -10 to 90 ‰

P 3.3 Gilliard D., Janssen D.J., Jaccard S.L.: Ocean circulation and hydrothermal activity control the cycling of dissolved Cr in the oligotrophic South Pacific Ocean

P 3.4 Hoffmann J., Anand A., Mezger K.: Mass-independent Ca and Cr isotope variations in chondritic components – Insights into Solar System evolution and planetary formation

P 3.5 Muesing K., Clarkson M.O., Vance D.: A new perspective on the constraints on marine carbonate Zn isotope records

P 3.6 Ulrich M., Rubatto D., Hermann J., Deloule E.: Isotopic disequilibrium during dehydration of subducted serpentinites (Zermatt-Saas unit)

P 3.7 Vesin C., Rubatto D., Pettke T., Deloule E.: Tracking fluid uptakes during abyssal serpentinization of passive margins by oxygen isotope analysis of the serpentine phases

3.1
Biogenic Carbonate Paleotemperature Records Biased by Grain Boundary Diffusion

Arthur Adams[1*], Lukas P. Baumgartner[2], Torsten Vennemann[2], Damien Daval[3], Sylvain Bernard[4], Deyanira Cisneros-Lazaro[1], Alain Baronnet[5], Olivier Grauby[5], Jinming Guo[1], Jarosław Stolarski[6], Anders Meibom[1]

[1] Laboratory for Biological Geochemistry, School of Architecture, Civil and Environmental Engineering, Ecole Polytechnique Fédérale de Lausanne (EPFL), Lausanne, CH-1015 Switzerland.
[2] Institute of Earth Surface Dynamics, University of Lausanne, CH-1009 Switzerland.
[3] Institut Terre et Environnement de Strasbourg, Université de Strasbourg / CNRS / ENGEES, 67084 Strasbourg, France.
[4] CNRS/Museum National d'Histoire Naturelle, 75005 Paris, France.
[5] CNRS, CINaM, Aix-Marseille Université, 13009 Marseille, France.
[6] Institute of Paleobiology, Polish Academy of Sciences, PL-00-818 Warsaw, Poland
[*] arthur.adams@epfl.ch

Oxygen isotope compositions of fossil marine organisms (e.g. foraminifera, molluscs, belemnites) have been successfully used to reconstruct surface and deep paleoseawater temperatures of the Mesozoic to the present. The reliability of this temperature record is predicated on the use of fossils that show no overt microscopic evidence of diagenesis. However, recent studies have demonstrated that the isotopic and chemical composition of many (bio)minerals can be altered at low temperatures without any ultrastructural signs of diagenesis. This suggests that paleotemperature records based on biomineral $\delta^{18}O$ values may be biased by "visually pristine" but diagenetically altered biominerals.

To quantify, correct, and determine the process behind this potential isotopic bias, we exposed modern foraminifera tests and bivalves to ^{18}O-enriched, artificial seawater, saturated with respect to calcite, for up to 60 days at 30–190 °C. Optical and scanning electron microscopy showed no changes to the original biomineral ultrastructures after the experiments. Bulk isotope measurements show that isotope exchange is linear with respect to the square root of time, which suggests a diffusive mechanism. Additionally, high temperature experiments reveal that isotope exchange plateaus after about 2 to 3% of the oxygen in a biomineral has exchanged, implying that biominerals contain a small but rapidly exchangeable reservoir of grain boundary oxygen. This reservoir will approach an isotopic equilibrium with any surrounding pore fluids in <100 years at any temperature over 0 °C.

Our results demonstrate that biominerals can rapidly exchange with pore fluids at low temperatures and on geologically short timescales. This reequilibration can bias paleotemperatures derived from biomineral $\delta^{18}O$ values and requires that these records be corrected for the effects of grain boundary diffusion.

3.2
Anoxic conditions of Proterozoic deep oceans: Evidence from recycled sediments in plume-influenced MORBs.

Qasid Ahmad[1], Martin Wille[1], Carolina Rosca[2], Jabrane Labidi[3], Stephan König[4]

[1] Insitute of Geological Sciences, University of Bern, Baltzerstrasse 1+3, CH-3012 Bern (qasid.ahmad@geo.unibe.ch)
[2] Isotope Geochemistry, Department of Geosciences, University of Tübingen, Schnarrenbergstrasse 94-96, DE-72076 Tübingen
[3] Université de Paris, Institut de physique du globe de Paris, CNRS, Paris, France
[4] Instituto Andaluz de Ciencias de la Tierra (IACT), CSIC & UGR, Avenida las Palmeras 4, Armilla, 18100 Granada, Spain

Subduction of ancient mafic oceanic crust and sediments is considered a major cause of the large-scale chemical heterogeneity in Earth's mantle. This is inferred from studies of mid-ocean ridge basalts (MORB) and ocean-island basalts (OIB), which show a large variability in their geochemical and isotope signatures.

Under present day oxidizing conditions, a light Mo isotope composition (down to δ98/95Mo = -1.5 ‰) compared to the depleted mantle (δ98/95Mo = -0.2 ‰) is preferentially retained in the residual subducted slab entering the deep mantle, where it is potentially recycled into the mantle source of OIBs (1, 2) such as oceanic crust and marine sediments, contribute to the Mo isotope signature of arc magmas and, hence, exert different controls on the terrestrial Mo cycle. Here we investigate Mo isotope systematics from input to output at the Tongan subduction zone: Arc lavas from different Tongan islands, pelagic sediments and altered oceanic crust (AOC. This is thought to reflect the redox—dependant aqueous mobility of Mo, causing Mo isotopic fractionation between different reservoirs before and during subduction. Molybdenum isotope ratios (δ98/95Mo) can therefore constrain the nature of recycled components in source of OIBs.

In this study, we present new Mo isotope data for MORB that partly interact with enriched mantle plumes. An increase towards heavier Mo isotopic values of up to -0.10 ‰ in δ98/95Mo is observed from the most depleted samples towards samples tapping a more enriched mantle source. The observed correlations between δ98/95Mo and radiogenic isotopes of Sr and Nd indicate recycling of sedimentary components with Mo isotopic composition that was not altered by Mo mobility under oxidizing conditions. Instead our new Mo isotope data, supporting and expanding on previous Se isotope evidence (3), suggest non-oxidizing conditions during deep sea sediment deposition and subduction metamorphism in the Proterozoic.

REFERENCES

1. Q. Ahmad, et al., The Molybdenum isotope subduction recycling conundrum: A case study from the Tongan subduction zone, Western Alps and Alpine Corsica. Chem. Geol. 576, 120231 (2021).
2. R. M. Gaschnig, et al., The impact of primary processes and secondary alteration on the stable isotope composition of ocean island basalts. Chem. Geol. 581, 120416 (2021).
3. A. Yierpan, S. König, J. Labidi, R. Schoenberg, Recycled selenium in hot spot–influenced lavas records ocean-atmosphere oxygenation. Sci. Adv. 6, eabb6179 (2020).

3.3
^{53}Mn-^{53}Cr chronological and ε^{54}Cr-Δ^{17}O geneological constrains on Erg Chech 002 parent body: source of the oldest andesite in the Solar System

Aryavart Anand[1], Pascal M. Kruttasch[1], Klaus Mezger[1]

[1] *Institut für Geologie, Universität Bern, Baltzerstrasse 1+3, 3012 Bern, Switzerland (aryavart.anand@geo.unibe.ch)*

Erg Chech 002 (EC 002) is the oldest magmatic rock analyzed to date and presents a unique opportunity to study the formation of felsic crusts that covered the earliest formed protoplanets after metal-silicate equilibration or core formation [Barrat et al., 2021]. Magmatic iron meteorites that represent the cores of such differentiated bodies have been extensively studied using ^{182}Hf-^{182}W chronometry [e.g., Kruijer et al., 2017] and more recently by ^{53}Mn-^{53}Cr systematics [Anand et al., 2021] and have dated the timing of metal segregation in magmatic iron meteorite parent bodies within 2.5 Myr after CAIs. This agrees with the ^{26}Al-^{26}Mg internal isochron defined by feldspars and pyroxenes in EC 002, giving an age of 2.255 Myr after CAIs, assuming a homogeneous distribution of ^{26}Al with an initial ^{26}Al/^{27}Al ratio of 5.23×10^{-5}; or 1 Myr after CAIs when anchored to the ^{26}Al chronology of D'Orbigny angrite [Barrat et al., 2021]. The short-lived ^{53}Mn-^{53}Cr ($t_{1/2} \approx 3.7$ Ma) chronometer can shed further light on the timing and extent of the formation process of a primitive igneous crust on the EC 002 parent body.

Manganese and Cr are minor elements in EC 002 components and these have variable and high Mn/Cr ratios, making them suitable for dating by constructing an isochron. Alternatively, the Cr isotopes can be used to obtain precise ''model ages" for chromite with a Mn/Cr ratio near zero. An additional advantage of Cr isotope study is that when combined with Δ^{17}O values, ε^{54}Cr-Δ^{17}O can provide a means for identifying the isotopic source reservoir of the parent body.

Here, we report on ^{53}Mn-^{53}Cr chronometry of EC 002 meteorite using both the isochron and model age approach. The chromite model age is in good agreement with the previously determined ^{26}Al-^{26}Mg age, however, the chromite-bulk rock-silicate-isochron gives an older age, possibly because of disturbances due to differences in the closure temperature of multiple phases and/or disturbance during core-formation processes. The ε^{54}Cr-Δ^{17}O data suggest EC 002 originates from the non-carbonaceous (NC) reservoir and point to its formation near the source reservoir of the acapulcoite-lodranite clan.

REFERENCES

[1] Barrat, J. A., Chaussidon, M., Yamaguchi, A., Beck, P., Villeneuve, J., Byrne, D. J., Broadley, M. W. and Marty, B. 2021: A 4,565-My-old andesite from an extinct chondritic protoplanet, PNAS 118(11).

[2] Kruijer, T. S., Burkhardt, C., Budde, G. and Kleine, T. 2017: Age of Jupiter inferred from the distinct genetics and formation times of meteorites, PNAS 114(26), 6712–6716.

[3] Anand, A., Pape, J., Wille, M., Mezger, K. and Hofmann, B. 2021: Early differentiation of magmatic iron meteorite parent bodies from Mn-Cr chronometry, submitted.

3.4
Strontium isotope analyses of matrix apatite and apatite incluions in zircon constrain the evolution of the Paleoarchean Singhbhum Craton

Sukalpa Chatterjee[1], Om Prakash Pandey[2], Klaus Mezger[1], Melanie Kielman-Schmitt[3], Ellen Kooijman[3]

[1] Institut für Geologie, Universität Bern, Baltzerstrasse 1+3, 3012 Bern, Switzerland
[2] Department of Earth Sciences, Indian Institute of Technology Kanpur, Kanpur 208016, India
[3] Department of Geosciences, Swedish Museum of Natural History, Stockholm, Sweden

The Rb-Sr isotope system is much more sensitive to mantle melting and fractionation processes than the Sm-Nd and Lu-Hf systems [1]. This strong Rb-Sr fractionation during geological processes can provide a higher temporal resolution for different differentiation processes and improve the understanding of Archean mantle differentiation. However, the strong fractionation can make it difficult to obtain precise initial Sr-isotope composition of rocks. In addition, the Rb-Sr isotope system is highly susceptible to later modification by alteration and metamorphic overprinting. Therefore, the application of Rb-Sr systematics in Archean rocks has not gained much attention. However, apatite has near zero Rb/Sr thus it has the potential to preserve its initial $^{87}Sr/^{86}Sr$, making it a suitable mineral to probe Archean crust-mantle evolution. Recent developments in in-situ techniques [2] are showing their suitability to obtain well-preserved initial $^{87}Sr/^{86}Sr$ in matrix apatite and apatite inclusions within zircon in Archean rocks.

A new laser ablation multi-collector inductively coupled plasma mass spectrometry method [2] was used to analyse matrix apatite and apatite inclusions in zircon in rocks from different lithological units of the Paleoarchean Singhbhum Craton (India) to obtain the best preserved initial $^{87}Sr/^{86}Sr$. Precision of up to 1□ (2SD of mean) unit was achieved on MAD apatite standard. A particular data filtering process has been applied to derive the least radiogenic Sr-isotope ratios, eliminating recrystallized and reset apatite grains with higher initial $^{87}Sr/^{86}Sr$ values. Lowest values from each of the samples were grouped for a representative initial value of a particular sample. Apatite inclusions in zircon systematically preserve less radiogenic initial $^{87}Sr/^{86}Sr$ values than their matrix counterpart, which advocates towards their chemically primary nature and efficiency in preserving initial $^{87}Sr/^{86}Sr$ ratios. Derived Rb/Sr ratios of the source coupled with initial $^{87}Sr/^{86}Sr$, constrains the Sr isotopic evolution of the craton and the mantle beneath.

Initial $^{87}Sr/^{86}Sr$ data from apatite of the 3.44 to 3.20 Ga Singhbhum granitoids show extraction either from a depleted mantle source with Rb/Sr of ~0.2 at 3.5 Ga or formation due to reprocessing of a mafic precursor with 49% SiO_2 and maximum age of 3.77 Ga. Irrespective of the process, the data indicates that no significant amounts of (mafic) crust older than 3.8 Ga was involved in formation of the voluminous Singhbhum granitoid suite and that the crustal rocks of the craton formed within a very narrow window of 200 Ma with very short crustal residence time.

REFERENCES

[1] Dhuime, B., Wuestefeld, A., & Hawkesworth, C. J. (2015). Emergence of modern continental crust about 3 billion years ago. Nature Geoscience, 8(7), 552-555.

[2] Emo, R. B., Smit, M. A., Schmitt, M., Kooijman, E., Scherer, E. E., Sprung, Peter., Bleeker, Wouter., & Mezger, K. (2018). Evidence for evolved Hadean crust from Sr isotopes in apatite within Eoarchean zircon from the Acasta Gneiss Complex. Geochimica et Cosmochimica Acta, 235, 450-462.

3.5
How to identify seafloor anoxia using carbonate U isotopes, despite oxidative diagenesis

Matthew O. Clarkson[1], Rick Hennekam[1,2], Tim C. Sweere[1], Morten B. Andersen[3], Gert-Jan Reichart[2,4] and Derek Vance[1]

[1] *Institut für Geochemie und Petrologie, ETH Zürich, Clausiusstrasse 25, CH-8092 Zürich (matthew.clarkson@erdw.ethz.ch)*
[2] *Department of Ocean Systems, NIOZ Royal Netherlands Institute for Sea Research, 't Horntje 1797 SZ, The Netherlands.*
[3] *School of Earth and Environmental Sciences, University of Cardiff, Cardiff, CF10 3AT, UK*
[4] *Department of Earth Sciences, Utrecht University, 3584 CB, Utrecht, the Netherlands*

The interpretation of local redox indicators in marine sediments relies on their preservation. By their nature, such biogeochemical tracers are susceptible to diagenetic alteration, particularly through post-depositional re-oxidation of the sediment. This can result in the mobilization and loss of distinctive redox dependant signatures, leading to the classical problem that the presence of oxygenated conditions cannot be robustly inferred by the absence of evidence for anoxia.

Authigenic uranium enrichments, and their isotope signatures ($\delta^{238}U$), are widely used to infer bottom-water and pore-water redox conditions but are susceptible to later oxidative diagenetic disturbance. Here we explore the preservation of authigenic $\delta^{238}U$ signatures in sediment samples from Sapropel S1 at Site 64PE406-E1 in the Eastern Mediterranean Sea, which was originally deposited under reducing conditions but severely affected by later oxidative diagenesis and the variable loss of authigenic U(IV) from the upper sapropel.

To this end, we compare U isotope signatures from bulk measurements ($\delta^{238}U_{bulk}$) with detrital corrected authigenic U ($\delta^{238}U_{auth}$) and carbonate associated U ($\delta^{238}U_{CAU}$). In contrast to open ocean carbonates deposited under fully oxic conditions and record seawater $\delta^{238}U$, sapropelic carbonate leachates yield $\delta^{238}U_{CAU}$ similar to calculated $\delta^{238}U_{auth}$, thus recording (predominantly) redox dependant isotope fractionation.

There is no evidence for significant isotope fractionation resulting from post-depositional oxidative diagenesis, but associated authigenic U(IV) removal results in larger relative detrital contributions to $\delta^{238}U_{bulk}$, and hence large uncertainties on $\delta^{238}U_{auth}$ estimates. By contrast, $\delta^{238}U_{CAU}$ successfully avoids detrital phases, and the uncertainty associated with detrital corrections, providing a primary record of changes in local redox conditions. Thus, we propose that $\delta^{238}U_{CAU}$ can be used for accurate reconstructions of benthic de-oxygenation in sediments with low U enrichments, including sediments with post-depositional U(IV) loss and less reducing environments.

3.6
Source-to-sink molybdenum (Mo) variability in the ultramafic bedrock-dominated catchment of Lake Towuti, Indonesia

Adrianus Damanik[1,2], Martin Wille[1], Qasid Ahmad[1], Martin Grosjean[2,3], Sri Yudawati Cahyarini[4], Hendrik Vogel[1,2]

[1] *Insitute of Geological Sciences, University of Bern, Baltzerstrasse 1+3, CH-3012 Bern (adrianus.damanik@geo.unibe.ch)*
[2] *Oeschger Centre for Climate Change Research, University of Bern, Hochschulstrasse 6, CH-3012 Bern*
[3] *Insitute of Geography, University of Bern, Hallerstrasse 12, CH-3012 Bern*
[4] *Paleoclimate & Paleoenvironment Research Group-Research Center of Geotechnology, Indonesian Insitute of Sciences (LIPI), Sangkuriang, ID-40135 Bandung*

Molybdenum (Mo) isotopes are known as sensitive recorders for changes in redox conditions in paleo-marine environments. In lake systems, the small dissolved Mo reservoir and the shorter Mo residence time require further investigation of Mo isotopic fractionation processes from source to sink to identify the impact of potential paleoenvironmental changes on Mo isotopic composition in lake sediments over time. Here we present Mo isotope and concentration data from (1) laterite profiles overlying ultramafic bedrock (source); (2) lake surface sediments (sink) and (3) a ~30 kyr downcore sediment succession (sink) from Lake Towuti, Indonesia. Variations in Mo concentration in Lake Towuti surface sediments can partly be explained by hydraulic sorting and deposition of fine, Mo-enriched lateritic detritus. However, higher Mo concentrations, particularly in the deeper, anoxic parts of the basin, compared to Mo concentrations measured in laterite and bedrock samples point towards an authigenic Mo enrichment from the water column. This is in line with an overall lighter and highly variable Mo isotope composition in lake sediments as compared to bedrock and laterite values. Interestingly, Mo isotope variability observed in Lake Towuti surface sediments is primarily a function of water depth, with Mo isotope composition from shallow, well-oxygenated sites being lighter and those originating from the deeper, anoxic parts of the basin being heavier. Likewise, sediments deposited under drier and colder climate conditions of the last glacial exhibit Mo isotope signatures similar to today's oxygenated shallow water sites making Mo isotope compositions a valuable quantitative indicator of past water column oxygenation.

3.7
Re-assessing the influence of particle-hosted sulphide formation on the marine cadmium cycle

Gregory F. de Souza[1], Derek Vance[1], Matthias Sieber[2], Tim M. Conway[2], Susan H. Little[3]

[1] ETH Zurich, Institute of Geochemistry and Petrology, Clausiusstrasse 25, CH-8092 (desouza@erdw.ethz.ch)
[2] College of Marine Science University of South Florida, St. Petersburg FL, USA
[3] Department of Earth Sciences, University College London, London, UK

It has been inferred that the marine distributions of the micronutrient cadmium (Cd) and its stable isotope composition (expressed as δ^{114}Cd) bear widespread and unambiguous evidence for loss of Cd from the water column through the formation of solid cadmium sulphide (CdS) in oxygen minimum zones (OMZs; Janssen et al., 2014). Recent research has suggested that this particle-hosted CdS formation may represent the largest Cd sink term in its whole-ocean budget (Guinoiseau et al., 2019). Here, by bringing together previously-published elemental and isotopic datasets from the dissolved and particulate Cd pools, we unravel the multiple, overlapping controls on the Cd and δ^{114}Cd distributions, demonstrating that the data challenge this view.

Our analysis reveals that the most important control on the marine Cd distribution is the extreme plasticity in the cadmium:phosphorus (Cd:P) stoichiometry of biological uptake, and thus particulate export. We show that the δ^{114}Cd systematics in low-latitude OMZs that have been taken to reflect Cd loss in fact mainly come about through the interaction between the physical circulation and the stoichiometric plasticity of biological Cd uptake at high and low latitudes. Water-column evidence for Cd loss is thus much less widespread than has previously been inferred.

Subtle but consistent signals in particulate elemental and dissolved isotopic data from the tropical Atlantic and Pacific Oceans do allow us to identify the signal of a Cd loss associated with the oxycline of the shallow tropical subsurface, as has been previously suggested (e.g. Janssen et al., 2014; Conway and John, 2015; Guinoiseau et al., 2019; Ohnemus et al., 2019; Xie et al., 2019). However, this Cd loss appears to be ubiquitous throughout the tropics, rather than confined to oxygen-poor waters, speaking against CdS formation as a driving mechanism. Although its true identity remains unknown, this tropical Cd loss may be related to biological activity. Most generally, our analysis bears upon the contribution of particle-hosted CdS formation to the whole-ocean mass balance of Cd, which is likely to be much smaller than recent estimates have suggested.

REFERENCES

Conway, T. M., & John S. G. 2015: Biogeochemical cycling of cadmium isotopes along a high-resolution section through the North Atlantic Ocean, Geochimica et Cosmochimica Acta, 148, doi: 10.1016/j.gca.2014.09.032.

Guinoiseau, D. et al. 2019: Importance of cadmium sulfides for biogeochemical cycling of Cd and its isotopes in oxygen deficient zones – a case study of the Angola Basin, Global Biogeochemical Cycles, 33, doi: 10.1029/2019GB006323.

Janssen, D. J. et al. 2014: Undocumented water column sink for cadmium in open ocean oxygen-deficient zones, PNAS, 111, doi: 10.1073/pnas.140238111.

Ohnemus, D. et al. 2019: Exposing the distributions and elemental associations of scavenged particulate phases in the ocean using basin-scale multi-element data sets, Global Biogeochemical Cycles 33, doi: 10.1029/2018GB006145.

Xie, R. C. et al. 2019: Limited impact of eolian and riverine sources on the biogeochemical cycling of Cd in the tropical Atlantic, Chemical Geology, 511, doi: 10.1016/j.chemgeo.2018.10.018.

3.8
Heavy Fe isotope signatures in micropyrites at the Smithian-Spathian boundary (Early Triassic)

Marie-Noëlle Decraene[1], Johanna Marin-Carbonne[1], Christophe Thomazo[2], Anne-Sophie Bouvier[1], Arnaud Brayard[2], Nicolas Olivier[3]

[1] *ISTE, Université de Lausanne, Switzerland (marie-noelle.decraene@unil.ch)*
[2] *Biogéosciences, Université de Bourgogne Franche Comté, Dijon, France*
[3] *LMV, Université Clermont Auvergne, Clermont-Ferrand, France*

The Early Triassic is a period marked of biotic crisis linked to environmental disturbances, such as oceanic redox changes, ocean acidification and strong temperature variations, after the end Permian mass extinction. These perturbations highly impacted geochemical cycles (O, C, S, N) that recorded isotopic swings, especially at the Smithian-Spathian boundary (SBB). However shallow environments were described to preserve favorable conditions for flourishing ecosystems. We propose here to explore regional paleoredox changes and the possible influence of biotic crisis through the analyze of iron isotopes in micropyrites from the Lower Webber Canyon (LWC) section in Utah. The depositional environment of the LWC section reflects a ramp system along which we analyzed, using SIMS technique, 8 samples representing 3 lithologies (siltstones, bioclastic limestones and silty marls). Large δ^{56}Fe fluctuations (~6‰) were evidenced from the late Smithian to the early Spathian, consistent with a local enhanced preservation of organic matter in microbial induced sedimentary structures deposited during the late Smithian and bioclastic limestones of the SSB. These results suggest a partial control of the depositional environment, as well as organic matter concentrations that is directly linked to microbial activity, on the iron cycling through the Smithian-Spathian crisis interval.

3.9
The oceanic budget of nickel: new concentration and isotope data from Mn-rich pelagic sediments

Sarah Fleischmann[1], Aditi Chatterjee[1], Jim McManus[2], Sridhar D Iyer[3] and Derek Vance[1]

[1]Institut für Geochemie und Petrologie, ETH Zürich, Clausiusstrasse 25, 8092 Zürich (sarah.fleischmann@erdw.ethz.ch)
[2]Bigelow Laboratory for Ocean Sciences, Maine, USA
[3]CSIR-National Institute for Oceanography, Dona Paula, Goa 403004, India

Nickel (Ni), like many other transition metals, plays an important role in ocean biogeochemistry (Archer et al., 2020). Recently, the advances in analyzing Ni isotopes (δ^{60}Ni), have opened new perspectives for their development as a tracer of the chemistry of past ocean environments. This application, however, requires, an understanding of its modern oceanic budget and biogeochemical cycling (Little et al., 2020; Vance et al., 2016).

The Ni isotope compositions of known inputs are lighter (+0.8‰) than Ni in the oceanic dissolved pool (+1.3‰), while most of the sedimentary outputs are isotopically similar to or heavier than seawater, resulting in an imbalance in the Ni budget in the ocean. Since there is no evidence for non-steady-state behavior of Ni, balancing the Ni budget requires an isotopically heavy Ni input or an isotopically light output flux, or both (Little et al., 2020; Vance et al., 2016). The heavy Ni sorbed to Fe-Mn crusts (+1.6‰) has been used as a proxy for the isotopic composition of the Fe-Mn oxide output flux of Ni from the dissolved pool of the ocean, creating the budgetary problem mentioned above. New data from Little et al. (2020) for Mn-rich oxide sediments from the eastern Pacific, however, show very light Ni isotopes (-0.2 to -0.8‰) compared to Fe-Mn crusts. These light signatures are attributed to diagenetic remobilization of isotopically heavy Ni, which could possibly lead to a heavy benthic Ni flux that would balance the oceanic budget.

In order to assess the extent to which the results from these sediments is general, we present new Ni data from Mn-rich pelagic sediments from different sites at different depths across the Pacific and from the Indian ocean. Nickel is enriched in these samples (~80-500 ppm), with little variation in data from the same site, and concentrations are of the same magnitude as the data presented by Little et al. (2020). The Ni isotope composition in our samples is generally lighter (δ^{60}Ni = 0.25-1.04‰) than seawater δ^{60}Ni (+1.3‰), but heavier than those in Little et al. (2020). Further analyses will investigate these site-specific δ^{60}Ni, including their relationship with diagenetic conditions driven by variable carbon oxidation rates. But, overall, the finding by Little et al. (2020), that the output flux of Ni associated with Mn oxides is in fact lighter than seawater, appears to be general.

REFERENCES

Archer, C., Vance, D., Milne, A., & Lohan, M. C. (2020). The oceanic biogeochemistry of nickel and its isotopes: New data from the South Atlantic and the Southern Ocean biogeochemical divide. Earth and Planetary Science Letters, 535, 116118.

Little, S., Archer, C., McManus, J., Najorka, J., Wegorzewski, A., & Vance, D. (2020). Towards balancing the oceanic Ni budget. Earth and Planetary Science Letters, 547, 116461.

Vance, D., Little, S. H., Archer, C., Cameron, V., Andersen, M. B., Rijkenberg, M. J., & Lyons, T. W. (2016). The oceanic budgets of nickel and zinc isotopes: the importance of sulfidic environments as illustrated by the Black Sea. Philosophical Transactions of the Royal Society A: Mathematical, Physical and Engineering Sciences, 374(2081), 20150294.

3.10
Local Melt Contamination and Global Climate Impacts: Geochronology of Karoo LIP Sills in Organic-Rich Shales

Sean P. Gaynor[1], Henrik H. Svensen[2], Stépane Polteau[2], Urs Schaltegger[1]

[1] *Earth Sciences, University of Geneva, Rue des Maraîchers 13, CH-1205 Genève (urs.schaltegger@unige.ch)*
[2] *Centre for Earth Evolution and Dynamics (CEED), University of Oslo, P.O. Box 1028, Blindern, 0315, Oslo, Norway*

Eruptions of Large Igneous Provinces (LIP) are commonly correlated with global climate change, and environmental and biological crises. However, establishing a causative link via chemical and physical proxies for global change is more complicated and often ambiguous. As technical improvements have allowed for increasingly higher precision dates, especially in U/Pb dating, it is possible to better test hypotheses connecting LIP's and environmental impact via their contemporaneity. Here, we focus on the early Jurassic period, which includes a period of global change known as the Toarcian oceanic anoxic event (TOAE), as well as the emplacement of the Karoo Large Igneous Province (K-LIP).

The K-LIP is comprised of a suite of basaltic lava flows, sills, dike swarms, centered in southern Africa. Approximately 340,000 km^3 of sills are interlaid within the Karoo Basin, and therefore served as significant heat source to the basin upon emplacement. While much of the sedimentary rocks of the basin are siliciclastic, the Permian Ecca Group contains organic-rich facies and hosts 160,000 km^3 of basaltic sills. Previous mass balance calculations indicate that between 7,000 and >50,000 Gt of CO_2 equivalents was released through metamorphic reactions of these shale bodies in contact aureoles within the Ecca Group. If intrusive magmatism was short lived within this formation than this event could represent a mechanism to drive a short pulse of global climate change due to rapid volatilization and degassing from the shales. Previous studies have shown that intrusions are coeval with the TOAE, however higher-precision geochronology data from the sills is necessary to determine if the flux and timing of thermogenic gases from the basin was sufficient to destabilize Earth's climate. In order to test the hypothesis, we present single crystal zircon and baddeleyite U-Pb dates and Hf isotopic compositions from sills across the Ecca Group. These data indicate that high-precision geochronology of intrusive LIP can be complicated by both inheritance and Pb-loss, and the thermogenic gas release of Ecca Group wall rocks was likely a rapid process, on the scale of 10's of ka, and therefore is a viable trigger for the observed environmental change during the Toarcian.

3.11
Chromium cycling in euxinic basins: Implications for the $\delta^{53}Cr$ paleoredox proxy from a modern system (Lake Cadagno, Ticino, Switzerland).

David J. Janssen[1,2], Jörg Rickli[1,3], Martin Wille[1], Christel S. Hassler[4,5], Hendrik Vogel[1,2], Samuel L. Jaccard[1,2,6]

[1] *Institute of Geological Sciences, University of Bern, Bern, Switzerland (corresponding author: janssen.davej@gmail.com)*
[2] *Oeschger Centre for Climate Change Research, University of Bern, Bern, Switzerland*
[3] *Institute of Geochemistry and Petrology, ETH Zürich, Zürich, Switzerland*
[4] *Department F.-A. Forel for Environmental and Aquatic Sciences, University of Geneva, Geneva, Switzerland*
[5] *Swiss Polar Institute, Sion, Switzerland*
[6] *Institute of Earth Sciences, University of Lausanne, Lausanne, Switzerland*

Chromium is present in two primary oxidation states in surface waters and marine and lacustrine sediments: the oxidized Cr(VI) and the reduced Cr(III) species. Due to the strong influence of redox cycling on Cr concentrations ([Cr]) and stable isotope distributions ($\delta^{53}Cr$), Cr has gained prominence as a potential paleoredox proxy. The fundamental underlying theory behind these applications – Cr(VI) is highly soluble, while Cr(III) is poorly soluble and readily scavenged onto particles, and redox cycling results in an enrichment of isotopicaly light Cr in Cr(III) – is generally supported by lab and field studies. However, few data for more direct assessments from modern anoxic systems are available. The meromictic Lake Cadagno (Ticino, Switzerland) has been used as a modern analog for euxinic systems throughout Earth's history to better understand geochemical cycling and paleoproxy applications. With this motivation, here we present $\delta^{53}Cr$ and [Cr] in Lake Cadagno from the water column and near-surface sediments. The euxinic monimolimnion is enriched in [Cr] relative to overlying oxic waters, in contrast to expectations from Cr(VI) and Cr(III) solubility. While dissolved $\delta^{53}Cr$ in euxinic water column samples is isotopically light relative to overlying oxic waters, deep waters are isotopically heavy relative to sediments. Furthermore, sediment $\delta^{53}Cr$ is indistinguishable from average upper continental crust $\delta^{53}Cr$. These data have important implications for [Cr] and $\delta^{53}Cr$ paleoproxy applications – namely that Cr may not be efficiently sequestered into sediments in euxinic systems, and that reconstructions of water column $\delta^{53}Cr$ from euxinic sediments may require additional corrections, which are unconstrained at present.

3.12
Temporal and spatial constraints on the ureilite-forming region inferred from Cr isotopes

Pascal M. Kruttasch[1], Aryavart Anand[1], Klaus Mezger[1]

[1] *Institut für Geologie, Universität Bern, Baltzerstrasse 1+3, 3012 Bern, Switzerland (pascal.kruttasch@geo.unibe.ch)*

The formation and evolution of meteorite parent bodies and their spatial distribution play a critical role in establishing early solar system processes and their chronology. The time difference between the accretion of the earliest differentiated meteorite parent bodies and most chondrite meteorite parent bodies is greater than ~2 Ma (e.g. Kruijer et al., 2014; Hellmann et al., 2019) with intermediate accretion ages of the ureilite parent bodie(s) at 1.4-1.7 Ma relative to CAI, as inferred by Hf-W chronometry (Budde et al., 2015).

Ureilites are ultramafic, carbon-rich primitive achondrites, highly depleted in feldspar-rich magma and sulfur-rich iron melt. However, despite their igneous textures, ureilites exhibit variable silicate compositions (e.g., Fo75 to Fo96) and show mass-independent isotope heterogeneities in O and ^{54}Cr, indicating incomplete equilibration of the ureilite parent body (UPB) or origin from more than one parent body. In order to investigate temporal and spatial constraints on the ureilite-forming region, Cr isotope systematics were applied to acid-leachates and chromite-silicate separates of a suite of monomict ureilites. Chromium isotopes were analysed with high precision using Thermal Ionization Mass Spectrometry (TIMS) at the University of Bern.

Internal ^{53}Mn-^{53}Cr isochrons of acid-leachates of individual ureilites are consistent with the chromite-bearing ureilite NWA 766 previously analysed by Yamakawa et al., (2010). Separated chromite grains with Mn/Cr ratios of ~0.01 and ε^{53}Cr $\approx$ -0.06, suggest an average Cr model age of ~3.3 Ma after CAI formation, asuming initial ^{53}Cr and ^{53}Mn abundances of the Solar System and chondritic Mn/Cr ratios reported in Anand et al., (2021). The variation in ε^{54}Cr ranges for individual ureilites from 1.0 to -0.6 and correlates with Mg# in olivine cores but exhibit internal homogeneity. The ε^{54}Cr-values are the lowest determined in any known meteorite group and suggest formation in the non-carbonaceous chondrite (NC) reservoir. Thus, the ureilites represent possibly a spatial endmember of the NC-reservoir.

REFERENCES

Anand, A., Pape, J., Wille, M., Mezger, K. 2021: Chronological constraints on the thermal evolution of ordinary chondrite parent bodies from the 53Mn-53Cr system, Geochimica et Cosmocimica Acta, 307, 281-301.

Budde, G., Kruijer, T.S., Fischer-Gödde, M., Irving, A. J. & Kleine, T. 2015: Planetesimal differentiation revealed by the Hf–W systematics of ureilites, Earth and Planetary Science Letters, 430, 316-325.

Hellmann, J. L., Kruijer, T. S., Van Orman, J. A., Metzler, K. & Kleine, T. 2019: Hf-W chronology of ordinary chondrites, Geochimica et Cosmocimica Acta, 258, 290-309.

Kruijer, T. S., Touboul, M., Fischer-Gödde, M., Bermingham, K. R., Walker R. J. & Kleine, T. 2014: Protracted core formation and rapid accretion of protoplanets, Sience, 344, 1150-1154.

Yamakawa, A., Yamashita, K., Makishima, A. & Nakamura, E. 2010: Chromium isotope systematics of achondrites: chronology and isotopic heterogeneity of the inner solar system bodies, The Astrophysical Journal, 720, 150-154.

3.13
Inter-mineral iron and oxygen isotope fractionation in eclogites of the Münchberg Massif (Germany).

Johannes E. Pohlner[1], Afifé El Korh[1], Massimo Chiaradia[2], Catherine McCammon[3], Daniela Rubatto[4], Reiner Klemd[5], Bernard Grobéty[1]

[1] Unit of Earth Sciences, Department of Geosciences, University of Fribourg, Chemin du Musée 6, 1700 Fribourg (johannes.pohlner@unifr.ch)
[2] Department of Earth Sciences, University of Geneva, Rue des Maraîchers 13, 1205 Genève
[3] Bayerisches Geoinstitut, University of Bayreuth, Germany
[4] Institute of Geological Sciences, University of Bern, Baltzerstrasse 1+3, 3012 Bern
[5] GeoZentrum Nordbayern, Universität Erlangen-Nürnberg, Schlossgarten 5a, 91054 Erlangen, Germany

In the absence of strong fluid-rock interactions, stable isotopes of oxygen ($\delta^{18}O_{V\text{-}SMOW}$) and iron ($\delta^{56}Fe_{IRMM\text{-}524a}$) are thought to behave conservatively during subduction zone metamorphism. High-pressure minerals may attain isotopic equilibrium, and preserve it in case of limited diffusion. High-$Fe^{3+}/\Sigma Fe$ minerals tend to enrich heavy Fe isotopes compared to coexisting low-$Fe^{3+}/\Sigma Fe$ minerals, but Fe coordination can also play an important role. The relative contributions of these two factors are poorly known for high-pressure minerals. Here, we test eclogites (without metamorphic vein networks) from the Variscan Münchberg Massif for oxygen isotope equilibrium, and characterize Fe isotope fractionation between eclogite facies minerals.

All minerals in the eclogites are homogeneous in major elements, except garnet, which mostly shows gradual zonations (rimward enrichment in MgO and depletion in CaO; FeO and MnO zonation is less common). Spatially resolved analyses of garnet were obtained by SIMS ($\delta^{18}O$), and microdrilling followed by solution ICP-MS ($\delta^{56}Fe$). Other minerals were conventionally separated and analyzed by laser fluorination mass spectrometry ($\delta^{18}O$) and solution ICP-MS ($\delta^{56}Fe$).

Within ca. ±0.5‰ uncertainties (2σ), garnet from all samples is homogeneous in $\delta^{18}O$ values. $\delta^{18}O$ values of garnet, omphacite, amphibole, kyanite, zoisite, phengite, and quartz mostly agree with predicted values for temperatures around 670-700°C. In contrast, $\delta^{18}O$ values for rutile are always ~3‰ lower than predicted. Despite lacking oxygen isotope zonations, garnet is zoned in $\delta^{56}Fe$ values with core-to-rim increases by up to 0.3‰. Being the most reduced mineral in the assemblage ($Fe^{3+}/\Sigma Fe \leq 0.03$), garnet yielded $\delta^{56}Fe$ values 0.1-0.3‰ lower than than those of coexisting omphacite ($Fe^{3+}/\Sigma Fe = 0.07$–0.56) and amphibole ($Fe^{3+}/\Sigma Fe = 0.07$–0.28), but 0.1-0.4‰ higher than pyrrhotite ($Fe^{3+}/\Sigma Fe = 0.29$ as Fe_7S_8).

It seems that the eclogites did not undergo major metasomatic events during high-pressure metamorphism and essentially retained inter-mineral oxygen isotope equilibria, except for diffusional resetting of rutile. With oxygen isotope equilibrium preserved, the assemblage is expected to be in Fe isotope equilibrium as well. Given closed-system behavior, we ascribe the $\delta^{56}Fe$ zonation in garnet to Rayleigh fractionation. Iron isotope fractionation between garnet, omphacite, and amphibole may result from both the different Fe oxidation states and bonding environments, whereas the low $\delta^{56}Fe$ values of pyrrhotite reflect its low Fe-S bond strength.

3.14
Robustness of the bornite (Cu_5FeS_4) rhenium-osmium (^{187}Re–^{187}Os) geochronometer for the quantification of geological and hydrothermal processes – Constraints from microscale spatial distribution and mineralogical residency of rhenium

Nicolas J. Saintilan[1], Christoph Neff[2], Simone Delessert[2], Paolo A. Sossi[1], Peter M. Tollan[1], Marcel Guillong[1], Bodo Hattendorf[2], Julien M. Allaz[1], Sylvain Petitgirard[1], Daniel Ariztegui[3], Stefan Farsang[3], Cyril Chelle-Michou[1], Detlef Günther[2]

[1] *Institute of Geochemistry and Petrology, Department of Earth Sciences, ETH Zürich, Clausiusstrasse 25, 8092 Zürich, Switzerland (nicolas.saintilan@erdw.ethz.ch)*
[2] *Laboratory of Inorganic Chemistry, Department of Chemistry and Applied Biosciences, ETH Zürich, Vladimir-Prelog-Weg 1, 8093 Zürich, Switzerland*
[3] *Department of Earth Sciences, University of Geneva, Rue des Maraîchers 13, 1205 Geneva, Switzerland*

The viability of rhenium-osmium (Re-Os) geochronology as a benchmark technique for accurate and high-precision time stamps of geological processes requires the characterization of the residency of Re and Os in all potential host phases (e.g., sulfides, organic-rich shale). Beyond the robust Re-Os geochronometer in molybdenite (Stein et al., 2000; Selby and Creaser, 2004; Takahashi et al., 2007), the exploration of the residency of Re and Os in other sulfides suitable for Re-Os geochronometry is only beginning (e.g., pyrite; Hnatyshin et al., 2020). Here, we develop a workflow to quantify the distribution and abundance of Re in bornite (Cu_5FeS_4) by using molybdenum (Mo) as proxy. This stepwise workflow includes: (1) reflected/transmitted light microscopy; (2) X-ray diffraction of individual bornite mineral separates; (3) major, minor and trace element mineral chemistry by combined electron microprobe and laser ablation inductively coupled plasma sector field mass spectrometry (LA-ICP-SFMS) to study the correlation between Mo and Re contents; and (4) laser ablation inductively coupled plasma time-of-flight mass spectrometry (LA-ICP-TOFMS) to map the distribution of Re in bornite leading to quantified maps of Mo in this mineral (detection limit of ≈ 1 mg kg^{-1} for Mo).

The Re and Mo concentrations quantified from individual, 43-µm-wide, LA-ICP-SFMS spots defined robust linear correlations in all studied bornite samples. The LA-ICP-TOFMS intensity maps of Re mimic the quantified distribution maps of Mo in these bornite samples. Micro-inclusions of molybdenite were not observed in bornite whereas inclusions of chalcopyrite and germanium sulfides do not host significant amounts of Re or Mo (Fig. 1). Thus, in epigenetic bornite associated with solid bitumen in dolomitized limestone, we explore:

i. Whether tetravalent Mo(IV) and Re(IV) are captured in sub-micron-scale, Re-bearing Mo-Fe-S cuboidal clusters that are scavenged during bornite growth;
ii. Or the coupled distribution of Mo and Re indicates that Mo(IV) and Re(IV) might both occupy vacancies in tetrahedral interstices of the cubic and orthorhombic crystalline structures of bornite when it precipitated as hydrothermal fluids cooled below 230°C.

Our work lends credibility for accurate and high-precision bornite Re-Os isochron dates obtained previously, as geologically significant ages of giant metal accumulations hosted in sedimentary rocks (Saintilan et al., under review).

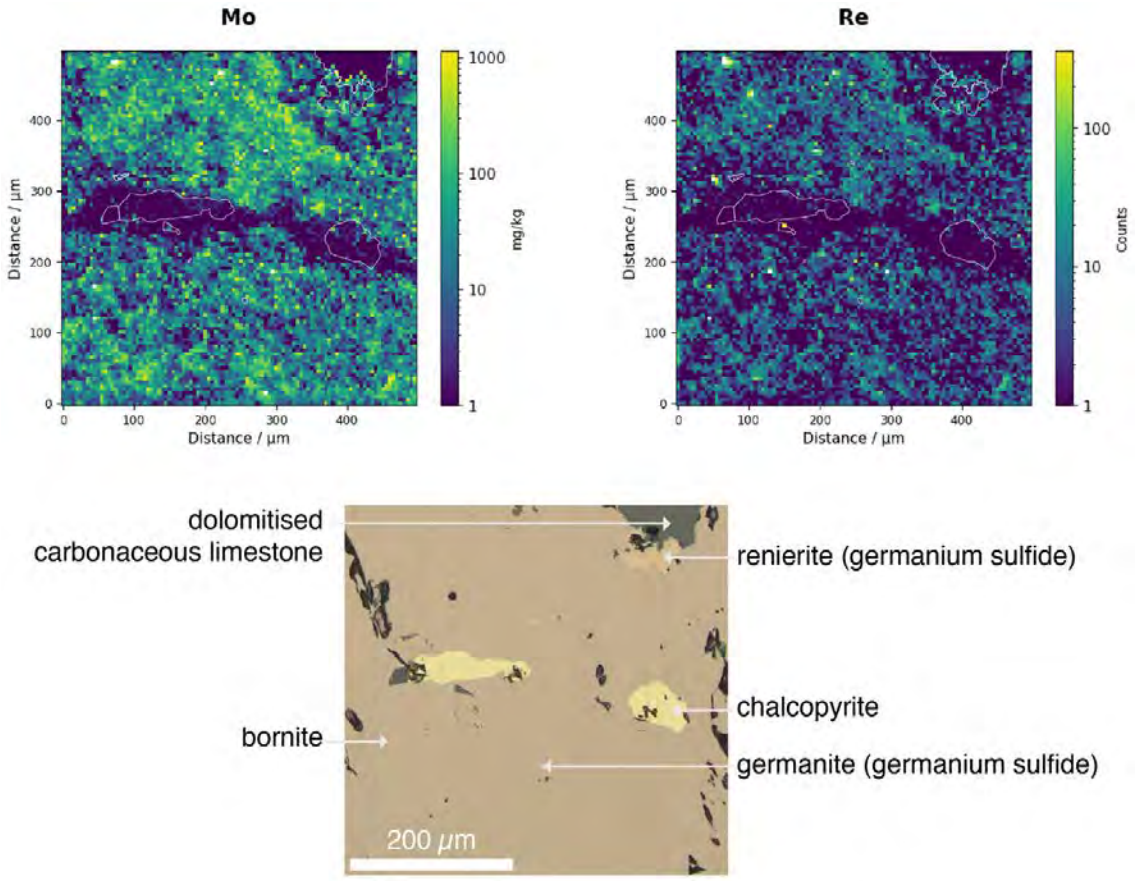

Figure 1. Sulfide paragenetic association (reflected light microscopy image of bornite sample ASK-03) compared with quantitative and qualitative maps of molybdenum (Mo) and rhenium (Re), respectively, generated by LA-ICP-TOFMS imaging of this sample. Laser ablation was carried out using a laser beam with a diameter of 5 µm represented each in one pixel.

REFERENCES

Hnatyshin, D., Creaser, R.A., Meffre, S., Stern, R.A., Wilkinson, J.J., & Turner, E.C., 2020: Understanding the microscale spatial distribution and mineralogical residency of Re in pyrite: Examples from carbonate-hosted Zn-Pb ores and implications for pyrite Re-Os geochronology. Chem. Geol. 533, 119427.

Saintilan, N.J., Archer, C., Maden, C., Samankassou, E., Bernasconi, S.M., Szumigala, D., Mahaffey, Z., West, A., & Spangenberg, J.E., under review at Nature Communications: Devonian greenhouse conditions drove giant metal accumulation in reef-bearing carbonate platform.

Selby, D. and Creaser, R.A., 2004: Macroscale NTIMS and microscale LA-MC-ICP-MS Re-Os isotopic analysis of molybdenite: testing spatial restriction for reliable Re-Os age determinations, and implications for the decoupling of Re and Os within molybdenite. Geochim. Cosmochim. Acta 68, 3897-3908.

Stein, H., Scherstén, A., Hannah, J., & Markey, R., 2003: Sub-grain scale decoupling of Re and 187Os and assessment of laser ablation ICP-MS spot dating in molybdenite. Geochim. Cosmochim. Acta 67, 3673-3686.

Takahashi, Y., Uruga, T., Suzuki, K., Tanida, H., Terada, Y., & Hattori, K.H., 2007: An atomic level study of rhenium and radiogenic osmium in molybdenite. Geochim. Cosmochim. Acta 71, 5180-5190.

3.15
New high-precision U-Pb zircon CA-ID-TIMS ages on the Paleoproterozoic Makganyene Formation, Griqualand West Basin, South Africa.

Senger, M.H.[1*]; Schaltegger, U.[1]; Rebeun, N.[2], Beukes, N.[2]

[1] *Department of Earth Sciences, University of Geneva, Rue de Marâichers 13, 1205 Geneva, Switzerland.*
[2] *Department of Geology, University of Johannesburg, Johannesburg, South Africa.*
** (martin.senger@etu.unige.ch)*

To improve the temporal correlation between changing environmental settings in the Paleoproterozoic and the Great Oxidation Event (GOE) at ca. ~2.4 Ga, we performed a detrital zircon study on six samples from glacial deposits of the Makganyene Formation, Griqualand West Basin, South Africa. It is hypothesized that these diamictites are the remnants of the oldest preserved Snowball Earth state. A potential overlap between this glacial period with the GOE makes this diamictite particularly interesting to evaluate links and causalities between both events.

The detrital zircon crystals were separated from hand and drillcore samples, which cover a large areal extent of the diamictites within the basin. Up to 150 zircon crystals per sample have previously been analyzed using laser ablation inductively coupled plasma mass spectrometry (LA-ICP-MS) techniques at University of Johannesburg, primarily to determine the maximum depositional age of these glacial sediments. At University of Geneva, we extracted zircon crystals with the youngest LA-ICP-MS dates from each sample, treated them with chemical abrasion, and analyzed the remaining zircon material with high precision and accuracy using isotope dilution thermal ionization mass spectrometry (ID-TIMS) technique. We take the result of the ID-TIMS method to be more robust, since the Pb loss bias has been significantly reduced.

The majority of the zircon crystals that defined an overly young ~2250 Ma peak from the LA-ICP-MS dating were completely dissolved after 4 hour of chemical abrasion at 210 °C. This observation indicates that the peak is possibly an artifact of Pb loss. Zircon crystals that survived the leaching procedure consistently returned older ages when analyzed with ID-TIMS; in many cases up to several tens to a hundred of millions of years. Moreover, the uncertainties of individual measurements were improved by one order of magnitude. All samples show a prominent, well-developed peak that spans from ~2460 to ~2480 Ma, which suggests that these zircons were likely sourced from the underlying upper Ghaap Group as previous work suggests. One sample (MAK-D), extracted nearby Griquatown, yielded multiple, concordant, single-grain analyses at 2420 Ma. Therefore, we confidently propose a new, robust, and reliable maximum depositional age of ~2420 Ma for the Makganyene Formation. We interpret this age to represent a post Snowball Earth state immediately after the melting and subsequent retreat of the hypothesized worldwide glaciation.

Our results support the already proposed hypothesis that the GOE pre-dates the Paleoproterozoic glaciations in the Griqualand West Basin. In addition, they also corroborate the age of the overlying Ongeluk lavas, and suggest that their extrusion was very fast within a few million years.

3.16
Sabkha dolomite as an archive for the magnesium isotope composition of seawater

Netta Shalev[1], Tomaso R.R. Bontognali[1,2,3], Derek Vance[1]

[1] *Institute of Geochemistry and Petrology, Department of Earth Sciences, ETH Zürich, Clausiusstrasse 25, CH-8092 Zurich* (*netta.shalev@erdw.ethz.ch*)
[2] *Space Exploration Institute, Faubourg de l'Hôpital 68, CH-2002 Neuchâtel*
[3] *Department of Environmental Sciences, University of Basel, Klingelbergstrasse 27, CH-4056 Basel*

Recent studies have uncovered the potential of Mg isotopes (δ^{26}Mg) for studying past ocean chemistry, but records of such data are still scarce. Dolomite has been suggested as a promising archive for δ^{26}Mg of seawater. However, its enigmatic formation mechanism and the difficulty in precipitating dolomite in the laboratory at surface temperatures decrease confidence in the interpretation of δ^{26}Mg values from the rock record. To evaluate factors determining the δ^{26}Mg of dolomite, we studied pore water and sediment from Dohat Faishakh Sabkha, Qatar – one of the rare environments where dolomite is currently forming. The δ^{26}Mg values of the dolomite (−2.56‰ to −1.46‰) are lower than that of seawater (−0.83‰), whereas δ^{26}Mg values of pore water (−0.71‰ to −0.14‰) are higher. The isotope fractionation accompanying dolomite formation is generally in accordance with an empirical fractionation from the literature, extrapolated to the sabkha's temperature (−1.84‰ to −1.51‰). The results suggest that evaporated seawater is the sole source of Mg, and isotopically light dolomite is the major sink, so that the δ^{26}Mg of the dolomite-forming pore water is equal to or greater than that of seawater. Thus, provided that the lowest δ^{26}Mg value among several dolomite samples is used, and the formation temperature is known, similar sabkha-type dolomites can be utilized as an archive for δ^{26}Mg values of ancient seawater.

REFERENCES

Shalev, N., Bontognali, T.R.R., & Vance D. 2021: Sabkha dolomite as an archive for the magnesium isotope composition of seawater, Geology, 49(3), 253–257.

3.17
Molybdenum and titanium isotopic data of arc derived differentiates and cumulates

Julian-Christopher Storck[1], Nicolas David Greber[1,2], Thomas Pettke[1] and Othmar Müntener[3]

[1] *Institute of Geological Sciences, University of Bern, Baltzerstrasse 1+3, CH-3012 Bern (julian.storck@geo.unibe.ch)*
[2] *Muséum d'histoire naturelle de Genève, Route de Malagnou 1, CH-1208 Genève*
[3] *Institute of Earth Sciences, University of Lausanne, Bâtiment Géopolis, CH-1015 Lausanne*

Differentiation of primitive basaltic magmas is a fundamental process contributing to the production of intermediate to silica-rich rocks and thus the continental crust. For many non-traditional stable isotope systems fractionation associated with igneous processes is documented, indicating their potential to (i) advance our understanding of magmatic differentiation, (ii) reconstruct past geodynamic regimes, and (iii) perform mass balance calculations for the amount of extracted continental crust (Teng et al. 2017).

The Mo and Ti isotope systems are particularly useful for such studies. The Mo isotopic composition of the upper continental crust (arc basalts and granites) is significantly heavier than the mantle, and Mo isotopes can therefore be used for mass balance calculations of the amount of extracted continental crust (McCoy-West et al. 2019). On the other hand, subduction-related and intraplate rocks have distinct Ti isotope signatures, making the δ^{49}Ti of magmatic rocks a potential proxy to reconstruct geodynamic settings of samples lacking such a context (e.g. Aarons et al. 2020; 2021). However, for both of these isotope systems important details for their stringent application to such questions are not well constrained. For example, Mo isotopes also fractionate during fractional crystallization, but data for the lower continental crust is not available, impacting mass balance calculations. For the Ti isotope system, the reason for the different composition of intraplate and subduction-related rocks is not well understood, partly because information about fractionation of Ti isotopes in mineral phases other than Fe-Ti oxides is rare. For both systems, data from cumulate rocks and rocks from the lower continental crust could help to overcome these unknowns, but these rock types are strongly understudied for the two isotopes systems.

We therefore present new Mo and Ti isotope data on calc-alkaline magmatic differentiation suites such as the Torres del Paine Intrusive Complex (TPIC, Patagonia) and compare their Mo and Ti isotope fractionation paths. The crustal derived mafic cumulates (hornblende gabbros, average $\delta^{98}Mo_{NIST} \approx -0.14 \pm 0.20$‰ (2 s.d.); $\delta^{49}Ti_{OL\text{-}Ti} \approx +0.01 \pm 0.06$‰) reported here are overall isotopically lighter than their granitic counterparts ($\delta^{98}Mo_{NIST} \approx +0.14 \pm 0.41$‰; $\delta^{49}Ti_{OL\text{-}Ti} \approx +0.45 \pm 0.03$‰), but heavier or identical to the depleted MORB mantle (DMM, $\delta^{98}Mo_{NIST} \approx -0.204 \pm 0.008$‰; $\delta^{49}Ti_{OL\text{-}Ti} \approx +0.002 \pm 0.007$‰).
The lack of Mo and Ti signatures lighter than DMM that would help to balance the isotopically heavy composition of felsic rocks may have several reasons: (i) the cumulates analyzed here may represent "late stage" relicts of progressive magma differentiation or (ii) they experienced overprinting (by mafic rejuvenation), while isotopically light and dense primary residuals remain (inaccessible) at deeper crustal levels. Large inter-sample spread in δ^{98}Mo contrasts the uniform δ^{49}Ti signatures of the mafic lithologies at TPIC, given the fact that one would expect some correlation between the two isotope systems as it is often suggested that Mo substitutes for Ti in oxides and eventually also silicate minerals. First order model calculations will show if this discrepancy can be the result of fractional crystallization or if additional processes need to be considered, such as sulfide segregation or metasomatism related to the redox sensitivity and fluid affinity of Mo.

REFERENCES

Aarons, S.M., Reimink, J.R., Greber, N.D., Heard, A.W., Zhang, Z. and Dauphas, N., 2020. Titanium isotopes constrain a magmatic transition at the Hadean-Archean boundary in the Acasta Gneiss Complex. Science advances, 6(50), p. eabc9959.

Aarons, S.M., Dauphas, N., Blanchard, M., Zeng, H., Nie, N.X., Johnson, A.C., Greber, N.D. and Hopp, T., 2021. Clues from Ab Initio Calculations on Titanium Isotopic Fractionation in Tholeiitic and Calc-Alkaline Magma Series. ACS Earth and Space Chemistry.

McCoy-West, A.J., Chowdhury, P., Burton, K.W., Sossi, P., Nowell, G.M., Fitton, J.G., Kerr, A.C., Cawood, P.A. and Williams, H.M., (2019): Extensive crustal extraction in Earth's early history inferred from molybdenum isotopes. Nature Geoscience, 12(11), 946-951.

Teng, F. Z., Dauphas, N., & Watkins, J. M. (2017). Non-traditional stable isotopes: retrospective and prospective. Reviews in mineralogy and geochemistry, 82(1), 1-26.

3.18
Titanium isotopes in detrital sediments: A reliable proxy for the protoliths composition?

Nicolas Vilela[1], Hendrik Vogel[1,2], Nicolas D. Greber[1,3]

[1] *Institut für Geologie, Universität Bern, Baltzerstrasse 1+3, CH-3012 Bern (nicolas.vilela@geo.unibe.ch)*
[2] *Oeschger Centre for Climate Change Research, Universität Bern, CH-3012 Bern*
[3] *Muséum d'histoire naturelle de Genève, Route de Malagnou 1, CH-1208 Genève*

In recent years Ti isotopes have received increasing attention as a tool to trace magmatic processes because the Ti isotopic composition of magmatic rocks increases with increasing fractionation of the system. This has been attributed to the formation of Fe-Ti-oxides, wich preferentialy incorporate light Ti isotopes. Due to the distinct $\delta^{49/47}$Ti signature of basalts and felsic rocks, the Ti isotopic composition of shales has been used to reconstruct the evolution of the average chemical composition of the continental crust throughout earths history (Greber et al., 2017). However, it has recently been suggested that hydrodynamic sorting of heavy mineral phases, which are one of the main hosts of Ti in igneous and metamorphic rocks, biases the $\delta^{49/47}$Ti of the sediment record, and in turn questiones the reliability of Ti isotope signatuers of marine sediments as a proxy for the catchment composition (Klaver et al., 2021).

To investigate potential biases and their extent in the sedimentary record, we measured the $\delta^{49/47}$Ti signature of lacustrine sediments and respective catchment bedrock and soil profiles from two study areas that represent geochemical and weathering endmembers; (i) Lake Grimsel in Switzerland displaying a felsic catchment dominated by mechanical weathering and (ii) Lake Towuti in equatorial Sulawesi, Indonesia, with an ultramafic to mafic catchment and strong chemical weathering. In both study areas we do not find evidence for a substantial bias introduced by hydrodynamic sorting in the sediments. Samples collected at Lake Grimsel composed of different particle sizes ranging from clay to gravel display a constant $\delta^{49/47}$Ti of +0.31 ± 0.03‰. This value is expected from the granodioritic protolith in the catchment. Samples from a sediment drill core from Lake Towuti spanning the past ~1 Myr display $\delta^{49/47}$Ti in a narrow range of +0.09 to +0.17 ‰ (both ± 0.03‰; 2SD), which matches the present Ti isotope signature present in soil and bedrock in the catchment, that range from +0.07 to +0.26‰ (both ± 0.03‰; 2SD). Our findings can be explained by variable rock mixing of catchment bedrocks and do not indicate that chemical weathering or hydrodynamic mineral sorting are able to push the $\delta^{49/47}$Ti values in sediments outside the range of bedrock signatures, at least for the here studied lake systems. However, further endmember and massbalance modeling together with measurments of individual mineral phases and comparison of isotopic variability through time combined with climate proxy data are required for a better understanding of the behaviour of Ti isotopes in the sedimentry cycle.

REFERENCES

Greber, N. D., Dauphas, N., Bekker, A., Ptáček, M. P., Bindeman, I. N., & Hofmann, A. (2017). Titanium isotopic evidence for felsic crust and plate tectonics 3.5 billion years ago. *Science, 357*(6357), 1271-1274.

Klaver, M., MacLennan, S. A., Ibañez-Mejia, M., Tissot, F. L., Vroon, P. Z., & Millet, M.-A. (2021). Reliability of detrital marine sediments as proxy for continental crust composition: The effects of hydrodynamic sorting on Ti and Zr isotope systematics. *Geochimica et Cosmochimica Acta*.

3.19
Neoarchean Continental Exposure and Hydrological Cycle Recorded in a 2.67 Ga Magmatic-Hydrothermal System from Kola Craton, Russia

David Zakharov[1], Dmitry Zozulya[2], Daniela Rubatto[3], Dylan Colón[4]

[1] *Institute of Earth Sciences, University of Lausanne, CH-1015 Lausanne (david.zakharov@unil.ch)*
[2] *Geological Institute, Kola Science Centre of the Russian Academy of Sciences, 184209 Apatity, Russia*
[3] *Institute of Geological Sciences, University of Bern, Baltzerstrasse 3, CH-3012 Bern*
[4] *Department of Earth Sciences, University of Geneva, CH-1205 Geneva*

Modern hydrological cycle includes precipitation of ^{18}O-depleted meteoric water over continental crust exposed above sea-level. How far back in the geological record can continental exposure be documented remains uncertain, particularly for the Archean. To investigate the extent of Archean continental exposure, we document a newly discovered low $\delta^{18}O$ magmatic-hydrothermal system that was emplaced in a subaerial environment of the Kola craton, Russia at 2.67 Ga. We present evidence for syn-emplacement incorporation of the local meteoric water signature with $\delta^{18}O$ at least as low as -11 ‰ VSMOW. The incorporation occurred via hydrothermal alteration of diverse Archean host rocks and concurrent emplacement of silicic alkaline magmas. The original meteoric water signature was reconstructed using the traditional and triple O isotope approaches, indicating that Archean crust was exposed to high-altitude climate with mean annual temperatures of around 4 °C. We employ detailed $\delta^{18}O$ mapping using mineral separates and bulk samples, as well as ion microprobe $\delta^{18}O$ measurements and U-Pb dating of zircon. The spatially extensive O-isotope dataset over 120 km in length intersects different lithological units including the granitic complex, the hosting gneiss and late-stage contact altered rocks. All analyzed samples show $\delta^{18}O$ below the normal mantle- and crustal derived values with the lowest $\delta^{18}O$ of ca. -7 ‰ measured in altered gneisses and granites near the intrusive contacts. We show that pristine low $\delta^{18}O$ zircon crystals yield an emplacement age for the magmatic complex of 2672±7 Ma. A subset of zircons was dated using CA-ID-TIMS geochronology placing the paleogeograpic record on geological timescale with high precision. Consequently, the studied here 2.67 Ga granitic complex provides the earliest quantitative record of low $\delta^{18}O$ precipitation that reflects mature hypsometry of Earth crust and precipitation patterns compatible with an active hydrological cycle over substantially exposed land.

P 3.1
Last Glacial Maximum Atlantic water mass provenance from a multi proxy compilation

Patrick Blaser[1,2], Frerk Pöppelmeier[3], Stefanie Kaboth-Bahr[2], Marcus Gutjahr[4], Martin Frank[4], Claire Waelbroeck[5], Samuel Jaccard[1], Jörg Lippold[2]

[1] Institute of Earth Sciences, University of Lausanne, Bâtiment Géopolis, CH-1015 Lausanne (patrick.blaser@unil.ch)
[2] Institute of Earth Sciences, Heidelberg University, Im Neuenheimer Feld 234, D-69120 Heidelberg
[3] Climate and Environmental Physics, Physics Institute and Oeschger Centre for Climate Change Research, University of Bern, CH-3012 Bern
[4] GEOMAR Helmholtz Centre for Ocean Research Kiel, Wischhofstrasse 1-3, D-24148 Kiel
[5] Laboratoire des Sciences du Climat et de l'Environnement, LSCE/IPSL, CEA–CNRS–UVSQ–Université Paris-Saclay, F-91198 Gif-sur-Yvette

During the Last Glacial Maximum (LGM) atmospheric CO2 concentrations were significantly lower than today and increased rapidly during the last deglaciation. This rapid increase is thought to be a finger print of the deep ocean that accumulated carbon during glacial times and released it in the course of deglacial reconfiguration of deep ocean circulation. The classical view of LGM deep Atlantic water mass structure is mainly derived from carbon isotopes and suggests that southern sourced water (SSW) masses occupied a much larger part of the deep ocean, thereby allowing the accumulation of carbon in this deep and isolated water layer. This expansion would have involved a reduction in the extent of northern sourced water (NSW) to intermediate depths.

Here we combine observations of neodymium, oxygen, and carbon isotopes, as well as foraminiferal B/Ca ratios from the LGM Atlantic to assess past water mass distribution. We find that a northern sourced deep water mass was probably also produced during the LGM, but had intermediate d13C signatures that mask its presence in investigations restricted to this proxy. This deep NSW spread across the whole deep Atlantic similar to North Atlantic Deep Water today, but was probably produced by different mechanisms. Overall, we find that LGM deep water mass provenance was probably not much different to today and can in fact not rule out equal northern vs. southern water mass distributions. This conclusion is relatively robust against systematic uncertainties in the different employed proxies. It therefore significantly alters the accepted idea of glacial deep ocean circulation.

P 3.2
Accuracy of stable oxygen isotope measurements from -10 to 90 ‰

Carolina F. M. de Carvalho[1], Sarah G. Pati[1],

[1] *Department of Environmental Sciences, University of Basel, Bernoullistrasse 32, CH-4056 Basel* (*carolina.carvalho@unibas.ch*, *sarah.pati@unibas.ch*)

Molecular oxygen (O2) is the most readily available oxidizing agent for enzymatic and abiotic redox reactions in the environment. Therefore, measuring oxygen (O) isotope fractionation in O2 can be an essential tool for investigating environmentally relevant redox reactions. During irreversible O2 consumption reactions, 16O16O reacts faster than 18O16O. Thus, in closed systems, the δ18O-value of the remaining O2 will increase as the reaction proceeds and O2 concentrations decrease. In these cases, δ18O-values can reach up to 90 ‰ with certain O2 consuming enzymes such as glucose oxidase. When measuring O isotope fractionation in O2, a one-point calibration with O2 from ambient air (δ18O = 23.88 ‰) is the most common approach. Measuring samples with δ18O-values higher than this standard can introduce measurement uncertainties, and the further away these values are from the standard, the larger the potential errors. A two-point calibration with O2 standards with different δ18O-values would improve stable isotope analysis of O2 when investigating O2 consumption processes. Obtaining additional O2 standards with elevated δ18O-values is challenging and a process that generates O2 from water without fractionation would be ideal. It has been suggested that photosynthesis generates O2 from water without causing oxygen isotope fractionation. Therefore, photosynthetically produced O2 gas with different δ18O-values could be generated from source waters with different δ18O-values. In this study, we tested the feasibility of this approach. Thylakoids were extracted from spinach leaves, suspended in O2-free buffered solutions with δ18O-values of the source water in the range of −10 to +90 ‰ and exposed to white light. Isotope analysis was performed on the photosynthetically produced O2 by sampling the headspace of the reactors at different time intervals of light exposure. The δ18O-values of the O2 in the headspace were analyzed with a GasBench-IRMS instrument. Comparison of the δ18O-values of the photosynthetically produced O2 with the δ18O-values of the different source waters, was used to determine the error introduced by the one-point calibration with O2 from air at increasing δ18O-values. δ18O-values of H2O were determined with a laser isotope analyzer, and water standards covering the whole range of δ18O-values. We found that there was no significant bias of the one-point calibration of the GasBench-IRMS system used in this study, compared to measurement uncertainties. We therefore conclude that our current set-up can be used to accurately determine oxygen fractionation in O2 consuming processes without bias from the one-point calibration. For other isotope analysis instruments, however, the errors introduced by a one-point calibration would have to be tested in a similar way to ensure accurate measurement across a large range of delta values.

P 3.3
Ocean circulation and hydrothermal activity control the cycling of dissolved Cr in the oligotrophic South Pacific Ocean

Delphine Gilliard[1], David J. Janssen[2], Samuel L. Jaccard[1]

[1]Faculty of Geosciences and Environment, Institute of Earth Sciences (ISTE), 1015 Lausanne (delphine.gilliard@unil.ch)
[2] Institute of Geological Sciences & Oeschger Centre for Climate Change Research, 3012 Bern

Over the last decade, stable chromium (Cr) isotope composition has emerged as a potentially useful paleo-proxy recording past oxygenation changes in the atmosphere and oceans. Although Cr is a promising paleo-proxy, the modern marine Cr cycle remains poorly understood. According to recent studies, biogeochemical transformations are potentially one of the main processes controlling Cr in modern oceans. This contribution reports on seawater Cr concentration ([Cr]) and its stable isotope composition (δ^{53}Cr) from the oligotrophic South Pacific Gyre. The seawater samples were collected during the GP 13 oceanographic transect, which extends from 155°E, 32°S to 170°W, 32.5°S and crosses the Tasman Basin and the South Pacific Basin. Influence of the biological pump on Cr is negligible, thus suggesting that the uptake and/or scavenging of Cr by phytoplankton is undetectable or insufficient to impact dissolved Cr distribution in severely oligotrophic conditions. Nonetheless, in the upper 750 m depth, a general increase in [Cr], concomitant with decreasing δ^{53}Cr values is associated with hydrographic features marking the boundary between Subtropical mode water and the West South Pacific Central Water/ Subantarctic Mode Water. This change in Cr behavior associated with water mass suggests a consequential influence of horizontal water mass advection on the regional distribution of Cr. At depth ~1500 to 3000 m, the easternmost stations record an unexpected increase in [Cr] and concomitant decrease of δ^{53}Cr, which correspond to the maximum [Cr] and minimum δ^{53}Cr in the dataset. The location of this feature, near the Kermadec ridge, and correlation with other dissolved metals (e.g., Fe) may be explained by a potential input of hydrothermal Cr and/or modified Upper Circumpolar Deep Water/Pacific Deep Water. The South Pacific Ocean data demonstrate a strong relationship between [Cr] and δ^{53}Cr with an isotope fractionation factor of -0.75 ‰. These observations are in general agreement with previous studies focusing on dissolved marine Cr, indicative of Rayleigh fractionation processes during which isotope fractionation is limited to a single or a limited number of processes.

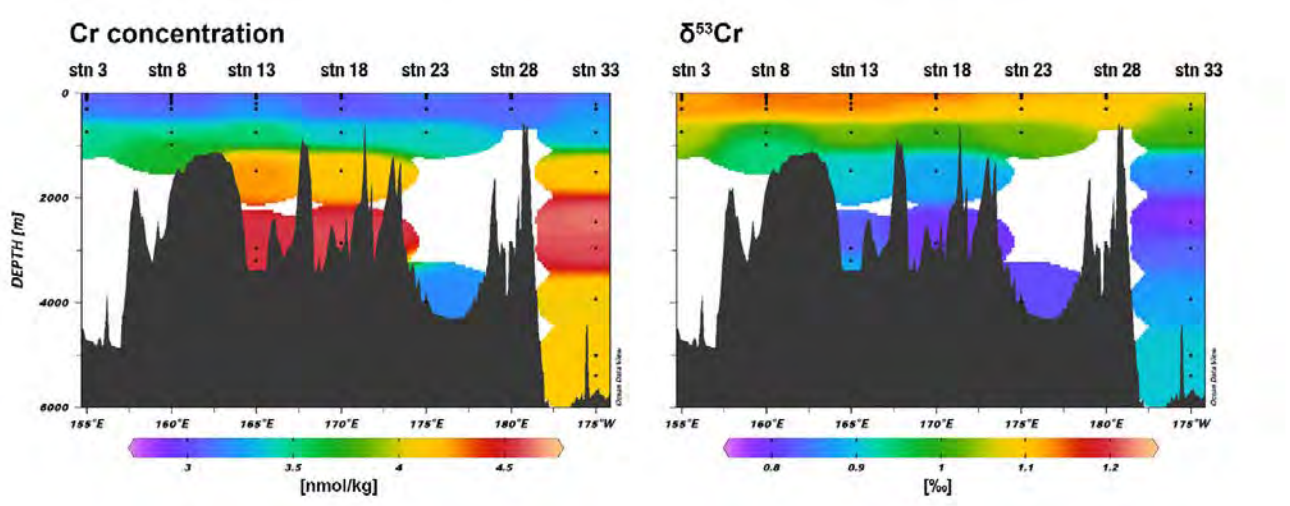

Figure1. Sections of GP 13 transect for Cr concentration and δ^{53}Cr. Black dots represent the sampling sites and the dark grey represent the topography of seafloor.

REFERENCES

Ellwood, M. J., Bowie, A. R., Baker, A., Gault-Ringold, M., Hassler, C., Law, C. S., Maher, W. A., Marriner, A., Nodder, S., Sander, S., Stevens, C., Townsend, A., van der Merwe, P., Woodward, E. M. S., Wuttig, K., & Boyd, P. W. (2018). Insights Into the Biogeochemical Cycling of Iron, Nitrate, and Phosphate Across a 5,300 km South Pacific Zonal Section (153°E–150°W). Global Biogeochemical Cycles, 32(2), 187–207.

Janssen, D. J., Rickli, J., Abbott, A. N., Ellwood, M. J., Twining, B. S., Ohnemus, D. C., ... & Jaccard, S. L. (2021). Release from biogenic particles, benthic fluxes, and deep water circulation control Cr and δ53 Cr distributions in the ocean interior.

Janssen, D. J., Rickli, J., Quay, P. D., White, A. E., Nasemann, P., & Jaccard, S. L. (2020). Biological Control of Chromium Redox and Stable Isotope Composition in the Surface Ocean. Global Biogeochemical Cycles, 34(1). https://doi.org/10.1029/2019GB006397

Frei, R., Gaucher, C., Poulton, S. W., & Canfield, D. E. (2009). Fluctuations in Precambrian atmospheric oxygenation recorded by chromium isotopes. Nature, 461(7261), 250–253. https://doi.org/10.1038/nature08266

Rickli, J., Janssen, D. J., Hassler, C., Ellwood, M. J., & Jaccard, S. L. (2019). Chromium biogeochemistry and stable isotope distribution in the Southern Ocean. Geochimica et Cosmochimica Acta, 262, 188–206. https://doi.org/10.1016/j.gca.2019.07.033

Scheiderich, K., Amini, M., Holmden, C., & Francois, R. (2015). Global variability of chromium isotopes in seawater demonstrated by Pacific, Atlantic, and Arctic Ocean samples. Earth and Planetary Science Letters, 423(2015), 87–97. https://doi.org/10.1016/j.epsl.2015.04.030

P 3.4
Mass-independent Ca and Cr isotope variations in chondritic components – Insights into Solar System evolution and planetary formation

Jan Hoffmann[1], Aryavart Anand[1], Klaus Mezger[1,2]

[1] *Institut für Geologie, Universität Bern, Baltzerstrasse 1+3, CH-3012 Bern*
[2] *Center for Space and Habitability, Universität Bern, Gesellschaftsstrasse 6, CH-3012 Bern*

Chondrules are small (0.1–2 mm), igneous spherules that are a major silicate constituent (≤ 80 vol.%) and eponymous for the most primitive meteorites in the terrestrial collections, the chondrites. Chondrites are considered leftovers of planetary formation in the Solar System and are today located in the astroid belt. Early formation ages of ca. 1.8–3.0 Ma after CAI (e.g. Pape et al. 2019) and their sheer abundance in undifferentiated meteorites make chondrules prime targets for studying dynamic processes in the emerging Solar System, such as transport across the evolving disk and mixing. Although they may have played a pivotal role during the time of condensation of the first solids in the solar nebula (CAI) and the accretion of planetary bodies, their significance during planetary accretion, their origin and formation mechanism(s) and their later incorporation into their host bodies remain elusive (e.g. Connolly & Jones, 2016).

Information on these processes can be derived from the distribution of isotope anomalies in chondrites and their components. These stable isotope variations in meteoritic components offer an opportunity to pin-point contributions of nucleosynthetic processes, that occur in specific stellar environments, and to potentially identify isotopically anomalous precursor materials that were injected into the solar nebula during its evolution.

Mass-independent isotope anomalies have been reported for several elements on the whole rock and component scale (e.g. Burkhardt et al. 2017), clearly indicating compositional heterogeneities in the protoplanetary disk. Currently, it is not unequivocally resolved if the non-carbonaceous–carbonaceous dichotomy (NC–CC) represents spatial or temporal isotopic gradients in the nebula or a combination of both and if there was any exchange of material after the dichotomy formed. The currently favoured model involves the rapid growth of Jupiter (≤1 Ma after CAI) which created an impenetrable barrier for radial migration and thereby mixing of material between the inner (NC) and outer (CC) Solar System (e.g. Nanne et al. 2019). A recent study revealed inconsistencies with this model (Williams et al. 2020) by reporting chondritic components that possess intermediate Cr, Ti and O isotopic compositions, possibly linking the NC and CC domains by a missing reservoir that was not represented in previous datasets.

Here, we investigate the mass-independent isotopic variations of Ca and Cr (MC-TIMS) in individual chondrules from various chondrite groups. We use the isotopic information to assess the efficiency of the proclaimed Jupiter barrier at the time of chondrule formation, i.e. after the formation of a first generation of planetesimals and before the final accretion of the chondrite parent bodies, thereby testing the NC–CC model.

The isotope data are complemented by petrological investigations in order to unravel possible systematics between the isotopic composition and mineralogical properties of the chondrules.

REFERENCES

Connolly, H.C. & Jones, R.H. 2016: Chondrules: The canonical and noncanonical views, Journal of Geophysical Research: Planets 121, 1885-1899.

Nanne, J., Nimmo, F., Cuzzi, J., Kleine, T. 2019: Origin of the non-carbonaceous–carbonaceous meteorite dichotomy, Earth and Planetary Science Letters 511, 44-54.

Pape, J., Mezger, K., Bouvier, A.-S., Baumgartner, L.P. 2019: Time and duration of chondrule formation: Constraints from ^{26}Al-^{26}Mg ages of indiviual chondrules, Geochimica et Cosmochimica Acta 244, 416-436.

Williams, C., Sanborn, M., Defouilloy, C., Yin, Q.-Z., Kita, N.T., Ebel, D.S., Yamakawa, A., Yamashita, K. 2020: Chondrules reveal large-scale outward transport of inner Solar System materials in the protoplanetary disk, Proceedings of the National Academy of Sciences of the United States of America 117, 23426-23435.

P 3.5
A new perspective on the constraints on marine carbonate Zn isotope records

Kim Müsing[1], Matthew O. Clarkson[1], Derek Vance[1]

[1] *Institut für Geochemie und Petrologie, ETH Zürich, Clausiusstrasse 25, CH-8092 Zürich (kim.muesing@erdw.ethz.ch)*

The marine carbonate sediment archive has long been recognised to hold valuable geochemical information on the past ocean. Zinc (Zn) isotopes in particular have recently seen a rise in the number of studies, due to their usefulness as tracers of marine biogeochemical cycles and redox processes. In order to robustly understand the meaning of Zn isotope trends extracted from bulk carbonate sediments, it is essential to understand how exactly these carbonate Zn isotope values relate to seawater Zn, and therefore how Zn is incorporated into carbonates.

According to recently published experimental findings, inorganic carbonate incorporates a Zn isotope composition distinctly heavier than the aqueous Zn^{2+} pool (Mavromatis et al., 2019). On the other hand, modern cold-water corals, representing the only biogenic carbonate $\delta^{66}Zn$ data to date, have been observed to record the ambient seawater Zn isotope composition (Little et al., 2021). The impact of this potential ambiguity in the interpretation of a Zn isotope composition measured in ancient bulk carbonates, that most likely contains both inorganic and organic carbonate components, has gone unrecognised but needs to be understood. Bulk carbonates also consist of multiple components, i.e. trace metal-rich contaminant phases, such as detrital silicates, Fe-Mn oxides, and metal-poor carbonate fractions, which further complicates trace metal isotope studies of the bulk carbonate record.

Here, using a detailed leaching study, we analyse mixing relationships between components within a bulk carbonate sample to identify endmembers with distinct chemistries and isotope compositions. Two primary contaminants (detrital silicates and Fe-Mn oxides) were identified that form clear mixing arrays with up to two carbonate phases. Both the latter have $\delta^{66}Zn$ values around 1‰, distinctly fractionated from modern seawater ($\delta^{66}Zn_{seawater}$ = 0.46 ± 0.08‰; e.g. Lemaitre et al., 2020). This latter result, showing that Zn isotope compositions extracted from bulk carbonates are heavier than the oceanic total dissolved pool of Zn, is consistent with aforementioned experimental data (Mavromatis et al., 2019) and the modern seawater isotopic composition.

Our data, together with recent findings on the incorporation of Zn and its isotopes into inorganic (with substantial fractionation) and biogenic carbonate (unfractionated), point towards another dimension in the interpretation of Zn isotope records in carbonate, potentially relevant for other metal isotope systems too. The variability in the Zn incorporation mechanisms into carbonates needs consideration in addition to the simpler and frequently invoked interpretation in terms of excursions in seawater, and thus source and sink related changes.

REFERENCES

Lemaitre, N., de Souza, G.F., Archer, C., Wang, R.-M., Planquette, H., Sarthou, G., & Vance, D. 2020: Pervasive sources of isotopically light zinc in the North Atlantic Ocean, Earth and Planetary Science Letters, 539, 116216.

Little, S. H., Wilson, D.J., Rehkämper, M., Adkins, J.F., Robinson, L.F. & van de Flierdt, T. 2021: Cold-water corals as archives of seawater Zn and Cu isotopes, Chemical Geology, 578, 120304.

Mavromatis, V., González, A. G., Dietzel, M., & Schott, J. 2019: Zinc isotope fractionation during the inorganic precipitation of calcite – Towards a new pH proxy. Geochimica et Cosmochimica Acta, 244, 99-112.

P 3.6
Isotopic disequilibrium during dehydration of subducted serpentinites (Zermatt-Saas unit)

Michelle Ulrich[1] , Daniela Rubatto[1,2], Jörg Hermann[1], Etienne Deloule [3]

[1] Institut für Geologie, University of Bern, Baltzerstrasse 1+3, CH-3012 Bern (michelle.ulrich@geo.unibe.ch)
[2] Institut Des Sciences de La Terre, University of Lausanne, Quartier Mouline, CH-1015 Lausanne
[3] CRPG, University of Lorraine, 15 Rue Notre Dame des Pauvres, 54500 Vandœuvre-lès-Nancy

During subduction of serpentinized oceanic lithosphere, the dehydration-reaction of brucite + antigorite forms metamorphic olivine and aqueous fluid is released. In the Zermatt-Saas unit this fluid release occurs at high pressures of ca. 2.5 GPa and temperatures between 550-600 °C (Kempf et al., 2020). This study presents in-situ oxygen isotopes of metamorphic olivine and antigorite measured with a secondary ion mass spectrometer (SIMS) at the University of Lorraine (CRPG) to constrain the isotopic signature of the fluid. Samples with different degrees of deformation within the Zermatt-Saas unit were selected: a) undeformed antigorite serpentinite still showing relict mantle fabrics with static olivine growth, b) serpentinite with olivine shear bands and c) an olivine shear zone that is supposed to represent the major fluid pathway.

Preliminary results show that the antigorite composition varies slightly from $\delta^{18}O$ = 7.38 ± 0.63 ‰ (2σ) in the undeformed sample, to $\delta^{18}O$ = 6.55 ± 0.63 ‰ in shear bands and $\delta^{18}O$ = 5.44 ± 0.47 ‰ in the shear zone. Olivine has significantly lower $\delta^{18}O$ values of 1.77 ± 0.69 ‰ in the undeformed sample and 1.57 ± 0.66 ‰ in most of the analysed grains from the shear bands. In these two samples, despite textural equilibrium, antigorite and olivine are not in isotopic equilibrium at the conditions of the dehydration reaction.

Olivine from the shear zone has a relative high $\delta^{18}O$-signature of 4.86 ± 0.23 ‰, similar to what is found in Mg-rich patches and rims in the olivine of the shear bands ($\delta^{18}O$ of 5.51 ± 0.83 ‰). In this case antigorite and olivine are in isotopic equilibrium at peak conditions.

Our results suggest that olivine formed during the brucite consuming reaction is in isotopic disequilibrium with reacting antigorite and due to a low fluid-rock ratio this disequilibrium is preserved in most of the samples. In the case of the shear zone with a higher fluid-rock ratio, isotopic equilibrium was achieved.

REFERENCES

Kempf, E. et al. 2020: The role of the antigorite + brucite to olivine reaction in subducted serpentinites (Zermatt, Switzerland), Swiss J Geosci, 113,16.

P 3.7
Tracking fluid uptakes during abyssal serpentinization of passive margins by oxygen isotope analysis of the serpentine phases

Coralie Vesin[1], Daniela Rubatto[1,2], Thomas Pettke[1], Etienne Deloule[3]

[1] *Institute of Geological Sciences, University of Bern, Bern CH-3012, Switzerland (coralie.vesin@geo.unibe.ch)*
[2] *Institut des Sciences de la Terre, University of Lausanne, Lausanne CH-1015, Switzerland*
[3] *Centre de Recherches Pétrographiques et Géochimiques (CRPG), CNRS, Université de Lorraine, 54501 Vandoeuvre-lès-Nancy, France*

Oxygen isotopes are commonly used in geochemistry to track the composition of hydrothermal fluids, such as those active during serpentinization of ultramafic rocks in oceanic settings. In the abyssal plains of passive margins, the successive stretching and thinning of the oceanic and continental crusts trigger the exhumation of the lithospheric mantle where fluid flow interacts along crustal faults to form serpentine phases, brucite and magnetite.

Investigated samples are from oceanic drill cores (Ocean Drilling Program) in the conjugate passive margins of Iberia and Newfoundland. We explore the variation in oxygen isotope composition of the serpentine phases formed at different stages of abyssal serpentinization based on textural relationships. Serpentine crystallizes in a mesh texture or as bastite after the hydration of olivine or pyroxene, respectively. The isotopic analyses are performed with a secondary ion mass spectrometer (SIMS) allowing for 20 µm spatial resolution, and using a serpentine standard (Schicchitano et al. 2018).

Our preliminary results show a significant variability in the oxygen isotope composition related to the serpentine texture, which emphasizes the importance of *in situ* data compared to bulk rock data. We observe an increase in the $\delta^{18}O$ of lizardite in the Iberia samples from the mesh rim texture with $\delta^{18}O$ = 4.4 ± 0.8 ‰ (2σ), to the mesh centers with a larger range of $\delta^{18}O$ = 4.0-7.7 ‰. Some bastite grains are chemically zoned and three groups can be distinguished: (i) Mg# = 87-91, $\delta^{18}O$ = 5.5-8.5 ‰; (ii) Mg# = 94-95, $\delta^{18}O$ = 8.5-10.6 ‰; (ii) Mg# = 92-94, $\delta^{18}O$ = 11.4-13.5 ‰. In two of the Newfoundland samples, we observe different trends with either a slight increase of the lizardite oxygen isotope composition from the mesh texture to the bastite, or a slight decrease between these two textures. Considering an initial seawater fluid composition ($\delta^{18}O_{fluid}$ = 0 ‰), a decrease in temperature during serpentinization (from ~190°C to ~60°C in the Iberia case, from ~140°C to 100°C in the Newfoundland case) can explain the increase in oxygen isotope composition of the serpentine phase. In a rock-buffered system, the serpentinizing fluid would be enriched in ^{18}O and would lead to higher calculated temperatures.

REFERENCES

Scicchitano, M. R., Rubatto, D., Hermann, J., Shen, T., Padrón-Navarta, J. A., Williams, I. S., & Zheng, Y. F. (2018). In situ oxygen isotope determination in serpentine minerals by ion microprobe: reference materials and applications to ultrahigh-pressure serpentinites. Geostandards and Geoanalytical Research, 42(4), 459-479.

04. Environmental Biogeochemistry of Trace Elements +

05. Natural Organic Matter, Trace Metals and Nanoparticle Biogeochemistry

Adrien Mestrot, Moritz Bigalke, Montserrat Filella, Marie Marques Fernandes,Vera I Slaveykova, Andreas Voegelin, Lenny Winkel, Isabelle A. Worms

TALKS:

4.1 Bachelder J., Tolu J., Wiggenhauser M., Winkel L., Frossard E.: Characterization of soil processes that impact Zn and Cd uptake in wheat plants treated with organic fertilizers

4.2 Barbosa N., Urquidi O., Jaquet J.-M., Adachi T., Filella M.: Understanding BaSO4 microcrystal formation in the freshwater algae Spirogyra with laser tweezer Raman microspectroscopy and SEM observations

4.3 Chávez-Capilla T., Mukherjee M., Coll-Crespi M., Deonarine A., Berniel-Latmani R., Hapfelmeier S., Mestrot A.: Microbiota-mediated transformations of arsenic species from rice in mammals

4.4 Filella M., Matoušek T.: Germanium in the environment: overview, equilibrium contant critical assessment and first lake chemical speciation study

4.5 Gressard T., Layglon N., Tercier-Waeber M.-L.: In situ autonomous voltammetric monitoring of the bioaccessible inorganic arsenic species

4.6 Jiskra Martin: Invited talk: Unravelling atmospheric mercury deposition to the Earth surface with mercury stable isotopes

4.7 Le Bras Z., Bouchet S., Thyssen M., Grosso O., Winkel L.H.E.: Seasonal variability in volatile selenium speciation at a coastal site in the Mediterranean Sea

4.8 Li C., Zhu W., Osterwalder S., Jiskra M., Nilsson M., Enrico M., Peng H., Bishop K.: Critical observations of Hg concentration and stable isotope signatures in ambient and soil pore air in a boreal peatland

4.9 Mahat S., Stanisic L., Weber A., Ryser M.P., Mestrot A.: Mercury in the terrestrial environment: bioaccumulation and biomonitoring in Switzerland

4.10 Schmidt F., Schäffer A., Lenz M.: Soil as a potent, natural matrix for sequestration of leached lead from perovskite solar cells

4.11 Tercier-Waeber M.-L., Abdou M., Dutruch L., Bossy C., Confalonieri F., Schäfer J.: In situ monitoring of the potentially bioavailable fraction of a range of trace metals and study of the processes influencing their temporal concentrations

4.12 Wielinski J., Jimenez-Martinez J., Göttlicher J., Steiniger R., Hug S., Berg M., Voegelin A.: Micromodel study on the removal of arsenic from drinking water using zerovalent iron / sand filters

4.13 Wiggenhauser Matthias: Invited talk: Metal isotope process tracing in plant science: a useful tool in plant science or just gymnastics for geochemists?

4.14 Worms I.A.M., Cossart T., Santos J., Trindade K., Slaveykova V.I.: Characterization of dissolved organic matter (DOM) produced by phytoplankton and its mercury binding capacities using asymmetrical flow field-flow fractionation with multi-detection (AF4-MD)

POSTERS:

P 4.1 Guan H., Caggìa V., Coll Crespi M., Liu X., Gomez Chamorro A., Chavez-Capilla T., Ramette A., Mestrot A., Schläppi K.B., Bigalke M.: The potential of indigenous microbes in supporting maize in the face of arsenic threats

P 4.2 Hul G., Ramseier Gentile S., Zimmermann S., Stoll S.: Adsorption of CeO2 Nanoparticles onto Sand used in Drinking Water Treatment Plant

P 4.3 Layglon N., Abdou M., Massa F., Castellano M., Povero P., Bakker E., Tercier-Weber M.-L.: Evaluation of dissolved Cu, Cd, Pb and Zn speciation in relation to Environmental Quality Guidance

P 4.4 Nenonen V., Kaegi R., Hug S.J., Mangold S., Göttlicher J., Winkel L.H.E., Voegelin A.: Effect of Si, Ca, and Mg on phosphate co-precipitation with Fe and on P retention during precipitate aging

P 4.5 Noyer R., Stoll S., Ramirez Arenas L.: Fate and removal efficiency of titanium oxide nanoparticles (TiO2 NPs) in a conventional drinking water treatment plant

P 4.6 Reusser J.E., Winkel L., Kretzschmar R., Wächter D., Meuli R.G.: Geochemical Soil Atlas of Switzerland

P 4.7 Worms I.A.M., Moulin E., Regier R., Kavanagh K., Slaveykova V.I.: Natural organic matter as a modifier of Hg bioavailability to green algae

P 4.8 Viacava K., Mestrot A.: Microbial Methylation of Antimony

P 4.9 Semeraro S., Rasmann R., Le Bayon C.: Swiss Mountain Soil Ecology Project

4.1
Characterization of soil processes that impact Zn and Cd uptake in wheat plants treated with organic fertilizers

Jill Bachelder[1,2,3], Julie Tolu[2,3], Matthias Wiggenhauser[1], Lenny Winkel[2,3], Emmanuel Frossard[1]

*[1]Institute of Agricultural Science, ETH Zurich, Zurich, Switzerland (*jbachelder [at] ethz.ch)
[2]Institute of Biogeochemistry and Pollutant Dynamics, ETH Zurich, Zurich, Switzerland
[3]Eawag, Swiss Federal Institute of Aquatic Science and Technology, Dubendorf, Switzerland

Zn is an essential micronutrient for humans and plants. Wheat grown in Zn-limiting conditions can exhibit Zn deficiency, which can limit biomass yields and decrease the nutritional value of resulting food products. Organic fertilizers can increase plant-available Zn in the soil, either through direct addition of available Zn or by solubilizing Zn immobilized in the soil solid phases (Figure 1). The effect of the organic fertilizer on Zn availability will depend on the chemical properties of the treatment, such as content of C, N, S, Zn, and Cd, as well as organic matter (OM) composition.

A potential limitation to the application of organic fertilizers is that they may also lead to an increase in plant uptake of Cd, a highly toxic element with similar chemical properties and biological uptake pathways as Zn. Because wheat-derived food products are a major source of Cd exposure in humans, it is essential to evaluate the impact of organic fertilizer application on both Zn and Cd availability. Our project aims (1) to understand the mechanism through which organic fertilizer application adds bioavailable Zn and Cd to the soil and (2) to determine how these underlying processes impact the subsequent uptake and transport of Zn and Cd within the wheat plant.

To better understand the effect of organic fertilizer application on Zn and Cd uptake by wheat, it is first necessary to evaluate how the differences in the composition of organic fertilizers may increase the bioavailability of soil Zn and Cd. In the first step of our project, we have analyzed the chemical composition of thirty organic fertilizers of diverse composition, including green manures, lignified crop residues, farmyard manures, and composts. OM molecular composition was determined by pyrolysis-gas chromatography-mass spectrometry (Py-GC/MS), and elemental concentrations were obtained using acid digestion and inductively-coupled-plasma-mass spectrometry (ICP-MS). Zn and Cd speciation were determined in the water-soluble fraction of our OMAO samples via size exclusion chromatography (SEC) coupled to UV and ICP-MS detectors to measure Zn and Cd bound to low vs. high molecular weight compounds.

Our analyses revealed that the OM molecular composition varied significantly among the thirty collected fertilizers. Using principal component and hierarchical cluster analyses, we identified six groups of fertilizers with distinct OM composition. We also observed trends in Zn and Cd speciation within the clusters, with samples that were clustered together based on OM composition also having similar Zn/Cd speciation. Zn and Cd were associated with OM fractions of lower molecular weight in green manure, lignified crop residues, and poultry manure as compared with cattle slurry, cattle and horse manure, and compost. Altogether, our data suggests that differences in chemical speciation of Zn and Cd may be observed between fertilizers with distinct OM composition. As a next step, we will select three organic fertilizers with distinct Zn/Cd speciation and OM composition and apply them in a pot experiment to evaluate their effect on Zn/Cd uptake in wheat.

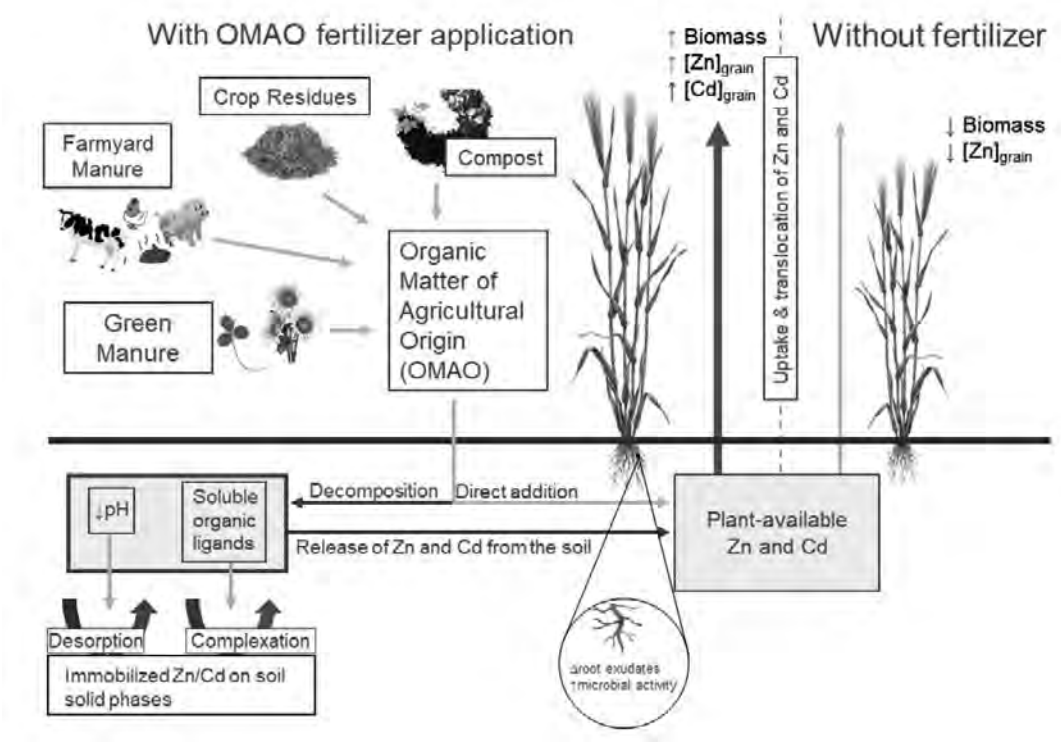

Figure 1. Summary of how we hypothesize OMAO application will add plant-available Zn/Cd to the soil and will increase uptake and translocation of Zn/Cd to wheat grains.

4.2
Understanding $BaSO_4$ microcrystal formation in the freshwater algae *Spirogyra* with laser tweezer Raman microspectroscopy and SEM observations

Natercia Barbosa[1], Oscar Urquidi[1], Jean-Michel Jaquet[2], Takuji Adachi[1], Montserrat Filella[3]

[1] Department of Physical Chemistry, University of Geneva, Quai Ernest Ansermet 30, CH-1211 Geneva 4 (natercia.barbosa@unige.ch)
[2] Department of Earth sciences, University of Geneva, rue des Maraîchers 13, CH-1205 Geneva
[3] Department F.-A Forel for Environmental and Aquatic Sciences, University of Geneva, Boulevard Carl-Vogt 66, CH-1211 Geneva 4

Biogeochemistry of Ba in seawater has been investigated for decades motivated by its unexplained nutrient-like distribution in the water column and its precipitation as barite in undersaturated conditions. The observation that Ba is removed from the water column during biological activity has led to a hypothesis that the degradation of sinking organic matter creates supersaturated microenvironments favorable to barite precitation. Yet, the precise mechanism of barite precipitation in globally undersaturated conditions remains unclear. For example, bacterium-mediated mineralization leads to barite precipitation in laboratory culture experiments and in natural extreme environments such as marine cold seep or sulfur springs where media and conditions strongly differ from seawater. In freshwaters, barite microcrystals are found intracellularly in green algae, used as a gravity sensor (e.g. *Loxedes* and *Chara*) or a detoxification strategy (e.g. *Closterium* and *Micrasterias* in peat bogs*)*. The ability of *Spirogyra*, a widespread filamentous green alga, to biomineralize Ba in undersaturated conditions has often been neglected. While Kreger and Boeré (1969) used XRD to identify barite microcrystals in *Spirogyra* cells and hypothesized that the diffusive particles observed by optical microscopy could be the microcrystals, this information got unnoticed and 30 years later Grolig (1990) assigned these particles as ‘’small vesicles of high refraction’’.

Using laser tweezer Raman microspectroscopy *in vivo*, we succeeded in proving the original hypothesis of Kreger and Boeré. Barite microcrystals are not fixed within the cells but are diffusing, and this character is common to the genus *Spirogyra*. Combining Raman results with SEM images of samples prepared and fixed at the critical point, we provide a description of the structure of *Spirogyra* and define the neighbouring environment in which crystals are present. The results obtained represent a key step forward in understanding the nucleation process of barite in *Spirogyra* and finding the answer to the fundamental question of how barite formation can take place in undersaturated conditions.

ACKNOWLEDGEMENTS. We thank Inés Segovia for her help in the lab. This research was supported by the Gebert Rüf Stiftung (Project Microbials Nr: GRS-071/17).

REFERENCES

Grolig, F. 1990: Actin-based organelle movements in interphase *Spirogyra*, Protoplasma, 155, 29–42.

Kreger, D. R. and Boeré, H. 1969: Some observations on barium sulphate in *Spirogyra*, Acta Botanica Neerlandica, 18, 143–151.

4.3
Microbiota-mediated Transformations of Arsenic Species from Rice in Mammals

Teresa Chavez-Capilla[1], Mohana Mukherjee[2], Miquel Coll-Crespi[1], Amrika Deonarine[3], Rizlan Berniel-Latmani[4], Siegfried Hapfelmeier[2], Adrien Mestrot[1]

[1] *Institute of Geography, University of Bern, Hallerstrasse 12, CH-3012 Bern*
[2] *Institute for Infectious Diseases, University of Bern, Friedbühlstrasse 51, CH-3010 Bern*
[3] *Department of Civil, Environmental and Construction Engineering, Texas Tech University, Lubbock, TX 79409-1023, United States*
[4] *Environmental Microbiology Laboratory, Swiss Federal Institute of Technology Lausanne, CH-1015, Lausanne*

According to the World Health Organization, arsenic is one of the ten pollutants of major health concern [1], with more than 200 million people worldwide being at risk of arsenic exposure from their diet [2]. In particular, rice accumulates up to 0.4 μg g^{-1} of arsenic, of which 85 – 90 % corresponds arsenous acid (As^{III}) and arsenic acid (As^{V}); and the remaining to methylarsonic acid ($MMAs^{V}$) and dimethylarsinic acid ($DMAs^{V}$) [3]. Although all four arsenic species are classified as carcinogens by the IARC [1], their specific modes of toxic action are strongly related to their metabolites once in the human body. In addition, interpopulation variability can influence arsenic metabolic products and excretion rates, which depend on human genetics and gut microbiome [4]. Understanding the effect of gut microbial communities on arsenic biotransformations can help to prevent the adverse effects of chronic arsenic exposure in humans [4]. This study aims to unveil the microbial-mediated transformations of As^{III}, As^{V}, $MMAs^{V}$, $DMAs^{V}$ from rice in the mammalian gut. Specific pathogen free (SPF) and germ free (GF) mice were fed rice-containing chow diets at varying concentrations of inorganic and organic arsenic species. After seven weeks of chronic arsenic exposure, mice were euthanized and all gut contents and key organs involved in arsenic metabolism were analysed for arsenic speciation. Our findings show how the gut microbiome plays an important role in the methylation of arsenic from diet but also promotes the transformation of arsenic into the more toxic thiolated arsenic species. In addition, we identified differences on the specific arsenic excretion pathways in the absence and presence of gut microbiota. The results from this study provide valuable insights to effectively understand how the mammalian gut can help in mitigating the pernicious effects of dietary exposure to arsenic.

REFERENCES

[1] World Health Organization 2010. Exposure to Arsenic: A Major Health Concern.
[2] Podgorski, J.E., Eqani, S.A.M.A.S, Khanam, T., Ullah, R., Shen, H., Berg, M. 2017. Extensive arsenic contamination in high-pH unconfined aquifers in the Indus Valley, Science Advances, 3(8), e1700935.
[3] Francesconi, K. 2010. Arsenic species in seafood: Origin and human health implications, Pure and Applied Chemistry, 82(2), 373-381.
[4] McDermott, T.R., Stolz, J.F., Oremland, R.S. 2020 Arsenic and the gastrointestinal tract microbiome, Environmental Microbiology Reports, 12(2), 136-159.

4.4
Germanium in the environment: overview, equilibrium contant critical assessment and first lake chemical speciation study

Montserrat Filella[1], Tomáš Matoušek[2]

[1] Department F.-A Forel for Environmental and Aquatic Sciences, University of Geneva, Boulevard Carl-Vogt 66, CH-1205 Geneva (montserrat.filella@ unige.ch)
[2] Institute of Analytical Chemistry of the Czech Academy of Sciences, Veveří 97, 60200, Brno, Czech Republic

Germanium is a chemical element of the Group 14 of the periodic table. The element was temporarily known as 'ekasilicon' because of its properties similar to silicon. Germanium is present as Ge(IV) in natural systems. The increasing use of Ge in state-of-the-art technology products has renewed the interest in studying its environmental behaviour and fate in the context of so-called Technology Critical Elements (TCEs) (Filella and Rodríguez-Murillo, 2017). In fact, however, the element has long been the object of attention of two scientific communities: as a proxy of silica when studying silicate rock weathering processes and in seawater where the uptake and regeneration profile of Ge mimics that of Si. Studies on freshwaters are however lacking. We followed 'dissolved' (0.22 μm pore filter size) germanium speciation in Lake Geneva water column by applying hydride generation and cryotrapping in combination with ICP-MS/MS (García-Figueroa et al. 2021). The study extended from January to June 2021, covering a whole spring bloom period. Results show that, as in seawater, inorganic germanium (iGe) has a nutrient-like profile while monomethylgermanium (MGe) is conservative but, in contrast with seawater, iGe is largely dominant while MGe, the main species in seawater, is present at the sub-trace level.
It is generally accepted that $Ge(OH)_4$ is the only species iGe existing over the pH range of interest but possible complexation by l.m.w. inorganic and organic ligands is unclear and our understanding mostly relies on old equilibrium studies. In particular, Ge interactions with organic ligands require attention because the element is known to be associated with organic matter in Ge-enriched coals and complexation by organic ligands containing vicinal OH groups (e.g., sugars) is proved. A summary of an exhaustive critical evaluation of published equilibrium constants will complete this communication.

ACKNOWLEDGEMENTS We thank Mathieu Coster, Jean-Luc Loizeau, Peter M. May and Sebastian Wey for their help and discussions.

REFERENCES

Filella, M., Rodríguez-Murillo, J.C. 2017. Less-studied TCE: are their environmental concentrations increasing due to their use in new technologies? Chemosphere, 182, 605–616.

García-Figueroa, A., Filella, M., Matoušek, T. 2021. Speciation of germanium in environmental water reference materials by hydride generation and cryotrapping in combination with ICP-MS/MS. Talanta, 225, 121972.

4.5
In situ autonomous voltammetric monitoring of the bioaccessible inorganic arsenic species

Tanguy Gressard, Nicolas Layglon, Mary-Lou Tercier-Waeber

Dept. of Inorganic and Analytical Chemistry, University of Geneva, 30 Quai E.-Ansermet, 1211 Geneva 4, Switzerland. (tanguy.gressard@etu.unige.ch)

Arsenic (As), from natural and anthropic sources, is a metalloid of global concern because of its prevalence, bioaccumulation, toxicity, and trophic transfer in the aquatic food chain. It is classified as a Group 1 human carcinogenic substance and acts as an endocrine disruptor. The international provisional guidelines for water quality and water quality criteria derived in an attempt to protect living species are all based on total dissolved As concentration. However, it is well known that the toxicity and bioavailability of As is highly dependent on its chemical form and oxidation state. Arsenic in the aquatic systems is mainly present in the form of inorganic trivalent (As(III) - more toxic) and pentavalent (As(V) - less toxic) oxyanions. Change in inorganic As speciation may occur continuously in space and time [1]. It is therefore important to closely monitor the concentrations of both inorganic As species *in situ* and at an appropriate time scale.

We report here on an innovative electrochemical technique enabling in-situ sequential quantification of the inorganic As(III) and As(V) species under their forms available for bio-uptake, the so-called dynamic metal fraction. The set-up consists on novel devices: an antifouling gel-integrated gold nanofilament microelectrode array [2] incorporated in a submersible multichannel probe [3]. An automated analytical procedure, based on substractive square wave anodic stripping voltammetry, was developed to enable autonomous sequential monitoring of the inorganic As species potentially bioavailble, i.e. the dynamic fractions of the inorganic As(III), As(V), and total As. Optimization of this procedure resulted of the first conducted in situ measurements of the these species in Lake Geneva, from which data are presented.

REFERENCES

[1] Barral-Fraga, L., Barral, M.T., MacNeill, K.L., Martiñá-Prieto, D., Morin, S., Rodríguez-Castro, M.C. 2020: Biotic and Abiotic Factors Influencing Arsenic Biogeochemistry and Toxicity in Fluvial Ecosystems: A Review, International journal of environmental research and public health, 17, 2331-

[2] Tercier-Waeber, M.-L., Fighera, M., Abdou, M., Bakker, E., van der Wal, P. 2021: Newly designed gel-integrated nanostructured gold-based interconnected microelectrode arrays for continuous in situ arsenite monitoring in aquatic systems. Sensors and Actuators B: Chemical, 328, 128996.

[3] Tercier-Waeber, M.-L., Confalonieri, F., Abdou, M., Dutruch, L., Bossy, C., Fighera, M., Bakker, E., Schäfer, J., 2021: Advanced multichannel submersible probe for autonomous high-resolution in situ monitoring of the cycling of the potentially bioavailable fraction of a range of trace metals, Chemosphere 282, https://doi.org/10.1016/j.chemosphere.2021.131014.

4.6
Unravelling atmospheric mercury deposition to the Earth surface with mercury stable isotopes

Martin Jiskra[1]

[1] *Environmental Geosciences, University of Basel, Bernoullistrasse 30, CH-4056 Basel (martin.jiskra@unibas.ch)*

Mercury (Hg) is a potent neurotoxin posing a health risk of global concern. Anthropogenic Hg emissions are deposited to the Earth surface far away from the emission sources due to the long residence time of gaseous elemental Hg (Hg(0)) in the atmosphere. The relation between anthropogenic Hg emission and atmospheric Hg deposition is complex, as Hg can be re-emitted from the Earth surface and cycle in the environment. Global chemical transport models are therefore key to assess the response of the Earth system to changes in anthropogenic emissions and climate conditions. The global Hg Earth system models are constrained by observations, which are largely restricted to Hg(0) measurements in the atmosphere and Hg wet deposition measurements to terrestrial surfaces. Other global fluxes like direct gasous Hg(0) deposition remain largely unconstrained due to limited observations, resulting in large uncertainties in the global Hg Earth system models. In this contribution, I will present Hg stable isotope fingerprinting as a new tool to constrain pathways of atmospheric Hg deposition. The photochemical redox transformations in the atmosphere result in distinct isotopic signatures of the elemental Hg(0) and oxidized Hg(II) species, allowing to quantitatively trace the deposition pathways to the Earth surface. Hg stable isotope results from terrestrial vegetation and soils reveal that 60 to 90 % of terrestrial Hg was deposited via direct Hg(0) deposition through the uptake by plants, rather than via the wet deposition pathway (Zhu et al., 2021). The first seawater Hg stable isotope mesaurements suggest that Hg(0) deposition to the ocean is equally important to Hg(II) deposition (Jiskra et al., accepted). Hg stable isotope fingerprinting therefore have revealed that the direct deposition of gaseous elemental Hg(0) both to terrestrial surfaces and the Ocean has previously been underestimates, which has implications for our understanding of global Hg cycling and ecosystem response to curbed Hg emissions and climate change.

REFERENCES

Zhou, J., Obrist, D., Dastoor, A., Jiskra, M., and Ryjkov, A.: Vegetation uptake of mercury and impacts on global cycling, Nature Reviews Earth & Environment, 2, 269-284, 10.1038/s43017-021-00146-y, 2021.

Jiskra, M., Heimburger-Boavida, L., Desgranges, M., Petrova, M., Dufour, A., Ferreira-Araujo, B., Masbou, J., Chmeleff, J., Thyssen, M., Point, D., Sonke, J. E. Mercury stable isotopes constrain atmospheric sources to the Ocean. Nature (accepted)

4.7
Seasonal variability in volatile selenium speciation at a coastal site in the Mediterranean Sea

Zoé Le Bras[1,2], Sylvain Bouchet[1,2], Melilotus Thyssen[3], Olivier Grosso[3], Lenny H.E. Winkel[1,2]

[1] *Institute of Biogeochemistry and Pollutant Dynamics, Department of Environmental Sciences, Swiss Federal Institute of Technology (ETH) Zurich, 8092 Zurich, Switzerland (zoe.lebras@usys.ethz.ch)*
[2] *Eawag, Swiss Federal Institute of Aquatic Science and Technology, Ueberlandstrasse 133, P.O. Box 611, 8600 Duebendorf, Switzerland*
[3] *Aix-Marseille Université, Université de Toulon, CNRS, IRD, Mediterranean Institute of Oceanography, UM110, 13288 Marseille, France*

Selenium (Se) is an essential trace element for humans and animals. The atmosphere represents an important reservoir of Se, in which yearly around 29'000 – 36'000 tons of Se are cycled. Marine biogenic emissions represent around 60% of the natural selenium emitted to the atmosphere (Feinberg et al., 2020). These marine biogenic emissions are dominated by the volatile selenium species dimethyl selenide (DMSe), dimethyl diselenide (DMDSe) and dimethyl selenyl sulphide (DMSeS) present at trace levels (fM-pM) in seawater (Amouroux and Donard, 1996). Despite their important contribution to the atmospheric selenium reservoir, the spatial and temporal variability of these volatile organic Se species remain poorly investigated due to a lack of sensitive and high throughput analytical methods for their analysis. Only a few studies have quantified volatile methylated Se compounds in aquatic ecosystems through cryogenic techniques coupled with gas chromatography inductively coupled plasma mass spectrometry (GC-ICP-MS) (Amouroux and Donard, 1996).

In this presentation, we will introduce a newly developed highly sensitive and selective analytical method dedicated to quantification of volatile Se and S species using thermal desorption coupled to GC-ICP-MS. We applied this method to measure the daily and seasonal variations of dissolved volatile Se species in seawater. Three sampling campaigns were conducted from March to July 2021 at a coastal station in the North Western Mediterranean Sea (Marine Station of Endoume). Seawater was sampled over six weeks three times per day at 3.5 m depth and analyzed for volatile organic selenium speciation by TD-GC-ICP-MS. Here, the results of these campaigns will be presented and obtained concentrations data will be linked to various biological and environmental parameters, giving new insights into the factors driving variability in volatile organic Se speciation.

REFERENCES

Amouroux, D. & Donard, O. F. X. Maritime emission of selenium to the atmosphere in Eastern Mediterranean seas. *Geophysical Research Letters* 23, 1777–1780 (1996).

Feinberg, A., Stenke, A., Peter, T. & Winkel, L. H. E. Constraining Atmospheric Selenium Emissions Using Observations, Global Modeling, and Bayesian Inference. *Environmental Science & Technology* 54, 7146–7155 (2020).

4.8
Critical observations of Hg concentration and stable isotope signatures in ambient and soil pore air in a boreal peatland

Chuxian Li[1], Wei Zhu[1], Stefan Osterwalder[2], Martin Jiskra[3], Mats Nilsson[1], Maxime Enrico[4], Haijun Peng[1,5], Kevin Bishop[6]

[1] Department of Forest Ecology and Management, Swedish University of Agricultural Sciences, 90183 Umeå, Sweden. (chuxian.li@slu.se)
[2] Institute of Agricultural Sciences, ETH Zurich, 8092 Zurich, Switzerland
[3] Environmental Geosciences, University of Basel, 4056 Basel, Switzerland.
[4] Universite de Pau et des Pays de l'Adour, E2S UPPA, CNRS, TOTAL, LFCR, IPREM, 64000 Pau, France.
[5] State Key Laboratory of Environmental Geochemistry, Institute of Geochemistry, Chinese Academy of Sciences, 550081 Guizhou, China
[6] Department of Aquatic Sciences and Assessment, Swedish University of Agricultural Sciences, 75007 Uppsala, Sweden

Mercury (Hg) is a global pollutant that threatens the health of human and wildlife (UN Environment, 2019). Peatlands, formed by decomposed vegetation, are generally hot spots of neurotoxic methylmercury production and contaminate adjacent aquatic ecosystems (St. Louis et al., 1996). Hg deposition to peatlands occurs in two main ways, by vegetation uptake of Hg^0 and rainfall Hg^{II} input (Enrico et al., 2016), while peat Hg^0 re-emission to the atmosphere can be caused by abiotic and biotic reduction, and photochemical reduction (Jiskra et al., 2015). Some studies find dominant Hg deposition to peatlands (e.g., Enrico et al., 2016)"ISSN":"0013-936X, 1520-5851","issue":"5","journalAbbreviation":"Environ. Sci. Technol.", "language":"en","page":"2405-2412","source":"DOI.org (Crossref. In contrast, a recent study investigating the net ecosystem exchange of Hg in a boreal peatland called "Degerö" reported that Degerö was a significant source of Hg to the atmosphere (Osterwalder et al., 2017). Here, we analyzed Hg concentration and Hg stable isotope signatures in ambient and soil pore air at Degerö, in order to improve our process understanding of Hg deposition and emission pathways in this boreal peatland. Our results show that Hg concentration in soil pore air (0.45 ± 0.12 ng m^{-3}, 1σ, n=38) is about three times lower than ambient Hg (1.31 ± 0.17 ng m^{-3}, 1σ, n=18). This might suggest a Hg diffusion pathway from the atmosphere to the peatland. In concert, preliminary Hg isotope data indicate that Hg oxidation by peat organic matter is the cause for atmospheric Hg diffusion to soil porewater. Subsequently, we will combine our newly gained knowledge on Hg diffusion pathways in peat with more direct Hg flux measurements to resolve the sink-source characteristics in boreal peatlands.

REFERENCES

Enrico, M., Roux, G.L., Marusczak, N., Heimbürger, L.-E., Claustres, A., Fu, X., Sun, R., Sonke, J.E., 2016. Atmospheric Mercury Transfer to Peat Bogs Dominated by Gaseous Elemental Mercury Dry Deposition. Environ. Sci. Technol. 50, 2405–2412.

Jiskra, M., Wiederhold, J.G., Skyllberg, U., Kronberg, R.-M., Hajdas, I., Kretzschmar, R., 2015. Mercury Deposition and Re-emission Pathways in Boreal Forest Soils Investigated with Hg Isotope Signatures. Environ. Sci. Technol. 49, 7188–7196. 2

Osterwalder, S., Bishop, K., Alewell, C., Fritsche, J., Laudon, H., Åkerblom, S., Nilsson, M.B., 2017. Mercury evasion from a boreal peatland shortens the timeline for recovery from legacy pollution. Sci Rep 7, 16022.

St. Louis, V.L., Rudd, J.W.M., Kelly, C.A., Beaty, K.G., Flett, R.J., Roulet, N.T., 1996. Production and Loss of Methylmercury and Loss of Total Mercury from Boreal Forest Catchments Containing Different Types of Wetlands. Environ. Sci. Technol. 30, 2719–2729.

UN Environment, 2019. Global Mercury Assessment 2018, UN Environment Programme Chemicals and Health Branch Geneva Switzerland.

4.9
Mercury in the terrestrial environment: bioaccumulation and biomonitoring in Switzerland

Sabnam Mahat[1], Lucija Stanisic[1], Andrea Weber[1], Marie-Pierre Ryser[2], Adrien Mestrot[1]

[1] *Institute of Geography, University of Bern, Hallerstrass 12, 3012 Bern (sabnam.mahat@giub.unibe.ch)*
[2] *Institute for Fish and Wildlife Health, University of Bern, Länggassstrasse 122, 3012 Bern*

The chemistry and biochemistry of mercury in aquatic environments has been studied extensively but the fate of mercury in all the terrestrial compartments is understudied, although the majority of atmospheric mercury is estimated to be deposited in terrestrial environments. As a result, data on the transfer and bioaccumulation of mercury and methylmercury and the associated risks in terrestrial environment is scarce, especially in Switzerland. Furthermore, the impact of the Minamata convention on mercury pollution signed in 2017 should be assessed, which implies the monitoring and quantification of the decline of mercury concentrations in terrestrial environments. The present study focuses on bioaccumulation of mercury and methylmercury in the terrestrial wildlife in Switzerland and aims to develop a long-term biomonitoring plan.
Firstly, an extensive literature review of European studies was conducted to determine the concentration of mercury and methylmercury in a range of animals and to assist for the selection of species and tissue samples for our study in Switzerland. Roe deer tissues (muscle, liver, kidney) were found as potentially good indicators for mercury pollution in Switzerland and therefore, secondly, tissue samples of roe deer were chosen for mercury analysis. Among the tissues analysed for roe deers, kidneys had the highest concentration of inorganic species of mercury, while more organic species of mercury was found to bioaccumulate in the muscles. A single-step methylmercury extraction in L-cysteine was used and the extracts were analyzed using high performance liquid chromatography in combination with inductively coupled plasma mass spectroscopy (Agilent) (Hight & Cheng, 2006). Direct mercury analyzer (Milestone) was used for total mercury quantification. High correlation was observed for the total mercury concentration among the tissues, inferring that any one of the tissues of the aforementioned organs can be used as a proxy for another. Thirdly, roe deer tissue samples were sampled and analyzed from different cantons in Switzerland. Results (figure 1) show cantonal variation in the total mercury concentration in muscles, with significatly higher concentrations in canton of Ticino and St. Gallen compared to cantons of Vaud, Neuchatel, Solothurn and Bern. Finally, the concentrations measured in the tissues are compared to the atmospheric mercury deposition in Switzerland (Ilyin et al., 2016).

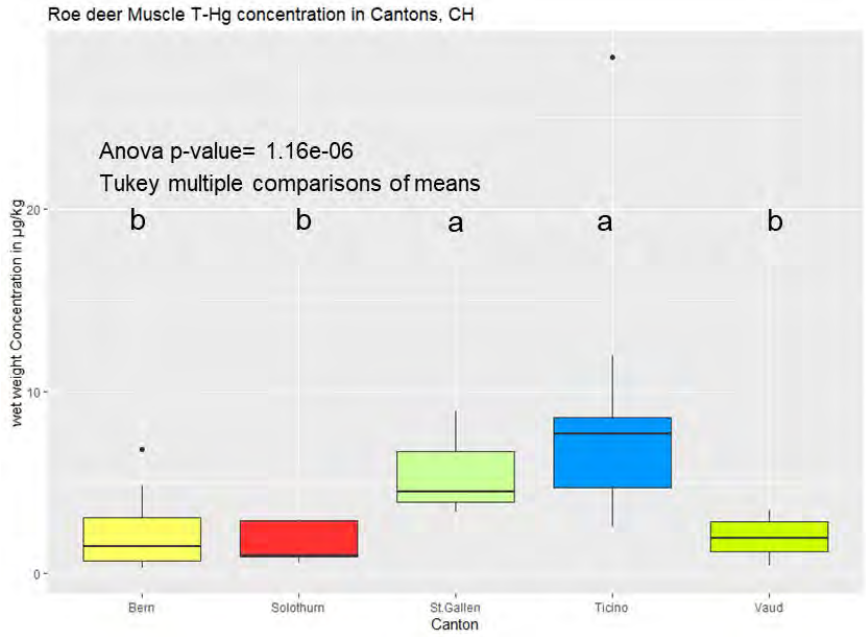

Figure 1.Cantonal variation for total mercury concentration in wet weight (µg/kg) in muscle tissue of roe deer samples in Switzerland collected between 2019-2020

REFERENCES

Hight, S. C., & Cheng, J. (2006). Determination of methylmercury and estimation of total mercury in seafood using high performance liquid chromatography (HPLC) and inductively coupled plasma-mass spectrometry (ICP-MS): Method development and validation. Analytica Chimica Acta, 567(2), 160-172.

Ilyin, I., Gusev, A., Rozovskaya, O., Strijkina, I, 2016. Transboundary Pollution of Switzerland by Heavy Metals in 2014 EMEP/MSC-E Report 5/2016.

4.10
Soil as a potent, natural matrix for sequestration of leached lead from perovskite solar cells

Felix Schmidt[1,2], Andreas Schäffer[2], Markus Lenz[1,3]

[1] *Institute for Ecopreneurship, School of Life Sciences, University of Applied Sciences and Arts Northwestern Switzerland, Hofackerstrasse 30, 4132 Muttenz, Switzerland (markus.lenz@fhnw.ch)*
[2] *Institute for Environmental Research, RWTH Aachen University, Worringerweg 1, 52074 Aachen, Germany*
[3] *Sub-Department of Environmental Technology, Wageningen University, 6700 AA, Wageningen, the Netherlands*

Solar cells based on so-called perovskite absorber materials have been a success story in scientific research (Grätzel, 2017). Within a decade after their discovery, the power-conversion efficiency of lab-scale perovskite photovoltaics has surpassed that of conventional thin-film solar cells, such as cadmium telluride (CdTe) or copper-indium-gallium selenide (Green, 2021). However, efficient and stable perovskite solar cells rely on the use of water-soluble Pb^{2+} species (such as $CH_3NH_3PbI_3$) potentially challenging the technologies' commercialisation (Rong, 2018). In this study, the environmental fate of Pb^{2+} species was assessed in soil-water microcosm experiments, simulating leaching under various biogeochemical conditions.

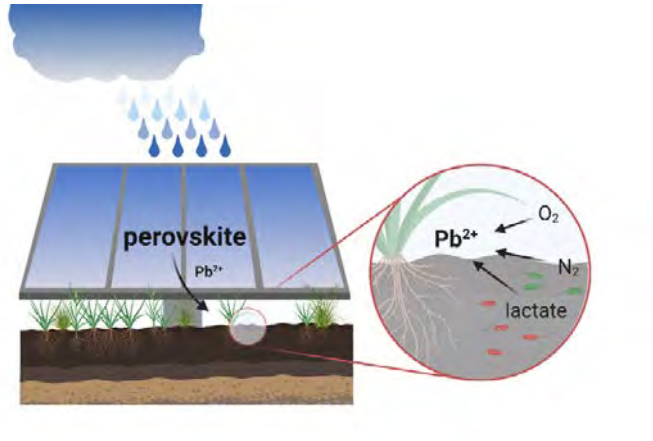

Figure 1. Graphical abstract of assessing environmental fate of perovskite solar cell constituents.

The rapid and efficient removal of Pb^{2+} from the aqueous phase is demonstrated by inductively coupled plasma mass spectrometry. Soil sequential extraction results reveal that a substantial amount of Pb^{2+} is associated with immobile fractions, whereas a minor proportion of Pb^{2+} may become available again in the long term, when oxygen is depleted. Thermodynamic, biogeochemical modelling pointed to favoured mineral formation (such as galena or pyromorphite) under the tested conditions, while X-ray absorption spectroscopy results indicate that the sorption of Pb^{2+} on mineral phases represents the most likely sequestration mechanism. The obtained results suggest that the availability of leached Pb^{2+} from perovskite solar cells is naturally limited in soils and that its adverse effects on soils are possibly negligible in oxic soils.

REFERENCES

Grätzel, M. 2017: The rise of highly efficient and stable perovskite solar cells. Acc. Chem. Res. 50, 487-491.
Green, M. et al., 2021: Solar cell efficiency tables (version 57). Prog. Photovoltaics Res. Appl. 27, 565-575.
Rong, Y. et al., 2018: Challenges for commercializing perovskite solar cells. Science. 361, 6408

4.11
In situ monitoring of the potentially bioavailable fraction of a range of trace metals and study of the processes influencing their temporal concentrations

Mary-Lou Tercier-Waeber[1], Melina Abdou[1,2], Lionel Dutruch[2], Cécile Bossy[2], Fabio Confalonieri[3], Jörg Schäfer[2]

[1] Dept. of Inorganic and Analytical Chemistry, University of Geneva, Sciences II, 30 Quai E.-Ansermet, 1221 Geneva 4, Switzerland (marie-louise.tercier@unige.ch)
[2] University of Bordeaux, UMR CNRS 5805 EPOC, 3315 Pessac, France
[3] Idronaut Srl, Via Monte Amiata 10, 20047 Brugherio (MB), Italy

Trace elements are ubiquitous elements playing critical roles in aquatic ecosystem function [1]. Some metals (e.g. Hg, Cd, Pb) and metalloids (e.g. As) have high toxicity even at very low concentrations, while others are either essential or toxic (e.g. Cu, Zn), depending on their concentrations and the nature of the organisms exposed. Trace metals are persistent and distributed under various chemical species (speciation). Only some specific metal species are potentially available for bio-uptake [1]. Bioavailability is therefore of primary concern when considering if a trace metal serves as micronutrient or toxicant.

We present here a unique submersible compact integrated multichannel trace metal sensing probe (TracMetal) [2]. Innovative antifouling gel-integrated microelectrode arrays (GIMEs) incorporated in this system enable in situ autonomous and simultaneous measurements of the dynamic (potentially bioavailable) fraction of a range of (priority) hazardous metals (Hg(II), As(III), As(V), Cd(II), Pb(II), Cu(II), Zn(II)) with sensitivity at the low picomolar to sub-nanomolar levels [2]. The TracMetal was applied in the Arcachon Bay that represents an important breeding ecosystem for regional seafood production, especially oysters. In parallel, master variables were monitored in situ, and water samples were collected for complementary analyses of particulate and total dissolved metal concentrations; water composition and proxies for primary production. Integration of all the data enabled to deeper understand the temporal behavior of the potentially bioavailable metal species and to identify abiotic and biotic processes that control their concentrations and cycling as reflected by selected examples of results.

REFERENCES

[1] Tercier-Waeber, M.-L., Stoll, S., Slaveykova, V.I. 2012: Trace metal behavior in surface waters: emphasis on dynamic speciation, sorption processes and bioavailability (Review), Archive of Sciences, 65, 119-142.
[2] Tercier-Waeber, M.-L., Confalonieri, F., Abdou, M., Dutruch, L., Bossy, C., Fighera, M., Bakker, E., Schäfer, J., 2021: Advanced multichannel submersible probe for autonomous high-resolution in situ monitoring of the cycling of the potentially bioavailable fraction of a range of trace metals, Chemosphere 282, https://doi.org/10.1016/j.chemosphere.2021.131014.

4.12
Micromodel study on the removal of arsenic from drinking water using zerovalent iron / sand filters

Jonas Wielinski[1], Joaquin Jimenez-Martinez[1,2], Jörg Göttlicher[3], Ralph Steiniger[3], Stephan Hug[1], Michael Berg[1], Andreas Voegelin[1]

[1] *Eawag, Swiss Federal Institute of Aquatic Science and Technology, 8600 Dübendorf, Switzerland* (*jonas.wielinski@eawag.ch*)
[2] *Department of Civil, Environmental and Geomatic Engineering, ETH Zürich, Zürich, Switzerland*
[3] *Institute of Photon Science, Karlsruhe Institute of Technology, Hermann-von-Helmholtz-Platz 1, 76344 Eggenstein-Leopoldshafen, Karlsruhe, Germany.*

Globally, about 80 - 220 million people consume drinking water with As concentrations exceeding the limit of 10 µg/L recommended by the World Health Organization (Podgorski & Berg, 2020). Various types of filters that contain zerovalent Fe (ZVI) between layers of sand are applied to remove As from anoxic As-rich groundwater (GW) for human consumption and other uses; as for example the commercial SONO filters (Hussam & Munir, 2007). In these filters, ZVI corrosion leads to the release of dissolved Fe^{2+}. During the filtration of oxygenated water, Fe^{2+} is oxidized to Fe^{3+} and precipitates as Fe(III)-(oxy)(hydr)oxides (FHO) while As(III) is oxidized to As(V) that strongly sorbs onto FHO. For the time between the filter uses, dissolved O_2 (DO) is depleted from stagnant water and continuing Fe^{2+} release can lead to the transformation of FHO into denser magnetite, thereby reducing the risk of pore-clogging.

To improve our understanding of pore-scale processes in ZVI / sand filters for As removal, we developed a micromodel to study intermittent water flow using light microscopy and synchrotron X-ray spectroscopy. The micromodel was 45 x 5 x 0.25 mm (length x width x depth) and contained ZVI and quartz grains (both 200 < *d* < 250 µm). Synthetic GW resembling groundwater in Bangladesh was pumped through the channel for 12 h at a flow rate of 300 µL/h, followed by a no-flow period for the next 12 h. Every 30 min, a microscope image (137x magnification) of the ZVI / quartz layer was recorded.

The images were collated into a movie to extract kinetic information on the transformation of Fe-phases determined by colour changes. During the flow period, transport is dominated by advection, whereas diffusion dominates during the no-flow period. The effluent was collected for the determination of elemental concentrations, and, after 13 days, the microfluidic channel was embedded in an epoxy resin for analysis by spatially-resolved synchrotron X-ray fluorescence spectrometry and X-ray absorption spectroscopy at the Fe and As K-edges. Results will be presented in this talk. Our goal is a comprehensive understanding of the physical (advection, diffusion) and chemical (redox reactions, sorption) processes occurring in ZVI / sand filters to identify relevant parameters for an improved filter design.

REFERENCES

Podgorski, J.; Berg, M., Global threat of arsenic in groundwater. Science 2020, 368 (6493), 845-850.

Hussam, A.; Munir, A. K. M., A simple and effective arsenic filter based on composite iron matrix: Development and deployment studies for groundwater of Bangladesh. Journal of Environmental Science and Health, Part A 2007, 42 (12), 1869-1878.

4.13
Metal isotope process tracing in plant science: a useful tool in plant science or just gymnastics for geochemists?

Matthias Wiggenhauser[1]

[1] *Institute of Agricultural Sciences, ETH Zurich, Eschikon 33, CH-8315 Lindau*

For almost two decades, geochemists have employed non-traditional stable isotope measurements to decipher chemical and physical processes that control trace metals and metalloids in plants. These attempts include plant nutrients such as Zn, Fe, Cu, Ca, and Mg, beneficial nutrients such as Si or non-essential pollutants such as Cd and Tl. Based on research results on Cd and Zn and on an ongonig interdisciplinary literature review on the use of metal stable isotope process tracing in plant science, I will i) provide basics of metal isotope process tracing, ii) show successful and 'poking in the fog' attempts, and iii) provide a critical evaluation on the effectiveness of isotope process tracing in plant science.

4.14
Characterization of dissolved organic matter (DOM) produced by phytoplankton and its mercury binding capacities using asymmetrical flow field-flow fractionation with multi-detection (AF4-MD)

I.A.M. Worms*, Thibaut Cossart*, Joao Santos*, Kevin Trindade* and V.I. Slaveykova*

**Department F.-A. Forel for environmental and aquatic sciences, Earth and Environmental Sciences, Faculty of Sciences, University of Geneva, 66, boulevard Carl-Vogt, CH-1211 Geneva 4, Switzerland (isabelle.worms@unige.ch).*

DOM is ubiquitous in aquatic environments and plays an essential role in regulating the water quality, the chemical speciation of metals, and thus toxic trace metals fate.
Among main DOM components, humic substances (HS) from pedogenic origin are by far the more studied in term of complexation capacities for metallic species, and thus in mitigating their persistence in watershed and in affecting bioavailability or toxicity of toxic metals for biota. However, much less information is available for the role of extracellular polymeric substances (EPS) released by phytoplankton. In this study we aimed to characterize and compare the production of EPS of three different phytoplanktonic species in terms of composition and molecular mass distribution, and to assess their binding capacity against mercury (Hg) species.

To this end we used a combination of bioassays with measurements by asymmetrical flow field-flow fractionation with multi-detection (AF4-MD). AF4-MD is able to separate on a size-basis component ranging from macromolecules to colloidal assemblages, and associate to the simultaneous on-line detection of several optical characteristics (UV-visible absorbance, Fluorescence) and elemental composition (ICP-MS), which makes it a technique of choice to characterize DOM composition and its metal binding capacity. The phytoplanktonic species were chosen to roughly cover natural diversity found in natural settings: *Synechocystis*, as representative for cyanobacteria (prokaryotes), *Chlamydomonas reinhardtii* representative of green algae (eukaryotes) and a diatom (eucaryotes), *Cyclotella meneghiniana*.

The excreted components were concentrated on 1kDa cut-off centrifugal-ultrafiltration devices and analyzed by using Excitation-Emission Matrices fluorescence. Our results show first that the secreted DOM components isolated from the extracellular media of three phytoplankton species differed in quantity and quality regarding the presence of HS-like fluorescent components (< 1kDa) and proteins (> 1kDa). In order to go deeper in details, AF4-MD with the addition of a multi-angle-light scattering detector (MALS) was used to differentiate the HS/protein size-patterns associated to each microorganism's EPS. Some proteins are of globular nature although other should occur more as inorganic-co-agglomerates in the culture media. In addition, some EPS present metallo-proteins that could be responsible of preferential binding of mono-methyl mercury (meHg) as compared to inorganic mercury (iHg), or depending on the phytoplankton involved. Additionally, HS-like components of low molecular mass are also involved in such preferential size-pattern interaction.

Our results illustrate how AF4-MD can be used to address the diversity in the composition, molecular mass distribution of the EPS released by phytoplankton species, in line with changes that could occur for DOM composition in productive lakes, subjected to seasonal cycling, or at the vicinity of microorganisms. Further work is needed to address how such differences could play a role in global Hg cycling, in term of (bio)-transformation, uptake or toxicity.

P 4.1
The potential of indigenous microbes in supporting maize in the face of arsenic threats

Hang Guan[1], Veronica Caggìa[2], Miquel Coll Crespi[1], Xiaowen Liu[1], Andrea Gomez Chamorro[3], Teresa Chavez-Capilla[1], Alban Ramette[3], Adrien Mestrot[1], Klaus Bernhard Schläppi[2] and Moritz Bigalke[1]

[1] *Institute of Geography, University of Bern, Hallerstrasse 12, CH-3012 Bern (hang.guan@giub.unibe.ch)*
[2] *Institute of Plant Sciences, University of Bern, Altenbergrain 21, CH-3013 Bern*
[3] *Institute for Infectious Diseases, University of Bern, Friedbühlstrasse 51, CH-3001 Bern*

Arsenic (As) is a trace metalloid known as “the king of poisons”. Arsenic is a class one carcinogen and its high toxicity causes various human diseases such as skin cancer. The speciation of As largely regulates its mobility, bioavailability and toxicity in the environment. Arsenic speciation is determined not only by abiotic parameters such as pH and DOC, but also by biotic factors such as soil microbiota. For example, soil microbiota can enzymatically transform As from inorganic to organic forms. Here, we performed a pot experiment in the greenhouse to analyze As concentrations and speciation in the soil-plant system and to investigate the potential of soil microbiota in supporting plant growth under As toxicity.

We formed nine experimental groups: three soil treatments (native soil (NS), disturbed soil (DS) and reconditioned soil (RS) intersecting with three As concentration groups (Asc, As100, and As200 mg kg-1). RS is first-sterilized soil reconditioned with indigenous microbial extracts. Since soil sterilization might have other effects such as nutrient release than microbial disturbance, RS treatment serves to distinguish the microbial processes from other effects. Asc is the control group without arsenic addition. We added corresponding levels of arsenate salt to prepare As100 and As200 soils. The soils were then incubated for two months to allow for As equilibrium between the soil and soil water phase. In each treatment group, we cultivated10 pots with maize plants and three pots without plants. We sampled soil water, soil, and plant samples to analyze multi-elements with ICP-MS, and As speciation with HPLC-ICP-MS. This experiment mainly aims to answer these two main research questions: 1) What is the influence of As, soil, and plant growth treatments on As concentrations and speciation in soil water? 2) What is the influence on plant health? Our hypothesis is that As concentrations in soil water is lowest in NS, followed by RS, and highest in DS, which is due to decreasing microbial abundance in the three soils. This is in line with the decreasing health status of maize plants grown on NS > RS > DS.

The results were mostly consistent with our hypothesis. Especially in uncontaminated soils (Asc group), total As concentrations and organic As species showed the concentration pattern NS < RS < DS. The sum of organic As species did not change over time, but were much higher in DS and RS soils at the beginning of the experiment, clearly indicating the effect of the soil microbiota. Moreover, plant health was also in agreement with our hypothesis. Plants in NS had the best health conditions, followed by plants in RS and last in DS. Due to higher As concentrations and soil microbiota disturbance in DS and RS, maize exhibited lower plant height, lower chlorophyll content, and a greater scale of spot disease on their leaves. Plants grwoing in DS were most affected by As toxin. This revealed that the soil microbiota has great potential to support plant growth even in enviroments with high As levels.

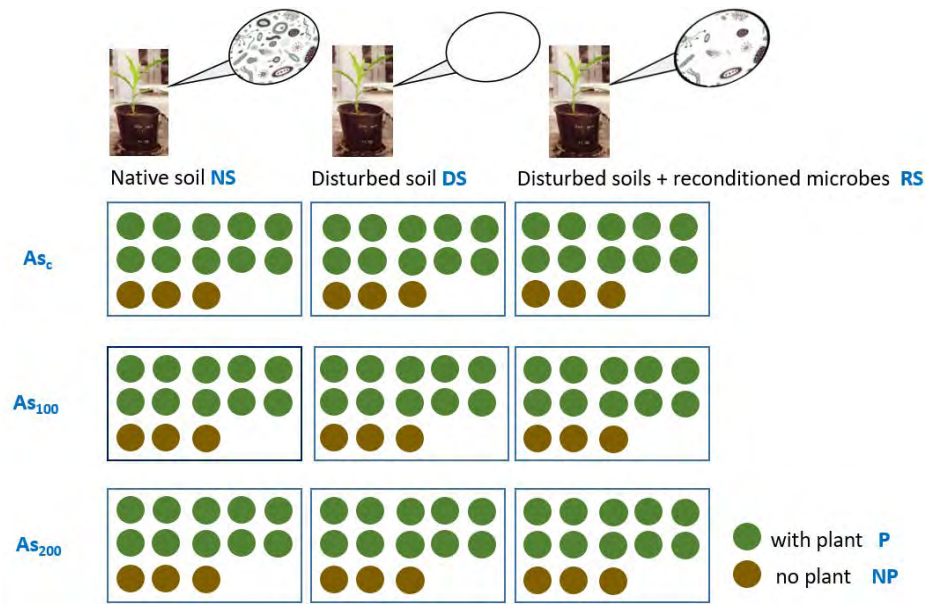

Figure 1. Overview of the experimental design.

P 4.2
Adsorption of CeO_2 Nanoparticles onto Sand used in Drinking Water Treatment Plant

Gabriela Hul [a], Stéphan Ramseier Gentile[b], Stéphan Zimmermann[b], Serge Stoll[a]

[a]Group of Environmental Physical Chemistry, Department F.-A. Forel for Environmental and Aquatic Sciences, Institute of Environmental Science, University of Geneva, Uni Carl Vogt 66, boulevard Carl-Vogt, CH-1211 Geneva 4, Switzerland; [b]SIG, Industrial Services of Geneva, Ch. du Château-Bloch, Le Lignon, 1211 Genève 2, Switzerland

Adsorption is considered as one of the most important processes controlling the fate and transport of nanomaterials in the environment and industrial filtration units. However, mechanisms and physical or chemical parameters influencing these processes are still poorly understood, especially in the case of porous materials used in water purification. In this study, mechanisms responsible for deposition and attachment of CeO_2 NPs onto quartz sand used as a filter medium in the drinking water treatment plant of Geneva (Switzerland) are examined. The batch experiments were performed using ultrapure water at pH of 3.0 ± 0.1 and filtered Geneva Lake water (pH ~8.6). Residual CeO_2 NPs concentrations in the supernatant after mixing with sand were determined with UV-vis spectroscopy. CeO_2 NPs were found to adsorb very well onto sand grains surfaces under acidic conditions due to electrostatic attractive interactions. The kinetics of adsorption followed well both pseudo-first-order model and pseudo-second-order model. The adsorption process was successfully described by Langmuir isotherm which indicated the formation of a monolayer, with a maximal adsorption capacity of 0.85 ± 0.2 mg g^{-1}, at the grains surface. The scanning electron microscopy (SEM) images showed individual CeO_2 NPs or small aggregates attached to the sand surface, thus confirming choice of the adsorption model. The results obtained from batch studies conducted using filtered Geneva Lake water showed that aggregation, caused by the presence of natural organic matter (NOM) and multivalent ions, and further aggregate sedimentation are the main processes responsible for CeO_2 NPs elimination under environmental conditions. Moreover, as CeO_2 NPs and sand grains both carried negative charges, electrostatic repulsion forces also hindered adsorption. SEM images confirmed these observations and revealed only limited adsorption in the vicinity of sand surface irregularities.

P 4.3
Evaluation of dissolved Cu, Cd, Pb and Zn speciation in relation to Environmental Quality Guidance

Nicolas Layglon[1], Melina Abdou[1], Francesco Massa[2], Michela Castellano[2], Paolo Povero[2], Eric Bakker[1], Mary-Lou Tercier-Waeber[1]

[1] University of Geneva, Sciences II, 30 Quai E.-Ansermet, 1221 Geneva 4, Switzerland (nicolas.layglon@unige.ch)
[2] University of Genoa, DISTAV-DCCI, 16132 Genoa, Italy

The EU Water Framework Directive (WFD-2008/105 / EC) established a list of priority hazardous chemicals and set thresholds for total dissolved concentrations (after filtration at 0.45 µm) which, if exceeded, indicate poor water quality. However, recent studies clearly demonstrated a flaw in the WFD environmental quality guidance (EQG) set for trace metals. As a matter of facts, while the maximal Pb and Cd concentrations allowed by the EQG are respectively 68 and 13.2 nM, lower Pb and Cd concentrations showed deleterious effects onto marine plankton (Echeveste et al., 2012; Ensibi and Daly Yahia, 2017). Furthermore, while Cu is not considered as a priority substance in the WFD, few nanomolar of dissolved Cu per liter could induced a negative response from some planktonic species (Coclet et al., 2020). Finally, it is assumed that the marine biota is more inclined to assimilate trace elements whose size is lower than 0.2 µm, especially the so-called truly dissolved metal species (≤ 1 nm). Thus, the determination of the bioavailable fraction is a primordial objective which requires innovative tools. Recently, a newly designed tool for simultaneous in situ measurements of a range of hazardous trace metals was developed (Tercier-Waeber et al., 2021). The present study aimed at evaluating the dissolved Cu, Cd, Pb and Zn speciation by measuring their total dissolved (after 0.2µm filtration), their “truly” dissolved (after 0.02 µm filtration) and their dynamic concentrations. The determined concentrations were compared to the EQG established by the EU as well as those determined by the Australia and New Zealand to protect 95 and 99 % of the species.

REFERENCES

Coclet, C., Garnier, C., Durrieu, G., D’onofrio, S., Layglon, N., Briand, J.-F., Misson, B., 2020. Impacts of copper and lead exposure on prokaryotic communities from contaminated contrasted coastal seawaters: the influence of previous metal exposure. FEMS Microbiology Ecology. https://doi.org/10.1093/femsec/fiaa048

Echeveste, P., Agustí, S., Tovar-Sánchez, A., 2012. Toxic thresholds of cadmium and lead to oceanic phytoplankton: Cell size and ocean basin-dependent effects. Environmental Toxicology and Chemistry 31, 1887–1894. https://doi.org/10.1002/etc.1893

Ensibi, C., Daly Yahia, M.N., 2017. Toxicity assessment of cadmium chloride on planktonic copepods Centropages ponticus using biochemical markers. Toxicology Reports 4, 83–88. https://doi.org/10.1016/j.toxrep.2017.01.005

Tercier-Waeber, M.-L., Confalonieri, F., Abdou, M., Dutruch, L., Bossy, C., Fighera, M., Bakker, E., Graziottin, F., van der Wal, P., Schäfer, J., 2021. Advanced multichannel submersible probe for autonomous high-resolution in situ monitoring of the cycling of the potentially bioavailable fraction of a range of trace metals. Chemosphere 282, 131014. https://doi.org/10.1016/j.chemosphere.2021.131014

P 4.4
Effect of Si, Ca, and Mg on phosphate co-precipitation with Fe and on P retention during precipitate aging

Ville Nenonen[1,2], Ralf Kaegi[1], Stephan J. Hug[1], Stefan Mangold[3], Jörg Göttlicher[3], Lenny H.E. Winkel[1,2] & Andreas Voegelin[1]

[1] Eawag, Swiss Federal Institute of Aquatic Science and Technology, Ueberlandstrasse 133, CH-8600 Duebendorf, Switzerland (ville.nenonen@eawag.ch)
[2] Department of Environmental Sciences, Institute of Biogeochemistry and Pollutant Dynamics, ETH, Swiss Federal Institute of Technology, Zurich, Switzerland.
[3] Karlsruhe Institute of Technology, Institute of Synchrotron Radiation, Hermann-von-Helmholtz Platz 1, D-76344 Eggenstein-Leopoldshafen, Germany

Phosphorus is an essential nutrient, but excessive inputs into surface waters may lead to the eutrophication and deterioration of aquatic ecosystems. The biogeochemical cycling of phosphorus is coupled to the cycling of Fe. The oxidation of dissolved Fe(II) in natural waters leads to the formation of Fe(III)-precipitates with a high sorption capacity for phosphate (P). Fresh Fe(III)-precipitates are metastable and can transform into more stable phases over time, which may lead to the release of initially bound P. Repartitioning of P into Ca-carbonates or –phosphates, on the other hand, could attenuate P release.

We performed time-resolved experiments on the structural transformation of Fe(III)-precipitates and the fate of co-precipitated P during aging, with a focus on the effects of Ca, Mg, Si, and P on Fe phase formation and transformation, Ca precipitation, and P retention. Expanding on earlier work (Senn et al., 2015, 2017, 2018), we determined changes in dissolved element concentrations and in the structure of the solids over time using X-ray absorption spectroscopy (XAS), X-ray diffraction (XRD), Fourier-transform infrared spectroscopy (FTIR), and transmission electron microscopy (TEM) for solids characterization.

The experiments were performed with 0.5 mM Fe in bicarbonate-buffered electrolytes with Na, Ca, or Mg as electrolyte cations without or with 0.5 mM Si at molar P/Fe ratios of 0.3 and 0.05. The initial precipitates were mixtures of amorphous Fe(III)-phosphate and poorly-crystalline lepidocrocite (no Si) or Si-ferrihydrite (with Si). Increases in dissolved P in the electrolytes without Si were linked to the formation of a higher share of more crystalline lepidocrocite. This transformation was slowed down by Ca and (to a lesser extent) Mg. The presence of Si inhibited P release during aging by promoting the formation of Si-ferrihydrite with a higher sorption capacity than lepidocrocite. The extent to which P was released during aging could be directly linked to the individual and coupled effects of Ca, Mg, and Si on Fe(III)-precipitate structure and transformation and to the P sorption capacity of the different solids.

REFERENCES

Senn, A.-C.; Kaegi, R.; Hug, S. J.; Hering, J. G.; Mangold, S.; Voegelin, A., *Composition and structure of Fe(III)-precipitates formed by Fe(II) oxidation in near-neutral water: Interdependent effects of phosphate, silicate and Ca.* Geochim. Cosmochim. Acta 2015, 162, 220–246.

Senn, A.-C.; Kaegi, R.; Hug, S. J.; Hering, J. G.; Mangold, S.; Voegelin, A., *Effect of aging on the structure and phosphate retention of Fe(III)-precipitates formed by Fe(II) oxidation in water.* Geochim. Cosmochim. Acta 2017, 202, 341–360.

Senn, A.-C.; Kaegi, R.; Hug, S. J.; Hering, J. G.; Voegelin, A., *Arsenate co-precipitation with Fe(II) oxidation products and retention or release during precipitate aging.* Water Res. 2018, 131, 334–345.

P 4.5
Fate and removal efficiency of titanium oxide nanoparticles (TiO2 NPs) in a conventional drinking water treatment plant

Robin Noyer, Serge Stoll and Lina Ramirez Arenas*

Group of Environmental Physical Chemistry, Department F.-A. Forel for environmental and aquatic sciences, University of Geneva, Uni Carl Vogt, 66, boulevard Carl-Vogt, CH-1211 Geneva 4, Switzerland.
**Corresponding author: Lina.RamirezArenas@unige.ch, Tel: +41 22 379 0332*

Owing to their physicochemical properties, titanium oxide nanoparticles (TiO_2 NPs) are widely used into a large number of industrial applications and consumer products. The intensive use of TiO_2 NPs results in their release into aquatic systems and consequently in drinking water resources, and represents a potential threat for ecosystems as well a potential health risk for humans.

NPs fate and removal efficiency in drinking water treatment plants (DWTP), which ensure water quality and supply drinking water for human consumption, have been by far less investigated. This study investigates the removal efficiency of TiO_2 NPs in a conventional water treatment plant providing drinking water for 500'000 consumers (Geneva, Switzerland). For that purpose, a pilot-scale DWTP reproducing at a small scale the different processes and conditions of the main treatment plant is used. The results show that filtration processes through sand and granular activated carbon (GAC) filters in the absence of coagulation achieves an overall TiO_2 NPs removal of 96%. The removal efficiency of filtration processes is mainly attributed to physical retention and adsorption mechanisms. On the other hand, the coagulation process greatly improves the removal efficiency and most of TiO_2 NPs are removed during sand filtration process with an effective removal efficiency equal to 99.5%. It should be pointed out that TiO_2 NPs were not found or detected in the drinking water after GAC filtration in presence of coagulant. The higher removal efficiencies with the addition of coagulant is related to TiO_2 NPs surface charge neutralization and large aggregate formation thus significantly increasing their retention in the filter media.

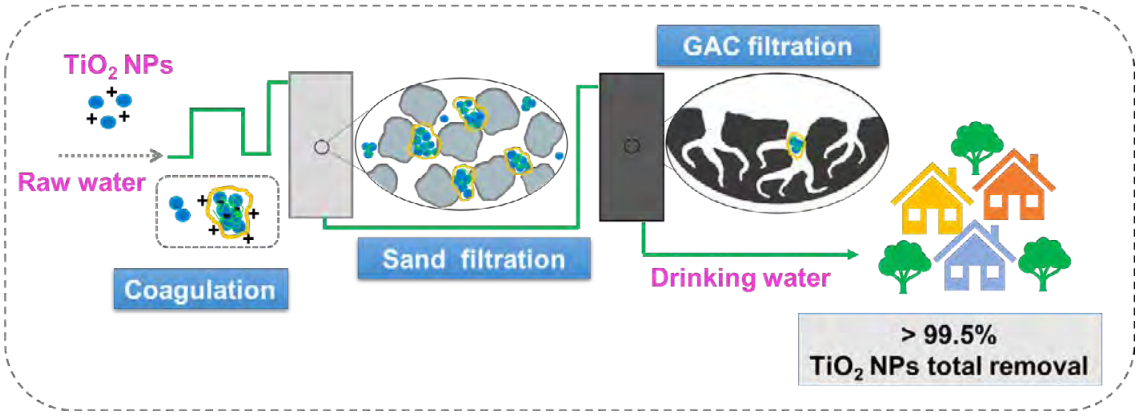

Figure 1. Overall performance of the conventional DWTP (Geneva, Switzerland) on the removal of TiO_2 NPs after coagulation, sand and GAC filtration.

P 4.6
Geochemical Soil Atlas of Switzerland

Jolanda E. Reusser[1], Lenny Winkel[2,3], Ruben Kretzschmar[2], Daniel Wächter[1], Reto G. Meuli[1]

[1] *Swiss Soil Monitoring Network NABO, Agroscope, CH-8046 Zurich (jolanda.reusser@agroscope.admin.ch)*
[2] *Institute of Biogeochemistry and Pollutant Dynamics, ETH Zurich, CH-8092 Zurich*
[3] *Department Water Resources and Drinking Water, Swiss Federal Institute of Aquatic Science and Technology, Eawag, CH-8600 Dübendorf*

Trace elements such as Se, Zn and Cu are essential for humans, animals and other organisms in a certain concentration range. Other trace elements such as Cd and Hg are potentially toxic to human health already at low concentrations. The concentration of trace elements in the soil and their bioavailability are main factors influencing the accumulation of these elements in crops and fodder.

Broad-scale distributions of trace element concentrations in soils are presented in geochemical soil atlases. Based on this information, regions with trace element deficiencies or soil contaminations can be assessed. However, in contrast to other countries (Rawlins et al., 2012; van der Veer, 2006), no nationwide geochemical soil atlas exists for Switzerland.

Between 2011 and 2015, samples of the topsoils (0-20 cm) have been collected along a regular 6 by 4 km grid within the framework of the Swiss Biodiversity Monitoring (BDM) program (Meuli et al., 2017). In total, 4'270 samples have been taken from 1'153 sampling sites covering whole Switzerland. The soil samples were dried, sieved at <2 mm, ground to powder and digested using an aqua regia solution. Concentrations of 53 elements were analysed in the soil extracts using ICP-MS. The dataset was complemented with an additional dataset on element concentrations measured in aqua regia digests of topsoils (291 sampling sites) compiled by the group of Dr. Moritz Bigalke (University of Bern) and the NABO soil database (105 sampling sites). The concentrations and spatial distributions of a subset of the complete dataset including the trace elements As, B, Ca, Cd, Co, Cr, Cu, Fe, Hg, Mg, Mn, Mo, Na, Ni, Pb, S, Sb, Se, Tl, U, V and Zn will be presented in the first Swiss geochemical soil atlas.

We hereby present the concept of the geochemical soil atlas as well as first statistical analyses of all elemental data.

REFERENCES

Meuli, R.G., Wächter, D., Schwab, P., Kohli, L., Zimmermann, R., 2017. Connecting Biodiversity Monitoring with Soil Inventory Data – A Swiss Case Study. Bulletin BGS 38, 65–69.

Rawlins, B.G., McGrath, S.P., Scheib, A.J., Breward, N., Cave, M., Lister, T.R., Ingham, M., Gowing, C., Carter, S., 2012. The advanced soil geochemical atlas of England and Wales. British Geological Survey, Keyworth.

van der Veer, G., 2006. Geochemical soil survey of the Netherlands: Atlas of major and trace elements in topsoil and parent material; assessment of natural and anthropogenic enrichment factors. Geografische Studies 347, 1–245.

P 4.7
Natural organic matter as a modifier of Hg bioavailability to green algae

Isabelle A.M. Worms*, Elodie Moulin*, Nicole Regier*, Killian Kavanagh* and Vera I. Slaveykova*

**Department F.-A. Forel for environmental and aquatic sciences, Earth and Environmental Sciences, Faculty of Sciences, University of Geneva, 66, boulevard Carl-Vogt, CH-1211 Geneva 4, Switzerland (vera.slaveykova@unige.ch).*

Mercury (Hg) is a priority pollutant of global concern, which is characterized by strong bioconcentration and biomagnification in the aquatic food webs. Mercury interaction with phytoplankton, central for its incorporation in the food webs, and in particular the role of various environmental modifying factors such as natural organic matter (NOM) is still to elucidate. The objective of this work is to get new insight in the role of the NOM on Hg bioavailability to phytoplankton. Since trace metal complexation by NOM is expected to reduce its bioavailability, we hypothesized that the reduction of the Hg bioavailability to *Chlamydomonas reinhardtii,* chosen as a model phytoplankton, will be proportional to the fraction of the Hg being complexed by NOM.

To get insight into the role of NOM in Hg uptake*, C. reinhardtii* was exposed to two concentrations of Hg in the presence of standard Suwannee River humic acid (SRHA) and in natural water rich in NOM from Onego Lake, Russia. Water was sampled from five sites representing the DOC gradient from River Shuya to open lake. Bioavailability was quantified by determining the intracellular mercury concentrations by Direct mercury analyzer on freeze-dried pellets. Concentrations of Hg in the exposure media were measured with the MERX Automated Total Mercury Analytical System. In addition the composition, molar mass distribution and binding of Hg to NOM was preformed by a combination of Assymetrical field flow fractionation coupled online to UV fluoresence detection and inductively coupled plasme mass spectrometry (AF4-UV-FL-ICPMS).

The results showed that adsorbed and intracellular Hg concentrations decreased as compared with exposure in the absence of SRHA only at 0.7nM IHg, when the estimated ratio between the reduced sulfur concentration and IHg is bigger than 100 (Beauvais-Flück, R. et al, 2019). A significant increase (1.5×) of Hg uptake in *C. reinhardtii* exposed to 70 nM Hg in the presence of 0.5 and 5 $mg \cdot L^{-1}$ DOC was found. In the DOC-rich water from lake Onega, a decrease of the bioavailability with respect to exposure in the absence of NOM was found. A negative correlatation between whole cell and intracellular Hg and DOC concentrations was found. This corelation was much stronger with the thiol concentrations, obtained by AF4-FL detection, fluorescence and humification indexes of NOM. Such relationships evidenced possible negative feedbacks with these NOM characteristics and Hg bioavailability to algae. The effect of the other factors such as the presence and concentration of different major cations and anions, present in natural waters, has to be taken into account in addition to the role of NOM. The significance and implications of the results are discussed with respect to the narrowing the gap in lab-to-field extrapolation, as well as with respect to the prediction of the mercury incorporation at the base of the food-webs and the impact in the environmental systems.

REFERENCES

Beauvais-Flück, R. Slaveykova, V.I.& U. Skyllberg, C. Cosio, 2019: Towards early-warning gene signature of *Chlamydomonas reinhardtii* exposed to Hg-containing complex media. Aquatic Toxicology 214, 105259.

P 4.8
Microbial Methylation of Antimony

Karen Viacava* & Adrien Mestrot*

**Institute of Geography, Univeristy of Bern, 3012, Bern, Switzerland (*correspondence: karen.viacava@giub.unibe.ch)*

Antimony (Sb) is a naturally occurring metalloid that can be remobilised from soils due to flooding. The released Sb can potentially expose the soil microorganisms to the metalloid. Sb shares common chemical and toxicological properties with arsenic (As), e.g. they are found in the same oxidation states in the environment and are potent genotoxines [1]. Thus, enzymes able to transform and detoxify from As might be able to transform and detoxify Sb. In deed, Sb entering the intracellular space can be pumped out of the cell by As membrane transporters [2][3]. The methylation of As has been subject of thorough study since the 1950's [4]. The reaction is catalysed by the enzyme arsenite methyltransferase (ArsM) and can lead to As volatilization. The gene encoding ArsM has been found to be phylogenetically diverse and extensively distributed in diverse microbial communities. To date, the phylogeny of the microbial drivers of As methylation in soils is still a subject of debate [5][6]producing mainly phytotoxic dimethylarsenate (DMAs. Methylated Sb species have been detected in pure and mixed microbial cultures [7][8]we focused on soils of different origin. Here, we describe the biogenic production of volatile metal(loid and it has been hypothesized that ArsM could be responsible for the methylation of Sb. However, the Sb methylated species have been detected only after long incubation periods or celullar lysis and with very low efficiencies, casting the doubt whether it is an active metabolic process, as it is the case of As methylation by ArsM, or an artifact driven by Sb chemical reaction with methyldonors. In our study, we investigated the potential of the aerobic heterotrophic strain *Arsenicibacter rosenii* SM-1, previously shown to efficiently methylate As [5][9], to actively methylate and volatilize Sb.

REFERENCES

[1] Gebel, 1997: Arsenic and antimony: comparative approach on mechanistic toxicology, Chem. Biol. Interact., 107, 3, pp. 131–144.

[2] Maciaszczyk-Dziubinska, *et al.*, 2010: The yeast permease Acr3p is a dual arsenite and antimonite plasma membrane transporter, Biochim. Biophys. Acta - Biomembr., 1798, 11, 2170–2175.

[3] Shi *et al.*, 2018: Efflux Transporter ArsK Is Responsible for Bacterial Resistance to Arsenite, Antimonite, Trivalent Roxarsone, and Methylarsenite, Appl. Environ. Microbiol., 84, 1842–1860.

[4] Challenger, *et al.* 1954: The formation of trimethylarsine and dimethy selenide in mould cultures from methyl sources containing 14C, Stud. Biol. Methylation. XIV, 1760–1771.

[5] Viacava *et al.,* 2020: Variability in Arsenic Methylation Efficiency across Aerobic and Anaerobic Microorganisms, Environ. Sci. Technol., 54, 14343–14351.

[6] Chen *et al.,* 2019: Sulfate-reducing bacteria and methanogens are involved in arsenic methylation and demethylation in paddy soils, ISME J., 13, 10, 2523–2535.

[7] Andrewes, *et al.*, 1999, Confirmation of the aerobic production of trimethylstibine by Scopulariopsis brevicaulis, Appl. Organomet. Chem., 13, 9, pp. 659–664.

[8] Meyer *et al.*, 2007: Volatilisation of metals and metalloids by the microbial population of an alluvial soil, Syst. Appl. Microbiol., 30, 3, 229–238.

[9] Huang *et al.*, 2016: Efficient Arsenic Methylation and Volatilization Mediated by a Novel Bacterium from an Arsenic-Contaminated Paddy Soil, Environ. Sci. Technol., 50, 6389–6396.

P 4.9
Swiss Mountain Soil Ecology Project

Sarah Semeraro[1], Sergio Rasmann[2], Claire Le Bayon[3]

[1] *Institute of biology, Functional Ecology Laboratory, University of Neuchâtel, Emile-Argand 11, CH-2000 Neuchâtel (sarah.semeraro@unine.ch)*
[2] *Institute of biology, Functional Ecology Laboratory, University of Neuchâtel, Emile-Argand 11, CH-2000 Neuchâtel (sergio.rasmann@unine.ch)*
[3] *Institute of biology, Functional Ecology Laboratory, University of Neuchâtel, Emile-Argand 11, CH-2000 Neuchâtel (claire.lebayon@unine.ch)*

Along with the current climatic crisis, terrestrial ecosystems are undergoing significant modifications, both above and belowground. The steep elevation gradients of the European Alps, because of their close connection to temperature gradients, might be particularly concerned. For example, climate warming might induce changes in vegetation community structure in the alpine environment; increase the metabolic rate of soil microbes, and active faster organic matter degradation. Thus, climate change might disrupt the role of mountain soils acting as carbon sinks. To address this question, we use a multiscalar approach, from the local vegetation patch to the Switzerland landscape level and apply both temporal-explicit and spatial-explicit experimental designs. Specifically, first, we use a >20 years-old soil collection to compare changes in soil properties and humus forms to date. Second, we perform reciprocal transplant common garden experiments at different elevations to assess the effect of local vegetation and soil biota and flora on soil organic matter degradation. Together, the results of this research address how climatic gradients, spanning collinear to alpine elevations, might affect the evolution of mountain soils, and it will allow deciphering the ecosystem components that will majorly drive these changes.

06. Palaeontology

Torsten Scheyer, Christian Klug, Lionel Cavin, Allison Daley

Schweizerische Paläontologische Gesellschaft,
Kommission des Swiss Journal of Palaeontology (KSJP)

TALKS:

6.1 Bath Enright O., Daley A.C., Lustri L., Antcliffe J.B.: Understanding the biases that control the preservation potential of different developmental stages in the marine shrimp, *Palaemon varians*

6.2 Cavin L., Ferrante C., Manuelli L.: News from Mesozoic coelacanths

6.3 Evers S.W., Joyce W.G., Choiniere J.N., Ferreira G.S., Foth C., Hermanson G., Honyu Y., Johnson C., Werneburg I., Benson R.B.J.: Ecomorphology and evolution of the vestibular organ of turtles

6.4 Foerster, F.: Crystallographic characterization of sea urchin skeletal elements

6.5 Hermanson G., Evers S.W., Farina B.M., Ferreira G.S., Langer M.C., Benson R.B.J.: Ecological and functional controls that correlate with skull shape in turtles

6.6 Jobbins M., Rüklin M., Ferron H., Klug C.: Anatomical description of a selenosteid placoderm from the Late Devonian of the eastern Anti-Atlas (Morocco) and its ecomorphological reconstruction

6.7 Joyce W.G., Landréat J.-L., Rollot Y.: The Unexpecting Discovery of Snapping Turtles (*Pan-Chelydridae*) in the Middle Eocene of France

6.8 Klug C., Lagnaoui A., Jobbins M., Haouz W.B., Najih A.: Marine vertebrates from Romer's Gap: a swimming trace from the latest Devonian of Morocco

6.9 Lustri L., Gueriau P., Daley A.C.: New specimens of *Bunaia woodwardi* Clarke 1919 (Euchelicerata, synziphosurine) provide insight into Euchelicerata and Vicissicaudata affinity

6.10 Manuelli L., Cavin L.: A new coelacanth from the Triassic of Lorraine

6.11 Ovtcharova M., Ivantsov A., Linnemann U., Ivleva A., Ershova V., Nagovitsin A.: U-Pb zircon ID-TIMS geochronology of the oldest biota of the Ediacaran White Sea assemblage (Summer Coast, NW Russia)

6.12 Pérez–Peris F., Adrain J., Daley A.C.: Phyologenetics and systematics of the trilobite subfamilies Cheirurinae and Deiphoninae: shedding light on the basal relationships

6.13 Potin G., Gueriau P., Daley A.C.: Unique assemblage of suspension-feeding radiodonts from the Early Ordovician Fezouata Biota

6.14 Rollot Y., Evers S.W., Joyce W.G.: Cranial anatomy and phylogeny of Late Jurassic to Early Cretaceous paracryptodiran turtles

6.15 Scheyer T.M., Kirwald K., Bregant P.: Revision of the Triassic placodont material (Sauropterygia) from Switzerland

6.16 Vasilyan D., Maul L., Becker D., Meyer M., Bukhskianidze M., Costeur L., Mayr G., Lazarev S.: First data on Pliocene continental fossil record of Armenia, Southern Caucasus

POSTERS:

P 6.1 Pople J., Daley A., Gueriau P.: 3D Taphonomy of Phosphatized Cambrian Arthropods

P 6.2 Stemmler D., Gerya T., Pellissier L., Stern R.J.: Influence of plate tectonics on biodiversity

6.1
Understanding the biases that control the preservation potential of different developmental stages in the marine shrimp, *Palaemon varians*

Orla G. Bath Enright[1], Allison C. Daley[1], Lorenzo Lustri[1], Jonathan B. Antcliffe[1]

[1] *Institut des sciences de la Terre, Université de Lausanne, Geopolis, CH-1015 Basel (orla.bathenright@unil.ch)*

The ontogeny of arthropods in the fossil record is well recognized to be highly biased towards the later ontogenic stages of their development. Larval and early juvenile stages are rarely preserved, with even the most impressive Lagerstätten either preserving large macroscopic or tiny fossils.The exception being the newly discovered Haiyan lagerstätte in China or the Orsten biota in Sweden. The Haiyan fossil assemblage has yielded rare and abundant larval and juvenile arthropod specimens making up 51% of all fossil specimens collected (Yang 2021). Such ontogenic data offers invaluable information about the developmental biology of this large group and opens a new line for taphonomic investigation into the biases controlling early juvenile stages of preservation.

In modern environments, many marine arthropods lay their eggs in specific maternal environements where the juveniles will stay until they reach a later stage of development. The newly grown adult shrimp will then leave that environment and enter an entirely different one. With so little juvenile data available in the fossil record, palaeontological recontructions may be biased towards considering most palaeo environments to be adult environments, but this may actually be the result of taphonomic biases within such assemblages.

Here we investigate the preservation potential of the common marine shrimp *Palaemon varians* at varying stages of its ontogeny. Decay was observed in an ovigerous female shrimp to fully grown specimens in their adult developmental stages. Understanding *Palaemon varians* decay at different growth stages and body sizes provides important information on the relationship between ontogeny and taphonomy, and the impacts on palaeocommunity reconstructions. Our first set of experimental results are presented here.

REFERENCES

Yang, X., Kimmig, J, Zhai, D., Liu, Y., Kimmig, S.R., & Peng, S. 2021: A juvenile-rich palaeocommunity of the lower Cambrian Chengjiang biota sheds light on palaeo-boom or palaeo-bust environments, *Nature Ecology & Evolution*, 5(8), 1082-1090.

6.2
News from Mesozoic coelacanths

Lionel Cavin[1], Christophe Ferrante[1,2], Luigi Manuelli[1,3]

[1] Natural History Museum of Geneva, 1 rue Malagnou, 1208-Geneva, Switzerland (lionel.cavin@ville-ge.ch)
[2] Department of Earth Sciences, University of Geneva, Rue des Maraîchais 13, 1205-Geneva, Switzerland.
[3] Department of Genetics & Evolution, University of Geneva, Boulevard D'Yvoy 4, 1205-Geneva, Switzerland.

Latimeria is the only extant representative of the coelacanth fish, with two species roaming the eastern coast of Africa and in Indonesia. These iconic fish are nicknamed "living fossils" because of their supposedly slow rate of morphological evolution. Fossil records of coelacanths are missing in the Cenozoic, but there was fair diversity during the Mesozoic. Most Mesozoic taxa belong to two families, the Mawsoniidae and the Latimeriidae, grouped together in the Latimeroidei. In this contribution, we review some recent discoveries in these two families studied by our team.

Mawsoniidae were first described from the Cretaceous of Western Gondwana (Africa and South America), then in the Triassic of North America. Recent discoveries have shown that this family was also present in marine deposits of the Triassic of Europe (Deesri et al., 2018) and in freshwater deposits of the Late Cretaceous of Europe (Cavin et al., 2016, 2020). Recently, a fragment of a giant Jurassic mawsoniid was discovered in the collection of the Natural History Museum of Geneva, and a re-examination of body-size reconstructions in the family showed that the low morphological disparity was counterbalanced by the disparity of body size (Cavin et al., 2021). A handful of bones referred to *Mawsonia* were recently discovered in the Late Cretaceous of Texas, USA, changing the evolutionary history of the genus. It now appears that this genus, and its sister genus *Axelrodichthys*, have stratigraphic ranges that may extend from the Late Jurassic to the end of the Cretaceous, or nearly 100 million years (Cavin et al., Submitted). The evolutionary history of *Mawsonia* is a model for understanding the evolutionary history of *Latimeria*, which has no fossil record but whose genome indicates the origin of the genus several tens of millions of years ago (Kadarusman et al. , 2021). Recent studies on the genetic origin of gigantism in vertebrates (Weber et al., 2020) and on the life cycle of *Latimaria* (Mahé et al., 2021) are avenues of exploratory research to understand the slow evolutionary rate and the large body size observed in some latimeroids.

The fossil record of Latimeriidae began in the Middle Triassic, notably with a middle Triassic coelacanth from Graubünden, eastern Switzerland, showing a very unusual morphology (Cavin et al., 2017). The recognition in the collection of the Paläontologisches Institut und Museum in Zurich of specimens of coelacanth from the Middle Triassic of Monte San Giorgio, sharing superficial characters with *Foreyia* from Graubünden, was the occasion to launch a detailed study of the anatomy and the relationships of this new form (Ferrante et al., 2017, in progress). Cladistic analysis revealed a close affinity with *Foreyia* and *Ticinepomis*, also from Monte San Giorgio, but the new taxon shows autapomorphic characters which are derived within the coelacanth clade.

Finally, three specimens of small complete and sub-complete articulated coelacanths preserved in nodules found in the Middle Triassic of Lorraine, France, were CT-scanned and are currently being described. The specimens show, among other features, an ossified lung visible in 3D. The taxon shares characters with *Diplurus*. Its inclusion in a cladistic analysis will help to understand the phylogenetic position of *Diplurus* and related taxa, since *Diplurus* is resolved as a mawsoniid in some analyzes (e.g. Cavin et al., 2017) and as a latimeriid in others (i.e. Toriño et al., 2017).

Although the taxonomic diversity of coelacanths has always remained very low during their 420 million years of history, these fish exhibit contrasting patterns in the rate and intensity of morphological transformation: some lineages display a slow evolution retaining a general coelacanth Bauplan, such as the Cretaceous *Mawsonia* or the extant *Latimeria*, while others exhibit short bursts of rapid morphological transformation, such as the basal Latimeriids from the Middle Triassic of the Alps or an as yet unstudied Late Jurassic specimen from Solnhofen.

REFERENCES

Cavin, L., Valentin, X., & Garcia, G. 2016: A new mawsoniid coelacanth (Actinistia) from the Upper Cretaceous of Southern France, Cretaceous Research, 62, 65-73.

Cavin, L., Mennecart, B., Obrist, C., Costeur, L., Furrer, H. 2017: Heterochronic evolution explains novel body shape in a Triassic coelacanth from Switzerland, Scientific Reports, 7, 13695.

Cavin, L., Buffetaut, E., Dutour, Y., Garcia, G., & Le Loeuff, J., et al. 2020: The last known freshwater coelacanths: New Late Cretaceous mawsoniid remains (Osteichthyes: Actinistia) from Southern France, PLOS ONE, 15, e0234183.

Cavin, L., Piuz, A., Ferrante, C., & Guinot, G. 2021: Giant Mesozoic coelacanths (Osteichthyes, Actinistia) reveal high body size disparity decoupled from taxic diversity, Scientific Reports, 11, 11812.

Deesri, U., Cavin, L., Amiot, R., Bardet, N., Buffetaut, E., et al. 2018: A mawsoniid coelacanth (Sarcopterygii: Actinistia) from the Rhaetian (Upper Triassic) of the Peygros quarry, Le Thoronet (Var, southeastern France), Geological Magazine, 155,

187-192.
Ferrante, C., Martini, R., Furrer, H., Cavin, L. 2017: Coelacanths from the Middle Triassic of Switzerland and the pace of actinistian evolution, Research and Knowledge, 3, 59-62.
Kadarusman, Sugeha, H.Y., Pouyaud, L., Hocdé, R., Hismayasari, I.B., et al. 2020: A thirteen-million-year divergence between two lineages of Indonesian coelacanths, Scientific Reports, 10, 192.
Mahé, K., Ernande, B., & Herbin, M. 2021: New scale analyses reveal centenarian African coelacanths, Current Biology.
Toriño, P., Soto, M., & Perea, D. 2021: A comprehensive phylogenetic analysis of coelacanth fishes (Sarcopterygii, Actinistia) with comments on the composition of the Mawsoniidae and Latimeriidae: Evaluating old and new methodological challenges and constraints, Historical Biology, 1-21.
Weber, J.A., Park, S.G., Luria, V, Jeon, S., Kim, H-M, et al. 2020: The whale shark genome reveals how genomic and physiological properties scale with body size, Proceedings of the National Academy of Sciences, 117, 20662-20671.

6.3
Ecomorphology and evolution of the vestibular organ of turtles

Serjoscha W. Evers[1,2], Walter G. Joyce[1], Jonah N. Choiniere[3], Gabriel S. Ferreira[4,5], Christian Foth[1], Guilherme Hermanson[1,6], Yi Honyu[7], Catherine Johnson[2], Ingmar Werneburg[4,5], Roger B. J. Benson[2,3]

[1] Department of Geosciences, University of Fribourg, Chemin du Musée 4, 1700 Fribourg, Switzerland (serjoscha.evers@googlemail.com)
[2] Department of Earth Sciences, University of Oxford, South Parks Road, Oxford, OX1 3AN, United Kingdom
[3] Evolutionary Studies Institute, University of the Witwaterrand, 1 Jan Smuts Avenue, Johannesburg 2000, South Africa
[4] Senckenberg Centre for Human Evolution and Paleoenvironment an der Universität Tübingen, Sigwartstrasse 10, 72076 Tübingen, Germany
[5] Fachbereich Geowissenschaften, Universität Tèbingen, Hölderlinstrasse 12, 72074 Tübingen, Germany
[6] Laboratório de Paleontogia de Ribeirão Preto, FFCLRP, Universidade de São Paulo, Ribereirão Preto, Brazil
[7] Institute of Vertebrate Paleontology and Paleoanthropology, Beijing 100044, China

The vestibular organ (= labyrinth) of amniotes consists of a series of semicircular ducts, which detect angular accelerations of the head and thus provide important sensory input for balance and orientation, by stabalizing the visual field of animals. This system is based on fluid dynamics, and morphological changes to the duct system have predicatble effects on the physics and thus the sensitivity of the system (e.g. Jones & Spells 1963). On this basis, strong form-function relationships have been hypothesized, which should be universally applicable among vertebrates if true. Specifically, these predict that some labyrinth attributes, such as the overall size of the system, are indicative of ecological specializations, particularly that agile amniotes have larger labyrinths. This relationship could be empirically supported by data from mammals (e.g., Spoor et al. 2007), but other groups have only recently been in the focus of studies, casting doubts on the universal applicability of most labyrinth form-function hypotheses. For instance, although labyrinth size variation in mammals is related to relative agility, the overall large labyrinth size of birds, traditionally linked to their ability to fly, evolutionary preceeded the origin of flight (Bronzati et al. 2021).

Turtles are a great case study in which to test the ecomorphology of the labyrinth: the group has an accellent fossil record extending over 230 Million years of evolution, and experienced numerous ecological transitions. These affect their locomotion behaviour, particularly secondary marine adaptations (e.g. sea turtles) and secondary terrestrial transitions (e.g. tortoises). The study of the turtle labyrinth is complicated by a strong mismatch of the membranous labyrinth organ and the endosseous labyrinth cavities that form its bony encasement. The latter can be studied in fossils, but the former determines vestibular function. We developed a reconstruction technique based on membranous-endossoeus labyrinth pairs from contrast-enhanced computed-tomography (CT) scans of living turtles, which allows us to faithfully reconstruct the endolmyphatic fluid flowpaths of the membranous labyrinth from endosseous data. We validated our method with statistical integration tests that document high co-variation between reconstructed and actual membranous labyrinths. We then apply this reconstruction technique to a large dataset of 168 digital turtle labyrinth specimens, which cover one fourth of extant turtle diversity and includes extinct representatives of all major fossil lineages. Our method also allows comparisons with the labyrinths of non-turtle amniotes (e.g. Bronzati et al. 2021). We landmarked our reconstructed labyrinth data, and tested ecological and other (allometric, spatial braincase constraint) effects on labyrinth size and shape in separate multiple phylogenetic regression models. In addition, we optimized residual relative labyrinth size over the phylogeny of turtles to study labyrinth size evolution. Turtle labyrinth sizes relative to skull size were further compared to other amniote lineages, including mammals, birds, lepidosaurs, and stem-archosaurs.

We find that turtles have unexpectedly large labyrinth sizes, comparable to those of birds. This seriously undermines ideas that labyrinth size can predominantly be explained by agility, as turtles are considerably less agile than birds. Evolutionary optimization of labyrinth size reveals that turtle labyrinths were ancestrally small, similar to those of stem-achosaurs. The labyrinth size increase in turtles coincides with their conquest of aquatic habitats, and may thus have an ecological explanation, likely linked to an increased need for visual stabilization during aquatic hunting of life prey. The size increase also coincides with the increase of otic capsule size in turtles, which is responsible for the appearance of the unique jaw adductor muscle system in turtles – one of the key anatomical trademarks of turtles among amniotes. As the otic size increase currently lacks an evolutionary explanation, we put increasing labyrinth sizes forward as a driver of this evolutionary development. The ecological interpretation of labyrinth size is supported by statistical models that relate secondary labyrinth size reductions to secondary terrestrial ecologies among extant tortoises and extinct terrestrial species. Unlike labyrinth size, labyrinth shape (i.e. geometry of the canals) shows no ecological signal. Instead, allometric effects as well as the shape of the braincase have significant effects on labyrinth shape. High unexplained residual variation nevertheless suggests that there are unknown influences on labyrinth shape. Our models challenge standing hypotheses that strongly relate labyrinth shape to ecology, and imply that the shape of the skull has a stronger impact on determining labyrinth shape than commonly recognized.

REFERENCES

Bronzati, M., Benson, R.B.J., Evers, S.W., Ezcurra, M.D., Cabreira, S.F., Choiniere, J., Dollman, K.N., Paulina-Carabajal, A., Radermacher, V.J., Roberto-da-Silva, L., Sobral, G., Stocker, M.R., Witmer, L.M., Langer, M.C., & Nesbitt, S.J. 2021: Deep evolutionary diversification of semicircular canals in archosaurs, Current Biology, 31, 1-10.

Jones, G., & Spells, K.E. 1963: A theoretical and comparative study of the functional dependence of the semicircular canal upon its physical dimensions, Proceedings of the Royal Society of London B, 157, 403-419.

Spoor, F., Garland Jr., T., Krovitz, G., Ryan, T.M., Silcox, M.T., & Walker, A. 2007: The primate semicircular canal systema and locomotion, Proceedings of the National Academy of Sciences, 104(26), 10808-10812.

6.4
Crystallographic Characterization of Sea Urchin Skeletal Elements

Frank Foerster[1]

[1] *Department für Geo- und Umweltwissenschaften, Ludwig-Maximilians-Universität München, 80333 Munich, Germany*

Echinoids (sea urchins) are marine organisms, which consist of numerous interlocked plates that form the shell. The so-called test protects the sea urchin's internal organs and often shows a five-fold symmetry. Attached to the test are primary and secondary spines. Sea urchins are one of many organsims to form calcite exoskeletons, functionalizing the calcite for structural stiffening and strengthening of the biological tissue (Addadi et al., 2003). The frequently reported lightweight properties in combination with special mechanical properties of the sea urchin skeleton originates from the three-dimensional highly-porous meshwork of calcite, termed stereom, forming test and spines. In between test plates and spines there are well-organized variations of the stereom architecture (Smith, 1980). Although the distinct microstructure may vary highly, sea urchins exhibit a highly ordered or almost perfect calcite crystal orientation and mineral organization (Goetz et al., 2014).

The present study describes the texture pattern of the magnesium calcite in test and spines of *Cidaris cidaris* in comparison to its microstructure and chemical composition. The sea urchin species *C. cidaris* is common in the Mediterranean Sea and lives in the epibenthos. Electron backscatter diffraction (EBSD) measurements reveal differences in crystallographic orientation of the test compared to the spines. The c-axes orientation of the single crystal-like test plates is tangential to the test curvature in aboral direction. The spine exhibits a bimodal-like texture. The highly co-oriented spine interior shows c-axes parallel to the longitudinal axis of the spine. The cortex, surrounding the spine's core, is polycrystalline with a weak co-orientation strength. The c-axes of the cortex forming biominerals are oriented perpendicular to the longitudinal spine axis. High-resolution EBSD identified the monocrystalline-like interior of the spine as mesocrystalline structure. Confocal laser microscopy and scanning electron microscopy (SEM) imaging reveal the main architectural features of the porous magnesium calcite. Test and spine show varying stereom fabrics, depending on the location within the plate and spine. Besides the changing texture in the spine's dense cortex, no correlation between crystallographic orientation and porosity pattern could be found. Energy-dispersive X-ray spectroscopy (EDS) detected Ca, Mg, S, Na and Cl in the test and in the spine of *C. cidari*s. All elements are homogenously distributed within the test. Mg concentration of the spines was calculated from results gained by X-ray powder diffractometry (XRPD). Similar Mg concentrations for the individual skeletal elements were obtained by energy-dispersive X-ray spectroscopy and XRPD. Results obtained by XRPD on pristine spines did not show differences between the low-magnesium calcite of primary and secondary spines. However, an additional phase, halite (NaCl) could be detected in the spines.

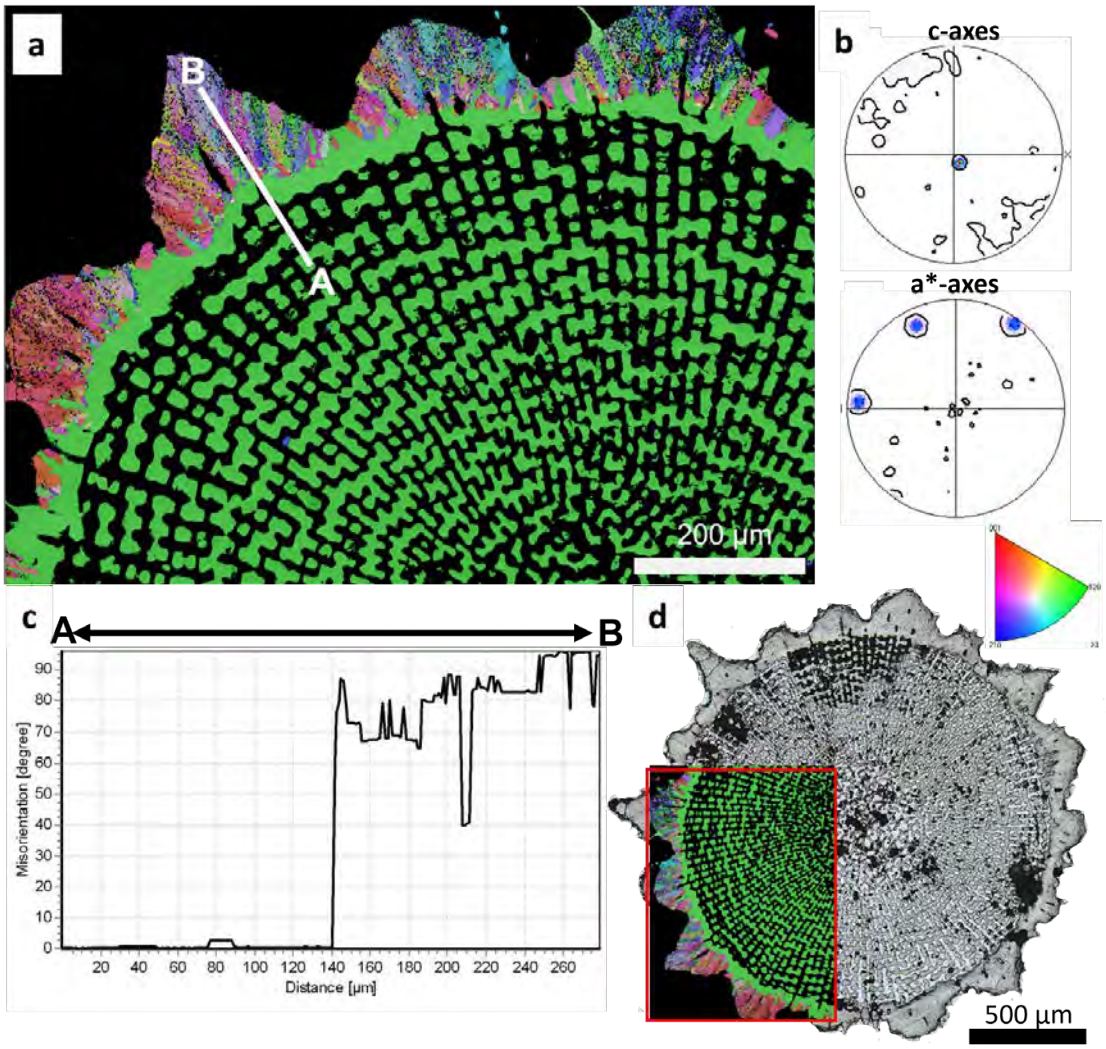

Figure 1. EBSD map on the cross section of a primary spine of *C. cidaris*. (a) Color coded orienation map, (b) density distribution pole figures with used color key along x1 direction, (c) misorientation profile between cortex and radiating layer, (d) measurement location on an image made by a confocal laser microscope.

REFERENCES

Addadi, L., Raz, S., Weiner, S. 2003: Taking Advantage of Disorder: Amorphous Calcium Carbonate and Its Roles in Biomineralization, Advanced Materials, 15, 959-970.

Goetz, A.J., Griesshaber, E., Abel, R., Fehr, T., Ruthensteiner, B., Schmahl, W.W. 2014: Tailored order: The mesocrystalline nature of sea urchin teeth, Acta Biomaterialia, 10, 3885-3898.

Smith, A.B. 1980: Stereom Microstructure of the Echinoid Test, Special Papers in Palaeontology, 25, pp. 81.

6.5
Ecological and functional controls that correlate with skull shape in turtles

Guilherme Hermanson[1,2,3], Serjoscha W. Evers[3], Bruna M. Farina[1,4], Gabriel S. Ferreira[5,6], Max C. Langer[1], Roger B. J. Benson[2]

[1] Laboratório de Paleontogia de Ribeirão Preto, FFCLRP, Universidade de São Paulo, Ribereirão Preto, Brazil (guilhermehermanson@gmail.com)
[2] Department of Earth Sciences, University of Oxford, South Parks Road, Oxford, OX1 3AN, United Kingdom
[3] Department of Geosciences, University of Fribourg, Chemin du Musée 6, 1700 Fribourg, Switzerland
[4] Department of Biology, University of Fribourg, Chemin du Musée 10, 1700 Fribourg, Switzerland
[5] Senckenberg Centre for Human Evolution and Paleoenvironment an der Universität Tübingen, Sigwartstrasse 10, 72076 Tübingen, Germany
[6] Fachbereich Geowissenschaften, Universität Tèbingen, Hölderlinstrasse 12, 72074 Tübingen, Germany

The 230-million year old history of turtles provides evidence of the evolution of a large diversity of habitat and feeding ecologies in the group. This diversity has been proposed to correlate with the great morphological disparity seen in the skulls of extant and extinct taxa. In fact, the well-preserved fossil record of turtles documents very distinct cranial architectures, some of which are no longer represented among modern representatives. In a similar way, functional aspects linked to their neck mobility have also been suggested to correlate with cranial shape in turtles, especially concerning the posterior skull region around the emarginations. For that reason, their cranial structure can be possibly understood as decoupled from their remaining skeletal parts: in addition to their necks, their skulls are the primary elements used to interact with the surrounding environment, and therefore key to understanding the diverse ecological feeding specialisations observed among representatives of the group. In this work, we use a three-dimensional geometric morphometrics approach to characterise shape aspects of turtle skulls. We created a new landmark concept to include single-point, sliding and surface landmarks that allowed us to capture the dimensions but also curves and fine surface details of their cranial geometry. We analyse all ecological and functional traits altogether under a phylogenetic framework to account for the non-independence of shared anatomical features, and assess what are the main factors that structure turtle skull shape.
We find that form-function relationships of turtle skulls involve size effects (allometry), habitat and diet preferences, feeding strategy, as well as their capacity to withdraw their necks. Turtle species that feed in the water have longer cranial shapes and more flattened palates than those that eat on land, and that the use of suction as a feeding strategy implies a slight lengthening of posterior skull parts in aquatic feeders. Furthermore, we show that their preferred type of food is associated with shape changes in skull height, width of the triturating surfaces of the palate and the position of the orbits. The lack of neck retraction in turtles correlates with extreme reduction of both emarginations simultaneously, alongside changes in overall skull dimensions. Our results can be applied to predict such explanatory traits to fossils and corroborate some previous qualitative palaeobiological inferences in literature. Our findings recognise that separate extinct lineages were not fully able to hide their necks, as well as that unrelated marine and estuarine groups evolved similar ecological diversity compared to extant sea turtles. These include multiple origins of durophagy, suction-feeding and preferences for more sedentary soft preys, and depict scnearios of ecomorphological convergence in these ecosystems throughout the group evolution.

6.6
Anatomical description of a selenosteid placoderm from the Late Devonian of the eastern Anti-Atlas (Morocco) and its ecomorphological reconstruction

Melina Jobbins[1], Martin Rücklin[2], Humberto G. Ferron[3,2], Christian Klug[2]

[1] *Palaeontological Institute and Museum, University of Zurich, Karl-Schmid-Strasse 4, 8006 Zürich, Switzerland (melina.jobbins@pim.uzh.ch)*
[2] *Naturalis Biodiversity Center, Leiden, The Netherlands*
[3] *Institut Cavanilles de Biodiversitat I Biologia Evolutiva, University of Valencia, Burjassot, Spain*
[4] *School of Earth Sciences, University of Bristol, Life Sciences Building, Tyndall Avenue, Bristol BS8 1TQ, United Kingdom*

Placoderms are an extinct group of early jawed vertebrates that play a key role in understanding the origin of the gnathostome body plan, including novelties like the jaws, teeth and pelvic fins. This makes them essential to elucidate the evolutionary success and early radiation of gnathostomes. As placoderms have a poorly ossified axial skeleton, preservation of the vertebral column and fins is extremely rare, unlike the well mineralised bones of the skull and thoracic armour. Therefore, the gross anatomy and body shape of placoderms are only known for a few taxa and reconstructions of the swimming function and ecology remain speculative. Here, we describe articulated skull roofs and shoulder girdles as well as body outlines of an arthrodire, a derived placoderm. Specimens of a new species of the selenosteid *Driscollaspis* reveal the pelvic girdle, the proportions and shape of the pectoral, dorsal and caudal fins as well as a laterally widened region at the base of the caudal fin resembling the lateral keel of sharks. This is the first record of a body outline preservation within selenosteids, and the second within Eubrachythoraci. This is also the first record of a preserved thoracic armour and inferognathal in *Driscollaspis*. The shape of its heterocercal caudal fin in combination with the pronounced laterally enlarged keel-like region is reminiscent of some modern pelagic sharks, thus suggesting this new selenosteid was an active swimmer.

6.7
The Unexpecting Discovery of Snapping Turtles (*Pan-Chelydridae*) in the Middle Eocene of France

Walter G. Joyce[1], Jean-Luc Landréat[2], Yann Rollot[1]

[1] *Department of Geosciences, University of Fribourg, Chemin du Musée 4, CH-1700 Fribourg (walter.joyce@unifr.ch)*
[2] *3 impasse de la Vigne Porale, F-02200 Soissons*

Snapping turtles (Pan-Chelydridae) are a species-poor clade of cryptodires that play a prominent role in extant ecosystems. The group has a particularly fragmentary fossil record, in part likely due to the fact that their shells disarticulate easily after death, but also a bias against collecting fragmentary turtle remains. As published, the record suggests that the clade originated in North America during the Late Cretaceous but dispersed to Asia and Europe no later than the late Oligocene and to South America no later than the Pleistocene. While a Neogene arrival in South America correlates well with the Great American Interchange, an Oligocene dispersal to Asia and Europe does not correlate well with other known turtle dispersal events, in particular the global dispersal event that took part across the Northern Hemisphere in concert with the Paleocene Eocene Thermal Maximum (PETM) that led to the complete replacement of the European turtle fauna.
A collection of 100 three-dimensionally-preserved pan-chelydrid shell fragments was collected near the turn of the millennium from a sandpit located near Chéry-Chartreuve, Department of Aisne, northern France. All fragments originate from a laterally constrained lens of sediments consisting of aeolian sands and clays that were deposited at the base of continental sediments that overlay marine sediments in this region. The rich, but poorly described mammalian fauna from this lens suggests an early Bartonian (MP15, Middle Eocene) age. The available material, which represents at least three different individuals, documents nearly the full plastron and peripheral series, but only aspects of the neurals and costals. Initial analysis of the material suggests close morphological affinities with Tullochelys montana from the Early Paleocene of Montana, USA and Chelydropsis decheni (a.k.a. Chelydropsis santihenrici) from the Late Oligocene of France. This is consistent with an arrival of the Chelydropsis lineage in Europe, perhaps directly from North America, no later than the Middle Eocene. The previously unanticipated arrival of pan-chelydrids in Europe by the Middle Eocene raises the possibility that pan-chelydrids may have arrived in Europe during the Early Eocene following the PETM, but remain undetected due to the above-mentioned collecting bias.

6.8
Marine vertebrates from Romer's Gap: a swimming trace from the latest Devonian of Morocco

Christian Klug[1], Abdelouahed Lagnaoui[2,3,4], Melina Jobbins[1], Wahiba Bel Haouz[4], Amine Najih[5]

[1] corresponding author, Paläontologisches Institut und Museum, Universität Zürich, Karl-Schmid-Strasse 4, 8006 Zürich, Switzerland. chklug@pim.uzh.ch, melina.jobbins@pim.uzh.ch
[2] Interdisciplinary Research Laboratory in Sciences, Education and Training, Higher School of Education and Training Berrechid (ESEFB), Hassan First University, Route de Casablanca Km 3.5, BP 539, 26100 Berrechid, Grand-Casablanca, Morocco.
[3] Working-Team on Geology of Mineral and Energy Resources, Research Laboratory Physico - Chemistry of Processes and Materials, Faculty of Sciences and Techniques, Hassan First University of Settat, Route de Casablanca Km 3.5, BP 539, 26000 Settat, Grand-Casablanca, Morocco.
[4] Laboratory of Stratigraphy of Oil-and-Gas Bearing Reservoirs, Department of Paleontology and Stratigraphy, Institute of Geology and Petroleum Technologies, Kazan (Volga Region) Federal University, Kremlyovskaya Str. 18, 420008, Kazan, Russian Federation
[5] Institut National Supérieur du Professorat et de l'Éducation de l'Académie de Poitiers, Université de Poitiers, 5 Rue Shirin Ebadi, 86073 Poitiers, France.

Taking the locally great abundance of body fossils of fishes such as, e.g., shark teeth into account, the scarcity of trace fossils prouced by these animals is surpising. Partially, this roots in the lower interest of researchers and the public in ichnofossils compared to fossil vertebrate skeletons. However, ichnofossils can provide valuable palaeobiological information about their producer such as, e.g., velocity, mode of locomotion, feeding behaviour etc.

We report an occurrence of swimming traces, which are known as the ichnogenus *Undichna*, from the youngest part of the Devonian of the eastern Anti-Atlas (Morocco). This is remarkable because the latest Devonian strata are usually very poor in tetrapod remains worldwide (Romer 1956; Coates and Clack 1995), but other vertebrates are also rare in this interval.

In the southern Tafilalt at the Jebel Aoufilal, the equivalent of the Hangenberg Sandstone consists of thin-bedded claystones, silstones, sandstones and rare coarser clastics (Kaiser et al. 2018). According to their ichnofauna and sedimentary structures, these sediments accumulated in a shalow marine setting. This is corroborated by abundant *Asteriacites*.

In our paper (Klug et al. 2021), we describe an over one meter long *Undichna britannica*, which was produced by an animal probably a little less than half a meter long. We cannot be certain about the producer, but Klug et al. (2016) documented teeth of ischnacanthid stem-chondrichthyans from the eastern Anti-Atlas. Thus, it appears possible that a moderate-sized acanthodian has produced this trace. It is planned to further study this rich ichnofossil-assemblage in the coming years.

REFERENCES

Coates, M. I., & Clack, J. A. 1995: Romer's gap: tetrapod origins and terrestriality. Bulletin du Muséum National d'Histoire Naturelle, 17, 373–388.

Kaiser, S. I., Becker, R. T., Hartenfels, S. & Aboussalam, Z. S. 2018: The global Hangenberg Crisis and Lower Alum Shale Event at El Atrous (southern Tafilalt Platform). Münstersche Forschungsberichte zur Geologie und Paläontologie, 110, 327-338.

Klug, C., Frey, L., Korn, D., Jattiot, R. & Rücklin, M. 2016: The oldest Gondwanan cephalopod mandibles (Hangenberg Black Shale, Late Devonian) and the Mid-Palaeozoic rise of jaws. Palaeontology, 59, 611-629. doi: 10.1111/pala.12248.

Klug, C., Lagnaoui, A., Jobbins, M., Haouz, W. B. & Najih, A. (2021): The swimming trace Undichna from the latest Devonian Hangenberg Sandstone equivalent of Morocco. Swiss Journal of Palaeontology, 140: 10 pp.

Romer, A. S., 1956: The early evolution of land vertebrates. Proceedings of the American Philosophical Society, 100(3), 151-167.

Sallan, L., & Galimberti, A. K. 2015: Body-size reduction in vertebrates following the end-Devonian mass extinction. Science, 350, 812–815. https://doi.org/10.1126/science.aac7373

6.9
New specimens of *Bunaia woodwardi* Clarke 1919 (Euchelicerata, synziphosurine) provide insight into Euchelicerata and Vicissicaudata affinity

Lorenzo Lustri[1], Pierre Gueriau[1,2], Allison C. Daley[1]

[1] *Institut des sciences de la Terre, Université de Lausanne, Geopolis, CH-1015 Basel (lorenzo.lustri@unil.ch)*
[2] *Université Paris-Saclay, CNRS, ministère de la Culture, UVSQ, MNHN, Institut photonique d'analyse non-destructive européen des matériaux anciens, 91192, Saint-Aubin, France*

Synziphosurine is an enigmatic paraphyletic clade including arthropod taxa of various affinities, such as stem members of Euchelicerata and of the lineages leading to Eurypterida, Xiphosura and Arachnida. Here we described new material that we ascribe to the Silurian synziphosurine *Bunaia woodwardi* Clarke, 1919, revealing previously unknown features of its ventral anatomy. The specimens have a first pair of uniramous appendages on the head, followed posteriorly by five pairs of biramous appendages in the prosoma. The pre-abdomen anteriorly bears at least two pairs of paddle-like uniramous appendages (exopods). Finally, the pre-telson segment is associated with a possibly membranous structure (post-ventral structure), that is open to a variety of interpretations. A similar structure is also present in undescribed synziphosurines from the early Ordovician Fezouata Biota, while several other Cambrian and Ordovician taxa bear an anal pouch or post-ventral appendages or plates in the pre-telson or anal region.

We undertook a phylogenetic analysis preformed with parsimony, to clarify the affinity of *B. woodwardi* together with the Fezouata synziphosurine using a dataset including an array of synziphosurines (Lamsdell et al. 2013). Both taxa are resolved together with *Offacolus kingi* Orr et al., 2000 and *Dibasterium durgae* Briggs et al,, 2012 from the Silurian Herefordshire Lagerstätte as a monophyletic group of stem-euchelicerates, and as sister group to all other Euchelicerata (Prosomapoda).

Given the stem-euchelicerates affinity of *B. woodwardia* and the Fezouata taxon, some possible interpretations of the post-ventral structures are here examined and we propose three alternative hypotheses: 1) the post-ventral structure is an "anal pouch", similar to that in the Cambrian *Habelia* (Aria et al. 2019); 2) the post-ventral structure is homologous to the post-ventral appendages characteristic of Vicissicaudata (Lerosey-Aubril et al. 2017); 3) all of the post-ventral structures (anal pouch, post ventral appendages and *B. woodwardi* post ventral structure) are homologous, and reflect the apomorphy state for a monophyletic group (Artiopoda) formed by Euchelicerata and the Cambrian Vicissicaudata.

The clade Artiopoda have already been retrieved in several phylogenetic analyses, and these new findings in the synziphosurines realm open new windows on the possible relationships within the clade, supporting a sister-group position of Vicissicaudata respective to the Euchelicerata.

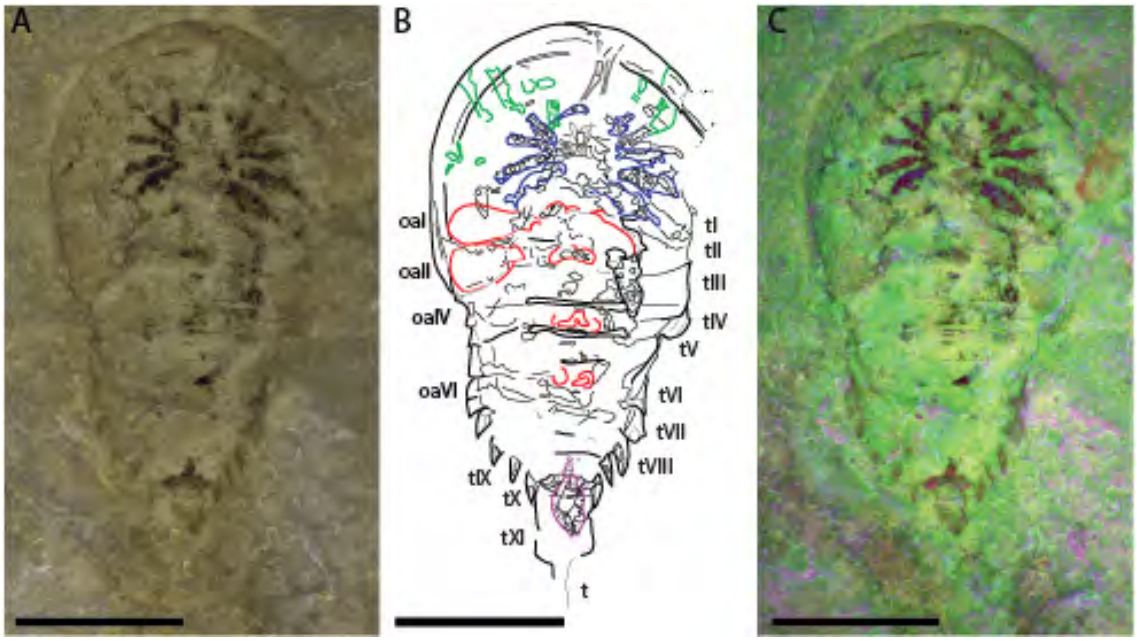

Figure 1. *Bunaia woodwardi* new specimen. A, optical photograph. B, interpretative drawing. C, multispectral false colour overlay of UV-visible reflection and luminescence images. oaI-VI, ophisthosomal appendages; tI–XI, opisthosomal targites; t, telson. Chelicerae are

highlighted in grey, endopods in blue, exopods in green, opisthosomal appendages in red and the post-ventral structure in purple. Scale bars, 1 mm.

REFERENCES

Aria, C., & Caron, J. B. 2017: Mandibulate convergence in an armoured Cambrian stem chelicerate, BMC Evolutionary Biology, 17(1), 1-20.

Briggs, D. E., Siveter, D. J., Siveter, D. J., Sutton, M. D., Garwood, R. J., & Legg, D. 2012): Silurian horseshoe crab illuminates the evolution of arthropod limbs, Proceedings of the National Academy of Sciences, 109(39), 15702-15705.

Lamsdell, J. C. 2013: Revised systematics of Palaeozoic 'horseshoe crabs' and the myth of monophyletic Xiphosura, Zoological Journal of the Linnean Society, 167(1), 1-27.

Lerosey-Aubril, R., Zhu, X., & Ortega-Hernández, J. 2017: The Vicissicaudata revisited–insights from a new aglaspidid arthropod with caudal appendages from the Furongian of China, Scientific Reports, 7(1), 1-18.

Lanphere, M., & Pamic J. 1992: K-Ar and Rb-Sr ages of Alpine granite-metamorphic complexes in northern Croatia, Acta Geologica, 22, 5-22.

Orr, P. J., Siveter, D. J., Briggs, D. E., Siveter, D. J., & Sutton, M. D. 2000: A new arthropod from the Silurian Konservat–Lagerstätte of Herefordshire, UK, Proceedings of the Royal Society of London. Series B: Biological Sciences, 267(1452), 1497-1504.

6.10
A new coelacanth from the Triassic of Lorraine

Luigi Manuelli[1,2], Lionel Cavin[1]

[1] *Natural History Museum of Geneva, 1 rue Malagnou, 1208-Geneva, CH*
[2] *University of Geneva, Department of Genetics & Evolution, 1205-Geneva, CH*
(luigi.manuelli@unige.ch)

A series of fossil coelacanths with unusual tridimensional preservation has been recently found in Triassic deposits near Saverne (East of France, Alsace), possibly representing a new species. We are currently describing the morphology of such specimens with classical paleontological tools and with modern approaches like MicroCT (Fig1). Our preliminary results, especially at the level of cranial morphology, consistently show a resemblance with the genus *Diplurus* (Schaeffer 1952). Its inclusion in a cladistic analysis will help to understand the phylogenetic position of *Diplurus*, since this genus is resolved as a mawsoniid in some analyzes (e.g. Cavin et al., 2017) and as a latimeriid in others (e.g. Toriño et al., 2017).

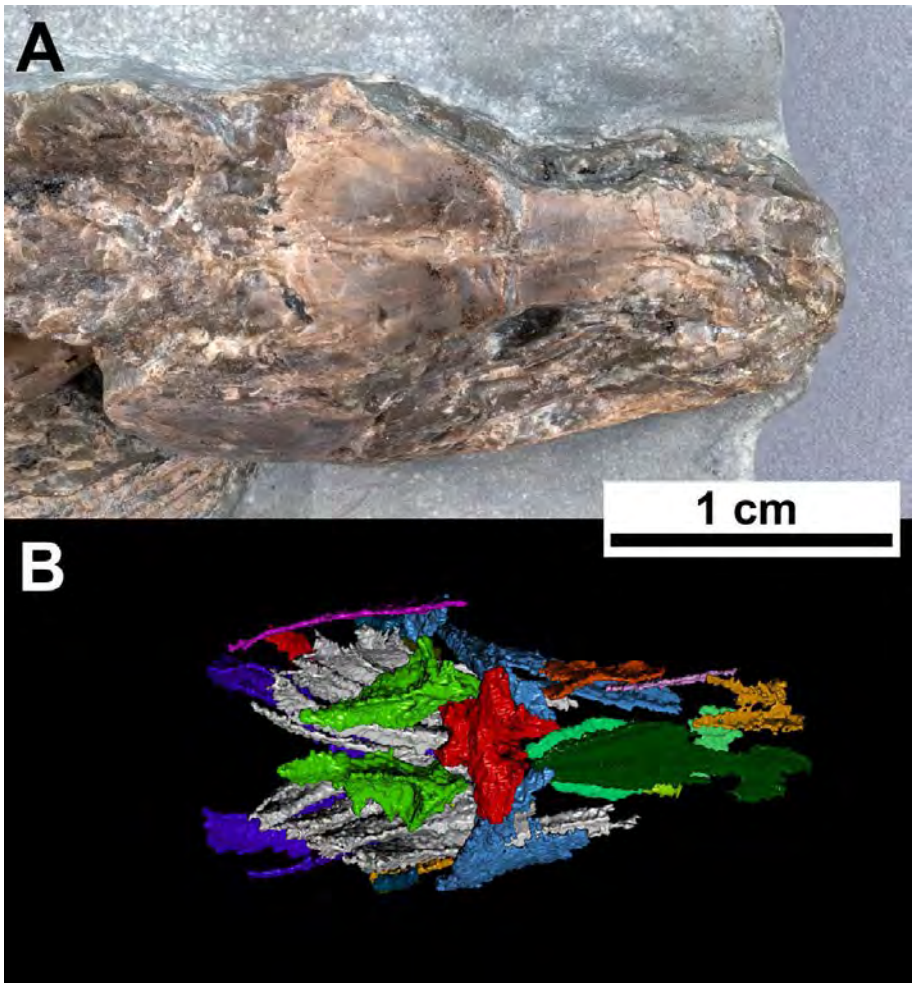

Figure 1 | A – dorsal view of the skull roof of one of the specimens. Anterior to right. B – dorsal view of the CTscan of the specimen in A.

REFERENCES

Cavin, L., Mennecart, B., Obrist, C., Costeur, L., Furrer, H. 2017: Heterochronic evolution explains novel body shape in a Triassic coelacanth from Switzerland, Scientific Reports, 7, 13695.

Schaeffer, B., 1952. The Triassic coelacanth fish Diplurus, with observations on the evolution of the Coelacanthini, Bulletin of the AMNH, 99, 2, 25-78.

Toriño, P., Soto, M., & Perea, D. 2021: A comprehensive phylogenetic analysis of coelacanth fishes (Sarcopterygii, Actinistia) with comments on the composition of the Mawsoniidae and Latimeriidae: Evaluating old and new methodological challenges and constraints, Historical Biology, 1-21.

6.11
U-Pb zircon ID-TIMS geochronology of the oldest biota of the Ediacaran White Sea assemblage (Summer Coast, NW Russia)

Maria Ovtcharova[1], Andrey Ivantsov[2], Ulf Linnemann[3], Anna Ivleva[4], Viktoria Ershova[4], Aleksey Nagovitsyn[5]

[1] Department of Earth Sciences, University of Geneva, Rue des Maraichers 13, 1205 Geneva (maria.ovtcharova@unige.ch)
[2] Paleontological Institute, Russian Accademy of Science, Moscow, Russia
[3] Senckenberg Natural History Collection, Dresden, Germany
[4] Department of Regional Geology, St. Petersburg State University, Russia
[5] Arkhangelsk Regional Lore Museum, Arkhangelsk, 163000 Russia

Establishing an absolute timeline for the evolution of Ediacaran (latest Neoproterozoic) biota is an outstanding challenge for the geochronology community. Ediacaran biota ("Vendian" in Russian literature; 580-539 Ma) are traditionally divided into three assemblages: Avalon, White Sea and Nama, considered as a partially overlapping evolutionary and temporal succession. The geochronological record of the White Sea assemblage is hampered by the lack of datable volcanic beds, with very few exceptions like along the Winter and Summer coast in northwestern Russia. There, we find examples of the most complete and diversified White Sea assemblage of the entire Russian platform.

We report here results from a field study and U-Pb geochronology on the the Lyamtsa, Verkhovka and Zimnie Gori formations along the Summer coast, more specifically on outcrops in river valleys on the Onega peninsula (Agma and Solza) in the area west of Arkhangelsk. The studied sedimentary successions consist mainly of fine-grained sandstone, mudstone and claystone, reflecting shallow marine conditions, influenced by a large river delta. The base of the Lyamtsa formation starts with conglomerates, overlain by a volcanic tuff (only in drillcore), which is predating the onset of the Ediacaran fossil assemblage. Further up in the section at the base of Verkhovka formation appear diverse trace fossils ("ichnofossils", e.g., Dickinsoniids, Trilobozoans, Kimberella, Charnodiskus, etc.), which are marking a major evolutionary step by the onset of bilaterian life forms.

We have sampled two ash layers, one at the base and one some 20m meters up section in the Verkhovka formation and can provide a date for the onset of bilaterian fossils in the White Sea assemblage. Our high precision U-Pb zircon CA-ID-TIMS age determinations yielded weighted mean $^{206}Pb/^{238}U$ ages of 555.68 ± 0.15 Ma and 555.10 ± 0.22 Ma for the two ash layers. This age provides evidence that the diverse assemblage of body and trace fossils and the oldest bilaterian fossil Kimberella occurred already 555.68 ± 0.15 million years ago. This new age information is in contradiction with an existing $^{207}Pb/^{206}Pb$ zircon age of 555.5 ± 0.3 Ma from a section at the Winter coast north of Arkhangelsk (Martin et al., 2000), which is considered to be stratigraphically younger than the volcanic levels dated here.

REFERENCES

Martin, M.W., Grazhdankin, D.V., Bowring, S.A., Evans, D.A.D., Fedonkin, M.A. & Kirschvink, J.L. 2000: Age of Neoproterozoic Bilaterian Body and Trace Fossils, White Sea, Russia: Implications for Metazoan Evolution, Science, 288, 841-845.

6.12
Phyologenetics and systematics of the trilobite subfamilies Cheirurinae and Deiphoninae: shedding light on the basal relationships

Francesc Pérez–Peris[1], Jonathan M. Adrain[2], Allison C. Daley[1]

[1]*Institute of Earth Sciences, University of Lausanne, Géopolis, CH-1015 Lausanne, Switzerland (francesc.perezperis@unil.ch; allison.daley@unil.ch)*
[2]*Department of Earth and Environmental Sciences, University of Iowa, 115 Trowbridge Hall, Iowa City, IA 52242, USA (jonathan-adrain@uiowa.edu)*

Cheiruridae is one of the most diverse families of trilobites during the Ordovician with 453 species assigned. Within Cheiruridae eight subfamilies (Acanthoparyphinae, Cheirurinae, Cyrtometopinae, Deiphoninae, Eccoptochilinae, Heliomerinae, Pilekiinae, and Sphaerexochinae) have been historically recognized. Although some subfamiles have been subjected to phylogenetic analysis (e.g., Acanthoparyphinae, Deiphoninae, Eccoptochilinae and Sphaerexochinae), no broader analyses involving different subfamilies have been performed. No information about the structure of the familiy and the basal nodes of the subfamilies in a phylogenetic context has yet been provided. A larger scale phylogenetic hypothesis is needed in order to assess the monophyly, the basal structure, the basal nodes and the relationships of the subfamilies.

In a first step to clarify early evolution of the family Cheiruridae, the subfamilies Cheirurinae, Deiphoninae and Cyrtometopinae were examined. These subfamiles have historically been defined by putative synapomorphies (e.g., anteroposterior constriction of the thoracic pleura, pleural furrow morphology, pygidial morphology) that differentiate them from the rest of Cheiruridae. Cheirurinae and Deiphoninae have been considered to be probably monophyletic. However, the phylogenetic status of Cyrtometopinae is unclear owing to a lack of obvious synapomorphies. It has been suggested to be a paraphyletic grade at the basal node of Deiphoninae (Adrain and Pérez–Peris, *in press*).

Here, we present phylogenetic analyses of Cheirurinae, Deiphoninae, and Cyrtometopinae. Mainly Ordovician species were selected for analysis, prioritizing older species in order to improve the resolution of basal nodes. Some younger taxa with well preserved morphological information were also included. Parsimony analyses were performed in T.N.T., under equal weight and implied weights (K= 3, 6, 9, 12), using the heursitic “Traditional Search” under tree bisection-reconnection (TBR) branch swapping with 100 replicates x 100 iterations. In addition, the dataset was also explored using the “New Technologies Search” algorithms “Ratchet” (1000 iterations), “Sectorial Searches” (1000 rounds), and “Tree Fusing” (100 rounds). The preliminary result indicates that both Cheirurinae and Deiphoninae are monophyletic. “Cyrtometopines” have been resolved as a paraphyletic grade rooted at the base of Deiphoninae and *Hemisphaerocoryphe* is the sister group of*Mainbrookia* + *Sphaerocoryphe*.

The new phylogenetic framework permits the reconstruction of the early evoltion of Cheiruridae. Better understanding of the timing of divergences and biogeography are provided by this analysis, resulting in new information crucial for the understanding of trilobites during the Ordovician Radation.

REFERENCES

Adrain, J.M. and Pérez–Peris, F. (in press): Middle Ordovician (Darriwilian) cheirurid trilobites from the Table Cove Formation, western Newfounland, Canada, Zootaxa.

6.13
Unique assemblage of suspension-feeding radiodonts from the Early Ordovician Fezouata Biota

Gaëtan J.-M. Potin[1], Pierre Guériau[2], Allison C. Daley[1]

[1] *Institute of Earth Sciences, University of Lausanne, Géopolis, CH-1015 Lausanne, Switzerland (gaetan.potin@unil.ch)*
[2] *Université Paris-Saclay, CNRS, ministère de la Culture, UVSQ, MNHN, Institut photonique d'analyse non-destructive européen des matériaux anciens, 91192, Saint-Aubin, France*

The Fezouata Shale is a Burgess Shale-like *lagerstätte* from the Early Ordovician of Morocco that is important for our understanding of the early evolution of animals, and the transition between the Cambrian Explosion and the Great Ordovician Biodiversification Event (GOBE) (Saleh et al. 2020). Located in the Anti-Atlas of Morocco, this site yield exceptionally well-preserved remains of invertebrates, including many arthropods (Saleh et al. 2020).

The Fezouata Shale has yielded a wide diversity of non-mineralized taxa and anatomical features of a mix between the Cambrian Explosion fauna and more common Palaeozoic animals, including a diverse assemblage of trilobites, chelicerates and radiodonts (Van Roy et al. 2015a). Radiodonts are an emblematic arthropod group best known by the famous *Anomalocaris canadensis*, a top predator in the Burgess Shale community. The first radiodont from the Fezouata Shale reported in publication is *Aegirocassis benmoulai*, a 2m-long suspension-feeding radiodont (Van Roy et al. 2015b). In reality more radiodonts, especially suspension-feeding taxa, have been found.

This study focusses on the frontal appendages of undescribed radiodonts from the Fezouata Biota, because it is this part of the body that has the highest preservation potential for radiodonts in general. All the frontal appendages examined belong to the family Hurdiidae, and the majority of them correspond to a suspension-feeding strategy. It reveals to us a unique assemblage of suspension-feeding radiodonts that allows us to create the clade Aegirocassisinae. This group includes *Aegirocassis benmoulai*, *Pseudoangustidontus duplospineus*, and *Pseudoangustidontus* sp. nov. (Fig.1). The genus *Pseudoangustidontus* was previously described as an unknown arthropod (Van Roy & Tetlie 2006), but the more complete material studied here identifies it as a suspension feeding radiodont. New material of *Aegirocassis benmoulai* allows us to refine the anatomical description of its appendage.

Owing to the study of around 100 specimens of frontal appendages, we can achieve a better understanding of radiodont paleoecology during the Ordovician, and its evolution implications. Mesh size measurement of the most complete Aegirocassisinae specimens permits us to estimate that the size of the prey was in the mesoplankton category. In term of evolutionary implications, this is the first time in the history of the group that we see such a high diversity and dominance of the suspension-feeding mode of life in radiodonts. It can be correlated with the "Ordovician Plankton Revolution", which provides more resources for these animals (Perrier et al. 2015). Finally, this study highlights the decline of radiodonts that were active predators, such as Anomalocarididae, with no specimens found in our collections so far. This could be explained by the emergence of more efficient predators such as eurypterid or orthocone cephalopods.

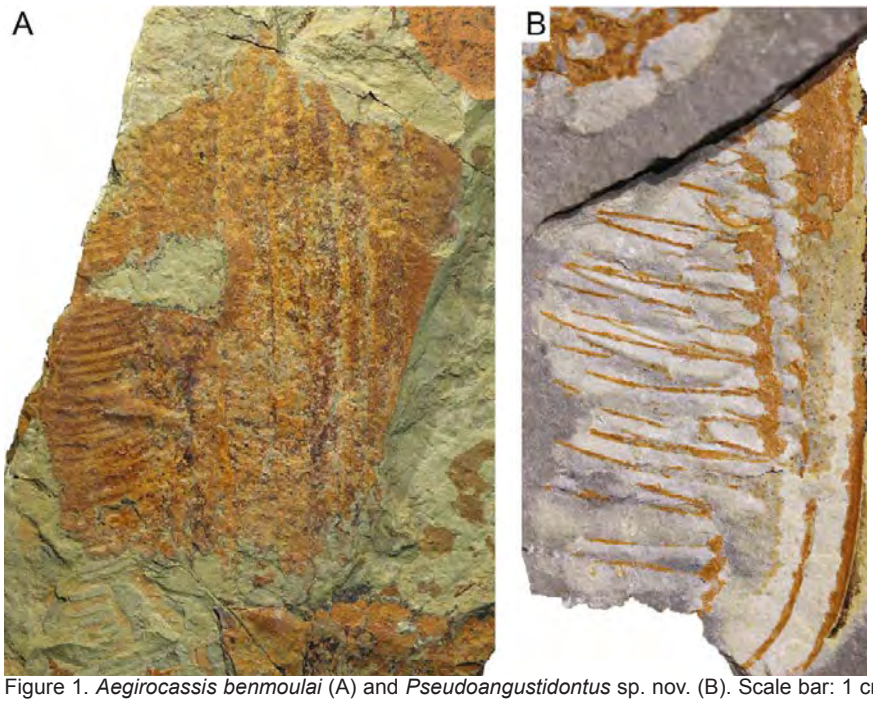

Figure 1. *Aegirocassis benmoulai* (A) and *Pseudoangustidontus* sp. nov. (B). Scale bar: 1 cm.

REFERENCES

Perrier, V., Williams, M., & Siveter, D.J. 2015: The fossil record and palaeoenvironmental significance of marine arthropod zooplankton, Earth-Science Reviews, 146, 146-162.

Saleh, F., Antcliffe, J.B., Lefebvre, B., Pittet, B., Laibl, L., Perez-Peris, F., Lustri, L., Gueriau, P., & Daley, A.C. 2020: Taphonomic bias in exceptionally preserved biotas, Earth and Planetary Science Letters, 529, 1-6.

Van Roy, P., Briggs, D.E.G., & Gaines, R.R. 2015a: The Fezouata fossils of Morocco; an extraordinary record of marine life in the Early Ordovician, Journal of the Geological Society, 172, 541-549.

Van Roy, P., Daley, A.C., & Briggs, D.E.G. 2015b: Anomalocaridid trunk limb homology revealed by a giant filter-feeder with paired flaps, Nature, 522, 77-80.

Van Roy, P., & Tetlie, O.E. 2016. A spinose appendage fragment of a problematic arthropod from the Early Ordovician of Morocco. Acta Palaeontologica Polonica 51 (2): 239–246.

6.14
Cranial anatomy and phylogeny of Late Jurassic to Early Cretaceous paracryptodiran turtles

Yann Rollot[1], Serjoscha W. Evers[1], Walter G. Joyce[1]

[1] Department of Geosciences, University of Fribourg, Chemin du Musée 6, CH-1700 Fribourg (yann.rollot@gmail.com; serjoscha.evers@googlemail.com; walter.g.joyce@gmail.com)

Paracryptodira is a clade of freshwater turtles that lived from the Late Jurassic to Eocene of North America and Western Europe. The clade was initially considered to be one of the three primary groups of turtles along with Pleurodira and Cryptodira and to consist of the North American and European Pleurosternidae and the North American Baenidae. While the phylogenetic placement of Paracryptodira within Testudinata is still under debate, recent phylogenies suggest the clade may include *Compsemydidae*, *Helochelydridae*, and *Kallokibotion bajazidi* as well. Although paracryptodiran fossils have been described since the 19th century, plenty of material remains poorly understood. Late Jurassic and Early Cretaceous pleurosternid shell material recently received greater attention, but the cranial anatomy of several taxa historically lacked detailed insights. Similarly, while about ten derived baenids skulls have been published over the last two decades, only one basal baenid benefited from a detailed study during that period.

As a better understanding of paracryptodiran cranial anatomy is crucial for more confidently assessing the phylogenetic relationships of that clade, we have described a series of skulls over the course of the last two years using micro-computed tomography, in particular the putative pleurosternids *Uluops uluops* from the Tithonian of Wyoming and *Pleurosternon bullockii* from the Berriasian of the United Kingdom, and the putative basal baenids *Arundelemys dardeni* from the Aptian-Albian of Maryland, *Lakotemys australodakotensis* from the Berriasian-Valanginian of South Dakota, and *Trinitichelys hiatti* from the Aptian-Albian of Texas (Fig. 1). Among the new features brought to light in our studies are the presence of a reduced basipterygoid process in *Pleurosternon bullockii* and *Uluops uluops*, which is interpreted as a symplesiomorphy for the latter two taxa, and the intriguing presence of a canal for the palatine artery in *Lakotemys australodakotensis* and *Uluops uluops*. The circulation system of turtles was used for decades to attempt improving our understanding of testudinatan relationships and the recent advent of computed-tomography technologies has allowed investigating in detail arterial and innervation patterns in turtle skulls. This led to a series of reinterpretations of cranial circulation within several turtle clades, including paracryptodires. While the palatine artery was initially thought to be universally present among that group, recent investigations suggested its loss in several taxa instead, if not for the entire group. Our studies of the five aforementioned paracryptodiran skulls reveal that the palatine artery is indeed absent in most representatives of Paracryptodira but remains present in *Lakotemys australodakotensis* and *Uluops uluops*, the most basal members of baenids and pleurosternids respectively, which suggests, for the moment, the independent loss of the palatine artery at the base of Baenidae and Pleurosternidae.

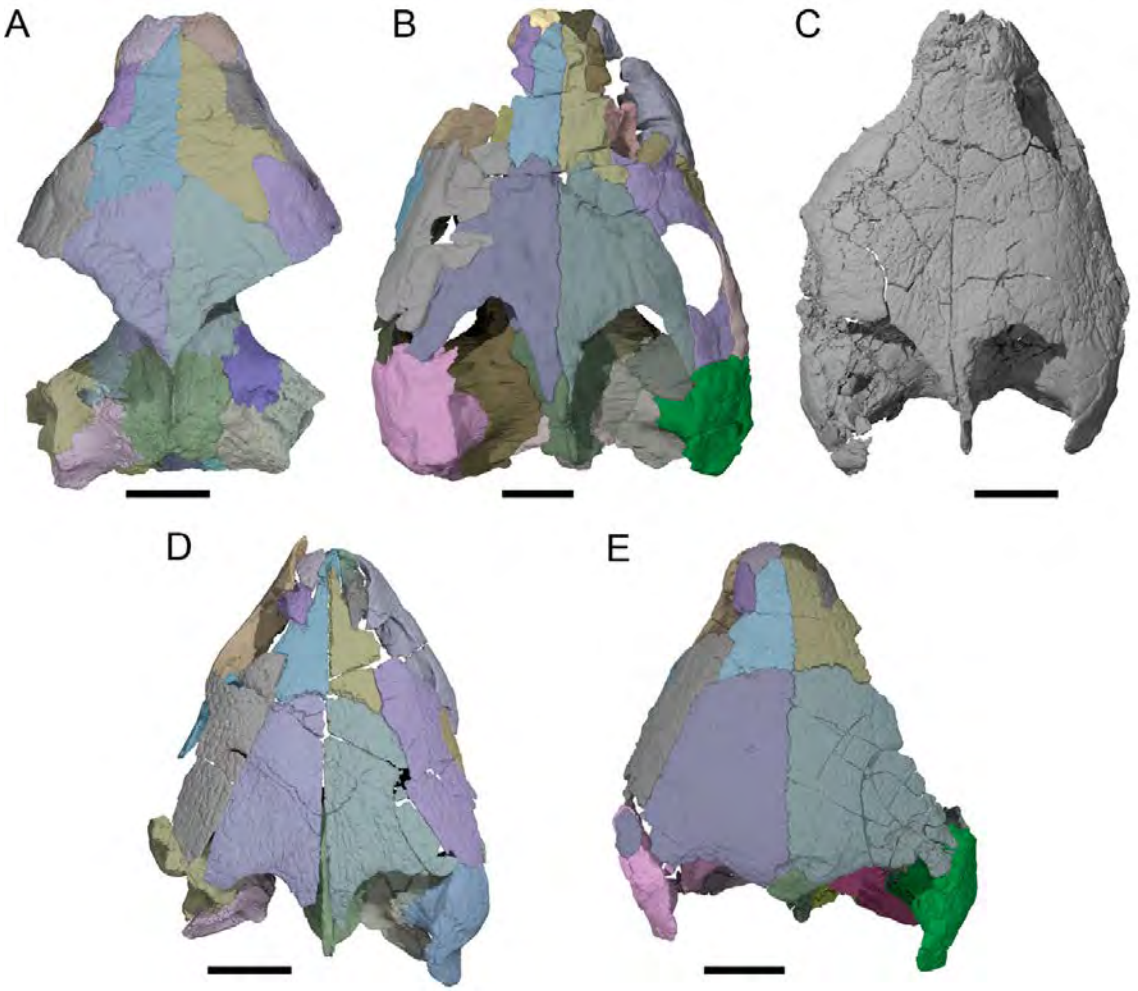

Figure 1. Selection of paracryptodiran skulls used for this project. Dorsal view of **A**, *Arundelemys dardeni*, **B**, *Lakotemys australodakotensis*, **C**, *Trinitichelys hiatti*, **D**, *Pleurosternon bullockii*, and **E**, *Uluops uluops*. Scale bars approximate 1 cm.

6.15
Revision of the Triassic placodont material (Sauropterygia) from Switzerland

Torsten M. Scheyer[1], Katrin Kirwald[1], Patrizia Bregant[1]

[1] *University of Zurich, Palaeontological Institute and Museum, Karl Schmid-Strasse 4, CH-8006 Zurich (tscheyer@pim.uzh.ch)*

Here we report on the revision of the Alpine placodont material from localities of Switzerland (and with an outlook to the neighboring countries Austria and Italy), namely specimens pertaining to the Middle Triassic *Paraplacodus broilii* and *Cyamodus hildegardis* and the Late Triassic *Psephoderma alpinum*. The former two species are prominently represented by several specimens each from the Besano Formation at the UNESCO world heritage site of Monte San Giorgio (Italy/Switzerland), whereas the latter species is found mainly in the Kössen Formation of Canton Grisons and the adjacent Vorarlberg region of Austria. We focussed on material that is mainly housed in the collections of the Palaeontological Institute and Museum of the University of Zurich (PIMUZ), and the Bündner Naturmuseum Chur (BNM). In the case of *Paraplacodus broilii*, all previously described fossils (mentioned in Rieppel, 2000) including the holotype PIMUZ T 2806 (not T 4773!) from Val Porina, Meride, and hitherto unpublished material stored at PIMUZ was inspected and (re-)described. The material includes a badly weathered skeleton of a small individual, which nevertheless preserved most of the skull in good condition so that the material could be used for computer-tomographic (CT) scanning and 3D reconstruction. Similarly, the CT scan of the 'Munich' exemplar (SNSB-BSPG 1953 XV 5, stored at the Bayerische Staatssammlung in Munich) of *P. broilii*, representing the most complete skull found to date, could be reconstructed. It confirmed the presence of two cranial osteoderms in the temporal region as was previously hypothesied by Rieppel (2000) and Maisch (2020), but also the presence of nine instead of eight crushing teeth in the maxilla. The skeleton of *Cyamodus hildegardis* was already the focus of several studies in the past (e.g., Kuhn-Schnyder, 1959; Pinna, 1980, 1992) and based on the best preserved skeletons, the skeletal reconstruction was revised by Scheyer (2010). Hitherto undescribed skull material in PIMUZ, however, includes a well presered and isolated skull roof, revealing an almost undistorted imprint of the dorsal part of the cranial vault and the parietal foramen. In addition, the osteoderm microstructure of the carapace of the holotype (PIMUZ T 4763) of *C. hildegardis* was recently reported on in Scheyer and Klein (2021).

For *Psephoderma alpinum*, numerous hitherto undescribed specimens are accessioned in the PIMUZ and BNM collections. These were used to supplement previous comparative works on the cranial and postcranial anatomy (e.g., Pinna, 1980; Pinna and Nosotti, 1989; Renesto and Tintori, 1995; Neenan and Scheyer, 2014) of the species. The new materials included several articulated armour pieces, including two very well preserved large fragments of adult individuals, but also armour pieces of subadult specimens, numerous isolated plates and teeth, as well as cranial remains of different ontogenetic stages. The latter include tiny jaw fragments of small juvenile specimens and subadults. Several cranial specimens could be CT scanned, allowing an updated view of the intracranial anatomy of the animals. The crushing teeth were also statistically evaluated and compared with the crushing teeth of *Macroplacus raeticus* from the Rhaetian of the Bavarian Alps in Germany, adding additional data to the phylogenetic discussion of the species. The results of the revisions are used to help with the determination of future collected material, summing up the study history and to discuss additional topics such as ontogeny, paleobiology and –ecology of placodonts. The study of the *Psephoderma* and *Paraplacodus* material was part of the MSc theses of two of us (K. Kirwald and P. Bregant, PIMUZ) and also of the diploma thesis of Grüter (2006).

REFERENCES

Grüter, M. 2006: *Psephoderma alpinum* - Placodontierreste aus der Kössen-Formation (späte Trias) der ostalpinen Decken von Graubünden. Unpublished Diploma Thesis, Universität Bern.

Kuhn-Schnyder, E. 1959: Über das Gebiss von *Cyamodus*, Vierteljahresschrift der Naturforschenden Gesellschaft in Zürich, 104 (Festschrift Steiner), 174-188.

Maisch, M. W. 2020: The evolution of the temporal region of placodonts (Diapsida: Placodontia) – a problematic issue of cranial osteology in fossil marine reptiles, Palaeodiversity, 13, 57-68.

Neenan, J. M., & Scheyer, T. M. 2014: New specimen of *Psephoderma alpinum* (Sauropterygia, Placodontia) from the Late Triassic of Schesaplana Mountain, Graubünden, Switzerland, Swiss Journal of Geosciences, 107, 349-357.

Pinna, G. 1980: Lo scheletro postcraniale di *Cyamodus hildegardis* Peyer, 1931 descritto su un esemplare del Triassico Medio Lombardo (Reptilia Placodontia), Atti della Società Italiana di Scienze Naturali e del Museo Civico di Storia Naturale di Milano, 121, 275-306.

Pinna, G. 1980: *Psephoderma alpinum* Meyer, 1858: rettile placodonte del Retico europeo, Volume Sergio Venzo, Università di Parma, 149-157.

Pinna, G. 1992: *Cyamodus hildegardis* Peyer, 1931 (Reptilia, Placodontia), Memorie della Società Italiana di Scienze Naturali e del Museo Civico di Storia Naturale di Milano, 26, 1-21.

Pinna, G., & Nosotti, S. 1989: Anatomia, morfologia funzionale e paleoecologia del rettile placodonte *Psephoderma alpinum* Meyer, 1858, Memorie della Società Italiana di Scienze Naturali e del Museo Civico di Storia Naturale di Milano, 25, 17-50.

Renesto, S., & Tintori, A. 1995: Functional morphology and mode of life of the Late Triassic placodont *Psephoderma alpinum* Meyer from the Calcare di Zorzino (Lombardy, N Italy), Rivista Italiana di Paleontologia e Stratigrafia, 101, 37-48.

Rieppel, O. 2000: *Paraplacodus* and the phylogeny of the Placodontia (Reptilia: Sauropterygia), Zoological Journal of the Linnean Society, 130, 635-659.

Scheyer, T. M. 2010: New interpretation of the postcranial skeleton and overall body shape of the placodont *Cyamodus hildegardis* Peyer, 1931 (Reptilia, Sauropterygia), Palaeontologia Electronica, 13(2), 15A.

Scheyer, T. M., & Klein N. 2021: Sauropterygia: Placodontia, pp. 425-434 in de Buffrénil, V., de Ricqlès, A., Zylberberg, L., Padian, K., Laurin, M. & Quilhac, A. (eds.), Vertebrate Skeletal Histology and Paleohistology, CRC Press, Boca Raton.

6.16
First data on Pliocene continental fossil record of Armenia, Southern Caucasus

Davit Vasilyan[1,2], Lutz Maul[3], Damien Becker[1,2], Marie Meyer[4], Maia Bukhskianidze[5], Loïc Costeur[6], Gerald Mayr[7], Sergei Lazarev[2,1]

[1] JURASSICA Museum, Route de Fontenais 21, Porrentruy, Switzerland (davit.vasilyan@jurassica.ch)
[2] University of Fribourg, Department of Geosciences, Chemin du Musée,1700 Fribourg, Switzerland (damien.becker@jurassica.ch)
[3] Senckenberg Research Station of Quaternary Palaeontology, Am Jakobskirchhof 4, 99423 Weimar, Germany (lutz.maul@senckenberg.de)
[4] École nationale vétérinaire Toulouse, 23 Chemin des Capelles, 31200, Toulouse, (marie.meyer_19@envt.fr)
[5] Georgian National Museum, Purtseladze street 3, Tbilisi 0105, Georgia, (maiabukh@gmail.com)
[6] Naturhisorisches Museum Basel, Augustinergasse 2, 4051 Basel (loic.costeur@bs.ch)
[7] Senckenberg Research Institute, Senckenberganlage 25, 60325 Frankfurt am Main, Germany (gerald.mayr@senckenberg.de)

Southern Caucasus with its geographic position at the crossroad of three continents is an important region in understanding of the past faunistic dispersals. In the few existing earlier works, this has been already partially demonstrated by its continental fossil record. However, despite the availability of Cenozoic continental deposits in Southern Caucasus, their potential for systematic studies of Cenozoic vertebrates and palaeoenvironmental and palaeoclimatic studies has hardly been used.

Here, we present our results of an interdisciplinary study on the Pliocene succession from Jradzor (Central Armenia, Lesser Caucasus). At least 15 horizons of vertebrate fossil faunas have been found in the 54-meter-thick continental succession comprises. The $^{40}Ar/^{39}Ar$ dating of abundant volcanic ashes along with an extensive palaeomagnetic sampling dated the section between 4.3 and 3.1 Ma.

Six sedimentological units can be identified in the section: Unit 1 (distal lacustrine setting) with white thinly-laminated diatomite succession; Unit 2 (palaeosol and downslope deposits) with brown mottled mudstones; Unit 3-4 (distal tail of pyroclastic flows) with mudstones containing extensive erosive sheet-like coarsening-upwards packages of scoria and pumice; Unit 5 (palaeosols and downslope deposition) with brown mottled mudstones; Unit 6 (alternating volcanoclastic and palaeosol environments).

The lacustrine unit 1 provides both aquatic (mainly fishes) and rare terrestrial forms. The fossiliferous horizons of units 3, 4, 6 contain vertebrate faunas including amphibians, reptiles, birds and mammals. Here, horizons JZ-3 and JZ-13 are the richest ones with a dominance of small sized vertebrates. Further, the horizon JZ-7 is remarkable with its rich large mammalian assemblage, including rare arvicolids, toads. All vertebrate groups suggest warm, rather dry and open habitats with very rare, forested regions. Based on a complex dating approach (biostratigraphy, $^{40}Ar/^{39}Ar$, and palaeomagnetic data) the age of the units is estimated as early Pliocene (unit 1-4), early/late Pliocene (unit 5) and late Pliocene (Unit 6).

P 6.1
3D Taphonomy of Phosphatized Cambrian Arthropods

Jonathan Pople[1], Allison Daley[1], Pierre Gueriau[1]

[1]*Institute of Earth Sciences, University of Lausanne, Lausanne, Switzerland*
(jonathan.pople@unil.ch)

Orsten-type Lagerstätten produce extremely detailed phosphatized fossils of microscopic arthropods and other minuscule organisms of the Cambrian period; while the animals themselves have been studied extensively, the exact processes that led to their exceptional preservation have yet to be described (Maas et al., 2006). Combining Synchrotron Radiation X-Ray Microtomography (SRXMT) with traditional Scanning Electron Microscopy (SEM), we undertake a 3-dimensional examination of the fossils of bivalved phosphatocopine arthropods collected from the Swedish Orsten (Upper Cambrian). We find that autolithified bacteria are frequently preserved inside the cuticle, forming masses of phosphate globules, along with remains of filamentous biofilms. This provides direct evidence for the involvement of microbial activity in Orsten-type preservation, and is consistent with taphonomy experiments (Butler et al., 2015) and other cases of exceptionally preserved soft tissues (Briggs, 2003). The fossils also contain pyrite framboids whose crystallization appears to have been simultaneous with or posterior to phosphatization. Average framboid size in examined specimens is positively correlated with quality of preservation; the level of growth may be linked to different environmental conditions (either in space or time) or biochemical variations at the scale of individual carcasses, which in turn also affected phosphatization.

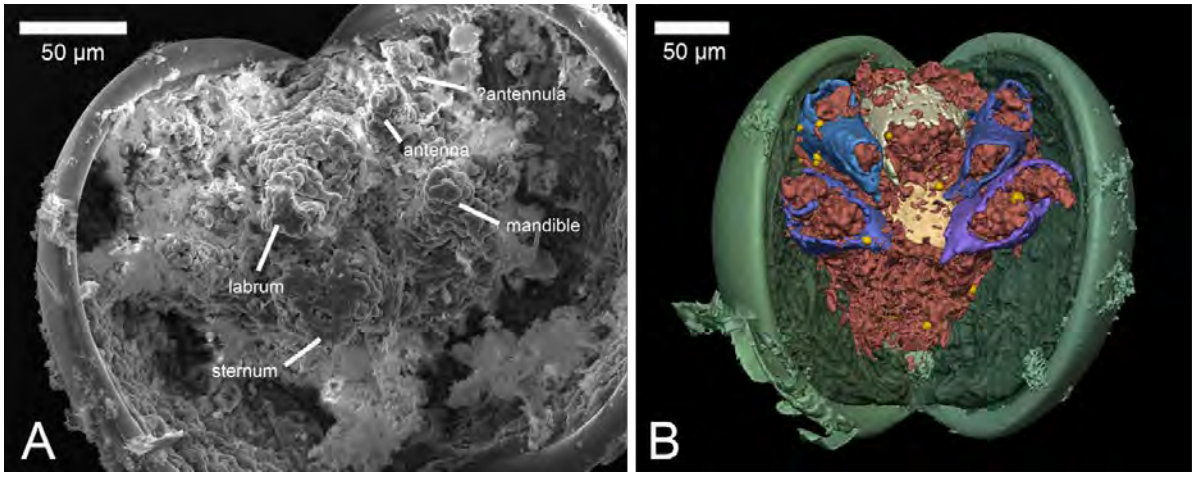

Figure 1. Fossils of phosphatocopines *Hesslandona* sp. with intact shield valves and varying degrees of preservation for softer parts. (A) SEM image of a specimen with trunk and appendages completely replaced by phosphatized bacteria. (B) Segmented 3D model of a specimen with partially preserved cuticle on the trunk and appendages (white and blue elements), filled with phosphatized bacteria (red) and pyrite framboids (bright yellow).

REFERENCES

Briggs, D. E. 2003: The Role of Decay and Mineralization in the Preservation of Soft-Bodied Fossils. Annual Review of Earth and Planetary Sciences, 31(1), 275-301.

Butler, A. D., Cunningham, J. A., Budd, G. E., & Donoghue, P. C. J. 2015: Experimental taphonomy of Artemia reveals the role of endogenous microbes in mediating decay and fossilization. Proceedings of the Royal Society B: Biological Sciences, 282(1808), 20150476.

Maas, A., Braun, A., Dong, X. P., Donoghue, P. C., Müller, K. J., Olempska, E., Repetski, J. E., Siveter, D. J., Stein, M., & Waloszek, D. 2006: The 'Orsten'—more than a Cambrian Konservat-Lagerstätte yielding exceptional preservation. Palaeoworld, 15(3-4), 266-282.

P 6.2
Influence of plate tectonics on biodiversity

Dominic Stemmler[1], Taras Gerya[1], Loïc Pellissier[2], Robert J. Stern[3]

[1] Departmentof Earth Sciences, ETH Zürich, Sonneggstrasse 5, CH-8092 Zürich (dominic.stemmler@erdw.ethz.ch)
[2] Department of Environmental Systems Science, ETH Zurich, Universitätsstrasse 16, CH-8092 Zürich
[3] Geosciences Department, University of Texas at Dallas, 800 West Campbell Road Richardson, USA-TX 75080-3021

The evolution of life on Earth is fundamentally linked to the dynamics of the lithosphere and deep mantle, and coupled to the Earth's surface, oceans and climate, but those dimensions are rarely studied together. We used a fast general circulation model for ocean and atmosphere (FOAM) (Jacob et al. 2001) with a paleo-digital elevation model (Scotese & Wright, 2018) for the timespan from 540 Ma up to recent times to generate climate model scenarios. Using variables like air surface temperature and precipitation combined with the digital elevation model considering different tectonics scenarios we show how simulations with gen3sis (Hagen et al. 2021), an eco-evolutionary biodiversity model, can inform about the conditions for the formation of biodiversity. By varying Earth dynamics e.g., the movement of tectonic plates, collisions, rifting we can investigate the causal connections between changes at Earth's surface like mountain building or creation of new oceans, the formation and destruction of habitats, we explore different scenarios generating specific biodiversity patterns. By combining these models and their respective results, we can develop a new methodology for understanding the feedback loops between geodynamics, climate and life evolution. In the current scenario, we investigate the differences in biodiversity between the natural movement of continental plates and a static Earth over the last 100 Ma.

Ultimately, we aim to apply our models to important events in Earth's history like supercontinent formation, continental breakup, large igneous province eruptions, and the transition from single lid to plate tectonics.

This project is funded by Fond National Suisse FNS: 192296

REFERENCES

Jacob, R., Schafer, C., Foster, I., Tobis, M. & Anderson, J. 2001:Computational design and performance of the fast ocean atmosphere model, version one. In Computational Science - ICCS 2001, pages 175–184. Springer Berlin Heidelberg, 2001.

Scotese, C.R. & Wright, N., 2018: PALEOMAP Paleodigital Elevation Models (PaleoDEMS) for the Phanerozoic PALEOMAP Project

Hagen O., Flück B., Fopp, F., Cabral, J. S., Hartig, F., Pontarp, M., Rangel, T. F., & Pellissier, L. 2021: gen3sis: A general engine for eco-evolutionary simulations of the processes that shape Earth's biodiversity. PLOSBiology, 19(7), e3001340. https://doi.org/10.1371/journal.pbio.3001340

07. Stratigraphy and Sedimentology: processes and deposits through time

Alain Morard, Sébastien Castelltort, Ursula Menkveld-Gfeller, Reto Burkhalter, Oliver Kempf

Swiss Committee for Stratigraphy (SKS/CSS)
Swiss Palaeontological Society (SPG/SPS)
Swiss Geological Survey – swisstopo

TALKS:

7.1 Banjan M., Crouzet C., Sabatier P., Jomard H., Bajard M., Demory F., Develle A.-L., Jenny J.-P., Findling N., Alain P., Clapot S., Messager E.: Increased seismicity in the Alps at the Younger Dryas–Holocene transition.

7.2 Carraro D., Ventra D., Moscariello A.: Architectural analysis of a large fluvial-fan succession: An example from the Paleogene–Eocene Wasatch Formation (Utah, USA).

7.3 Fucelli A. & Martini R.: Sedimentology and stratigraphy of the Upper Triassic carbonates from Hosselkus Limestone and Luning Formation (Western USA).

7.4 Harlet D., Douillet G.A., Ghienne J.-F., Razin P., Bouscary C., Dietrich P., Schlunegger F.: Stratigraphic architecture of a siliciclastic shallow-marine platform: Insights from the Late Ordovician of Southern Morocco (Anti-Atlas).

7.5 Karabeyoglu A.U, Adatte T., Lorenzo V., Spangenberg J., Özkan-Altiner S., Altiner D.: The Deccan volcanic activity and its environmental and ecologic consequences across the Cretaceous–Paleogene (K-Pg) boundary: Examples from Neo-Tethys in Turkey.

7.6 Lazarev S., Sahakyan L., Kuiper K., Vasiliev I., Caves J., Vasilyan D.: Volcanoclastic trap of the Pliocene fauna in the Lesser Caucasus: Depositional environments and integrated stratigraphy of the new locality Jradzor (Armenia).

7.7 Mair D., Do Prado A.H., Garefalakis P., Lechmann A., Schlunegger F.: Uncertainty of grain size data from close-range UAV imagery in fluvial gravel bars.

7.8 Nibourel L., Galfetti T., Grazioli S., Schumacher I., Schläfli S., Morgenthaler J., Heuberger S.: Towards a semi-automated and faster identification of potential mineral resources.

7.9 Paul A.N., Edward O., Adatte T., Vennemann T., Schaltegger U., Bucher H.: Temporal bracketing of geochemical excursions in stratigraphic sequences by ID-TIMS U-Pb zircon dating.

7.10 Ruchat A., Lathuilière B., Wohlwend S., Deplazes G., Madritsch H., Eberli G., Eruteya O., Samankassou E.: The Bajocian coral reefs of the “Herrenwis Unit” in North-Eastern Switzerland.

7.11 Sharma N., Valero L., Watkins S., Vérité J., Prieur M., Puigdefabregas C., Whittaker A., Garces M., Guillocheau F., Adatte T., Castelltort S.: Middle Eocene Climatic Optimum, fluvial paleohydraulic reconstruction and geochemical signals from the Escanilla sediment routing system (Spain).

7.12 Tournier N., Vogel H., Fabbri S.C., Anselmetti F.S., Russell J.M., Bijaksana S., Cahyarini S.Y.: Seismic event stratigraphy of tectonic Lake Towuti (Sulawesi, Indonesia): A 60 kyrs record of seismo-turbidites.

7.13 Tremblin M., Minoletti F., Hermoso M., Desmares D.: Evolution of the Atlantic meridional temperature gradient during the Paleogene: New insights from coccolith-derived temperatures.

7.14 Vaucher R., Dashtgard S.E., Horng C.-H., Zeeden C. Dillinger A., Pan Y.-Y., Ari Setiaji R., Chi W.-R., Löwemark L.: Sea level and sediment supply in Taiwan during the Early Pleistocene: A matter of precession.

POSTERS:

P 7.1 Moscariello A., Ventra D., Cervelli M., Eruteya O.E., Omodeo Salé S., Makhloufi Y.: Revisiting the origin of the Carboniferous infill of Swiss post-Hercynian troughs: Insights from the Weiach-1 borehole (northern Switzerland).

P 7.2 Frund F.E., Fellin M.G., Picotti V., Willet S.D.: Provenance of the Habkern Granite and the Wilfdflysch based on an integrated geo-thermochronologic approach.

P 7.3 Bekonga B.G.S., Yem M., Atangana J.Q.Y., Nkoa E.P.N., Biouele S.E.A., Yakufu Niyazi Y., Eruteya O.E.: Evolution and morphology of a Late Cretaceous submarine channel system in the Kribi/Campo sub-basin, offshore Cameroon.

P 7.4 Prieur M., Whittaker A.C., Schlunegger F., Sømme T.O., Braun J., Castelltort S.: Impact of an abrupt climate change on sediment fluxes from source to sink: An example from the PETM in the Southern Pyrenees (Spain).

P 7.5 Jaimes-Gutierrez R., Adatte T., Puceat E., Braun J., Castelltort S.: Chemical weathering intensity linked with extreme global warming during PETM: Insights from the Southern Pyrenees (Spain).

P 7.6 Kobakhidze N., Lebanidze Z., Beridze T., Makadze D., Uchman A., Chagelishvili R., Lobzhanidze K., Khutsishvili S., Koiava K., Khundadze N.: Trace fossils in Paleocene–Lower Eocene deep-sea sediments of the eastern segment of the Achara–Trialeti fold-and-thrust belt.

P 7.7 Lebanidze Z., Uchman A., Beridze T., Kobakhidze N., Lobzhanidze K., Khutsishvili S., Makadze D., Chagelishvili R., Khundadze N., Koiava K.: The trace fossil Polykampton Georgianum Horizon in the Paleocene deposits of the Achara–Trialeti fold-and-thrust belt (Georgia).

P 7.8 Maqadze D., Rice S., Maqadze M., Kobakhidze N.: The study of main lithofacies types of Bertakari low-sulphidation epithermal deposit (Bolnisi ore field, Southern Georgia).

7.1
Increased seismicity in the Alps at the Younger Dryas –Holocene transition

Banjan Mathilde [1,3], Crouzet Christian[1], Sabatier Pierre[2], Jomard Hervé[3], Bajard Manon[4], Demory Francois[5], Develle Anne-Lise[2], Jenny Jean-Philippe[6], Findling Nathaniel[7], Alain Philippe[8], Clapot Sylvain, Messager Erwan[2]

[1] *Université Savoie Mont Blanc, Université Grenoble Alpes, CNRS, IRD, Université Gustave Eiffel, ISTerre, Chambéry, France (mathilde.banjan@univ-smb.fr)*
[2] *Université Savoie Mont Blanc, CNRS, EDYTEM, Chambéry, France*
[3] *IRSN - Bureau d›évaluation des risques sismiques pour la sûreté des installations, Fontenay-aux-Roses, France*
[4] *Department of Geosciences, MetOs, CEED, University of Oslo*
[5] *Aix Marseille Univ, CNRS, IRD, INRAE, Coll France, CEREGE, Aix-en-Provence, France*
[6] *Université Savoie Mont Blanc, INRAE, CARRTEL, Thonon-les-Bains, France*
[7] *Univ. Grenoble Alpes, Univ. Savoie Mont Blanc, CNRS, IRD, Université Gustave Eiffel, ISTerre, Grenoble, France*
[8] *Sonar Systems Division, iXblue, La Ciotat, France*

In the NW Alps, several glacial origin lakes present several mass movement deposits (MMD) within their sedimentary sequences. These anomalies could be the result of lake sediment destabilization triggered by earthquakes. Based on sedimentological, geochemical, magnetic data and high-resolution seismic and bathymetric survey, we identify a 1.15-meter thick MMD in the deepest Lake Aiguebelette basin and synchronous to a 2cm-thick deposit in the shallow basin. Radiocarbon based age-depth models constrain the age of this event in Lake Aiguebelette at the Younger Dryas-Early Holocene climatic transition (i.e. 11 500 cal BP). At the same time, in Lake La Thuile (located 30 km away), a translational slide was recorded in the sedimentary sequence. The analyses of these two lakes highlight a possible regional synchronicity of large MMD. The comparison with high-resolution seismic profiles previously acquired in Lake Annecy and previous Swiss Alpine lakes studies supports this hypothesis of a significant MMD occurrence at the YD-EH transition *(Strasser et al. 2008; Kremer et al 2017; Strasser et al 2013)*. Based on these results, we discuss the impact of climate change in triggering earthquakes at the occidental Alps scale, with driving processes such as glacial triggering crustal rebound and erosional unloading.

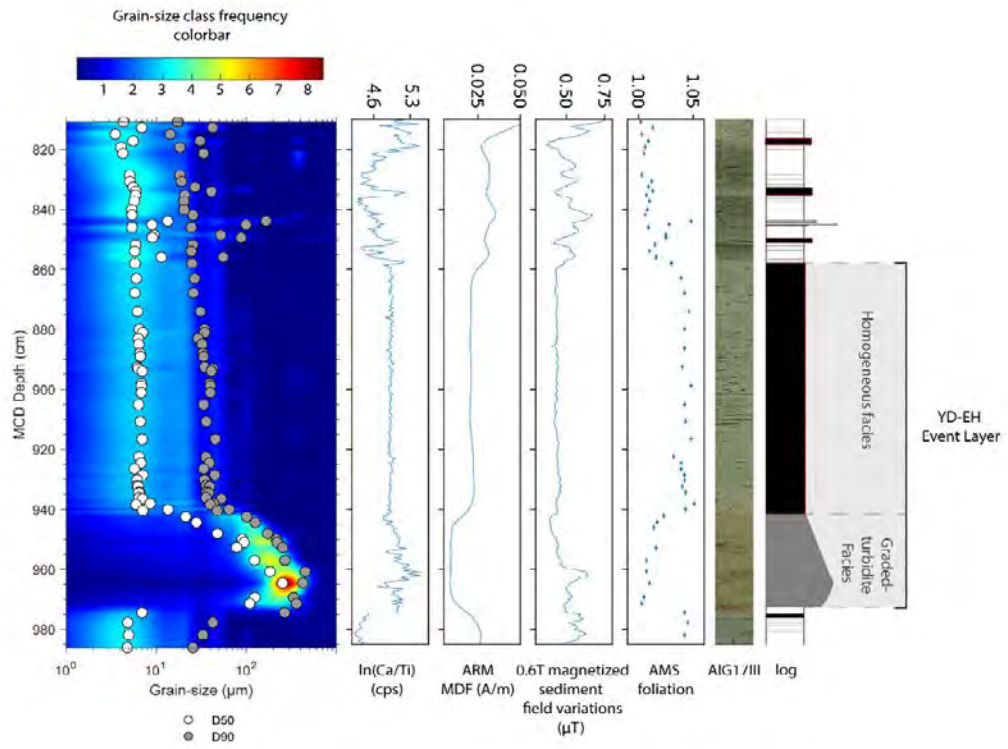

Figure 1. Sedimentological, geochemical and magnetic results at depths covering the large EL of the Lake Aiguebelette deep basin sequence. From left to right: grain-size measurements presented in a contourplot. D50 and D90 values (white and grey dots respectively) are superimposed on the grain-size frequency contourplot; ln(Ca/Ti) ratio; ARM; magnetized sediment low field variations (equivalent to low Isothermal Remanent Magnetization, *Demory et al. 2019*); AMS foliation; photography and macroscopic log description of the different facies types observed (plain black lines: laminated facies; black rectangles: homogenite facies; grey graded symbol: graded-turbidite facies with inverse-graded base topped with a main normal-graded facies).

REFERENCES

Demory, F., Uehara, M., Quesnel, Y., Rochette, P., Romey, C., Tachikawa, K., ... & Andrieu-Ponel, V. (2019). A new high-resolution magnetic scanner for sedimentary sections. Geochemistry, Geophysics, Geosystems, 20(7), 3186-3200.

Kremer, K., Wirth, S. B., Reusch, A., Fäh, D., Bellwald, B., Anselmetti, F. S., ... & Strasser, M. (2017). Lake-sediment based paleoseismology: Limitations and perspectives from the Swiss Alps. Quaternary Science Reviews, 168, 1-18.

Strasser, M., Schindler, C., & Anselmetti, F. S. (2008). Late Pleistocene earthquake-triggered moraine dam failure and outburst of Lake Zurich, Switzerland. Journal of Geophysical Research: Earth Surface, 113(F2).

Strasser, M., Monecke, K., Schnellmann, M., & Anselmetti, F. S. (2013). Lake sediments as natural seismographs: A compiled record of Late Quaternary earthquakes in Central Switzerland and its implication for Alpine deformation. Sedimentology, 60(1), 319-341.

7.2
Architectural analysis of a large fluvial-fan succession: an example from the Paleogene-Eocene Wasatch Formation (Utah, U.S.A.).

Davide Carraro[1], Dario Ventra[1], Andrea Moscariello[1]

[1] Geoscience Department, University of Geneva, 13 rue des Maraichers, CH-1205 Geneva (davide.carraro@unige.ch)

Recent developments in fluvial geomorphology and sedimentology suggest that fluvial fans might be responsible for the accumulation of great volumes of clastic successions in continental basins. The possibility of identifying a “typical” stratigraphic signature for aggrading fluvial fans opens a new perspective to interpret continental records, where distinguishing the effects of autogenic dynamics from those of allogenic forcing remains a major challenge. Furthermore, due to the intrinsic heterogeneity displayed by this type of depositional system, the success of exploration for subsurface resources relies greatly on the reliability of the chosen stratigraphical model. From geological and economic perspectives, hydrocarbon exploration and development along continental basin margins have been classically considered as high-risk, low-pay endeavors, given the scarcity of viable conceptual models to address their supposed architectural unpredictability. This research consists of an outcrop-based analysis of architectural patterns and spatio-temporal trends in avulsion mechanisms through the Palaeocene-Eocene Colton-Wasatch fluvial-fan system of the Uinta Basin (central Utah). Three-dimensional digital outcrop models were created from a set of high-quality photos acquired by drone fly-bys over circa 35km long, laterally continuous outcrop belts, ground-truthed by composite stratigraphic logs which cover the full extent of the Wasatch Formation. This allowed the reconstruction of the system’s depositional history correlated with a detailed description of the internal organization of architectural elements identified in the field such as ribbon-shaped channel-fills, amalgamated channel-belt sandstones, mudstone-dominated floodplain muds, and heterolithic succession of overbank fines. Along a downfan radial transect, three main fan segments are distinguished here based on the stratigraphic organization and proportion of architectural elements, ultimately defining the net-to-gross trend. High net-to-gross values and latero-vertical connectivity define the proximal sector, where channel-belt deposits are highly amalgamated, with only minor preservation of mudstone-prone lenses representative of overbank deposition. The relative volume and amalgamation of channel-fill deposits decrease in the medial sector in which channel-belt units are laterally extensive but vertically compartmentalized by thick, mud-rich floodplain units. Net-to-gross values decrease drastically in the distal sector of the system, where isolated, ribbon-shaped channel-bodies are encased in a claystone-dominated succession. Textural, compositional, and primary porosity trends documented by QEMSCAN analysis of petrographic thin sections further accompany the definition of net-to-gross values at the system scale. Outcrop observations will be complemented by analyses of publicly available well-log and core data to test the recognition of architectural elements in the subsurface and to better define the regional extent of fluvial-fan sectors in areas where natural exposures are absent or inaccessible. The research approach described here emphasizes the efficacy of digital outcrop models, supported by ground-based surveys, as a tool to describe and quantify architectural complexity in clastic successions. The regional-scale stratigraphic trends provide a first-order validation of the expected fluvial-fan model, with observed differences possibly related to the influence of step-wise transgression during the onset of the Green River lacustrine system.

7.3
Sedimentology and stratigraphy of the Upper Triassic carbonates from Hosselkus Limestone and Luning Formation (Western USA)

Andrea Fucelli* & Rossana Martini*

**Department of Earth Sciences, University of Geneva, Rue des Maraichers 13, CH-1205 Genève (andrea.fucelli@unige.ch)*

Although the significant research carried out during the last years, knowledge about Panthalassan shallow-water carbonates remains distinctly minor than their Tethyan counterparts. Considering the broad diffusion of these limestones, the comprehension of their depositional environment, ecologic conditions and geographic extent, represents a unique way to better assess life evolution and recovery after the main Permo-Triassic biological crisis. Hosselkus Limestone and Luning Formation, respectively located in Northern California and Western Nevada, represent two completely different scenarios of limestone deposition during Upper Triassic. The first, deposited on a volcanic arc far from the coast of the American craton, shows a rapid change from shallow water facies to deep marine deposits, offering a wide spectrum of calcareous and siliceous organisms. The second, deposited in a large embayment attached to the continent, represents a much wider and homogeneous environment, where calcareous organisms thrive for a long period. Paleontological studies started at the beginning of the last century, but focused exclusively on large-dimension fauna, mainly because of the poor preservation of the rocks. Now, thanks to targeted fieldworks and a significant amount of collected samples, the two formations are described in terms of microfacies and microorganisms, allowing a more exhaustive picture of the depositional environments and a sharper comparison of biological contents. Ages have been revised too, thanks to numerous Conodont specimens, allowing a high temporal resolution and thus a better correlation with other terrane-based carbonates from the Panthalassan domain.

7.4
Stratigraphic architecture of a siliciclastic shallow-marine platform: Insights from the Late Ordovician of Southern Morocco (Anti-Atlas)

Déborah Harlet[1], Guilhem Amin Douillet[1], Jean-François Ghienne[2], Philippe Razin[3], Chloé Bouscary[4], Pierre Dietrich[5], Fritz Schlunegger[1]

[1] Institut für Geologie, Universität Bern, Baltzerstrasse 3, CH-3012 Bern (deborah.harlet@geo.unibe.ch)
[2] EOST, Centre de Géochimie de la surface, CNRS-UMR 7517, 1 rue Blessig, FR-67084 Strasbourg
[3] Institut ENSEGID, Université Bordeaux 3, FR-33607 Pessac
[4] Institut des Dynamiques de la Surface Terrestre (IDYST), Université de Lausanne, CH-1015 Lausanne
[5] Géosciences Rennes, Université de Rennes, UMR 6118, FR-35000 Rennes

Since the latest Precambrian (Ediacaran), sediments have been deposited on the northern Gondwana shallow marine platform, now exhumed as the Moroccan Anti-Atlas. The Ktawa Group, of early Late Ordovician in age (Mid-Sandbian to Katian), outcrops as marked cuestas with different orientations along the Jbel Bani mountain range. This field-based study focuses on a ca. 175 km long transect in the western Central Anti-Atlas, where “3D” stratigraphy is used to constrain the platform history during deposition of the Ktawa Group. Forty-two stratigraphic logs were correlated by satellite and drone images. The latter also enables calibration of the logs by photogrammetry.

The Ktawa Group is subdivided into three formations (Fm): Lower Ktawa, Rouïd-Aïssa and Upper Ktawa. Here, focus is put on the Lower Ktawa Fm, consisting of silty shale to fine to very coarse sandstones in the studied region. In contrast, the Rouïd-Aïssa Fm is dominated by medium to coarse sandstones with a strong fining eastward trend whereas the Upper Ktawa Fm do not outcrop in the area, eroded during the Late Ordovician (Hirnantian) glaciation.

Within the Lower Ktawa Fm, the silty-shale background is punctuated by several sandstone cuestas continuous over tens of kilometers. These cuestas represent regressive excursions and are analyzed individually hereafter.

The lowermost cuesta (Foum-Zguid Member) outcrops continuously over more than 100 km. It marks the top of a shallowing up parasequence and consists of facies oscillating between amalgamated Hummocky-Cross-Stratifications (HCS) and bioturbated sandstones. Its flatness and monotonic changes in facies point towards a flat prograding clinoform deposited during a normal regression, pinching out towards the ENE.

The second cuesta («Tissint Member») outcrops only in the western part of the transect. This 20 to 30 m thick sand-body has a sharp base located ca. 20 m above the top of the Foum-Zguid Member. It consists of medium sandstones and thin horizons of granules organized in channelized to amalgamated beds containing obliques and trough-cross-beds. The 30 m thick sand-body laterally disappears within ca 3.5 km towards the NE. The sharp base and proximal facies associations may indicate a downward shift and forced regression. The NE confined extension results either from a channelized morphology or from a transgressive ravinement eroding the north-eastern part of the sand-body. This sudden disappearance together with the observed high-energy facies associations could further suggest deposition in a river mouth environment.

Above the Foum-Zguid Member’s eastern part, two minor superimposed sand-bodies, ca. 70 and 100 m above the first, thin out and dip towards the NNE. The evolution of facies associations ranges from channelized sandstones in the W to bioturbated silty sand towards the NE, thus suggesting a distalization towards the NE. Hence, these two sand-bodies may be shaped as subaquatic clinoforms with an overall basinward direction to the NE.

The thickest and uppermost cuesta in the region is the Bou-Hajaj Member, a prominent sand-body ranging from 5 to 60 m in thickness and outcropping over ca. 60 km eastward from the Foum-Zguid Member. The Bou-Hajaj cuesta marks a step in elevation, lower towards the N. Furthermore, it is separated in two parts with distinct facies associations. The lower part represents a regressive parasequence from silts to HCS to channelized sandstones. This sequence is cut to the East and overlaid by a thick body of medium to very coarse sandstones showing granule beds and trough to oblique beddings with *Diplocraterion Parallelum* burrows. This abrupt change of the upper sequence suggests an incision and downward shift to a river mouth environment.

To the East of the Bou-Hajaj Member, another sand-body (“Abbas Member”), 5 to 30 m thick, outcrops at an elevation slightly lower than the Bou-Hajaj cuesta, yet with a 10 km lateral gap in physical correlation with the Bou-Hajaj Member. This cuesta is dominated by HCS sandstones to the S and bioturbated sandstones to the N, and could laterally correlate to the lower or upper part of the Bou-Hajaj Member. The Bou-Hajaj and Abbas cuestas laterally disappear abruptly towards, leaving no trace but a shale dominated series further eastward, thus suggesting their truncation by a transgressive ravinement.

Overall, the Ktawa Group stratigraphy suggests a S-N to SW-NE basinward orientation. This part of the margin exhibits a flat and stable geometry except for narrow zones that may represent the rollover point of clinoforms.

7.5
The Deccan volcanic activity and its environmental and ecologic consequences across the Cretaceous-Paleogene (K-Pg) boundary: examples from Neo-Tethys, Turkey

A. Uygar Karabeyoglu [1] (aliuygar.karabeyoglu@unil.ch), Thierry Adatte [1], Valentin Lorenzo [1], Jorge Spangenberg [2], Sevinç Özkan-Altiner [3], Demir Altiner [3]

[1] ISTE, Institute of Earth Sciences, University of Lausanne, Lausanne, Switzerland
[2] IDYST, Institute of Surface Dynamics, University of Lausanne, Lausanne, Switzerland,
[3] Department of Geological Engineering, Middle East Technical University, Çankaya/Ankara, Turkey

Decades of studies have shown the causation between continental flood basalt volcanism and the mass extinction events. Among those, the end-Cretaceous mass extinction has a special standing in possessing the junction of two mega Earth-rendering events: The Deccan volcanism and the Chicxulub impact. Among them, the role of the Deccan volcanism is critical in understanding the interplay between large volcanic activity and associated environmental stress. Here we show this relation with high-resolution biostratigraphy, quantitative species counts, and geochemical data from two sections (Haymana and Mudurnu-Göynük basins) in Central Anatolia, Turkey.

The high-resolution quantitative study in the Haymana Basin reveals that planktonic foraminiferal community in the latest Maastrichtian is dominated by ecological generalists with small, simple morphologies. It also shows a systematic reduction in the species richness. Similar in both sections, the K-Pg boundary is characterized by a 2-3 mm thick reddish oxidized layer corresponding a sudden annihilation of large, ornamented species. It also represents enrichment in some critical elements, such as Ir, Te, Hg, Ba, Ni, Cr, Co. Right above the boundary, acmes of *Thoracosphaera*, and *Guembelitria cretacea* indicate the ecosystem collapse during post-K-Pg environment. The same levels correspond to a surge in the number of fecal pellets.

Overall, our multiproxy approach highlights the influence of the Deccan volcanism by releasing high amounts of atmospheric CO_2 and SO_2 gases, leading to climatic changes, and hence enabling a biotic stress which predisposes faunas to the eventual extinction at the K-Pg boundary.

7.6
Volcanoclastic trap of the Pliocene fauna in the Lesser Caucasus: depositional environments and integrated stratigraphy of the new locality Jradzor (Armenia)

Sergei Lazarev[1,2] , Lilit Sahakyan[3], Klaudia Kuiper[4], Iuliana Vasiliev[5], Jeremy Caves[6], Davit Vasilyan[1,2],

[1] *University of Fribourg, Department of Geosciences, Chemin du Musée,1700 Fribourg, Switzerland (sergei_lazarev@outlook.com)*
[2] *JURASSICA Museum, Route de Fontenais 21, Porrentruy, Switzerland*
[3] *Institute of Geological Sciences, National Adacemy of Republic of Armenia, 24A, Marshall Baghramian Avenue, Yerevan 0019, Armenia*
[4] *Department of Earth Sciences, Faculty of Science, Vrije Universiteit Amsterdam, De Boelelaan 1085, 1081HV Amsterdam, the Netherlands*
[5] *Senckenberg Biodiversity and Climate Research Centre (SBiK-F), Senckenberganlage 25, D-60325 Frankfurt am Main, Germany*
[6] *Department of Geosciences, Colorado State University, Fort Collins, CO 80523, USA*

Aridification of climate and development of open landscapes at the Mio-Pliocene transition of the Northern Hemisphere enabled active faunal migrations between Africa and Eurasia that consequently formed the modern ecosystems. Reconstruction of such complex biogeographic history relies on very fragmented continental fossil records that makes the new paleontological localities across Eurasia of a high interest.

The Lesser Caucasus is a mountain range with unique geographic position at the crossroad between Africa, Europe and Asia that makes the regional geological record highly potential for reconstruction of Eurasian paleobiogeographic history. However, the regional Pliocene fossil record remains very poorly studied due to the lack of both rich vertebrate fauna localities and well-dated geological records.

Here, we present our first geological data of the new faunal locality Jradzor (Central Armenia, Lesser Caucasus). Being discovered in 2009 and actively studied since 2016, the 58-meter succession revealed at least 15 fossil horizons of vertebrate fauna with more than 30 taxa of various groups (birds, mammals, reptiles, fishes, amphibians etc.), most of which are associated with volcanoclastic deposits. Combination of $^{40}Ar/^{39}Ar$ dating of five volcanic ash layers along with magnetostratigraphy allowed creating a high resolution age constants dating the section between 4.3 and 3.1 Ma.

Sedimentological analysis allowed to subdivide the section into six sedimentary units: Unit 1 represented by white thinly-laminated diatomite succession (distal lacustrine setting); Unit 2 build of brown, mottled mudstones (palaeosols and downslope deposits); Unit 3-4 made of pale yellow mudstones with rootlets and extensive erosive sheet-like coarsening-upwards packages of scoria and pumice (distal and medial tails of pyroclastic flows); Unit 5 with brown mottled mudstones (palaeosols and downslope deposits); Unit 6 with alternating packages of pumice, volcanic ashes and paleosols.

The rich taxonomic content of the locality, burned surfaces on bones and their frequent clumping with pumice fragments suggest that the local fauna was often killed and buried by hot and rapid pyroclastic flow and surges. The ongoing research on the site will help to better understand the Pliocene interregional faunal migrations and to trace their link with dynamic volcanic environments of the Lesser Caucasus.

7.7
Uncertainty of grain size data from close-range UAV imagery in fluvial gravel bars

David Mair[1], Ariel Henrique Do Prado[1], Philippos Garefalakis[1], Alessandro Lechmann[1] and Fritz Schlunegger[1]

[1] *Institute of Geological Sciences, University of Bern, Bern, 3012, Switzerland (david.mair@geo.unibe.ch)*

The grain size distribution of channel bars in gravel-bed rivers is a key quantity for the understanding and managing of a river system. Standard methods that have been developed to quantify the size of gravels in rivers involve time-intensive fieldwork (e.g., the method of Wolman, 1954), and bear the risk to introduce sampling biases. Recently, the collection of grain size data has been achieved from photos that have been taken by low-cost UAV (unmanned aerial vehicle) platforms. Several methods to extract grain size estimations from such imagery have been developed (e.g., Carbonneau et al., 2018; Purinton and Bookhagen, 2019). Despite the avialbility of information on the precision and accuracy of an UAV survey (e.g., James et al., 2020), a systematic analysis of the uncertainty that is introduced into the resulting grain size distribution is still missing.

Here we present the results of three close-range UAV surveys conducted along Swiss gravel-bed rivers with a consumer-grade UAV. We use these surveys to assess the dependency of grain size measurements and associated uncertainties from topographic models, in turn generated from the UAV imagery. In particular, we assess (i) the effect of different image acquisition formats, (ii) specific survey designs recommended by previous authors, and (iii) how geo-referencing methods impact the resulting topographic data. To do so, we determine how the different photogrammetric models and their uncertainties influence the statistical uncertainty of the collected grain size data through a combined bootstrap and Monte Carlo (MC) modelling approach.

Our preliminary results reveal that the quality of an UAV model is fairly insensitive to the image acquisition format, but strongly varies for different UAV survey choices. Most precise and accurate results are obtained with single altitude surveys, the inclusion of oblique camera angles and the use of independently measured ground control points. Least precise and accurate results, with 1 to 2 orders of magnitude higher uncertainties, are obtained with self-referenced images that were acquired in nadir-only and gridded surveys. However, the MC modelling of grain size distributions with propagated UAV uncertainties as input, shows that grain size uncertainty is mainly dominated by counting statistics and the choice of the measurement method.
These results indicate that even relative imprecise and not accurate UAV image data can yield acceptable grain size data for some applications. Furthermore, the use of a MC modelling strategy can be employed to estimate the grain size uncertainty for any image-based method with which individual grains are measured.

REFERENCES

Carbonneau, P. E., Bizzi, S. and Marchetti, G. 2018: Robotic photosieving from low-cost multirotor sUAS: a proof-of-concept, Earth Surf. Process. Landforms, 43(5).

James, M. R., Antoniazza, G., Robson, S. and Lane, S. N. 2020: Mitigating systematic error in topographic models for geomorphic change detection: accuracy, precision and considerations beyond off-nadir imagery, Earth Surf. Process. Landforms, 45(10).

Purinton, B. and Bookhagen, B. 2019: Introducing PebbleCounts: A grain-sizing tool for photo surveys of dynamic gravel-bed rivers, Earth Surf. Dyn. Discuss., 1–33.

Wolman, M. G. 1954: A method of sampling coarse river-bed material, Trans. Am. Geophys. Union, 35(6), 951.

7.8
Towards a semi-automated and faster identification of potential mineral resources

Lukas Nibourel*, Thomas Galfetti**, Sandra Grazioli*, Isabel Schumacher*, Salome Schläfli**, Joël Morgenthaler & Stefan Heuberger*

**Fachgruppe Georessourcen Schweiz, Departement Erdwissenschaften, ETH Zürich, Sonneggstrasse 5, 8092 Zürich (lukas.nibourel@erdw.ethz.ch)*
***Bundesamt für Landestopografie swisstopo, Seftigenstrasse 264, 3084 Wabern*

The goal of mineral occurrence maps is to display the spatial distribution of a given raw material of potential economic value. Spatial planners and the private sector depend on these maps to secure the access to the raw material of interest and to resolve or reduce the conflicts associated with its extraction. We present a semi-automated Matlab- and GIS-based routine to locate hard siliceous limestone and sandstone, which can potentially be suitable for the production of hard rock aggregates – a material essential for the construction and maintenance of Swiss railway and road infrastructure. From the Swiss geological vector dataset GeoCover (1:25'000), the routine locates and plots hard rock occurrences based on (1) the true thickness of a target unit and (2) the estimated proportion of high quality hard rock within the same unit. The true thickness is computed by our Matlab-script, which extracts orientation and thickness data from GeoCover and combines it with thickness data from published geological cross-sections. The quality of the target unit is estimated from published stratigraphic descriptions. Our GIS routine selects occurrences which are estimated to fullfill our quantitative thickness and quality boundary conditions. This allows a clear focus on relevant areas for spatial planners and for further invesigations. The flexibility of the method and the automation of the routine ensures reproducibility and auditability of the results as well as the production of new results as new data becomes available. With relatively small adjustments, the routine may be applicable to a wide range of other mineral resources.

7.9
Temporal bracketing of geochemical excursions in stratigraphic sequences by ID-TIMS U-Pb zircon dating

André Navin Paul[1], Oluwaseun Edward[2], Thierry Adatte[2], Torsten Vennemann[2], Urs Schaltegger[1], Hugo Bucher[3]

[1] Department of Earth Sciences, Université de Genève, Rue des Maraîchers 13, CH-1205 Genève (Andre.Paul@unige.ch)
[2] Faculty of Geoscience and Environment, Université de Lausanne, Quartier UNIL-Mouline, Batîment Géopolis, CH-1015 Lausanne
[3] Paläontologisches Institut und Museum, Universität Zürich, Karl-Schmidt-Strasse 4, CH-8006 Zürich

Correlation of geographically disparate sedimentary sections is of fundamental importance to most stratigraphic studies. First order approaches to achieve a correlation is by comparing lithostratigraphy, backed up by a comparison of geochemical features and ultimately verifying the temporal consistency.The precise and accurate U-Pb dating of accessory minerals such as zircon from individual volcanogenic ash beds in sedimentary sucessions is the preferred method for temporally calibrating, for example, the early Triassic (Widmann et al., 2020) or the Permian-Triassic transition (Baresel et al., 2017). Some studies, however, base their correlations on diachronous first occurrences of index species and on visual matching of geochemical time-series only, without robust criteria (e.g. Shen et al. 2021). This may lead to diachronous correlations between different sedimentary records and eventually to wrong lithostratigraphic or biochronologic calibration. This study presents preliminary data obtained from two Lower Triassic sections in the Pintang syncline of the southern part of the Nanpanjiang basin, S. China, which apparently have equivalent C isotope and Hg concentration curves. It is expected that the geochemical excursions of interest in this study are short in nature, possibly <200kyrs. Such short timescales are difficult to resolve in the Triassic, unless extended stratigraphic sections are available and a statistically sufficient number of temporal analyses can be generated. Nonetheless, previous studies arrived at high-precision temporal resolutions at the 50 ky level using zircon U-Pb geochronology (e.g., Baresel et al. 2017). Furthermore, the chemical characteristics of accessory minerals in the ash beds can support temporal correlations from geochronology (Baresel et al. 2017), bulk sediment geochemistry and biochronology. Based on these two deep water sections, our new zircon U-Pb and apatite geochemical data demonstrate that the largest Hg anomaly clearly postdate the Permian-Triassic boundary and coincides with the peak of the protracted negative C-isotope excursion that initiated within the late Permian (Bagherpour et al. 2020 GSA Bull).

REFERENCES

Bagherpur, B., Bucher, H., Vennemann, T., Schneebli-Hermann, E., Yuan, D.-X., Leuu, M., Zhang, C. & Shu-Zhong, S. 2021: Are late Permian carbon isotope excursions of local or of global significance?, GSA Bulletin, 132(3-4), 521-544.

Baresel, B., Bucher, H., Brosse, M., Cordey, F., Guodun, K. & Schaltegger, U. 2017: Precise age for the Permian–Triassic boundary in South China from high-precision U-Pb geochronology and Bayesian age–depth modeling, Solid Earth, 8, 361-378.

Baresel, B., D'Abzac, F.-X., Bucher, H. & Schaltegger, U. 2017: High-precision time-space correlation through coupled apatite and zircon tephrochronology: An example from the Permian-Triassic boundary in South China, Geology, 45(1), 83-86.

Shen, J., Chen, J., Algeo, T.J., Feng, Q., Yu, J., Xu, Y.-G., Xu, G., Lei., Y., Planavsky, N.J., & Xie., S. 2021: Mercury fluxes record regional volcanism in the South China craton prior to the end-Permian mass extinction, Geology, 49(4), 452-456.

Widmann, P., Bucher, H., Leu, M., Vennemann, T., Bagherpour, B., Schneebli-Hermann, E., Goudemand, N. & Schaltegger, U. 2020: Dynamics of the Largest Carbon Isotope Excursion During the Early Triassic Biotic Recovery, Frontiers in Earth Science, 8, 196.

7.10
Bajocian coral reefs of the "Herrenwis Unit" in North-Eastern Switzerland

Arnaud Ruchat[1], Bernard Lathuilière[2], Stephan Wohlwend[3], Gaudenz Deplazes[4], Herfried Madritsch[4], Gregor P. Eberli[5], Ovie E. Eruteya[1], Elias Samankassou[1]

[1] Department of Earth Sciences, University of Geneva, Rue des Maraîchers 13, 1205 Geneva, Switzerland
[2] Université de Lorraine, CNRS, Lab. GeoRessources, UMR 7359, BP 70239, 54506 Vandoeuvre-lès-Nancy Cedex, France
[3] Geological Institute, ETH Zürich, Sonneggstrasse 5, 8092 Zürich, Switzerland
[4] National Cooperative for the Disposal of Radioactive Waste (Nagra), Hardstrasse 73, 5430 Wettingen, Switzerland
[5] Department of Marine Geosciences, Rosenstiel School of Marine and Atmospheric Science, University of Miami, FL 33149, USA

Within the framework of the "Sachplan Geologische Tiefenlafer" (SGT), Nagra is currently investigating three sites in northern Switzerland as potential repositories for radioactive waste. The host rock, the Opalinus Clay, and its containment stratigraphic units are being explored by deep drilling and 3D seismic analysis.

In the Nördlich Lägern study area, 2D seismic data have already revealed a rounded paleohigh in the Middle Jurassic upper confining units of the Opalinus Clay (Meier & Deplazes, 2014) and later confirmed by 3D seismic data. The recently drilled Nagra borehole Bülach-1 within this paleohigh shows well-preserved corals above the Wedelsandstein Formation respectively a thin "Humphriesi-Oolith Formation". This new unit is informally named "Herrenwis Unit."

This unit is further investigated in the presented study by an integrative analysis of the currently available 3D seismic reflection data and well data and cores available from the study area.

Seismic geomorphological interpretation of the 3D seismic reflection data reveals a unique cluster of mound-shape structures interpreted as coral patch reefs. The development of these features on a pre-existing paleohigh indicates topographic control on their evolution. The individual mound structures are comparable in morphology and size.

The main coral genera identified are *Isastrea*, *Periseris*, *Thamnasteria* and *Dendraraea*. Preliminary assessment of the growth features and orientation of the corals, the presence of surrounding microbialites and the scarcity of transport features indicates that most corals are upright and occur in growth position. This reef is typical of the Bajocian, based on quantitative data using the coral diversity and abundance (Lathuilière, 2000a, b).

The identified "Herrenwis Unit" shows that coral reefs developed in Northern Switzerland, along with the Middle Jurassic marine oolitic carbonates and marly basinal deposits reported by Gonzalez & Wetzel (1996). This finding extends the occurrence of coral reefs, widely reported in the Tethyan realm and displaying comparable geometries (e.g., France and Morocco).

Ongoing research will help characterize the reef facies and its large-scale distribution.

REFERENCES

Gonzalez, R., & Wetzel, A. 1996: Stratigraphy and paleogeography of the Hauptrogenstein and Klingnau Formations (middle Bajocian to late Bathonian), northern Switzerland]. Eclogae Geologicae Helvetiae, 89(1), 695-720. https://doi.org/10.5169/SEALS-167921

Lathuilière, B. 2000a: Coraux constructeurs du Bajocien inférieur de France. Geobios, 33(1), 51–72. https://doi.org/10.1016/S0016-6995(00)80149-7

Lathuilière, B. 2000b: Coraux constructeurs du Bajocien inférieur de France. Geobios, 33(2), 153–181. https://doi.org/10.1016/S0016-6995(00)80013-3

Meier, B., & Deplazes G. 2014: Reflexionsseismische Analyse des ‚Braunen Doggers'. Nagra Arbeitsbericht. NAB 14-058. Nagra, Wettingen. 51 pp.

7.11
Middle Eocene Climatic Optimum, fluvial paleohydraulic reconstruction and geochemical signals from the Escanilla sediment routing system, Spain

Nikhil Sharma[1] , Luis Valero[1] , Stephen Watkins[1] , Jean Vérité[2] , Marine Prieur[1] , Cai Puigdefabregas[3] , Alexander C Whittaker[4] , Miguel Garces[5] , Francois Guillocheau[6] , Thierry Adatte[7] and Sebastien Castelltort[1]

(1) University of Geneva, Department of Earth Sciences, Geneva, Switzerland,
(2) Université du Maine LPG - Le Mans, Bât. Sciences Naturelles UFR Sciences et Techniques, Le Mans cedex 9, France,
(3) University of Barcelona, Departament de Dinàmica de la Terra i l'Oceà, Barcelona, Spain,
(4) Imperial College London, Department of Earth Science & Engineering, London, United Kingdom,
(5) Universitat de Barcelona, Departament de Dinàmica de la Terra i l'Oceà, Barcelona, Spain,
(6) Université de Rennes, Géosciences Rennes, Rennes, France,
(7) University of Lausanne, Institute of Earth Sciences, Lausanne, Switzerland

The Middle Eocene Climatic Optimum (MECO) is a global warming event that started at 40.5 Ma and lasted nearly 500 kyr. Unlike the previous hyperthermals such as the Paleocene- Eocene Thermal Maximum (PETM) where a distinct negative carbon isotopic peak is observed, the MECO only shows a negative shift of ~0.5‰ in δ13C. In parallel, however, the MECO is marked by a decrease of ~1.0‰ in oxygen isotope (δ18O) suggesting a rise in sea surface temperatures by 6ºC, and a widespread dissolution of deep-sea carbonates attributed to increased ocean acidification. The MECO has been identified and studied in oceanic sediments, however, data from continental sections is sparse but crucial to understand the MECO conundrum.

To provide narratives of the impact of MECO in the continental realm, we focus on the Escanilla sediment routing system in the south-central Pyrenees, Spain. The system consists of ca. 1000 m thick middle to upper Eocene deposits that grade from alluvial (Coll de Vent) to proximal fluvial (Lascuarre) and distal fluvial (Olson). We present here a multi-proxy approach involving paleohydraulic reconstructions from sandstone channel bodies and geochemical data from floodplain deposits, based on bulk rock and clay mineralogy, weathering indices, Mean Annual Precipitation (MAP) estimates and stable isotope analyses. Based on magnetostratigraphic age constraints, the warming peak of the MECO in the Escanilla system corresponds to a thick, sheet-like amalgamated conglomeratic body of basin-wide extent which we call the 'Olson sheet'. The Olson sheet and several other smaller scale laterally extensive sheet like channel bodies which overlie several meters of floodplain below form the base of our fining upward sequences. These are overlain by several isolated channel bodies until the base of our next sequence with each sequence having a thickness of at least 50–80 m.

Our paleohydraulic results depict the evolution of paleoslope, which is empirically related to grain size and flow depth estimates, in three fining-upward sequences. Our reconstructed alluvial / fluvial slopes are lower in the amalgamated intervals, whilst non-amalgamated intervals have higher slope values. Our paleoslope results thus suggest a link between the observed stratigraphic cyclicity and changes in upstream factors (sediment supply, water discharge and sediment calibre). We also make use of the compensation index and compensational stacking patterns to interpret the possible role of autogenic signals in our fluvial stratigraphic sequences. Our bulk rock and clay mineralogy results indicate a poorly developed floodplain with high silicious content. This is interpreted as high sedimentation rates resulting in poorly developed paleosoils. Mean Annual Precipitation rate estimates are in the range of 200 – 300 mm/yr with a peak of 650 mm/yr corresponding to the MECO warming peak. This most likely indicates ephemeral high discharge events with peak discharge occurring at the peak warming event. Based on this multi-proxy approach, we will thus discuss the temporal evolution of a fluvial system in response to a global warming event.

7.12
Seismic event stratigraphy of tectonic Lake Towuti, Sulawesi, Indonesia: a 60 kyrs record of seismo-turbidites

Nicolas Tournier[1], Hendrik Vogel[1,2], Stefano C. Fabbri[1,2], Flavio S. Anselmetti[1,2], James M. Russell[3], Satria Bijaksana[4], Sri Yudawati Cahyarini[5]

[1] Institute of Geological Sciences, University of Bern, CH-3012 Bern, Switzerland (nicolas.tournier@geo.unibe.ch)
[2] Institute of Geological Sciences and Oeschger Centre for Climate Change Research, University of Bern, CH-3012 Bern, Switzerland
[3] Department of Earth, Environmental, and Planetary Sciences, Brown University, Providence, RI 02912, USA
[4] Faculty of Mining and Petroleum Engineering, Institut Teknologi Bandung, Bandung 40132, Indonesia
[5] Indonesian Institute of Sciences (LIPI), Research Centre for Geotechnology, Sangkuriang, Bandung 40135, Indonesia

Located at the triple junction of the Pacific, Eurasian and Sunda plates, the Island of Sulawesi in Indonesia is one of the most tectonically active places on Earth. This is highlighted by the recurrence of devastating earthquakes, such as the 2018 Mw 7.5 earthquake that destroyed the city of Palu and caused several thousand fatalities. The majority of large-magnitude earthquakes in Sulawesi are related to stress release along major strike-slip faults, such as the Palu-Koro fault and its southern extensions, the Matano and Lawanopo faults. To date, information on the frequency and magnitude of major seismic events on these and associated faults is limited to instrumental records covering a time span of roughly 50 years, while information from historical sources and natural archives are completely lacking. Considering the increase in population density on Sulawesi and the extension of villages into remote areas, it is important to better quantify the seismic hazard and its associated risk on the island. Therefore, a systemic catalog of past earthquakes is essential for understanding the tectonic dynamics of the region.

Lake Towuti, located in East Sulawesi, is a key site to study the paleoseismology of the island. The lake is located 20 km north of the strike-slip Matano Fault and thus provides an ideal archive for past earthquakes that occurred in the surrounding area. In addition, the large and particularly deep basins of the lake allow for a temporally continuous sediment succession and preserve deposits related to seismic activity. We combine high-resolution Chirp seismic data with lithostratigraphic and petrophysical data of sediment piston cores to identify earthquake-triggered Mass Wasting Deposits (MWD) and to compile a co-seismic event stratigraphy. This will ultimately help to assess the recurrence of major earthquakes (Mw > 6) in the region. Three major seismo-stratigraphic units are identified in the upper 150 ms TWT (~60 m) of sedimentary infill. MWDs and associated seismoturbidites can be readily distinguished in the seismic data and are well preserved in the cored sedimentary successions of the uppermost Unit 1.1. Chronologically, Unit 1.1 covers the last ~15 kyr and allows the establishment of an event chronostratigraphy for the recent past of Lake Towuti. Underlying Unit 1.2, roughly comprising last glacial deposits of MIS 2, reveals frequent event deposits reaching vast volumes in some basins of the lake. This higher recurrence may on the one hand indicate stronger and/or more frequent activity of the surrounding faults, but may on the other hand indicate the influence of a dry MIS 2 lake-level lowstand, which impacts the sensitivity of the slopes to fail under seismic stress. Finally, Unit 1.3, comprising sediments deposited at higher lake-levels under wet interstadial MIS 3 climate conditions, appears similar to Unit 1.1 with less frequent MWDs, possibly indicative for extended periods of quiescence or an episode of reduced event recording sensitivity in Lake Towuti.

7.13
Evolution of the Atlantic meridional temperature gradient during the Paleogene: New insights from coccolith-derived temperatures

Maxime Tremblin*, Fabrice Minoletti**, Hermoso Michaël***, Delphine Desmares****

** Département des Sciences de la Terre, Université de Genève, 13 rue des Maraîchais, 1205 Genève, Suisse*
*** Institut des Sciences de la Terre de Paris, Sorbonne Université, 4 place Jussieu, 75005 Paris, France*
**** Laboratoire d'Océanologie et de Géosciences, Univ. Littoral Côte d'Opale, 32 avenue du Maréchal Foch, 62930 Wimereux, France*
***** Centre de recherche en paléontologie, MNHN, Sorbone Université, 4 place Jussieu, 75005 Paris, France*

The Paleogene represents the last period of extremely high temperatures and CO_2 levels of the Cenozoic and represents a possible analog for the climate settings and changes of the Anthropocene. Climate reconstructions of this greenhouse interval are thus essential to provide benchmarks to climate models and better understand future climate change. However, if many studies have focused on the sudden hyperthermal events that punctuated the climate history of the Eocene, the mechanisms that shifted the Earth's system from a greenhouse to an icehouse climate regime remain poorly constrained.

Two main contrasting hypotheses for the inferred long-term Eocene cooling are put forward: (1) change in circulation and meridional heat transport associated with the opening of ocean gateways, (2) a long-term decline in atmospheric CO_2 levels. During the warm Paleogene, significant uncertainties affect the reconstruction of sea surface temperature (SST), hampering accurate reconstruction of the meridional temperature gradient (MTG). This gradient reflects the processes associated with heat distribution on the planet's surface and, therefore, has significant implications for our understanding of the climate system under a greenhouse world. During the Eocene, the available low-resolution dataset shows a reduced latitudinal temperature gradient compared to present-day settings. However, despite improved model–proxy agreement in the terrestrial realm, climate models struggle to reproduce a putative low equator-to-pole gradient, even under high pCO_2 conditions.

In this study, we take advantage of the developments in the biogeochemistry of coccolithophores to exploit the isotopic signals of their calcite biominerals - the coccoliths - as a new source of paleoclimatic information. Coccoliths are produced in the mixed layer, and their good preservation even in warm and high pCO_2 settings may overcome methodological caveats associated with the absence or frequent recrystallization of foraminiferal shells.

Four latitudinally distributed sites across the Atlantic Ocean are investigated to generate new equator-to-poles SSTs throughout the Eocene.

Our new coccolith-derived SSTs evolutions indicate significantly warm SSTs during the early to middle Eocene, followed by significantly cooler temperatures immediately after the EOT and the entrenchment of permanent ices over Antarctica. The most striking feature of our dataset is that coccolith-derived SSTs record a strong asymmetry in the SSTs evolutions amongst the various study sites during the late Eocene and the EOT. Indeed, despite a progressive decline in the pCO_2 values, equatorial SSTs warm up while a significant cooling is recorded in the southern latitudes. This interval that predated the EOT is characterized by the progressive development of a stronger Atlantic MTG. This observation supports the hypothesis that ocean circulation changed played an essential role in the long-term Eocene climate change.

Furthermore, our results provide evidence for the existence of a relatively strong MTG in the Atlantic Ocean since the early Eocene ($\Delta SSTs > 19°C$). From a modeling perspective, this larger MTG than this derived from organic proxies is more in line with the modeled Eocene temperatures gradients. This new dataset may help to resolve the proxy-model discrepancy without invoking a "missing physics" in the models or fundamental changes in heat transport mechanisms. Altogether, these new data will contribute to the refinement of climate models and finally better constrain greenhouse climatic states that may prevail in the future.

7.14
Sea level and sediment supply in Taiwan during the early Pleistocene: a matter of precession

Romain Vaucher[1,2*], Shahin E. Dashtgard[2], Chorng-Shern Horng[3], Christian Zeeden[4], Antoine Dillinger[5], Yu-Yen Pan[6], Romy A. Setiaji[7], Wen-Rong Chi[8,9], Ludvig Löwemark[5]

[1]Institute of Earth Sciences (ISTE), University of Lausanne, Geopolis, CH-1015 Lausanne, Switzerland (romain.vaucher@unil.ch)
[2]Applied Research in Ichnology and Sedimentology (ARISE) Group, Department of Earth Sciences, Simon Fraser University, Burnaby, Canada
[3]Institute of Earth Sciences, Academia Sinica, Taipei, Taiwan
[4]LIAG – Leibniz Institute for Applied Geophysics, Geozentrum Hannover, Hannover, Germany
[5]School of Mining and Geosciences, Nazarbayev University, 53 Kabanbay Batyr Ave, Nur-Sultan, Kazakhstan
[6]Centre for Natural Hazards Research, Department of Earth Sciences, Simon Fraser University, Burnaby, Canada
[7]Department of Geosciences, National Taiwan University, Taipei, Taiwan
[8]Department of Earth Sciences, National Central University, Taoyuan, Taiwan
[9]Department of Earth Sciences, National Cheng-Kung University, Taïnan, Taiwan

Global marine archives from the early Pleistocene indicate that glacial-interglacial cycles, and their corresponding sea-level cycles, have predominantly a periodicity of ~41 kyrs driven by Earth's obliquity. Here, we present a clastic shallow-marine record from the early Pleistocene in Southeast Asia (Cholan Formation, Taiwan). The studied strata comprise stacked cyclic successions deposited in offshore to nearshore environments in the paleo-Taiwan Strait. The stratigraphy was compared to both a δ18O isotope record of benthic foraminifera and orbital parameters driving insolation at the time of deposition. Analyses indicate a strong correlation between depositional cycles and Northern Hemisphere summer insolation, which is precession-dominated with an obliquity component. Our results represent geological evidence of precession-dominated sea-level fluctuations during the early Pleistocene, independent of a global ice-volume proxy. Preservation of this signal is possible due to the high-accommodation creation and high-sedimentation rate in the basin enhancing the completeness of the stratigraphic record.

P 7.1
Revisiting the origin of the Carbonifeorus infill of Swiss post-Hercynian Throughs: Insights from the Weiach-1 borehole (northern Switzerland)

Andrea Moscariello[1], Dario Ventra[1], Martina Cervelli[1,2], Ovie Emmanuel Eruteya[1], Silvia Omodeo Salé[1], Yasin Makhloufi[1]

[1] GE-RGBA Group, Department of Earth Sciences, University of Geneva, Rue des Maraichers 32, CH-1201 Geneva (andrea.moscariello@unige.ch)
[2] Dipartimento di Geologia, Universta di Padova, Via G. Gradenigo n.6 - 35131- Padova, Italy

The Weiach-1 borehole (north-central Switzerland) provides a unique sedimentary and petrophysical record of the Carboniferous infill of one of the largest structural depression in the subsurface of the Swiss Plateau, thought to be formed during the post-Hercyinian tectonic extensional phase. The extensive high-quality core recovered from this borehole displays ~600 m of Carboniferous deposits, assigned to the Stephanian A to C time intervals (i.e. Pennsylvanian).

The examination of petrophysical data, consisting mostly of gamma ray, density, sonic, neutron and resistivity logs, is supported by the availability of the core, which can be interpreted as an alternation of conglomerates, sandstones, shales and coal-rich or organic-rich intervals. Sedimentologically the studied core interval is characterized by a persistent facies assemblage indicative of dominant deposition associated with a braided delta front prograding periodically into a relatively deep (below wave base) lacustrine environment. Dark-grey, locally organic-rich claystones and silty claystones are volumetrically prevalent. These are intercalated by two principal facies associations: 1) thin-bedded alternations of very fine to fine sandstones, representing turbiditic (possibly hyperpycnal) transfer of sediments to a distal setting, and 2) decimetric to metric associations of massive, plane-bedded or cross-bedded coarse to gravelly sandstones resting on erosional bases and frequently including muddy and peaty intraclastic debris, indicative of more energetic transport along shallow subaqueous distributary channels. The constant occurrence of diffuse soft-sediment deformation features (liquefaction structures, microfaults, homogenized beds), together with the frequent occurrence of tilted sedimentary intervals capped by erosional surfaces, suggest frequent instability associated with i) water-saturated sediment at the depositional interface, possibly triggered also by seismic events, ii) processes of gravitational instability possibly associated with sliding of subaqueous slopes.

The examination of 2D seismic data also suggests a strong discontinuity of reflectors and the occurrence of surfaces which can be interpreted as intraformational faults affecting the entire succession.

Overall these observations suggest: 1) a different depositional environment than previously envisaged (anastomosing fluvial systems); 2) a conceptual model which would indicate that a large part of the coals encountered in the succession might be reworked and resedimented in a sublacustrine environment; 3) a strong influence or syndepositional tectonics and deformation, probably related to active faults at the basin margin.

The revisited depositional model for the Carboniferous portion of the Weiach-1 well has important implications for the prediction of coal and sandstone distribution within the P-C throughs of central Switzerland, affecting the presence of potential hydrocarbon source rocks and reservoirs, respectively. Predicting these elements of possible petroleum systems in the region is the main objective of the UNCONGEO project*, as hydrocarbon occurrences represent a risk for deep geothermal exploration.

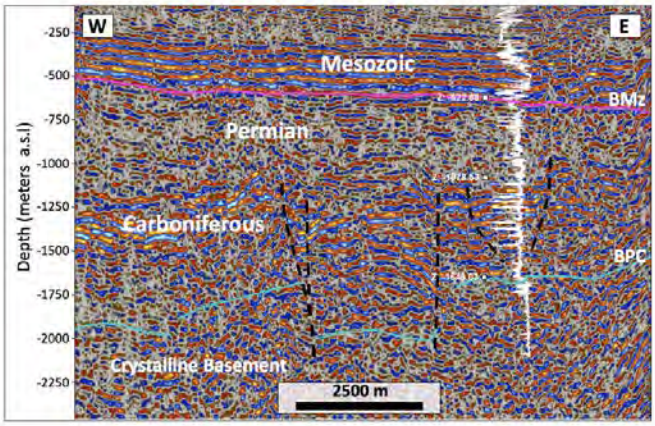

Figure 1. West-East 2D seismic data with indication of the Weiach well position displaying sonic log (seismic data kindly provided by NAGRA) and the depth below ground surface of key stratigraphc markers. BMz: Base Mesozoic; BPC: Base Permo-Carbonifeorus.

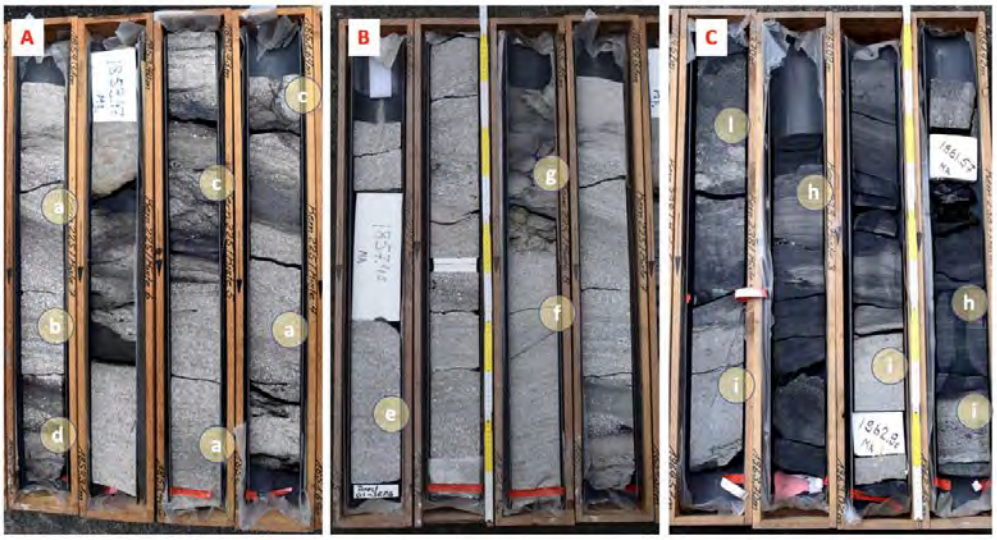

Figure 2: Examples of facies associations recorded in the Weiach-1 core in the Carboniferous section. **A**: assemblage of a) cross-laminated gravelly sandstone characterised by frequent b) dewatering, alternated to c) organic-rich slumps and d) diamicton generated by high-density flow; **B**) alternation of low-angle e) laminated sandstone and f) tilted unit characterised by lamination i.e. higher than the angle of repose and g) slumped heterolithic intervals; **C**) heterolithic assemblage of h) irregular finely horizontally laminated or massive mudstone alternated with i) dewatered organic-debris rich sandstone and l) diamicton. Each core box in 1 m long.

**The UNCONGEO project is funded by Swisstopo, the Federal Office of Energy, Canton of Geneva, Canton of Vaud and NAGRA*

P 7.2
Provenance of the Habkern Granite and the Wilfdflysch based on an integrated geo-thermochronologic approach

Florence Emanuelle Frund[1], Maria Giuditta Fellin[2], Vincenzo Picotti[1], Sean D. Willett[1]

[1] *Geologisches Institut, ETH Zurich, Rämistrasse 101, CH-8092 Zürich (frundf@ethz.ch)*
[2] *Institut für Geochemie und Petrologie, ETH Zurich, Rämistrasse 101, CH-8092 Zürich*

The Wildflysch and Habkern Granite outcrop locally in central Switzerland near Habkern. The Habkern Granite is characterized by yellowish to greenish quartz and it consists of blocks, up to tens of meters large, embedded in the Wildflysch. The provenance of the Habkern Granite and of the Wildflysch is unknown; in the Alpine basement rocks no example of Habkern Granite is found but boulders similar to the Habkern Granite are known in other Alpine clastic units that are both older (Basaler Schlieren Flysch, Gurnigel Flysch) and younger than the Widlflysch (Subalpine Flysch) (Bayer, 1982). The Wildflysch was deposited in the upper Lutetian to Priabonian (Bayer, 1982) in front of the Alpine accretionary wedge. It comprises turbiditic sandstones, conglomerates and broken formations with exotic blocks and sandstones lenses in deformed shales. Besides the Habkern Granite, the olistoliths in the Wildflysch include Campanian and Maastrichtian sandstones and limestones, Liassic limestones, Triassic dolomites and gypsum (Bayer, 1982; Paul, 1913). The Wildflysch is exposed next to large slabs of Schlieren Flysch (Maastrichtian-lower Eocene) and Leimern Leimstone (Upper Cretaceous). These blocks and the Wildflysch are laterally juxtaposed to the Lutetian-Priabonian marls and shales of the Stad Formation (Kuhn, 1972) with a poorly exposed contact that has been interpreted so far as tectonic. During the last 50 years, contrasting interpretations have been proposed for the depositional environment, paleogeographic position and tectonic history of Wildflysch. According to Bayer (1982), the Wildflysch is a tectonic melange, where the exotic blocks were included during thrusting within the Alpine accretionary wedge.Thus, Wildflysch, Leimern Formation and Schlierenflysch as exposed near Habkern were interpreted as a stack of multiple nappes.

We contribute to the long-standing debate about the Wildflysch and the Habkern Granite with new field observations and with double-dating analysis of detrital zircons. We aim at providing new constraints on the supplying source terranes of the Wildflysch basin and new insights into the tectono-stratigraphic relationships between the Wildflysch and the surrounding units. We dated with both the U-Pb and fission-track techniques the zircons from three samples, including: a piece of Habkern Granite, a glauconite-bearing turbiditic sandstone above a breccia bearing Habkern Granite boulders near Habkern and an upper Eocene sandstone exposed in Obersuld, southwest of Interlaken. These three samples show very different U-Pb age distributions, with major populations in the early Permian-Carboniferous and in the Ordovician, but very similar zircon-fission track age distributions, with the largest populations centered in the late Jurassic and a minor populations in the late Cretaceous. This indicates that the detrital zircons were sourced from different basement and/or detrital rocks that were affected by the same pre-alpine (Tethyan) and early alpine thermal overprints. The youngest zircon-fission track ages in the Wildflysch is 65 Ma old indicating that syn-to-post depositional burial conditions were low enough that they did not affect the fission-tracks in the detrital zircons. We find no evidence of a tectonic contact either between the Wildflysch and the Stad Formation or between the Wildflysch and the Schlieren Flysch and Leimern Limestones. Locally we find olistostromic shales and sandstones in between these units. Thus, we infer that the Habkern Granite blocks and the other olistoliths are recycled material from older units that entered the accretionary wedge earlier than the deposition of the Wildflysch and we interpret also the large slabs of Schlieren Flysch and Leimern Limestone near Habkern as olitstoliths embedded in the Wildflysch.

REFERENCES

Bayer, A. A. (1982). *Untersuchungen im Habkern-Melange ('Wildflysch') zwischen Aare und Rhein* [PhD Thesis, ETH Zurich]. https://doi.org/10.3929/ethz-a-001660103

Kuhn, J. a. (1972). Stratigraphisch-mikropaläontologische Untersuchungen in der Äusseren Einsiedler Schuppenzone und im Wägitaler Flysch E und W des Sihlsees (Kt. Schwyz). In *Eclogea Geologicae Helvetiae* (Vol. 65).

Paul, B. (1913). Definition der Niesen-Habkerndecke. *Eclogea Geologica Helvetiae*, *12*.

P 7.3
Evolution and morphology of a Late Cretaceous submarine channel system in the Kribi/Campo sub-basin, offshore Cameroon

Boris Gouott Secke Bekonga [1], Mbida Yem [1], Joseph Quentin Yene Atangana [1], Eric Pierre Nkoa Nkoa[2], Serge Edouard Angoua Biouele [2], Yakufu Niyazi[3], Ovie Emmanuel Eruteya[4]

[1] University of Yaoundé I, Faculty of Science, Department of Earth Sciences, P.O. Box: 812, Yaoundé, Cameroon (bsecke@yahoo.fr)
[2] National Hydrocarbon Corporation (NHC), P.O. Box: 955, Yaoundé, Cameroon
[3] School of Life and Environmental Sciences, Deakin University, Warrnambool 3280, Victoria, Australia
[4] GE-RGBA Group, Department of Earth Sciences, University of Geneva, Rue des Maraîchers 13, CH-1205 Geneva, Switzerland

Submarine channels are vital components of ancient and modern deep-water settings responsible for transporting sediments into the deep sea. In this study, we integrated a 3D seismic reflection data and well data to characterise the internal architecture and evolution of an ancient deep-water channel systems in the Kribi-Campo sub-basin, offshore Cameroon. Morphometric parameters such as thalweg depth (lowest point on a channel's base), thalweg gradient, channel width, and aspect ratio (width/depth) of the submarine channel system were measured at intervals of 1 km perpendicular to the channel pathways.

Our results show that the submarine channel system in the study area devolved in two stages. The main channel has a relatively straight morphology, and its width ranges from 3 to 5 km, and its depth varies from 89 to 197 m. However, the later stage channel is characterized by a narrower (1 to 3 km) and shallower (41 to 103 m) incision with sinuous morphology carved into the main channel. The entire channel system is divided into three windows with different gradients (i.e., "Segments x, y and z") according to the range of thalweg depth variations in profiles (Fig. 1). The submarine channel is mainly filled with fine-grained sediments in the later stage, and the main channel is dominated by coarse-grained sediments in the southwest of the channel and some fine-grained in the northeastern segment of the channel (Fig. 2).

The findings from this study demonstrates that decreasing slope gradient favours coarser-grained deposits primarily along the axis of the channel system, while a strong slope gradient leads to the deposition of fine-grained sediments. Additionally, sediment transport models indicate that grain size and grain-size distribution, as well as slope gradients, are key variables dictating the presence of good quality sand reservoirs. Systems with gentle slopes and relatively fine maximum grain sizes likely offer the highest potential for hydrocarbon discoveries. Such a thorough understanding of channel morphology is of great importance for facies prediction and efficient development of deep-water channel reservoirs, especially as hydrocarbon exploration transits into deeper waters.

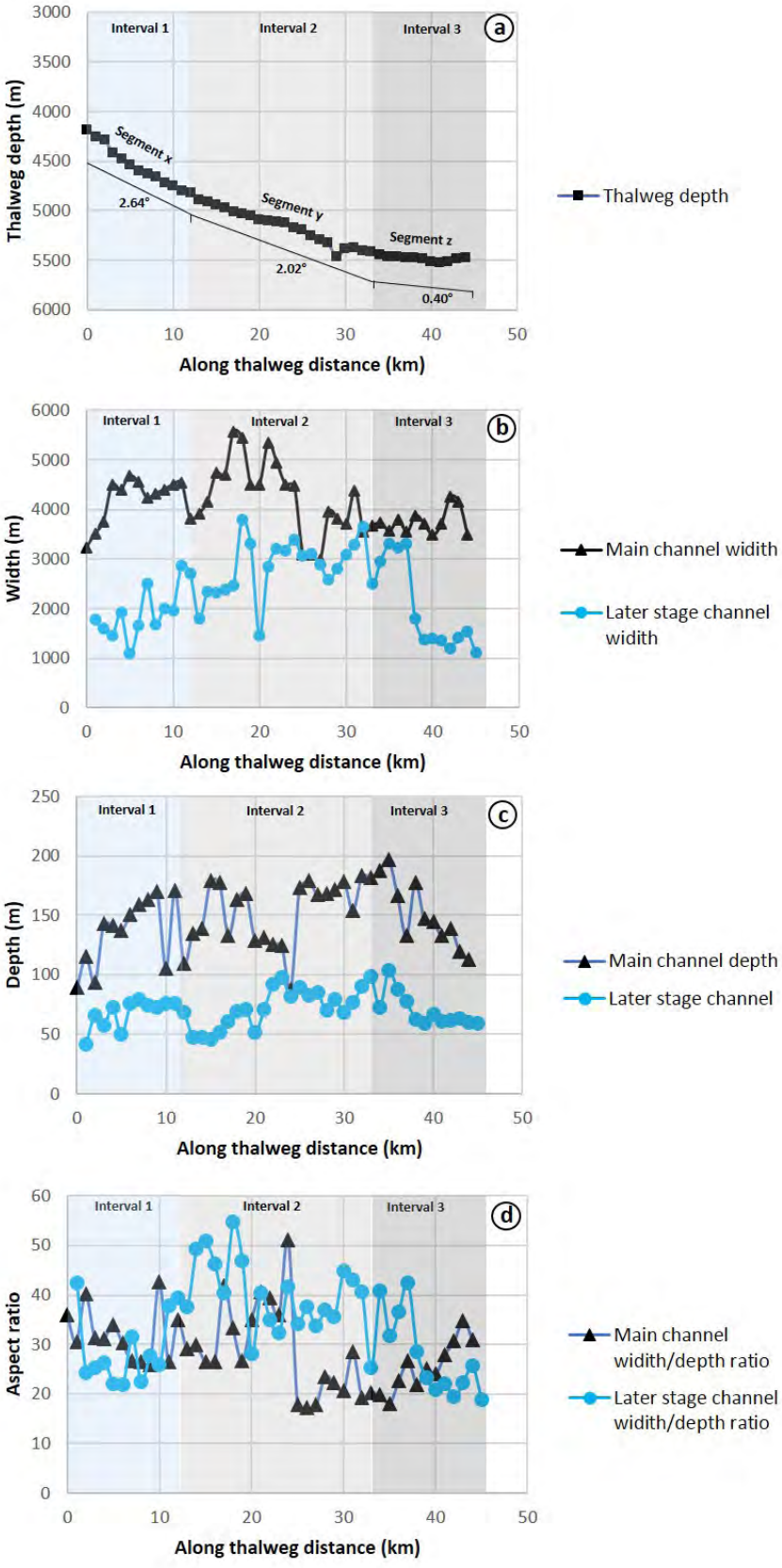

Figure 1: Quantitative analysis of the submarine channel system. a) Width of main channel and later stage channel. b) Main channel and later stage channel depth profile. c) Aspect ratio (width/depth) of the main channel and later stage channel. d) Depth profile of channel thalweg along the channel.

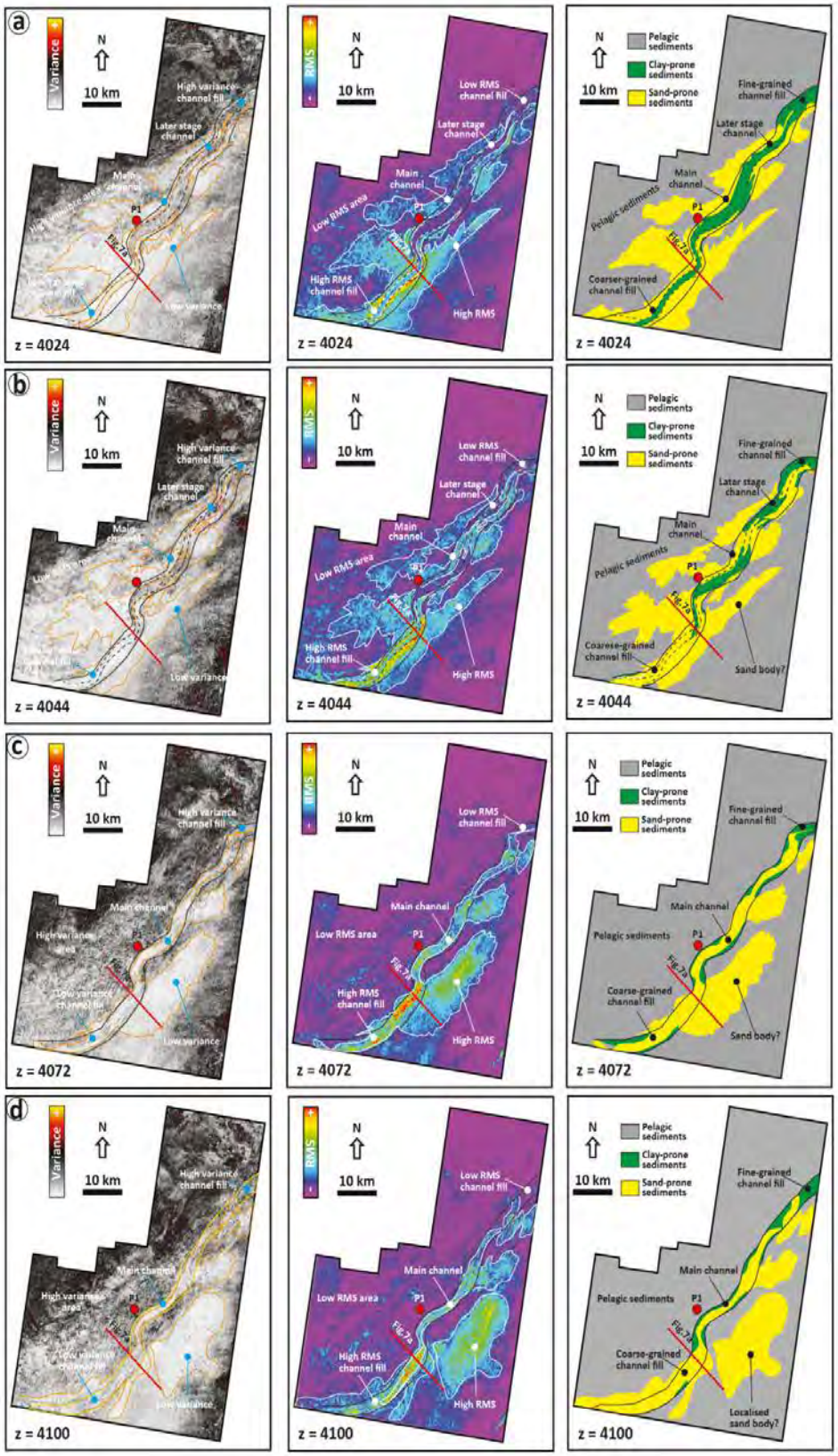

Figure 2: Variance and root mean square amplitude maps of the submarine channel time slices and their corresponding interpretations.

P 7.4
Impact of an abrupt climate change on sediment fluxes from source to sink: An example from the PETM in the Southern Pyrenees (Spain)

Marine Prieur [1], Alexander C. Whittaker [2], Fritz Schlunegger [3], Tor O. Sømme [4], Jean Braun [5], Sébastien Castelltort [1]

[1] *Université de Genève, Département des Sciences de la Terre, Rue des Maraîchers 13, 1213 Genève, Switzerland (marine.prieur@unige.ch)*
[2] *Imperial College, Department of Earth Science and Engineering, London, UK*
[3] *University of Bern, Institute of Geological Sciences, Baltzerstrasse 1+3, 3012 Bern, Switzerland*
[4] *EQUINOR Oslo, Martin Linges vei 33, 1364 Fornebu, Norway*
[5] *GFZ Helmholtz Centre, Wissenschaftpark „Albert Einstein“, Telegrafenberg, 14473 Potsdam, Germany*

Sedimentological processes are dependent on external conditions, namely climate and tectonics. While these forcings are constantly varying through time and space, the way sedimentary systems adapt to those variations depends on their intensity and time-scale. Today global warming occurs over a very short time-scale and therefore has to be approached as a “rapid” event. Studying the rock record provides insights on the consequences of a climate change on Earth surface processes. Because it is one of the fastest (170 kyrs) and most intense (5 to 8°C increase in temperature) event, the Paleocene-Eocene Thermal Maximum (PETM, 56 Myr ago) is one of the best examples that can be studied from the rock record.

Our study focuses on the Paleocene-Eocene boundary in the South-Pyrenean Foreland Basin (Spain), where excellent outcrops show the whole sedimentary system from continental to deep marine depositional areas. The PETM corresponds to an abrupt increase in siliciclastic deposits over the whole system. Here we present a description of the changes in transport processes through observations of the physical characteristics and architecture of the continental channels (flow type, channel dimensions and stacking). Grain-size data allow to discuss the evolution of sediment transport capacity. Provenance analyses based on petrography and U-Pb and (U-Th)/He double dating of detrital zircons are in progress in order to better characterise the continuity of the system down to the sink and to provide information about the source area evolution.

We propose both qualitative and quantitative estimations of the variations in sediment transport capacity under a rapidly changing climate. The study of the response of a whole source-to-sink system to an abrupt climate perturbation in deep time will provide a tangible perspective of possible future landscape change that may be expected with current global warming.

This research is carried out in the scope of the lead author’s PhD project and is part of the S2S-FUTURE European Marie Skłodowska-Curie ITN (Grant Agreement No 860383).

P 7.5
Chemical Weathering Intensity Linked with Extreme Global Warming During PETM, insights from the Southern Pyrenees, Spain

Jaimes-Gutierrez, Rocio[1]; Adatte, Thierry[2]; Puceat, Emmanuelle[3]; Braun, Jean[4]; Castelltort, Sebastien[1]

[1] Department of Earth Sciences, University of Geneva, Rue des Maraîchers 13, 1205, Geneva, Switzerland
[2] Institute of Earth Sciences, Géopolis, University of Lausanne, 1015 Lausanne, Switzerland
[3] Biogéosciences, UMR 6282, UBFC/CNRS, Université Bourgogne Franche-Comté, 6 boulevard Gabriel, F-21000 Dijon, France
[4] Helmholtz Center Potsdam, GFZ German Research Center for Geosciences Institute of Earth and Environmental Science, Universität Potsdam, Potsdam, Germany

The latest Paleocene and early Eocene were periods yielding multiple hyperthermal events. The most pronounced of them was the Paleocene-Eocene Thermal Maximum (PETM), which was characterized by an abrupt increase in global temperature (5–8 °C) over a short period (20 ka). A negative carbon isotope excursion marks the onset of the PETM, which reflects the fast injection of CO_2 into the ocean-atmosphere system, triggering global climatic changes. Geochemical, mineralogical, and sedimentological markers record the resulting increase in physical and chemical erosion. Chemical weathering of silicates is a sink of CO_2, that may have acted as a negative feedback mechanism, allowing for the recovery of the climate to pre-PETM conditions. In this project, we aim to quantify the intensity of chemical weathering of detrital material, as well as the lag time between the onset of the PETM and the chemical weathering response in a source-to-sink system. We focus on three sections located in the Spanish Pyrenees: Esplugafreda, Campo, and Zumaia corresponding to continental, transitional, and deep marine environments along the source-to-sink system, respectively. We will utilize clay minerals as climate-sensitive proxies, using oxygen and hydrogen stable isotopes as indicators of paleo-precipitation, temperature, and elevation of the catchment areas. Further, we will combine Lu-Hf and Sm-Nd isotopes in the clay-sized fraction to track chemical weathering intensity. Unlike other weathering proxies, this approach may provide important insights into the pedogenetic processes prevailing in the floodplains and the transported signal to the basin. This method will help us constrain the weathering regime and its response time relative to the onset and the body of the PETM. This topic is of relevance, as the PETM and its sedimentological and geochemical response may serve as a natural analog for the current climatic change. The results obtained in this project will serve to test numerical models of landscape evolution incorporating the chemical weathering response to climatic changes. The project has received funding from the European Union's Horizon 2020 research and innovation program under the Marie Sklodowska-Curie Grant Agreement No 860383.

P 7.6
Trace fossils in Paleocene-Lower Eocene deep-sea sediments of the eastern segment of the Achara-Trialeti Fold-Thrust Belt

N. Kobakhidze[1], Z. Lebanidze[2], T. Beridze[1], D. Makadze[4], A. Uchman[5], R. Chagelishvili[3], K. Lobzhanidze[1], S. Khutsishvili[1], K. Koiava[2], N. Khundadze[4]

[1]Al. Janelidze Institute of Geology, Tbilisi State University, Tbilisi, Georgia
[2]Department of Geology, Faculty of Exact and Natural Sciences, Tbilisi State University, Tbilisi, Georgia
[3]Department of Geology and Paleontology, Georgian National Museum, Tbilisi, Georgia
[4]Alexander Tvalchrelidze Caucasian Institute of Mineral Resources, Tbilisi State University, Tbilisi, Georgia
[5]Institute of Geological Sciences, Jagiellonian University, Kraków, Poland

The Achara-Trialeti Fold-Thrust Belt (ATFTB) is located in the northernmost part of the Lesser Caucasus and is associated with the Arabian and Eurasian plate convergence. Deposits constituting the ATFTB accumulated in the Achara-Trialeti Trough (rift), which was formed within the Transcaucasian Massif (island arc) during Late Cretaceous–Eocene times (Adamia et al., 2010).

The Paleocene-Lower Eocene flysch deposits (”Borjomi Suite” or ”Borjomi Flysch”) are traced as a latitudinal zone/belt in the central and eastern segments of the ATFTB. In the eastern segment the “Borjomi Flysch” is 900–1000 m thick and is represented by alternations of calcareous sandstones, marls and mudstones. Sandstone beds are grouped into 30–50 m thick packages.

According to previous investigations, Trace fossils were found on the southern far reach of the village Kvemo Nichbisi, in 50 m-thick package of thin- and rarely medium-bedded, fine- to medium-grained sandstones at the base of the Borjomi Suite. The rich ichno assemblage belongs to the *Paleodictyon* ichnosubfacies of the deep-sea *Nereites* ichnofacies, which is typical of thin-bedded sandy turbidites deposited in various parts of the depositional system (Lebanidze et al., 2017).

During the 2021 fieldwork, two new sections containing of trace fossils have been investigated in the eastern segment of the ATFTB at the same stratigraphic level (the base of the Borjomi Suite). The first section is located north of the village Zaridzeebi, on the right bank of the river Satovle and adjacent slope. The second section is located SW of the village Dzegvi, on the left bank of the river Darbazula and adjacent slope.

In the first section, the Paleocene conformably lies over Danian varicolored marls and limestones and is represented by the packages formed by alternation of very thin bedded and medium bedded sandstones with thin intercalations of mudstones. The trace fossils assemblage here consists of *Chondrites intricatus* (Brongniart), *Ch. targionii* (Brongniart), *Cochlichnus isp., Gyrophyllites multiradiatus* Heer, *Helminthopsis* isp., *Megagrapton irregulare* Ksi□żkiewicz, *Megagrapton isp., Ophiomorpha annulata* (Ksi□żkiewicz), *O. rudis* (Ksi□żkiewicz), *Paleodictyon italicum* Vialov & Golev, *P. hexagonum* (van der Marck), *P. minimum (Sacco), Planolites* isp., *Protopaleodictyon incompositum* Ksi□żkiewicz, *Scolicia strozzii* (Savi & Meneghini), *S. isp.,* and *Zoophycos isp.*

In the second section, the Borjomi suite lies over Maastrichtian limestones and marls with angular unconformity and is composed of grey calcareous siltstones and mudstones intercalated with thin bedded, fine-grained calcareous sandstones. These deposits contain trace fossils: *Chondrites intricatus* (Brongniart), *Ch. targionii* (Brongniart), *Halopoa imbricata, Helicodromites* isp., *Nereites irregularis* (Schafhäutl), *Ophiomorpha annulata* (Ksi□żkiewicz), *O. rudis* (Ksi□żkiewicz), *Planolites* isp., *Scolicia isp*. and *Zoophycos isp.*
Trace fossils from all three sections belong to the deep-sea *Nereites* ichnofacies. The assemblage from Darbazula represents the *Nereites* ichnosubfacies, which is typical of mud-rich distal turbidites. Abundance of graphoglyptids identified in Kvemo Nichbisi and Satovle points to the *Paleodictyon* ichnosubfacies, which is typical of thin-bedded sandy turbidites (Uchman & Wetzel 2012).

Apparently, the Darbazula turbidites are related to the distal part of a deep-sea turbiditic depositional system (outer fan), while Kvemo Nichbisi and Satovle turbidites - to the deep-sea fan environments, such as the channel margin, depositional lobe or fan fringe.
Finally, it should be assumed that Paleocene-Lower Eocene deposits of the eastern segment represent the deep-marine turbiditic sedimentation in the Achara-Trialeti rift basin.

This works was supported by Shota Rustaveli National Science Foundation of Georgia (SRNSFG) [Grant number FR-18-3765 – Ichnology and Sedimentology of the Paleocene–Lower Eocene Sediments in the Achara-Trialeti Fold-and-Thrust Belt, Georgia].

REFERENCES:

Adamia Sh., Alania V., Chabukiani A., Chichua G., Enukidze O., Sadradze N. 2010: Evolution of the Late Cenozoic basins of Georgia (SW Caucasus): a review. Geological Society of London, Special Publication no. 340, 239–259.

Lebanidze Z., Beridze T., Koiava K., Khutsishili S., Chagelishvili R., Khundadze N. 2017: Trace fossils from deep sea sediments of the Palaeocene-Lower Eocene Borjomi Suite Exposed in the Eastern Part of the Achara-Trialeti Fold-Thrust Belt, Georgia. 15th Swiss Geoscience Meeting, on-line abstract volumes (https://geoscience-meeting.ch/sgm2017)

Uchman, A. & Wetzel, A. 2012: Deep-sea fans. In: Bromley, R. G. & Knaust, D. (Eds.), Trace Fossils as Indicators of Sedimentary Environments. *Developments in Sedimentology* 64, 643–671. Elsevier, Amsterdam.

P 7.7
The trace fossil *Polykampton georgianum* horizon in the Paleocene deposits of the Achara-Trialeti fold-and-thrust belt (Georgia)

Zurab Lebanidze*, Alfred Uchman**, Tamar Beridze***, Nino Kobakhidze***, Koba Lobzhanidze***, Sophio Khutsishvili***, Rusudan Chagelishvili****, Davit Makadze*****, Kakha Koiava*, Nino Khundadze*****

** Department of Geology, Faculty of Exact and Natural Sciences, Iv. Javakhishvili Tbilisi State University, University str. 13, Tbilisi, 0186, Georgia*
***Jagiellonian University, Faculty of Geography and Geology, Institute of Geological Sciences, Gronostajowa 3a, Kraków PL-30-387, Poland.*
****Alexander Janelidze Institute of Geology, Iv. Javakhishvili Tbilisi State University, Politkovskaia 31, Tbilisi 0186, Georgia*
*****Department of Geology and Paleontology, Georgian National Museum, Purtseladze str. 3, Tbilisi 0105, Georgia*
******Alexander Tvalchrelidze Caucasian Institute of Mineral Resources, Tbilisi State University, Mindeli str. 12, Tbilisi 0186, Georgia*

The present study focuses on the results of integrated ichnological-sedimentological analysis of the Paleocene-Lower Eocene strata in the central part of the Achara-Trialeti Fold-and-Thrust Belt undertaken in 2019–2020. The extensional (rift) Achara-Trialeti Basin was formed in the Late Cretaceous–Paleocene–Eocene within the Transcaucasian Massif (island-arc system). The central part of the Achara-Trialeti Fold-and-Thrust Belt is the typical locality for the Paleocene-Lower Eocene Borjomi Flysch/Borjomi Suite. The Borjomi Suite is subdivided into the Tusrebi, the Boshuri and the Bolevani subsuites. According to its lithofacies architecture, the Paleocene (Thanetian) Tusrebi Subsuite consists of three lithofacies units: lower shaly, middle sand-rich and upper shaly units. The volcanogenic-sedimentary Boshuri and the shaly Bolevani subsuites are dated to the Lower Eocene (Ypresian) (Adamia et al.,2010, Mrevlishvili N., 2003).

In 2019, the trace fossil *Polykampton georgianum* (new ichnospecies) was discovered in the section Ardagani 1 on the steep, southern flank of the Borjomi Anticline (environs of Ardagani settlement, Borjomi region, along the Borjomi-Bakuriani motorway, the left bank of the river Gujareti). It occurs abundantly in the uppermost part of lower shaly unit of Tusrebi Subsuite. The trace fossil is composed of a median tunnel and side lobes that are filled with material differing from the host sediment. It is interpreted as a sequestrichnion, wherein the tracemaker stored organic-rich mud in the lobes as a food resource for times of food deficiency. The recent ferruginization of the median tunnel resulting from the former presence of pyrite suggests strong chemical gradient between lumen of the median tunnel and the surrounding. Chemichnial behaviour is not excluded as nutritional strategy of the worm-like tracemaker (a polychaete?). It occupies a middle tier and is commonly crosscut by *Trichichnus, Chondrites* and *Scolicia.* Rare or absent other trace fossils typical of deep-sea fine-grained deposits suggest slight dysoxia. The trace fossil assemblage is atypical, but in general it resembles the *Nereites* ichnosubfacies of the *Nereites* ichnofacies, which characterizes distal parts of the turbiditic depositional systems.
During the fieldwork undertaken in 2020, several occurrences of the trace fossils with predominance of *Polykampton georgianum* were identified at the same stratigraphic levels in the central part of the Achara-Trialeti Fold-and-Thrust Belt. These are: the river Kvabiskhevi gorge (15 km west of Ardagani I section), and environs of villages Mukhileti and Gagluantubani (accordingly 30 and 40 km east of the Ardagani I section). All the three localities show atypical trace fossil assemblages, but in general they resemble the *Nereites* ichnosubfacies of the *Nereites* ichnofacies.
In addition, on the left bank of the river Gujareti, stratigraphically 500 m below the Ardagani I section, a specimen of *Polykampton georgianum* has been found. Apparently, this is the level where the producer of *Polykampton georgianum* occurred for the first time, reached its peak in the end of the deposition of the lower shaly unit of the Tusrebi Subsuite and spread from this place in the remaining parts of the Achara-Trialeti Fold-and-Thrust Belt territory.
Based on the abovementioned we suggest to define the *Polykampton georgianum* horizon in the uppermost part of lower shaly unit of Tusrebi Subsuite, central Achara-Trialeti fold-and-thrust belt. This horizon is of great importance for the regional stratigraphy (Uchman et al., 2020).
This works was supported by Shota Rustaveli National Science Foundation of Georgia (SRNSFG) [Grant number FR-18-3765 – Ichnology and Sedimentology of the Paleocene–Lower Eocene Sediments in the Achara-Trialeti Fold-and-Thrust Belt, Georgia].

REFERENCES

Adamia Sh., Alania V., Chabukiani A., Chichua G., Enukidze O., Sadradze N. (2010) Evolution of the Late Cenozoic basins of Georgia (SW Caucasus): a review. Geological Society of London, Special Publication no. 340, 239–259.

Mrevlishvili, N., 2003. Regional correlative stratigraphic scheme of Paleogene of the north-western part of the Minor Caucasus. Proc. I. Javakhishvili Tbilisi State Univ. 355, 49–62 (In Russian.).

Uchman A., Lebanidze Z., Beridze T., Kobakhidze N., Lobzhanidze K., Khutsishvili S., Chagelishvili R., Makadze D., Koiava K., Khundadze N. (2020) Abundant trace fossil Polykampton in Palaeogene deep-sea flysch deposits of the Lesser Caucasus in Georgia: Palaeoecological and palaeoenvironmental implications. Palaeogeography, Palaeoclimatology, Palaeoecology, 558, 09958.

P 7.8
The Study of Main Lithofacies Types of Bertakari Low-Sulphidation Epithermal Deposit (Bolnisi Ore Field, Southern Georgia)

Davit Maqadze [1], Samuel Rice[3], Mirian Maqadze [1], Nino Kobakhidze[2]

[1] *Caucasian Al. Tvalchrelidze Institute of Mineral Recourses of Tbilisi State University, Tbilisi, 12, Mindeli Str. (Maqadze9292@gmail.com)*
[2] *Al. Janelidze Institute of Geology of Tbilisi State University, Tbilisi, 12, Politkovskaia Str*
[3] *Geology, Independent Consulting Geologist and Director, SR, Geoscience limited,Glasgow, United Kingdom*

The Study area (Bertakari low-sulfidation epithermal deposit) is located in Bolnisi ore field in southern Georgia which is part of the globally significant Tethyan-Eurasian Metallogenic Belt.

The Bolnisi ore field is well known for the existence of both Kuroko-type volcanogenic massive sulphide and volcanogenic epithermal ore deposits primarily associated with hydrothermal processes. There is a large variation in the style of epithermal deposits, including the associated alteration minerals, that is related to tectonic setting, magmatic affiliation, lithologic and structural features, and other potential variables.

The Bertakari deposit are host by Upper Cretaceous Gasandami suite which in the Bertakari area is subdivided into two - the lower Gasandami and upper Gasandami subsuites (Adamia et all. 2012). Gold-base metals mineralization within the lower Gasandami subsuite is related to pervasively hydrothermally altered rocks – hydrothermal breccias (Sillitoe, R, 1985) The upper Gasandami subsuite postdates mineralization and does not contain any of significance ore occurenses. It is introduced by volcanogenic, magmatic and normal marine rocks (Adamia et all. 2012).

The lower subsuite of the Gasandami suite, (K2gn1) is constituted by the altered rocks with diverse textures, chemical and mineralogical compositions and mechanic properties mainly formed after ryolite-dacitic lavas, volcaniclastic and extrusives rocks. The upper Gasandami subsuite breccia-conglomarates are affected by quartz-sericite, adularia, argillic phyllic and propylitic alteration (Fig.1).

As above mentioned, the Bertakari deposite is hosted by Gasandami felsic formation. The clear tendency is that mineralization here is related to phreatic, phreatomagmatic and hydrothermal breccias along with rhyolite and rhyodacite domes. Depositional environment of Upper Cretaceous volcanic formations varies from shallow-marine to subaerial settings. Major lithofaces type of Bertakari deposite are Polymict breccia-conglomerate, Volcaniclastic turbidities, Pumice tuffs and ignimbrites, Pumice breccias, Volcaniclastic breccias and Hydrothermal breccias (Sadradze et all. 2017).

The work was supported by Shota Rustaveli National Science Foundation of Georgia (PHDF-18-630 – Bertakari and Bneli-Khevi Low sulphidation Epithermal Gold Deposits: Geological Setting, Structure, Petrology and Peculiarities of Gold Forming Processes)

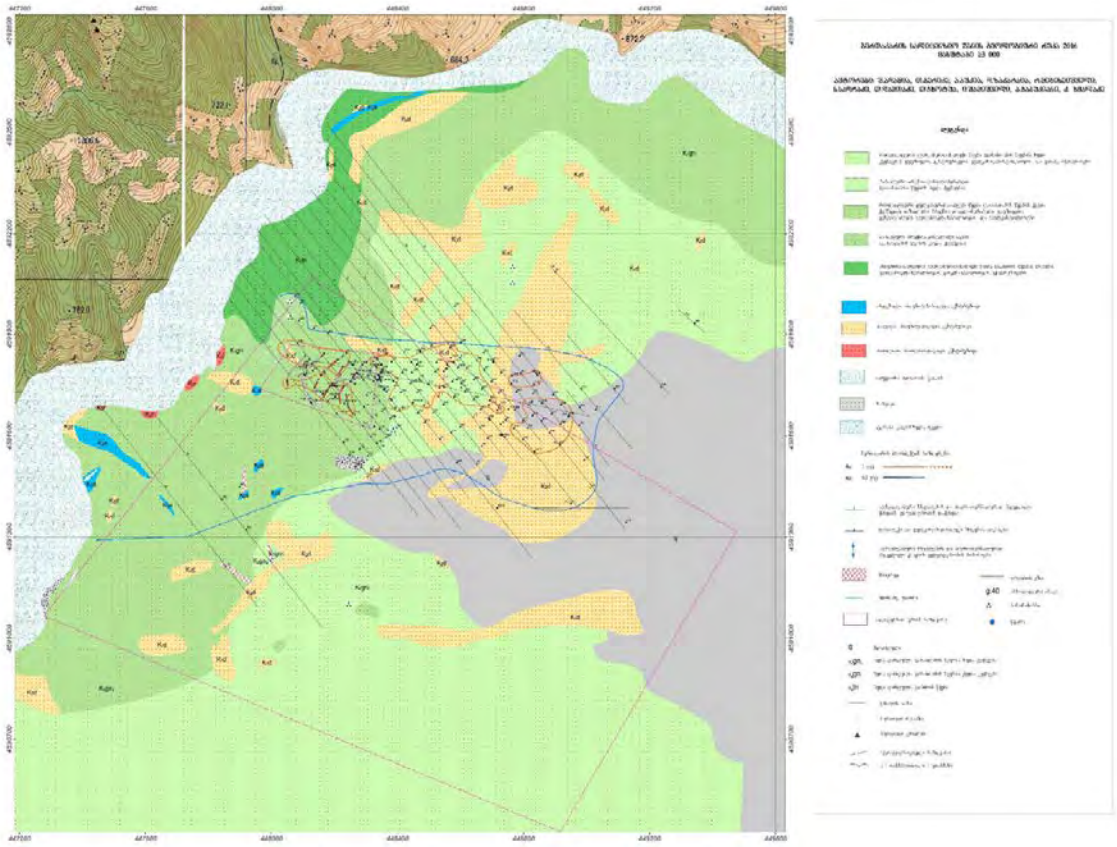

Figure.1. 1:2000 Scale Geological Map of Bertakari Deposit Area (CMG Funds)

REFERENCES

Adamia Sh, Bukia A, Gelasvili N, Goderdzishvili N, Zaqaraia D, Zaqariadze G, Migineishvili R, Muladze I, Sadradze N, Gavtadze T, Chkhotua T, Shavishvili I, Chabukiani A, Javaxidze D. (2012) The geology and structure of Bertakari area of the Bolnisi ore field. Explanatory note on 1:2000 and 1:4000 geological map and cross-sections of Bertakari area. Tbilisi. [in Georgian]

Sillitoe, R. 1985. Ore-related breccias in volcanoplutonic arcs. Economic Geology, vol. 80, p. 1467-1514

Sadradze N., Adamia Sh., Beridze T., Gavtadze T., Migineishvili R. (2017) Magmatism and ore formation on the example of Upper Cretaceous Bertakari and Bneli Khevi Ore deposits, Bolnisi ore district, Georgia Final Workshop of IRG South Caucasus Geosciences

08. Seismic Hazard and Risk in Switzerland: From Science to Mitigation

Donat Fäh, Katrin Beyer, Blaise Duvernay

TALKS:

8.1 Bergamo P., Janusz P., Panzera F., Perron V., Imtiaz A., Fäh D.: National and local site amplification models from the Earthquake Risk Model for Switzerland project

8.2 Glueer F., Fäh D., Mreyen A.-S., Cauchie L., Havenith H.-B.: Comparison of the seismic response of different compartments within the very slow-moving Heinzenberg Landslide, Switzerland

8.3 Imtiaz A., Panzera F., Hallo M., Dresmann H., Steiner B., Fäh D.: Application of multizonal transdimensional Bayesian inversion method for developing a 3D geophysical model in Basel, Switzerland

8.4 Janusz P., Perron V., Knellwolf C., Imperatori W., Bonilla L.F., Fäh D.: The currect state of the local site amplification model for the city of Lucerne

8.5 Reuland Y., Bodenmann L., Martakis P., Stojadinovic B., Chatzi E.: Improving early post-earthquake regional damage assessment in Switzerland

POSTERS:

P 8.1 Hallo M., Bergamo P., Fäh D.: Depth-to-surface ground motion amplification as revealed by our stochastic model and empirical data from Japanese KiK-net stations

P 8.2 Häusler M., Gischig V., Thöny R., Glueer F., Fäh D.: The dynamic response of the Brienz/Brinzauls rock slope instability

P 8.3 Lontsi A.M., Shynkarenko A., Hobiger M., Bergamo P., Kremer K., Fäh D.: Full microtremor horizontal-to-vertical spectral ratio inversion for the characterization of Swiss borehole and OBS sedimentary sites

P 8.4 Panzera F., Bergamo P., Chieppa D., Danciu L., Hallo M., Imperatori W., Fäh D.: Design-compatible waveforms for Switzerland: preliminary results

P 8.5 Toledo T., Kraft T., Simon V., Herrmann M., Villiger L., Antunes V., Diehl T.: The QuakeMatch Toolbox: the swiss-army-knife approach to a nearly automatic analysis for microearthquake sequences

8.1
National and local site amplification models from the Earthquake Risk Model for Switzerland project

Paolo Bergamo[1], Paulina Janusz[1], Francesco Panzera[1], Vincent Perron[1], Afifa Imtiaz[1], Donat Fäh[1]

[1] *Swiss Seismological Service (SED) at ETH Zurich, Sonneggstrasse 5, CH-8092 Zürich (paolo.bergamo@sed.ethz.ch)*

The “Earthquake Risk Model for Switzerland” (ERM-CH) project aims at delivering a complete assessment of the seismic risk for the Swiss territory (http://www.seismo.ethz.ch/en/research-and-teaching/ongoing-projects/). A key component of the project is the site response module, which has been developed in previous years working at different scales and resolutions: the national level model is accompanied by several regional and local level studies achieving a higher resolution and precision, allowing a verification of the coarser national model. The first national amplification model developed within ERM-CH has been delivered in 2020, and it consists of three macroseismic aggravation maps to be plugged in the risk model workflow (Bergamo et al. 2020). As intermediate products, a series of maps representing the site amplification at T=2, 1, 0.4, 0.35, 0.3, 0.25 and 0.2 s have been prepared (Fig. 1). These maps have been obtained combining geophysical measurements of the soil properties, earthquake site amplification measured at instrumented sites (Fig.1a), and a bespoke lithological classification of Switzerland (Fig.1b). Observed trends of amplification *vs* morphology or geological data for each lithotype (e.g. Fig. 1c) were extrapolated to the national territory (e.g. Fig. 1d).

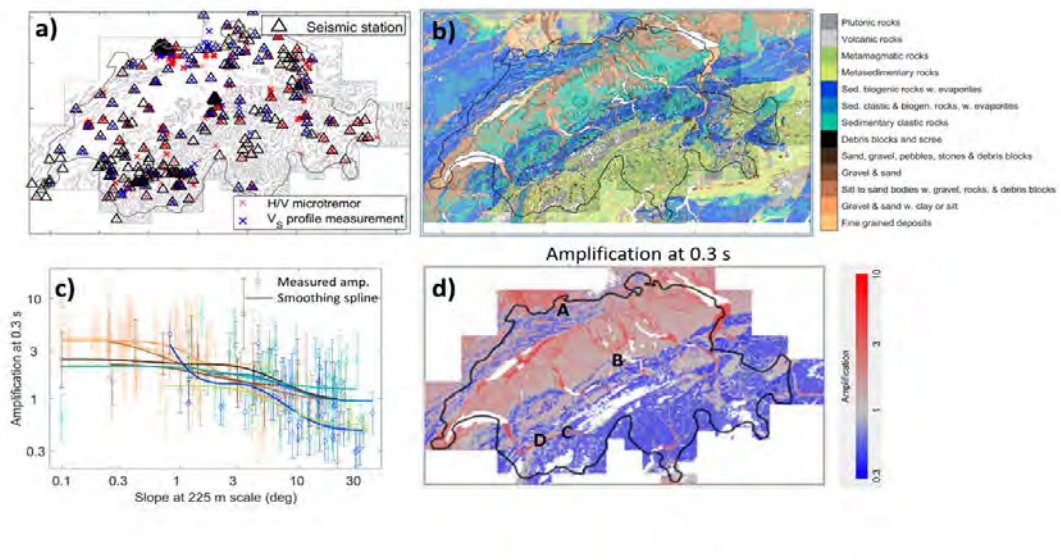

Figure 1. National site-amplification model. a) geophysical data; b) geological classification; c) derived site-amplification (at 0.3 s) *vs* slope relations (color code is the same as in (b)); d) obtained national amplification map at 0.3 s and location of local models: A=Basel, B=Lucerne, C=Visp, D=Sion.

In parallel, local models have been recently developed for the areas of Sion (Perron et al., 2020), Lucerne (Janusz et al. 2021), and Visp (Panzera et al. 2020) from dedicated regional datasets and with the application of different refined techniques, such as the canonical correlation between microtremor and earthquake response (Panzera et al., 2021) and the hybrid site-to-reference spectral ratio (Perron 2017). As validation of the national model, we have systematically compared it with the local amplification maps (e.g. Fig. 2). In the comparison, we have also included the site response model for Basel of Michel et al. (2017). On the whole, the collation national *vs* local amplification layers has evidenced a satisfactory agreement, particularly for the lithotypes hosting a wide number of seismic stations (e.g. alluvial deposits). Discrepancies mostly relate to *i)* lithotypes whose representation in the national model is constrained by few stations (e.g. fine-grained lacustrine deposits); and to *ii)* the local inaccuracy of the lithological map employed for the national model, based on the large-scale (1:500000) Swiss geological map GK500.

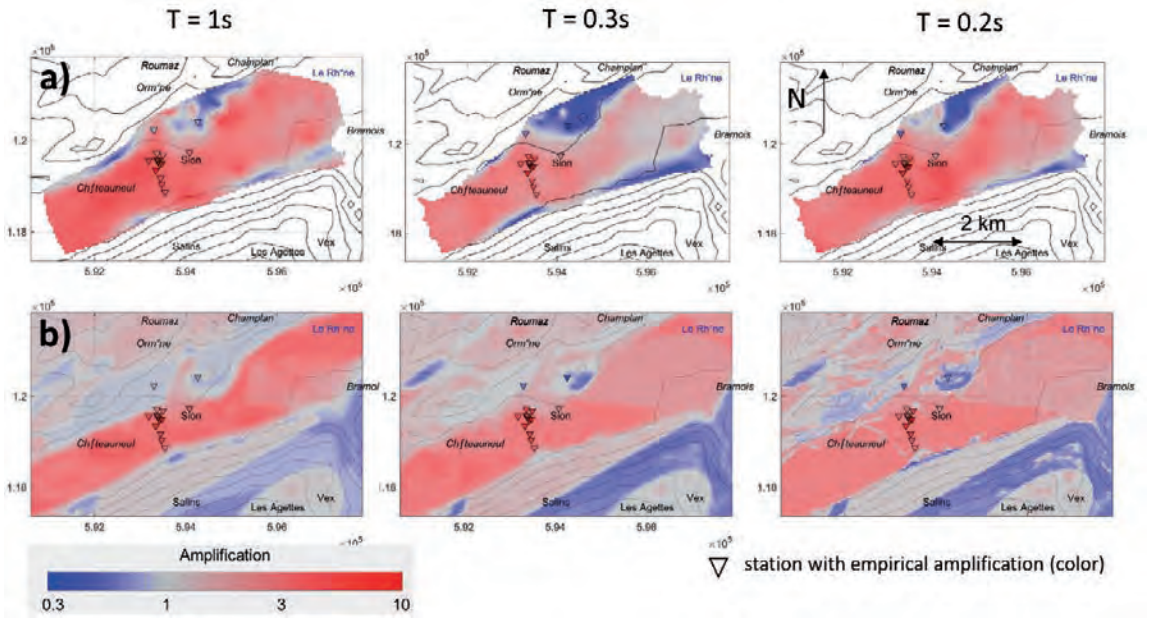

Figure 2. Example of comparison between a) a local amplification model (Sion, Perron et al 2020), and b) national amplification model for the same area.

REFERENCES

Bergamo et al. 2020. Progress in the compilation of multi-frequency seismic site amplification maps for the Earthquake Risk Model Switzerland project, 18th Swiss Geoscience Meeting 2020.

Janusz et al. 2021. Combining recordings of earthquake ground-motion and ambient vibration analysis to estimate site response variability in the city of Lucerne, Switzerland, EGU General Assembly 2021 EGU21-4380

Michel et al. 2017. Probabilistic mechanics-based loss scenarios for school buildings in Basel (Switzerland), BEE 15:1471–1496

Panzera et al. 2021. Canonical Correlation Analysis Based on Site-Response Proxies to Predict Site-Specific Amplification Functions in Switzerland, BSSA 111 (4): 1905–1920

Panzera et al. 2020. Reconstruction of site amplification functions through canonical correlation with site proxies, 18th Swiss Geoscience Meeting 2020.

Perron et al. 2020. Empirical earthquake's site response assessment in the Sion area, Switzerland, 18th Swiss Geoscience Meeting 2020.

Perron 2017. Apport des enregistrements de séismes et de bruit de fond pour l'évaluation site-spécifique de l'aléa sismique en zone de sismicité faible à modérée. PhD thesis, Université Grenoble Alpes.

8.2
Comparison of the seismic response of different compartments within the very slow-moving Heinzenberg Landslide, Switzerland

Franziska Glueer[1], Donat Fäh[1], Anne-Sophie Mreyen[2], Lena Cauchie[2], Hans-Balder Havenith[2]

[1] *SED - Schweizerischer Erdbebendienst, ETH Zürich, Sonneggstr. 5, CH-8092 Zürich (franziska.glueer@sed.ethz.ch)*
[2] *Geologisches Institut, Universität Liège, B-4000 Sart Tilman, Liège*

For more than 200 years, Heinzenberg (GR) has been known as an active moving landslide, causing also damage to buildings. Geodetic surveys from 1910-1931 show movements up to 0.25 m/a for this period (Jäckli 1948). A set of mitigation measures (drainage of the lake Lüschersee, torrent control) have slowed down movements to 0.04 m/a as proved by the long-term time series of geodetic displacement measurements (1927-2017) (Osten et al. 2020). A potential re-flooding of the lake Lüschersee with an economic (snowmaking system), scenic and biological value (Naturpark Beverin Geschäftsstelle 2019), has drawn recent attention on the Heinzenberg Landslide. Reactivation of the landslide movements might be expected, increasing as well the potential for earthquake-triggering of a mass movement.

In 2019, we conducted a large experiment to characterize the seismic response of different slope areas. These measurements serve as a baseline to map future changes in the ground water table and the associated changes in the seismic response. We used two sets of instruments for the acquisition of ambient vibration data and one set for seismic refraction and electrical resistivity measurements. For the ambient vibration experiments, 21 identical three-components portable seismometers with an eigenperiod of 5s and lower cut-off frequency of 0.2 Hz (Lennartz Le-3D/5s) with Centaur digitizers (Nanometrics) and seven seismometers GURALP (CMG-6TD) with a lower cut-off frequency of 0.033 Hz were used. For the seismic refraction tomographic profiles (SRT), 48 4.5 Hz geophones were connected to two 16-bit 24 channel seismographs (DAQLinkII). Sledgehammer impacts on a metal plate provided the required seismic energy.

We now represent the results from the ambient vibration and the active seismic measurements at five different locations around the Heinzenberg Landslide in the area around Lüschersee and Bischolapass. The configurations and locations are shown in Figure 1. We applied polarization analysis (Burjanek et al. 2012; Burjanek et al. 2014), site to reference spectral ratios (SRSR; e.g. Kleinbrod et al. 2017; Perron et al. 2018), surface wave analysis methods using three component high resolution beamforming techniques (e.g. Poggi and Fäh 2010; Hobiger et al. 2021; Kleinbrod et al. 2019) as well as MASW techniques (e.g. Socco and Strobbia 2004). The results show that ambient vibration analysis compare well to the active seismic methods at Lüschersee and Bischolapass. Several geophysical sections and 1D Vs logs could be established for the large Heinzenberg landslide to characterize the seismic reponse in the different compartments.

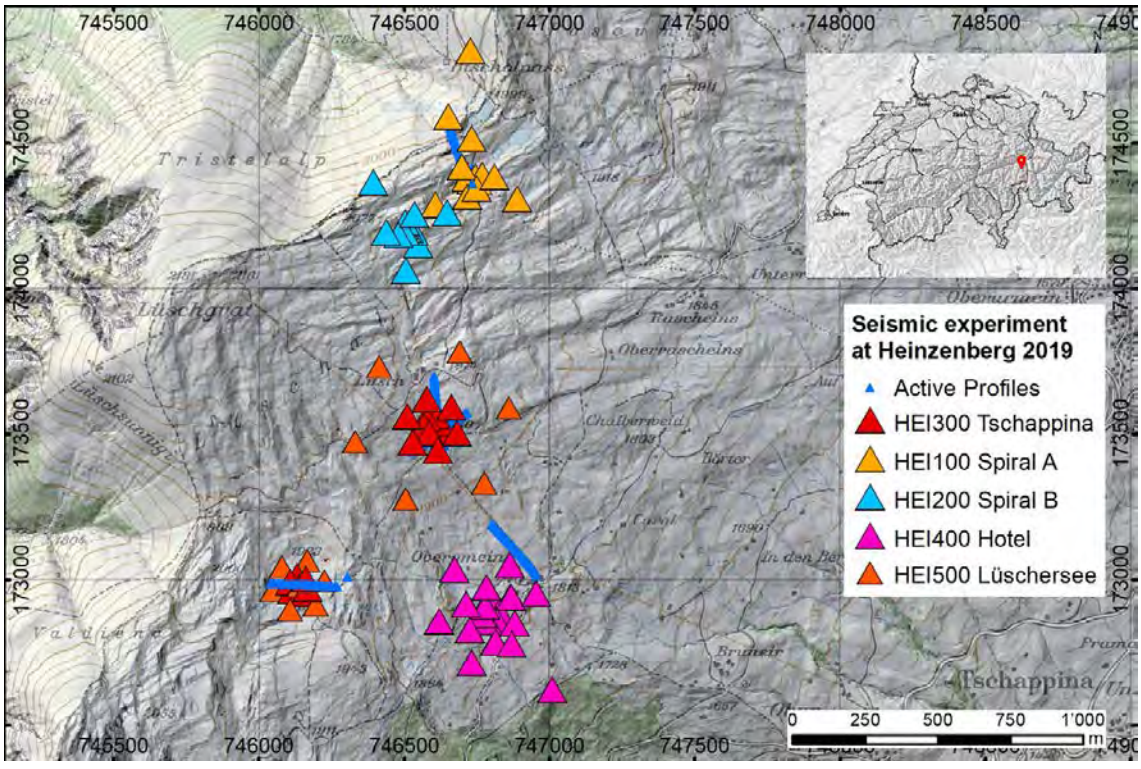

Figure 1. Location of the different arrays and refraction tomographic profiles profiles for the seismic experiment at Heinzenberg.

REFERENCES

Burjanek J et al. (2012) Toward reliable characterization of sites with pronounced topography and related effects on ground motion. Paper presented at the 15th World Conference on Earthquake Engineering (15WCEE), Lisbon, Portugal, September 24-28, 2012,

Burjanek J, Edwards B, Fäh D (2014) Empirical evidence of local seismic effects at sites with pronounced topography: a systematic approach. Geophys J Int 197:608-619 doi:10.1093/gji/ggu014

Hobiger M et al. (2021) Site Characterization of Swiss Strong-Motion Stations: The Benefit of Advanced Processing Algorithms. Bulletin of the Seismological Society of America

Jäckli H (1948) Die Bodenbewegungen im Hinterrhein-Tal und ihre bautechnischen Auswirkungen. Schweizerische Bauzeitung 66, H 37:5

Kleinbrod U, Burjanek J, Fäh D (2017) On the seismic response of instable rock slopes based on ambient vibration recordings. Earth Planets and Space 69 doi:10.1186/s40623-017-0712-5

Kleinbrod U, Burjanek J, Fäh D (2019) Ambient vibration classification of unstable rock slopes: A systematic approach Engineering Geology 249:198-217 doi:10.1016/j.enggeo.2018.12.012

Naturpark Beverin Geschäftsstelle N (2019) Gesuch um globale Finanzhilfen Kapitel C: Projektblätter 2020 – 24:75

Osten J, Küppers J, Dufresne A, Huwiler A, Amann F (2020) Deep seated gravitational slope deformation of the southern Heinzenberg (Grison, Switzerland) 13:74-87 doi:https://doi.org/10.1002/geot.201900065

Perron V, Laurendeau A, Hollender F, Bard PY, Gelis C, Traversa P, Drouet S (2018) Selecting time windows of seismic phases and noise for engineering seismology applications: a versatile methodology and algorithm. Bulletin of Earthquake Engineering 16:2211-2225 doi:10.1007/s10518-017-0131-9

Poggi, V., Fäh, D. (2010). Estimating Rayleigh wave particle motion from three-component array analysis of ambient vibrations. Geophys. J. Int. 180, 251–267.

Socco LV, Strobbia C (2004). Surface-wave method for near-surface characterization: a tutorial 2:165-185 doi:https://doi.org/10.3997/1873-0604.2004015

8.3
Application of multizonal transdimensional Bayesian inversion method for developing a 3D geophysical model in Basel, Switzerland

Afifa Imtiaz[1], Francesco Panzera[1], Miroslav Halo[1], Horst Dresmann[2], Brian Steiner[2], Donat Fäh[1]

[1] *Swiss Seismological Service (SED), ETHZ, Switzerland (afifa.imtiaz@sed.ethz.ch)*
[2] *Applied and Environmental Geology (AUG), University of Basel, Switzerland*

Local shear-wave velocity (Vs) structure and sedimentary thickness are considered to be the controlling parameters in seismic amplification. Using dispersion characteristics of surface waves from ambient vibration array data has proven to be an effective tool for imaging Vs profiles in the subsurface. However, the conventional optimization inversion techniques are limited in their ability to account for the inherent non-uniqueness of this inverse problem solution and related uncertainty of the profiles. Therefore, we apply a novel Bayesian inversion approach based on a Multizonal Transdimensional Inversion (MTI) developed by Hallo et al. (2021), with the aim of developing a 3D model of subsurface velocity structure for the city of Basel, Switzerland. The MTI method is based on a joint inversion of multimodal Rayleigh- and Love-wave dispersion curves (DCs) along with Rayleigh-wave ellipticity. The key advantages of the method are that the number of layers is determined self-adaptively from the measured data, and model uncertainties can be assessed quantitatively. Moreover, the solution of the Bayesian inversion is the posterior Probability Density Function (PDF) that results from the prior expectations and the observed data supplemented by an expected distribution of data errors. Hence, the model uncertainty can be duly propagated from DCs to Vs profiles.

We apply MTI to retrieve 1D Vs profiles from 26 passive arrays located within an area of about 130 square km (marked by the red polygon on the top panel of Figure 1) by using single-zone transdimensional model space with homogeneous prior assumptions on models. It delivered a major improvement in our results because such joint inversions of surface wave dispersion and ellipticity curves could be performed only for a few sites in Basel in the past. Our work leads to a more robust identification of the interfaces corresponding to major velocity contrasts, especially in the complex sedimentary structure of the Rhine Graben formation. In the bottom panel of Figure 1, we present results from 6 array sites located along a NW-SE cross-section. For each array site, we compare a summary of outputs from the MTI in terms of marginal posterior average profile (AMP), maximum likelihood (ML) model and maximum a posteriori (MAP) model with 1D geological profile (VBH) obtained from the newly updated 3D geological model of Basel (Dresmann et al., 2013). For these sites, we consistently observe relatively stronger velocity contrasts at the base of the Meletta layer. The thickness of this layer increases from the northwest to the southeast. At the next stage, additional constraints on the depths of intermediate layers will be drawn from the 3D geological model for performing so-called multizonal inversion. A 3D geophysical model will be constructed by assigning elastic properties (i.e. shear- and compressional-wave velocities and mass density) to the corresponding geologic units and depths. Uncertainties associated with the dispersion and ellipticity curves, elastic parameters of the inverted models, and thickness of different layers will be extensively evaluated.

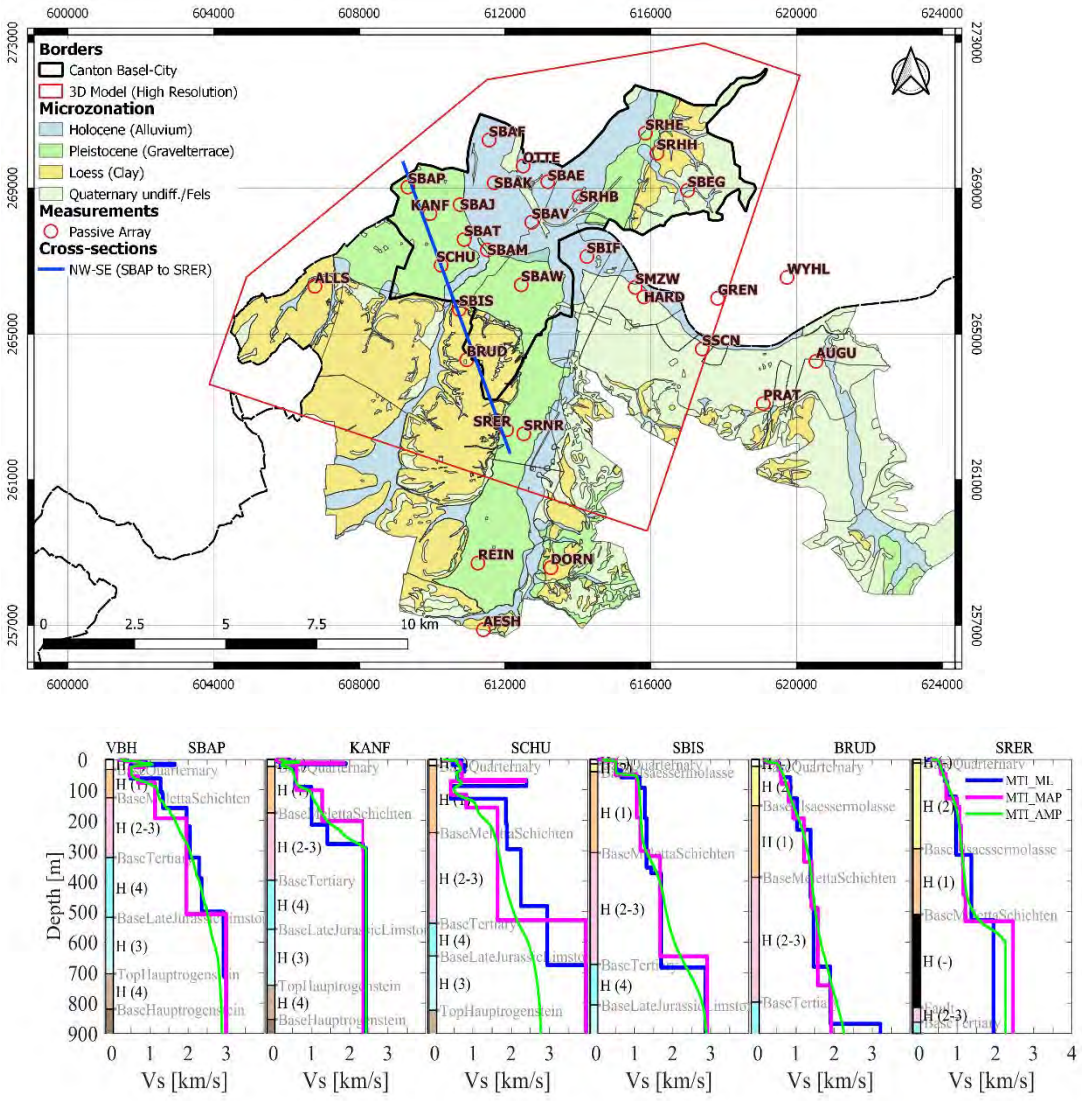

Figure 1. Top: Locations of passive array measurements in Basel. Bottom: Vs models (ML, MAP and AMP) from MTI and geological profiles (VBH) for the arrays, located along the cross-section (marked by the blue line on the top panel). H values represent the hardness of the layer (1=soft, 4=hard).

REFERENCES

Dresmann H., Huggenberger P., Epting J., Wiesmeier S., Scheidler S., GeORG - project team 2013: A 3D spatial planning tool – application examples from the Basel region. Proceedings of the 33rd GOCAD Meeting, 17.-20. Sep. 2013, Nancy, France.

Hallo, M., Imperatori, W., Panzera, F., Fäh, D. 2021: Joint multizonal transdimensional Bayesian inversion of surface wave dispersion and ellipticity curves for local near-surface imaging, Geophys. J. Int., 226,1, 627–659, https://doi.org/10.1093/gji/ggab116.

8.4
The currect state of the local site amplification model for the city of Lucerne

Paulina Janusz[1], Vincent Perron[1], Christoph Knellwolf[2], Walter Imperatori[1], Luis Fabian Bonilla[3], Donat Fäh[1]

[1] *Swiss Seismological Service, ETH Zürich, Sonneggstrasse 5, 8092 Zürich, Switzerland (paulina.janusz@sed.ethz.ch)*
[2] *Verkehr und Infrastruktur, Abteilung Naturgefahren, Kanton Luzern, Arsenalstrasse 43, 6010 Kriens, Switzerland*
[3] *Université Gustave Eiffel, 14-20 Boulevard Newton, Cité Descartes, 77447 Marne-la-Vallée Cedex 2, France*

Estimation of site response variability is an essential part of seismic hazard and risk assessment, in particular in densely populated urban areas that are especially vulnerable due to the concentration of exposed elements and high population density. We present the current state of the local site amplification model for the city of Lucerne in central Switzerland, which is located in a glacial basin filled with soft sediments. The seismicity in the area is low-to-moderate, however, several strong earthquakes occurred there in the past (i.e. Mw 5.9 in 1601), hence the long-term seismic risk cannot be neglected. During the last two years, we carried out measurement campaigns in the Lucerne area. Firstly, we deployed a temporary seismic monitoring network which was operating in total for about one year. Then, two surveys were performed (in June 2020 and April 2021) to record ambient vibration at 100 densely distributed points. In addition, our dataset was supplemented by recordings from seismic stations of the Swiss Strong Motion Network (SSMNet) and by more than 200 single-station ambient vibration measurements performed in Lucerne in the past (e.g. Poggi et al., 2012).

We first calculated the H/V spectral ratios and mapped the fundamental frequency of resonance across the area. We employed also polarization analysis by analysis Burjánek et al., (2010) to check for any directional effects. Secondly, we have combined the ground motion from low-magnitude or distant earthquakes and ambient vibration recordings to map the amplification factors with respect to local rock site using a hybrid site-to-reference spectral ratio method (SSRh - Perron et al. 2018, 2020, Janusz et al. 2021). To refer our local amplification model to the Swiss reference bedrock conditions (Poggi et al., 2011), we corrected our results using the amplification functions (EAF) derived with empirical spectral modelling (Edwards et al., 2013)due to the heterogeneity of the upper crust, the site amplification effect is highly variable over scales of kilometers or less (e.g., Boore, 2004 which are routinely computed for the stations of the Swiss seismic network. At selected urban sites, we compared the SSRh amplification function with the classical Standard Spectral Ratio approach (SSR - Borcherdt, 1970) obtaining good agreement (Figure 1). However, due to the variability of the noise wavefield, the uncertainty for the hybrid method is much higher than for the SSR approach (Figure 1). We present and discuss also the influence of daily variation of the noise wavefield on our local amplification model as well as the impact of the distribution of the temporary seismic network stations in the basin. The local model for the city of Lucerne shows the peak amplification of more than 10 at about 1.2 Hz in the deepest part of the basin. The results indicate a significant local increase in seismic hazard.

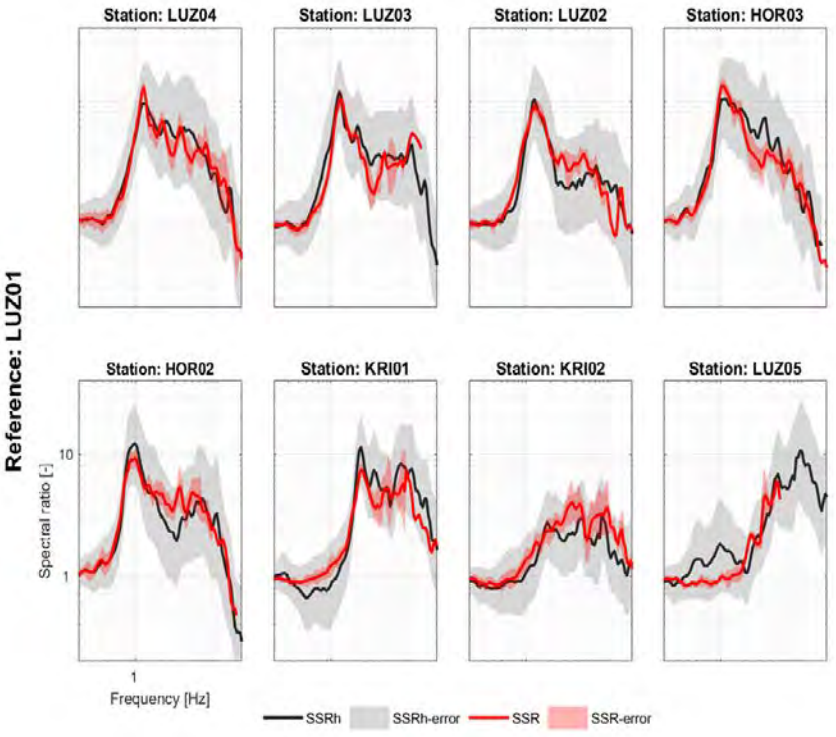

Figure 1. Relative amplification function using the SSR and SSRh methods at eight sites in the Lucerne area.

REFERENCES

Borcherdt, R.D., 1970. Effects of local geology on ground motion near San Francisco Bay. Bull. Seismol. Soc. Am. 60, 29–61.

Burjánek, J., Gassner-Stamm, G., Poggi, V., Moore, J. R., & Fäh, D., 2010. Ambient vibration analysis of an unstable mountain slope. Geophys. J. Int., 180(2), 820–828.

Edwards, B., Michel, C., Poggi, V., Fäh, D., 2013. Determination of Site Amplification from Regional Seismicity: Application to the Swiss National Seismic Networks. Seismol. Res. Lett. 84, 611–621.

Janusz, P., Perron, V., Knellwolf, C., Imperatori, W., Bonilla, L. F., and Fäh, D., 2021, Combining recordings of earthquake ground-motion and ambient vibration analysis to estimate site response variability in the city of Lucerne, Switzerland, EGU General Assembly 2021, EGU21-4380

Perron, V., Gélis, C., Froment, B., Hollender, F., Bard, P.-Y., Cultrera, G., Cushing, E.M., 2018. Can broad-band earthquake site responses be predicted by the ambient noise spectral ratio? Insight from observations at two sedimentary basins. Geophys. J. Int. 215, 1442–1454.

Perron V., Bergamo P. Panzera F., Hammer C. & Fäh D., 2020. Empirical earthquake's site response assessment in the Sion area, Switzerland. Abstract booklet, Swiss Geoscience Meeting 2020

Poggi, V., Edwards, B., & Fäh, D., 2011. Derivation of a Reference Shear-Wave Velocity Model from Empirical Site Amplification Derivation of a Reference Shear-Wave Velocity Model from Empirical Site Amplification. Bulletin of the Seismological Society of America, 101(1), 258–274.

Poggi, V., Fäh, D., Burjanek, J. and Giardini, D., 2012. The use of Rayleigh wave ellipticity for site-specific hazard assessment and microzonation. Application to the city of Lucerne, Switzerland. Geophys. J. Int., 188(3), pp 1154–1172

8.5
Improving early post-earthquake regional damage assessment in Switzerland

Yves Reuland[1], Lukas Bodenmann[1], Panagiotis Martakis[1], Bozidar Stojadinovic[1], Eleni Chatzi[1]

[1] *Dept. of Civil, Environmental and Geomatic Engineering, ETH Zurich, Wolfgang-Pauli-Str. 27, CH-8093 Zürich (reuland@ibk.baug.ethz.ch)*

Despite being rare in Switzerland, earthquakes carry potential for disastrous and long-lasting societal consequences. This is a consequence of the increased vulnerability of the ageing Swiss building stock. The processes of performance-based seismic design of new buildings and risk-informed seismic retrofitting of vulnerable buildings lay the foundation for long-term risk mitigation, yet adequate post-earthquake decision-making is a crucial enabler for rapid post-earthquake recovery. Current practice relies on visual screening during post-earthquake inspection for ensuring safe building re-occupancy and functional recovery. However, the task of visually inspecting all affected structures is non-trivial and, depending on available resources, could require several weeks. To ensure rapid loss assessment and early recovery regional seismic risk models of exposure and vulnerability are typically combined with ground-motion estimates that are computed on the basis of seismic recordings (Erdik et al., 2011). Despite the large uncertainties related to such early estimates, these are required for directing important decisions that may shape the recovery process.

Regional risk models provide rapid, yet uncertain, damage predictions at regional scale. However, economic and technical constraints often hinder the collection of in-depth information prior to a seismic event and the exhaustive simulation of the complete building stock of a region. Instead, buildings are clustered into predefined classes with a pre-allotted average vulnerability that are made for exposure models at very large scale (Crowley et al., 2020).

Several aspects of these regional risk models and their use for rapid post-earthquake regional risk assessment can be improved, either in a pro-active manner, before any earthquake strikes, or in the early aftermath of an earthquake.

While machine-learning tools have previously been used to classify buildings into typologies (Diana et al., 2019) on the basis of publicly available data, such as construction year and height, building typologies are not defined based on expected-performance metrics. In addition, numerous properties that govern the capacity to resist seismic loads, such as the percentage of openings and the stiffness repartition, are ignored. Vibration measurements, model updating (Martakis et al., 2021), and machine learning allow to overcome such limitations.

The occurrence of damaging earthquakes will inevitably trigger inspection activities, which will result in a continuous stream of information regarding the extent of damage. Machine-learning approaches are used to leverage the inspection outcome of a subset of damaged buildings to improve upon early regional damage assessments and reduce their uncertainty (Bodenmann et al., 2021). Such a scheme allows to simultaneously update the estimated shaking intensity map, building exposure, and even typological vulnerability curves.

In addition, highly sensitive sensors, such as accelerometers, are increasingly available at relatively low costs and thus, enable a permanent monitoring of numerous buildings within a region. Damage-sensitive features, which are derived from acceleration time histories recorded during an earthquake, allow for near-real time estimation of the damage sustained by a building. Combined with visual inspections and a regional damage-updating approach, such sensing data carry the potential to improve early regional damage estimates.

In this contribution, we review the potential of such a proactive approach, as investigated within the framework of the DynaRisk and RISE projects, to improve rapid damage estimates. In addition, the alleviation of the adverse consequences of seismic events will be discussed by providing an outlook on how such an approach may influence recovery of the housing capacity over time and possibly enhance the resilience of Switzerland with respect to earthquakes.

REFERENCES

Bodenmann, L., Reuland, Y., Stojadinovic, B. 2021: Dynamic Updating of Building Loss Predictions using Regional Risk Models and Conventional Post-Earthquake Data Sources. Proc. of 31st European Safety and Reliability Conference, Angers, France.

Crowley, H., V. Despotaki, D. Rodrigues, V. Silva, D. Toma-Danila, E. Riga, A. Karatzetzou, S. Fotopoulou, Z. Zugic, L. Sousa, S. Ozcebe, and

P. Gamba. 2020: Exposure model for European seismic risk assessment. Earthquake Spectra, 36(1), 252–273.

Diana, L., Thiriot, J., Reuland, Y. & Lestuzzi, P. 2019: Application of Association Rules to Determine Building Typological Classes for Seismic Damage Predictions at Regional Scale: The Case Stufy of Basel. Frontiers in Built Environment, 5.

Erdik, M., Sesetyan, K., Demircioglu, M. B., Hancilar, U. & Zülfikar, C. 2011: Rapid earthquake loss assessment after damaging earthquakes. Soil Dynamics and Earthquake Engineering, 31(2), 247–266.

Martakis, P., Reuland, Y. & Chatzi, E. 2021: Amplitude-dependent model updating of masonry buildings undergoing demolition. Smart Structures and Systems, 27(2), 157-172.

P 8.1
Depth-to-surface ground motion amplification as revealed by our stochastic model and empirical data from Japanese KiK-net stations

Miroslav Hallo[1], Paolo Bergamo[1], Donat Fäh[1]

[1] *Swiss Seismological Service (SED), ETH Zürich, Sonneggstrasse 5, CH-8092 Zürich (miroslav.hallo@sed.ethz.ch)*

The site-specific high-frequency (>1Hz) amplification and attenuation observed in earthquake recordings have various contributions coming from the path- and site-terms. Advancements in the prediction of these parameters are essential for improving the accuracy of the ground motion prediction on a local scale. Moreover, there is a need to characterize a possible ground motion at depth for long return periods in the seismic hazard assessment of deep geological disposals (e.g. nuclear waste repositories). This highlights the importance of the advancements to characterize high-frequency ground motion at depth.

Recently, we proposed a theoretical stochastic model to characterize the high-frequency ground motion at depth. This model is constructed by a three-step procedure as follows: 1) We derive a set of local 1D velocity profiles considering various possible effects of the near-surface geology on ground motions. Particularly, we consider possible random perturbations in S-wave velocity, medium density, and the damping ratio of layers. Alternatively, we might use a set of 1D velocity profiles resulting from a Bayesian inversion (e.g. Hallo et al. 2021). 2) Then these random profiles are used for the computation of an ensemble of theoretical depth-to-surface SH-wave transfer functions in the spectral domain (e.g. Kramer 1996). As the plane SH-waves are polarized perpendicularly to the direction of propagation, we include also possible random variations of the wave incidence angle at the onset at depth. 3) The ensemble of such transfer functions is used for the construction of the stochastic model by means of Gaussian statistics in the energy spectral density (amplification term) and envelope delay (temporal term, Boore 2003).

To demonstrate the applicability of this stochastic model, we retrieve surface-to-borehole amplitude spectral ratios (S/B ratios) and envelope delays (S-B delays) from borehole installations of the Japanese KiK-net network (Aoi et al. 2011, NIED 2019). For this purpose, we use three-component acceleration waveforms of local earthquakes (depth <=25 km) recorded between the years 1997 and 2008 with the sampling frequency of 200 Hz. These records are rotated into the transverse component and transformed into the spectral domain. Then, pairs of surface and borehole record spectra with a sufficient signal-to-noise ratio are used for the computation of S/B spectral ratios and S-B envelope delays. The set of these spectral curves from multiple earthquake records are statistically evaluated on individual stations (i.e. data median, mean, 16th percentile, 84th percentile).

Finally, we use 1D velocity profiles provided by NIED and compute theoretical S/B spectral ratios and S-B envelope delays by using our stochastic model. The comparison of predicted and empirical spectral curves in Fig.1 shows, that our stochastic model can reasonably predict the ground motion at dept from surface recordings for sites characterized by 1D amplification effects.

REFERENCES

Aoi, S., Kunugi, T., Nakamura, H., Fujiwara, H. 2011: Deployment of new strong motion seismographs of K-NET and KiK-net, In: Akkar, S., Gülkan, P., van Eck, T. (eds) Earthquake data in engineering seismology geotechnical, geological, and earthquake engineering, vol. 14., pp. 167–186, Springer, Dordrecht.

Boore, D.M. 2003: Phase Derivatives and Simulation of Strong Ground Motions, Bull. Seismol. Soc. Am., 93, 1132–1143.

Hallo, M., Imperatori, W., Panzera, F., Fäh, D. 2021: Joint multizonal transdimensional Bayesian inversion of surface wave dispersion and ellipticity curves for local near-surface imaging, Geophysical Journal International, 266, 627–659.

Kramer, S.L. 1996: Geotechnical Earthquake Engineering, 653 pp., Prentice Hall, Upper Saddle River, NJ.

National Research Institute for Earth Science and Disaster Resilience 2019: NIED K-NET, KiK-net, National Research Institute for Earth Science and Disaster Resilience, doi:10.17598/NIED.0004.

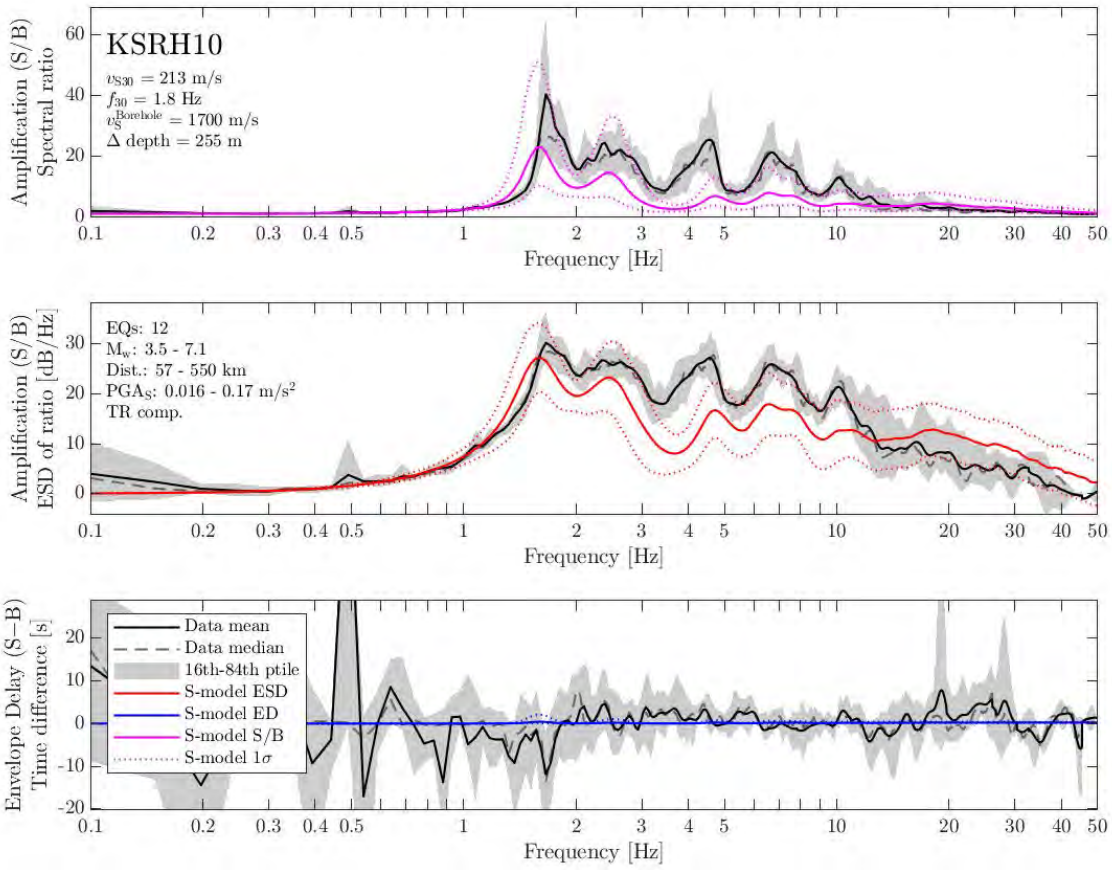

Figure 1. A comparison of empirical (black lines) and predicted (coloured lines) depth-to-surface spectral curves of station KSRH10 (KiK-net; Hokkaido, Japan). Surface and borehole receivers are installed in 0 and 255 m depth, respectively. Upper panels: S/B spectral ratio; bottom panel: S-B envelope delay.

P 8.2
The dynamic response of the Brienz/Brinzauls rock slope instability

Mauro Häusler[1], Valentin Gischig[2], Reto Thöny[3], Franziska Glueer[1], Donat Fäh[1]

[1] *Swiss Seismologial Service, Institute of Geophysics, ETH Zurich, Sonneggstrasse 5, CH-8092 Zürich (mauro.haeusler@sed.ethz.ch)*
[2] *CSD Ingenieure AG, Hessstrasse 27d, CH-3097 Liebefeld*
[3] *BTG Büro für Technische Geologie AG, Grossfeldstrasse 74, CH-7320 Sargans*

Unstable slopes exhibit very specific dynamic site response, with strong seismic wavefield amplification and ground motion polarization perpendicular to dominant fracture networks (e.g., Kleinbrod et al., 2019). Therefore, measuring the dynamic response by ambient vibrations and earthquake recordings enables geophysical characterization of slope instabilities, including structural landslide compartmentalization. In addition, such measurements provide basic input data for modeling earthquake-induced failure.

Here, we present the seismological characterization of the currently active, large Brienz/Brinzauls rock slope instability in Canton of Grisons, Switzerland (e.g., Krähenbühl and Nänni, 2017). We characterize the dynamic response in terms of relative seismic amplification and normal mode behavior and show how these findings can support geologists to subdivide the unstable rock mass into structural compartments (Figure 1).

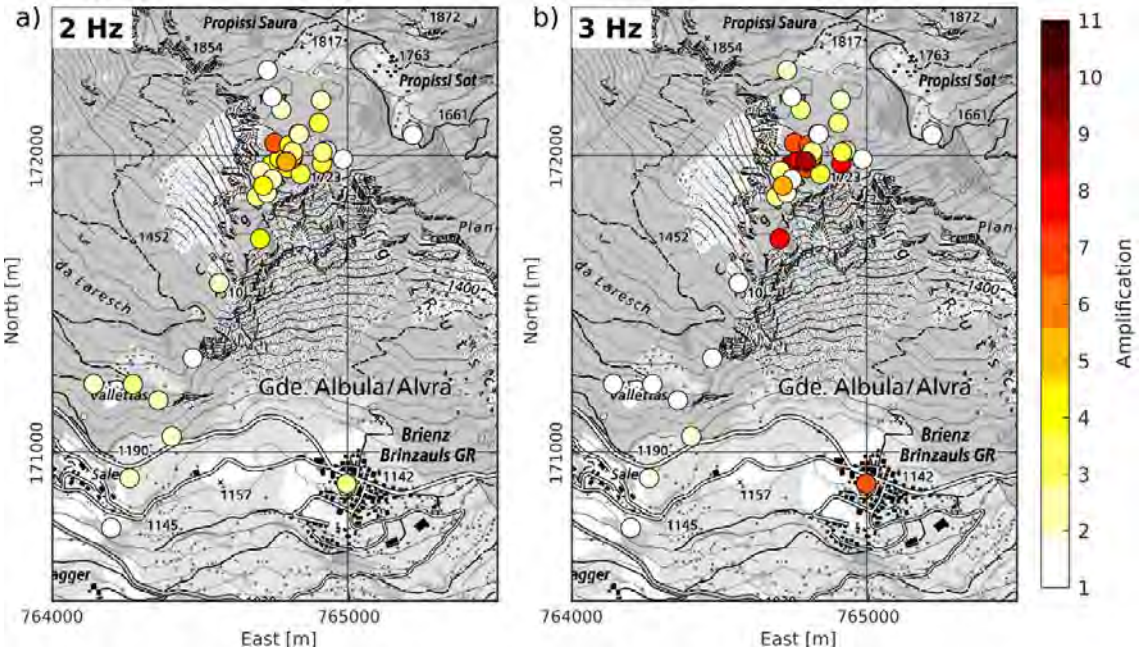

Figure 1. Seismic amplifications across the rock slope instability above the village Brienz/Brinzauls at a) 2 Hz and b) 3 Hz. High amplification factors correlate with the extent of the instability and can reach values of up to 11 in areas dominated by persisting, sub-vertical fractures.

In addition, we present the continuous monitoring of the dynamic response since 2018 by a permanently installed seismometer. We observed changes in ground motion polarization correlating with the surface displacement field and found a direct connection between the local precipitation history and seismic amplification (Häusler et al., 2021).

REFERENCES

Häusler, M., Gischig, V., Thöny, R., Glueer, F. & Fäh, D. 2021: Monitoring the changing seismic site response of a fast-moving rockslide (Brienz/Brinzauls, Switzerland), Geophysical Journal International (in review).

Kleinbrod, U., Burjánek, J., & Fäh, D. 2019, Ambient vibration classification of unstable rock slopes: A systematic approach. Engineering Geology, 249, 198-217.

Krähenbühl R. and C. Nänni. 2017, Ist das Dorf Brienz-Brinzauls Bergsturz gefährdet? Swiss Bulletin für angewandte Geologie, 22, 2, 33-47.

P 8.3
Full microtremor horizontal-to-vertical spectral ratio inversion for the characterization of Swiss borehole and OBS sedimentary sites

Agostiny Marrios Lontsi[1], Anastasiia Shynkarenko[1], Manuel Hobiger[2], Paolo Bergamo[1], Katrina Kremer[1], Donat Fäh[1]

[1] *Swiss Seismological Service, ETH Zürich, Sonneggstrasse 5, 8092 Zürich, Switzerland (agostiny.lontsi@sed.ethz.ch)*
[2] *Federal Institute for Geosciences and Natural Resources, Stilleweg 2, 30655 Hannover, Germany*

The microtremor horizontal-to-vertical (H/V) spectral ratio has emerged as a single-station method due to its capability to estimate the frequency of resonance at a site. Moreover, using additional constraints and sufficiently long recording times, a shear-wave velocity profile can be derived from H/V spectral ratios (Lontsi et al. 2015). The extracted information are of importance for seismic hazard assessment both onshore and offshore. We estimate the shear wave velocity profiles at two sedimentary sites in Switzerland. One site is located onshore at Buochs and is equipped with three strong motion sensors: one is located at the surface and two are located in boreholes at 26 and 100 m depths (Hobiger et al., 2021). We first analyzed the temporal variability of the estimated microtremor H/V spectral ratio for the receiver at the surface (Figure 1) and select an appropriate H/V curve, combined with H/V measurements at depths, for the inversion. The second site is located offshore Weggis (Lake Lucerne). With the advances in seismic instrumentation offshore, high quality data were recorded to help us characterize the internal sediment structure of the lake/ocean bottom, and to assess the volume of the sediment cover that could fail in case a seismic event occur. As we know that failed slopes could potentially lead to tsunamis (e.g. Hilbe and Anselmetti, 2015). Between 2018 and 2020, we used ocean bottom seismometers (OBS) and performed ambient-vibration measurements at selected sites in Lake Lucerne where sediments are susceptible to failure or have failed before (Figure 1). Here we show preliminary inversion results at Weggis. The inversion considers one station only. The inversion would be much better constrained by adding for example H/V spectral ratio measured at depth, phase velocity dispersion curves obtained by array analysis (Shynkarenko et al., 2021), or layer thicknesses from seismic surveys. This is subject to further investigation.

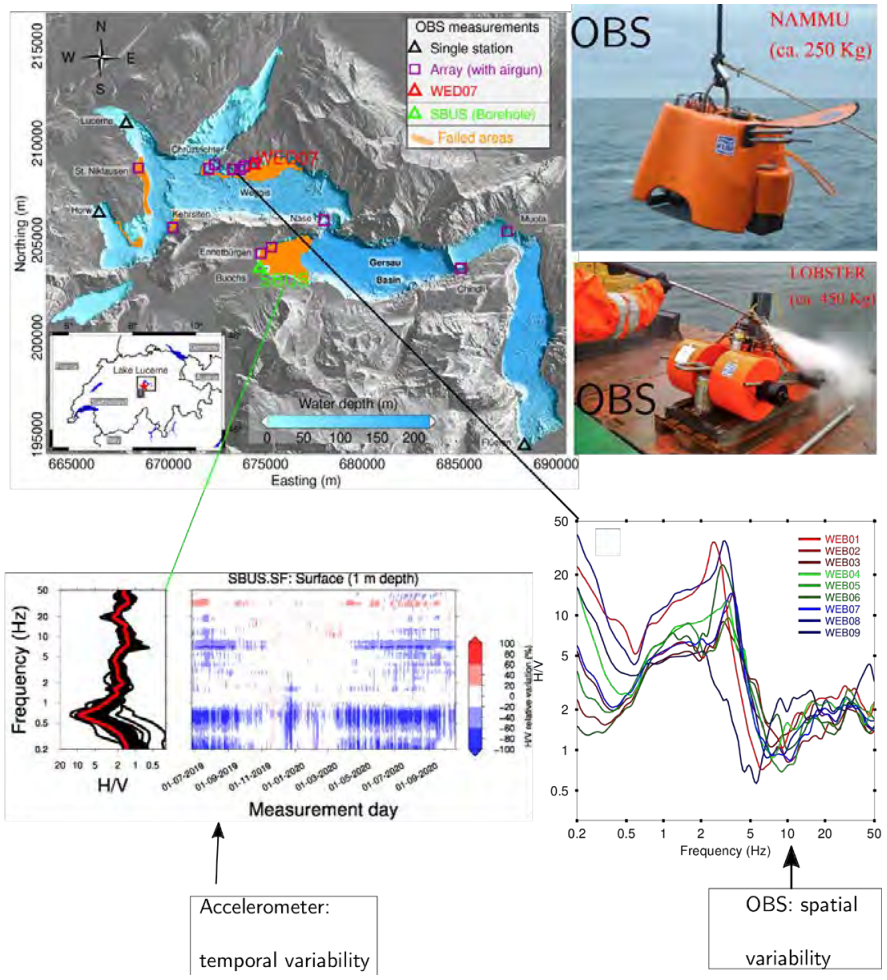

Figure 1. Lake Lucerne: Bathymetry and nearby geomorphology. In total: more than 169 OBS deployments and recoveries between 2018 - 2020. The OBS station WED07 is later used in the inversion. The location of the borehole station SBUS is indicated with green color. NAMMU and LOBSTER indicate the two OBS types that were used in Lake Lucerne. The spatial variability of the H/V spectral ratio for one array at Weggis is shown. For the borehole station, the temporal variability for the surface station is presented.

REFERENCES

Hilbe, M., & Anselmetti, F.S., (2015). “Mass Movement-Induced Tsunami Hazard on Perialpine Lake Lucerne (Switzerland): Scenarios and Numerical Experiments”, Pure Appl. Geophys. 172, 545–568.

Hobiger, M., Bergamo, P., Imperatori, W., Panzera, F., Lontsi, A. M., Perron, V., Michel, C., Burjánek, J., & Fäh, D. (2021). “Advanced site characterization as part of the renewal project of the Swiss Strong Motion Network (SSMNet)”, Bull. Seismol. Soc. Am., 111 (4), 1713–1739.

Lontsi, A.M., Sánchez-Sesma, F.J., Molina-Villegas, J.C., Ohrnberger, M., & Krüger, F., (2015). “Full microtremor H/V(z, f) inversion for shallow subsurface characterization”, Geophysical Journal International, 202(1), 298-312.

Shynkarenko, A., Lontsi, A.M., Kremer, K., Bergamo, P., Hobiger, M., Hallo, M., & Fäh, D., (2021). “Investigating the subsurface in a shallow water environment using array and single-station ambient vibration techniques”, *Geophysical Journal International*, 227 (3), 1857 – 1878.

P 8.4
Design-compatible waveforms for Switzerland: preliminary results

Francesco Panzera[1], Paolo Bergamo[1], Dario Chieppa[1], Laurentiu Danciu[1], Miroslav Hallo[1], Walter Imperatori[1], Donat Fäh[1]

[1] *Swiss Seismological Service, ETH Zurich, Sonneggstrasse 5, CH-8092 Zürich (francesco.panzera@sed.ethz.ch)*

Selection of design-compatible ground motions is a topic of great interest in engineering seismology. It consists in searching time series inside a ground motion database, having appropriate response spectral values in an predefined earthquake magnitude and distance range, and soil class. The selection and use of earthquake ground motion recordings must be consistent with the selected seismic hazard level and ideally able to capture the variability and contributions of both local and distant earthquakes.

We summarize the preliminary results of our work to inspect available databases of waveforms and to select waveforms compatible with the requirement defined in the Swiss building codes SIA261. In a first step the available databases of waveforms and related metadata were inspected (reliability of magnitude, distance, site condition information, free-field recording, etc.). We defined standards linked to the quality of 3C-waveforms (compatibility to GMPE, adequate frequency content, absence of non-physical drift in velocity and displacement). Among the available strong motion databases, we scrutinized the Engineering Strong Motion database (https://esm-db.eu/#/home), the Japanese database of K-NET and KiK-net (https://www.kyoshin.bosai.go.jp/) and the recordings from NGA-West2 (https://ngawest2.berkeley.edu/). From each database, we extract a subset of stations suitable for the purposes of the project classified in terms of SIA261 soil classes (A-E), focussing on the provided V_S profiles. Therefore, the waveform metadata of the selected stations were checked, and high-quality waveforms were sorted in terms of magnitude and Joyner-Boore distance. Finally, using the results of seismic hazard disaggregation for the five Swiss national seismic zones, we select a subset of waveforms covering the range of magnitude and distance combinations relevant for each seismic zone and soil class (Fig. 1).

This subset of waveforms is then used to perform an unconditional selection of waveforms by using the geometric mean of the two horizontal components response spectra. The targets are the SIA261 response spectra for building importance class III (~975 years return period) and the selected soil class. The period range used for the selection is 0.06-2.0s to cover the range generally used in site-specific seismic soil amplification analyses as suggested by the draft version of the revision of Eurocode 8. From the database, we select two sets of 11 three-component waveforms. The selection was made using horizontal components of unscaled waveforms, but if necessary a scalar factor between 0.5 and 2 was allowed (Fig. 2). Nevertheless, the number of strong-motion earthquake records especially in the near-source distance range and for soil class A are limited. To overcome this problem, we are working on a procedure to numerically simulate synthetic ground motions compatible with the design response spectra and earthquake scenarios in terms of magnitude, distance and site geological conditions.

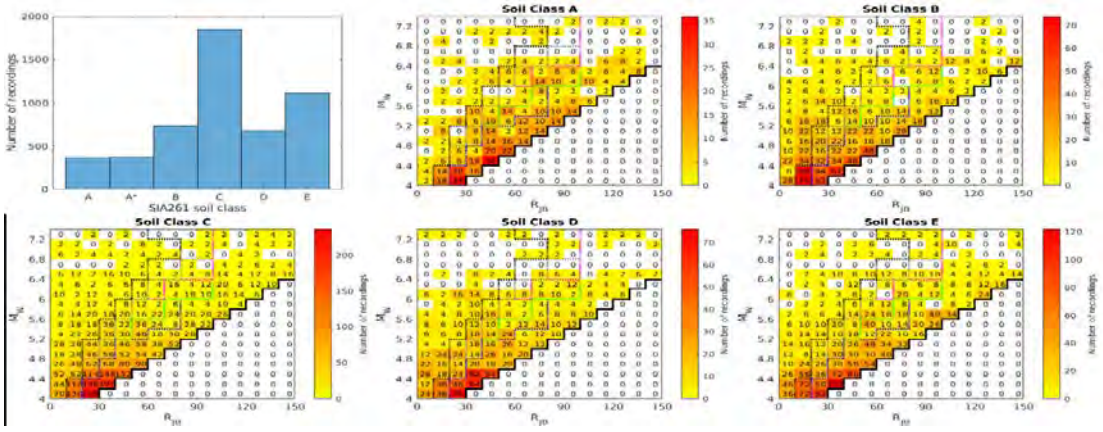

Figure 1. Left panel: subset of the selected number of recordings for each SIA261 soil class. Right panel: Plot showing number of horizontal component waveformsfor bins in distance (10 km width) and moment magnitude M_W (0.2 unit) for SIA261 soil class A. The coloured dotted lines indicate the ranges where deaggregation gives contributions above 0.1% for the five seismic zones (blue=Z1a; green=Z1b; magenta=Z2; grey=Z3a; black=Z3b). The black solid line indicates our limit for the first selection of waveforms.

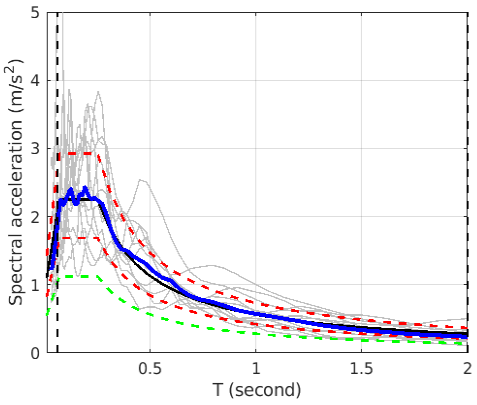

Figure 2. Example of sets of ground motions (grey lines) selected according to the target spectum (black line) for the zone Z1a of the national zonation in SIA261. The red dashed lines correspond to 0.75 and 1.3 times the target spectrum, whereas the green line is the lower limit (0.50 times the target spectrum) above which all the selected response spectra need to be.

REFERENCES

Eurocode8, 2004: Design of structures for earthquake resistance—part 1: general rules, seismic actions and rules for buildings, European Committee for Standardization (CEN), EN 1998-1. www.eurocodes.jrc.eceuropa.eu/

SIA261, 2020: SIA261 Azioni sulle strutture portanti. Compiled by: Società svizzera degli ingegneri e degli architetti (SIA).

P 8.5
The QuakeMatch Toolbox: the swiss-army-knife approach to a nearly automatic analysis for microearthquake sequences

Tania Toledo[1], Toni Kraft[1], Verena Simon[1], Marcus Herrmann[2], Linus Villiger[1], Veronica Antunes[1], Tobias Diehl[1]

[1] *Swiss Seismological Service at ETH Zurich, Switzerland (tania.toledo@sed.ethz.ch)*
[2] *Università degli Studi di Napoli, Federico II, Italy*

Many Swiss microearthquake sequences have been studied using relative location techniques, which often allowed to constrain active fault planes and the tectonic processes that drive the seismicity. Yet, in some cases, the number of located earthquakes was too small to infer the details of the space-time evolution of the sequences or their statistical properties. Therefore, it has often been impossible to resolve clear patterns in the seismicity of individual sequences, which are needed to improve our understanding of their driving mechanisms.

Here we present a nearly automatic workflow that combines well-established seismological analysis techniques and allows to significantly improve the completeness of detected and located earthquakes of a sequence. We start from the manually timed routine catalog of the Swiss Seismological Service (SED) containing the larger events of a sequence in Switzerland (Mc~1.5 on average and Mc < 1.0 for densely instrumented regions). From these well-analyzed earthquakes we assemble a template set and perform a matched filter analysis on a single station with the best SNR; and a recording history of at least 10-15 years, our typical analysis period. This usually allows us to detect events of magnitude below 0. The waveform similarity of the events is then further exploited to derive precise and consistent magnitudes. The enhanced catalog is then analyzed statistically to derive high-resolution temporal evolutions of the a- and b-value and consequently the occurrence probability of larger events. Many of the detected events are strong enough to be located using relative double-difference methods. No further manual interaction is needed; we simply time-shift the manual arrival-time pattern of the detecting template to the associated automatic detection. Waveform similarity assures a good approximation of the expected arrival-times, which we use to calculate event-pair differential times by cross correlation. After a SNR and cycle-skipping quality check these are directly fed into the hypoDD algorithm. With this procedure, we usually improve the number of well-relocated events by a factor 2-5. Weak events that cannot be relocated using the DD method, can still be related to well-located events via waveform similarity. With our simloc technique, we use this information to estimate single-station locations for these events with a precision close to that reached by the DD technique in the previous step.

With **QuakeMatch**, we aim to provide an open-source Python toolbox for the workflow outlined above. **QuakeMatch** will contain a GUI for easy step-by-step visualization of the data processing:

- Fetching event and inventory data from different data centers
- Database initialization for handling large sets of seismicity
- Parallel computing for template matching
- Earthquake relocation and accurate templet-family-based magnitude estimates
- High-resolution statistical earthquake analysis
- Relocation by the DD and simloc techniques

Adapting the toolbox's techniques to the laboratory or deep-underground-lab scales can be achieved by scaling time and space axis accordingly and was tested on hydraulic fracturing data from the Grimsel Rock Lab.

09. Deep geothermal energy, CO_2-storage and energy-related exploration of the subsurface

Marie Violay, Christophe Nussbaum, Benoît Valley, and Larryn Diamond

TALKS:

9.1 Eruteya O.E., Omodeo Salé S., Makhloufi Y., Guglielmetti L., Moscariello A.: Unravelling the 3D geometry and nature of sedimentary infill of the Permo-Carboniferous Grabens in St Gallen, Northern Switzerland: Implication on Geo-energy prospectivity

9.2 Hau K.P., Games F., Lathion R., Saar M.O.: Conceptual study about isolating CO_2 in the geological subsurface of the greater Eclépens area while producing geothermal energy

9.3 Guglielmetti L., Danillidis A, Valley B, Moscariello A: Favourability assessment for high temperature aquifer thermal energy (HT-ATES) storage in Switzerland based on play fairway analysis approach

9.4 van den Heuvel D.B., Richards J.P., Alt-Epping P., Wanner Ch., Diamond L.W.: Sandstones of the Lower Freshwater Molasse as reservoirs for high-temperature aquifer thermal energy storage (HT-ATES) – properties and expected mineral reactions

9.5 Lecampion B., Sáez A., Lu G.: Numerical modeling of fluid-induced crack growth for hydraulic stimulation design

9.6 Castilla R., Dyer B., Bethmann F., Alcolea A., Christe F., Serbeto F., Meier P., Hertrich M.: Preliminary analysis of hydraulic shear stimulations in the Bredretto Lab: The link with natural fractures

9.7 Ritz V.A., Rinaldi A.P., Wiemer S.: Evaluating injection strategies for EGS from the temporal evolution of the Gutenberg-Richter b-value.

9.8 Peruzzo C., Capron J., Lecampion B.: The breakthrough time of a hydraulic fracture contained between two tough layers.

9.9 Fryer B., Giorgetti C., Passelègue F., Violay M.: The Effect of Fault Roughness on Bare Surfaces in Load-Controlled Biaxial Experiments

9.10 Giorgetti C., Violay M.: The effect of fluid chemistry on the friction of carbonate faults

9.11 Shi P., Tuinstra K., Lanza F., Grigoli F., Rinaldi A.P., Fichtner A., Wiemer S.: Towards Real-time Monitoring of Induced Microseismicity in Enhanced Geothermal Systems

POSTERS:

P 9.1 Alt-Epping P., Diamond L.W., van den Heuvel D.B., Wanner C.: System-scale simulation of the thermal evolution and geochemical processes of the planned aquifer heat-storage (HT-ATES) project at Forsthaus, Bern, Switzerland

P 9.2 André M., Valley B., Sohrabi R.: Characterization of fractured and karstified limestone reservoir for Aquifer Thermal Energy Storage (ATES)

P 9.3 Richards J.P., di Lorenzo F., van den Heuvel D.B., Diamond L.W.: Experimental assessment of calcite scaling occurring during high-temperature aquifer thermal energy storage (HT-ATES)

P 9.4 Carbajal D., Peiffer L., Diamond L.W., Wanner C.: Exploration of amagmatic orogenic, fault-hosted geothermal systems using coupled thermal-hydraulic simulations

P 9.5 Crinière A., Moscariello A.: Reservoir geology of the Cretaceous-Cenozoic Transition in the context of geothermal exploration in the Geneva Basin and neighbouring France (Switzerland & France)

P 9.6 Guglielmetti L., Mondino F., Moscariello A., Perozzi L., Strobbia C.: Improved onshore subsurface seismic imaging: examples from the geothermal province of Tuscany (Italy)

P 9.7 Milo A., Valley B., Sohrabi R.: Thermo-Hydraulic behaviour in fractured limestone for Aquifer Thermal Energy Storage (ATES)

P 9.8 Figura F., Giorgetti C., Lebihain M., Violay M.: Evolution of the rate and state frictional parameters of carbonate bearing faults at the brittle-to-ductile transition

P 9.9 Guggisberg A., Passelègue F., Violay M.: Micromechanical Modelling of Elastic Wave Velocity Variations for Intact Brittle Rocks

P 9.10 Paglialunga F., Passelègue F., Lebihain M., Violay M.: On the scale dependence in the dynamics of frictional rupture

P 9.11 Zabihian F., Sohrabi R., Valley B.: Preliminary results from the analysis of stress profiles in deep geothermal reservoirs

P 9.12 Bröker K., Ma X., Doonechaly N.G., Wenning Q., Zhang S.,Hertrich M., Giardini D.: Hydro-geomechanical characterisation for upcoming hydraulic stimulation experiments at the Bedretto Underground Laboratory

P 9.13 Antunes V., Kraft T., Roth P., Toledo T., Wiemer S.: Results from the GEOEBST2020+ baseline seismic monitoring in the cantons of Vaud and Geneva

P 9.14 Houlie N., Martin F., Guglielmetti L., Meyer M.: Monitoring geothermal field Geo-01 using GPSs, seismometer and inclinometers.

P 9.15 Kraft T., Antunes V., Roth P., Wiemer S.: GEOBEST2020+: a framework for cantonal authorities to deal with induced seismicity risk in deep geothermal energy

P 9.16 Lanza F., Wiemer S.: The DEEP Project: Innovation for De-Risking Enhanced Geothermal Energy Projects

P 9.17 Lei Q., Brixel B.: Fluid Injection-Induced Off-Fault Deformation and Seismicity in Shallow Crustal Faults: Preliminary Results from Fully-Coupled Hydro-Mechanical Simulations

P 9.18 Moein MJA: Linkage between seismogenic index and fault network during fluid injections

P 9.19 Momeni S., Lu G., Lecampion B.: Automatic passive acoustic emission-microseismic monitoring using a parallel algorithm; A case study of a hydraulic-fracturing experiment

P 9.20 Muñoz F., Calò M., Lupi M., Reyes V.: Dedicated seismic study of the Domo de San Pedro geothermal field Nayarit, Mexico

P 9.21 Passarelli L., Rinaldi A.P.,Grigoratos I., Ciardo F., Broccardo M., Lanza F., Wiemer S.: How good are existing seismicity models at forecasting induced seismicity in EGS?

9.1
Unravelling the 3D geometry and nature of sedimentary infill of the Permo-Carboniferous Grabens in St Gallen, Northern Switzerland: Implication on Geo-energy prospectivity

Ovie Emmanuel Eruteya[1], Silvia Omodeo Sale[1], Yasin Makhloufi[1], Luca Guglielmetti[1], Andrea Moscariello[1]

[1] GE-RGBA Group, Department of Earth Sciences, University of Geneva, Rue des Maraîchers 13, CH-1205 Geneva, Switzerland (ovie.eruteya@unige.ch)

The nature and structural characteristics of most Late Palaeozoic basins in the Northern Alpine Foreland related to the Post-Variscan orogeny is associated with uncertainties and poorly constrained. This is related to the complexity of their deep structure buried by thick Mesozoic and Cenozoic sediments, coupled with the masking effect of the younger tectonic events. In addition to this is scarcity of deep boreholes penetrating the entire interval down to the crystalline basement.

Under the framework of the UNCONGEO project*, we have developed a new workflow to characterize the deeply buried Pre-Mesozoic grabens developed in the Swiss Plateau. In this presentation, we focus specifically on the St Gallen area in Northern Switzerland. Previous study in the St Gallen area suggested the presence of Permo-carboniferous sediments in the pre-Mesozoic graben-like structures separated by a horst. However, the size and nature of the infill of these grabens, was unresolved up to now. Here, the availability of the time-migrated St Gallen 3D seismic reflection dataset permits a robust 3D interpretation and visualization of these grabens aided by complex seismic attribute workflow (Fig. 1a).

We present an uncertainty-based 3D geometry of these grabens and the associated bounding and internal faults structures (Fig. 1b). For the first time, we attempt a subdivision of the grabens infill into Permian infill and Carboniferous infill using the Weiach-1 borehole tied to the Permo-Carboniferous seismic facies from the newly available depth-migrated seismic data from the Constance Frick trough as an analogue. This permitted providing a separate volumetric estimate of the Permian and Carboniferous sediments in the grabens (Fig. 1c). Subsequently, using a net-to-gross cut-off derived from the Weiach-1 borehole, volumes of source rock and reservoir rock in the Permian and Carboniferous infill across these grabens are estimated.

The findings from this study provide new insights into nature of the sedimentary infill in the St. Gallen Grabens. Importantly, the workflow developed reduces the uncertainties associated with constructing geological and reservoir models for geo-energy application here in Switzerland and elsewhere characterized by the presence of similar grabens. Accurate volumetric estimation of the graben infill as to either composed of source rock related to coals in the Carboniferous infill or lacustrine shales in the Permian infill and the tight siliciclastic reservoirs units have implication for the success of geothermal exploration project and sequestration capabilities of this region. Ultimately, the presence of these Permo-Carboniferous troughs within this segment of the Swiss Molasse Basin indicate unexplored post-Variscan geo-energy plays.

**The UNCONGEO project is funded by Swisstopo, the Federal Office of Energy, Canton of Geneva, Canton of Vaud and NAGRA*

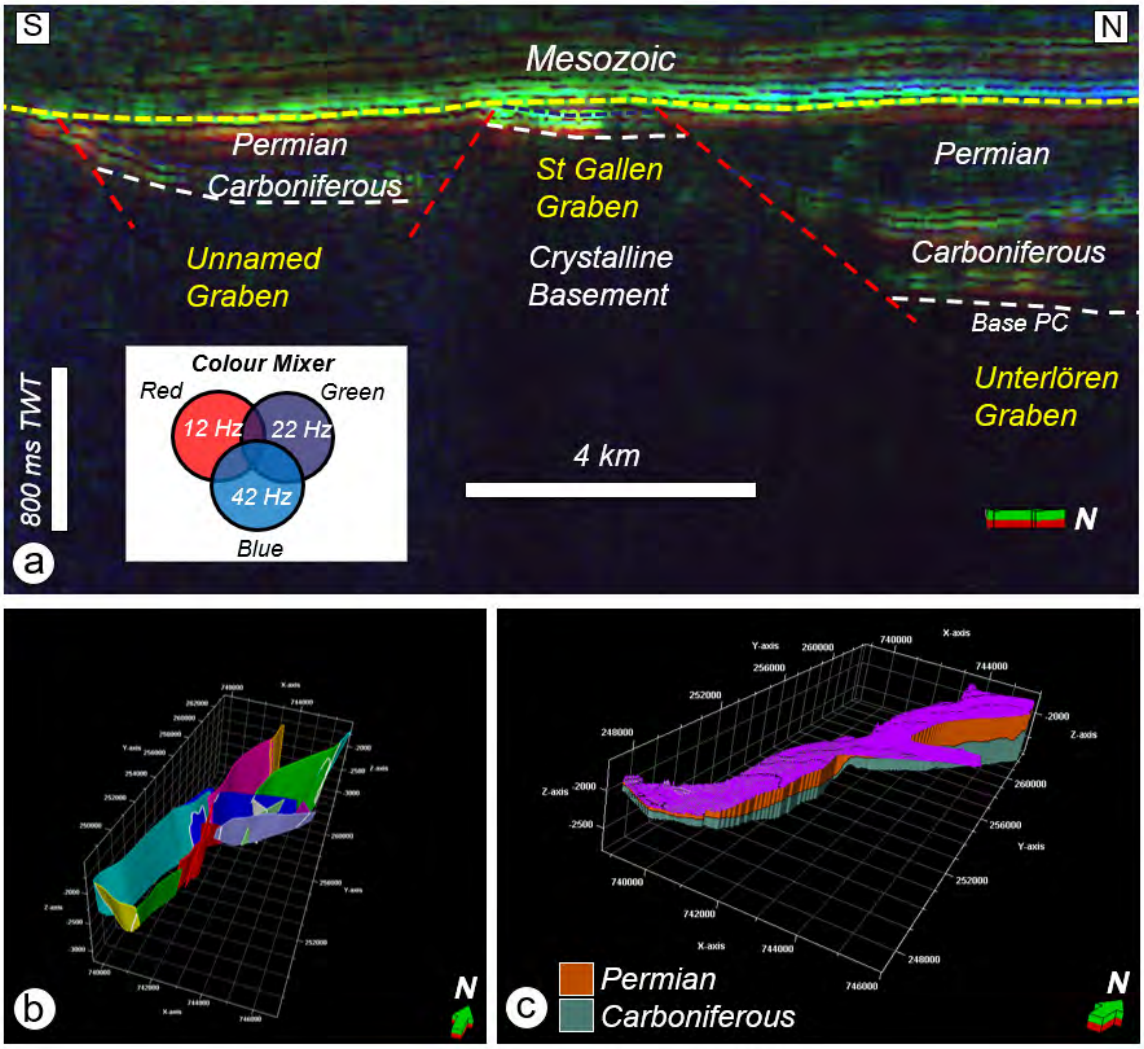

Figure 1.(a) Interpreted spectrally decomposed volume of the St Gallen 3D seimsic reflection dataset revealing the configuration of the grabens and infill. (b) Structural framework showing the bounding graben faults and internal faults. (c) Geological model showing the Permian and Carbonifeorus fill of the grabens.

9.2
Conceptual study about isolating CO_2 in the geological subsurface of the greater Eclépens area while producing geothermal energy

Kevin P. Hau[1], Federico Games[2], Rodolphe Lathion[2], Martin O. Saar[1,3]

[1] *Geothermal Energy and Geofluids, Department of Earth Sciences, ETH Zurich, Zurich, Switzerland; (hauk@ethz.ch)*
[2] *Swiss Geo Energy S.A., Payerne, Switzerland;*
[3] *Department of Earth and Environmental Sciences, University of Minnesota, MN, USA*

The heavy rainfall events during July 2021 in Western and Central Europe can be linked to human caused global warming. Among others, the occurring frequency of such events will increase if global greenhouse gas emissions are not drastically reduced soon (IPCCC, 2021).

Carbon, Capture and Storage (CCS) is considered essential for reaching a substantial reduction of the global CO_2 emissions. Capturing CO_2, from e.g. point sources, and injecting it in the geological subsurface, permanently isolates the greenhouse gas from the atmosphere. By circulating the injected CO_2 in a closed loop system - also known as CO_2 Plume Geothermal (CPG) systems - to extract geothermal energy, the disposed CO_2 can be utilised while permanently isolating the CO_2 from the atmosphere. (Figure 1). Moreover, the stable baseload of geothermal energy produced can possibly reduce the high costs normally associated with CCS (Randolph and Saar, 2011).

Our conceptual study first estimates the potential subsurface CO_2 storage capacity range within a seismic interpreted anticline structure in the Triassic sediments of the Swiss Molasse Basin in the greater Eclépens area (Allenbach et al., 2017). Secondly, we investigate numerically whether any of the injected CO_2 could possibly be circulated in a CPG-system. Finally, we aim to provide a first order estimate of the possible expected geothermal power of the site.

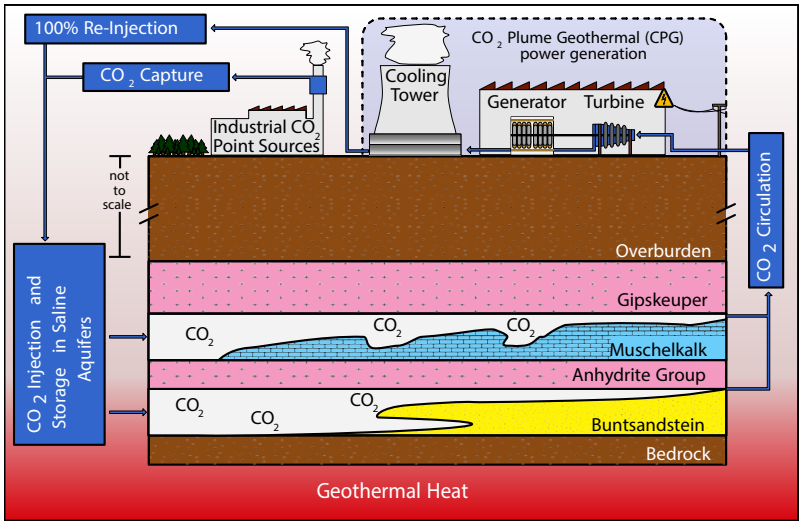

Figure 1. Schematic sketch visualising the combination of a conventional CCS-site with an integrated CPG-system in the Swiss Molasse Basin.

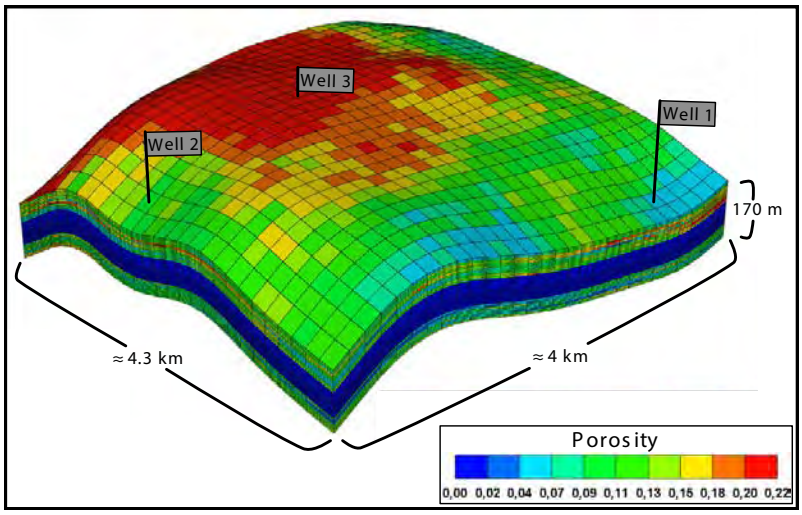

Figure 2. Arial view of the used geological model

The here presented study results are based on a concepual geological model covering an area of more than 17 km^2 (Figure 2). CO_2 injection was simulated at multiple locations with a minimum injection depth of 2 km. Multiple heterogeneous model realisations were obtained by geostatistcally distributing the possible expected porosity ranges. The porosity scales up the absolute permeability. Consequently, a “heterogeneous” absolute permeabilty distribution was obtained.
Among others, our simultaions include two-phase fluid flow with brine and CO_2 and the Peng-Robinson equation of state for dynamic modelling. Moreover, structural, hysteresis and solubilty trapping effects are inclduded in our simulations.

Overall, this study presents a first order assessment of the assumed anticline structure’s CO_2 storage capacity. Additionally, our study investigates reliable well operation constraints over multiple decades, and analyses the expected well flow regime in a potential CO_2 circulation operation.

ACKNOWLEDGMENTS

The first (Hau) and last (Saar) author thank the Werner Siemens Foundation (Werner Siemens-Stiftung) for its support of the Geothermal Energy and Geofluids (GEG.ethz.ch) group at ETH Zurich. Swiss Geo Energy S.A. thanks swisstopo for providing the geological 3D-Model for Switzerland - GeoMol.

REFERENCES

Allenbach, R., R. Baumberger, E. Kurmann, C. Michael, and L. Reynolds (2017*). GeoMol: Geologisches 3D-Modell des Schweizer Molassebeckens: Schlussbericht*. Vol. 10. Wabern: Bundesamt für Landestopographie swisstopo, p. 128. isbn: 978-3-302-40109- 6.

IPCC (2021). “Summary for Policymakers”. In: *Climate Change 2021: The Physical Science Basis. Contribution of Working Group I to the Sixth Assessment Report of the Intergovernmental Panel on Climate Change*, Cambridge University Press. In Press.

Randolph, J. B. and M. O. Saar (2011). “Combining geothermal energy capture with geologic carbon dioxide sequestration”. In: *Geophysical Research Letters* 38.10, n/a– n/a. doi: 10.1029/2011gl047265.

9.3
Favourability assessment for high temperature aquifer thermal energy (HT-ATES) storage in Switzerland based on play fairway analysis approach

Luca Guglielmetti[1], Alexandros Danillidis[1], Benoît Valley[2], Andrea Moscariello[1]

[1] Department of Earth Sciences, University of Geneva. Rue des Maraichers 13, 1205 Geneva (luca.guglielmetti@unige.ch)
[2] Centre d'hydrogeologie et geothermie, Université de Neuchatel. Rue Emile Argand 11, 2000 Neuchatel

This study is carried out in the framework of the ERA-Net/GEOTHERMICA project HEATSTORE and focuses on the development of a framework for the assessment of the favourability for HT-ATES development in the Swiss Molasse Plateau (SMP) centered on multi-criteria spatial analysis. The assessment is based on the combination of subsurface favourability indicators with energy system components including availibility of excess heat,heat demand as well as proximity to thermal networks and waste incineration plants. The choice of focussing on the SWM was driven by the availability of public subsurface data (3D geologic model available from Swisstopo), which at present only cover this region. The two targets for which favourability is assessed are the Cenozoic Molasse (e.g. target of the Bern pilot site) and the Upper Mesozoic carbonates (e.g. target of the Geneva pilot site). A minimal temperature threshold is set to 25˚C which is the temperature commonly considered as separating low temperature ATES from HT-ATES systems. These two units show different lithological, petrophysical and hydraulic conditions, locally enhanced by lithological heterogeneities in the Cenozoic Molasse and by enhanced fracture conditions thanks to the presence of fault corridors in the Mesozoic. In addition, a maximal depth of 2000m was set as boundary as it was arbitrarily considered as a reasonable largest depth for the techno-economic favourable implementation of HT-ATES systems

In this study we applied a five-step method to locate favourable areas in SMP according to the following steps:

1. First, a geothermal play analysis approach was applied to identify and weight the subsurface elements controlling the circulation of fluids in the area.
2. Second a data reliability assessment was carried out based on the proximity from the main source of subsurface data (i.e. exploration wells and 2D-3D seismic surveys).
3. Third the storage capacity was computed according to the 3D geometries and temperature distribution from the GeoMol model and petrophysics properties from literature data
4. The fourth step, was to embed int eh workflow heat demand and excess heat data
5. The final step was then to integrate the different favourabilities into a combined favourability index, calculated, multiplying the proximity scores of each compoenent by their weight

$$I(x_{ij}) = x'_{ij} \cdot w$$

The final favorability index that combines all the individual favorability indexes is given by the weighted average scheme:

$$I_{comb} = \frac{\sum_{i=1}^{n} I(x_{ij})}{\sum_{i=1}^{n} w}$$

The results reveal different levels of favourability in the Cenozoic sediments and in the faulted Upper Mesozoic Carbonates (Figure 1).

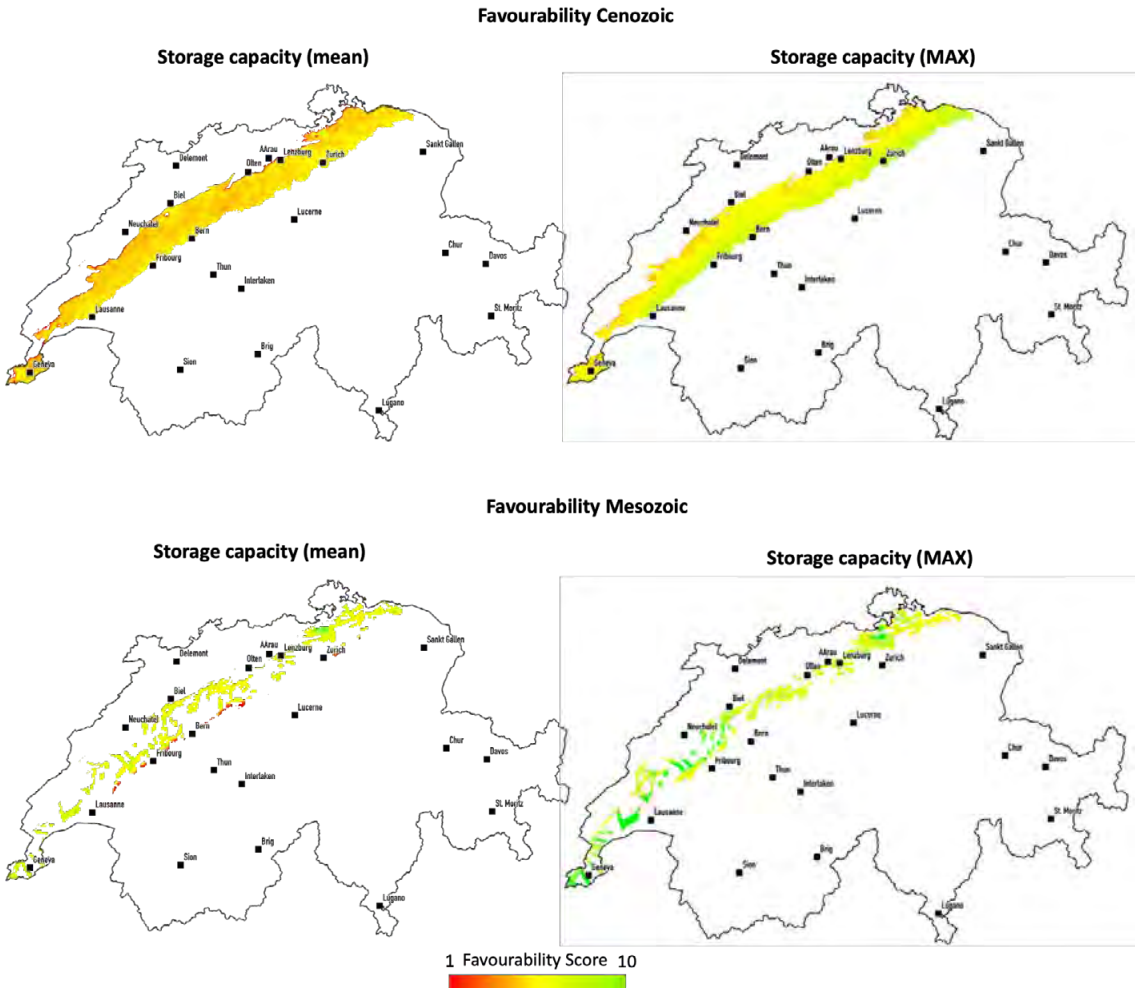

Figure 1. Favourability maps implemented in this study for the Cenozoic (upper maps) and Mesozoic units (lower maps)

9.4
Sandstones of the Lower Freshwater Molasse as reservoirs for high-temperature aquifer thermal energy storage (HT-ATES) – properties and expected mineral reactions

Daniela B. van den Heuvel, Joshua P. Richards, Peter Alt-Epping, Christoph Wanner, Larryn W. Diamond

Institut für Geologie, University of Bern, Baltzerstrasse 3, CH-3012 Bern (daniela.vandenheuvel@geo.unibe.ch)

Usage of excess thermal energy (e.g. process heat from industry) is a way to reduce the carbon footprint of the heating sector. While the heat supply is relatively constant year round, the demand for energy for spatial heating is highly seasonal. To cover this gap, thermal energy needs to be stored throughout the warm months. One approach is high-temperature aquifer thermal energy storage (HT-ATES) where hot water is injected into a geological reservoir over summer and retrieved and fed into a district heating network during winter. During the storage period, the injected water will interact with the minerals in the reservoir formation, leading to dissolution and potential precipitation. As these processes can affect permeability and integrity of the formation as well as change the composition of the working fluid, understanding them is crucial when making site-specific predictions.

One geological reservoir under consideration in the Bern area is the meander belt sandstones of the Lower Freshwater Molasse. We have compiled relevant properties from the literature and characterised additional samples to obtain information on the composition and reservoir properties of these units. In addition, we have performed batch experiments where a disaggregated sandstone was mixed with an artificial USM groundwater and left to react for 3 months at 25, 60 and 90°C. Based on the compositional differences of the solution before and after the experiments and coupled kinetic modelling, the following crucial processes could be identified: (1) Dissolution dominates over precipitation, likely increasing the overall permeability of the reservoir; (2) albite, K-feldspar, quartz/chalcedony, various sheet silicates and calcite dissolve to increase the concentrations of Na, K, Si, Ca and HCO_3; (3) an as yet unidentified solid (likely poorly crystalline Mg-alumosilicate) precipitates to remove Mg from solution.

In the long-term, these results will be used to calibrate the 3D reactive transport simulations presented by Alt-Epping et al. (abstract also submitted to this session) and the reaction rates will be used to assess the scaling potential of the groundwater equilibrated during the storage interval.

9.5
Numerical modeling of fluid-induced crack growth for hydraulic stimulation design

Brice Lecampion[1], Alexis Sáez[1], Guanyi Lu[1]

[1] *Geo-Energy Lab – Gaznat chair on Geo-Energy, EPFL, Lausanne, CH 1015*

Hydraulic stimulation of deep geothermal reservoirs (in crystalline rocks) is necessary in order to establish economical flow rates between the injector and producer wells. Previous field experience in deep crystalline reservoirs have highlighted the importance to stimulate the well by zones in order to create several fractures along the well instead of carrying out a single large stimulation which typically results in the reactivation of very few fractures along the open-hole section – thus resulting in poor reservoir coverage and low flow transmissivity. Localized hydraulic stimulation can be performed via packer-systems, and although different in their details, share similarities with stimulation operations performed in unconventional oil and gas reservoirs. The main differences are that i) propping agents are not typically used in deep geothermal reservoirs, ii) the injection pressure often remains lower than the minimum in-situ stress and iii) the long-term increase of permeability relies on the self-propping effect associated with the shear dilatant behaviour of pre-existing fractures. The type of fractures propagated during hydraulic stimulation thus exhibit both shear and tensile modes of deformation (different than the purely tensile hydraulic fractures).

Physics-based models are necessary in order to design the injection sequence and are typically used in conjunction with uncertainty analysis. We report our developments of a three-dimensional numerical model for the hydraulic stimulation of pre-existing fractures accounting for both shear and opening modes of deformation. The fracture behavior is modelled via a non-associated Mohr-Coulomb frictional elasto-plastic law with possible weakening/hardening of friction and dilatancy with slip, while the host rock is assumed linearly elastic. The fluid flow behaviour of the fracture accounts for opening and the associated permeability / storativity changes (with the possibility to use different type of permeability law). We solve in a fully coupled manner the resulting non-linear moving boundary hydromechanical problem. The mechanical balance of momentum is solved using a collocation boundary element method while fluid flow in the fractures is discretized with finite elements. The non-linear coupled problem is solved using a Newton-Raphson scheme at each increment of time, and the tangent coupled system is solved by a block conjugate gradient solver. The non-linear elastoplastic relation of the fracture is integrated using an implicit elasto-plastic return mapping scheme, and the consistent tangent operator for the fracture deformation is consistently used to build the jacobian of the tangent system.

We present several verification tests for the growth of a shear crack growth in the plane of a pre-existing frature under the injection of fluid at constant rate in both 2D and 3D. Especially, we compare our numerical results with recent analytical solutions for the case of constant friction and constant hydraulic properties of the pre-existing fracture. We then discuss several examples combining shear dilatancy and its effect on flow properties as well as the possible tensile opening of the pre-existing stimulated fracture. Accuracy, robustness and numerical performance – critical for the use of the solver for engineering design - will be discussed as well as future improvements.

This work is sponsored by Geo-Energie Suisse A.G. and the Swiss Federal Office of Energy.

REFERENCES

Ciardo F. and Lecampion B. 2019: Effect of dilatancy on the transition from aseismic to seismic slip due to fluid injection in a fault. Journal of Geophysical Research: Solid Earth, 124:3724—3743.

Garagash D. I. and Germanovich L. N. Nucleation and arrest of dynamic slip on a pressurized fault. Journal of Geophysical Research: Solid Earth (1978–2012), 117(B10), 2012.

Viesca R. C. 2021: Self-similar fault slip in response to fluid injection. arXiv preprint arXiv:2102.03123.

Bhattacharya P. and Viesca R. C. 2019: Fluid-induced aseismic fault slip outpaces pore-fluid migration. Science, 364(6439):464–468

Sáez, A. and Lecampion, B. and P. Bhattacharya and R. C. Viesca 2021: Three-dimensional fluid-driven stable frictional ruptures, under review - Journal of the Mechanics and Physics of Solids.

9.6
Preliminary analysis of hydraulic shear stimulations in the Bredretto Lab: The link with natural fractures.

Raymi Castilla[1], Ben Dyer[1], Falko Bethmann[1], Andrés Alcolea[1], Fabien Christe[1], Francisco Serbeto[1], Peter Meier[1], Marian Hertrich[2].

[1] Geo-Energie Suisse, Reitergasse 11, 8004 Zürich (r.castilla@geo-energie.ch)
[2] ETH Zürich, Dep. of Earth Sciences. BULGG - Bedretto Underground Lab

Three stimulation treatments were performed in the Bedretto Lab during 2020 by Geo-Energie Suisse. The locations of microseismic events as well as image logs taken before and after were analyzed to characterize the results of these stimulations.

Millimetric, permanent displacements were identified in pre-existing, natural fractures after stimulation treatments. The measured displacement vectors are consistent between different structures. The deformation can be measured weeks after the end of the stimulation indicating the permanent character of shear displacements.

Micro-seismicity clouds were analyzed to find links with the previously established structural model. Simple linear fitting methods were used to find planes formed by seismicity clusters. The search for planes was carried out using 3 different methods: 1) A “brute force” method was used to find statistically dominant orientations, 2) A semi-manual method fitting one plane to events grouped by clusters or stimulation intervals and, 3) A fully-manual method, fitting planes to lineaments identified by visual inspection of the clouds.

In general, a dominant orientation approximately perpendicular to the boreholes was found in all clouds across all three methods. This direction is present in the lab, especially near the bottom of long boreholes. The orientations found in this analysis represent general trends and alignments at the scale of the whole cloud. Individual events might be associated with different orientations.

The observations described here show the effectiveness of a multistage stimulation protocol to reactivate pre-existing structures

9.7
Evaluating injection strategies for EGS from the temporal evolution of the Gutenberg-Richter b-value.

Vanille A. Ritz*, Antonio P. Rinaldi*, and Stefan Wiemer*

** Swiss Seismological Service at ETH, Sonneggstrasse 5, CH-8092 Zürich, Switzerland (vanille.ritz@sed.ethz.ch)*

Induced seismicity is a hot topic within geo-applications, however the physical mechanisms driving the induced ruptures is yet to be fully understood. The injection of fluid in the subsurface in particular has been shown to cause changes in the stress field leading to the induction of eqarthquakes. Recent events in Switzerland (Basel, Sankt-Gallen) and abroad (Pohang) have shown that such injection operations can have dramatic consequences. The hazard associated with these earthquakes thus needs to be managed to prevent infrastructure damages and protect both the population and viability of the project. The Gutenberg-Richter b-value has been used as a proxy for the state of stress in the subsurface. The temporal evolution of the b-value provides statistical tools to estimate the seismic hazard posed by an earthquake sequence. Thus, monitoring and forecasting changes in the b-value could be used as a proxy in a near-real-time mitigation context (Adaptive Traffic Light System). Several studies have looked at the evolution of the b-value both in time and space, for example in Basel, where the observed b-value dropped before shut-in and further away from the injection well□. We present a numerical approach coupling a fluid flow simulator with a geomechanical-stochastic formulation (TOUGH2-Seed) to simulate injection-induced seismicity-sequences. We model a Hot Dry Rock-type setting, and we investigate the variation of b-value during injection-induced seismic sequences with different injection scenarios and levels of complexity as to the geological features.

REFERENCES

Bachmann, C. E., Wiemer, S., Goertz-Allmann, B. P. & Woessner, J. *Influence of pore-pressure on the event-size distribution of induced earthquakes.* Geophys. Res. Lett.39, 1–7, DOI: 10.1029/2012GL051480 (2012).

Rinaldi, A. P. & Nespoli, M. *TOUGH2-seed: A coupled fluid flow and mechanical-stochastic approach to model injection-induced seismicity.* Comput. Geosci.DOI: 10.1016/j.cageo.2016.12.003 (2016).

Herrmann, M., Kraft, T., Tormann, T., Scarabello, L. & Wiemer, S. A *Consistent High-Resolution Catalog of Induced Seismicity in Basel Based on Matched Filter Detection and Tailored Post-Processing*. J. Geophys. Res. Solid Earth124,8449–8477, DOI: 10.1029/2019JB017468 (2019).

9.8
The breakthrough time of a hydraulic fracture contained between two tough layers

Carlo Peruzzo[1], Judith Capron[1], Brice Lecampion[1]

[1] *Geo-Energy Lab - Gaznat chair in Geo-Energy, EPFL, EPFL-ENAC-IIC-GEL, Station 18, CH-1015 Lausanne (carlo.peruzzo@epfl.ch)*

Hydraulic fracturing is a widespread technology used to enhance reservoir production but also to measure the in-situ stress field. It consists of growing a tensile (mode I) fracture via the injection of a viscous fluid (usually at a constant rate) from a wellbore. Hydraulic fracturing treatments vary widely in scales, rates and volumes injected. For example, a well stimulation operation typically consists in injecting up to 100'000 liters at a rate of about 20-50 liters per second, while only ~5 liters are injected over the two-three minutes of the duration of an injection cycle of a micro-hydraulic fracturing stress measurement. The main risk associated with hydraulic fracturing treatment relates to vertical fracture growth above the desired formation of interest, toward environmentally sensitive layers. In sedimentary basins, characterised by rock strata at different scales, hydraulic fractures are typically observed to be contained at depth and propagate horizontally in a "finger-like" geometry (Economides & Nolte 2000, Bunger & Lecampion 2017). Such containment is usually explained by the increase of the horizontal confining stress in the layers above and below the stimulated reservoir. Of course, variation of material properties such as elastic modulus, permeability, fracture toughness can also contribute to containment (Simonson et al. 1978, Thiercelin et al. 1989).

In this work, we consider the symmetric scenario where the injection point is located at the center of a layer of height H bounded by two layers of similar properties. We investigate the case where the material fracture toughness in the central layer is lower than in the bounding layers, assuming the other properties to be uniform (see Fig. 1). We focus on the so-called toughness dominated regime, where the fluid viscous energy is negligible compared to the energy spent in creating new fracture surfaces. By means of numerical simulations and scaling analysis, we establish whether, or not, a fluid-driven fracture can remain confined between the two tough layers. We show that a ratio of fracture toughness between the layers larger than is sufficient to contain indefinitely the growing hydraulic fracture. For toughness ratios lower than that limit, we estimate the amount of time the propagating fracture remains contained before breaking through. Finally, we discuss how a finite amount of fluid viscous energy affects containment in that configuration.

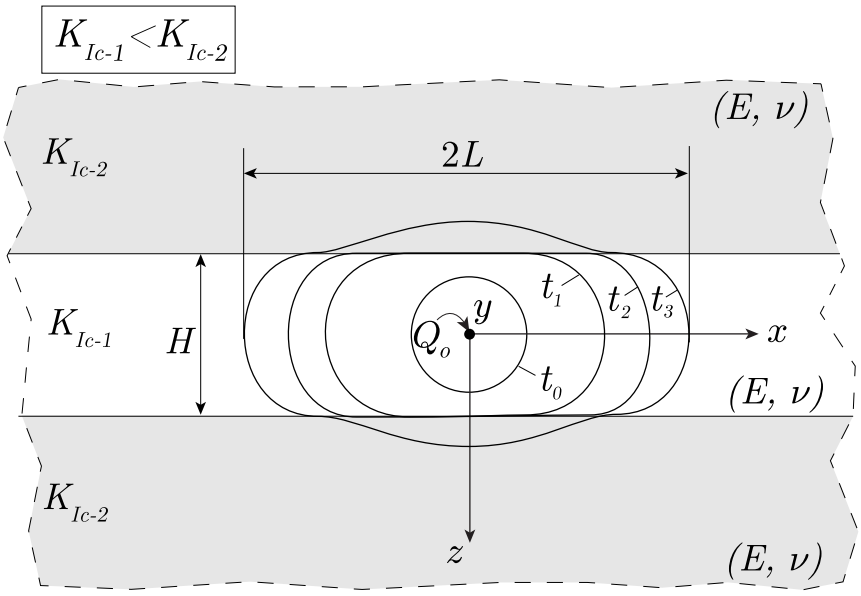

Figure 1. Sketch of a three-layer scenario with fracture footprints at times t_0 , t_1, t_2 and t_3. The central layer of height is characterized by a fracture toughness . It is bounded from both sides by two semi-infinite layers of fracture toughness >. All layers are assumed to be impermeable and to behave as a linear elastic material with the same Young›s modulus and Poisson›s ratio . A radial fracture propagates from the center of layer 1 driven by the injection of an inviscid fluid at a constant rate . The fracture propagates radially (footprints) until it reaches the bounding layers. From that moment, the propagation continues only along with the central layer (footprints), before possibly breaking through into the bounding layers (footprint).

REFERENCES

Bunger, A. P. & Lecampion B. 2017: Four critical issues for successful hydraulic fracturing applications. In X.-T. Feng, editor, Rock Mechanics and Engineering, volume 5 (Surface and Underground Projects), chapter 16. CRC Press/Balkema.

Economides, M. J. & Nolte K. G. 2000: Reservoir Stimulation. John Wiley & Sons.

Simonson, E.R., Abou-Sayed, A.S. & Clifton, R.J. 1978: Containment of Massive Hydraulic Fractures. SPEJ 18 (1): 27–32. SPE-6089-PA.

Thiercelin, M., Jeffrey, R.G. & Ben Naceur, K. 1989: Influence of Fracture Toughness on the Geometry of Hydraulic Fractures. SPEPE 4 (4):435–442; Trans., AIME, 287. SPE-16431-PA.

9.9
The Effect of Fault Roughness on Bare Surfaces in Load-Controlled Biaxial Experiments

Barnaby Fryer[1], Carolina Giorgetti[1], François Passelègue[1], Marie Violay[1]

[1] *Laboratory of Experimental Rock Mechanics, EPFL, Station 1018, 1015 Lausanne (barnaby.fryer@epfl.ch)*

Induced seismicity has become a key talking point point in CO_2 sequestration and especially Enhanced Geothermal Systems. Fault slip behavior and earthquake nucleation are often framed within the context of velocity-dependent friction, ranging from velocity-strengthening to velocity-weakening behaviour. Previous studies have shown that fault roughness controls the fault slip behavior, with rougher faults having a greater tendency to be velocity-strengthening. However, it is not clear how the spontaneous transition from velocity-strengthening to velocity-weakening occurs nor what the role of roughness is.

Using the High Strain TEmperature Pressure Speed (HighSTEPS) low to high velocity biaxial friction apparatus located at the EPFL in Switzerland, this transition has been investigated with load-controlled experiments. Creep in biaxial apparatuses has rarely been investigated, but this approach allows for a development of slip which is spontaneous and a loading which is more readily compared to natural seismicity.

The investigation concerns bare surface norite samples with customized roughnesses. The samples were loaded to a normal stress of 20 MPa and then a shear stress of 8 MPa. The applied shear stress was held for 1000 seconds before the shear stress was increased in a step-wise fashion by 0.4 MPa, until the sample achieved a shear displacement of 25 mm (typically around 18 MPa). Typical mechanical data, such as the horizontal and vertical displacements and forces, were collected. The samples/sample holder were also equipped with 12 P-wave acoustic sensors.

Smoother samples exhibited larger and more frequent stress drops than rougher samples, with reactivation at lower strength. Slip velocity was also observed to be higher for smooth samples. Localized acoustic emissions were used to assess the degree of localization and provide insight into the relative magnitude distributions for each roughness.

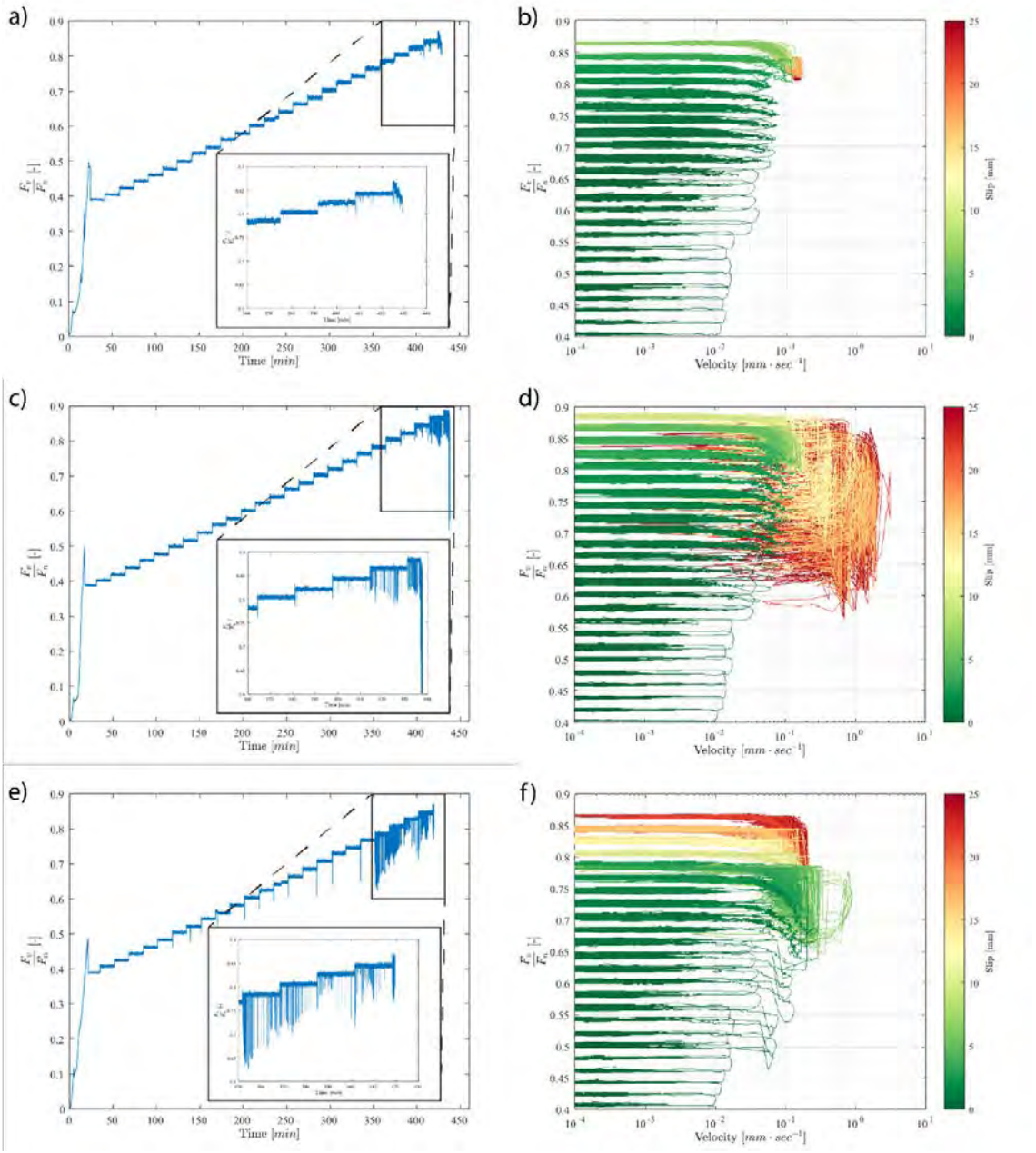

Figure 1. (a,b) represent the roughest, (c,d) the intermediate, and (e,f) the smoothest sample tested. (a,c,e) An overview of the development of the ratio between vertical and horizontal force on the sample throughout the experiment. The inset shows the final few steps of each experiment. (b,d,f) The shear velocity development as the ratio between vertical and horizontal force was increased. The accumulated slip is given by the color bar.

9.10
The effect of fluid chemistry on the friction of carbonate faults

Carolina Giorgetti[1], Marie Violay[1]

[1]*Laboratory of Experimental Rock Mechanics, EPFL, Rte Cantonale, CH-1015 Lausanne, Svizzera (carolina.giorgetti@epfl.ch)*

Pressure-solution is a key deformation mechanism in carbonate faults. The role of water pH and dissolved ions on the kinetics of calcite pressure-solution has long been investigated under static conditions. However, how water chemistry influences the frictional properties of carbonate rocks is still not fully constrained. To investigate this, we have conducted shear experiments on experimental faults, both bare surfaces and gouge, of Carrara Marble at 5 MPa of normal stress. The faults have been sheared with different fluids: 0.4 M $MgSO_4$ solution using $CaCO_3$-equilibrated water as solvent (pH ≈ 9), 0.4 M Na_2SO_4 solution using $CaCO_3$-equilibrated water as solvent (pH ≈ 9), $CaCO_3$-equilibrated water (pH ≈ 9), and acidic water prepared adding HCl to water (pH ≈ 4). Slide-hold-slide (SHS) sequences (1 - 3000 s) and velocity-stepping sequences (1 - 100 µm/s) have been conducted to evaluate respectively the ability of the fault to regain strength during the interseismic periods and the potential for earthquake nucleation. Additionally, we have conducted creep experiments under the same boundary conditions, increasing the shear stress step-wise by 0.3 MPa each 20 minutes.

Interestingly, the frictional behavior is influenced more by the Mg^{2+} ions dissolved in water at the equilibrium with the rock than by the pH, i.e. water at the disequilibrium with the rock. Particularly, when Mg^{2+} is dissolved in the water the frictional healing is low and the *(a-b)* parameter is high. The presence of Na^+ affects less the frictional behavior, leading to high healing and slightly velocity-strengthening behavior, similarly to $CaCO_3$-equilibrated and acidic water. Fault compaction and/or dilation during SHSs and shear-stress-controlled expriments is smaller when the water is at the disequilibrium with calcite (acidic water) suggesting that in this case pressure-solution is not an efficient mechanism. Consistently, in shear-stress-controlled experiments in the presence of $CaCO_3$-equilibrated water and Na^+ ions, the minimum creep rate increases with the increasing applied shear stress. In the presence of Mg^{2+} ions, the creep rate tends to increase with increasing shear stress as well, but it is more variable and the fault slip shows slow acceleration pulses also at shear stress values that are lower than the maximum shear stress. In contrast, in the presence of acidic water, the minimum creep rate is constant and it does not depend on the shear stress value, until the maximum shear stress is achieved and the fault slip accelerates.

Although it is well known that Mg^{2+} slows down pressure-solution, we show how this mechanism can stabilize carbonate faults. In natural carbonate-bearing faults, dissolved ions can derive from the alteration of other minerals, potentially changing the efficiency of pressure-solution and the overall fault frictional behavior. Our study has also implications for acidic fluids injections in geo-reservoirs and the related induced seismicity.

9.11
Towards Real-time Monitoring of Induced Microseismicity in Enhanced Geothermal Systems

Peidong Shi[1], Katinka Tuinstra[1], Federica Lanza[1], Francesco Grigoli[2], Antonio Pio Rinaldi[1], Andreas Fichtner[3], Stefan Wiemer[1]

[1] Swiss Seismological Service, ETH Zurich, Sonneggstrasse 5, CH-8092 Zurich (peidong.shi@sed.ethz.ch)
[2] Department of Earth Sciences, Università di Pisa, Lungarno Pacinotti 43, 56126 Pisa
[3] Institute of Geophysics, ETH Zurich, Sonneggstrasse 5, CH-8092 Zurich

In Enhanced Geothermal systems (EGS), real-time monitoring of the induced seismic events is crucial for assessing the stimulation effects as well as mitigating the induced seismic risk. Here we develop a new framework to detect micro-seismic events and simultaneously build earthquake catalogs directly from continuous seismic data. The new framework combines machine learning (ML) and waveform migration techniques (Grigoli et al. 2018), and harnesses the advantages provided by both methods. The proposed method does not require phase detection nor association, instead the probabilities of P- and S-phases generated by ML models are directly back-projected into the space and time domain to obtain source location and origin time. The automated nature and parallel efficiency make it capable of real-time monitoring. We present a real-data application to continuous data from the Hengill geothermal site in Iceland. To obtain accurate relative event locations, we further propose an innovative high-resolution earthquake relative relocation technique that makes use of the emergent Distributed Acoustic Sensing (DAS) sensors. In this new approach, we adapt the software package HADES (Grigoli et al. 2021) to work for the multitude of channels that DAS offers and compute the relative distance between clustered earthquakes from the S- and P-wave arrival time differences, leading to event locations in a relative frame. The correct orientation and position of seismic cluster are found by minimising the differences between observed and calculated S- and P-wave arrival times. Tests show that with a good estimate of the local velocity, the location and orientation of the seismic cluster can be retrieved.

We will apply the proposed approaches to the data set from the Utah FORGE EGS site and test the real-time performance of induced seismicity monitoring during the upcoming enhanced geothermal stimulation. The developed methods and operational experience will offer a unique opportunity for testing an operational real-time seismic monitoring system in EGS and could have a profound impact on the geothermal energy exploitation in Switzerland.

REFERENCES

Grigoli, F., Ellsworth, W. L., Zhang, M., Mousavi, M., Cesca, S., Satriano, C., Beroza, G. C., & Wiemer, S. 2021: Relative earthquake location procedure for clustered seismicity with a single station, Geophysical Journal International, 225(1), 608-626.

Grigoli, F., Scarabello, L., Böse, M., Weber, B., Wiemer, S., & Clinton, J. F. 2018: Pick-and wavform-based techniques for real-time detection of induced seismicity. Geophysical Journal International, 213(2), 868-884.

P 9.1
System-scale simulation of the thermal evolution and geochemical processes of the planned aquifer heat-storage (HT-ATES) project at Forsthaus, Bern, Switzerland

Peter Alt-Epping, Larryn W. Diamond, Daniela B. van den Heuvel & Christoph Wanner

Institute of Geological Sciences, University of Bern, Baltzerstrasse 3, CH-3012 Bern (alt-epping@geo.unibe.ch)

The “Geospeicher Forsthaus” project in Bern aims to develop a HT-ATES (High Temperature Aquifer Thermal Energy Storage) system within the Tertiary sediments of the Lower Freshwater Molasse (USM). The system will use excess heat from the nearby “Energiezentrale Forsthaus” to produce hot water that is injected into USM during warm months of the year and will retrieve hot water from the aquifer during times of heat demand during winter. Heat will be retrieved via a heat exchanger and fed into the district heating network.

The USM is a fluvial sequence of alternating permeable medium- to coarse-grained channel sandstones and clay-rich low-permeability floodplain deposits. The permeable sandstones constitute the reservoir rock. The layout of the planned HT-ATES consists of a central injection/ production well surrounded by up to five peripheral supporting wells. The supporting wells are used to regulate the flow, to maintain the desired reservoir pressure and to provide a connection to the surface installation, so that the reservoir, the wells and the surface installation (e.g. the heat exchanger) form a closed circulation system.The main well extends to a depth of 500 m, penetrating 150 m of Quaternary sediments and 350 m of USM. Individual sandstone channels of the USM have a thickness of 2 to 15 m and a substantial porosity (6 – 25 vol.%) and permeability (≤ 5.6e-12 m^2), but limited spatial extent.

As part of the planning stage, a system-scale 3D coupled thermal-hydraulic-chemical model of the Forsthaus HT-ATES was constructed to assess, among other things, the implications of mineral reactions on the porosity and permeability of the reservoir rock and of mineral scaling in the wells and the heat exchanger. The model includes a generic succession of sandstone and clay layers of variable thickness and the envisaged arrangement of wells (Figure 1A). The main and supporting wells are spaced 50 m apart. Formation water from the sandstones is heated to 90 °C at the surface and reinjected into the reservoir. The sandstone is composed of quartz, feldspars, mica/clay minerals, calcite and minor dolomite. The following yearly pumping schedule was applied over a simulated operation period of 2 years:

- 214 days injection of 90 °C water at 25 l/s
- 2 days rest
- 147 days extraction at 25 l/s
- 2 days rest

Results show that the ATES is feasible in principle (Figures 1B and 2). Upon injection of hot water into the permeable sandstone layers, the low-permeability clay units are heated conductively. As a result the reservoir heats up over time. Calcite is the most reactive mineral, showing a complex pattern of dissolution and precipitation in the reservoir after several injection/extraction cycles (Figure 1C). Silicate minerals dissolve as the reservoir is heated. Overall, the amounts of minerals dissolving/precipitating in the reservoir are small and not expected to degrade permeability or injectivity. There is, however, a potential for significant scaling in the heat exchanger during the loading cycle owing to the retrograde solubility of calcite. Low-temperature clay/amorphous silicate minerals precipitate in the heat exchanger during unloading due to their prograde solubility, but their amount is negligible. Based on these simulations, there is no indication of a severe problem related to chemical processes that would call for abandoning the project at this stage.

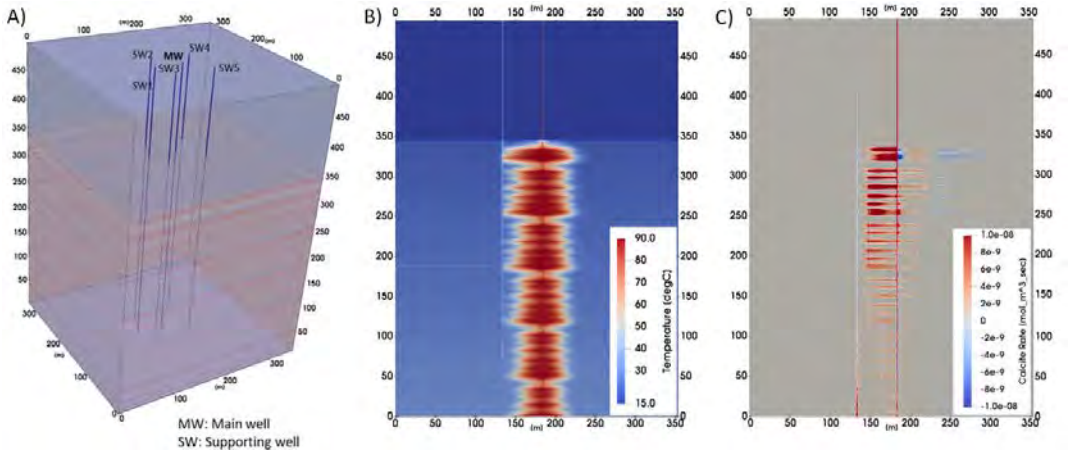

Figure 1. Panel A: 3D domain with stratigraphic succession of the USM (sandstones in red) overlain by 150 m of homogeneous Quaternary deposits and the arrangement of wells. Panel B: Temperature distribution after the first loading cylce. Panel C: Distribution of rates of calcite dissolution (< 0) and precipitation (> 0) after the second unloading (i.e. after two years of operation).

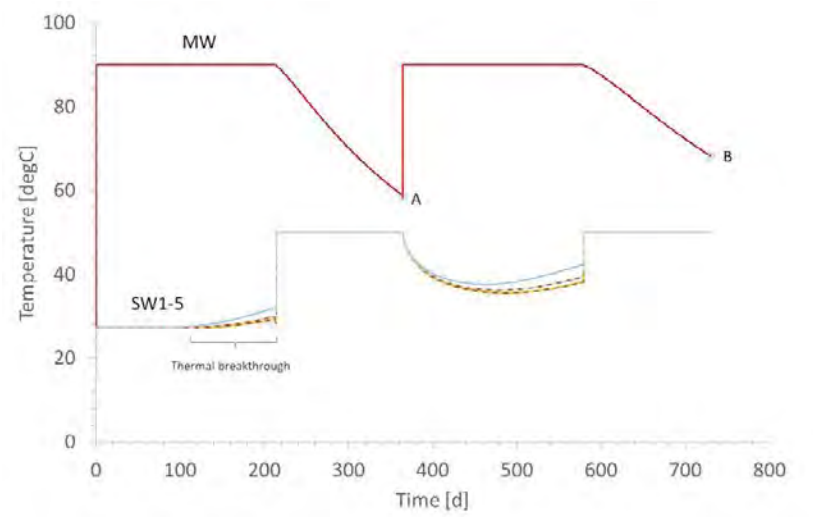

Figure 2. Temperature evolution at the wellheads. The temperature of the water extracted through the main well (MW) increases over time (see points A and B marking the ends of two successive extraction cycles), and so does the water discharging from the supporting wells (SW) during injection through the MW. This indicates a gradual heating of the reservoir. Note the temperature increase of the water discharging from the supporting wells during injection into the MW. This is indicative of a slight “thermal short circuit”, which can be remedied by increasing the spacing between the wells.

P 9.2
Characterization of fractured and karstified limestone reservoir for Aquifer Thermal Energy Storage (ATES)

Matthieu André, Benoît Valley, Reza Sohrabi

Centre for Hydrogeology and Geothermics (CHYN), University of Neuchâtel, Neuchâtel, Switzerland (matthieu.andre@unine.ch)

In order to support the transition to sustainable, low-carbon energy systems, it is essential to use all available options to reduce fuel consumption for heat production. To make efficient use of available heat, it is necessary to be able to store surplus heat during periods of low demand and high availability. One solution with great potential is the storage of heat in aquifers (Aquifer Thermal Energy Storage, ATES). In order to enable a wide use of this potential, it is necessary to broaden the type of aquifers in which heat storage is possible. Fractured and karstified limestone aquifers are widely available. However, the very heterogeneous nature of flows in these media implies that heat transport and exchange is complex. In order to establish the feasibility and design of heat storage in this type of aquifer, it is necessary to develop characterization strategies for these media that are relevant for heat transport and storage.

The specificity of heat transport in fractured and karstified media is the combination of dominant advective transport in fracture planes and karst conduits with conduction toward the bulk of the rock matrix for storage. The geometry and contact area between the fracture/karst system and the matrix dominate the efficiency of the later. Furthermore, when considering flow in deep systems, a strong coupling between fracture aperture, fluid pressure and fluid flow is possible which requires the consideration of the mechanical conditions in the reservoir. A challenge for the development of ATES in fractured and karstified limestone reservoir is to develop relevant characterization strategies for acquiring the necessary parameters for simulating the complex combinations of these processes.

As part of the HEATSTORE project (www.heatstore.eu), we used data from deep exploration borehole in the Geneva area (GEo-01 and GEo-02) and we developed an analogue shallow test site in Concise (VD) where characterization strategies can be developed and tested. At the Concise test site, three boreholes were drilled in fractured limestones in the Cretaceous (Barremian and Hauterivian formations; Sohrabi & Valley, 2021). We used core logging, borehole imaging, and acoustic logging for deriving a detailed understanding of the characteristics of the fracture network at the site. We complemented this data with photogrammetric studies on outcrops in the test site vicinity. We also measured thermal conductivity, permeability and porosity on core sample in order to evaluate matrix parameters. In the Geneva boreholes, we focused our study on the integration of borehole imaging and hydraulic testing data in order to characterize the stress state in the target reservoirs. Observation of borehole breakouts combined with mechanical parameters estimation from sonic logs and punctual stress measurements with minifrac allow us to propose a first in-situ stress characterization in the Geneva basin. We complemented these analyses with stress modelling approaches for assessing the influence of stiffness contrast.

Our final objective is to create different 3D numerical models that include all the properties determined experimentally and that best reproduce the hydrogeological context. We incorporate mechanical structures as fractures, elastic modulus, density, stress conditions, and thermal properties in order to perform thermo-hydraulic simulations. These models will allow to estimate the capacity to perform ATES in this environment regarding the geomechanical characteristics determined experimentally. The Concise site gives a notion of the expected results for ATES in fractured and karstified limestone reservoir for projects at larger scale, and this work gives leads for exploration drilling campaigns in Geneva as both systems share hydrological similarities.

REFERENCES

Sohrabi, R. & Valley, B. (2021). Rapport hydrogéologique des forages RSBV. Canton de Vaud, Commune de Concise. Centre d'Hydrogéologie et de Géothermie, Université de Neuchâtel. p.20.

P 9.3
Experimental assessment of calcite scaling occurring during high-temperature aquifer thermal energy storage (HT-ATES)

Joshua P. Richards[1], Fulvio di Lorenzo[1], Daniela B. van den Heuvel[1], Larryn W. Diamond[1]

[1] *Institut für Geologie, University of Bern, Baltzerstrasse 3, CH-3012 Bern (joshua.richards@geo.unibe.ch)*

Whilst there has been a large shift to renewable electricity sources throughout Europe, only 10% of the continent›s heat energy is produced by renewables. This is partly due to renewable heat production often being caught in a seasonal mismatch of supply and demand. To close this gap, High Temperature Aquifer Thermal Energy Storage (HT-ATES) systems aim to store excess heat during summer in sandstone and carbonate aquifers, to be retrieved for use in the winter. Operation of such systems, however, can be impeded by geochemical issues arising in the surface installations, where scaling of calcium carbonate can occur, clogging pipes and heat exchangers.

To assess the effect of temperature and aqueous chemical composition on the nucleation and growth of calcium carbonate, laboratory titration experiments were performed.

Previous nucleation experiments using pure $CaCO_3$ solutions (Di Lorenzo et al., 2017) have determined the supersaturation of calcite required for instantaneous, homogeneous nucleation at 25 °C. We have used the same approach at temperatures up to 90 °C, finding that the critical supersaturation decreased from SI = 1.8 at 25 °C to SI ~ 1 at 90 °C. The same experiments were repeated using a $CaCO_3$ solution containing Mg, SO_4 or both. These ions are well known to inhibit the nucleation of calcite. However, the inhibitory effect weakened rapidly when raising the temperature stepwise to 40 °C. This effect was primarily due to the increased stability of aqueous $MgCO_3$ species versus Mg^{2+}, which enhanced incorporation of Mg in the nucleating phases. Growth rates were measured with the constant composition method and with an Atomic Force Microscope (AFM).

The growth rate of calcite at 25 °C was determined to be 1.41×10^{-8} mol/cm^2/s. In the presence of Mg^{2+} ions this rate reduced slightly to 1.34×10^{-8} mol/cm^2/s. The effect of temperature on growth inhibition was not assessed.
The experimental data can be used to better constrain numerical simulations of mineral reactions, especially calcite scaling, during HT-ATES operations. The results suggest that the inhibitory effects of Mg and SO_4 on calcite precipitation do not need to be taken into account in such simulations at temperatures of interest in HT-ATES (> 40 °C).

REFERENCES

Di Lorenzo, F., Burgos-Cara, A., Ruiz-Agudo, E., Putnis, C. V., & Prieto, M. (2017). Effect of ferrous iron on the nucleation and growth of $CaCO_3$ in slightly basic aqueous solutions. CrystEngComm, 19(3), 447–460. https://doi.org/10.1039/c6ce02290a.

P 9.4
Exploration of amagmatic orogenic, fault-hosted geothermal systems using coupled thermal-hydraulic simulations

Daniel Carbajal[1], Loïc Peiffer[2], Larryn W. Diamond[1], Christoph Wanner[1]

[1] *Institut für Geologie, Universität Bern, Baltzerstrasse 1+3, CH-3012 Bern (daniel.carbajal@geo.unibe.ch)*
[2] *Departamento de Geología, CICESE, Ensenada, Baja California, México.*

Amagmatic, fault-hosted orogenic geothermal systems offer great potential for geothermal energy and hence for reduction of greenhouse gas emissions. This study focuses on the amagmatic geothermal system hosted by the Agua Blanca fault (ABF), Baja California (B.C.), Mexico (Figure 1a). The ABF is a 140 km long transtensional structure with five segments recording up to 11 km of dextral strike-slip displacement and normal throws of up to 0.65 km (Wetmore et al., 2019). We have identified at least seven geothermal areas along the ABF manifested by hot springs discharging at temperatures ranging from 38 to 102 °C (Figure 1b). These systems involve topography-driven infiltration of meteoric water deep into the ABF and exfiltration of the heated Na-Cl water at valley floors and along a local beach on the Pacific coast known as La Jolla, where we have measured discharge temperatures of up to 94 °C.

Here, we present 3D coupled thermal-hydraulic simulations carried out with the software Toughreact (i) to assess the role of surface topography and nearshore seafloor bathymetry in controlling regional water circulation in the ABF, and (ii) to obtain a fundamental understanding of the processes that cause the strong thermal anomaly at La Jolla beach.

Our numerical model covers a large 3D domain of 20x10x14 km (x, y, z). It consists of ca. 200,000 grid blocks and explicitly considers the topography (max. 1 km) and bathymetry (max. 0.3 km) of the model domain. All simulations were run by specifying hydrostatic pressure and conductive temperature distributions as initial conditions, while the pressure and temperature were fixed at all model boundaries. For the initial and boundary temperatures we assumed an average annual temperature of 16 °C at the coast, an adiabatic cooling rate of -5.5 °C/km over the continent, a cooling gradient of -3.1 °C/100 m depth in the seawater column, and a regional geothermal gradient of 24 °C/km. Over the continent, the boundary pressure was fixed at 1 bar, while on the seafloor it was set according to the seawater depth and salinity.

In our simulations we have tested different configurations of permeability and width (50–200 m) for the ABF plane to reproduce the surface temperature (94 °C) and the surface extent (200 x 60 m) of the thermal anomaly at La Jolla beach, as well as the seawater contribution (30%) to the thermal springs (Figure 2). Simulation results indicate that high permeabilities above $2x10^{-14}$ m^2 create vigorously convecting systems exceeding the temperature and size of the thermal anomaly. To avoid convection, the ABF permeability must be below $6x10^{-14}$ m^2. To reproduce the observed geothermal features, it is necessary to consider a heterogeneous permeability distribution along the ABF. An enhanced permeability close to the coast agrees with structural evidence, such as uplifted marine terraces and an elevated extensional component of the ABF. Consequently, a one-dimensional tube with a high permeability of $k = 7x10^{-13}$ m^2 was defined below La Jolla beach. Together with permeabilities of $1x10^{-15}$ and $1x10^{-17}$ m^2 for the remaining ABF fault and the host rock, respectively, this eventually allowed matching of all key observations (Figure 2).

In conclusion, the strong thermal anomaly at La Jolla is mainly caused by a highly permeable structural anomaly, which coincides with the location of the highest pressure gradient along the entire ABF. Owing to this favorable setting, the thermal anomaly has potential to be used for seawater desalination or electricity production (at ~ 2 km depth).

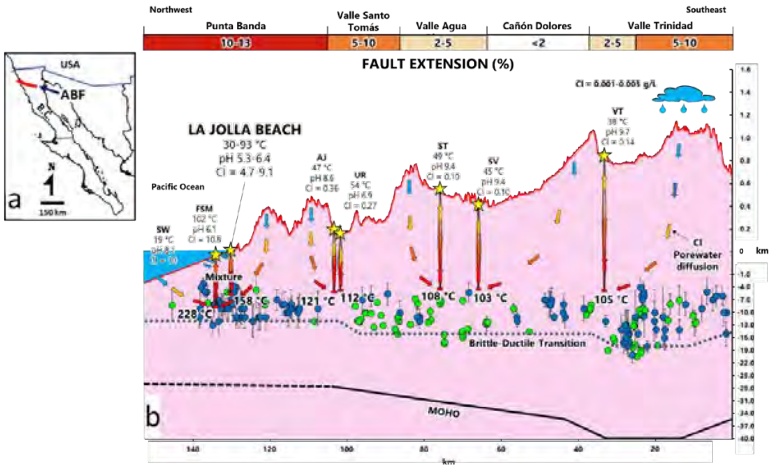

Figure 1. a) Study area location. b) Conceptual model of the amagmatic orogenic geothermal systems hosted by the Agua Blanca fault (ABF).

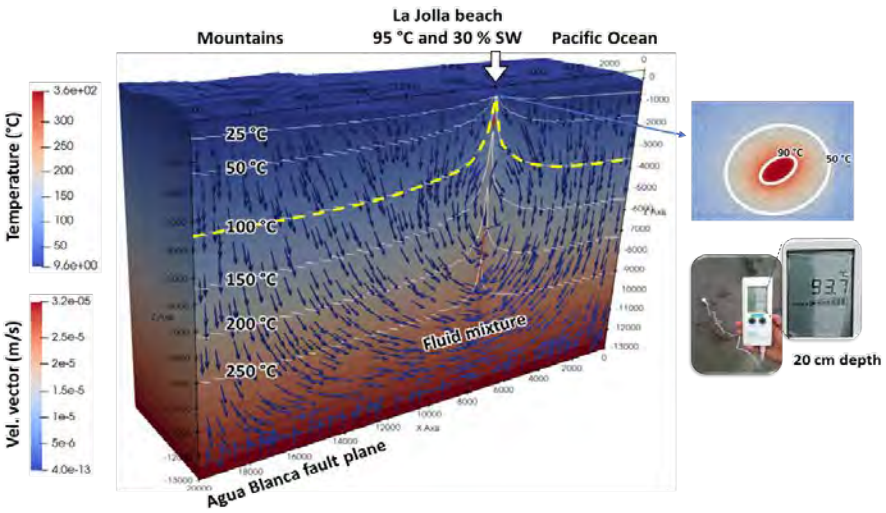

Figure 2. Simulation of the temperature distribution along ABF for one specific permeability configuration: host rock $1x10^{-17}$ m^2, fault $1x10^{-15}$ m^2, and a tube $7x10^{-13}$ m^2.

REFERENCES

Wetmore, P. H., Malservisi, R., Fletcher, J. M., Alsleben, H., Wilson, J., Callihan, S., ... & Gold, P. O. (2019). Geosphere, 15(1), 119-145.

P 9.5
Reservoir geology of the Cretaceous-Cenozoic Transition in the context of geothermal exploration in the Geneva Basin and neighbouring France (Switzerland & France)

Aurélia Crinière[1], Andrea Moscariello[1]

[1]GE-RGBA Group, Department of Earth Sciences, University of Geneva, Rue des Maraîchers 13, CH-1205 Geneva (Aurelia.Criniere@unige.ch)

Enhancing geothermal exploration in sedimentary basin for thermal production is part of the GEothermies program in the Geneva Basin including the south-westernmost part of Switzerland and neighbouring France (Fig. 1). Results from the hydrocarbon exploration carried out since the early 60's and subsequent geothermal drilling campaigns (Moscariello, 2019) confirmed the presence of five stratigraphic intervals for geothermal projects: Lower Cretaceous, Kimmeridgian, Bajocian, Muschelkalk, Buntsandtein (Rusillon, 2017).

This study focuses on the shallowest, the Cretaceous-Cenozoic Transition (CCT), identified in 35 wells (Fig. 1) and seismic signatures (2D-3D) that displaying a good geothermal potential for its flow rate due to karstified Lower Cretaceous. The karst substratum is mostly low porosity carbonates, but the Eocene and Oligocene units that fill the karst exhibit good reservoir characteristics due to their coarse texture:

- the '*Sidérolithique*', a quartz-rich sandstone facies,
- the Gompholite, a polygenic conglomerate facies.

The CCT is marked by a sedimentary hiatus related to the tectonic phase and the climate that dominated the area at this period. This study will provide a better understanding of this poorly known stratigraphic interval by tackling the following aspects:

1. Sedimentological framework and diagenetic history of the Cenozoic sediments based on field survey and description of cores, further refined by geochemical and mineralogical analyses and reconstruct their depositional environment,
2. Petrophysical study to characterize the reservoir properties with regard to their use as geothermal reservoirs,
3. Regional 2D conceptual model based on the 35 wells recording CCT and 2D and 3D seismic interpretation to predict their lateral and vertical distribution.

These units have been recorded in a depth range between 31.20 m (well SPM-3) and 1376 m (well Thônex; Fig. 1). A few outcrops are observed in the Salève (Fig. 2), the Vuache and the Jura. The most significant '*Sidérolithique*' deposit of 130 m thickness was recorded at 630 m depth in the geothermal exploration well GEo-02 (near Lully) drilled in 2019. According to cores and outcrops observations, the '*Sidérolithique*' facies have a variable clay content of kaolinite and chlorite as well as a variable abundance of siderite (Fig. 2). In the Gex wells, porosity values in the CCT deposits ranges from 0 to 20 % while permeability values can reach up several hundred mD.

Ultimately, this study aim at improving the predictive capability of the geological model of the Canton of Geneva and neighbouring France and provide new useful insights on the potential of the CCT deposits as geothermal reservoirs.

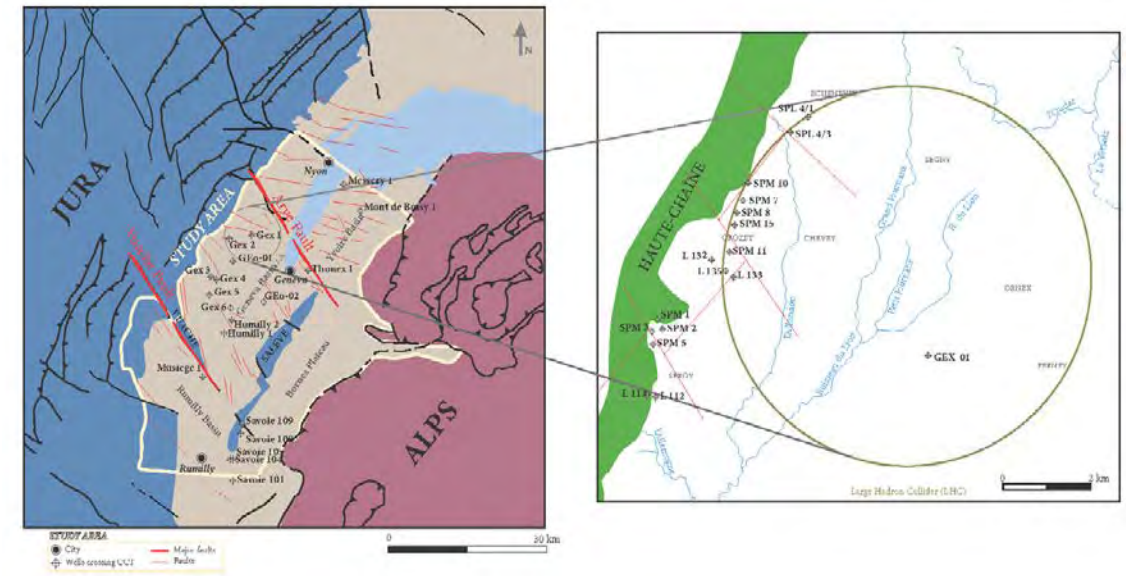

Figure 1. Location of the study area over the trans-border Geneva Basin and neighbouring France with wells location crossing the CCT.

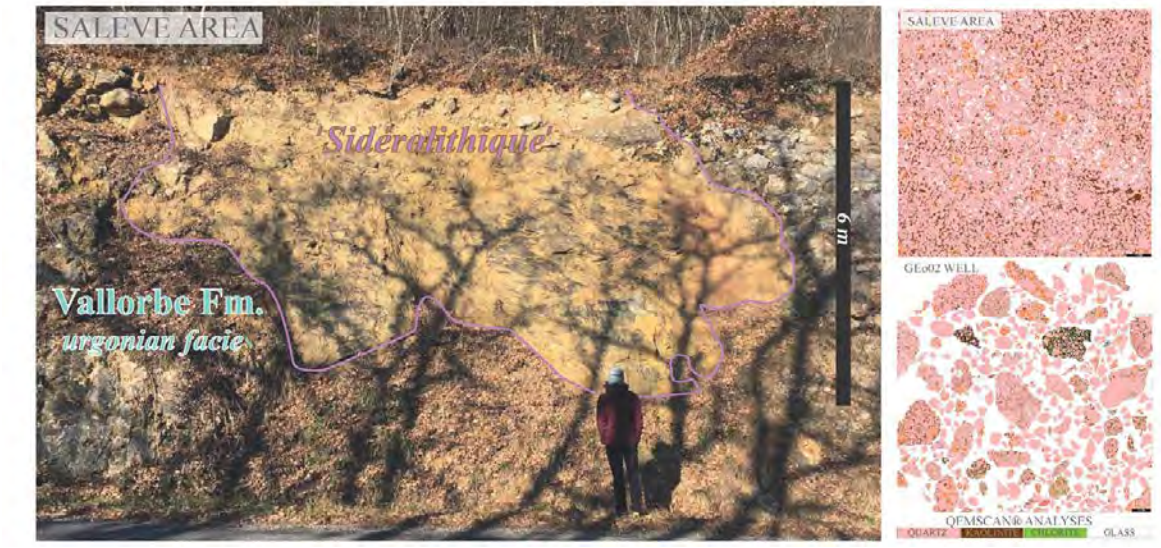

Figure 2. '*Sidérolithique*' deposit observed in outcrops filling karst (Salève area) with two samples analyzed with QEMSCAN from the outcrop and compared with cuttings from GEo-02 well (752 m in depth).

REFERENCES

Moscariello, A. 2019: Exploring for geo-energy resources in the Geneva Basin (Western Switzerland): opportunities and challenges. Swiss Bull. angew. Geol., 24/2, 105-124.

Rusillon, E. 2017: Characterisation and rock typing of deep geothermal reservoirs in the Greater Geneva Basin (Switzerland & France). Thesis. Université de Genève.

P 9.6
Improved onshore subsurface seismic imaging: examples from the geothermal province of Tuscany (Italy)

Luca Guglielmetti[1], Fiammetta Mondino[2], Andrea Moscariello[1], Lorenzo Perozzi [1,2], Claudio Strobbia[3]

[1] GE-RGBA Group, Department of Earth Sciences, University of Geneva, Rue des Maraîchers 13, CH-1205 Geneva (luca.guglielmetti@unige.ch)
[2] Geneva Earth Resources sA, Rue Jean jaquet 10, 1201 Geneva, Switzerland
[3] Real Time Seismic, Av. du Pdt ANGOT Technopole Helioparc, 64000 Pau, France

Successful geothermal exploration often depends on the quality of the images obtained by 2D and 3D seimic data which strongly control the ability to carry a reliable geoligical interpretation of the subsurface. In several sedimentary basins where geothermal exploration is focusing at the moment, legacy seismic data, typically aquired between the late 60s and 80s for hydrocarbon exploraiton often exists but is difficult to use because of its scarce quality.
Advanced seismic re-processing and imaging techniques combined with increased computing power, for instance, allow the extraction of increased bandwidth from field data, especially low frequencies which are often lacking in legacy images. The latter can help extracting more detail by increasing the span of seismic signal and thus extracting more information from the same data. Moreover, the preservation of low frequencies in the reprocessed legacy data, although not as reliable and rich as in modern broadband can help to improve the definition of velocity model like Full Waveform Inversion and support the generation of improved velocity models, and more reliable and detailed images of the subsurface.

Innovative seismic re-processing techniques have been applied ot the CROP03 seimic data crossing E-W the eastern part of the southern Geothermal Province of Tuscany. Based on the new image, a clear identification of a series of tilted blocks bounded by high-angle fault likely passing to sa listric geometry at depth have been identified. The lack of boreholes in the area does not allow a unique stratigraphic interpretation. However, based on outcrop geology and previous studies the area is charcaterisd by the superposition of a number of tectonic nappes associated with the Appennine compressional tectonic, later affected by back-thrust extension (orogenic collapse). The mesozoic Tuscan Nappe units containing carbonate and marly limestones, later overthrusted by Ligurian Units form the tilted block. Some of them, isolated, covered by Ligurian units and connected with target for deeply rooted fault systems, can represent interesting geothermal exploration targets. The staggering difference between the seismic presented in Giustiniani et al., (2015) and the results presented in this work, indicates the importance of the continued advances made in seismic re-pocessing techniques can bring to a new life legacy seismic data. The latter, as they were treated and displayed, were allowing model-driven interpretations based on a large degree of imagination and have frequently charcaterised the scientific literature in the past years.

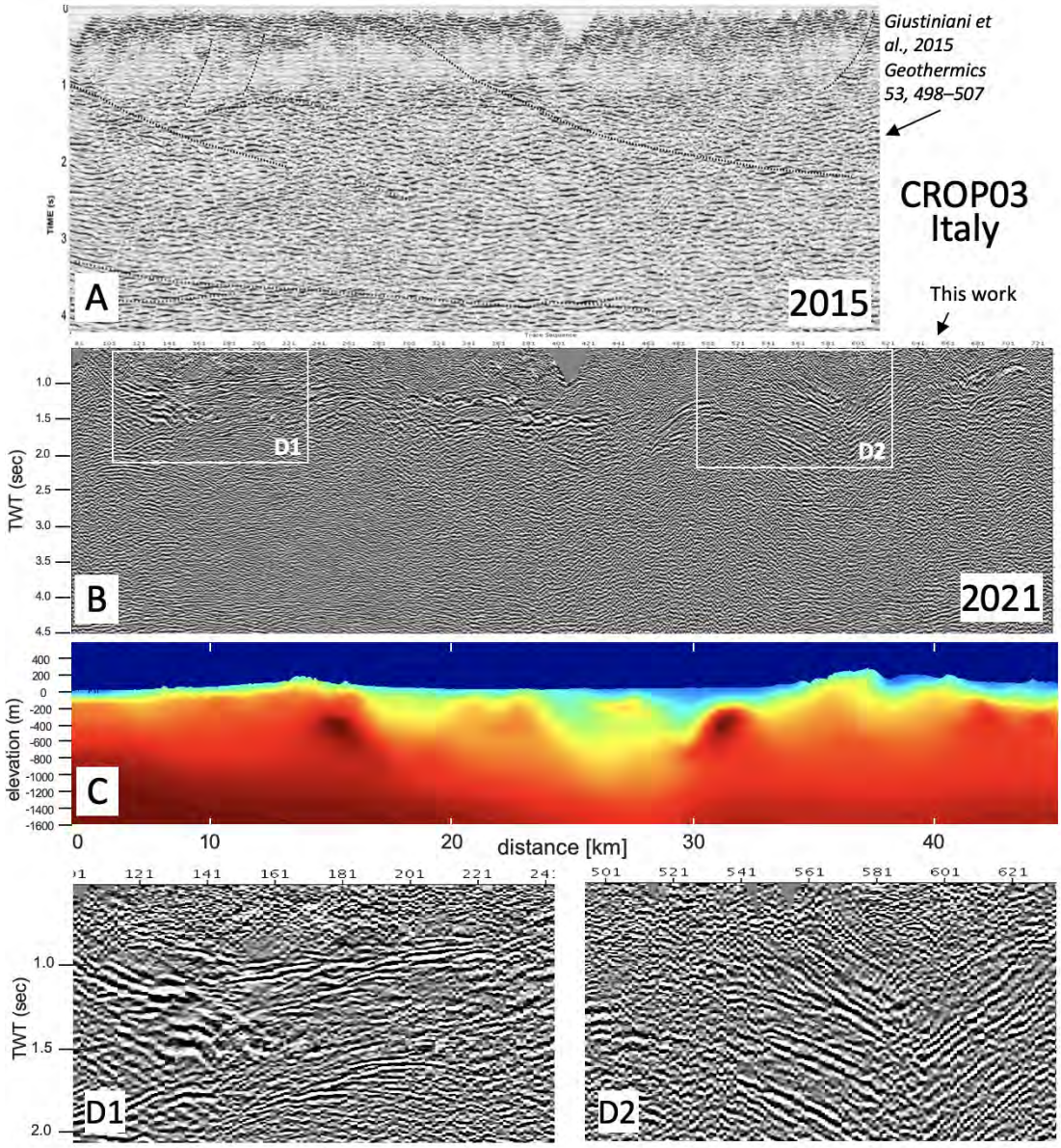

Figure 1. A) Re-processed CROP03 seismic data as presenmted by Giustiniani et al., (2015); B) re-processed CROP03 sesmic data in 2021 (this work); C) velocity model displaying strong velocity contrast suggesting the occurrence of high-velocity areas (basement high) limiting slower packages (i.e. sedimentary basin ?) at the center of the profile; D) detailed view of 2021's reprocessd CROP03 seismic where reflectors indicating vertical stacking of stratigraphc units, their gemetry and dipping, lateral discontinuity and structural complexity are visible.

REFERENCES

Giustiniani M., Tinivella U. Nicolich R. 2015, Reflection seismic sections across the Geothermal Province of Tuscany from reprocessing CROP profiles Geothermics 53, 498–507.

P 9.7
Thermo-Hydraulic behaviour in fractured limestone for Aquifer Thermal Energy Storage (ATES)

Alessandro Milo, Benoît Valley, Reza Sohrabi

Centre for Hydrogeology and Geothermics (CHYN), University of Neuchâtel, Neuchâtel, Switzerland (alessandro.milo@unine.ch)

Aquifer Thermal Energy Storage (ATES) is a promising technology for compensating seasonal unbalance between heat demand and availability in district heating systems. The first ATES experiment was performed by the Centre for Hydrogeology and Geothermics (CHYN) at the University of Neuchâtel (Switzerland) in 1974 (Saugy et al., 1984; Saugy et al., 1992; Tsang & Hopkins, 1982), followed by a three-stage experimental project at Auburn University (USA) in 1976 (Moltz et al., 1978; Moltz et al., 1979; Moltz et al., 1983; Tsang et al., 1981). Further countries such as France, Japan, Germany, or Canada started participating in ATES research with their own experimental field sites. Current applications of ATES are essentially limited to shallow classic aquifers. In order to broaden the potential of ATES, it is essential to develop this technology in a wider range of aquifer types.

Heat transport and storage is particularly complex in fractured and karstified aquifers because the hydraulic flow predominates the heat transfer process. A karstified aquifer is difficult to understand due to the presence of many fractures and conduits. The complicated hydraulic interaction between the fractures leads to determine which one dominates the system within the time scale of tests. A challenge for the development of ATES is thus to develop thermo-hydraulic test protocol that allow for assessing relevant reservoir characteristics for performing thermo-hydraulic simulation and predict reservoir performance to heat storage cycles.

In this study, we developed a new test site in fractures and karstified limestone in Concise (Vaud, Switzerland) in order to develop thermo-hydraulic test protocols. The site consists of three boreholes drilled in Creteceous limestones to 50 m deep with a 4.5 m spacing (Sohrabi & Valley, 2021). Two boreholes have major fractures while the last one seems to be disconnected. The boreholes were extensively logged and core samples were analysed in order to develop a detailed local understanding of the fracture network and the characteristics of the rock mass (André et al., 2021). We performed pulse, slug, pumping and injection test in open hole configuration and between packers as well as flow logging (spinner) in order to obtain a detailed characterization of the hydraulic features of the rock mass and to identify the prominent flow path. Analyses of these data with different analytic solutions as Theis, Barker, and Warren & Root equations help to develop a conceptual understanding of the system behaviour and to estimate relevant hydraulic parameters. We then performed push pull test with 50°C hot water (natural aquifer temperature is about 11°C) and with conservative tracers for characterizing the transport characteristics of our aquifer. Finally, we calibrated finite element models with different geometrical reservoir characteristics to our data in order to identify key parameters influencing heat storage features of the reservoir.

The comparison of hydraulic conductivity results allows to check the validity of these solutions, even if the assumptions are not completely respected. The double porosity model gives interesting storativity results because laboratory tests on cores illustrate the very low porosity of the matrix. So, it seems that it is not the matrix providing the recharge but the others fractures around playing the role of the matrix instead. The hydraulic tests give a range of hydraulic conductivity around 10-6 to 10-5 m/s with a storativity between 10-5 to 10-2 [-]. The hydraulic conceptual model is driven by a high density of fractures interacting via major fractures going through a part of the system. The flow dimension differs according to the nature of the test. Using Theis and Barker solutions, the production tests give a 2-D radial flow around the wells which can be interpolated as a fracture plane. For the recovery, the dimension is close to a 3-D flow around the wells.

For the heat experiments, two conservative tracers are used as Uranine and Sulforhodamine-B. Each one is associated with a heat injection test. The aim is to compare the heat recovered with the amount of conservative tracer. As a result of an injection during 6 hours with the Sulforhodamine-B, around 39 % of the thermal energy is retrieved at the pumping end sequence after a recovery of 14 hours. Unexpectedly, the observation wells do not receive relevant temperatures increase. Moreover, the disconnected observation well is the place where the temperature steps up the most with a rise of 2°C.

The challenges about the climate crisis needs to find innovative ways to consume and store energy. Data collection lead to numerical modeling. This is why, we used numerical simulation to fully coupled the physics involved and understand the geometry of the system. Four conceptual models are used in order to find the most reliable geometry of fractures, as equivalent porous media, bedding only, Discrete Fracture Network (DFN) and deterministic fractures. This permits a better comprehension of the aquifer system with the use of heat as an indicator for different geometries. The thermo-hydraulic method used at Concise (VD) could be fundamentals ways to test this kind of groundwater systems.

REFERENCES

André M., Valley B., & Sohrabi R. (2021). Characterization of fractured and karstified limestone reservoir for Aquifer thermal Energy Storage (ATES). Swiss Geoscience Meeting 2021, Geneva, Switzerland.

Molz, F. J., Warman, J. C., & Jones, T. E. (1978). Aquifer storage of heated water: Part I—a field experiment. Groundwater, 16(4), 234-241.

Molz, F. J., Parr, A. D., Andersen, P. F., Lucido, V. D., & Warman, J. C. (1979). Thermal energy storage in a confined aquifer: Experimental results. Water Resources Research, 15(6), 1509-1514.

Molz, F. J., Melville, J. G., Parr, A. D., King, D. A., & Hopf, M. T. (1983). Aquifer thermal energy storage: a well doublet experiment at increased temperatures. Water Resources Research, 19(1), 149-160.

Saugy, B., Doy, R., Mathey, B., Aragno, M., Geister, M., Rieben, C., et al. (1984). Accumulateur de chaleur en nappe souterraine SPEOS - Bilan de deux ans d'exploitation. SEATU: Société des éditions des associations techniques universitaires.

Saugy, B. (1992). Speos-dorigny and associated projects on aquifer thermal energy storage: Annex III des Programms der Internationalen Energieagentur: Energy conservation through energy storage.

Sohrabi, R. & Valley, B. (2021). Rapport hydrogéologique des forages RSBV. Canton de Vaud, Commune de Concise. Centre d'Hydrogéologie et de Géothermie, Université de Neuchâtel. p. 20.

Tsang, C. F., Buscheck, T., & Doughty, C. (1981). Aquifer thermal energy storage: a numerical simulation of Auburn University field experiments. Water Resources Research, 17(3), 647-658.

Tsang, C. F. & Hopkins, D.L. (1982). Aquifer thermal energy storage: a survey: Recent trends in hydrogeology. Geological Society of America. p. 427–42.

P 9.8
Evolution of the rate and state frictional parameters of carbonate bearing faults at the brittle-to-ductile transition

Francesco Figura[1], Carolina Giorgetti[1], Mathias Lebihain[1], Marie Violay[1]

[1]*École polytechnique fédérale de Lausanne, Laboratory of Experimental Rock Mechanics, Lausanne, Switzerland (francesco.figura@epfl.ch)*

The majority of the seismic events in the Mediterranean region are hosted in carbonate-bearing rocks at depths representative of the semi-brittle regime. Within this regime, a complex interplay between brittle (localized) and ductile (distributed) deformation mechanisms co-exists. Despite its relevance for seismic hazard, the influence of this interplay on the nucleation and propagation of seismic events is poorly studied. Up to now, most experimental work has been conducted far from *in-situ* conditions, mostly at room temperature and low confining pressure.

Here we constrain the frictional behavior of faults in carbonate rocks under conditions relevant for their brittle to ductile transition. Velocity-step experiments are performed through the HighSTEPS (High Strain Temperature Pressure Speed) biaxial apparatus installed at EPFL, investigating sliding velocities from 10 µm/s to 0.01 m/s. Experiments are conducted under different values of confining pressure (0 – 50.0 MPa) and normal stress (9.5 – 95.0 MPa), keeping constant the ratio between $\sigma_n/P_c \sim 2$. Local strain field along the fault is measured with strain gauges. Experimental results are modelled with rate-and-state friction laws (RSFLs) to define the rate and state parameters relate to the critical conditions for fault stability. Moreover, microstructural observations of the post mortem samples are conducted at the SEM, to investigate the deformation mechanisms active during the experiments.

We show that with increasing the confining pressure, the rate-and-state parameter *a* and *b* decrease. Whereas the critical distance D_c and the value of *(a-b)* both increase with increasing the confining pressure and the sliding velocity.

These results shed light on the evolution of rate-and-state frictional parameters with depth, as well as their dependence on the strain partitioning between on-fault slip and bulk-accommodated deformations (elastic and plastic) with increasing depth.

P 9.9
Micromechanical Modelling of Elastic Wave Velocity Variations for Intact Brittle Rocks

Antoine Guggisberg, François Passelègue, Marie Violay

École Polytechnique Fédérale de Lausanne, LEMR, Lausanne, Switzerland

In the upper crust, where brittle mechanisms are predominant, the growth and coalescence of microcracks play a key role in lithosphere deformations and earthquakes propagation. Micromechanical models such as the wing crack model developed by Ashby and Sammis aim to describe the compressive strength of brittle rocks. This model has only been used for failure predictions; however, it gives relevant information regarding the crack opening process continuously during loading, so this model is extended to compute elastic wave velocities according to the cracked solid theory of Kachanov. Laboratory experiments at various confining pressures on Westerly granite were realised to fit its parameters and test this extension. A decent correlation between modelled and measured velocities shows that this model might be used for seismic velocities and crack-induced anisotropy computation. Furthermore, the validity of the model is discussed through an energy budget and comparisons with in-situ measurements of velocity changes..

P 9.10
On the scale dependence in the dynamics of frictional rupture

Federica Paglialunga[1], François Xavier Thibault Passelègue[1], Mathias Lebihain [1], Marie Violay[1]

[1] *Laboratory of Experimental Rock Mechanics, École Polytechnique Fédérale de Lausanne, Switzerland*

When an earthquake nucleates in the earth crust, the potential energy accumulated during the inter-seismic period is released into breakdown work, heat energy and radiated energy. Often the breakdown work is considered a seismological equivalent of the fracture energy. However, discrepancies related to the definition of the two are not yet fully solved. To this end, we reproduced frictional ruptures in the laboratory to study the relationship between these two energies. A dual strength weakening is observed, reflected in a scale dependent evolution of breakdown work with fault' slip, contrarily to fracture energy which is, by definition, scale independent. This behavior shows to be probably caused by thermal weakening (i.e. flash heating) activated during slip and to be well described by the recently developed unconventional theory of frictional ruptures (i.e. rupture driven by a non-square root singularity). Importantly, these results highlight, from an experimental point of view, the presumable unconventional nature of earthquakes, solving the discrepancies between breakdown work and fracture energy. Moreover, it suggests that an analysis of the propagating rupture in the framework of linear elastic fracture mechanics could prove to be not always sufficiently exhaustive when frictional weakenings occur, as it is expected along crustal faults.

P 9.11
Preliminary results from the analysis of stress profiles in deep geothermal reservoirs

Farid Zabihian, Reza Sohrabi, Benoît Valley

Center for Hydrogeology and Geothermics (CHYN), University of Neuchâtel, Neuchâtel, Switzerland (farid.zabihian@unine.ch)

Achieving the energy turn-around requires the mobilisation of all possible energy sources. Geothermal could contribute much largerly to the renewable energy porto-folio, if the enhanced geothermal system (EGS) technology would gain maturity. EGS would allow exploiting deep rock mass heat by creating permability where it is naturally insuficient. Hydraulic fracturing and shearing are typically applied to achieve this goal. However, such activities will perturb the stress regime in the rock mass, producing seismic events in various magnitudes. Therefore, it is essential to develop techniques to reduce the risks and anticipate EGS reservoir behavior in different scenarios.

EGS requires to engineer a reservoir with the largely critically stressed earth crust. Earth crust criticallity could be explained by the fact that the crust is a self-organised critical system (Bak et al., 1987). The specificity of such system is that the point of criticallity is an attractor and thus criticallity tends to be the rule. In addition, self-similar processes tend to emerge in such systems. Gutenberg-Richter law of earthquake magnitude distribution is one example of these self-similar processes. It is also likely that other important parameters like fracture size distribution and stress variation tend to follow self-similar statisitics.

We will focus on this contribution on the statitics of the stress variability state and its self-scaling charateristics. There are two different terms for defining scaling patterns, self-similar and self-affine. The conservation of statistical characteristics, while they are being magnified, clarifies which pattern they are following. When shapes are being repeated during magnification, they are self-similar; on the other hand, when shapes require a constant scaling factor to keep their original properties, they are called self-affine. If the observed variabilities in stress properties follow self-affinity scaling approaches, they could be attributed to the natural fractures network and earthquake magnitude-frequency. In this case, in order to constrain statistical attributes of the fracture network and to predict the seismic response of a rock mass, the measurable variations in stress orientation could be employed. Geometries that do not have a particular size or length can be described by fractal mathematical models. Fractal distributions are parameterized by the fractal dimension, D, which measures how the pattern details change within the observation scale.

One of the main sources for studying the characteristics of the stress field in deep boreholes, is the observation of the borehole failure profiles. Borehole failure is typically discontinuous. Nevertherless, the scaling characteristics of stress variability must be determined in a trustworthy manner. The fractal dimension of stress orientation variations indicated by wellbore failure data can be evaluated by taking advantage of various techniques. At first, these techniques were applied to synthetic data of known fractal dimensions produced by different methods. Because gaps and noise are always present in most of borehole datasets, in the next step, some biases were introduced by their presence in the data and then they were reassessed.

Finally, the methods were applied to the borehole failure data obtained from the Soultz-sous-Forêts and Basel projects. Preliminary results indicate that estimates of D were found, for various methods applied to the same dataset, with significantly differences. In this study, the best explaination for this deviation could be accredited to the gaps in the wellbore measured data. In the further step, the methodology will be extended for considering the tensorial characterisic of the stresses.

REFERENCES

Bak, P., Tang, C., Wiesenfeld, K. 1987: Self-organized criticality: An explanation of the 1/f noise. Physical Review Letters, 59, 381–384.

P 9.12
Hydro-geomechanical characterisation for upcoming hydraulic stimulation experiments at the Bedretto Underground Laboratory

Kai Bröker*, Xiaodong Ma*, Nima Gholizadeh Doonechaly*, Quinn Wenning*, Shihuai Zhang*, Marian Hertrich*, Domenico Giardini*, & the Bedretto Lab team*

**Institute of Geophysics*, ETH Zürich, *Sonneggstrasse 5*, CH-8092 Zürich (kai.broeker@erdw.ethz.ch)

The global interest in engineered geothermal systems (EGS) has increased in recent years as they are considered a low emission, renewable energy source. EGS reservoirs with sufficiently high temperatures are located at several kilometres depth, where the permeability of the crystalline basement rocks is too low to allow feasible geothermal energy extraction. Permeability enhancement is achieved by hydraulic stimulation, either through hydraulic shearing of natural fractures or shear zones, or through hydraulic fracturing of intact rock. The Bedretto Underground Laboratory for Geoenergies (Bedretto Lab) serves as an in situ test-bed where meso-scale hydraulic stimulation experiments will be conducted (Gischig et al. 2020; Ma et al. 2021). It is anticipated that the experiments will bridge the knowledge gap between laboratory and reservoir scale to better understand the hydro-seismo-mechanical response of fractured crystalline rock masses.

The Bedretto Lab is located in a 100 m long enlarged section of the Bedretto tunnel (Ticino, Switzerland), with an overburden of more than 1000 m of granite. Several characterization, monitoring, and stimulation boreholes were drilled over the past 2 years. In this work, we focus on a 400 m long, 45°-dipping stimulation borehole (referred to as ST1), which was equipped with a multi-packer system that partitions the borehole into different intervals. These intervals will later be used for a multi-stage hydraulic stimulation. A prerequisite for this stimulation is to characterize the natural hydraulic conditions, i.e. transmissivities and ambient pore pressures, and sets of pre-existing natural fractures. Additionally, the slip tendencies, which describes how likely these natural fractures are to be reactivated under ambient stress conditions, were evaluated in a deterministic and stochastic manner.

The results indicate a strong heterogeneity of the rock volume, which is dominated by a number of fault zones that were intersected and mapped across multiple boreholes. Although open fractures and fault zones with high slip are present in all intervals of ST1, transmissivities differ by orders of magnitude. This indicated that compartmentalized hydro-structures exist and that the hydraulic connectivity between some pre-existing fracture sets can potentially be increased by hydraulic shearing. In addition, the results will inform the design of the stimulation protocol to plan the required injection flow rates and injection pressures.

REFERENCES

Ma, X., Hertrich, M., Bröker, K. et al. 2021: Multi-disciplinary characterizations of the Bedretto Lab - a unique underground geoscience research facility. Submitted to Solid Earth.

Gischig, V. S., Giardini, D., Amann, F., et al. 2020: Hydraulic stimulation and fluid circulation experiments in underground laboratories: Stepping up the scale towards engineered geothermal systems. Geomechanics for Energy and the Environment, 24. https://doi.org/10.1016/j.gete.2019.100175

P 9.13
Results from the GEOEBST2020+ baseline seismic monitoring in the cantons of Vaud and Geneva

Verónica Antunes[1], Toni Kraft[1], Philippe Roth[1], Tania Toledo[1], Stefan Wiemer[1]

[1] *Swiss Seismological Service at ETH Zurich, Switzerland (veronica.antunes@sed.ethz.ch)*

Within the GEOBEST2020+ project, funded by the Federal Office of Energy's SwissEnergy program, the Swiss Seismological Service at ETH Zurich (SED) can support cantonal authorities in adequately handling the risk of induced seismicity associated with deep geothermal projects. One pillar of this support is that the SED can provide operator-independent baseline seismic monitoring for deep geothermal projects to GEOBEST2020+ partner cantons. In Summer 2021, the cantons of Vaud and Geneva signed the GEOBEST2020+ agreement, allowing the SED to provide such baseline seismic monitoring for the projects Lavey-les-Bains (AGEPP), Vinzel (EnergeO), Yverdon-les-Bains (Malmenergie Naturelle) in Vaud as well as the GEOTHERMIES (SIG) in the Geneva Basin.

GEOBEST2020+ Baseline Seismic Monitoring aims to ensure the minimum monitoring requirements for deep geothermal projects defined in SED's "Good-Practice Guide for Managing Induced Seismicity in Deep Geothermal Energy Projects in Switzerland" (Kraft et al., 2020). To reach this goal, the SED may install additional seismic stations in the vicinity of the monitored projects to improve the network geometry of the existing national seismic network. The hardware is provided by the GEOBEST2020+ instrumentation pool and can be reused in future projects. All monitoring stations are integrated into the automatic seismic processing system of the SED, and a group of experienced SED seismologists performs manual reviews of detected seismic events. Earthquake alarms for all earthquakes located in the vicinity of the monitored projects are immediately sent to the concerned cantonal authority and operator via SMS and email. The operators use these alarms in their traffic light systems and can access the seismic waveform data to perform additional analysis. The baseline seismic monitoring data can be accessed freely in near-real-time via the data portals of the SED.

Here we introduce the current baseline seismic monitoring networks of the GEOBEST2020+ program. We outline our workflow from network planning, to site survey, to station installation and discuss the network performance and first monitoring results. At the example of the Lavey-les-Bains network, we demonstrate how we use template matching analysis, daily spectrograms, probabilistic power spectra density plots, theoretical Brune source spectra, Bayesian Magnitude of Completeness (BMC) maps, and records of local and regional earthquakes to evaluate network performance. Finally, we estimate theoretical location uncertainties of the network, considering the network geometry, 3D velocity model, and the observed noise level at the stations and compare it to results obtained for recorded earthquakes and quarry blasts. Parts of our analysis workflow have been implemented as Python tools and will be made available via SED's gitlab platform.

REFERENCES

Kraft, T., Roth, P., & Wiemer, S. (2020). Good-Practice Guide for Managing Induced Seismicity in Deep Geothermal Energy Projects in Switzerland (Version 2). SED-Report. https://doi.org/10.3929/ethz-b-000453228

P 9.14
Monitoring geothermal field Geo-01 using GPSs, seismometer and inclinometers.

Nicolas Houlié[1], Francois Martin[2], Luca Guglielmetti[3], Michel Meyer[2]

[1] *Nicolas Houlié Geologie GmbH, Zurich, Switzerland*
[2] *Services Industriels de Geneve, Geneva, Switzerland*
[3] *University of Geneva, Geneva, Switzerland*

Geothermal production from deep reservoirs allows delivering energy in the form of heat and/or power to final users. Additionally, one application that is recently emerging is seasonal storage of excess heat from industrial and civil processes into the subsurface such as deep aquifers. Stored heat can then be delivered in high heat demand periods according and has the potentially to contribute decarbonizing the energy system by partially replacing fossil fuels that are commonly used for heat production in winter. The potential of storage of excess heat in deep aquifers in Geneva is under investigation in the framework of the European ERA-Net GEOTHERMICA HEATSTORE project.

Heat production and storage are the main applications that are investigated in the framework of the GEOTHERMIES program developed by the Services Industriels de Geneve (SIG) and the Canton of Geneva. The GEo-1 exploration well is the first deep wells drilled by SIG in the Geneva area, it is 744m deep, produces 50l/s of thermal water at 34°C with 8-10 bars wellhead pressure. One of the environmental effects associated with geothermal production is ground deformations which usually occurs due to reservoir depletion because of excessive withdrawn of fluid with respect to the recharge. This effect has been observed in several industrial geothermal fields (Bromley et al. 2010, Mossop and Segall,1997) but has never been investigated for heat storage applications where rather frequent production and injection cycles are operated seasonally. The GEo-01 well is providing a great opportunity to assess the effects of fluid extraction from the reservoir as production tests are planned to be performed in the near future. Therefore, to establish the background noise that can and use it to establish a quiet baseline, before production tests, the GEo-01 well has been monitored using a wide range of geophysical instruments and the combination of truly collocated instruments (inclinometer, GPS and seismometer) allowing for the monitoring of ground motion and local vibration. This study presents the results from the data collection over 12 months, for all parameters of the local context at two locations close to GEo-1. The data time series are discussed in the context of regional tectonics.

REFERENCES

Houlié, N., Woessner, J., Giardini, D., and Rothacher, M.: Lithosphere strain rate and stress field orientations near the Alpine arc in Switzerland, Sci. Rep., 8, 1–14, https://doi.org/10.1038/s41598-018-20253-z, 2018.

P 9.15
GEOBEST2020+: a framework for cantonal authorities to handle induced seismicity risk in deep geothermal energy projects

Kraft, T.[1], V. Antunes[1], Ph. Roth[1], and S. Wiemer[1]

[1] *Swiss Seismological Service at ETH Zurich, Sonneggstr. 5, CH-8092 Zurich (geobest@sed.ethz.ch)*

As a local, versatile, clean, and renewable energy source, geothermal energy can contribute to achieving Switzerland's energy and climate objectives. Worldwide, numerous geothermal projects have been successfully operating for decades. Unfortunately, some have also been aborted during the reservoir construction or operation phase. Today, adequate risk governance of induced seismicity is perceived as essential for establishing safe and economically viable geothermal projects.

In Switzerland, the subsurface is under the sovereignty of the cantons. Therefore, the cantonal authorities in charge of the permitting, concessioning, and regulatory oversight must have access to independent, state-of-the-art seismological expertise. Furthermore, independent seismic monitoring and competent project oversight are important contributions to risk governance and can build and maintain public acceptance of geothermal projects.

GEOBEST2020+ ensures that the Swiss Seismological Service (SED), the federal agency for earthquakes, can provide seismological expertise and baseline seismic monitoring services to the cantons at no cost and independently of the operators of geothermal projects:

Seismological consulting:
SED experts can support the cantonal authorities with:

- defining induced-seismicity-related content requirements for all relevant cantonal authorizations mandatory for geothermal projects,
- reviewing seismological aspects of permit and concession requests submitted by the project operators,
- providing independent, canton-specific information on geothermal energy and seismicity to the public.

Seismic monitoring and earthquake alarming:
SED can provide the baseline seismic monitoring, including:

- installation of a customized seismological monitoring network,
- automatic real-time earthquake analysis, rapidly reviewed by experienced seismologists,
- earthquake alerting via SMS and email to defined stakeholders,
- providing a rapid preliminary assessment of the natural or human-made origin of seismic events,
- operation of a public, project-specific web page with real-time earthquake and background information,
- operation of a public-access archive of the recorded seismological data.

P 9.16
The DEEP Project: Innovation for De-Risking Enhanced Geothermal Energy Projects

Federica Lanza[1], Stefan Wiemer[1]

[1] *Swiss Seismological Service, Swiss Federal Institute of Technology, ETH Zurich, Sonneggstrasse 5 CH-8092 Zurich (federica.lanza@sed.ethz.ch)*

The Swiss Energy Strategy 2050 anticipates that by 2050 up to ~7% of the future energy production will come from deep geothermal energy. In order to meet this target, it is critical to gain more experience with the technologies of Enhanced Geothermal Systems (EGS), and to demonstrate that safe and sustainable development of deep geothermal energy projects is possible.

The DEEP (Innovation for De-risking Enhanced geothermal Energy Projects) project is an international collaboration whose research-goal is to establish a full-scale protocol for real-time monitoring and risk analysis of potential seismicity triggered by EGS operations. To this end, the project will employ innovative seismic sensors, improved event-cataloguing techniques, fully probabilistic seismicity forecasts, and loss assessment strategies. The resulting Adaptive Traffic Light System (ATLS) will be continuously updated with real-time data-feeds, providing an integrated and dynamic assessment of the seismic risk to the operators. The development and testing of the ATLS will take advantage of unique parallel field investigations at the Frontier Observatory for Research in Geothermal Energy (FORGE) in Utah (USA), as well as at EGS sites in Germany and France. Key to the project is also the definition of next-generation good-practice guidelines and risk assessment procedures in order to reduce commercial costs and enhance the safety of future projects, such as the planned Haute-Sorne EGS project in the canton Jura. Here, we will present an overview of the DEEP project to provide a framework for other DEEP presentations. We will also showcase a selection of results from new event detection and location algorithms using machine learning and Distributed Acoustic Sensing (DAS), together with a seismicity simulation for an upcoming FORGE stimulation strategy.

P 9.17
Fluid Injection-Induced Off-Fault Deformation and Seismicity in Shallow Crustal Faults: Preliminary Results from Fully-Coupled Hydro-Mechanical Simulations

Qinghua Lei, Bernard Brixel

Department of Earth Sciences, ETH Zürich, Sonneggstrasse 5, CH-8092 Zürich
(qinghua.lei@erdw.ethz.ch)

We conduct fully-coupled hydro-mechanical simulations (Lei et al., 2021) to study fluid injection-induced pressure diffusion, poroelastic response, fracture deformation, damage growth, and the onset of microseismicity in shallow (<1 km deep) crustal faults, which are comparable analogues to fault zones recently targeted by stimulation experiments at the Grimsel Rock Laboratory, Switzerland (Amann, 2018; Brixel, 2021). In this study, we conceptualise a fault as a two-component system consisting of a low-permeability fault core and a high-permeability damage zone characterised by an exponential decay in fracture density with the off-fault distance (Brixel et al. 2020). Special attention is paid to the complex nature of off-fault damage and we employ the discrete fracture network approach (Lei et al. 2017) to explicitly represent the geometrical distribution and multiphysics response of fractures in both damage zones and host rocks. We use the finite element method to solve the coupled system of governing equations of fluid flow, solid deformation, and damage evolution in the rock mass system. To constrain our results, numerical simulations are parameterised and compared to a set of comprehensive, high-resolution field data characterising the in-situ stress state, pore pressure level, rock and fracture properties, as well as injection protocols applied as part of the stimulation experiments carried out in Grimsel (Krietsch, 2018, 2020; Brixel, 2020a,b). Preliminary results show that the seismo-hydro-mechanical response of stimulated faults in crystalline rock is complex, and controlled by interactions of multiple factors including fracture network geometry, in-situ stress state, and injection location. Insights from our research findings may help develop safer and more efficient stimulation protocols for enhanced geothermal systems and hazard assessment of induced seismicity.

REFERENCES

Amann, F., Gischig, V., Evans, K., Doetsch, J., Jalali, R., Valley, B., Krietsch, H., Dutler, N., Villiger, L., Brixel, B., Klepikova, M., Kittilä, A., Madonna, C., Wiemer, S., Saar, M.O., Loew, S., Driesner, T., Maurer, H., Giardini, D. 2018. The seismo-hydromechanical behavior during deep geothermal reservoir stimulations: Open questions tackled in a decameter-scale in situ stimulation experiment. Solid Earth 9:115-37.

Brixel, B. 2021. Fluid flow in sparse fracture systems, prior to and after fault slip. PhD Thesis. ETH Zürich, Zürich.

Brixel, B., Klepikova, M., Jalali, M.R., Lei, Q., Roques, C., Krietsch, H., & Loew, S. 2020a. Tracking fluid flow in shallow crustal fault zones: 1. New in situ permeability measurements. Journal of Geophysical Research: Solid Earth 125: e2019JB018200.

Brixel, B., Klepikova, M., Lei, Q., Roques, C., Jalali, M.R., Krietsch, H., & Loew, S. (2020b). Tracking fluid flow in shallow crustal fault zones: 2. Insights from cross-hole forced flow experiments in damage zones. Journal of Geophysical Research: Solid Earth 125: e2019JB019108.

Krietsch H, Gischig V, Evans K, Doetsch J, Dutler NO, Valley B, Amann F. 2019. Stress measurements for an in situ stimulation experiment in crystalline rock: Integration of induced seismicity, stress relief and hydraulic methods. Rock Mechanics and Rock Engineering 52:517-42.

Krietsch, H., Gischig, V.S., Doetsch, J., Evans, K.F., Villiger, L., Jalali, M.R., Valley, B., Loew, S., & Amann, F. 2020. Hydromechanical processes and their influence on the stimulation effected volume: Observations from a decameter-scale hydraulic stimulation project. Solid Earth 11: 1699-1729.

Lei, Q., Latham, J.-P., & Tsang C-F. 2017. The use of discrete fracture networks for modelling coupled geomechanical and hydrological behaviour of fractured rocks. Computers and Geotechnics 85: 151-176.

Lei, Q., Gholizadeh Doonechaly, N., & Tsang, C.-F. 2021. Modelling fluid injection-induced fracture activation, damage growth, seismicity occurrence and connectivity change in naturally fractured rocks. International Journal of Rock Mechanics and Mining Sciences 138: 104598.

P 9.18
Linkage between seismogenic index and fault network during fluid injections

Mohammad Javad Afshari Moein[1]

[1] *Institute of Geoscience and Geopgraphy, von-Seckendorff-Platz 3-4, 06120 Halle, Germany (javad.afshari@geo.uni-halle.de)*

Hydraulic stimulation of Enhanced Geothermal Systems (EGS) is carried out to create a commercially exploitable heat exchanger at the target depths (i.e., 2-5 km) with favorable temperatures (i.e., above 120°C). This operation is typically accompanied by injection-induced earthquakes that are manifestations of strain energy release over pre-existing discontinuities such as fractures and faults. Fluid over-pressure disturbs the in-situ stress/strength of the fault system and if the resulting shear stress exceeds the strength of the fault surfaces, the failure would occur. The task of seismic risk and hazard assessment of injection operations requires reliable estimates of the maximum possible magnitude M_{max}. Despite the recent developments in physical understanding of induced seismicity at various scales (laboratory-, intermediate- and large-scale experiments), anticipating M_{max} is still a challenging task. Current M_{max} models do not properly address the site-specific geological conditions including the pre-existing fault network. Moreover, they are often based on the hypothesis that the magnitude of induced events is always below a deterministic upper limit. Among them, the theory proposed by McGarr (2014) is widely applied to estimate maximum seismic moment M_0 by $M_0=GV$ (where, G is the shear modulus and V is the net injected volume). However, this deterministic limit was exceeded in several case histories such as M_w *5.5* in Pohang EGS site in South Korea.

This research incorporated the statistical attributes of fault system (such as fracture length distribution) into the existing seismicity models to constrain the M_{max} estimates. Hence, it adopted an alternative approach and assumed that the largest possible magnitude is identical to that of the natural earthquakes in the region. Moreover, the tectonics and pre-existing fault network likely controlled the magnitude distribution of induced events in critically-stressed regions (van der Elst et al., 2016). Assuming the pore-pressure diffusion as the dominant triggering mechanism, theoretical relations were derived between seismogenic index (a parameters that quantifies the seismotectonic activity of the study site and larger values indicate high level of seismic activity) and fault network attributes (e.g., length distribution) by combining two seismicity models:

1) seismogenic-index theory relating the number of induced events to the injection volume (Shapiro et al., 2010) and,
2) fractal model of induced seismicity relating the number of events to the location and magnitude of seismic events by a dual power-law model (Afshari Moein et al., 2018). Note that the fractal model was originally developed in the context of discrete fracture networks modeling to simulate faulting in the earth's crust (e.g., Afshari Moein et al., 2019).

Eventually, theoretical relations were applied to define conservative estimates of M_{max} as a function of net injection for perturbing a given volume of rock volume. The estimates were based on the reported values of seismogenic index and fracture network attributes in literature. Further investigations revealed that the reported magnitudes of injection-induced earthquakes were below the 90% confidence range of theoretical estimates.

REFERENCES

Afshari Moein, M.J., Tormann, T., Valley, B., Wiemer, S., 2018: Maximum Magnitude Forecast in Hydraulic Stimulation Based on Clustering and Size Distribution of Early Microseismicity. Geophysical Research Letters 45(14), 6907-6917.

Afshari Moein, M.J., Valley, B., Evans, K.F., 2019: Scaling of Fracture Patterns in Three Deep Boreholes and Implications for Constraining Fractal Discrete Fracture Network Models. Rock Mechanics and Rock Engineering.

McGarr, A., 2014: Maximum magnitude earthquakes induced by fluid injection. J Geophys Res-Sol Ea 119(2), 1008-1019.

Shapiro, S.A., Dinske, C., Langenbruch, C., Wenzel, F., 2010: Seismogenic index and magnitude probability of earthquakes induced during reservoir fluid stimulations. The Leading Edge 29(3), 304-309.

van der Elst, N.J., Page, M.T., Weiser, D.A., Goebel, T.H.W., et al., 2016: Induced earthquake magnitudes are as large as (statistically) expected. J Geophys Res-Sol Ea 121(6), 4575-4590.

P 9.19
Automatic passive acoustic emission-microseismic monitoring using a parallel algorithm; A case study of a hydraulic-fracturing experiment

Seyyedmaalek Momeni*, Guanyi Lu, Brice Lecampion

Geo-Energy Laboratory, Gazant chair on Geo-Energy, EPFL. Station 18, CH-1015, Lausanne, Switzerland.
*(seyyedmaalek.momeni@epfl.ch)

Acoustic emission and microseismic (AE-MS) monitoring are similar seismic techniques to study the transient elastic wave signals of acoustic emissions and microseisms produced at seismic sources with low magnitudes (usually <1) compared to natural earthquakes. AE-MS monitoring is an effective way to study the spatio-temporal distribution of fractures. This technique has several applications including monitoring of hydraulic fracturing growth, flow mobilities in oil and gas production, geothermal reservoir stimulation, induced seismicity for hazard assessment purposes, and laboratory experiments for understanding the physics of fracturing phenomena (Vera Rodriguez et al, 2017). In the context of hydraulic fracturing, AE-MS is due to the sudden occurrence of i) tensile cracks (mode I) and ii) frictional sliding along grain boundaries (mode II) around the propagating fracture (Mogi, 2007).

AE-MS monitoring provides source locations of a significant number of micro-cracking events occurring within an observable frequency bandwidth that helps in imaging the fracture process zone and understanding mechanisms of the associated source ruptures. The abundance (usually > 1000 per minute of data) and high-frequency content (usually in scale of KHz) of AE-MS events during fracturing phenomena, make their datasets large (usually in the order of hundreds of GB) and lead to some significant challenges for data acquisition, processing, and localization.

We present an automatic Acoustic Emission-MicroSeismic detection-localization algorithm suitable for both laboratory and field AE-MS monitoring (see Momeni et al., 2021 for details). The algorithm is fast, parallelized, and flexible in defining all parameters that control the detection, phase reading, and localization sub-algorithms. Seismic and acoustic data with various formats can be used and isotropic and transversely isotropic materials are implemented in the code.

We show the AE localization results for a hydraulic fracturing test on a transversely isotropic Slate rock sample. Applying the described localization algorithm on three minutes of continuous data acquired (at a sampling rate of 10 MHz) from this test and recognized as rupture time from an active acoustic method (see Liu et al., 2020 for details), we detect and locate more than 3100 AEs. To have reliable locations, we then select AEs that are recorded by at least six sensors, have an azimuthal gap of <180◦, and an RMS of <1 microsecond. The new set contains 789 AEs. Their spatio-temporal distribution during the HF experiment is displayed in Figure 1. Parallel to the passive monitoring system, active acoustic measurements have been performed and allow to reconstruct the fracture fronts using P-wave diffracted signals. The passive AEs related to the fracture process zone correlates well with the fracture fronts obtained from active acoustic measurements (Fig. 1).

For the mentioned study case, the processing, detection, and localization of > 100 GB of acoustic data took less than 4 hours on a laptop computer using three 2.3 GHz processors and 16 GB of RAM. The spatio-temporal distribution of AEs is relatively consistent with active acoustic measurements of the fracture front using diffracted P-waves. It is notable that the AEs distribute ahead of the reconstructed fracture front, most likely in relation to the fracture process zone. The cloud of seismicity on top of the main fracture is mainly related to the activated bedding planes.

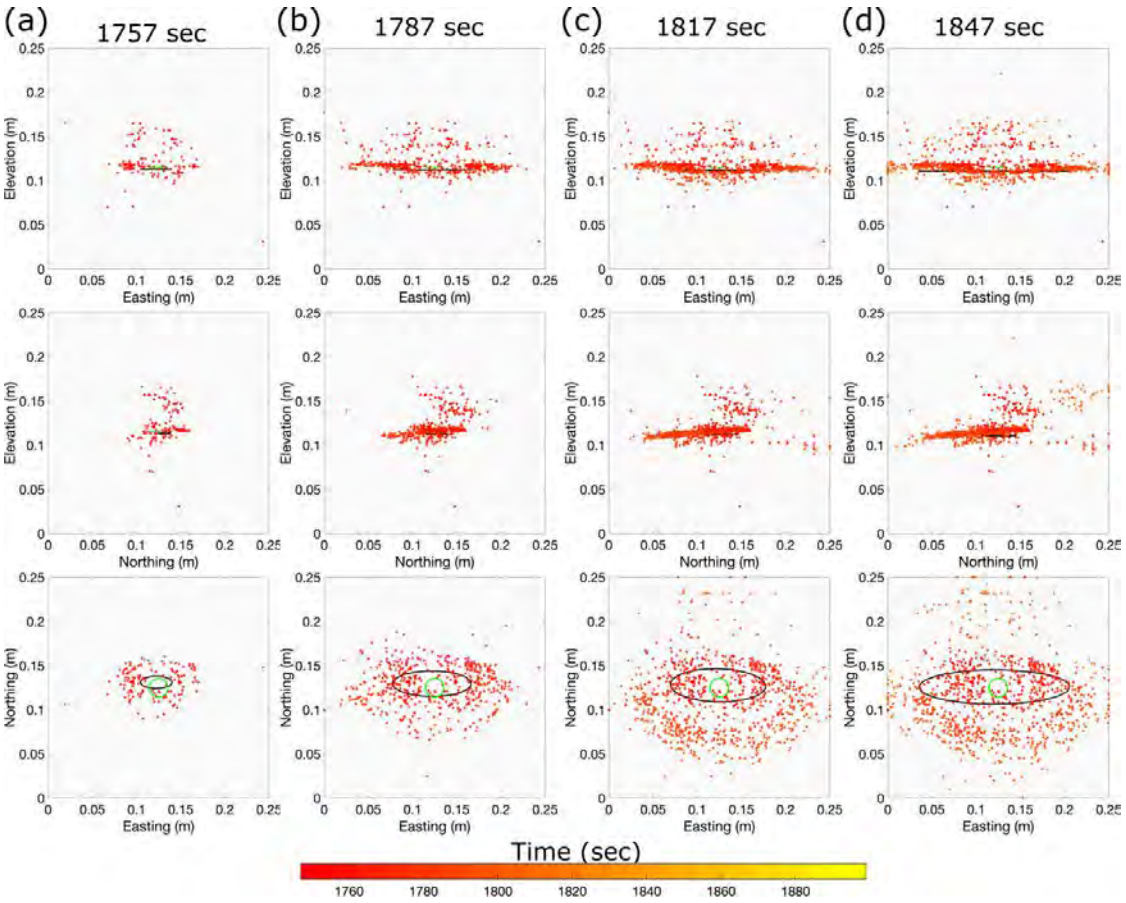

Figure 1. Snapshots of the spatio-temporal distribution of hydraulic fracture growth and occurred AEs during the Slate-K104 experiment. Black ellipses represent the fracture fronts estimated from the active acoustic measurements (see Liu et al., 2020) at specific times for each column. The green circles show the injection(notch) location. Color-filled circles are the AEs occurred until that time. The three rows show different views of the results from the north, east, and top, respectively.

REFERENCES

Vera Rodriguez, I., Stanchits, S., Burghardt, J. [2017] Data-Driven, In Situ, Relative Sensor Calibration Based on Waveform Fitting Moment Tensor Inversion. *Rock Mech Rock Eng, 50:891–911.*

Liu, D., Lecampion, B. and Blum, T. [2020] Time-lapse reconstruction of the fracture front from diffracted waves arrivals in laboratory hydraulic fracture experiments. *Geophys. J. Int.*, 223, 180– 196.

Mogi, K. Experimental rock mechanics. London: Taylor & Francis; 2007. p. 361.

Momeni, S., Liu, D. and Lecampion, B. [2021] Combining active and passive acoustic methods to image hydraulic fracture growth in laboratory experiments. *Eurock21*.

P 9.20
Dedicated seismic study of the Domo de San Pedro geothermal field Nayarit, Mexico

F. Muñoz[1], M. Calò[2], M. Lupi[1], V. Reyes[3]

1 Université de Genève UNIGE, 13 Rue des Maraîchers, 1205, Genève, Suisse
(francisco.munozburbano@unige.ch, matteo.lupi@unige.ch)
2 Universidad Nacional Autónoma de México UNAM, Ciudad Universitaria, 04510, México, México
(calo@igeofisica.unam.mx)
3 Grupo Dragón, Km 12 Carr. Chapalilla-Compostela. San Pedro Lagunillas, Nayarit. México
(vreyeso@gdragon.com.mx)

The Domo de San Pedro is part of a silicic volcanic complex located in the westernmost part of the trans-Mexican volcanic belt. The dome is a hydrothermal magmatic driven system of high enthalpy with probed geothermal potential. Early studies have suggested the existence of active seismic sources product of the crustal deformation of the region. A collaboration between the UNIGE, UNAM, Grupo Dragón, and the Swiss agency REPIC* resulted in the retrieval of six months of seismic data from a new temporary seismological network deployed in the vicinity of the Domo de San Pedro geothermal field in the state of Nayarit, Mexico in 2021. The network consists of 20 broadband seismological stations covering approximately 400km^2 with a detection capacity of earthquakes from a magnitude of 0.5. The new seismic dataset also registered low magnitude earthquakes with events ranging from 0 to 1.1 likely associated with the local fault systems trending NW-SE. The network has also registered high-frequency signals with frequencies from 10 to 20 Hz, in some cases turning to harmonic with a dominant frequency of 15 Hz. Those events seem to be produced by the intervention of the wells in the Domo de San Pedro power plant. During the study, none of the local earthquakes seem triggered by the operations of the power plant. We aim to complete at least one year of data acquisition to focus our investigation on the effective use of affordable passive seismic methods for geothermal exploring in two ways. First, to characterize the seismic behavior of the region and second, to derive tomographic images from ambient noise up to 5km depth to shed light on the 3D velocity structure of the Domo de San Pedro that in combination with the currently available information lead to refining the conceptual model of the geothermal field.
We introduce an earthquakes catalog and advances in obtaining a new 1D velocity model for local earthquakes location derived by simultaneous hypocenter-velocity inversion.

* Renewable Energy, Energy and Resource Efficiency Promotion in Developing and Transition Countries. https://www.repic.ch/en

P 9.21
How good are existing seismicity models at forecasting induced seismicity in EGS?

Luigi Passarelli[1], Antonio Pio Rinaldi[1], Iason Grigoratos[1], Federico Ciardo[1], Marco Broccardo[2], Federica Lanza[1], Stefan Wiemer[1]

[1] *Schweizerischer Erdbebendienst (SED), ETH Zürich, Switzerland.*
[2] *Dept. Civil, Environmental, and Mechanical Engineering, University of Trento, Italy*

Enhanced Geothermal Systems (EGS) usually employ hydraulic fracturing (HF) to increase the rock permeability and favor a more efficient exploitation of deep hydrothermal reservoirs when local geology does not favor natural pathways for fluid circulation. HF can at times cause seismicity that can be felt by nearby residents and, if earthquakes are large enough, it can cause structural damages to properties. The adoption of EGS thus requires a careful assessment of seismic hazard to mitigate the occurrence of large earthquakes. Induced seismicity models able to assess future earthquake occurrences are a key aspect of the seismic hazard analysis associated with EGS. An objective evaluation of the forecasting performance of these seismicity models is thus desirable in order to assess the models' capability to produce plausible probabilistic scenarios for a given HF injection-strategy. For this reason, we have developed a statistical methodology to compare seismicity models and have integrated it in a pseudo real-time strategy with a data assimilation scheme. The statistical comparison of the models we propose is flexible enough to include any seismicity model and can be tested a posteriori on existing datasets or implemented in real-time monitoring operations.

We based the model-comparison algorithm on the information theory by directly comparing the logarithm of the probability of models to reproduce the observed seismicity rate. We tested two statistical models and a hydromechanical model; all three use seismicity and hydraulic data as input-parameters. We employed two HF injection experiments in Switzerland with different seismological characteristics and data quality; the Basel stimulation in 2006 and the Bedretto Lab injection in November 2020. We split the datasets into two parts, one for learning and one for validation. On the learning data we derive the parameters of the seismicity models, and their associated uncertainties. We then produced forecasts and compared the model-performances to reproduce the observed data in the validation part. The forecasts are simulated on either the whole validation period and on a finer time bin discretization with progressive data assimilation. The results indicate that regardless of the quality of data, the model with larger uncertainties of the parameters performs better at forecasting the observed earthquake occurrence. This preliminary analysis on model-comparison suggests that seismicity models that are able to produce large variability of earthquake occurrence scenarios do not have to be deemed inaccurate in real-time applications and in a priori studies of the seismic hazard during HF operations.

10. Scientific Drilling is Going Strong, Scientific Drilling Matters!

Miriam Andres, Anders McCarthy, Judith McKenzie, Camille Thomas, Helmut Weissert

TALKS:

10.1 Früh-Green G.L, Orcutt B.N, Bernasconi S.M, Lilley M.D, Kelley D.S., IODP Expedition 357 Science Party: Magmatism, hydrothermal alteration and life at slow-spreading ridges: Insights from Lost City and drilling the Atlantis Massif

10.2 Haas M., Plötze M., Moscariello A.: Geo-engineering feasibility study of CERN's 90-100 km subsurface infrastructure in the Geneva Basin

10.3 Hernández-Almeida I., Saavedra-Pellitero M., Cabarcos E., Flores J.A., Sierro F.J., Baumann K.H.: Coupled coccolith-based temperature and productivity reconstructions in the Eastern Equatorial Pacific during the last deglaciation and the Holocene

10.4 Le Houedec S., Mojtahid M., Ciobanu M., Jorry S.J., Bouhdayad F.Z., Guyonneau E., Sourice S., Toucanne S.: Deglacial to Holocene environmental changes in the northern Ligurian Sea (core KESC9-14)

10.5 Liu Y., Greenwood A., Hetényi G., Baron L., Scarponi M., Müntener O., Holliger K.: Geophysical surveys in the Ivrea-Verbano Zone: Novel approaches for interpreting steeply dipping structures

10.6 Magnabosco C.: Life in the Swiss underground and implications for the habitability of other planets

10.7 Schaller S., Anselmetti F., Buechi M.W., Fiebig M., Gabriel G., Kroemer E., Preusser F., Reitner J., Schuster B., Tanner D., Wielandt-Schuster U.: ICDP Project DOVE (Drilling Overdeepened Alpine Valleys): First results from the Basadingen Borehole

10.8 Vogel H., Haberzettl T., Kipfer R., Daut G., Wonik T., Ariztegui D., Berg J., Thomas C., Magnabosco C., Wang J., Zhu L., Spiess V., Barbolini N., Clarke L., Henderson A., van der Woerd J., Waldmann N.: The Nam Co Drilling Project, Tibet (NamCore): towards retrieving a one million year sedimentary record from the third pole

10.9 Zhang H., Liu C., Hernández-Almeida I., Mejía L.M., Stoll H.M.: High and low latitude controls on Mid-Brunhes Coccolithophore Bloom and implications on ocean carbon cycle

POSTERS:

P 10.1 Müntener O., Hétenyi G., Rubatto D., Hermann J., Holliger K.: Exploring the lower continental crust: geology, geophysics, and the Ivrea drilling project DIVE

P 10.2 Greenwood A., Baron L., Hetényi G., DIVE Site Survey 2019 Field Team & project DIVE Team: Siting the DIVE DT-1a drillhole – from geology and geomorphology to modeling and seismic imaging

P 10.3 Pasiecznik D., Greenwood A., Baron L., Hetényi G., Bleibinhaus F.: A high-resolution seismic survey across the Balmuccia Peridotite, Ivrea Zone, Italy – Project DIVE phase two, site investigation

P 10.4 Pistone M., Ziberna L., Hetényi G., Scarponi M., Zanetti A., Müntener O.: Joint Geophysical-Petrological Modeling on the Ivrea Geophysical Body Beneath Valsesia, Italy: Constraints on the Continental Lower Crust prior to Drilling the Ivrea-Verbano zonE (DIVE)

P 10.5 Fiebig M., Anselmetti F., Buechi M.W., Gabriel G., Kroemer E., Preusser F., Reitner J., Schaller S., Schuster B., Tanner D.C., Wielandt-Schuster U.: Drilling overdeepened Eastern Alpine valleys and basins

P 10.6 Schuster B., Tanner D.C., Gabriel G., Burschil T., Wonik T., Preusser F., Anselmetti F., Buechi M.W., Schaller S., Fiebig M., Wielandt-Schuster U.: Drilling Overdeepened Alpine Valleys: First results from the Tannwald Borehole

P 10.7 Montillier A., Pappalardo G., Samankassou E., Spezzaferri S. & the RESILIENCE Project Partners: undeRstanding coral thErmal bleaching threSholds during past InterglaciaL extremes: Insight into thermal strEss dyNamics on tropical Coral reef Ecosystems (RESILIENCE)

P 10.8 Stoll H.M., Guitian J., Hernandez-Almeida I., Palike H., Pena L.: $^{87}Sr/^{86}Sr$ to reconcile chronology and weathering through the Oligocene

P 10.9 Guitián J., Hernández-Almeida I., Fuertes M.A., Flores J.A., Stoll H.: Response of Coccolithophores to the Oligocene – Miocene Dynamic System: Size and Degree of Calcification

P 10.10 Weidlich R., Bialik O.M., Rueggeberg A., Grobéty B., Vennemann T., Makovsky Y., Foubert A.: Morphological and Geochemical Characterisation of south-eastern Mediterranean Seep Carbonates

P 10.11 Thomas C., Vogel H., Ariztegui D.: Microbes as probes of past and present environmental changes recorded in lake sediments

P 10.12 Rodriguez P., Berg J., Deng L., Vogel H., Lever M.A. , Magnabosco C.: Vertical variation of the microbial community structure and functional potential in an 8000-year sediment sequence from Lake Cadagno (Piora Valley, Switzerland)

10.1
Magmatism, hydrothermal alteration and life at slow-spreading ridges: Insights from Lost City and drilling the Atlantis Massif

Gretchen L. Früh-Green[1], Beth N. Orcutt[2], Stefano M. Bernasconi[1], Marvin D. Lilley[3], Deborah S. Kelley[3], IODP Expedition 357 Science Party

[1] *Department of Earth Sciences, ETH Zurich, Sonneggstrasse 5, CH-8092 Zurich (frueh-green@erdw.ethz.ch)*
[2] *Bigelow Laboratory for Ocean Sciences, East Boothbay, Maine, 04544, USA*
[3] *School of Oceanography, Univ. of Washington, Seattle, Washington, 98105, USA*

Ultramafic and lower crustal rocks are exposed on the seafloor in different tectonic settings and have been the target of a number of expeditions throughout the history of ocean drilling. Progressive interaction of seawater with mantle-dominated lithosphere during serpentinization is a fundamental process that controls rheology and geophysical properties of the oceanic lithosphere and has major consequences for heat flux, geochemical cycles and microbial activity. At slow spreading ridge environments, serpentinization occurs along detachment faults (major, large-scale offset normal faults), as mantle rocks are uplifted to the seafloor and are incorporated in dome-shaped massifs known as oceanic core complexes. The processes controlling hydrothermal activity and a deep biosphere are intimately linked, however, the spatial scale of lithological variability, the implications for geochemical cycles and the consequences for subsurface ecosystems supported by these systems remain poorly constrained. This presentation will provide an overview of magmatic and alteration processes at the Atlantis Massif (Mid-Atlantic Ridge, 30°N, Fig. 1A) and will highlight the importance of the discovery of the spectacular Lost City hydrothermal field (Kelley et al., 2005) and recent results of drilling during IODP Expedition 357.

The Atlantis Massif is one of the best-studied oceanic core complexes and hosts the low-temperture Lost City hydrothermal field on its southern wall (Fig.1). Serpentinization reactions in the underlying mantle rocks produce clear, “non-smoking”, high pH fluids that form intricate carbonate-brucite structures upon venting on the seafloor. The fluids have high concentrations of hydrogen, methane and formate that support novel microbial communities dominated by methane-cycling archaea in the hydrothermal carbonate deposits (Kelley et al., 2005). Understanding the links between serpentinization processes and microbial activity in the shallow subsurface of the Atlantis Massif was one focus of IODP Expedition 357, which used seabed rock drilling technology for the first time in the history of ocean drilling to recover ultramafic and mafic rock sequences and fluids along a detachment fault zone (Früh-Green et al., 2017). The expedition also successfully applied new technologies that provide insights into active serpentinizing systems at slow-spreading ridges. An *in-situ* sensor package and water sampling system recorded real-time variations in dissolved methane and hydrogen, oxygen, pH, oxidation reduction potential, temperature and conductivity during drilling and sampled bottom water after drilling. Systematic excursions in these parameters together with elevated hydrogen and methane concentrations in post-drilling fluids provide evidence for active serpentinization at all sites (Früh-Green et al., 2018). A major achievement of Expedition 357 was to obtain microbiological samples along a west–east profile to better understand how microbial communities are sustained as ultramafic rocks are altered and emplaced on the seafloor. The presence of a limited biosphere in this subseafloor environment is confirmed by cell counts, which revealed cell densities on the order of 10-10^4 cells per cubic centimetre of rock.

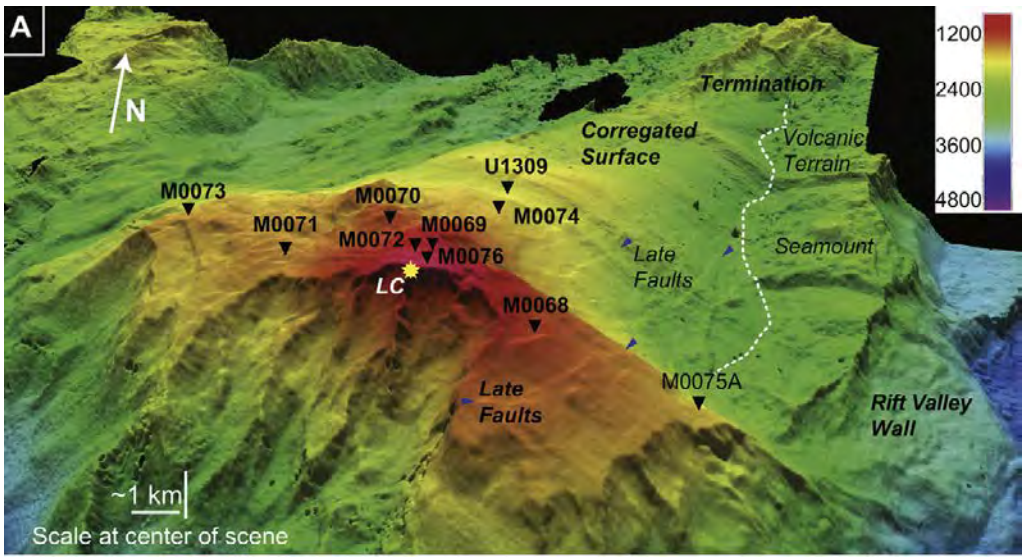

B.

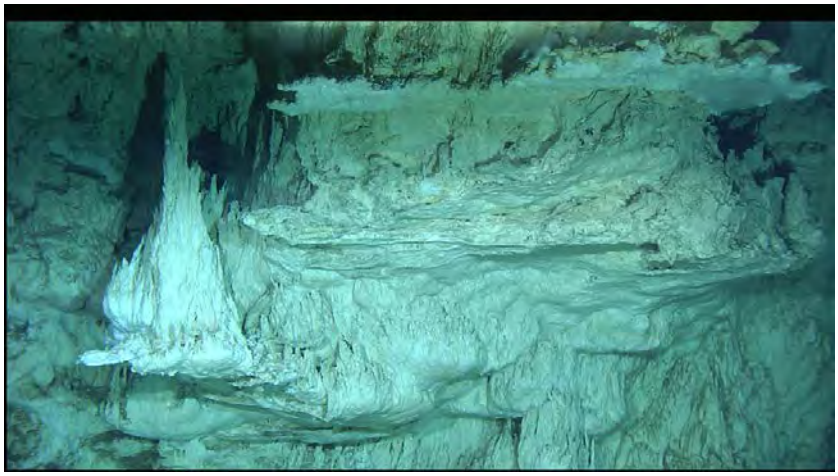

Figure 1. (A): 3-D bathymetric model of the Atlantis Massif with a northward view of the detachment fault surface showing striations associated with detachment faulting and locations of IODP Expedition 357 drill sites, the Lost City hydrothermal field (LC: yellow star) and Site U1309 (drilled in during IODP Exps. 304 & 305 and, primarily recovering gabbroic rocks). (B): Carbonate-brucite minerals are deposited from high pH fluids at temperatures of 40-95°C, forming elaborate towers and structures of the Lost City hydrothermal field.

REFERENCES

Früh-Green, G. L., et al. 2017: Atlantis Massif Serpentinization and Life, Proceedings of the International Ocean Discovery Program, College Station, TX, http://dx.doi.org/10.14379/iodp.proc.357.2017.

Früh-Green, G.L., et al. 2018: Magmatism, serpentinization and life: Insights through drilling the Atlantis Massif (IODP Exp. 357): Lithos, 323, 137–155.

Kelley, D.S., et al., 2005, A serpentinite-hosted ecosystem: The Lost City Hydrothermal Field: Science, 307, 1428–1434.

10.2
Geo-engineering feasibility study of CERN's 90-100 km subsurface infrastructure in the Geneva Basin

Maximilian Haas[1,2,3], Michael Plötze[4], Andrea Moscariello[3]

[1] *European Organization for Nuclear Research (CERN), Esplanade Des Particules 1, CH-1211 Geneva (maximilian.mathias.haas@cern.ch)*
[2] *Subsurface Engineering, Montanuniversität Leoben, Erzherzog-Johann-Strasse 3, AT-8700 Leoben*
[3] *GE-RGBA Group, Department of Earth Sciences, University of Geneva, Rue des Maraîchers 13, CH-1205 Geneva*
[4] *Institute for Geotechnical Engineering (ClayLab), ETH Zurich, Stefano-Franscini-Platz 3, CH-8093 Zurich*

The European Organization for Nuclear Research (CERN) is currently undertaking a feasibility study to build the next-generation particle accelerator, named the Future Circular Collider (FCC) to be hosted in a 90-100 km subsurface infrastructure in the Geneva Basin, extending across western Switzerland and adjacent France between depth intervals of 100 to 300 m above sea level (Figure 1). Geo-engineering feasibility concepts require detailed subsurface investigations to address tunnelling construction hazards as well as environmental impact assessment to pave the way for FCC's subsequent technical design phase.

The Geneva Basin (GB) constitutes the most south-western part of the Northern Alpine Foreland Basin (NAFB) and has been the object of intensive research over the past fifty years with a particular focus on its tectono-sedimentary evolution and associated potential for mineral and geo-energy resources, both at regional (Ziegler, 1990) and local scales (Doppler, 1989). During the past decade, research concentrated on the potential importance of carbonate formations for geothermal exploration and subsurface heat storage (Moscariello, 2019). A distinct lack of shallow stratigraphic analyses and lithotype identification remains for the subsurface of the GB; in particular, the identification of geo-engineering hazards such as swelling rocks, karstic intervals, aquifer horizons and traces of hydrocarbons considering environmental impact, and active fault regimes.

This article aims to provide an extracted overview of the subsurface interval across the Geneva Basin based on the review of 660 existing wells from former research and industrial activities, digitizing and analysing associated well documentation and geophysical well-logs and identifying lithotypes substantiated by available inspected core material and petrophysical calculations for a detailed evaluation of FCC's subsurface conditions for subsequent underground construction. These core and geophysical well-log data are further integrated with mineralogical, geochemical and petrophysical laboratory analyses using a multi-disciplinary approach across several geoscientific domains to decipher the extent of inferred geological hazards and serve as a basis for a robust predictive approach for FCC's large-scale subsurface construction to address current engineering uncertainties and optimize well placement prior to high-hazard site investigations.

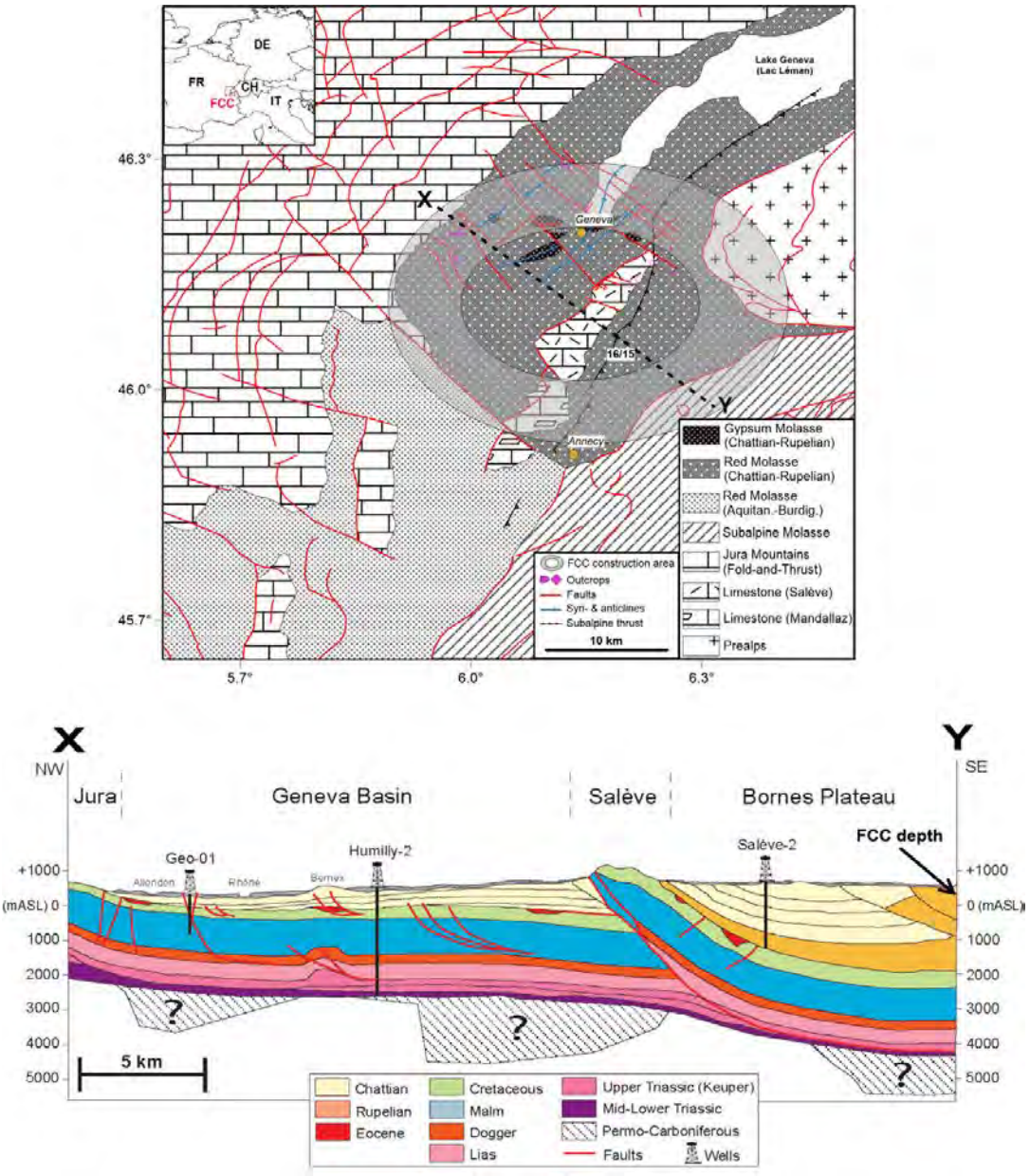

Figure 1. Top: Layout of FCC's current tunnel perimeter in the Geneva Basin. Bottom: cross section X-Y of intersecting geological formations. Modified after Haas et al. (submitted).

REFERENCES

Doppler, G., 1989. Zur Stratigraphie der nördlichen Vorlandmolasse in Bayrisch-Schwaben. Geol. Bavarica 94, 83– 133.

Haas, M., Carraro, D., Ventra, D., Plötze, M., De Haller, A., Moscariello, A. 2021: Multidisciplinary geo-engineering characterisation for CERN's proposed Future Circular Collider subsurface infrastructure in the Geneva Basin (Switzerland-France) from well-log, laboratory and field data, submitted.

Moscariello, A., 2019. Exploring for geo-energy resources in the Geneva Basin (Western Switzerland): Opportunities and challenges. Swiss Bull. Appl. Geol. 24, 105–124.

Ziegler, P.A. 1990. Geological Atlas of Western and Central Europe, Geological Atlas of Western and Central Europe. Shell Internationale Petroleum Maatschappij B.V.

10.3
Coupled coccolith-based temperature and productivity reconstructions in the Eastern Equatorial Pacific during the last deglaciation and the Holocene

Iván Hernández-Almeida[1], Mariem Saavedra-Pellitero[2], Eloy Cabarcos[3], Jose-Abel Flores[3], Francisco Javier Sierro[3], Karl-Heinz Baumann[4]

[1] Geological Institute, Department of Earth Science, ETH, 8092, Zürich, Switzerland (ivan.hernandez@erdw.ethz.ch)
[2] University of Birmingham, School of Geography, Earth and Environmental Sciences, Birmingham B15 2TT, UK
[3] Department of Geology, University of Salamanca, 37008, Salamanca, Spain
[4] University of Bremen, Department of Geosciences, P.O. Box 33 04 40, 28334 Bremen, Germany

We present a new high-resolution reconstruction of sea-surface temperatures (SST) and net primary productivity (NPP) based on novel coccolithophore-based models developed for the Easter Equatorial Pacific (EEP). We combined published coccolithophore census counts from core-tops in the Eastern Pacific with 32 new samples from the Equatorial region, to derive a new statistical model to reconstruct annual SST (SSTa). Results show that the addition of the new EEP samples improves existing SST-calibrations, and allow reconstructing SSTa in the EEP with higher confidence. We also merged the relative abundance of deep-photic living coccolithophore *Florisphaera profunda* with existing calibration datasets for tropical regions, to reconstruct NPP. Both temperature and productivity calibrations were successfully applied to fossil coccolith data from ODP Site 1240, in the EEP. The coccolith-based SSTa estimates show a clear cooling during the LGM and the Younger dryas, and warming at the start of the Holocene. This pattern differs in the timing and magnitude of the temperature changes from other available SST-reconstructions based on biogeochemical and faunal proxies. We discuss these discrepancies to be the result of different responses of the proxies to forcings, seasonal bias, or preservation artefacts. The NPP shows a general decreasing trend from the late last glacial period to recent times, which we relate to the weakening of wind-driven upwelling during the Holocene. We also calculated carbon export using our SSTa and NPP reconstructions, and compared to other geochemical-based reconstructions for the same location. Our coupled SSTa-NPP reconstruction provides key data to properly assess the evolution of primary and export productivity as well as organic carbon burial in the EEP.

10.4
Deglacial to Holocene environmental changes in the northern Ligurian Sea (core KESC9-14)

Sandrine Le Houedec[1], Meryem Mojtahid[2], Maria Ciobanu[3], Stephan J. Jorry[3], Fatima Zohra Bouhdayad[5], Emma Guyonneau[2], Stéphane Sourice[2], Samuel Toucanne[3]

[1] University of Geneva, Department of Earth Sciences, Rue des Maraîchers 13, CH-1205 Genève, Switzerland (sandrine.lehouedec@unige.ch)
[2] LPG-BIAF UMR-CNRS 6112, UNIV Angers, CNRS, 2 bd Lavoisier 49045, Angers Cedex 01, France.
[3] IFREMER, Unité de Recherche Géosciences Marines, Laboratoire Géodynamique et enregistrement Sédimentaire, CS10070, F-29280 Plouzané, France.
[4] Institute of Geology and Mineralogy, Faculty of Mathematics and Natural Sciences, University of Cologne, Otto-Fischer-Straße 14, 50674 Cologne, Germany.

The sedimentary archives of the Mediterranean Sea record periodic deposits of organic-rich deposits, called sapropels in the eastern basin (e.g. Rossignol-Strick, 1985; Rohling et al., 1994; 2015) and organic-rich layers (ORL) in the western basin (e.g. Rogerson et al., 2008; Incarbona and Sprovieri, 2020; Pérez-Asensio et al., 2020). Changes in both the Mediterranean circulation and inputs of fresh water through borderlands rivers under more humid climate, are important mechanisms to explain those events (e.g., Rossignol-Strick et al., 1982, 1985; Rohling et al., 2002, 2015; Casford et al., 2003; Marino et al., 2009; Hennekam et al., 2014; Weldeab et al., 2014). The last ORL and sapropel S1 have different timing, respectively from ~14.5 to 9 Ka and from ~10 to 6 Ka, presumably due to different forcing factors in the western basin (Bard et al., 2002; Toucanne et al., 2015; Wagner et al., 2019). Here we present high-resolution studies of marine sediment core located off the Var River, one of the most dynamic river systems of the northern borderland of the western Mediterranean Sea. A multi-proxy approach based on benthic foraminiferal assemblages, foraminiferal δ18O and δ13C, and sedimentological data was applied to decipher the regional climate signals from the basin-scale intermediate circulation signature.

Our results do not point to major change in the regional hydrology at the time period corresponding to the deposit of the last ORL. However, foraminiferal and geochemical evidence indicate that the 11-6 kyr period, concomitant to Sapropel S1 event in the Eastern Mediterranean, was characterised by high river activity and low ventilated bottom waters at the studied location. In such case, the contribution of western Mediterranean rivers to the development of east Mediterranean sapropel should be further considered. Additionally, our results characterized the last 6 ka with large scale episodes of more active bottom water ventilation due perhaps to enhanced wind activity under an overall cooler climate.

REFERENCES

Bard, E., Delaygue, G., Rostek, F., Antonioli, F., Silenzi, S., & Schrag, D. P. (2002). Hydrological conditions over the western Mediterranean basin during the deposition of the cold Sapropel 6 (ca. 175 kyr BP). Earth and Planetary Science Letters, 202(2).

Casford, J. S. L., Rohling, E. J., Abu-Zied, R. H., Fontanier, C., Jorissen, F. J., Leng, M. J., et al. (2003). A dynamic concept for eastern Mediterranean circulation and oxygenation during sapropel formation. Palaeogeography, Palaeoclimatology, Palaeoecology, 190, 103–119.

Hennekam, R., Jilbert, T., Schnetger, B., & de Lange, G. J. (2014). Solar forcing of Nile discharge and sapropel S1 formation in the early to middle Holocene eastern Mediterranean. Paleoceanography, 29(5), 343–356.

Incarbona, A., & Sprovieri, M. (2020). The Postglacial Isotopic Record of Intermediate Water Connects Mediterranean Sapropels and Organic-Rich Layers. Paleoceanography and Paleoclimatology, 35(10).

Marino, G., Rohling, E. J., Sangiorgi, F., Hayes, A., Casford, J. L., Lotter, A. F., et al. (2009). Early and middle Holocene in the Aegean Sea: interplay between high and low latitude climate variability. Quaternary Science Reviews, 28(27), 3246–3262.

Pérez-Asensio, J. N., Frigola, J., Pena, L. D., Sierro, F. J., Reguera, M. I., Rodríguez-Tovar, F. J., et al. (2020). Changes in western Mediterranean thermohaline circulation in association with a deglacial Organic Rich Layer formation in the Alboran Sea. Quaternary Science Reviews, 228, 106075.

Rogerson, M., Cacho, I., Jimenez-Espejo, F., Reguera, M. I., Sierro, F. J., Martinez-Ruiz, F., et al. (2008). A dynamic explanation for the origin of the western Mediterranean organic-rich layers. Geochemistry, Geophysics, Geosystems, 9(7).

Rohling, E., Mayewski, P., Abu-Zied, R., Casford, J., & Hayes, A. (2002). Holocene atmosphere-ocean interactions: records from Greenland and the Aegean Sea. Climate Dynamics, 18(7), 587–593.

Rohling, E. J., Marino, G., & Grant, K. M. (2015). Mediterranean climate and oceanography, and the periodic development of anoxic events (sapropels). Earth-Science Reviews, 143, 62–97.

Rohling, Eelco J. (1994). Review and new aspects concerning the formation of eastern Mediterranean sapropels. Marine Geology, 122(1), 1–28.

Rossignol-Strick, M. (1985). Mediterranean Quaternary sapropels, an immediate response of the African monsoon to variation of insolation. Palaeogeography, Palaeoclimatology, Palaeoecology, 49(3), 237–263.

Rossignol-Strick, M., Nesteroff, W., Olive, P., & Vergnaud-Grazzini, C. (1982). After the deluge: Mediterranean stagnation and sapropel formation. Nature, 295(5845), 105–110.

Toucanne, S., Soulet, G., Freslon, N., Silva Jacinto, R., Dennielou, B., Zaragosi, S., et al. (2015). Millennial-scale fluctuations of the European Ice Sheet at the end of the last glacial, and their potential impact on global climate. Quaternary Science Reviews, 123, 113–133. ht

Wagner, B., Vogel, H., Francke, A., Friedrich, T., Donders, T., Lacey, J. H., et al. (2019). Mediterranean winter rainfall in phase with African monsoons during the past 1.36 million years. Nature, 573(7773), 256–260.

Weldeab, S., Menke, V., & Schmiedl, G. (2014). The pace of East African monsoon evolution during the Holocene. Geophysical Research Letters, 41(5), 1724–1732.

10.5
Geophysical surveys in the Ivrea-Verbano Zone: Novel approaches for interpreting steeply dipping structures

Yu Liu[1], Andrew Greenwood[1,2], György Hetényi[1], Ludovic Baron[1], Matteo Scarponi[1], Othmar Müntener[1], Klaus Holliger[1]

[1] Institute of Earth Sciences, University of Lausanne, Lausanne, Switzerland (yu.liu@unil.ch)
[2] Chair of Applied Geosciences, Montanuniversität Leoben, Leoben, Austria

A high-resolution seismic reflection survey has been conducted across the Insubric Line from the Sesia Zone into the Ivrea-Verbano Zone (IVZ), where a remarkably complete cross-section of lower continental crust is exposed. The survey was carried out in preparation for the DIVE (Drilling the Ivrea-Verbano zonE) project, which was recently approved by the International Continental Scientific Drilling Program (ICDP). DIVE aims to gain new insights into the characteristics of the lower continental crust through targeted drilling, sampling, and borehole logging. A key borehole is planned near the Insubric Line at Balmuccia, where the deepest parts of the lower continental crust are exposed. As such, the primary objective of this seismic survey was to explore whether the sub-vertical structures prevailing at the surface can be expected to continue at depth or whether there are any indications for major flattening or fault-related offsets. Correspondingly, the acquisition and processing of the seismic reflection data were geared towards revealing weak backscattered events from local heterogeneities associated with the prevailing sub-vertical structural grain. The migrated sections, contain coherent backscattered events to a depth of ~1 km, which form numerous short lineaments that do indeed seem to align sub-vertically. To substantiate this observation, we have generated synthetic seismic reflection surveys for canonical models of sub-vertical structures associated with Gaussian- and binary-distributed heterogeneities. Both the observed and synthetic seismic data were then subjected to energy-based attribute analysis as well as geostatistical estimations of the structural aspect ratios and associated dips. The results of these quantitative interpretation approaches are indicative of the overall consistency between the synthetic and the observed seismic data and, hence, support the original qualitative interpretation of the latter in that the sub-vertical structural grain evident at the surface seems to prevail throughout the imaged part of the uppermost crust. Further down, structural and compositional constraints are provided by newly acquired gravity and passive seismic data. These point to a marked increase of both density and seismic velocity at shallow depth (~1-3 km b.s.l) and a sub-vertical continuation of the associated anomaly, interpreted as the protruding Ivrea Geophysical Body (IGB), across the remainder of crust.

10.6
Life in the Swiss underground and implications for the habitability of other planets

Cara Magnabosco, ETH Zurich

The continental subsurface holds more bacteria and archaea than any other habitat on Earth yet the origins, eco-evolutionary dynamics and behaviours of these organisms are still largely unknown. As Swiss policies increasingly turn towards CO2 mitigation strategies that form new and innovative interactions with subsurface environments, there is an urgent need to understand how subsurface microorganisms respond to physical-chemical changes in natural and human-altered environments. The underground laboratories of Switzerland provide a unique opportunity to study subsurface life in a controlled environment and perform experiments to test hypotheses related to subsurface microbial responses to changes in the environment. This presentation will prove an overview of the history of subsurface geobiology research in Switzerland, new findings surrounding the microbial biomass, biodiversity and biogeochemical cycles throughout the Bedretto Underground Laboratory for Geosciences and Geoenergies (BULGG) and conclude with a discussion on how studying life in the Swiss subsurface helps us understand the potential for life on other planets and design missions to explore other subsurface worlds.

10.7
ICDP Project DOVE (Drilling Overdeepened Alpine Valleys): First results from the Basadingen Borehole

Sebastian Schaller[1], Flavio Anselmetti[1], Marius W. Buechi[1], Markus Fiebig[2], Gerald Gabriel[3], Ernst Kroemer[4], Frank Preusser[5], Jürgen Reitner[6], Bennet Schuster[5], David Tanner[3], Ulrike Wielandt-Schuster[7]

[1] *Institute of Geological Sciences, University of Bern, Switzerland (sebastian.schaller@geo.unibe.ch)*
[2] *Department of Civil Engeneering and Natural Hazards, University of Natural Resources and Life Sciences Vienna, Austria*
[3] *Department for Seismic, Gravimetry, and Magnetics, Leibniz Institute for Applied Geophysics, Hannover, Germany*
[4] *Bayrisches Landesamt für Umwelt, Augsburg, Germany*
[5] *Institute of Earth and Environmental Sciences, University of Freiburg, Germany*
[6] *Geologische Bundesanstalt für Österreich, Vienna, Austria*
[7] *Landesamt für Geologie, Rohstoffe und Bergbau, Baden-Württemberg, Germany*

The panalpine project 'DOVE' (Drilling Overdeepened Alpine Valleys), co-funded by the International Continental Scientific Drilling Program (ICDP), is drilling a series of overdeepened glacial troughs around the Alps that were formed by subglacial erosion during past glaciations. The sedimentary fill of these troughs, consisting of multiple stacked and nested glacial sequences, provides the best archives of when and where glaciers reached the Alpine forelands. The combined data from all DOVE sites comprising synchronous or asynchronous ice advances and ice extents in the different regions, will eventually provide a critical database to evaluate the various patterns in glacial-interglacial paleoclimates and landscape evolution back to the Mid-Pleistocene.

One of the DOVE sites drilled the overdeepened Basadingen Trough, located in Northern Switzerland, within the extents of several Middle–Late Pleistocene foreland glaciations of a lobe of the Rheine Glacier. The trough is a narrow, ca. 250–300 m deep structure that runs SSE–NNW, forming a so-far poorly understood, old overdeepened valley system that connected the present-day Thur Valley with the Rhine Valley – a connection that does not exist in the present surface morphology and that was probably only active during the Middle Pleistocene. New high-resolution 2-D seismic displays a detailed seismic stratigraphy with several depositional sequences, indicating that the valley fill consists of deposits from multiple glaciations, making the Basadingen Trough an ideal target for DOVE. We aim to establish a chronostratigraphic and sedimentological model to identify and understand the older glaciations that affected the Basadingen Trough and the Northern Alpine foreland in general.

10.8
The Nam Co Drilling Project, Tibet (NamCore): towards retrieving a one million year sedimentary record from the third pole

Hendrik Vogel[1], Torsten Haberzettl[2], Rolf Kipfer[3], Gerhard Daut[4], Thomas Wonik[5], Daniel Ariztegui[6], Jasmine Berg[7], Camille Thomas[6], Cara Magnabosco[8], Junbo Wang[9], Liping Zhu[9], Volkhard Spiess[10], Natasha Barbolini[11], Leon Clarke[12], Andrew Henderson[13], Jerome van der Woerd[14], Nicolas Waldmann[15]

[1] Institute of Geological Sciences & Oeschger Centre for Climate Change Research, University of Bern, Baltzerstr. 1+2, CH-3012 Bern (hendrik.vogel@geo.unibe.ch)
[2] Institut für Geographie und Geologie, University of Greifswald, F.-L.-Jahn-Str. 16 D-17487 Greifswald, Germany
[3] Eawag, Überlandstr. 133, CH-8600 Dübendorf
[4] Institut für Geographie, University of Jena, Löbdergraben 32, D-07743 Jena, Germany
[5] Leibniz-Institut für Angewandte Geophysik (LIAG), Stilleweg 2, D-30655 Hannover, Germany
[6] Department of Earth Sciences, University of Geneva, Rue des Maraichers 133, CH-1205 Geneva
[7] Institut des dynamiques de la surface terrestre, University of Lausanne, Batiment Geopolis, CH-1015 Lausanne
[8] Department of Earth Sciences, ETH Zürich, Sonneggstrasse 5, CH-8092 Zürich
[9] Institute of Tibetan Plateau Research, Chinese Academy of Sciences, China
[10] Fachbereich Geowissenschaften, University of Bremen, Germany
[11] Department of Biological Sciences, University of Bergen, Norway
[12] Department of Natural Sciences, Manchester Metropolitan University, UK
[13] School of Geography, Politics and Sociology, Newcastle University, UK
[14] Institut de Physique du Globe de Strasbourg, Université de Strasbourg, France
[15] Deptartment of Marine Geosciences, University of Haifa, Israel

The Tibetan Plateau (TP) is highly sensitive to climate change. Its isolated high-altitude setting makes it home to unique ecosystems characterized by endemic species. Understanding tectonic and climatic controls on the TP's hydroclimate and linking them to ecosystem functioning, will help unravel factors controlling the resilience of life in extreme environments. The TP is also of key societal relevance because it is the source of major rivers providing freshwater to a large portion of the Asian population. Future climate change will disproportionately impact the hydrological cycle in this region and consequently its water resources, ecology and economies. In order to evaluate model-based future climate change scenarios, long and continuous proxy time-series will be fundamental to establish forcing and response relationships to enhance our understanding of atmospheric westerly-monsoon and associated environmental responses.

The multinational and multidisciplinary ICDP NamCore project aims at producing a long and continuos sediment record from one of the largest, deepest and oldest lakes of the TP – Nam Co. Owing to its location in the modern monsoon regime and its documented recent and past sensitivity to hydrological changes Nam Co records the temporal development of large-scale atmospheric circulation systems. Comprehensive seismic reflection data covering the entire lake clearly show an infill of >700 m of well-layered, widely undisturbed sediments in the central part of the lake, spanning several glacial/interglacial cycles. Sediment accumulation rates from piston cores for the past 24 ka and seismostratigraphic investigations suggest a lake formation of >1 Ma. This makes Nam Co's sedimentary record an exemplar archive to fill the paleoclimate data gap between two ICDP/IODP transects that will allow comparisons of climate evolution/behaviour on a continental scale. Continuous, high-resolution Nam Co paleoenvironmental records for these long time scales will further allow to study sediment budget changes under varying climatic and tectonic settings and contribute to a better understanding of the Quaternary geomagnetic field, since capturing rates of change and defining dynamic features can only be preserved in the highest resolution records. The high altitude Tibetan Plateau also is unique as it has a high degree of endemism in aquatic organisms that were dependent on persistent water bodies; Nam Co likely served as a dispersal centre, because most other lakes desiccated during dry glacial periods. Therefore, Nam Co is a first-class site to study the links between climate and biological evolution within isolated Tibetan Plateau ecosystems. These studies will also include the unknown geomicrobiological communities and processes in the high altitude lacustrine deep biosphere.

10.9
High and low latitude controls on Mid-Brunhes Coccolithophore Bloom and implications on ocean carbon cycle

Hongrui Zhang[1,2], Chuanlian Liu[2], Iván Hernández-Almeida[1], Luz María Mejía[1], Heather M. Stoll[1]

[1] *Department of Earth Sciences, ETH, Zurich, Sonnegstrasse 5, 8092 Zurich, Switzerland (zhh@ethz.ch)*
[2] *State Key Laboratory of Marine Geology, Tongji University, Siping Road 1239, Shanghai 200092, China*

Periodic ~400 thousand years (kyr) variations in the ocean carbon cycle, manifest in carbonate dissolution and benthic carbon isotope, have been observed throughout the Cenozoic but the driving mechanisms remain under debate. Some evidence suggests that coccolithophore bloom events potentially contribute to these ~400 kyr oscillations. However, there is no consensus on the mechanism responsible for blooms. In this study, we investigate the timing and spatial pattern of the coccolithophore bloom events during the Mid-Brunhes period. We find that peak coccolithophore productivity in the Southern Ocean coincided with minimum eccentricity, whereas coccolithophore productivity peaked in the Western Pacific ~80 kyr later. We propose a dual high and low latitude control on blooms whereby at minimum eccentricity, increased high-latitude diatom silica consumption lowers the Si/P, leading to coccolithophorid blooms in the Southern Ocean. Subsequently as eccentricity increased, stronger tropical monsoons deliver higher fluvial nutrients to surface waters and mix the upper ocean more intensely, increasing coccolithophore productivity. We hypothesize that high latitude processes have intensified over the Pleistocene, extending the 400 kyr carbon cycle to ~500 kyr.

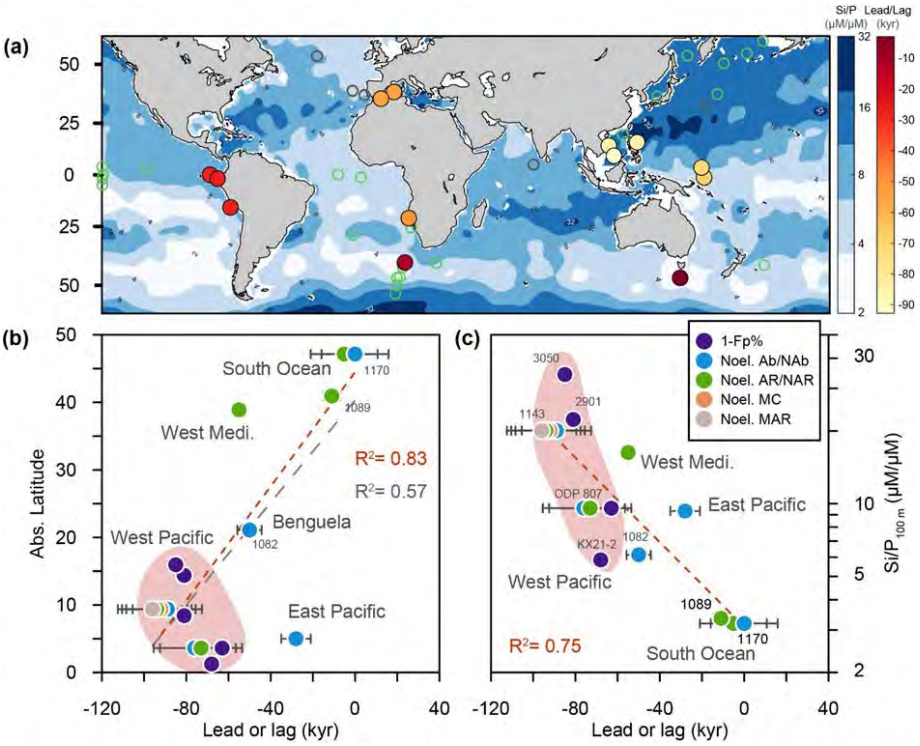

Figure1. Coccolithophore bloom timing vs site location and nutrient ratio. a Coccolithophore bloom peak timing (relative to eccentricity minimum) against the core latitude and Si/P ratio at the modern location of each core. Other diatom (green) or coccolithophore (gray) productivity records cited in this work are plotted as circles. b The timing of coccolithophore blooms (relative to eccentricity minimum) against absolute latitude of cores (only sites with significant bloom during eccentricity minimum are plotted here). The red dashed line represents the linear regression of data without Western Mediterranean and Eastern Pacific stacks (R^2 = 0.83 and p-value<<0.001) and the gray dashed line is the regression of all data (R^2 = 0.57 and p-value<<0.001). A negative x-axis value indicates where the peak of coccolithophore productivity happened later than the eccentricity minimum. c Timing of coccolithophore bloom (relative to eccentricity minimum) versus Si/P ratio in 100 m depth (from World Ocean Atlas).The red dashed line is the linear regression of the lead-lag result to nutrient ratio (R^2 = 0.75 and p-value<<0.001). The shaded areas in (b) and (c) highlight results from Western Pacific. Noel. MC and Noel. MAR in legend refer to the Noelaerhabdaceae mass content and Noelaerhabdaceae mass accumulation rate, respectively.

P 10.1
Exploring the lower continental crust: geology, geophysics, and the Ivrea drilling project DIVE

Othmar Müntener[1],György Hetényi[1], Daniela Rubatto[1,2], Jörg Hermann[2], Klaus Holliger[1]

[1] *Institute of Earth Sciences, University of Lausanne, Geopolis Building, CH-1015 Lausanne (othmar.muntener@unil.ch)*
[2] *Geologisches Institut, University of Bern, Baltzerstrasse 1+3, CH-3012 Bern*

Amongst the known post-archean crustal exposures with continental (e.g., Sila Massif, Calabria, Italy; Prince Rupert, BC, Canada; Doubtful Sound, Fiordland, New Zealand; Sierra de Famatina, Argentina) and paleo-island arc signatures (e.g., Kohistan, Pakistan; Talkeetna, Alaska, USA), the Ivrea-Verbano Zone (IVZ) in the southern Alps is considered as the archetypal lower continental crustal section. Characterized by pronounced geophysical anomalies, the Ivrea Geophysical Body (IGB) below the exposed IVZ served as a calibrating benchmark for other lower continental crustal sections. Indeed, the large gravity, seismic, and magnetic anomaly associated with the IGB has sparked worldwide interest as it indicates that dense, mantle-type rocks are located locally as shallow as 1-3 km below the surface (e.g., Berckhemer 1968; Lanza 1982; Kissling, 1984; Scarponi et al. 2020, 2021; Liu et al. 2021).

Here, we provide a synopsis of the planned Swiss research activities as a part of the drilling project DIVE (Drilling Into the Ivrea-Verbano zonE) funded by the International Continental Drilling Program (ICDP). Key requirements for this multidisciplinary research program are that (i) different techniques are applied to the same samples and (ii) the corresponding point-type information from boreholes and hand-specimens can be upscaled to reconstruct 3D sections of the lower continental crust and uppermost mantle. This, in turn, requires detailed geological and geophysical information on a regional scale. The IVZ meets these requirements to take full advantage of the unique archive provided by DIVE. We outline how these investigations provide a mechanistic link between observed rock properties (seismic velocity and anisotropy, thermal structure and radiogenic heat production, density, electrical conductivity, and chemical composition) and the geological processes that shaped the lower continental crust (melting and fluid release, heating by burial, metamorphic reactions, crustal differentiation, and deformation).

REFERENCES

Berckhemer H (1968) Topographie des «Ivrea-Körpers» abgeleitet aus seismischen und gravimetrischen Daten. Schweiz Mineral Petrogr Mitt 48:235-246.

Kissling E, Wagner J, Müller S (1984) Three-dimensional gravity model of the northern Ivrea-Verbano Zone, *In:* Geomagnetic and Gravimetric Studies of the Ivrea Zone (eds. Wagner J-J, Müller S) Matér Géol Suisse Géophys 21:55-61.

Lanza R (1982) Models for interpretation of the magnetic anomaly of the Ivrea body. Géol Alpine 58:85-94.

Liu Y, Greenwood A, Hetényi G, Baron L, Holliger K (2021) High-resolution seismic reflection surveys crossing the Insubric Line into the Ivrea-Verbano Zone: Novel approaches for interpreting the seismic response of steeply dipping structures. Tectonophys 816:229035. doi:10.1016/j.tecto.2021.229035

Scarponi M, Hetényi G, Berthet T, Baron L, Manzotti P, Petri B, Pistone M, Müntener O (2020) New gravity data and 3D density model constraints on the Ivrea Geophysical Body (Western Alps). Geophys J Int 222:1977-1991

Scarponi M, Hetényi G, Plomerová J, Solarino S, Baron L, Petri, B (2021) Joint seismic and gravity data inversion to image intra-crustal structures: the Ivrea Geophysical Body along the Val Sesia profile (Piedmont, Italy). Front Earth Sci 9:671412. doi:10.3389/feart.2021.671412

P 10.2
Siting the DIVE DT-1a drillhole - from geology and geomorphology to modeling and seismic imaging

Andrew Greenwood[1,2], Ludovic Baron[1], György Hetényi[1], DIVE Site Survey 2019 Field Team[3], project DIVE Team[4]

[1] *Institut des sciences de la Terre, University of Lausanne, Batiment Géopolis, CH-1015 Lausanne (andrew.greenwood@unil.ch)*
[2] *Chair of Applied Geophysics, Montanuniversität Leoben, Peter Tunner Strasse 25, A-8700 Leoben*
[3] The full list of field participants will be listed on the poster
[4] *http://www.dive2ivrea.org/*

High-resolution seismic surveys have been conducted in Val d'Ossola, in the Western Alps of Italy, to site the stage 1 boreholes of the recently funded ICDP project Drilling the Ivrea-Verbano zonE (DIVE). The DIVE project aims at unravelling long-standing fundamental questions on the nature of the lower continental crust, its lithological expression in iconic geophysical anomalies and the characteristics of the underlying physical and chemical rock properties. The DIVE DT-1a drillhole near Megolo di Mezzo locality is planned to intersect a pre-Permian part of the continental lower crust characterized by peridotite-gabbro-metasedimentary interfaces that lie within the broad Proman Antiform, ca. 2.5 km form the Insubric Line. Seismic data acquisition utilised 295 geophones and a 20,000 lb Vibrator truck allowing imaging to ca. 1 km depth.

Accurate seismic imaging is reliant on a detailed velocity model of the subsurface. To achieve this, refracted ray travel-time tomography was performed to determine the vertical velocity structure along the main seismic profile (Fig. 1a and b), and a seismic velocity volume encompassing the seismic survey area was generated by continuing the topographic profile of the mountain flanks (Fig. 1c and d). Features within both the refraction tomography image and the velocity volume agree well with observations seen in the normal-moveout corrected seismic stacked volume (Fig. 2). The derived velocity volume is then used as the starting basis for 3D pre-stack-depth-migration imaging.

Unravelling the structure of the underlying crystalline rocks is challenging as they are seismically somewhat featureless compared to overlying sediments, however a seismic fabric dipping eastward is observed in the seismic profile (Fig. 2). The lack of strong reflectivity within the crystalline rocks suggests that the metagabbros and pyroxenites are massive with little open fractures or faults. The sedimentary cover is approximately 50 m thick and the underlying crystalline rock contact dips steeply at 30° to the N-NE. This dip agrees with the topographic slope of the mountain flanks on either sides of Val d'Ossola in Megolo and Premosello. Based on these observations, drilling at ca. 20° from vertical towards the West is proposed.

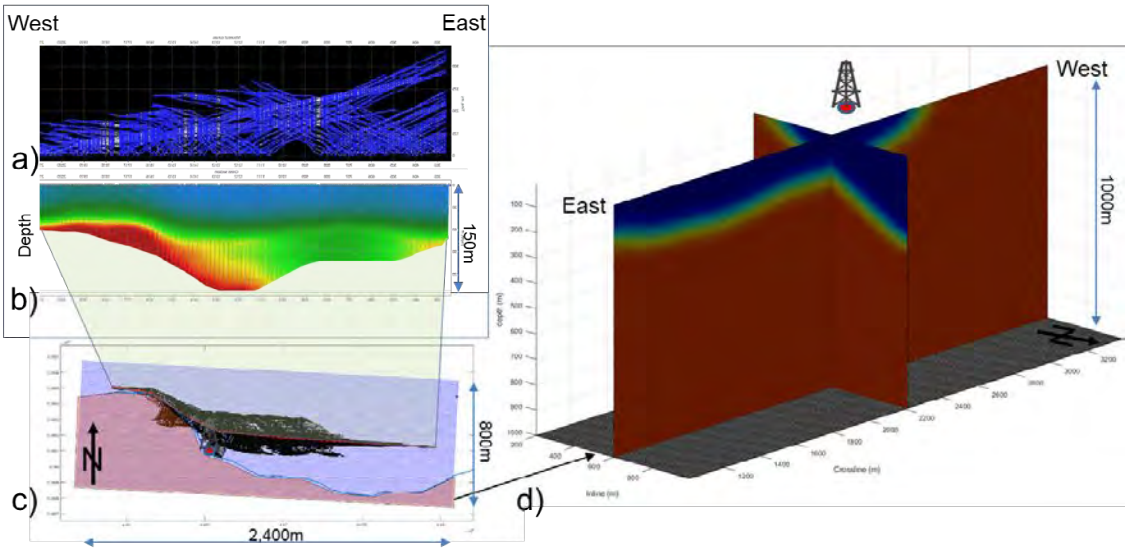

Figure 1. Refracted ray travel-time tomography and geomorphology based modeling. a) Travel-time curves from first-arrival analysis; b) velocity tomogram; c) surface layer of the seismic velocity model showing all nodes that correspond to either valley walls (red) or valley sediments (blue), locations of the theoretical seismic traces (black) and seismic receivers (red-dotted line); and d) seismic velocity volume with a 30° dipping valley structure. The proposed location of DT-1a is shown in c) and d)

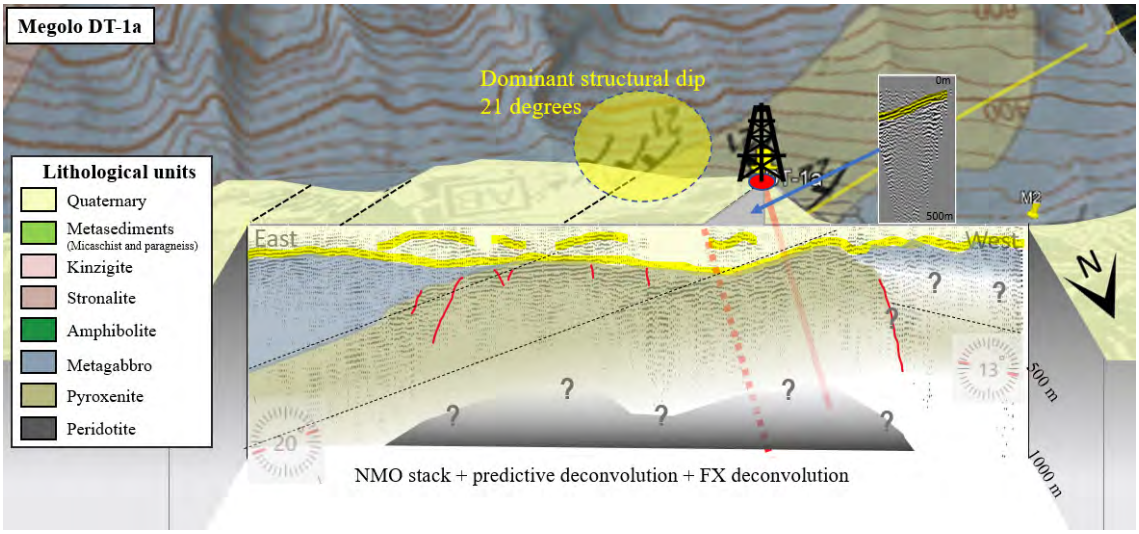

Figure 2. Megolo site (DT-1a) high resolution seismic reflection survey overview: below the sediment cover (yellow), the crystalline basement is shown as a transition from mafic to ultramafic units dipping east at 20° (red dashed lines). The seismic section is inserted into 3D topography overlain with geology that shows the main lithologies and structures mapped at surface.

P 10.3
A high-resolution seismic survey across the Balmuccia Peridotite, Ivrea Zone, Italy - Project DIVE phase two, site investigation

Damian Pasiecznik[1], Andrew Greenwood[1,2], Ludovic Baron[2], György Hetényi[2], Florian Bleibinhaus[1]

[1] Chair of Applied Geophysics, Montanuniversität Leoben, Peter-Tunner-Straße 25, 8700 Leoben, Austria (damian.pasiecznik@unileoben.ac.at)
[2] Institut des Sciences de la Terre, Université de Lausanne, Quartier Mouline, CH-1015 Lausanne, Switzerland

The Ivrea Verbano Zone (IVZ) is one of the most complete crust–upper mantle geological references in the world, and the Drilling the Ivrea-Verbano zone project (DIVE) aims to resolve the uncertainties below this area. Geophysical anomalies detected across the IVZ indicate that dense, mantle-like rocks are located at depths as shallow as ca. 1-3 km (Scarponi et al., 2020, 2021). Thus, within DIVE several geological, geochemical and geophysical studies are planned, including the drilling of a 4 km deep borehole that will penetrate the Balmuccia Peridotite (Val Sesia, Italy) to approach, and possibly cross, the crust–mantle transition zone, and provide for the first time geophysical in-situ measurements of the deepest rocks of the IVZ.

One of the primary requirements before drilling is a seismic site characterization, to define with precision the correct positioning and orientation of the borehole, to assess potential drilling hazards and to allow for the spatial extrapolation of the borehole logs. For that goal, two joint geophysical surveys were performed in October 2020 in a collaboration between GFZ Potsdam, Université de Lausanne and Montanuniversität Leoben: (1) a deep seismic survey performed by GFZ Potsdam, entitled SEismic imaging of the Ivrea ZonE (SEIZE), consisting of two approximately orthogonal 15 km-long seismic lines, that aim to resolve the deeper structure of the IVZ in the area, and (2) a smaller seismic survey at the proposed drill site, entitled High-resolution SEismic imaging of the Ivrea ZonE (HiSEIZE), geared towards providing high-resolution seismic images of the uppermost few km at the proposed drill site.

The HiSEIZE survey (Figure 1), the subject of this study, was performed with a fixed spread of 200 vertical geophones and 160 3C-sensors, spaced at ca. 11m along three sub-parallel lines spaced 50-80 m apart. A 17’000 kg Vibroseis was utilized as a source at 22 m spacing along a 2.4 km line emitting a 10 s linear sweep (from 12 to 140 Hz) with 3 s listening time.

The presence of high-velocity crystalline rocks and sub-vertical structures throughout the study area (Liu et al., 2021) make seismic processing challenging. Important processing steps applied include:

- P- and S-wavefield separation,
- Generation of a high-resolution near-surface velocity model through refraction tomography. Merging with low-resolution velocity model from the SEIZE survey,
- Pre-Stack Depth Migration (PSDM).

This project will not only provide site characterization for the DIVE project, but also contribute to understanding the structure of the Balmuccia Peridotite, its changes in depth and its relationship with the crustal-mantle transition.

In this contribution, we will present the newly acquired data and first results.

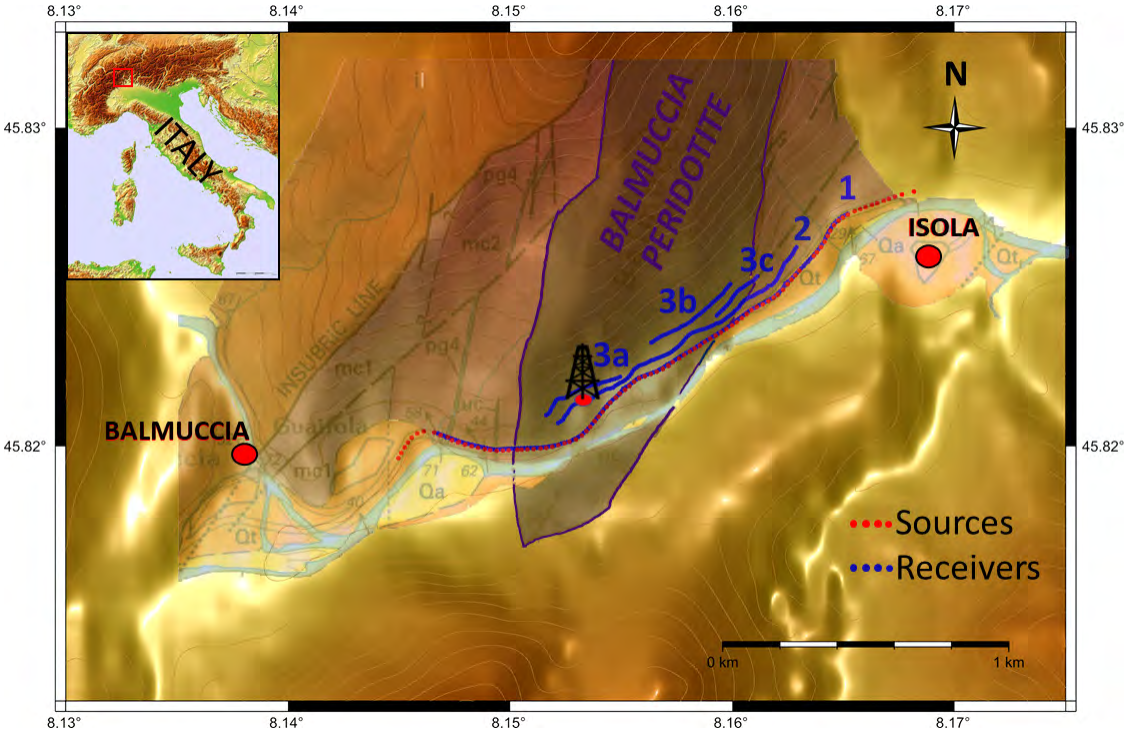

Figure 1. Digital Elevation Model of the study area between Balmuccia and Isola, with overlaid geological features (modified from Quick et al. 2003), plausible drill site and position of receivers and sources. Numbers 1, 2 and 3 indicate the three sub-parallel lines.

REFERENCES

Liu, Y., Greenwood, A., Hetényi, G., Baron, L., Holliger, K. 2021: High-resolution seismic reflection surveys crossing the Insubric Line into the Ivrea-Verbano Zone: Novel approaches for interpreting the seismic response of steeply dipping structures. Tectonophysics, 816, 229035. doi:10.1016/j.tecto.2021.229035

Quick, J.E., Sinigoi, S., Snoke, A.W., Kalakay, T.J., Mayer, A., Peressini, G. 2003: Geologic map of the Southern Ivrea–Verbano Zone, Northwestern Italy. US Geological Survey I-Map, vol. 2776.

Scarponi, M., Hetényi, G., Berthet, T., Baron, L., Manzotti, P., Petri, B., Pistone, M., Müntener, O. 2020: New gravity data and 3D density model constraints on the Ivrea Geophysical Body (Western Alps). Geophysical Journal International, 222, 1977-1991. doi:10.1093/gji/ggaa263

Scarponi, M., Hetényi, G., Plomerová, J., Solarino, S., Baron, L., Petri, B. 2021: Joint seismic and gravity data inversion to image intra-crustal structures: the Ivrea Geophysical Body along the Val Sesia profile (Piedmont, Italy). Frontiers in Earth Sciences, 9, 671412. doi:10.3389/feart.2021.671412

P 10.4
Joint Geophysical-Petrological Modeling on the Ivrea Geophysical Body Beneath Valsesia, Italy: Constraints on the Continental Lower Crust prior to Drilling the Ivrea-Verbano zonE (DIVE)

Mattia Pistone[1], Luca Ziberna[2], György Hetényi[3], Matteo Scarponi[3], Alberto Zanetti[4], Othmar Müntener[3]

[1] *Department of Geology, The University of Georgia (UGA), Franklin College of Arts and Sciences, Geography-Geology Building, 210 Field Street, Athens, GA 30602-2501, United States of America. (Mattia.Pistone@uga.edu)*
[2] *Department of Mathematics and Geosciences, University of Trieste, Via Weiss 2, 34128 Trieste, Italy.*
[3] *Institute of Earth Sciences, University of Lausanne (UNIL), Bâtiment Géopolis, Quartier UNIL-Mouline, 1015, Lausanne, Switzerland.*
[4] *Institute of Geosciences and Earth Resources, IGG-CNR, Unità di Pavia, Via Ferrata 1, I-27100 Pavia, Italy.*

One of the few near-complete continental crustal sections exposed on Earth's surface is the Ivrea-Verbano Zone (Western Alps, Italy), which is considered as a petro-geophysical benchmark of the continental lithosphere. Exposed peridotite slivers embedded in lower crustal rocks at the surface and large density, seismic velocity anomalies of the Ivrea Geophysical Body in the subsurface suggest that mantle-like rocks are located as shallow as a few kilometers depth, but the actual composition of the rocks producing these anomalies is unknown. As detailed in the work of Pistone et al. (2020), we investigated how the published seismic data (seismic compressional wave velocity, V_P) and new gravimetric data (rock density, ρ) beneath Valsesia could be reconciled with existing petrologic data and models of the Ivrea-Verbano Zone. We used Perple_X software to calculate densities and compressional wave velocities for a range of possible deep crustal rock types. We argue that amphibole gabbros (<18 km depth) and pyroxene hornblendites (>18 km depth) provide the best fit to the joint geophysical and petrologic constraints, whereas residual ultramafic rocks and anhydrous gabbros are inconsistent with the existing data. This indicates that the Ivrea Geophysical Body beneath the Valsesia area in the Ivrea-Verbano Zone preserves the structure of an igneous complex formed during magmatic underplating from the crystallization of hydrous mafic magmas. This would imply melting of a damp mantle source that produced a continental crust of an original thickness of up to ~48 km in the Permian, of which ~30 km are exposed at Earth's surface today. The ultimate question on whether the top of the Ivrea Geophysical Body is composed of mantle or crustal rocks will be addressed in the framework of the project DIVE (Drilling the Ivrea-Verbano zonE; Pistone et al., 2017), which has been recently approved by the International Continental Drilling Program (ICDP).

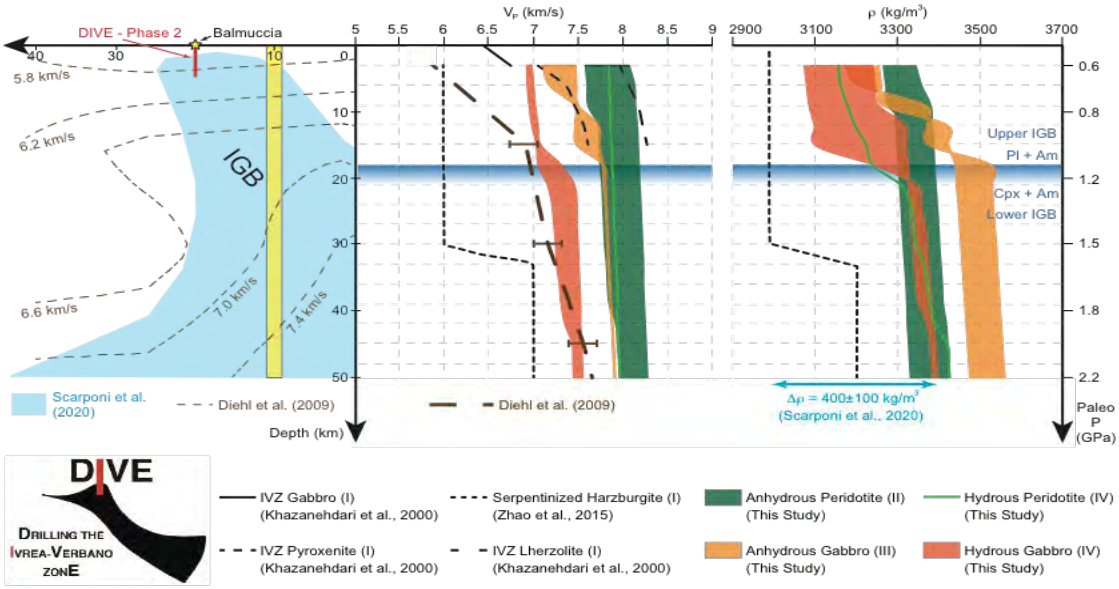

Figure 1. V_P and ρ profiles along a depth-structure profile (yellow) beneath Valsesia. (I) Laboratory constraints for gabbro (0–3 km), serpentinized harzburgite, pyroxenite, and lherzolite (3–15 km), and Perple_X calculations for (II) anhydrous ultramafic rocks and (III) gabbros, and (IV) hydrous lherzolite and gabbros of the Ivrea-Verbano Zone (IVZ) (3–50 km). V_P uncertainties (every 15 km of depth) (Diehl et al., 2009) (brown) and ρ variation range (Δρ) (Scarponi et al., 2020) (light blue) are reported. The Ivrea Geophysical Body (IGB) is made of upper amphibole gabbros (plagioclase [Pl] + amphibole [Am]) and lower pyroxene hornblendites (clinopyroxene [Cpx] + amphibole [Am]). The DIVE - Phase 2 borehole is 4 km deep (red). Modified after Pistone et al. (2020).

REFERENCES

Diehl, T., Husen, S., Kissling, E., & Deichmann, N. 2009. High resolution 3D VP model of the Alpine crust, Geophysical Journal International, 179, 1133–1147.

Khazanehdari, J., Rutter, E.H., & Brodie, K.H. 2000. High pressure/temperature seismic velocity structure of the mid- and lower-crustal rocks of the Ivrea-Verbano zone and Serie dei Laghi, NW Italy, Journal of Geophysical Research, 105, 13843–13858.

Pistone, M., Müntener, O., Ziberna, L., Hetényi, G., & Zanetti, A. 2017. Report on the ICDP workshop DIVE (drilling the Ivrea–Verbano zone), Scientific Drilling, 23, 47–56.

Pistone, M., Ziberna, L., Hetényi, G., Scarponi, M., Zanetti, A., & Müntener, O. (2020). Joint geophysical-petrological modeling on the Ivrea geophysical body beneath Valsesia, Italy: Constraints on the continental lower crust, Geochemistry, Geophysics, Geosystems, 21, e2020GC009397.

Scarponi, M., Hetényi, G., Berthet, T., Baron, L., Manzotti, P., Petri, B., Pistone, M., & Müntener, O. 2020. New gravity data and 3D density model constraints on the Ivrea geophysical body (Western Alps), Geophysical Journal International, 222, 1977–1991.

Zhao, L., Paul, A., Guillot, A., Solarino, S., Malusà, M.G., Zheng, T., Aubert, C., Salimbeni, S., Dumont, T., Schwartz, S., Zhu, R., & Wang, Q. 2015. First seismic evidence for continental subduction beneath the Western Alps, Geology, 43, 815–818.

P 10.5
Drilling overdeepened Eastern Alpine valleys and basins

Markus Fiebig[1], Flavio Anselmetti[2], Marius W. Büchi[2], Gerald Gabriel[3], Ernst Kroemer[4], Frank Preusser[5], Jürgen Reitner[6], Sebastian Schaller[2], Bennet Schuster[5], David C. Tanner[3], Ulrike Wielandt-Schuster[7]

[1] Institute of Applied Geology, University of Natural Resources and Life Sciences Vienna, Peter Jordan Str. 82, A-1190 Wien (markus.fiebig@boku.ac.at)
[2] Institute of Geological Science, University of Berne, Baltzerstr. 1-3, CH-3012 Bern
[3] Leibniz-Institut für Angewandte Geophysik, Stilleweg 2, D-30655 Hannover
[4] Landesanstalt für Umwelt (LfU), Haunstetter Str. 112, D-86161 Augsburg
[5] Institute of Earth and Environmental Science, Universität Freiburg, Tennbacherstr. 4, D-79106 Freiburg
[6] Geologische Bundesanstalt, Neulinggasse 38, A-1030 Wien
[7] Landesamt für Geologie, Rohstoffe und Bergbau, Albertstr.5, D-79104 Freiburg

The panalpine project “DOVE” (Drilling Overdeepened Alpine Valleys), co-funded by the International Continental Scientific Drilling Program (ICDP), Leibniz-Institut für Angewandte Geophysik (LIAG), Deutsche Forschungsgemeinschaft (DFG), Universität für Bodenkultur (BOKU), Landesanstalt für Umweltschutz (LfU), Regierungspräsidium Freiburg (RP), Nationale Genossenschaft für die Lagerung radioaktiver Abfälle (NAGRA), Eidgenössisches Nuklearsicherheitsinspektorat (ENSI) is drilling a series of overdeepened glacial basins around the Alps that were formed by glacial erosion during past glaciations.

In the eastern section of the DOVE project Phase 1, we reinvestigate the inneralpine trough of Bad Aussee (Pleistocene Traun glacier area, Austria), the subalpine basin of the Pleistocene Salzach Foreland glacier (Neusillersdorf, Bavaria), and the tongue basin of the Pleistocene Isar-Loisach-Foreland glacier (Schäftlarn, Bavaria).

During the Quaternary, depth of glacial erosion below Bad Aussee reached down to 400 m below sea level (comparable to the level of the Dead Sea in the Levant, the lowest part of today’s surface topography on Earth). 880 m of core material have been drilled and will be reinvestigated and physically dated by methods of luminescence and burial age dating.

In Neusillersdorf (Bavaria), we continue to study the cores of a drilling through a branch basin of the Pleistocene Salzach Foreland glacier area. Fom first luminescence dating results we already know that sediments from the penultimate glaciation and older occur.

Finally, the sequence in the former tongue basin area of the Pleistocene Isar Loisach Foreland glacier area, close to Munich, offers about 100 m of lake sediments, which are interpreted to contain sediments from Middle Pleistocene glaciations.

All available cores will be studied with state-of-the-art tools and methods in modern sedimentology and dating technics. Especially the combined investigation and interpretation of several drillholes will offer the opportunity to develop a modern reconstruction of past Eastern Alpine glacial environments.

P 10.6
Drilling Overdeepened Alpine Valleys: First results from the Tannwald Borehole

Bennet Schuster[1,3], David C. Tanner[2], Gerald Gabriel[2], Thomas Burschil[2], Thomas Wonik[2], Frank Preusser[1], Flavio Anselmetti[3], Marius W. Büchi[3], Sebastian Schaller[3], Markus Fiebig[4], Ulrike Wielandt-Schuster[5]

[1] Institute of Earth and Environmental Sciences, University of Freiburg, Tennenbacher Str. 4, 79106 Freiburg, Germany (bennet.schuster@geologie.uni-freiburg.de)
[2] Leibniz Institute for Applied Geophysics, Stilleweg 2, 30655 Hannover, Germany
[3] Institute of Geological Science, University of Bern, Baltzerstrasse 1+3, 3012 Bern, Switzerland (bennet.schuster@geo.unibe.ch)
[4] Department of Civil Engineering and Natural Hazards, BOKU Vienna, Peter-Jordan-Straße 82, 1190 Wien, Austria
[5] Landesamt für Geologie, Rohstoffe und Bergbau (LGRB), Albertstraße 5, 79104 Freiburg im Breisgau, Germany

The panalpine project “DOVE” (Drilling Overdeepened Alpine Valleys), co-funded by the International Continental Scientific Drilling Program (ICDP), is drilling a series of overdeepened glacial troughs around the Alps that were formed by subglacial erosion during past glaciations. The sedimentary fill of these troughs, consisting of multiple stacked and nested glacial sequences, provide the best archives of when and where glaciers reached the Alpine forelands. The combined data from all DOVE sites, comprising synchronous or asynchronous ice advances and ice extents in the different regions, will eventually provide a critical database to evaluate the various patterns in glacial-interglacial paleoclimates and landscape evolution back to the Mid-Pleistocene.

The Tannwald Basin forms a distal, overdeepened part of the Rhine glacial landscape, ca. 50 km north of Lake Constance, and has a maximum depth of 250 m (Burschil et al. 2018). Core and flush drilling on the western flank of the basin began in April 2021 and reached the bedrock, i.e. top Tertiary Molasse, at a depth of 154 m. The glacial basin is filled by 100 m-thick fine clastics of the Dietmanns Formation (Hosskirchian – Rissian age; Ellwanger et al. 2011). This is overlain by 42 m coarse clastics of the Illmensee Formation (Rissian - Wurmian age; Ellwanger et al. 2011). We aim to chronologically date the sediments using borehole and core geophysics, OSL, pollen, and noble gases from pore water. Together with detailed sedimentology, these data will be used to constrain the glacial history of the basin. We show the preliminary results of the flush and core drilling, together with the borehole geophysics.

REFERENCES

Burschil T., Buness H., Tanner D., Wielandt-Schuster U., Ellwanger D., Gabriel G. 2018: High-resolution reflection seismics reveal the structure and the evolution of the Quaternary glacial Tannwald Basin, Near Surf. Geophy., 16, 593-610.

Ellwanger D., Wielandt-Schuster U., Franz M. and Simon T. 2011: The Quaternary of the southwest German Alpine Foreland (Bodensee-Oberschwaben, Baden-Württemberg, Southwest Germany), Quaternary Science Journal, 60, 306–328.

P 10.7
undeRstanding coral thErmal bleaching threSholds during past InterglaclaL extremes: Insight into thermal strEss dyNamics on tropical Coral reef Ecosystems (RESILIENCE)

Adrien Montillier[1], Gioele Pappalardo[1], Elias Samankassou[1], Silvia Spezzaferri[2] and the RESILIENCE Project Partners*

[1] *Département des Sciences de la Terre, Université de Genève, Rue des Maraîchers 13, CH-1205 Genève*
[2] *Département des Géosciences, Université de Fribourg, Chemin du Musée 6, CH-1700 Fribourg*

Tropical and subtropical coral reefs are globally distributed biodiversity hotspots presently threatened by unprecedented environmental forcing. Their ecological functioning and ultimate survival depend on their sensitivity to climatic perturbations and in addition to anthropogenic forcing. One of the main visual signs for thermal stress is bleaching, a predominant stressor on reefs, i.e. the loss of the photosynthetic symbionts that live within their tissues. The increase in magnitude, duration and frequency of coral bleaching events over the last few decades has seriously compromised the resilience of these vulnerable ecosystems. Future bleaching events are predicted to become even more frequent and, therefore, will likely not ensure reef persistence in the Anthropocene. The best approach to gain insights to how global climate change will impact reef ecosystems is to learn from the past. However, in the fossil record, bleaching cannot be observed! The Earth's paleo-climatic record found in deep sea sediments adjacent to coral reefs can provide us with relevant information on multiple prospective analogues for modern times. In particular, some interglacial periods in the Earth's history were characterized by climatic conditions similar to modern-day marine environmental conditions, whereas others were warmer. We will investigate deep-sea sedimentary records in basins adjacent to coral reef-bearing carbonate platforms from the Atlantic (IODP Leg 166-Bahamas), Indian (IODP Expedition 359-Maldives) and Pacific Oceans (ODP Leg 130-Ontong Java Plateau; ODP Leg 133 and IODP Leg 194-Marion Plateau; Expedition 320-Tahiti); in the interval spanning the Present to Marine Isotope Stage (MIS) 31 in the Pleistocene (a time span of around 1100 kyr) and compare these with their shallower sedimentary counterparts.

The overarching objective of this research is to evaluate the magnitude and frequency of interglacial periods characterized by anomalously high temperatures that may have produced coral bleaching in the past and to test if nutrients have also contributed to this process. This objective will be achieved by an initial assessment of the modern benthic habitat in the target regions, and evaluating photo-inhibition caused by photo-oxidative stress using the large benthic foraminifer *Amphistegina* (which similarly to corals can undergo bleaching). The modern habitat will be used as a baseline for past evaluation of potential stressors (temperature and nutrients). The resolution of the long-range isotope curves available for the "deep sea" sites will be increased to identify the more negative $\delta^{18}O$ signals indicating the warmest condition during interglacial MISs. A common age model will be applied to all "deep-sea" sites. $\delta^{18}O$ of single specimens of the planktonic foraminifer *Globigerinoides ruber* (white) and the large benthic *Amphistegina* will be measured across the thermal maxima of each interglacial MIS in the investigated regions. The parallel use of $\delta^{18}O$ composition and the Mg/Ca ratio, as temperature proxies, will help disentangle which fraction of the $\delta^{18}O$ signal is due to ice volume and will help to reconstruct more accurate paleo-temperature estimates. The combination of Sr/Ca, Mg/Ca and U/Ca ratios, along with corrected Sr-U and Li/Mg on the coral *Porites*, accurately dated by U/Th, from the "shallow" sites, will allow us to constrain paleo-temperature for a direct comparison with the "deep" sites. Reactive (bioavailable) phosphorus and $\delta^{13}C$ from the "deep" sites will be used to trace nutrient availability that, coupled with anomalously high temperatures, may trigger coral bleaching. The temperatures obtained from past interglacial extremes will serve to extract the relative frequency and magnitude of temperature extreme events, which went beyond the modern-day bleaching thresholds to gain insight into possible scenarios for a warmer world. Novelties of this project are the use of $\delta^{18}O$ on single foraminiferal specimens from the Present down to MIS31 to identify the magnitude and frequency of thermal excess through time and the exploration of chemical elements, whose enrichment or depletion in coral skeletons during bleaching can be used as a potential marker signal in fossil counterparts.
This project contributes to the understanding of climate dynamics in tropical and subtropical regions, and to understand the cause of the survival and or decline of coral reefs, which is presently a serious global concern.
An additional contribution of this project is to highlight the importance of the Swiss access to IODP samples recovered during past expeditions and stored in core repositories around the world.

We acknowledge the Swiss National Science Foundation Project 200020_201106 for the generous support to make this research possible.

*Project Partners:
Daniela Basso and Giovanni Coletti (University of Milano-Bicocca, Italy),
Anton Eisenhauer (GEOMAR Helmholtz-Zentrum für Ozeanforschung, Kiel, Germany)
Dick Kroon and Erica de Leau (University of Edinburgh, UK)

Michael Martinez-Colon (Florida A&M University, Tallahassee, USA)
Chiara Pisapia (KAUST-King Abdullah University of Science and Technology, Saoudi Arabia)
Stephanie Stainback (Kudala Environmental Ecology, South Africa)
Zoltan Zajacz (University of Geneva, Switzerland)

P 10.8
$^{87}Sr/^{86}Sr$ to reconcile chronology and weathering through the Oligocene

Heather Stoll[1], Jose Guitian[1], Ivan Hernandez[1], Heiko Palike[2,] Leo Pena[3]

[1] Geologisch Institut, ETH Zürich, Sonnegstrasse 5, CH-8092 Zürich (heather.stoll@erdw.ethz.ch)
[2] MARUM Univ. Bremen, Bibliothekstrasse 1 D-28359
[3] Marine Science Group, Univ. Barcelona,c/ Marti I Franques, Barcelona, ES-08028

The Oligocene is characterized by extremely rapid change in the marine $^{87}Sr/^{86}Sr$ ratio, which is helpful for stratigraphic correlation and which suggests very significant changes in the dominant sources of Sr to the ocean. We report new MC-ICPMS $^{87}Sr/^{86}Sr$ determinations on well preserved foraminifera from the Newfoundland Margin ODP 1406, as well as the Equatorial Pacific ODP Site 1218. At ODP 1406, results clarify the most likely stratigraphic position of 1-2 million year long depositional hiatuses, which were poorly resolved by biostratigraphy. New analyses at ODP 1218 provide an anchor Sr isotope stratigraphy, because site 1218 features an orbitally resolved age model based on benthic oxygen isotope record. From this site, we an confidently assess million year scale rates of change in the Sr isotope evolution, independent of temporal variations in sedimentation rate. We compare rate of change in Sr isotope evolution with key events such as intensification of glaciation during the Middle Oligocene Glacial interval, the Late Oligocene Warming, and the Oligo-Miocene Transition.

P 10.9
Response of Coccolithophores to the Oligocene – Miocene Dynamic System: Size and Degree of Calcification

José Guitián[1], Iván Hernández-Almeida[1], Miguel Ángel Fuertes[2], José-Abel Flores[2], Heather Stoll[1]

[1] Geological Institute, ETH Zürich, Zürich, Switzerland (jose.paleocean@gmail.com)
[2] Departamento de Geología, Universidad de Salamanca, Salamanca, Spain

Coccoliths formed by coccolithophores, the dominant group of marine calcifying phytoplankton, play a key role in the marine carbon cycle. Culture experiments have shown a strong sensitivity in size and their calcification to changing CO2 and ocean acidification. Therefore, there is significant interest in quantifying these physiological parameters of these calcite plates on geological time scales in response to changing ocean-atmosphere conditions.

Here, we firstly present coccolith size records of reticulofenestrid —the dominant coccolithophore family of the Cenozoic— over the Oligocene to Early Miocene time interval. Contrasting latitudes and environmental settings are compared using updated age models in order to identify globally synchronous trends in cell size from regional trends. Size results confirm several changes in coccolith size that are seen at all study sites, within the ~1 Myr age uncertainty, including a reduction in mean size by >2 µm from 30.2 to 27 and 24.5 to 23 Ma, and then increase in mean size after 20 Ma. Main differences among regions is the presence/absence of coccoliths larger than 8 µm. Changes in carbon dioxide, temperature, and nutrient availability are evaluated as potential drivers of the observed size trends at each studied site.

Secondly, in order to estimate the mass of coccoliths of any thickness, we have implemented the previous microscope methodology based on calcite wedge as thickness reference, into a precise modification of the original image processing routines allowing automatically analysis of coccoliths of any thick. With this application, we provide the first evaluation of the thickness and shape factor of coccoliths over temporal trends in the Cenozoic. Secondary calcite overgrowth or dissolution are discussed in the original dataset to final identify temporal thickness changes coincident with significant environmental trends, relationships that may entail specific adaptation of the degree of calcification.

These million-year scale morphological adaptations of ancient coccolithophores contribute to the understanding of phytoplankton physiology in the transition to the modern “icehouse” world.

P 10.10
Morphological and Geochemical Characterisation of south-eastern Mediterranean Seep Carbonates

Reinhard Weidlich[1], Or M. Bialik[2,3], Andres Rüggeberg[1], Bernard Grobéty[1], Torsten Vennemann[4], Yizhaq Makovsky[3,5], Anneleen Foubert[1]

[1] University of Fribourg, Department of Geosciences, Chemin du Musée 6, CH-1700 Fribourg (reinhard.weidlich@unifr.ch)
[2] Marine Geology & Seafloor Surveying, Department of Geosciences, University of Malta, Msida, MSD, 2080 Malta
[3] The Dr. Moses Strauss Department of Marine Geosciences, Leon H. Charney School of Marine Sciences, University of Haifa, ISR-3498838 Haifa
[4] University of Lausanne, Institut des dynamiques de la surface terrestre, Bâtiment Géopolis, CH-1015 Lausanne
[5] The Hatter Department of Marine Technologies, Leon H. Charney School of Marine Sciences, University of Haifa, ISR-3498838 Haifa

Authigenic seep carbonates, which are found globally at continental margins, can serve to characterise the seepage of hydrocarbon-enriched fluids into the oceans. In this study, we aim to identify past seepage activity on the south-eastern margin of the Mediterranean, based on the analysis of authigenic seep carbonates that were collected during the 2016 EUROFLEETS 2 SEMSEEP expedition aboard the RV AEGEO. Here we report results of sediment petrography (fluorescence, CL and standard optical microscopy), X-ray diffraction and stable isotope analyses of distinct seep-carbonate morphologies. The samples collected include three different carbonate morphologies: chimneys, crusts and pavements. Recurrent cement phases identified are associated with varying amounts of aragonite, low-magnesium calcite, high-magnesium calcite and dolomite. Carbonate chimneys consist of a sediment matrix with barite crystals and low-Mg calcite replacements, which act as nuclei for aragonite growth. Aragonite fans grow in several stages, with intermittent dissolution marks, indicating several phases of hydrocarbon seepage. Fe-Mn phases are often present at the edges of the aragonite fans and the low-Mg calcite replacements. Small dolomite rhombs occur within the sediment matrix. Carbonate crusts consist mainly of a matrix, which is rich with fossils and detritus- with low-Mg calcite breccias and high-Mg calcite nodules. Fan-shaped aragonites show several growth stages, which are separated by dissolution horizons and Fe-Mn crusts. These indicate several pulses of hydrocarbon seepage, which is similar to the chimneys. Carbonate pavements consist mainly of micritic dolomite and high-Mg calcite. Low-Mg calcite microsparite can be identified as well. Fan-shaped aragonites are locally present as pore-lining cement. Fe-oxides are coating the low- and high-Mg calcitic and dolomitic cements. The high amount of dolomite indicates a formation process under sulfate-reducing conditions. Stable carbon isotope data reveal a cluster between -10 and +5 $‰_{VPDB}$ for the sediment matrix, a ^{13}C-depleted cluster of about -20 to -35 $‰_{VPDB}$ for the replacements (low- and high-Mg calcite) and dolomites, and a highly ^{13}C-depleted cluster of about -30 to -52 $‰_{VPDB}$ for the aragonite fans.
Sediment petrography, combined with the XRD and stable isotope data hence support several phases of methane seepage through time. Furthermore, different carbonate formation processes, inferred from the dolomite content, can be identified within the different seep carbonates from the Eastern Mediterranean Sea.

P 10.11
Microbes as probes of past and present environmental changes recorded in lake sediments

Camille Thomas[1], Hendrik Vogel[2], Daniel Ariztegui[1]

[1] *Department of Earth Sciences, University of Geneva, rue des Maraichers 13, CH-1205 Geneva (camille.thomas@unige.ch)*
[2] *Institute of Geological Sciences & Oeschger Centre for Climate Change Research, University of Bern, Baltzerstrasse 1+3, CH-3012 Bern, Switzerland*

Specific microbial communities have inhabited past depositional settings, ecosystem and environments under precise conditions (i.e. environmental parameters). Limnogeological studies aim at reconstructing these conditions through the use of today's sediments and "proxy" that can only be interpretable if the path they have taken between their recording and their recovery (i.e. diagenesis, Fig. 1) is understood.

Microbes react to every change in environmental conditions (temperature, source of organic matter, conductivity, nutrient input) in an incredibly sensitive way. Tools such as ancient DNA (Thomas and Ariztegui, 2019; Capo et al., 2021), pigments, metal enrichments, can be used to reconstruct these original environmental conditions. Microbes are also actors of the diagenesis that transform these climatic archives, and leave an imprint that can be retraced to better inform paleoclimatic and paleoenvironmental reconstructions. The use of isotopes, lipid biomarkers (Thomas et al., 2019), bio- and organominerals Thomas et al., 2016) can permit to unravel these diagenetic processes. Finally, while these climatic archives are recovered, microbial communities still inhabit these environments and offer the opportunity to study the trajectory of an ecosystem, and potentially to inform on the response of life to changing climatic patterns. OMICS methods (Thomas et al., 2020; Kanellopoulos et al., 2018) along with traditional incubation and cultivation methods (Thomas et al., 2018) can provide key information regarding biogeochemical cycling in varied environments (i.e. fate of greenhouse gases, toxic element mobility) and potential advances for biotechnological applications or exobiology research.

Within this work, we provide examples showing that the integration of studies of the subsurface biosphere within geo- and paleo-limnology investigations can help unlock or secure the potential of multiproxy analysis for reconstructing the paleoenvironments, paleoclimates and paleo-ecology of lake basins while fostering new discoveries in the field of the deep biosphere.

REFERENCES

Capo, E. et al., 2021, Lake sedimentary DNA research on past terrestrial and aquatic biodiversity : Overview and recommendations Lake sedimentary DNA research on past terrestrial and aquatic biodiversity : Overview and recommendations: Quaternary, p. 0–75

Kanellopoulos, C., Thomas, C., Xirokostas, N., and Ariztegui, D., 2018, Banded Iron Travertines at the Ilia Hot Spring (Greece): An interplay of biotic and abiotic factors leading to a modern Banded Iron Formation analogue ? The Depositional Record, p. 1–23

Thomas, C., Frossard, V., Perga, M., Tofield-Pasche, N., Hofmann, H., Dubois, N., Belkina, N., Zobkova, M., Robert, S., Lyautey, E., 2018, Lateral variations and vertical structure of the microbial methane cycle in the sediment of Lake: Inland Waters, p. 1–22

Thomas, C., and Ariztegui, D., 2019, Fluid inclusions from the deep Dead Sea sediment provide new insights on Holocene extreme microbial life: Quaternary Science Reviews,.

Thomas, C., Ebert, Y., Kiro, Y., Stein, M., and Ariztegui, D., 2016, Microbial sedimentary imprint on the deep Dead Sea sediment: The Depositional Record, p. 1–21

Thomas, C., Francke, A., Vogel, H., Wagner, B., and Ariztegui, D., 2020, Weak influence of paleoenvironmental conditions on the subsurface biosphere of lake ohrid over the last 515 ka: Microorganisms, v. 8, p. 1–20

Thomas, C., Grossi, V., Antheaume, I., and Ariztegui, D., 2019, Recycling of Archaeal Biomass as a New Strategy for Extreme Life in the Dead Sea Deep Sediment: Geology

P 10.12
Vertical variation of the microbial community structure and functional potential in an 8000-year sediment sequence from Lake Cadagno (Piora Valley, Switzerland)

Paula Rodriguez[1], Jasmine Berg[2], Longhui Deng[2], Hendrik Vogel[3], Mark A. Lever[2], Cara Magnabosco[1].

[1] Department of Earth Sciences, ETH-Zurich, Zurich, Switzerland.
[2] Department of Environmental Systems Science, ETH-Zurich, Zurich, Switzerland.
[3] Institute of Geological Sciences, University of Bern, Bern, Switzerland & Oeschger Centre for Climate Change Research, University of Bern, Bern, Switzerland.

This study investigates the relationships between the geochemical properties of Lake Cadagno sediment deposits and the functional potential of the associated prokaryotic assemblages. Here, we use whole-genome and genome-resolved metagenomics to identify the changes in the microbial community profile in an 8000-year sedimentary sequence deposited throughout the Holocene. The study aims to predict the metabolic functions of the sediment-dwelling microbial groups to assess their potential role in the biogeochemical cycling of sulfur and carbon.

Results show that 16S rRNA gene abundance peaks in the upper 1-32 cm of the sedimentary sequence (10^8 copies per gram of sediment) and decreases with depth. The decline in bacterial and archaeal cell abundance is concomitant with a change in the microbial community structure. Moreover, a clear differentiation between surface and deep sediment communities is observed. Results from 16S rRNA gene sequencing show that in surface sediments the microbial community is dominated by Gamma and Deltaproteobacteria, Bacteroidetes, and Chloroflexi. In the first 40 cm of euxinic sediments, microbial respiration is fueled by sulfate reduction, as most of the Deltaproteobacteria representatives belong to the orders of sulfate-reducing bacteria Syntrophobacterales, Desulforomonadales, Desulfobacterales, and Desulfovibrionales. In contrast, the microbial community in mid-column sediments is dominated by Chloroflexi, Planctomycetes, Firmicutes, Bathyarchaeota, Euryarchaeota, and Aminicenantes. The presence of these groups indicates that fermentation and methanogenesis may be common metabolic strategies at these depths.

Whole-genome and genome-resolved metagenomic analyses (currently in progress) will give information on the presence of complete pathways and/or genes related to sulfur and carbon cycling in these microbial groups. By reconstructing the genomes of microbial populations throughout the sediments, we will investigate whether there are genomic changes associated with the main geochemical trends. This work will enable us to assess the influence of a changing lake on the structure of sediment-dwelling prokaryotic communities over thousands of years.

11. Quaternary environments: landscapes, climate, ecosystems and human activity during the past 2.6 million years

Marc Luetscher, Stefanie Wirth, Catharina Dieleman, Loren Eggenschwiler, Jean-Nicolas Haas, René Löpfe and Bigna Steiner

Swiss Society for Quaternary Research (CH-QUAT)

TALKS:

11.1 Gegg L., Anselmetti F.S., Deplazes G., Fuelling A., Madritsch H., Mueller D., Preusser F., Buechi M.W.: The Mid-Pleistocene Record of the Lower Aare Valley (northern Switzerland)

11.2 Hächler L., Beffa G., Zander P., Tinner W., Grosjean M.: High resolution record of primary productivity and anoxia in the context of the environmental history of Lago di Mezzano, Central Italy, since the Late Glacial

11.3 Islam N., Vennemann T., Lane S.N.: Changes in the growth of tree-rings and their water sources in relation to climatic changes in the Turtmanntal catchment, Switzerland

11.4 Martin C., Richter N., Schubert C., Dubois N.: Alkenones in Swiss lakes: first results and future applications

11.5 Mokatse T., Vainer S., Irving J., Schmidt C., Shemang E., Verrecchia E.P.: Geometry and nature of landforms in the Chobe Enclave, Northern Botswana: evidence from near-surface geophysical surveys and optically-stimulated luminescence (OSL)

11.6 Rapuc W., Bouchez J., Sabatier P., Gaillardet J., Arnaud F.: Quantitative evaluation of the impact of human and climate forcing on erosion in the Alpine Critical Zone over the Holocene

11.7 Roattino T., Buoncristiani J.-F., Crouzet C., Vassallo R., Carcaillet J., Gribenski N., Valla P.: Cosmogenic exposure dating of the last glacial extension in western French Alps.

11.8 Serra E., Valla P.G., Gribenski N., Magrani F., Carcaillet J., Deline P.: Post-LGM glacial history of the Dora Baltea catchment (western Italian Alps)

11.9 Studer A.S., Wörmer L., Vogel H., Dubois N., Bartosiewicz M., Hinrichs K.-U., Lehmann M.F.: First application of the diatom-bound nitrogen isotope paleo-proxy to reconstruct lacustrine eutrophication in Lake Lugano

11.10 Vainer S., Matmon A., Ben Dor Y., Verrecchia E., ASTER Team: Eolian chronology reveals causal links of tectonics and climate with coeval erg generation

11.11 Zander P.D., Żarczyński M., Tylmann W., Rainford S.-K., Grosjean M.: Seasonal climate signals preserved in biochemical varves: insights from novel high-resolution biogeochemical imaging techniques

POSTERS:

P 11.1 Flöter S., Fietzke J., Frank N., Freiwald A.: The potential of the deep-sea bamboo coral Acanella arbuscula (Octocorallia: Isididae) for environmental reconstruction

P 11.2 Gabriel I., Plunkett G., Abbott P., Oladottir B., McConnell J., Hoerhold M., Sigl M.: Unlocking the secrets of past Icelandic volcanism with tephra

P 11.3 Lloren R., Cochrane E., Augustinus P., Prebble M., Dubois N.: The voyage of Humans in the South Pacific: the view from Lake Lanotō, Sāmoa

P 11.4 Kremer K., Betschart S., Bernet N., Mitrano D.M.: Lake sediments as archives of microplastic pollution

P 11.5 Dziomber L., Gurtner L., Leunda M., Schwörer C.: A palaeoecological reconstruction of Holocene vegetation dynamics in the Eastern Swiss Alps

P 11.6 Kaelin D., Thew N., Cuenca-Bescós G., Urresti I., Buechi M.W., Deplazes G.: The Hasli Formation – an exceptional record of Early Pleistocene interglacial sediments in Northern Switzerland

P 11.7 Bolliger D., Buechi M.: Early retreat of Thur Glacier: New insights form mapping the sediment-landform assemblage in the tongue basin of Andelfingen

P 11.8 Lechleitner F.A., Day C.C., Kost O., Wilhelm M., Haghipour N., Henderson G.M., Stoll H.M.: Increasing soil respiration over the last deglaciation reconstructed from stalagmites – a coupled multi-proxy and forward modelling approach

P 11.9 Luetscher M., Jeannin P.-Y.: Tracking extreme flood records in speleothems

P 11.10 Rowan S., Luetscher M., Szidat S., Lechleitner L.: Stalagmite organic carbon as a novel paleoecosystem proxy? Implications from a high resolution cave process study.

11.1
The Mid-Pleistocene Record of the Lower Aare Valley (northern Switzerland)

Lukas Gegg[1], Flavio S. Anselmetti[1], Gaudenz Deplazes[2], Alexander Fuelling[3], Herfried Madritsch[2], Daniela Mueller[3], Frank Preusser[3], Marius W. Buechi[1]

[1] Institute of Geological Sciences and Oeschger Centre for Climate Change Research, University of Bern, Baltzerstrasse 1+3, CH-3012 Bern (lukas.gegg@geo.unibe.ch)
[2] Swiss National Cooperative for the Disposal of Radioactive Waste (Nagra), Hardstrasse 73, CH-5430 Wettingen
[3] Institute of Earth and Environmental Sciences, University of Freiburg, Albertstraße 23b, D-79104 Freiburg

During the Pleistocene, Alpine glaciers repeatedly advanced into the foreland, temporarily covering the majority of northern Switzerland in ice. Despite their severe environmental and geomorphic impact, the number, the timing, and the extent of the individual glaciations – especially of those predating the last glacial maximum – are still poorly constrained. This is a consequence of the fragmentarity of the geological record, and difficulties in resolving, interpreting, and dating it.

Subglacial overdeepenings trapped sediment below the fluvial base level, significantly increasing its preservation potential, and thus contain promising archives of Quaternary environmental change. We investigate the infill of the overdeepened Gebenstorf-Stilli Trough and the glaciofluvial paleochannel system of the Lower Aare Valley, in the confluence area with the rivers Reuss and Limmat.

In four scientific boreholes, we recovered ~350 m of drill cores, that are complemented with outcrop studies. Sedimentological and petrographic analyses combined with luminescence dating provide new insights into the regional glaciation history. The depositional record of the Lower Aare Valley reaches back well into the Middle Pleistocene. It reveals multiple phases of glacial / glaciofluvial reactivation of both overdeepening and paleochannel, and allows inferences of ice-margin positions and relative sediment yields from the Limmat, Reuss, and Aare(/Rhone) glaciers.

11.2
High resolution record of primary productivity and anoxia in the context of the environmental history of Lago di Mezzano, Central Italy, since the Late Glacial

Luc Hächler[1], Giorgia Beffa[2], Paul Zander[1], Willy Tinner[2], Martin Grosjean[1]

[1] Institute of Geography & Oeschger Centre for Climate Change Research, University of Bern, Switzerland (luc.haechler@students.unibe.ch)
[2] Institute of Plant Sciences & Oeschger Centre for Climate Change Research, University of Bern, Switzerland

Anthropogenic impact is seen as the main cause for current global warming, which is influencing nature and human societies on earth. Climate change and direct anthropogenic impacts are now harming lake ecosystems globally, especially from high nutrient loads. Woolway & Merchant (2019) showed that with ongoing climate change, most lake mixing regime changes worldwide are projected (RCP 6.0) to be from currently warm-monomictic (only mixing in winter) to meromictic (permanent stratification). This puts additional pressure on freshwater ecosystems in the Mediterranean. Long-term data provide unique insights to the state of ecosystem degradation. Which in turn is needed to develop sound restoration and management strategies. Lake sediments provide an unique archive that unlocks valuable long-term information on how lake ecosystems reacted in the past to natural variability and human pressure.

In this study, we used, for the first time in the Mediterranean, a high resolution series of calibrated pigment concentrations based on hyperspectral imaging (HSI). This recently developed, rapid, non-destructive scanning technique with 83 µm spatial resolution allows us to reconstruct the primary productivity and anoxia since the late Glacial for the nowadays warm-monomictic Lago di Mezzano in Central Italy. To disentangle influences from either natural variability or human pressure these HSI data on lake productivity and anoxia were related to the lake catchment's environmental history and postglacial climate change. Information on the environmental history (erosion, land cover, vegetation changes, fire dynamics, and anthropogenic impact) was derived from X-ray fluorescence (XRF) elemental proxies and palynological investigations. Data were validated with conventional geochemical analysis done by researchers two decades ago. The effect of climate was assessed using independent climate proxy data on temperature and humidity.

In the late Glacial, we found low lake productivity and high erosion. During the Bølling/Allerød, we observed an increase in production and lower erosion. This trend was paused at the Younger Dryas. The early-Holocene shows very high production, prolonged meromixis, and low erosion. During the mid-Holocene, production peaks, anoxia is less stable, and erosion is slightly increasing. With the onset of the Bronze Age, humans transformed the catchment through deforestation. At the same time, we observe high erosion, low production, and an end of prolonged meromixis.
First results, show a tendency to meromixis at higher temperatures, supporting model results. However, a more detailed analysis is ongoing to disentangle cause and effect of natural variability and human pressure. This should allow us as well to assess the current state of the lake ecosystem degradation. In summary, this record provides unprecedented detail on the past-environmental history of a present day warm-monomictic lake with implications to the present and future.

REFERENCES

Woolway, R. I. & Merchant, C. J. 2019: Worldwide alteration of lake mixing regimes in response to climate change. Nature Geoscience, 12(4), 271–276. https://doi.org/10.1038/s41561-019-0322-x

11.3
Changes in the growth of tree-rings and their water sources in relation to climatic changes in the Turtmanntal catchment, Switzerland

Nazimul Islam*, Torsten Vennemann and Stuart N. Lane

**presenting author's email: nazimul.islam@unil.ch*

Climate change has important impacts both on water-related risks (e.g., flooding) and water-related resources, notably the reduction of glacial meltwater in mountain regions including Alpine catchments. Water-related risks (e.g. extreme events) can be identified by detecting the unexpected growth changes in tree-rings (often called pointer years), whereas water-related resources (e.g. changing water sources) can be traced by isotopic compositions analysed for cellulose extracted from tree-rings. A pilot study in the Turtmänna river catchment (110 km^2), south-western Switzerland, indicates distinctive patterns of climate change via the tree-rings in two different species. The tree-ring width (TRW) chronologies from cores of Larix decidua (larch) and Picea abies (spruce) collected from four different zones (at 3 km intervals) along the 18 km long Turtmänna river, downstream of the Turtmannsee reservoir, shows that in the last two decades (2000-2020) the trees have experienced a steady decline in their growth (approx. 50%) with higher fluctuations in year-to-year growth that correlate strongly with recent climate warming. The longest TRW chronology was constructed for 146 years (dated back to 1874) in site-4, which demarcates a strong positive correlation with reference chronology (Gleichläufigkeit or GLK = 73%, $p < 0.001$). Furthermore, the results also provide evidence that the growth of tree-rings even of the same species within the same zone differs significantly from trees next to the river compared to the trees that are more distal to the river. This supports the hypothesis that the growth of the trees that have direct access to the proglacial streams likely depend on glacier-meltwater induced runoff, whereas the trees that are distal to the river predominantly depend on groundwater accessibility that may decrease with decreasing amounts of precipitation. In comparison to picea abies, larix decidua shows higher sensitivity to regional climate fluctuations and some years of unexpected growth changes are well correlated with the years of rockfall events. However, this research work is currently at a preliminary stage. Further work will trace water sources by trees that are even more distal to the river and hence further assess the impacts of water intake from the stream on the tree-ring growth in the Turtmänna river catchment.

11.4
Alkenones in Swiss lakes: first results and future applications

Céline Martin[1], Nora Richter[2], Carsten Schubert[3], Nathalie Dubois[1]

[1] Surface Waters Research + Management, Eawag, Überlandstrasse 133, CH-8600 Dübendorf, Switzerland (celine.martin@eawag.ch)
[2] Department of Marine Microbiology and Biogeochemistry, NIOZ Royal Netherlands Institute for Sea Research, AB Den Burg, The Netherlands
[3] Surface Waters Research + Management, Eawag, Seestrasse 79, CH-6047 Kastanienbaum, Switzerland

Past temperature records are important tools for inferring climate dynamics and provide empirical data for testing climate models to improve our mechanistic understanding of natural climate variability. Unfortunately, very few quantitative records of pre-historic continental temperatures exist in Europe. Moreover, existing paleothermometers only provide mean annual or warm season temperatures, limiting our understanding of climate variability during the transitional seasons and winter. In this project we surveyed Swiss lakes for a promising sedimentary paleothermometer, the alkenone biomarker, and we found it! Alkenones are temperature-sensitive lipids produced by different groups of haptophyte algae, which have been used for decades to reconstruct quantitative changes in sea-surface temperatures. Increased reporting of alkenones in both saline and freshwater lakes worldwide suggests that there is great potential for alkenone-based paleotemperature reconstructions in lacustrine settings. And in fact, among the 58 Swiss lakes studied, 33 contain alkenones in their sediments. Most of these lakes seem to host a particular group of lacustrine alkenone producers that have been reported to bloom during the spring season and produce alkenones that are well correlated with changes in winter-spring temperatures. Lake St Moritz has been equipped with a surveying system that will allow to determine the seasonality of alkenone production. Our first results suggest that we will be able to improve the understanding of alkenone production in freshwater lakes and to develop the first winter-spring lake temperature reconstruction in Switzerland that extends beyond existing historical records.

11.5
Geometry and nature of landforms in the Chobe Enclave, Northern Botswana: evidence from near-surface geophysical surveys and optically-stimulated luminescence (OSL)

Thuto Mokatse[1], Shlomy Vainer[1], James Irving[2],Christoph Schmidt[1], Elisha Shemang[3], Eric P. Verrecchia[1]

[1] Institute of Earth Surface Dynamics – IDYST, FGSE, University of Lausanne, Switzerland (thuto.mokatse@unil.ch)
[2] Institute of Earth Sciences – ISTE, FGSE, University of Lausanne, 1015 Lausanne, Switzerland
[3] Earth and Environmental Sciences, Botswana International University of Science and Technology, Botswana

The imprint of neotectonics is frequently obscured in low-relief environments by the sedimentary cover, hindering distinction between landforms of different origin. This study utilizes near surface geophysical surveys and optically-stimulated luminescence (OSL) dating in the Chobe Enclave, an area that offers unique opportunities of relating landscape development with (neo)tectonic activity. The Chobe Enclave is part of a pristine region of the Middle Kalahari Basin in northern Botswana, which preserves fossil landforms, such as sand dunes, pans, sand ridges, and carbonate islands, as a result of paleo-environmental and paleo-drainage changes through the Quaternary and associated to (neo)tectonics processes. Particularly, sand ridges are seen from electrical resistivity tomography (ERT) data to be characterized by high resistivity values and they overly the conductive silt-rich floodplains. Ground penetrating radar (GPR) show continous reflectors corresponding to possible bounding surfaces of either lacustrine (paleolakes) or aeolian origin. The resultant OSL ages are Holocene age of two clustered age groups that range between 23.4 ka and 20.8 ka and between 6.2 ka and 4.4 ka, attesting to different depositional environments, indicating a period of non-deposition with possible erosion phase, which could be related to (neo)tectonics. The tectonic influence on the landscape and drainage is evidenced by incisions of sand ridges forming fluvial watergaps.

REFERENCES

Diaz, N., Armitage, S. J., Verrecchia, E. P., & Herman, F. 2019: OSL dating of a carbonate island in the Chobe Enclave, NW Botswana. Quaternary Geochronology, 49, 172-176.

Eckardt, F. E., Flügel, T., Cotterill, F., Rowe, C., & McFarlane, M. 2016: Kalahari tectonic landforms and processes beyond the Okavango Graben. Quaternary International, 404, 194.

Mokatse, T., Diaz, N., Shemang, E., Van Thuyne, J., Vittoz, P., Vennemann, T., & Verrecchia, E.P. (in press) Landscapes and landforms of the Chobe Enclave, Northern Botswana.

Otvos, E. G. 2000: Beach ridges—definitions and significance. Geomorphology, 32(1-2), 83-108.

11.6
Quantitative evaluation of the impact of human and climate forcing on erosion in the Alpine Critical Zone over the Holocene

William Rapuc[1,2,3], Julien Bouchez[3], Pierre Sabatier[2], Jérôme Gaillardet[3,4], Fabien Arnaud[2]

[1] *Université Grenoble Alpes, Université Savoie Mont Blanc, CNRS, IRD, IFSTTAR, Grenoble, France (william.rapuc@hotmail.fr)*
[2] *Université Grenoble Alpes, Université Savoie Mont Blanc, CNRS, EDYTEM, 73000 Chambéry, France*
[3] *Université de Paris, Institut de physique du globe de Paris, CNRS, F-75005 Paris, France*
[4] *Institut Universitaire de France*

The Critical Zone (CZ), defined as the thin active layer at the Earth's surface is at risk due to climate change and anthropogenic pressure increase. This represents a potential threat to the future of humanity as the CZ is the locus of developing human societies. CZ's soil erosion is now considered as one of the geosciences/society central issues. Understanding the influence of both forcing factors is key to improve our management of the CZ's soil resource, especially in mountainous areas where erosion is highest. Only studies combining large spatial and temporal approaches allow to assess the effect of the different forcing factors on soil erosion rates. Here, we apply a retrospective approach based on lake sediments to reconstruct the long-term evolution of erosion in alpine landscapes. Lake Bourget and Lake Iseo, located in the northern French and Italian Alps, respectively, acts as natural sinks for all the erosion products from their large catchments. We combined a multiproxy study of lacustrine sediment sections covering the Holocene (Lake Bourget) and the last 2 kyrs (Lake Iseo) with a source-to-sink method, using isotopic geochemistry (εNd, $^{87}Sr/^{86}Sr$). The applied methodology allows us to disentangle the role of climate and land use as erosion forcing factors through their differential impact on the various rock types present in the catchment. Indeed, high-altitude areas of the two study sites, where the erosion is dominated by precipitation and glacier advances, present isotopic signature different from those of the sedimentary rocks located in the rest of the catchment, where both human activities and precipitations impact erosion through time. To understand the effect of human activities, erosion signals from high-altitude and the rest of the catchment were compared to local and regional erosion chronicles. During the Early Holocene and until 3.8 kyr cal BP, the erosion signal is dominated by climate fluctuations. Since 3.8 kyr, climate fluctuations alone cannot explain measured erosion trends. From then, human activities by modifying the soil erodibility through land-use become the dominant forcing factor of the physical erosion in mountainous environment of the European Alps.

11.7
Cosmogenic exposure dating of the last glacial extension in western French Alps.

Thibault Roattino[1], Jean-François Buoncristiani[2], Christian Crouzet[1], Riccardo Vassallo[1], Julien Carcaillet[3], Natacha Gribenski[4], Pierre Valla[3]

[1] *Savoie Mont-Blanc University, Grenoble Alpes University, CNRS, IRD, IFSTTAR, ISTERRE, France*
[2] *Biogéosciences, UMR 6282 CNRS, Bourgogne Franche-Comté University, France*
[3] *Grenoble Alpes University, Savoie Mont-Blanc University, CNRS, IRD, IFSTTAR, ISTERRE, France*
[4] *Bern University, Institute of Geological Sciences, Switzerland*

According to paleoclimate proxies, two temperature minima occurred throughout the last ice age and correspond to the marine isotope stages MIS 4 and MIS 2. The Last Glacial Maximum (LGM) corresponds to the coldest period during MIS 2. In the European Alps, glaciers formed large foothill lobes reaching maximum extent during this period. This study focuses on the foreland moraines of the western French Alps located about 20 km east of the city of Lyon. These numerous moraine ridges, well preserved in the piedmont landscape, are bounded to the north by the southern Jura and to the south by Miocene hills. OSL dating of glacio-fluvial deposits in front of the western French Alps glaciers reveals large ancient advances in the foreland during MIS 4 and the end of MIS 3. However, the extension of the LGM has not yet been recorded by chronological data. In the study area, we sampled quartz-rich boulders to obtain exposure ages. We performed in-situ beryllium-10 (10Be) cosmogenic ages on quartz from 21 sampled boulders in order to reconstruct the palaeogeography of these glaciers during the LGM. 17 of the 21 samples give exposure ages between 23.81 ± 1.12 and 12.94 ± 0.85 ka, covering the LGM and Lateglacial periods. 4 outliers are much older or younger, involving pre- or post-depositional processes. The Lateglacial exposure ages are synchronous with the radiocarbon dates of the postglacial deposits and human occupations within the study area. Therefore, Lateglacial exposure ages are probably the result of exhumated erratic boulders following the degradation of moraines. Our results clearly show that during the LGM, the glaciers of the western French Alps reached the foothills again, where the palaeogeography of glacial extensions is complex. The old advances and the LGM extension are superimposed in the southern Jura and the Miocene hill areas. In the foreland plain, the LGM advance is less important than the old extensions (MIS4-MIS3). This new LGM palaeogeography of the western French Alps shows an interesting similarity with the western Italian Ivrea and Rivoli-Avigliana glacier lobes, sharing the same accumulation zone with the studied glaciers.

11.8
Post-LGM glacial history of the Dora Baltea catchment (western Italian Alps)

Elena Serra[1,2], Pierre G. Valla[1,2,3], Natacha Gribenski[1,2], Fabio Magrani[1,2], Julien Carcaillet[3], Philip Deline[4]

[1] *Institute of Geological Sciences, University of Bern, Baltzerstrasse 1-3, CH-3012*
[2] *Oeschger Centre for Climate Change Research, University of Bern, Hochschulstrasse 4, CH-3012 Bern*
[3] *Univ. Grenoble Alpes, Univ. Savoie Mont Blanc, CNRS, IRD, IFSTTAR, ISTerre, F-38000 Grenoble*
[4] *EDYTEM, Université de Savoie, CNRS, F-73000 Chambéry*

Fluctuations of mountain glaciers in response to climate variations have been recognised worldwide, both for modern and past time periods. Across the European Alps, several post-Last Glacial Maximum (LGM; 26.5-19.0 ka) ice retreat and re-advance stages have been identified and related to short-term climate oscillations, independently constrained in the paleoclimate record. However, due to the scarcity of continuous glacial deposits and landforms preserved along Alpine valleys, only few studies have succeeded in providing detailed Lateglacial deglaciation sequences from the LGM to the Holocene along an individual catchment.

We present a thorough reconstruction of the post-LGM glacial history of the Dora Baltea catchment (north-western Italy) which hosted one of the main Quaternary glacial systems of the western European Alps. By combining existing and new chronological constraints (^{10}Be surface-exposure and optically-stimulated luminescence burial dating) from glacial and postglacial landforms/deposits with ice surface reconstructions, we quantitatively reconstruct the timing and ice-configuration of six (pre-)LGM to early Holocene paleoglacial stages in the main Dora Baltea valley. In addition, we combined our chronology data with calibrated numerical ice modeling (iSOSIA) to simulate Lateglacial glacier evolution in three main lateral tributary valleys and investigate forcing paleoclimatic conditions.

Our deglaciation sequence brings new information in line with post-LGM glacier reconstructions from other Alpine areas, and can be correlated with specific Lateglacial paleoclimatic periods. Tributary glaciers fluctuated synchronously after disconnecting from the main Dora Baltea glacier (ca. 16 ka), demonstrating similar sensitivity to Lateglacial climate variations.

11.9
First application of the diatom-bound nitrogen isotope paleo-proxy to reconstruct lacustrine eutrophication in Lake Lugano

Anja S. Studer[1], Lars Wörmer[2], Hendrik Vogel[3], Nathalie Dubois[4], Maciej Bartosiewicz[1], Kai-Uwe Hinrichs[2], Moritz F. Lehmann[1]

[1] Department of Environmental Sciences, University of Basel, Basel, Switzerland (anja.studer@unibas.ch)
[2] MARUM – Center for Marine Environmental Sciences, University of Bremen, Bremen, Germany
[3] Institute of Geological Sciences and Oeschger Centre for Climate Change Research, University of Bern, Bern, Switzerland
[4] Department of Surface Waters Research and Management, Eawag, Dübendorf, Switzerland

Past changes in the input/output, and internal cycling, of bioavailable nitrogen (N) in marine and lacustrine environments can be reconstructed by analyzing the N isotopic composition (i.e., the $^{15}N/^{14}N$ ratio, or $\delta^{15}N$) of organic matter in the sedimentary record. Bulk sedimentary $\delta^{15}N$ signatures, however, can be biased by secondary alteration and external (e.g., terrestrial) N inputs. Such a bias can be overcome by measuring the $\delta^{15}N$ of organic N trapped and protected in the mineral structure of (micro-)fossils, such as diatoms, foraminifera and corals, which is thought to record the pristine $\delta^{15}N$ signature of nitrate in the ambient water. While the diatom-bound N isotope paleo-proxy is widely used in the marine environment, it has not yet been applied to the lacustrine realm. In this study, investigating a sediment core from eutrophic Lake Lugano (Switzerland), we reconstruct nutrient cycling and paleoenvironmental conditions in the lake over the past 150 years through a combination of diatom-bound $\delta^{15}N$ measurements, X-ray fluorescence scanning and molecular biomarker analysis. Our data indicate that primary productivity, as inferred from the barium/titanium ratio, increased at the beginning of the 1960s, coeval with the period of severe eutrophication in Lake Lugano. At the same time, diatom-bound $\delta^{15}N$ values increased as well, which could either point to (i) a rise in the $\delta^{15}N$ of the nitrate input to the lake, e.g., through manure, (ii) enhanced nitrate utilization, or (iii) enhanced water column denitrification. In order to differentiate among these possibilities, we also determined the concentration of heterocyst glycolipids (HG) in the sediments, which is a diagnostic biomarker for N_2 fixing cyanobacteria. HG concentrations increased in parallel with the other proxy variables, implying that N_2 fixation is closely coupled to water column denitrification (and thus, N loss) in Lake Lugano. We hypothesize that greater primary productivity during eutrophication led to anoxic conditions as a result of enhanced organic matter remineralization, causing higher water column denitrification in Lake Lugano. At the same time, the nitrogen-to-phosphorous (N:P) ratio in the lake declined due to enhanced N loss and remobilization of P from the sediments under anoxic conditions, fostering N_2 fixation in surface waters.

11.10
Eolian chronology reveals causal links of tectonics and climate with coeval erg generation

Shlomy Vainer[1,2,3*], Ari Matmon[2], Yoav Ben Dor[2], Eric Verrecchia[1], ASTER Team[3,a]

[1] *Institute of Earth Surface Dynamics, University of Lausanne, 1015 Lausanne, Switzerland*
[2] *Institute of Earth Sciences, The Hebrew University of Jerusalem, 919040 Jerusalem, Israel*
[3] *Aix-Marseille Université, CNRS, Collège de France, IRD, INRA, CEREGE, 13545 Aix-en-Provence, France.* [a]*Georges Aumaître, Didier L. Bourlès, Karim Keddadouche*

The onset and intensification of eolian activity mark climatic transitions that promote wide-scale aridification, recorded by the generation and preservation of massive sand deposits. Evaluating the impact and implications of such repositories on Earth systems requires knowledge about the timing of their emplacement and the mechanisms responsible for their generation, which remain highly uncertain. Here we provide time constraints for the establishment of the Kalahari Erg, which is the largest continuous body of sand on Earth. We apply cosmogenic nuclide dating of sand from the Kalahari Desert combined with numerical modeling to determine when sand was introduced into the interior of southern Africa. Through the consideration of several scenarios, we show that major events of eolian sand transport and accumulation occurred between ~2.5 and 1 Myr ago (Fig. 1). This substantial activity, which significantly altered environmental settings, corresponds to regional, continental, and global scale morphotectonic and climatic changes (Fig. 2) that contributed to the mass production and widespread dispersion of sand. These changes substantially altered existing habitats, thus constituting a crucial milestone for hominin evolution and migration throughout the African continent during the Pleistocene.

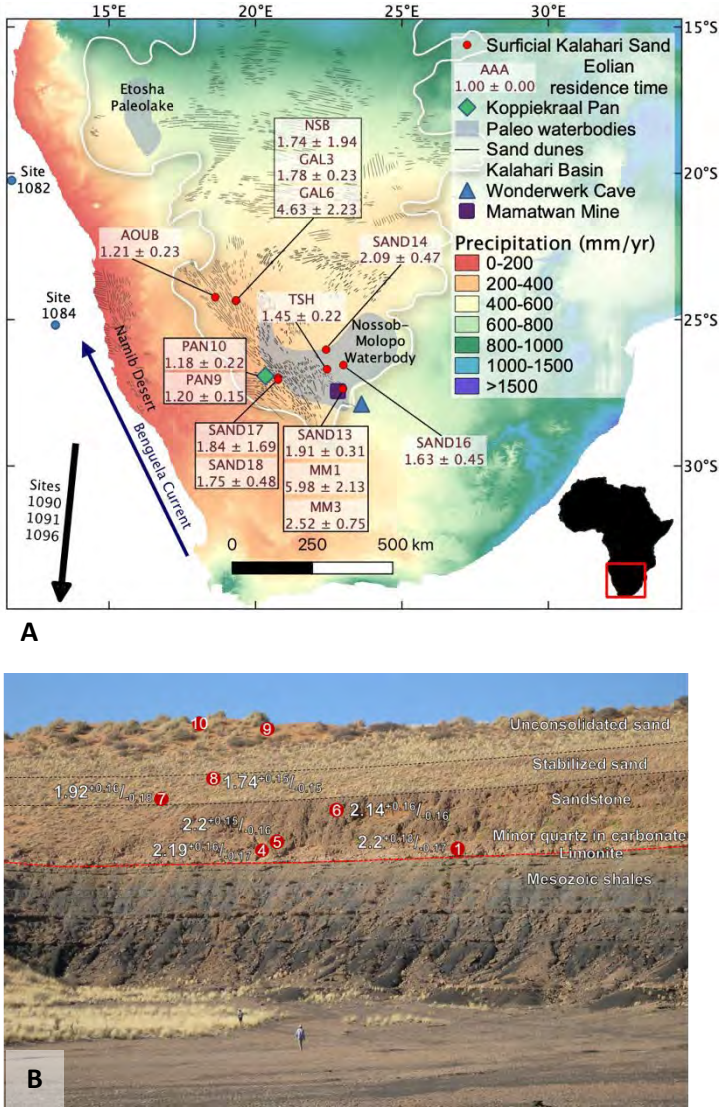

Figure 1. Eolian chronology of the Kalahari Desert Sand. (a) Locations of sand samples and sites mentioned in the text are superimposed on the modern precipitation map of southern Africa (www.worldclim.org). Eolian residence time is the weighted average of the simulated duration in which agreement between simulated and measured radionuclides was achieved (Vainer et al 2018, Vainer and ben Dor 2021). Burial ages (reported in Ma with 1σ uncertainty) were calculated assuming pre-burial $^{26}Al/^{10}Be$ between 5.03 and 5.15 (estimated iteratively after Granger et al., 1997). Inset: The red rectangle depicts the area of the main figure within the African continent. (b) A 60 m thick exposure at the northeastern wall of Koppieskraal Pan (see location in Fig. 1a) where ~40 m of consolidated Kalahari Sand overlies Mesozoic shales of the Karoo supergroup. Burial ages (reported in Ma with 1σ uncertainty) were calculated assuming pre-burial $^{26}Al/^{10}Be$ between 5.56 and 5.79 (estimated iteratively after Granger et al., 1997). Numbers in red circles correspond to the sample's serial number in the supplementary data.

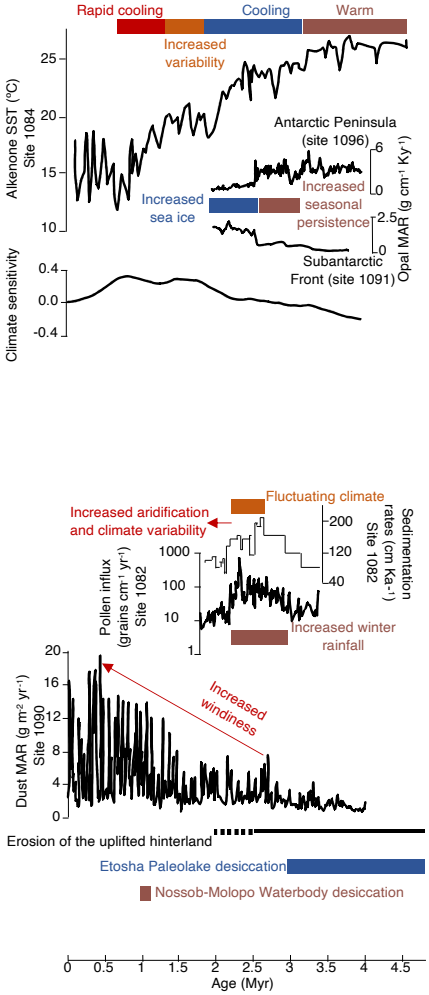

Figure 2. The timing of eolian activity in the Kalahari Desert (shaded gray rectangle) displayed on top of environmental settings and key events in southern Africa and proximate oceans. The text provides interpretation of the records and is colored in accordance with colored bars and arrows. (a) Sea Surface Temperature (SST) record offshore Namibia (ODP site 1084) derived from alkenone unsaturated index (), which reflects the strengthening of upwelling along the west African margins throughout the Pleistocene (Marlow et al. 2000). (b) Primary productivity based on biogenic opal Mass Accumulation Rates (MAR) shows coeval increase in the Southern Ocean (ODP site 1091) and decrease in the Antarctic Peninsula (ODP site 1096) due to the onset of Antarctic Sea Ice (McKay et al. 2012). (c) Climate sensitivity in high latitudes, calculated as the ratio between the deconvoluted records of the obliquity component of the scaled oxygen isotope and the solar forcing (Ravelo et al. 2004). (d) Reconstructed atmospheric CO_2 record showing a decrease below the bioclimatic threshold for the expansion of C_4 plants at ~2.7 Ma (Van de Wal et al. 2011). (e) Sedimentation rates and pollen Influx at ODP Site 1082 indicating a transition from a mixed fluvial and eolian input to predominantly eolian transport at 2.2 Ma (Dupont 2006). (f) Dust MAR at site 1090 derived from Ti MAR recording increased windiness since ~2.7 Ma (Martínez-Garcia et al. 2011).

REFERENCES

Dupont, L.M., 2006. Late Pliocene vegetation and climate in Namibia (southern Africa) derived from palynology of ODP Site 1082. *Geochemistry, Geophysics, Geosystems*, 7(5).

Granger, D.E., Kirchner, J.W. and Finkel, R.C., 1997. Quaternary downcutting rate of the New River, Virginia, measured from differential decay of cosmogenic 26Al and 10Be in cave-deposited alluvium. Geology, 25(2), pp.107-110.

Marlow, J.R., Lange, C.B., Wefer, G. and Rosell-Melé, A., 2000. Upwelling intensification as part of the Pliocene-Pleistocene climate transition. *Science*, 290(5500), pp.2288-2291.

Martínez-Garcia, A., Rosell-Melé, A., Jaccard, S.L., Geibert, W., Sigman, D.M. and Haug, G.H., 2011. Southern Ocean dust–climate coupling over the past four million years. *Nature*, 476(7360), pp.312-315.

McKay, R., Naish, T., Carter, L., Riesselman, C., Dunbar, R., Sjunneskog, C., Winter, D., Sangiorgi, F., Warren, C., Pagani, M. and Schouten, S., 2012. Antarctic and Southern Ocean influences on Late Pliocene global cooling. *Proceedings of the National Academy of Sciences*, 109(17), pp.6423-6428.

Ravelo, A.C., Andreasen, D.H., Lyle, M., Lyle, A.O. and Wara, M.W., 2004. Regional climate shifts caused by gradual global cooling in the Pliocene epoch. *Nature*, 429(6989), pp.263-267.

Vainer, S & Ben Dor, Y, 2021. The Cosmolian program for simulating aeolian dynamics and its application to central Australia. *Earth Surface Processes and Landforms*, 46 (9), pp. 1631-1639.

Vainer, S., Ben Dor, Y. and Matmon, A., 2018a. Coupling cosmogenic nuclides and luminescence dating into a unified accumulation model of aeolian landforms age and dynamics: The case study of the Kalahari Erg. *Quaternary Geochronology*, 48, pp.133-144.

Van de Wal, R.S.W., De Boer, B., Lourens, L., Köhler, P. and Bintanja, R., 2011. Reconstruction of a continuous high-resolution CO_2 record over the past 20 million years. *Climate of the Past*, 7, pp.1459-1469.

11.11
Seasonal climate signals preserved in biochemical varves: insights from novel high-resolution biogeochemical imaging techniques

Paul D. Zander[1], Maurycy Żarczyński[2], Wojciech Tylmann[2], Shauna-kay Rainford[3], Martin Grosjean[1]

[1] *Institute of Geography & Oeschger Centre for Climate Change Research, University of Bern, Switzerland*
[2] *Faculty of Oceanography and Geography, University of Gdansk, Poland*
[3] *Institute of Plant Sciences & Oeschger Centre for Climate Change Research, University of Bern, Switzerland*

Varved sediments are recognized as uniquely valuable archives of paleoenvironmental information, and have been used for studies of paleoclimate for over a century. However, quantitative paleoclimate reconstructions derived from the geochemical composition of biochemical varves are rare, due to the challenge of obtaining biogeochemical data at sufficiently high-resolution, as well as complicated and diverse possible climate-proxy relationships. Recently developed high-resolution spectroscopic imaging techniques make it possible to acquire biogeochemical data with unprecendented resolution, providing oppurtunities to investigate how climate signals affect varve structure and composition at (sub)seasonal resolution.

In this study, we use hyperspectral imaging (HSI) to measure sedimentary pigments, and micro X-Ray fluorescence (µXRF) imaging to measure elemental abundances in sediments of Lake Żabińskie, Poland. Both techniques provide spatially resolved data at 60 µm resolution, yielding ca. 100 data points per varve year on average. Additionally, C, N and S, were measured at annual resolution. We focus on the period 1966-2019 because during this time varve preservation is excellent, and varve counts show no uncertainty. A hierarchical clustering algorithm was used to classify varve years into four varve types based on the dissimilarity of the within-varve multivariate geochemical time series. Analysis of variance shows that the four varve types formed in years with significantly different seasonal meteorological conditions, with windiness and temperature showing the strongest influence on varve geochemical patterns. Seasonal climate conditions were reconstructed from sedimentary variables using generalized additive models (GAMs). Spring and summer (MAMJJA) temperature was inferred using Ti and total C (R^2_{adj} = 0.55; cross-validated root mean square error (CV-RMSE) = 0.7 °C, 14.4 %). The number of windy days from March to December (mean daily wind speed > 7 m/s) were inferred using mass accumulation rate (MAR) and Si (R^2_{adj} = 0.48; CV-RMSE = 19.0 %). This study shows the potential of high-resolution sediment scanning techniques to clarify our understanding of varve formation processes and improve our understanding of climate proxy-relationships in biochemical varves. This information provides a foundation for high-resolution paleoclimate reconstruction, and here we provide examples of calibration models for annual resolution seasonal weather reconstruction from biogeochemical proxies.

P 11.1
The potential of the deep-sea bamboo coral *Acanella arbuscula* (Octocorallia: Isididae) for environmental reconstruction

Sebastian Flöter[1,2], Jan Fietzke[2], Norbert Frank[3], André Freiwald[4]

[1] *Department of Earth Sciences, University of Geneva, Rue des Maraîchers 13, 1205 Genève, Switzerland (sebastian.floeter@unige.ch)*
[2] *GEOMAR Helmholtz Centre for Ocean Research, Wischhofstr. 1-3, 24148 Kiel, Germany*
[3] *Institute of Environmental Physics, Heidelberg University, 69120 Heidelberg, Germany*
[4] *Marine Research Department, Senckenberg by the Sea, Südstrand 40, 26382 Wilhelmshaven, Germany*

The calcitic parts of bamboo corals show a layered internal structure that can be used for high resolution environmental reconstruction or dating. To evaluate this potential of the corals two neighbouring specimens of the genus *Acanella* were collected on the Great Meteor Seamount in 975 m water depth. Multiple internodes in each specimen were sectioned for chemical mapping with Electron Microprobe Mapping and Backscattered Electron Imaging for visualising the internal growth structure. These structures were investigated on their similarity in banding pattern between different internodes of each specimen and between the two specimens. Our data show no obvious common banding pattern. Thus, the detailed processes of skeletal formation of each individual must be understood carefully prior to regional environmental reconstructions.

P 11.2
Unlocking the secrets of past Icelandic volcanism with tephra

Imogen Gabriel[1*], Gill Plunkett[2], Peter Abbott[1], Bergrún Óladóttir[3,4], Joseph McConnell[5], Maria Hörhold[6] and Michael Sigl[1,7]

[1] Climate and Environmental Physics & Oeschger Centre for Climate Change Research, University of Bern, 3012 Bern, Switzerland (imogen.gabriel@climate.unibe.ch)
[2] School of Natural and Built Environment, Queen's University Belfast, Belfast, BT9 5AG, UK
[3] Institute of Earth Sciences, University of Iceland, Reykjavík, Iceland
[4] Icelandic Meteorological Office, Bústaðavegur 9, 150 Reykjavík, Iceland
[5] Desert Research Institute, Nevada System of Higher Education, Reno, USA
[6] Alfred-Wegener-Institut Helmholtz-Zentrum für Polar- und Meeresforschung, Am Handelshafen 12, 27570 Bremerhaven, Germany
[7] Department of Geosciences, University of Oslo, em Sælands vei 1, 0371, Oslo, Norway

The associated climatic cooling following a volcanic eruption has resulted in these events being considered as one of the key natural drivers for oscillations in the global climate system (Robock, 2000; Sigl et al., 2015). It is therefore important that we fully understand the nature (duration and magnitude) of these events to robustly assess their climatic-societal impacts.

Evidence of past eruptions (i.e. volcanic ash and sulphate aerosols) may be preserved in high-resolution archives, such as the Greenland ice cores (Abbott and Davies, 2012). Analysis of these records has highlighted a period of increased Icelandic volcanism between 500-1250 AD, coincidental with climatic changes in the North Atlantic region (Massé et al., 2008). However, the nature of these Icelandic events (duration and magnitude) is poorly constrained. Correlations have been further hindered by the high number of eruptions and geochemical similarity of events during this time period (Óladóttir et al., 2011; 2018).

To resolve this, we have adopted a high-resolution targeted sampling strategy on two Greenland ice cores (TUNU2013 and B19). From undertaking EPMA geochemical analysis on tephra from the events in the ice core records, alongside proximal material, precise correlations can be made to their volcanic centres. When utilised with other key proxies (i.e. Sulphur isotopes), the overall nature of the eruption can be constrained, allowing the effects of Icelandic volcanism on the North Atlantic climate during this period of increased eruption activity to be robustly assessed.

REFERENCES

Abbott, P. M., & Davies, S. M. 2012: Volcanism and the Greenland ice-cores: the tephra record. Earth-Science Reviews, 115(3), 173-191.

Massé, G., Rowland, S. J., Sicre, M. A., Jacob, J., Jansen, E., & Belt, S. T. 2008: Abrupt climate changes for Iceland during the last millennium: evidence from high resolution sea ice reconstructions. Earth and Planetary Science Letters, 269(3-4), 565-569.

Óladóttir, B. A., Larsen, G., & Sigmarsson, O. 2011: Holocene volcanic activity at Grímsvötn, Bárdarbunga and Kverkfjöll subglacial centres beneath Vatnajökull, Iceland. Bulletin of Volcanology, 73(9), 1187-1208.

Óladóttir, B. A., Sigmarsson, O., & Larsen, G. 2018: Tephra productivity and eruption flux of the subglacial Katla volcano, Iceland. Bulletin of Volcanology, 80(7), 1-16.

Robock, A. 2000: Volcanic eruptions and climate, Reviews of Geophysics, 38(2), 191-219.

Sigl, M., Winstrup, M., McConnell, J.R., Welten, K.C., Plunkett, G., Ludlow, F., Büntgen, U., Caffee, M., Chellman, N., Dahl-Jensen, D. and Fischer, H. 2015: Timing and climate forcing of volcanic eruptions for the past 2,500 years, Nature, 523(7562), 543-549.

P 11.3
The voyage of Humans in the South Pacific: the view from Lake Lanotō, Sāmoa

Ronald Lloren*[1,2], Ethan Cochrane[3], Paul Augustinus[4], Matthew Prebble[5,6], Nathalie Dubois[2]

[1] Department of Earth Sciences, ETH Zürich, Sonneggstrasse 5, CH-8006 Zürich
[2] Department of Surface Waters Research and Management, Eawag, Überlandstrasse 133, CH-8600 Dübendorf
[3] Anthropology, School of Social Sciences, The University of Auckland, New Zealand, Private Bag 92019, Auckland 1142, New Zealand
[4] School of Environment, University of Auckland, Private Bag 92019, Auckland 1142, New Zealand
[5] School of Earth and Environment, University of Canterbury, Christchurch, New Zealand,
[6] School of Culture, Australian National University, History and Languages, Canberra, Australia
**ronald.lloren@eawag.ch*

Archaeological data suggests that humans commenced inhabiting the remote islands in the South Pacific around 3000 yr BP. Human occupation brought tremendous modifications to these small islands: clearing forests through burning, introduction of new flora and fauna, horticulture practices and the like. These practices were either drastic or gradual in some areas in the region, and may have been related to patterns of climate change. To better understand the peopling of this area, a 4.75 m composite sediment core, encompassing the period of human settlement, was retrieved from Lake Lanotō, Sāmoa. A multi-proxy approach, including micro-XRF scanning of the cores, grain size distribution, organic carbon content and molecular biomarkers from human and plant remains engraved in the sediment, is used to reconstruct past environmental changes. Combining these biomarker and elemental proxies will help us advance our knowledge on the timing of human expansion in Sāmoa, and in the South Pacific region. The generated data will shed valuable light on Pacific prehistory and complement the knowledge gained from archaeological data.

P 11.4
Lake sediments as archives of microplastics pollution

Katrina Kremer[1], Silvan Betschart[1], Nora Bernet[2], Denise M. Mitrano[2]

[1] *Swiss Seismological Service at ETH Zurich, Sonneggstrasse 5, 8092 (katrina.kremer@sed.ethz.ch)*
[2] *Department of Environmental Systems Science, ETH Zurich, Universitätstrasse 16, 8092 Zurich*

Plastics are ubiquitous in our daily lives, and this has a profound yet poorly understood impact on our environment. Since the 1950, plastics consumption has increased across the globe, yet the mismanagement of plastics waste and leakage into the environment have been well documented both in urban and rural locations. Through various aging and weathering processes, plastics can be chemically or mechanically weathered into smaller size fraction, including microplastics (<1mm). Sediments serve as environmental integrators and thus can serve as archives to better understand the history and legacy of plastic pollution. Through fluvial systems, plastics are transported and are deposited in reservoirs such as lakes and oceans where the plastics accumulate in the sedimentary systems. Thus, sediments which contain these plastic fragments can be used to assess their fate pathways, mass loads and accumulation rates in different environmental systems. This study aims to assess the burden of plastics contamination in lake sediments, particularly for the microplastic size fraction. Here we aim to understand its temporal deposition and elucidate accumulation areas and hot spots based on specific fate pathways which govern the sedimentation processes. In order to accurately quantify microplastics in sediments, the particles must first be extracted from the complex matrix of lake sediments before further identification and characterization. In this contribution, we present (i) the workflow adopted to separate microplastics particles from the sediments and (ii) the first preliminary data for the temporal evolution of the microplastics contamination recorded within one sediment core retrieved from the deep basin of Lake Zurich. Using these first results, we plan to further expand the study to better understand the pathways of microplastics into Lake Zurich over a watershed scale to assess specific release scenarios and mass concentrations of plastics from different areas surrounding Lake Zurich, from urban to natural.

P 11.5
A palaeoecological reconstruction of Holocene vegetation dynamics in the Eastern Swiss Alps.

Laura Dziomber[1,2], Lisa Gurtner[1], Maria Leunda[1,2,3], Christoph Schwörer[1,2]

[1] Institute of Plant Sciences, University of Bern, Altenbergrain 21, 3013 Bern, Switzerland (laura.dziomber@ips.unibe.ch)
[2] Oeschger Centre for Climate Change Research, University of Bern, Hochschulstrasse 4, 3012 Bern, Switzerland
[3] WSL Swiss Federal Research Institute, Zürcherstrasse 111, 8903 Birmensdorf, Switzerland

Human-induced global warming is affecting natural ecosystems in many different aspects. The scientific community has been informing decision-makers and the public on this topic since decades. Thus, it is still essential to better understand the impact of climate change on natural systems, in order to prevent or mitigate negative effects on fragile ecosystems.

Plant populations are, as a result of climate change, forced to shift their range to more suitable areas, adapt to changing conditions or suffer decline. Despite the growth of monitoring programs assessing the impacts of global change in ecological processes, there is in general an insufficient use of long-term studies in conservation biology to understand long-scale responses.

The last climate change of a similar magnitude and rate as projected for this century occurred during the transition between the last Ice Age and the Holocene interglacial (ca. 11,700 years ago). Studying this time period will provide new insights into vegetation changes resulting from climatic drivers, since it represents a potential analogue to the present-day and future climate change. Understanding the response of vegetation to rapid temperature increase is a fundamental prerequisite to produce accurate and reliable predictions.

We are currently investigating a palaeoecological archive from a high-altitude mountain lake, Lai da Vons (1991 m a.s.l), located in Eastern Switzerland. We present results of macrofossil and pollen analyses which allow us to reconstruct local to regional vegetation changes. In a next step, we will use novel molecular methods, in order to track adaptive and neutral genetic diversity of conifer populations through the Holocene by analyzing ancient DNA from subfossil conifer needles. The overarching goal of this large-scale, multiproxy study is to better understand past vegetation dynamics and the impact of future climate change on plants at multiple scales; from the genetic to the community level.

P 11.6
The Hasli Formation – an exceptional record of Early Pleistocene interglacial sediments in Northern Switzerland

Daniel Kälin[1], Nigel Thew[2], Gloria Cuenca-Bescós[3], Isabel Urresti[3], Marius W. Buechi[4], Gaudenz Deplazes[5]

[1] Federal Office of Topography swisstopo, Seftigenstrasse 264, CH-3084 Wabern (daniel.kaelin@swisstopo.ch)
[2] Rue Paul-Bouvier 2, CH-2000 Neuchâtel (nigelmthew@gmail.com)
[3] Aragosaurus-IUCA-EIA, Earth Sciences, University of Zaragoza, Pedro Cerbuna 12, E-50009 Zaragoza (cuencag@unizar.es), (isaperez@unizar.es)
[4] Institute of Geological Sciences & Oeschger Centre for Climate Change Research, University of Bern, Baltzerstrasse 1+3, CH-3012 Bern (marius.buechi@geo.unibe.ch)
[5] National Cooperative for the Disposal of Radioactive Waste (Nagra), Hardstrasse 73, CH-5430 Wettingen (gaudenz.deplazes@nagra.ch)

The Höhere Deckenschotter («upper cover gravels») is considered to be the oldest body of Quaternary sediments in Northern Switzerland (Graf 1993). It forms the highest of four morphostratigraphic units (top down: Höhere Deckenschotter, Tiefere Deckenschotter, Hochterrassenschotter and Niederterrassenschotter). The Höhere and Tiefere Deckenschotter units in Switzerland consist of glaciofluvial gravels with intercalated overbank and other fluvial sediments deposited in broad channels. They lie directly on Molasse or Mesozoic bedrock. Due to subsequent erosion, the Deckenschotter are preserved as relic deposits on top of hills. There is an ongoing debate about the age of the Deckenschotter as cosmogenic nuclide dating (Claude et al. 2017) has produced younger ages than those derived from biostratigraphic dating (Bolliger et al. 1996).

On the Irchel Plateau (northern canton of Zurich), the Höhere Deckenschotter gravels are well exposed along the edge of the plateau. Within these exposures, a characteristic layer of fine-grained, mostly beige or grey overbank sediments (Hasli Formation) can be traced across much of the Irchel Plateau. Based on mapping and high-precision surveying at five locations, the base of the Hasli Formation can be shown to be a floodplain deposit that dips slightly to the NW. Six profiles through the Hasli Formation have been excavated, documented and sampled in detail.

Lithologically, the Hasli Formation consists mainly of characteristic light beige silts and fine sands with sporadic cemented sand layers and carbonate concretions. In places the Hasli Formation also includes thin gravel layers. Thin lignite layers were also observed at Irchel Hasli. The Hasli Formation reaches its greatest thickness of c. 7 m at the south-eastern end of the Irchel Plateau, and its least thickness of c. 2 m in the central part and at its north-western end. Locally the Hasli Formation seems to be missing due to subsequent erosion.

A rich (several thousand specimens) and diverse molluscan fauna (>80 different species) has been recovered from all of the investigated profiles. In addition, small numbers of Chara and ostracods were also found. Small mammal teeth were discovered at several sites, but only the already known site at Irchel Hasli (Bolliger et al. 1996, Cuenca-Bescòs 2015) has yielded a well-preserved and identifiable fauna.

For age determination, both the small mammal and molluscan remains provide important data. For the small mammals, the fauna from Irchel-Hasli falls into the Borsodia-Villanyia Superzone (Fejfar & Heinrich 1989), whose upper limit lies at ca. 1.8 Ma. In particular, *Mimomys pliocaenicus* and *Mimomys reidi/pitymyoides* are marker species characteristic for the small mammal unit MN 17 (Mein 1989, ca. 2.6–1.8 Ma). This confirms the previous biostratigraphic study of Bolliger et al. (1996), although a further analysis of the first occurrences of the mammalian species in the assemblage allows a more precise age classification in the time range of ca. 2.2/2.0–1.8 Ma.

The molluscan faunas identified from the Irchel sites give important new biostratigraphical information for the first part of the Early Pleistocene. The presence of several key indicator species typical of Tiglian faunas strongly suggests that the Hasli Formation dates from between c. 2.2 and 1.8 Ma. The molluscs also confirm that the Hasli Formation represents a floodplain accumulation at the margin of a large meandering river.

The uniquely rich and diverse faunas from the Hasli Formation represent interglacial conditions that were significantly warmer than today, during the first part of the Early Pleistocene.

REFERENCES

Bolliger, T., Fejfar, O., Graf, H.R. & Kälin, D. 1996: Vorläufige Mitteilung über Funde von pliozänen Kleinsäugern aus den höheren Deckenschottern des Irchels (Kt. Zürich). Eclogae geol. Helv. 89/2, 1043−1048.

Claude, A., Akçar, N., Ivy-Ochs, S., Schlunegger F., Kubik W.P., Dehnert A., Kuhlemann J., Rahn M. & Schlüchter, C. 2017:

Timing of early Quaternary gravel accumulation in the Swiss Alpine Foreland. Geomorphology 276, 71−85.
Cuenca-Bescòs, G. 2015: The Pleistocene small mammals from Irchel, Switzerland. A taxonomic and biostratigraphic revision. Expertenbericht Eidgenössisches Nuklearsicherheitsinspektorat.
Fejfar, O. & Heinrich, W. 1989: Muroid rodent biochronology of the Neogene and Quaternary in Europe. European Neogene Mammal Chronology (Lindsay, E. H., Fahlbusch, V. & Mein, P., Eds.). NATO ASI Series, Series A: Life Sciences 180, 91−118.
Graf, H.R. 1993: Die Deckenschotter der zentralen Nordschweiz. Diss. ETH Zürich.
Mein, P. 1975: Résultats du groupe de travail des vertébrés: Biozonation du Néogène méditerranéen à partir des mammifères. In: Report on Activity of the RCMNS Working Groups (1971–1975), Bratislava, 78–81.

P 11.7
Early retreat of Thur Glacier: New insights form mapping the sediment-landform assemblage in the tongue basin of Andelfingen

Daniel Bolliger[1] and Marius W. Buechi[1,2]

[1] Institute of Geological Sciences, University of Bern, Baltzerstrasse 1+3, CH-3012 Bern (daniel.bolliger@geo.unibe.ch)
[2] Oeschger Centre for Climate Change Research, University of Bern, Hochschulstrasse 4, 3012 Bern

After peak glaciation, many of the northern Alpine foreland glaciers retreated in a down wasting-stagnation pattern: Phases of rapid glacier disintegration are interrupted by periods of ice-front stagnation or minor re-advances. We study the glacial sediment-landform assemblage in the area of Andelfingen (Canton of Zurich, N Switzerland) to better characterize this type of retreat dynamics for the Thur Valley Glacier at the end of the Birrfeld Glaciation. The detailed sedimentological field work focussed on a series of moraines ridiges encircling a tongue basin, all of which have been correlated with the ice marginal complex Stein am Rhein/Zürich (Keller & Krayss 2005). With maps and profiles, we analyzed the geomorphology and internal structure of these exposed sediment successions.

Our results indicate that two to three glacial advances with moraine formation, flooding of the tongue basin and basin sedimentation can be distinguished. At last, 'Lake Thurtal' formed after the final retreat of the glacier and extended over a length of about 30 km (Müller 2014). It seems likely that these observed advances are oscillations of the ice-front but may reflect a more wide-spread behavior of the Thur Glacier at that time.

REFERENCES

Keller, O. & Krayss, E. 2005: Der Rhein-Linth-Gletscher im letzten Hochglazial. 1. Teil: Einleitung, Aufbau und Abschmelzen des Rhein-Linth-Gletschers im Oberen Würm, Vierteljahrsschrift der Naturforschenden Gesellschaft in Zürich, 150, 19-32.

Müller, E. R. 2014: Frauenfeld ab dem ausgehenden Eiszeitalter, Mitteilungen der Thurgauischen Naturforschenden Gesellschaft, 67, 7-45.

P 11.8
Increasing soil respiration over the last deglaciation reconstructed from stalagmites – a coupled multi-proxy and forward modelling approach

Franziska A. Lechleitner[1,2], Christopher C. Day[1], Oliver Kost[3], Micah Wilhelm[4], Negar Haghipour[3,5], Gideon M. Henderson[1], Heather M. Stoll[3]

[1] Department of Earth Sciences, University of Oxford, South Parks Road, OX1 3AN Oxford, UK
[2] Department of Chemistry, Biochemistry and Pharmaceutical Sciences & Oeschger Centre for Climate Change Research, University of Bern, Freiestrasse 3, 3012 Bern, Switzerland
[3] Department of Earth Sciences, ETH Zurich, Sonneggstrasse 5, 8006 Zürich, Switzerland
[4] Swiss Federal Institute for Forest, Snow and Landscape Research, Zürcherstrasse 111, 8903 Birmensdorf, Switzerland
[5] Laboratory for Ion Beam Physics, ETH Zürich, Otto-Stern-Weg 5, 8093 Zürich, Switzerland

Soil respiration is a critical but poorly constrained part of the global carbon cycle. In particular, not much is known about how soil respiration responded to past episodes of climatic change, but this knowledge would be informative for projections of terrestrial ecosystem responses to current and future anthropogenic warming scenarios.

Here we present a new reconstruction of soil respiration from stalagmites from the northern Iberian Peninsula over the last deglaciation. The record is based on stable carbon isotopes ($\delta^{13}C$), which closely track millennial scale temperature changes. This similarity has previously been noted across the temperate Western European region, suggesting that the dominant process driving stalagmite $\delta^{13}C$ is closely linked to regional temperatures.

Stalagmite $\delta^{13}C$ is a mixed signal from soil respiration, carbonate bedrock dissolution, and in-cave processes. To disentangle these effects and extract the soil respiration signal, we use i) a multi-proxy approach using Ca-isotopes and radiocarbon measurements, which are sensitive to different parts of the cave carbon cycle and ii) forward modelling of conditions in soil, karst and cave, generating large simulation ensembles that allow us to find the initial conditions best matching the proxy data. This approach is the first to quantify and remove the effects of carbonate dissolution and in-cave processes from the bulk stalagmite $\delta^{13}C$ signature, allowing us to derive temporal changes in soil pCO_2, linked to respiration.

Our results show a robust trend of increasing soil respiration over the period of the last deglaciation, consistent with increasing temperatures in the region.

P 11.9
Tracking extreme flood records in speleothems

Marc Luetscher[1], Pierre-Yves Jeannin[1]

[1] *Swiss Institute for Speleology and Karst Studies (marc.luetscher@isska.ch)*

Because they are well-preserved from surface erosion, speleothems have emerged as a promising archive for the reconstruction of paleofloods on short and long time-scales (Denniston and Luetscher, 2017). The identification and interpretation of hydrological proxy records is, however, subject to a good understanding of a system's response to precipitation events. Based on a detailed cave survey we model the hydraulic response of Milandre cave using pipe-flow models and calibrate our results with recent monitoring data to provide a quantitative approach for the interpretation of speleothem paleoflood layers.

Model results are compared with recently deposited stalagmites to reconstruct a sequence of paleoflood extremes in the late Holocene. We evaluate the significance of these results on a regional scale and discuss their potential to provide original information about the maximal discharge rates anticipated under contrasting climate scenarios.

REFERENCES

Denniston, R.F., & Luetscher, M., 2017: Speleothems as high-resolution paleoflood archives, Quaternary Science Reviews, 170, 1-13.

P 11.10
Stalagmite organic carbon as a novel paleoecosystem proxy? Implications from a high resolution cave process study.

Sarah Rowan[1], Marc Luetscher[2], Sönke Szidat[1], Franziska Lechleitner[1]

[1] Department of Chemistry, Biochemistry, and Pharmaceutical Sciences & Oeschger Centre for Climate Change Research, University of Bern, Freiestrasse 3, 3012 Bern, Switzerland, (sarah.rowan@unibe.ch)
[2] Swiss Institute for Speleothem and Karst Studies, Rue de la Serre 68, 2301 La Chaux-de-Fonds, Switzerland.

Stalagmites are popular climate proxy archives as they form from incremental depositional layers and are easily dated with U-Th and U-Pb chronometers (Hellstrom & Pickering, 2015). Well recognised stalagmite based proxies focus on the dominant inorganic carbon fraction (Shah et al. 2013; Fohlmeister et al. 2020). Over the past 20 years, interest in the organic carbon (OC) fraction of stalagmites has increased due to its potential to offer information about past ecosystem dynamics. OC sourced from the overlying soil, vadose zone, or within the cave itself may be preserved within stalagmites through the link between cave and outside environment via rainwater percolating through the soil and karst (Blyth et al. 2016). Hence, the isotopic characterisation ($\delta^{13}C$ and ^{14}C) of the small fraction of OC present in stalagmites has the potential to give information about past ecosystem processes in the surrounding catchment (Blyth et al. 2013).

Stalagmite OC typically comprises 0.01-0.3% of its total carbon, the overwhelming majority being inorganic calcium carbonate (Blyth et al. 2016). Recent advancements in accelerator mass spectrometry (AMS), and the method of OC extraction from stalagmites has allowed for the extraction and ^{14}C analysis of small speleothem OC samples (Lechleitner et al. 2019). These preliminary studies have shown its potential as a sensitive counterpart to other proxies such as carbonate and OC $\delta^{13}C$.

Here we present first results from an ongoing high frequency process study at Milandre cave (Switzerland) which will analyse the isotopic composition of inputs and fluxes of OC to the karst system over the course of two years. Preliminary results of total organic carbon (TOC) quantification of cave drip and river water are also discussed. This study will assist in constraining the source of OC within stalagmites from this and other caves and allow assessment of its suitability as a proxy for ecosystem change.

REFERENCES

Blyth, A., Hartland, A. and Baker, A., 2016. Organic proxies in speleothems – New developments, advantages and limitations. Quaternary Science Reviews, 149, pp.1-17.

Blyth, A., Smith, C. and Drysdale, R., 2013. A new perspective on the ^{13}C signal preserved in speleothems using LC–IRMS analysis of bulk organic matter and compound specific stable isotope analysis. Quaternary Science Reviews, 75, pp.143-149.

Fohlmeister, J., Voarintsoa, N., Lechleitner, F., Boyd, M., Brandtstatter, S., Jacobson, M. and L. Oster, J., 2020. Main controls on the stable carbon isotope composition of speleothems. Geochimica et Cosmochimica Acta, 279, pp.67-87.

Hellstrom, J. and Pickering, R., 2015. Recent advances and future prospects of the U–Th and U–Pb chronometers applicable to archaeology. Journal of Archaeological Science, 56, pp.32-40.

Lechleitner, F., Lang, S., Haghipour, N., McIntyre, C., Baldini, J., Prufer, K. and Eglinton, T., 2019. Towards Organic Carbon Isotope Records from Stalagmites: Coupled ^{13}C and ^{14}C Analysis Using Wet Chemical Oxidation. Radiocarbon, 61(03), pp.749-764.

Shah, A., Morrill, C., Gille, E., Gross, W., Anderson, D., Bauer, B., Buckner, R. and Hartman, M., 2013. Global Speleothem Oxygen Isotope Measurements Since the Last Glacial Maximum. Dataset Papers in Geosciences, 2013, pp.1-9.

13. Geomorphology

Cristian Scapozza, Nikolaus Kuhn, Dorota Czerski, Caroline Bolliger, Reynald Delaloye, Isabelle Gärtner-Roer, Elisa Giaccone, Christoph Graf, Isabelle Kull, Mario Kummert, Christophe Lambiel, Géraldine Regolini, Julie Wee

Swiss Geomorphological Society (SGmS)

TALKS:

13.1 Aarnink J., Vuaridel M., Ruiz-Villanueva V.: Monitoring instream large wood transport in rivers, using video cameras, deep learning and RFID

13.2 Bandou D.T., Schlunegger F., Kissling E., Marti U., Schwenk M., Schläfli P., Douillet G.A., Mair D.: Gravity modelling of overdeepenings fill in the Bern area

13.3 del Hoyo J., Vennemann T., Vauridel M., Ruiz-Villanueva V.: Using stable isotopes to fingerprint the origin of instream wood at the river basin scale

13.4 Del Siro C., Lambiel C., Scapozza C., Perga M.E.: Water origin and quality of rock glacier springs. Case studies in the Swiss Alps.

13.5 Giaccone E., Oriani F., Tonini M., Lambiel C. Mariéthoz G.: Semi-automated geomorphological mapping: a first attempt in the Swiss Alpine environment

13.6 Mourey J., Ravanel L., Lambiel L: Mapping climate-change related processes affecting mountaineering itineraries. Application to the Valais Alps (Switzerland)

13.7 Peleg N., Skinner C., Ramirez J.A., Fatichi S., Molnar P.: Rainfall heterogeneity accelerates hydro-morphological processes

13.8 Shynkarenko A., Kremer K., Stegmann S., Bergamo P., Lontsi A.M., Roesner A, Hammerschmidt S., Kopf A., Fäh D.: Geotechnical investigations and slope stability analysis in Lake Lucerne

13.9 Vos H.C., Fister W., Kuhn N.J.: The surface conditions of dust emission from the sandy croplands in the Free State, South Africa

POSTERS:

P 13.1 De Pedrini A., Giacomazzi D., Scapozza C., Ambrosi C., Manconi A.: Role of the last deglaciation on the timing of collapsing of large rock slope failures in the Southern Swiss Alps

P 13.2 Finch B., Ruiz-Villanueva V.: Application of the Graph Theory to instream large wood supply and transfer to define the wood cascade in fluvial networks

P 13.3 Schmidt C., Laag C., Whitehead M., Kereszturi G., Profe J.: The complexities assessing volcanic hazards along the Cameroon Volcanic Line using spatial distribution of monogenetic volcanoes

13.1
Monitoring instream large wood transport in rivers, using video cameras, deep learning and RFID

Janbert Aarnink[1], Marceline Vuaridel[1], Virginia Ruiz-Villanueva[1]

[1] *IDYST, Universite de Lausanne, Quartier Mouline, CH-1005 Lausanne*
(*janbert.aarnink@unil.ch*, *marceline.vuaridel@unil.ch*, *virginia.ruiz-villanueva@unil.ch*)

This work is supported by the SNSF Eccellenza project PCEFP2-186963 “Towards a new understanding of fluvial ecosystems: integrating wood regime across multiple scales “ and the University of Lausanne.

Wood’s role in the River ecosystem The influence of instream large wood (10cm diameter & 1m long minimal) recruited from forested river catchments on fluvial processes has in early studies generally been disregarded. In more recent years, research shows that instream wood influences morphodynamics and its presence results in a more diverse river, creating habitats for aquatic and terrestrial species (Wohl et al., 2019). Wood transport may also cause damages to infrastructures during floods. Thus, an increasing interest in wood transport quantification has led to the use of techniques like aerial imagery, carbon dating, Radio-Frequency Identification (RFID) and video monitoring (MacVicar et al., 2009). Currently a few sites are equipped with video cameras (Ghaffarian et al., 2020), but a fully automated detection system is still absent.

Objective The main objective of the research is to increase our understanding of transport processes of large wood in rivers. To achieve this understanding, we are designing a monitoring framework to quantify wood transport.

Study sites

- **Vallon de Nant**: An area located in the Swiss mountains in canton Vaud. The valley is a dedicated natural reserve. On the downstream end, there is already a station that measures water flow and sediment transport.
- **Spoel**: In the east of Switzerland at the town of Zernez (Canton Graubünden), the Spoel river is located in a Swiss national park. The hydropower dam upstream releases experimental floods every year during which wood is transported.
- **Zulg**: After several floods caused severe damage, the Zulg river (Canton Bern) was provided with a flood warning system. Amateur images show a high amount of wood transported.
- **Sense**: Located in Gantrisch Nature Parc (Canton Bern & Fribourg), the Sense river is a dynamic wide braided river, which allows it to have a large wood storage capacity.

Methods

- **Detection**: We are developing a camera observation system based on deep learning to detect large wood and quantify wood transport in rivers. The first camera is already recording at the *Vallon de Nant* area. To create an object detection algorithm based on deep learning, so-called training data was obtained by manually adding wood to the river and having multiple cameras record it. As a result, we now have thousands of manually identified wood observations.
- **Tracking**: In the *Spoel* river, in recent years we have created a database of large wood pieces. From 2018 onwards, pieces were tagged with a unique number. This was done pre- and post-flood. As the sizes and locations of the pieces are known, a comprehensive wood transport analysis can be created. The same will be done at the *Vallon de Nant* area, with the addition of RFID tags that are put in every piece of large wood in the channel. This will allow us to have an even more precise database that can be correlated with the hydrographs and sediment transport already measured (figure 1).

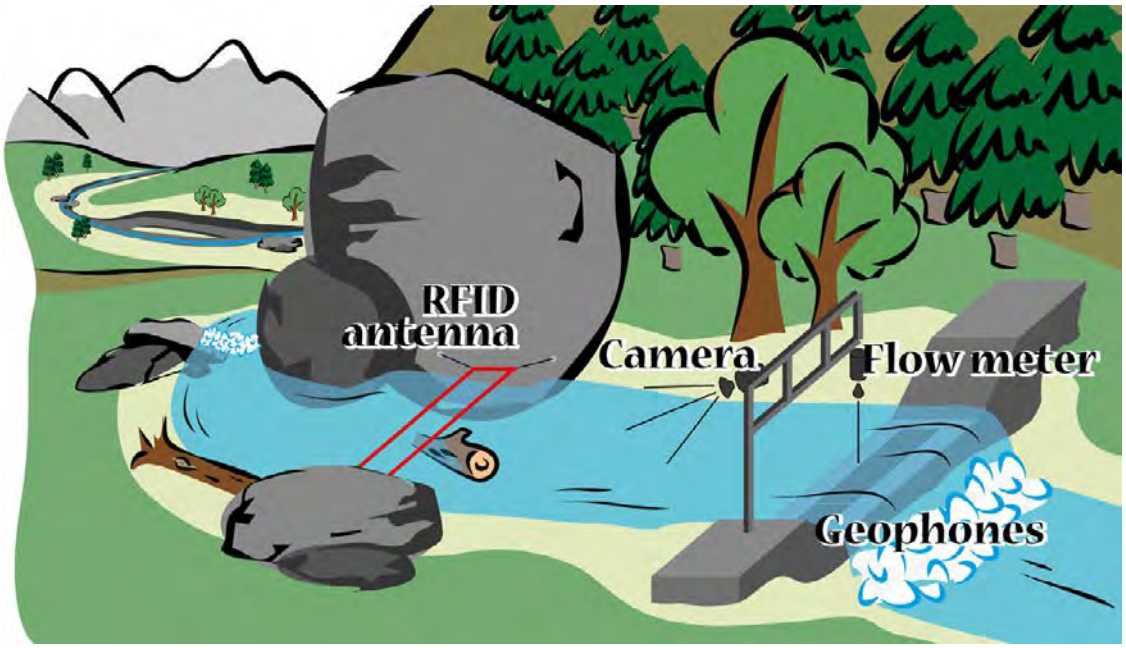

Figure 1. Setup of the Vallon de Nant measuring station. An RFID antenna scans tags in large wood. A camera is monitoring for large wood using deep learning. Sonar measures flow and geophones measure sediment transport.

Results and Outlook

First results show that the deep learning approach has the potential to become a more effective detection approach than current computer vision solutions. The challenge now is to make the system robust and efficient enough to expand the observation network (e.g. to other Swiss rivers like the Zulg or Sense) and to increase our database whilst keeping the data quantity minimal. Also, preliminary tests have proven the capacity of RFID tags to accurately track pieces of wood. Additional work will be done to tag a large number of pieces along the studied streams.

REFERENCES

Wohl, E., Kramer, N., Ruiz-Villanueva, V., Scott, D., Comiti, F., Gurnell, A., Piégay, H., Lininger, K., Jaeger, K., Davis, W., Fausch, K., 2019: The natural wood regime in rivers. Bioscience 69, 259–273.

MacVicar, B., Piegay, H., Henderson, A., Comiti, F., Oberlin, C., & Pecorari, E. 2009: Quantifying the temporal dynamics of wood in large rivers: fieldtrials of wood surveying, dating, tracking, and monitoring techniques. Earth Surface Processes and Landforms, 34.

Ghaffarian, H., Piegay, H., Lopez, D., Riviere, N., MacVicar, B., Antonio, A., & Mignot, E. 2020: Video-monitoring of wood discharge: first inter-basin comparison and recommendations to install video cameras. Earth Surface Processes and Landforms, 45(10): 2219–2234.

13.2
Gravity modelling of overdeepenings fill in the Bern area

D. Bandou[1], F. Schlunegger[1], E. Kissling[2], U. Marti[3], M. Schwenk[1], P. Schläfli[1,4], G. A. Douillet[1], D. Mair[1]

[1]*Institute of Geological Sciences, University of Bern*
[2]*Department of Earth Sciences, ETH Zürich*
[3]*Landesgeologie Swisstopo, Bern*
[4]*Institute of Plant Sciences, University of Bern*

The geometry of glacial overdeepenings on the Swiss Plateau close to Bern was inferred through a combination of gravity data with a 3D modelling software, named Gravi3D (Bandou et al., in prep). To achieve these goals, we conducted a gravity survey across the Gürbe and Aare valleys near Bern which also included the Belpberg mountain ridge in-between these valleys. This strategy also allowed us to obtain the density of the bedrock independently which was required for the modelling. This survey yielded residual anomalies of -2.9 mGal and -4.1 mGal in the Gürbe and Aare valleys, respectively, where the occurrence of overdeepenings has been disclosed through drillings (Reber & Schlunegger, 2016).
Modelling shows that these overdeepenings have depths between 160 m and 235 m and that the density of the overdeepening fill is 2'000 kg/m3.

This contrasts to the density of 2'500 kg/m3 of the Molasse bedrock which we determined using Nettleton's method across the Belpberg (Nettleton, 1939). The models also show that the overdeepenings can be characterized by U-shaped cross-sectional geometries composed of a wider top segment and a narrower shape towards the base. In addition, the lateral flanks are steep, with dip angles up to 80°.

Stratigraphic and sedimentological data (Zwahlen et al.,2021), extracted from drillings, disclose that the overdeepenings were formed and then filled during at least two major glacial periods. These are the LGM during MIS 2, and possibly a glacial cycle around MIS 6 or before.

The U-shape geometries, together with the over steepened flanks suggest that glacial erosion was the main process for the carving of the troughs. Interestingly, the combination of the geometries with stratigraphic data suggests that the MIS 6 (or older) glaciers deeply carved the bedrock, whereas the LGM ice sheet only widened the existing valleys but did not further deepen the trough. We explain these differences by the ice thicknesses where a thick MIS 6 glacier had a greater potential for eroding the bedrock compared to a thinner LGM glacier. Gravity data in combination with forward modelling discloses details of how a landscape evolved during the Quaternary.

REFERENCES

Bandou, D., Kissling, E., Schlunegger, F. 2021: Gravi3D – an openly accessible software for the modelling of the gravity effect of geological bodies. BORIS (in prep.).

Nettleton, L.L. 1939: Determination of density for the reduction of gravimeter observations. Geophyscics, 4, 176-183.

Reber, R. & Schlunegger, F. 2016: Unravelling the moisture sources of the Alpineglaciers using tunnel valleys as constraints. Terra Nova, 28, 202-211.

Zwahlen, P., Tinner, W. & Vescovi, E. 2021: Ein neues EEM-zeitliches Umweltarchiv am Spiezberg (Schweizer Alpen) im Kontext der mittel- und spätplesitozänen Landschaftsentwicklung. Mitt. Naturf. Ges. Bern, 78, 92-121.

13.3
Using stable isotopes to fingerprint the origin of instream wood at the river basin scale

Javier del Hoyo[1*], Torsten Vennemann[1], Marceline Vauridel[1], Virginia Ruiz-Villanueva[1]

[1] Institute of Earth Surface Dynamics, University of Lausanne, Quartier Mouline, 1015 Lausanne. *Javier.delhoyo@unil.ch

Fluvial geomorphology has classically been based on the study of the interactions of two elements: water flow and sediments. In the last decades, other key constituents, such as the riparian vegetation and the instream large wood (LW), have been included to better understand geomorphological processes. LW refers to pieces of wood larger than one meter long and ten centimetres in diameter, which influence fluvial and sediment dynamics and have the capacity to alter the river geomorphology (Keller & Swanson, 1979).

In addition to its geomorphological and ecological effects, large amounts of LW may also pose a risk during flood events. Flow alteration caused by the presence of woody material in rivers and transportation of this material during a flood event, may result in impacts on infrastructures (i.e., bridges) and population, making proper management of LW essential (De Cicco et al., 2018).

Knowing the origin and sources of wood is crucial to better understand wood dynamics at the catchment scale, to manage forest stands and thus to control the inputs of wood into the rivers. This project aims to develop a methodology to decipher the provenance of LW in large catchments (e.g., >1000 km^2). This will be carried out by using tracers in wood and applying fingerprinting techniques, to identify LW sources from tributaries and along the river continuum, similarly to methods done within the field of sedimentology (e.g., Collins et al., 2017).

The first tracers tested so far were the stable isotope ratios of the wood cellulose that are known to be sourced from the water molecule Stable isotopes of hydrogen (D/H) and oxygen ($^{18}O/^{16}O$) have been used as hydrological tracers for decades, but never applied to study instream wood sources before. The isotopic composition is related to the fractionation during evaporation-precipitation processes and reflect local conditions and thus spatial variations (longitudinal, latitudinal and altitudinal) of the water´s origin. The water taken up by a tree contains this isotopic information about its provenance and the information is stored in the growth rings cellulose . Thus, we hypothesize that the isotopic composition of LW pieces whose source is unknown can be used to infer their origin (Figure 1).

Our study area is a reach of the Rhone River between Lake Geneva, close to the city of Geneva, and the Genissiat dam (France), 50 km downstream from the lake, where all incoming woody material is retained. This reach has two main tributaries, the Arve and the Valserine (coming from two different mountain systems, the Jura and the Alps), which are the main suppliers of wood. The objective of the study is to infer the origin of the LW that arrives to the dam by differentiating between these two tributaries and along the rivers.

Preliminary results showed significant differences in the isotopic composition (δD and $\delta^{18}O$ values) between the tree samples from the two tributaries. These differences are higher when the most recent tree rings are analysed.

Additional tracers, such as other isotopes or major elements reflecting the contrasting geology and land use within the river basin will also be tested, and multivariate analyses (e.g., mixed models) will be applied to better capture the variability, reduce uncertainties and better decipher the origing of LW.

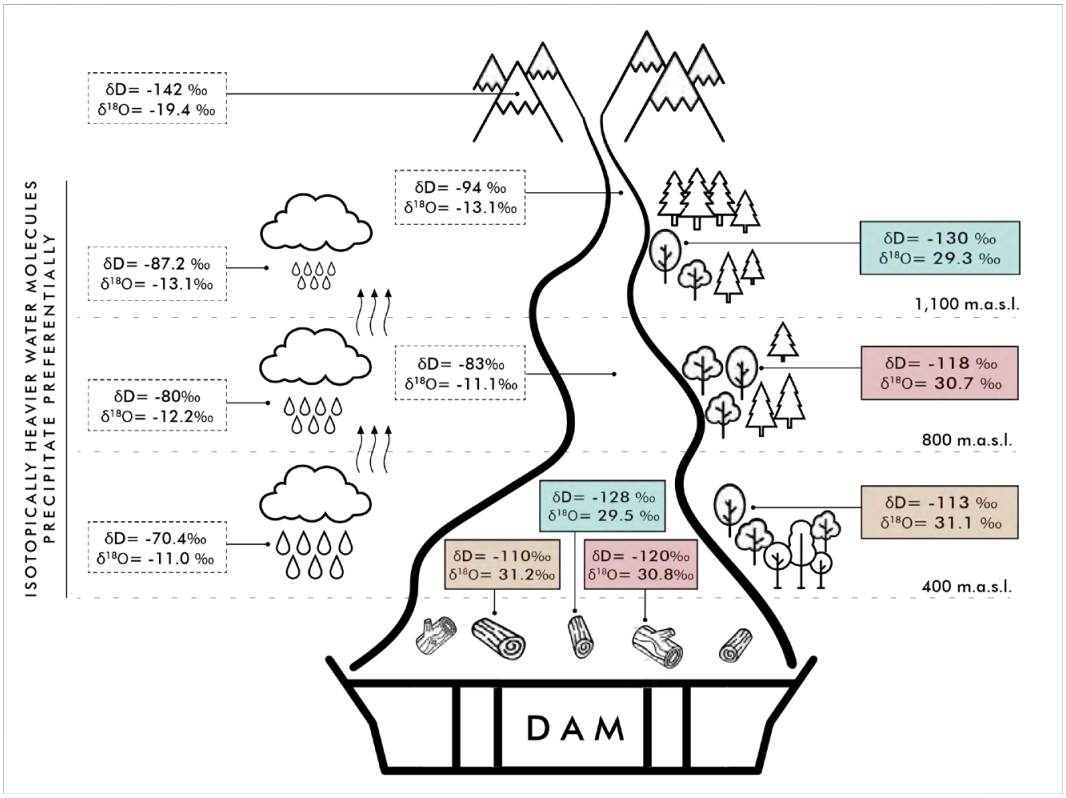

Figure 1. Conceptual diagram showing the method devoloped to infer the origin of instream large wood arriving at Genissiat dam, using hydrogen and oxygen stable isotope compositions of wood cellulose. δD reffers to the standarized ratio $^{2}H/^{1}H$ (deuterium/hydrogen) and $\delta^{18}O$ to the standarized ratio $^{18}O/^{16}O$.

ACKNOWLEDGEMENTS

This work is supported by the SNSF Eccellenza project PCEFP2-186963 and the University of Lausanne.

REFERENCES

Collins, A. L., Pulley, S., Foster, I. D. L., Gellis, A., Porto, P. & Horowitz, A. J. (2017). Sediment source fingerprinting as an aid to catchment management: a review of the current state of knowledge and a methodological decision-tree for end-users. *Journal of Environmental Management* 194:86–108.

Crouzet, E., Hubert, P., Olive, P., Siwertz, E. & Marce, A. (1970) Le tritium dans les mesures d'hydrologie de surface. Determination experimentale du coefficient de ruissellement. Journal of Hydrology, Vol 11, Issue 3, p. 217-229.

De Cicco, P. N., Paris, E., Ruiz-Villanueva, V., Solari, L., & Stoffel, M. (2018). In-channel wood-related hazards at bridges: A review. River Research and Applications, 34(7), 617–628.

Keller E. A. & Swanson F.J. (1979). Effects of large organic material on channel form and fluvial processes. Earth Surf. Process. Landforms 4: 361–380.

13.4
Water origin and quality of rock glacier springs. Case studies in the Swiss Alps.

Chantal Del Siro[1], Christophe Lambiel[1], Cristian Scapozza[2], Marie-Elodie Perga[1]

[1] Institut des dynamiques de la surface terrestre, Université de Lausanne, Quartier UNIL-Mouline, CH-1015 Lausanne (chantal.delsiro@unil.ch)
[2] Istituto scienze della Terra, Scuola universitaria professionale della Svizzera italiana (SUPSI), Via Flora Ruchat-Roncati 15, CH-6850 Mendrisio

While the knowledge on the dynamics and internal structure of rock glaciers is well developed, a lack of understanding of their hydrological functioning is observed in the scientific literature. In particular, the origin and the quality of the water that emerges from the rock glacier snouts are not well known, together with its contribution to aquatic systems. This study aims therefore to explore the contribution of ground ice melting in the water supply of rock glacier springs and its impact on the hydrochemistry of Alpine water systems. Isotope analyses were combined with physico-chemical analyses of six rock glacier outflows in the Swiss Alps, in order to investigate the origin and the quality of the water during the warm season. The chemical composition (SO_4^{2-}, Ca^{2+}, Mg^{2+}, NO_3^-) was found to be significantly different between rock glacier springs and streams not fed by rock glaciers. Water from the springs of active rock glaciers and ice-patches was characterised by an increase in electrical conductivity and in ionic (SO_4^{2-}, Ca^{2+}, Mg^{2+}) and isotopic content during the warm season. This seasonal evolution of the physico-chemical and isotopical composition of the water could indicate the progressive ground ice melting. It is hypothesized that the cryosphere stored atmospheric pollutants and other chemical elements during a colder period in the recent past (1960-1980) and that the current melting of rock glacier ice allows the release of these chemical compounds into the Alpine water systems.

13.5
Semi-automated geomorphological mapping: a first attempt in the Swiss Alpine environment

Elisa Giaccone[1], Fabio Oriani[1], Marj Tonini[1*], Christophe Lambiel[1], Grégoire Mariéthoz[1]

[1] *Institute of Earth Surface Dynamics, University of Lausanne, Lausanne, Switzerland (* marj.tonini@unil.ch)*

Geomorphological maps are traditionally elaborated by manually digitalization, based on field observations, topographic data, orthoimagery or remote sensing imagery. This approach is time-consuming, particularly for large areas with limited accessibility, and thus motivates the recent development of different supervised and unsupervised numerical approaches for the automated mapping of key landforms. Among them, the recent implementation of advanced mapping techniques based on geostatistics and machine learning exhibit improved classification performance, also thank to the increasing availability of high-resolution terrestrial images.

To demonstrate the potential of the latest-generation supervised classification techniques on geomorphological mapping, in the present study we compare two data-driven algorithms: Direct Sampling and Random Forest. The main objective is to perform a semi-automated geomorphological mapping (SAGM) in an alpine environment. The results have been assessed against an existing geomorphological map elaborated on the field and considered as the ground truth.

The study area corresponds to a rectangular domain of 70 km^2 in the Arolla valley, located in the southwest Swiss Alps. The dataset is composed of 13 variables: the geomorphological classes (8 classes were finally retained), representing the target variable, and 12 predictor variables, including topographical (slope, sine aspect, cosin aspect, normal curvature, plan curvature, profile curvature, solar radiation, flow accumulation, roughness) and remote-sensing indicators (RGB bands).

Direct Sampling (DS) is part of the multiple-point geostatistics family of techniques. The algorithm generates a random variable on a simulation grid (SG), representing the study zone, by resampling the training image (TI) under pattern-matching constraints and calculating the distance D(d→(X),d→(y))(i.e., the measure of dissimilarity) between two data events. Random Forest (RF) is an ensemble-learning algorithm based on decision trees and capable of learning from and making predictions on data, by modelling the hidden relationships between a set of input and output variables. RF was trained on the TI and results predicted on the SG. This selection of the training and the testing dataset (i.e., corresponding to the TI and SG respectively) allowed comparing RF and DS results in identical conditions. To this end, the predictions made on the SG and resulting from the two implemented models were compared with the original geomorphological map through a confusion matrix. This allowed evaluating the performance for each class and computing the overall accuracy and Kappa value.

As a result, DS and RF show similar performances. The overall accuracy has only one point percentage of difference (~0.55), and about three for the Kappa value, with values in the range of what is considered as a moderate agreement (~0.45). Both methods are deemed appropriate for SAGM, albeit with different trade-offs in terms of spatial smoothness and computational performance. The map elaborated using RF presents a noisier spatial distribution of classes, but it gives more insights on the importance of the predictor variables and it is more efficient in terms of computation time compared to DS. Some geomorphological classes, such as the Lateglacial deposits, glaciers and rock outcrop areas, resulted in high detection scores, highlighting the suitability of the employed methods in alpine environment. However, other classes such as alluvial fans and alluvial plains were weakly detected, indicating that not all landforms can be appropriately classified with the proposed strategies and algorithm setup, especially for classes that are underrepresented in the TI.

The present study identified a potential to use data-driven algorithms for SAGM at a regional scale in alpine environment. Nevertheless, the methodology employed in the current analysis can be improved upon and future research can be devoted to the optimal choice of the input geomorphological dataset and predictor variables.

REFERENCES

Giaccone, E., Oriani, F., Tonini, M., Lambiel C., Mariéthoz G., 2021: Using data-driven algorithms for semi-automated geomorphological mapping, Stoch Environ Res Risk Assess. https://doi.org/10.1007/s00477-021-02062-5

13.6
Mapping climate-change related processes affecting mountaineering itineraries. Application to the Valais Alps (Switzerland)

Jacques Mourey[1], Ludovic Ravanel[1,2], Christophe Lambiel[1]

[1] Interdisciplinary Centre for Mountain Research, University of Lausanne, Ch. de l›Institut 18, CH-1967 Bramois, Switzerland
[2] EDYTEM, Savoie Mont-Blanc University, CNRS, 73000 Chambéry, France

Climate change leads to deep changes on high Alpine environments, especially because of glacier shrinking and permafrost degradation. Associated glaciological and geomorphological processes have significant consequences on recreational mountain activities.

Although a growing number of studies has recently documented the effects of climate change on mountaineering itineraries (Ritter *et al.* 2011; Temme, 2015; Purdie and Kerr, 2018; Mourey *et al.* 2019), they only list the processes affecting them and do not document their characteristics or location. It is therefore impossible to produce maps of the processes affecting the itineraries even though this would be a very useful document, particularly to disseminate knowledge to mountaineers and to promote adaptive behaviours. In addition, they use different methodologies making the comparison and compilation of results difficult. Therefore, the main objective of the present study is to develop a specific legend to map the processes related to climate change that affect high mountain areas and modify climbing parameters. Such a legend should (i) ease data collection, (ii) make the data analysis simpler, (iii) favor the knowledge transfer to the mountaineer's community, and (iv) participate in improving knowledge on processes related to climate change in high mountains. More generally, this legend would provide a common methodological basis, destined to be completed and to be relevant out of the European Alps. It would also enable the comparability and compilation of results from different research.

The method used to map the processes is divided in 4 stages:
1) We first built a legend on the basis of the 25 processes previously identified in the Mont Blanc massif. 21 symbols were defined, following the UNIL geomorphic legend and using the same colour code.
2) Then, Alpine guides and refuge keepers were asked during a first set of semi-structured interviews to draw on the most recent topographic map available and with the help of the legend the long-term modifications of the itineraries (since the 1980s) they were able to identify.
3) The changes mapped during the interviews were then mapped in QGIS, completed by a diachronic analysis of aerial images.
4) Finally, an evaluation of the map was carried out through a second set of 5 interviews.

In order to evaluate the applicability and interest of the legend, we present a first application in the Valais Alps (Switzerland), allowing to assess the modification of mountaineering itineraries for this Alpine region.

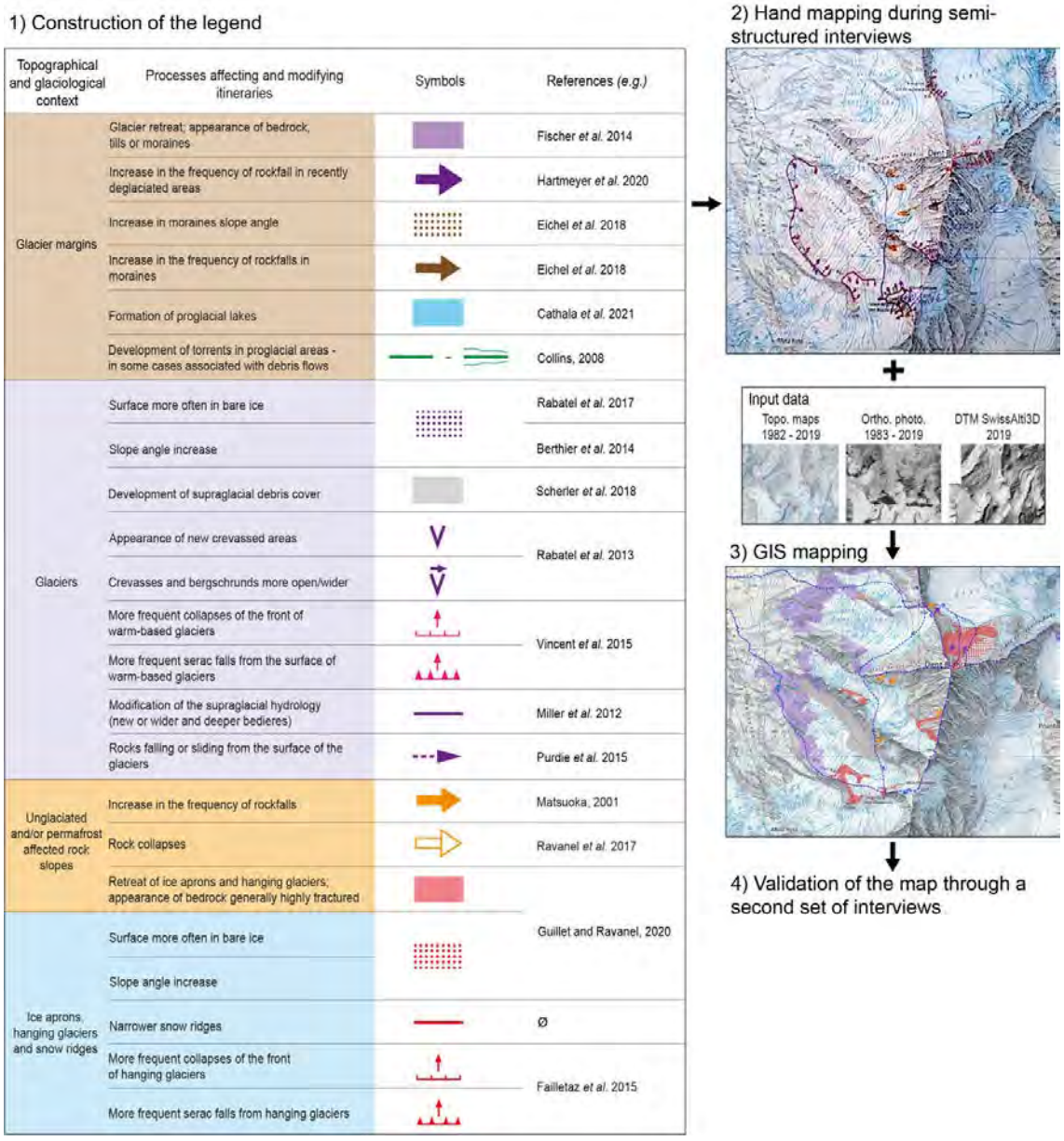

Figure 1. The 4 stages of the mapping work of climate related processes affecting mountaineering itineraries.

REFERENCES

Mourey, J., Marcuzzi, M., Ravanel, L., Pallandre, F. 2019: Effects of climate change on high Alpine environments: evolution of mountaineering routes in the Mont Blanc massif (Western Alps) over half a century. Arctic, Antarctic and Alpine Research 51(1), 176-189.

Purdie, H. and Kerr, T. 2018: Aoraki Mont Cook : Environmental change on an iconic mountaineering route. Mountain Research and Development 38(4), 364-379.

Ritter, F., Fiebig, M., Muhar, A. 2011: Impacts of Global Warming on Mountaineering: A Classification of Phenomena Affecting the Alpine Trail Network. Mountain Research and Development 32, 4–15.

Temme, A.J.A.M. 2015: Using Climber's Guidebooks to Assess Rock Fall Patterns Over Large Spatial and Decadal Temporal Scales: An Example from the Swiss Alps. Geografiska Annaler: Series A, Physical Geography 97(4), 793-807.

13.7
Rainfall heterogeneity accelerates hydro-morphological processes

Nadav Peleg[1], Chris Skinner[2], Jorge Alberto Ramirez[3], Simone Fatichi[4], Peter Molnar[5]

[1] *Institute of Earth Surface Dynamics, University of Lausanne, CH-1015 Lausanne (nadav.peleg@unil.ch)*
[2] *Energy and Environment Institute, University of Hull, UK-HU6 7RX Hull*
[3] *Geography Department, Université du Québec à Montréal, CA-H3C 3P8 Montréal*
[4] *Department of Civil and Environmental Engineering, National University of Singapore, SG-117576 Singapore*
[5] *Institute of Environmental Engineering, ETH Zurich, CH-8093 Zurich*

Hydro-morphological response of a catchment is highly dependent on rainfall properties, including rainfall intensity, storm duration and frequency, and the timing of those events. Additionally, rainfall spatial variability is a major determinant of streamflow, erosion, and sediment transport and is explored largely in the context of heavy rainfall triggering floods and rapid morphological changes on hillslopes and in channels. To explore the potential effects of climate change on hydro-morphological responses, we first examined how the spatial structure of rainfall is changing as a result of changes in air temperature (Peleg et al., 2018). Then, we explored the sensitivity of the hydro-morphological response to an extreme rainfall event, focusing on the 2005 flood in the K. Emme (Peleg et al., 2020). Our last study examined how changes in rainfall patterns affect landscape evolution at the catchment scale over hundreds of years (Peleg et al., 2021). Multiple realizations of hourly rainfall fields, each with a different spatial distribution but identical in all other respects, were simulated using a weather generator. We assessed the impact of storm heterogeneity on catchment morphology using a landscape evolution model (CAESAR-Lisflood). We demonstrate the importance of including the rainfall spatial structure in geomorphological impact studies as it is often more important than simply knowing the magnitude of the extreme rainfall event. We also found that erosion and deposition rates increased and net erosion and deposition areas changed (increased and decreased, respectively) when the rain became less uniform in space. As a result of increased rainfall heterogeneity, new gullies were found to be longer, deeper, and more branched. Even when rainfall volumes and temporal structures are identical, the results suggest that heterogeneity in rainfall spatial patterns accelerates landscape development. It appears that the spatial structure of rainfall may play a greater role than previously thought in shaping catchment morphology.

REFERENCES

Peleg, N., Marra, F., Fatichi, S., Molnar, P., Morin, E., Sharma, A. & Burlando P. 2018: Intensification of Convective Rain Cells at Warmer Temperatures Observed from High-Resolution Weather Radar Data, Journal of Hydrometeorology, 19, 715-726.

Peleg, N., Skinner, C., Fatichi, S. & Molnar, P. 2020: Temperature effects on the spatial structure of heavy rainfall modify catchment hydro-morphological response, Earth Surface Dynamics, 8, 17-36.

Peleg, N., Skinner, C., Ramirez, J.A. & Molnar, P. 2021: Rainfall spatial-heterogeneity accelerates landscape evolution processes, Geomorphology, 390, 107863.

13.8
Geotechnical investigations and slope stability analysis in Lake Lucerne

Anastasiia Shynkarenko[1], Katrina Kremer[1,2], Sylvia Stegmann[3], Paolo Bergamo[1], Agostiny Marrios Lontsi[1], Alexander Roesner[3], Steffen Hammerschmidt[3], Achim Kopf[3], Donat Fäh[1]

[1] Swiss Seismological Service (SED), ETH Zürich, Sonneggstrasse 5, CH-8092 Zürich (a.shynkarenko@sed.ethz.ch)
[2] Geological Institute & Oeschger Centre for Climate Change Research, University of Bern, Baltzerstr. 1+3, CH-3012 Bern
[3] MARUM - Center for Marine Environmental Sciences, University of Bremen, Leobener Strasse 8, DE-28359 Bremen

Sublacustrine mass movements and associated lake tsunamis represent a natural hazard that needs to be assessed, especially in the context of the growing, vulnerable population at the lake shores and potential damage to infrastructure. For proper hazard assessment, a comprehensive geotechnical study of the sediment properties and the consecutive slope stability analysis are required.

Lake Lucerne in Central Switzerland has experienced tsunamis in the past. In 1601, a lake tsunami was induced by subaquatic slope failures and subaerial rockfall from Bürgenstock during the Mw 5.9 Unterwalden earthquake, and in 1687 - by a spontaneous failure of the Muota delta (Hilbe and Anselmetti, 2014). The tsunami waves locally reached heights of about 5 m. Lake Lucerne, therefore, can serve as a "field laboratory" for a comprehensive geotechnical characterization of the lake sediments and an assessment of the stability of submerged slopes. The presented geotechnical study is a part of the ongoing research that includes also seismological site characterization in Lake Lucerne (e.g. Shynkarenko et al., 2021; Lontsi et al., 2021).

To define the most failure-prone areas, we interpreted available reflection seismic data and analyzed the bathymetric map of the lake floor. Then, we performed 152 in-situ Cone Penetration Tests with pore pressure measurements (CPTu) and retrieved 49 sediment cores at the selected locations in the lake for analysis in the laboratory (Figure 1). These experiments provided us with the undrained shear strength profiles and main geotechnical index properties of the lake sediment (e.g. density, Atterberg limits, grain size distribution). The collected dataset allowed us to derive also the generalized models of the depth-dependent undrained shear strength of the sediment which can be transferred to other lakes with similar sediments. Finally, we carried out a static limit-equilibrium slope stability analysis at the locations tested with CPTu. Some of these locations are metastable to potentially unstable and require a more detailed investigation. The areas with a steeper slope angle and thicker, gas-bearing, unconsolidated sediment drape usually show lower static stability.

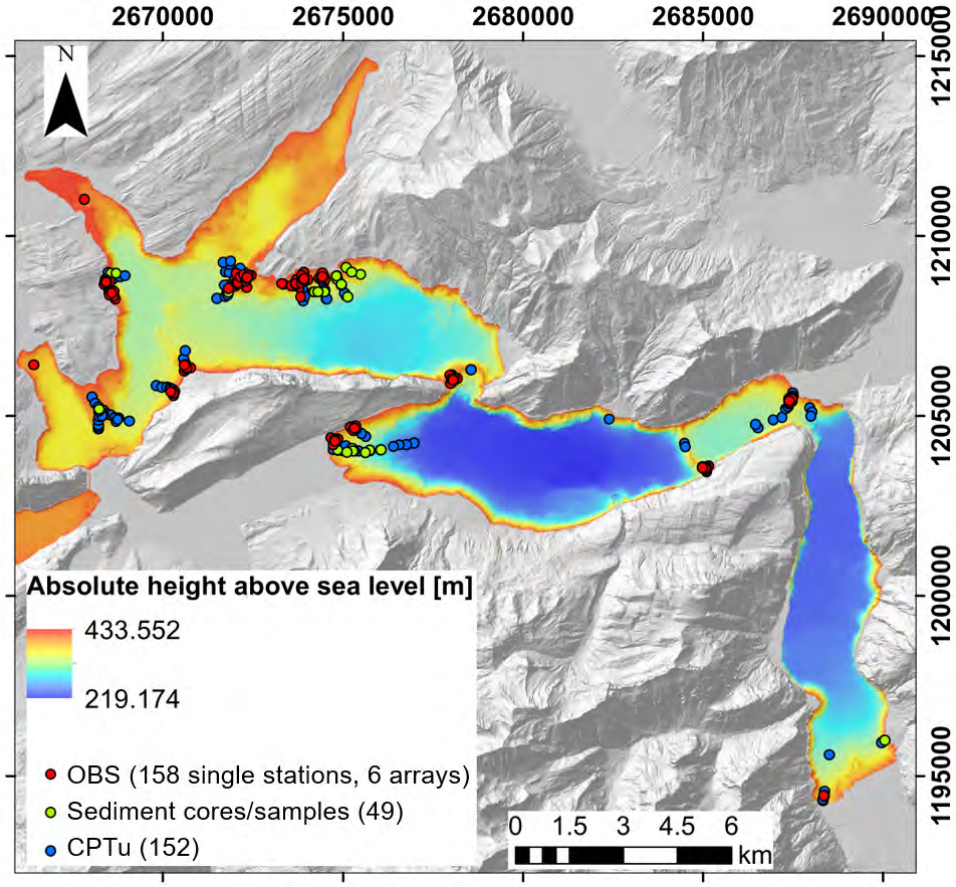

Figure 1. Measurement sites in Lake Lucerne, including seismic measurements with Ocean Bottom Seismometers (OBS), in-situ CPTu measurements and sediment sampling for geotechnical laboratory analysis.

REFERENCES

Hilbe, M., & Anselmetti, F.S. 2014: Signatures of slope failures and river-delta collapses in a perialpine lake (Lake Lucerne, Switzerland), Sedimentology, 61(7), 1883-1907, https://doi.org/10.1111/sed.12120.

Lontsi, A.M., Shynkarenko, A., Kremer, K., Hobiger, M., Bergamo, P., Fabbri, S.C., Anselmetti, F.S., & Fäh, D. 2021: Workflow for robust Scholte and Love waves phase-velocity estimation from small aperture Ocean Bottom Seismometer arrays in Lake Lucerne: deployment, location, orientation, and clock error correction, Pure and Applied Geophysics (submitted).

Shynkarenko, A., Lontsi, A.M., Kremer, K., Bergamo, P., Hobiger, M., Hallo, M., & Fäh, D. 2021: Investigating the subsurface in a shallow water environment using array and single-station ambient vibration techniques. Geophysical Journal International, doi: https://doi.org/10.1093/gji/ggab314.

13.9
The surface conditions of dust emission from the sandy croplands in the Free State, South Africa

Heleen C. Vos[1], Wolfgang Fister[1], Nikolaus J. Kuhn[1]

[1] *Physical Geography and Environmental Change, Department of Environmental Sciences, University of Basel, Klingelbergstrasse 27, CH-4056 Basel (heleen.vos@unibas.ch)*

The emission, transport, and deposition of dust particles affect human health, climate, and the global dust flux, and can lead to the degradation of soil. The emission of dust can come from natural sources, but a significant amount of dust is created by human impact. One of such sources is the Free State province in South Africa, where the agricultural fields are the biggest emitters of dust in the country. This dust has the potential to reach the densely populated Gauteng province, where the negative impact on human health can be significant. The amount of dust events differs greatly per year, and the geomorphological surface characteristics that influence this variation are not well understood. Understanding the processes and influencing factors that lie behind this phenomenon is crucial for protecting the soil against degradation and preventing negative impacts on human health.

This study uses a combination of small-scale experimental measurements and field monitoring to determine the surface conditions that control the emission of dust. These measurements were performed on a range of agricultural fields. Measurements from the Portable In-Situ Wind Erosion Laboratory (PI-SWERL) showed a higher dust emission from loose, disturbed surfaces compared to crusted surfaces. Hereby it is notable that the emission from loose surfaces is controlled by the texture of the soil, and the emission from crusted surfaces by the presence of saltating sand grains.

The percentage of vegetation and stubble cover and its influence on the erodibility of a surface was determined using UAV image analyses and combined with field monitoring data. The wind erosion was quantified using Big Spring Number Eight (BSNE) sediment samplers from which the horizontal sediment flux was calculated. These measurements showed a clear influence from vegetation, whereby the sediment flux was the highest on the highly disturbed, low vegetated peanut field and the lowest on the maize field, where a lot of stubble is left after harvest. The sediment flux on the fallow field was still significant, which indicates that abrasion is an active process on these fully crusted fields. This indicates that there is an interplay of geomorphological characteristics which needs to be considered when predicting or minimizing dust emission from these surfaces.

P 13.1
Role of the last deglaciation on the timing of collapsing of large rock slope failures in the Southern Swiss Alps

Alessandro De Pedrini[1,2], Daphné Giacomazzi[1], Cristian Scapozza[1],Christian Ambrosi[1], Andrea Manconi[2]

[1] Institute of Earth Sciences, University of Applied Sciences and Arts of Southern Switzerland, Via Flora Ruchat-Roncati 15, CH-6850 Mendrisio (alessandro.depedrini@supsi.ch)
[2] Department of Earth Sciences, Swiss Federal Institute of Technology, Sonneggstrasse 5, CH-8092 Zürich, Switzerland

The occurrence of large rock slope failures in the Southern Swiss Alps shows high temporal variability, governed by a combination of local factors such as the valley shape, slope morphology, glacial history (thickness of the ice on the slope during the last glaciation and age of slope exposure during the deglaciation), and the geological and structural framework of each site.

In Canton Ticino several inherited large rock slope failures (prehistorical, historical, recent) and still active rock slope instabilities can be observed. In the territory between the five valleys north of Bellinzona (Riviera, Valle Leventina and Valle di Blenio in Canton Ticino, Val Calanca and Valle Mesolcina in Canton Graubünden), several of these phenomena are present, with failure dates ranging from 13.50 ka cal BP (some millennia after the deglaciation of the lower Leventina Valley, which occurred around 19.85–17.64 ka cal BP, during the Bølling/Allerød interstadial of the Lateglacial), to today, referring to phenomena that have not yet collapsed (Figure 1). The rock slope failures and instabilities in this territory show a similar geological and morpho-structural context, while a more significant variability can be found regarding the glacial history (age of deglaciation). We provide here an insight of the glacial retreat in the Southern Swiss Alps (Scapozza, et al., 2014; Scapozza, 2016; Bernoulli, et al., 2018; Kamleitner, et al., 2020), flanked by the failure dating of each rockslide already known in literature, and the new dating performed in summer 2021 with Schmidt hammer exposure-age dating (SHD, e.g. Goudie, 2006; Scapozza, 2013; Scapozza, et al., 2014) on the deposit of the undated rockslides.

Our observations suggest independence between the timing of deglaciation and the occurrence of the large rock slope failures, opening questions on which combination of local factors can lead to the rockslide development, evolution, and collapsing in the Southern Swiss Alps.

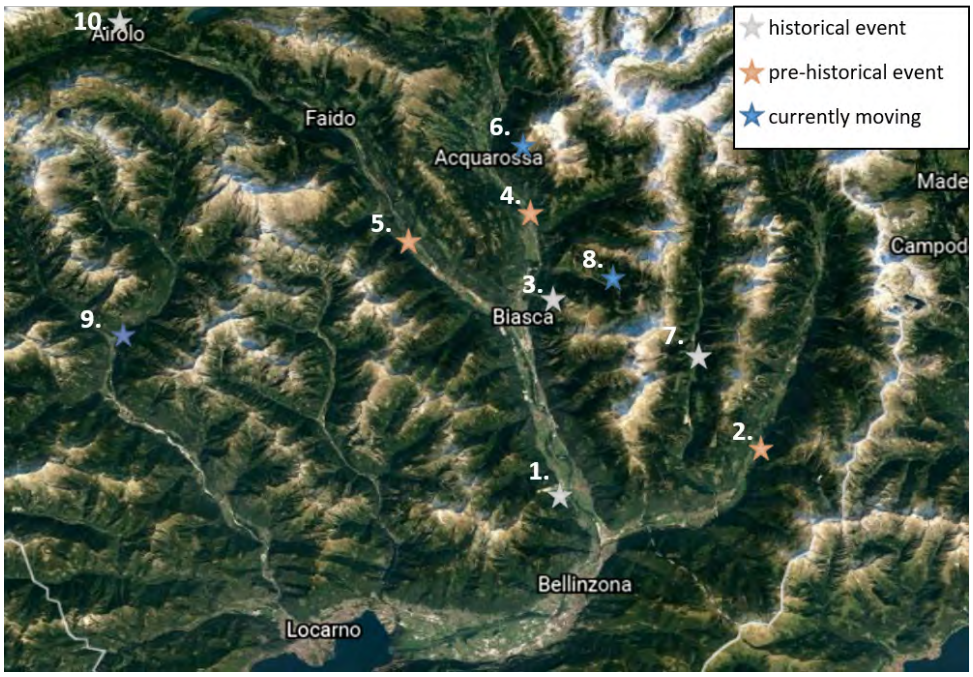

Figure 1. Location of the study cases: 1. Preonzo rockslide, 2. Norantola rockslide, 3. Monte Crenone rock avalanche, 4. Ludiano rockslide, 5. Chironico rock avalanche, 6. Simano instability, 7. Bodio-Cauco rockslide, 8. Fontana rockslide, 9. Peccia instability, 10. Sasso Rosso rockslide

REFERENCES

Bernoulli, D., Ambrosi, C., Scapozza, C., Stockar, R., Schenker, F. L., Gaggero, L., Antognini, M. and Bronzini, S. 2018: Foglio 1373 Mendrisio-Como, Explanatory notes 152, Geological Atlas of Switzerland 1:25'000, Federal Office of Topography swisstopo, Berna, Switzerland.

Goudie, A. S. 2006: The Schmidt Hammer in geomorphological research, Prog. Phys. Geog., 30, 703–718.

Kamleitner, S., Ivy-Ochs, S., Scapozza C., and Christl, M. 2020: Early Lateglacial ice decay in Swiss main Valleys. Glacier retreat into Rhine & Ticino Valley at the end of the last glaciation, Annual Report 2020, Ion Beam Physics, ETH Zurich, Switzerland.

Scapozza, C. 2013: Stratigraphie, morphodynamique, paléoenvironnements des terrains sédimentaires meubles à forte déclivité du domaine périglaciaire alpin, Université de Lausanne, Lausanne, Suisse, Géovisions, 40, 551 pp.

Scapozza, C., Lambiel, C., Bozzini, C., Mari, S., and Conedera, M. , 2014: Assessing the rock glacier kinematics on three different timescales: a case study from the southern Swiss Alps. Earth Surf. Proc. Land., 39, 2056–2069.

Scapozza, C. 2016: Evidence of paraglacial and paraperiglacial crisis in Alpine sediment transfer since the Last Glaciation (Ticino, Switzerland), Quaternaire, 27, 139–154.

P 13.2
Application of the Graph Theory to instream large wood supply and transfer to define the wood cascade in fluvial networks

Bryce Finch[1], Virginia Ruiz-Villanueva[1]

[1] *Institute of Earth Surface Dynamics, University of Lausanne, Quartier Mouline, CH-1015 Lausanne (bryce.finch@unil.ch)*

Large wood (LW) has become an increasingly studied constituent of fluvial systems as its ecological and physical benefits as well as its contributions to damages during flood events have been realized (Ruiz-Villanueva et al. 2016). Numerous approaches have been explored to identify contributing areas and conditions which permit wood transfer within fluvial networks and depositional areas (Mazzorana et al. 2009, Zischg et al. 2018). LW is known to be supplied through processes such as treefall (e.g., wind-thrown, snow loading), landslides, bank erosion, avalanches, and fluvial entrainment. These processes can occur concurrently or independently and vary spatially and temporally. For example, wood supply via avalanche recruitment becomes pertinent concurrently with snow loading during colder seasons of the year but is not relevant in absence of snow/ice. Analogous challenges exist in sediment dynamics, which have used the Graph Theory to materialize new insights regarding sediment supply (Heckmann & Schwanghart 2013). Therefore, we propose to explore wood supply and transfer through novel application of the Graph Theory.

A network of nodes representing wood sources are connected by edges representing pathways of wood exchange between nodes within the study of area of Vallon de Nant, Vaud, Switzerland. Nodes are classified according to the presence of wood and the likelihood to supply wood based on related geomorphic processes. As these conditions will change spatially, additional nodes are formed to seamlessly capture all sources of wood within a catchment. Directed edges connect nodes if there is an exchange or wood flux between nodes and are classified according to the type of exchange such as direct entry through treefall or entrainment during mass wasting events (see figure 1).

To properly account for seasonal variation, we propose to include separate scenarios based on the presence and absence of snow. For all scenarios, connections between wood sources and the network are materialized to identify which sources of wood are connected to the main fluvial network and which of those remain on hillslopes or within a separate, disconnected feature. Thus permitting, identification of primary and secondary contributors of LW based on multiple scenarios while maintaining information such as the quantity and species class of wood supplied.

The study basin, Vallon de Nant, envelops an unconfined, braided network at the upper-most section of the valley and progressively transitions into a slightly sinuous single thread channel to a confined, high-gradient reach. Coniferous trees appear to the be predominant species at lower elevations and nearest the river while broadleaved trees comprise the majority of trees found in higher elevations and the upper-most section of the valley. The valley's hillslopes have significantly different structure with the presence of cragged, jagged peaks producing large, conical depositional features and entrenched debris flow paths, on one side of the valley. Meanwhile, narrow, debris flow pathways are lightly scoured into bedrock along the opposite valley wall.

Currently, digital surface models (DSM) and digital terrain models (DTM) with 0.5m resolution have been used to produce the fluvial network and identify the heights of trees. Tree type and abundance have been realized with the addition of raster files available for all of Europe at 10m resolution. The Fluvial Corridor toolbox (Roux et al. 2013), has been used to delineate the extent of the riparian zone which serves as the main fluvial network. Simple algebraic equations have been used to determine the proximity of tree locations to the fluvial network which can then be related to the heights of the trees to determine whether a direct connection exists simulating treefall. Additional work needs to be done to develop the precise classification system for nodes and edges, to delineate the avalanches, landslides or debris flows, and areas prone to bank erosion during each defined scenario. The final work will accurately reflect wood availability, potential fluxes and levels of connectivity which may be useful for defining a local monitoring strategy.

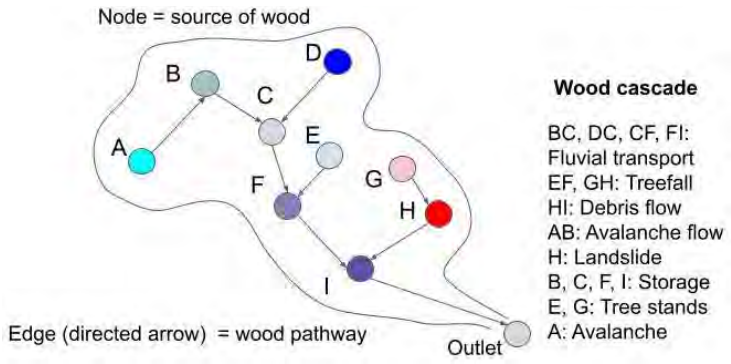

Figure 1. Conceptual model of the wood cascade.

"This work is supported by the SNSF Eccellenza project PCEFP2-186963 «Towards a new understanding of fluvial ecosystems: integrating wood regime across multiple scales « and the University of Lausanne."

REFERENCES

Heckmann, T. & Schwanghart, W. 2013: Geomorphic coupling and sediment connectivity in an alpine catchment – Exploring sediment cascades using graph theory. Geomorphology 182, 89-103.

Mazzorana, B., Zischg, A., Largiader, A. & Hubl, J. 2009: Hazard index maps for woody material recruitment and transport in alpine catchments. Natural Hazards and Earth System Sciences 9, 197-209.

Roux, C., Alber, A., & Piegay, H. 2013: Valley bottom guideline for the FluvialCorridor toolbox, a new ArcGIS toolbox package for exploring multiscale riverscape at a network scale. Sedalp (Sediment management in alpine basins) and CNRS (UMR5600).

Ruiz-Villanueva, V., Piegay, H., Gurnell, A.M., Marston, R.A. & Stoffel, M. 2016: Recent advancements quantifying the large wood dynamics in river basins: New methods and remaining challenges. Reviews of Geophysics 54, 611-652.

Zischg, A.P., Galatioto, N., Deplazes, S., Weingartner, R. & Mazzorana, B. 2018: Modelling spatiotemporal dynamics of large wood recruitment, transport, and deposition at the river reach scale during extreme events. Water 10, 1134.

P 13.3
The complexities assessing volcanic hazards along the Cameroon Volcanic Line using spatial distribution of monogenetic volcanoes

Christoph Schmidt[1], Christian Laag[2], Melody Whitehead[3], Gabor Kereszturi[3], Joern Profe[4]

[1] Institute of Earth Surface Dynamics, University of Lausanne, Géopolis, CH-1015 Lausanne (christoph.schmidt@unil.ch)
[2] Institut de Physique du Globe de Paris, Université de Paris, CNRS, F-75005 Paris
[3] Volcanic Risk Solutions, School of Agriculture and Environment, Massey University, Private Bag 11 222, NZ-Palmerston North
[4] Department of Geography, Geoinformatics and Remote Sensing, Justus-Liebig-University Giessen, Schlossgasse 7, DE-35390 Gießen

Volcanic eruptions represent hazards for local communities and infrastructure. Spatio-temporal patterns in the occurrence of these eruptions can provide valuable information on locations more likely to host future eruptions within monogenetic volcanic fields (MVFs). Monogenetic volcanoes (usually) erupt only once, and then volcanic activity moves to another location, making quantitative assessment of eruptive hazards challenging.

While the eruption history of many stratovolcanoes along the Cameroon Line (CL) is comparatively well studied, only fragmentary data exists on the distribution and timing of monogenetic volcanism (scoria, spatter and tuff cones, maars). Here, we present for the first time a catalogue of monogenetic vents for the CL. These were identified by their characteristic morphologies using field knowledge, Digital Elevation Models and high-resolution satellite imagery. More than ~1100 scoria cones and 50 maars were registered and divided into eight MFVs based on assessment of clustering and geological information.

Robust point-process based spatial analyses show a large range of areal densities from >0.2 km^{-2} to 0.02 km^{-2} from the southwest towards the northeast. This finding is in general agreement with previous observations, indicating closely spaced edifices typical for fissure-fed eruptions on the flanks of Bioko and Mt. Cameroon. High vent densities in these areas might be associated with generally younger and hence more visible structures. Spatial patterns were smoothed via kernel density estimates (KDE) with a set of bandwidth estimators, the results from which may provide an uncertainty range for a first-order hazard assessment of vent opening probability along the CL. Due to the scarce chronological data, and the complex structural controls across the region, it was not possible to estimate the number of vents formed during the same eruptive events, and similarly, the percentage of hidden (buried, eroded) vents could not be assessed with any acceptable statistical result. Finally, the impact of different approaches (convex hull, minimum area rectangle and ellipse, KDE isopaches) to define MVF boundaries on the spatial organization of vents was tested and the volume of scoria cones (approximated by their basal diameters) across the CVL contrasted to available data on their geochemical composition. This region presents a complex problem for volcanic hazard analysis that cannot be solved through basic statistical methods and thus, provides a potential testbed for novel, multi-disciplinary approaches.

14. Hydrology and Hydrogeology

Peter Molnar, Daniel Hunkeler, Christophe Lienert, Sandra Pool, Michael Sinreich, Massimiliano Zappa, Sanja Hosi

Swiss Hydrological Commission CHy,
Swiss Society for Hydrology and Limnology SGHL,
Swiss Hydrogeological Society SGH

TALKS:

14.1 Becker D., Epting J.: Thermal impact of urban subsurface structures on groundwater temperatures in the city of Basel

14.2 Brett-Adams A.C., Diamond L.W.: Permeability available for hydrothermal fluid flow in altered and fractured lavas in the oceanic crust, Semail ophiolite, Oman

14.3 Brunner M. et al.: Shedding light on the extreme precipitation-flood paradox in a warming climate using a hydro-SMILE

14.4 Collin R. et al.: Development of a Forecasting Tool for Groundwater Levels in Valais Using Artificial Intelligence

14.5 Jeannin P.-Y., Sinreich M.: Managed Aquifer Recharge (MAR) by karst groundwater on the Swiss plateau

14.6 Jola S. et al.: Hybrid Hydrological Modeling for Sub-seasonal Droughts Forecasts – A Combination of Traditional Models and Machine Learning Techniques for Streamflow and Lake Level Predictions For the Alpine Aare Basin

14.7 Kong X.-Z. et al.: Laser-induced fluorescence study of solute mixing in 3D-printed fractured porous media

14.8 Moeck C. et al.: Joint use of $^{3}H/^{3}He$ apparent age and on-site helium analysis to identify groundwater flow dynamics and transport of PCE

14.9 Müller T. et al.: Hydrogeomorphological Assessment of Future Water Availability for Ecosystem Development in Proglacial Catchments

14.10 Sonney R. et al.: Mapping piezometric fluctuations in the Rhone valley: results of over 40 year of monitoring

14.11 Walder S. et al.: Application of soil water potential threshold in Swiss landslide early warning systems

14.12 Wechsler T. et al.: Implementing lake regulations into a hydrological model to disentagle climatic and regulatory impacts

POSTERS:

P 14.1 Acciardo A. et al.: Initial investigations into microbial dynamics and biogeochemical cycling in the Bedretto Tunnel

P 14.2 Arnoux M. et al.: Geostatitical piezometric products in the Rhone valley: tools for groundwater management and protection

P 14.3 Collenteur R.A. et al.: Exploratory study on the application of time series models to simulate groundwater levels and estimate recharge in Switzerland

P 14.4 Fluixa-Sanmartin J. et al.: Impacts of climate change-influenced hydrology on dam failure risks

P 14.5 Moeck C.: CH-GNet – Swiss Groundwater Network

P 14.6 Moradi H. et al.: Mobilization of toxic elements in high-alpine streams of the Eastern Alps: monitoring strategy and first results

P 14.7 Shekhar A. et al.: Understanding sources of isotopic mismatch of tree water and soil water of a sub-alpine coniferous forest

P 14.8 Wiersma P. et al.: The Value of Synthetic High-resolution Daily Snow Cover Maps for Long-term Hydrological Modeling

P 14.9 Zhao C. et al.: Groundwater Drainage-Induced Rock Mass Deformation during the Gotthard Base Tunnel Excavation in the Swiss Alps: 3D Modelling and Comparison to Field Measurements

14.1
Thermal impact of urban subsurface structures on groundwater temperatures in the city of Basel

Dominic Becker[1], Jannis Epting[1]

[1] *Angewandte und Umweltgeologie, Departement Umweltwissenschaften, Universität Basel, Bernoullistrasse 32, CH-4056 Basel, Schweiz (dominic.becker@unibas.ch)*

In Basel (CH), the thermal impact of various subsurface structures on urban groundwater resources, including five underground parkings and a freeway tunnel, were investigated by monitoring systems. Data were analyzed together with meteorological and groundwater temperature data and results from heat-transport modelling.
Significantly elevated temperatures between 18.8 and 21.1 °C were recorded in the underground parkings, even in winter. Accordingly, underground parkings emit heat into the subsurface all year. In comparison, data recorded in the freeway tunnel indicate that in the winter months heat can also be absorbed from the subsurface.
In addition, the temperatures of underground parkings show a clear dependence on the type of use: with a higher number of daily entrances and exits, greater daily temperature increases were detected, with differences of up to 2 °C. This became particularly clear in the “lockdown” period during the COVID-19 pandemic between March and May 2020.

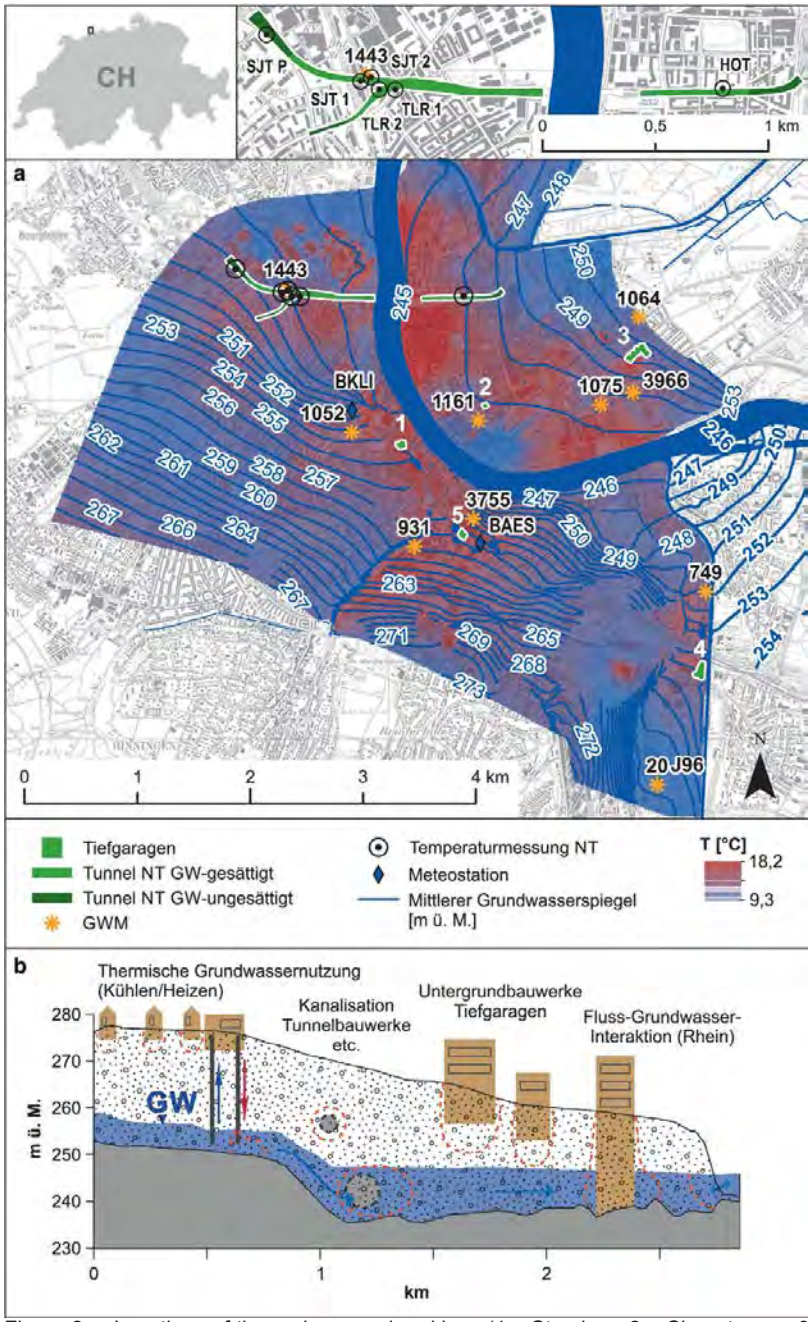

Figure 2. **a** Locations of the underground parkings (1 – Storchen; 2 – Clarastrasse; 3 – St. Claraspital; 4 – St. Jakob Park; 5 – Anfos), the

freeway tunnel Nordtangente, the selected groundwater observation wells and the meteorological stations BKLI and BAES in the study area. Mean simulated groundwater temperatures [°C] and the hydrogeological regime for the years 2010–2015 (according to Mueller et al. 2018) are also shown. **b** Characteristic hydrogeologic profile through the urban aquifer.

REFERENCES

Becker, D., & Epting J. 2021: Thermischer Einfluss urbaner Untergrundstrukturen auf die Grundwassertemperaturen im Kanton Basel-Stadt, Grundwasser - Zeitschrift der Fachsektion Hydrogeologie. https://doi.org/10.1007/s00767-021-00483-1

Epting, J., Scheidler S., Affolter A., Borer P., Müller M.H., Egli L., García-Gil A., Huggenberger P. 2017: The thermal impact of subsurface building structures on urban groundwater resources – A paradigmatic example. Science of The Total Environment 596-597, 87-96. Doi.10.1016/j.scitotenv.2017.03.296

Müller, M.H., Huggenberger P., Epting J. 2018: Combining monitoring and modelling tools as a basis for city-scale concepts for a sustainable thermal management of urban groundwater resources. Science of the Total Environment 627, 1121-1136. Doi.10.1016/j.scitotenv.2018.01.250

14.2
Permeability available for hydrothermal fluid flow in altered and fractured lavas in the oceanic crust, Semail ophiolite, Oman

Alannah C. Brett-Adams[1], Larryn W. Diamond[1]

[1] *Institute of Geological Sciences, University of Bern, Bern, Switzerland (alannah.brett@geo.unibe.ch)*

The distribution of permeability in the upper oceanic crust controls hydrothermal circulation and the induced water-rock interactions that feed seafloor vents and sulphide ore deposits. A prevailing view is that the lavas behave as a fractured aquifer in which permeability is dominated by extensional faults and fracture networks. However, little is known about the nature and hydraulic efficiency of fracture networks and the rock-matrix in the km-wide blocks of hydrothermally altered crust that lie between major faults and damage zones.

To bridge this gap this study characterises the distribution of permeability in fault-distal blocks during greenschist-facies hydrothermal alteration of the upper oceanic crust. We base this on rock-matrix porosity and permeability measurements, and on field mapping of hydrothermal veins in pervasively altered ridge-axis lavas in the Semail ophiolite, Oman. Rock-matrix permeability was upscaled from measurements of 25 mm plugs to yield outcrop-scale values of ~2.5×10^{-16} m^2. Fracture intensities in distal blocks are only ~0.005 m of fracture per m^2 of outcrop (Fig. 1a), compared to an order of magnitude higher in fault zones. We have peformed numerical hydraulic simulations of our measurements to calculate bulk permeability, including the simultaneous contributions of the porous and permeable rock matrix and the sparse fracture sets. Coupled fracture- and matrix flow using dfnWorks software (Hyman et al., 2015; Sweeney et al., 2019) yielded a bulk permeability of ~5×10^{-16} m^2 in crustal blocks distal from seafloor faults (Fig. 1b).

These models demonstrate that in distal blocks the rock matrix is as permeable as the sparse and unconnected fracture network. This result is consistent with the thoroughly pervasive, rather than fracture-controlled, nature of greenschist-facies hydrothermal alteration observed in the Semail lavas. Our observations and calculated bulk permeabilities provide an updated view of fluid flow through the upper oceanic crust, in which matrix-flow controls circulation through large blocks of lavas, enhanced by fault-damage zones at km-scale intervals. This new perspective explains how the layer of oceanic lavas is accessible for rock-matrix leaching of metals for seafloor sulphide deposits.

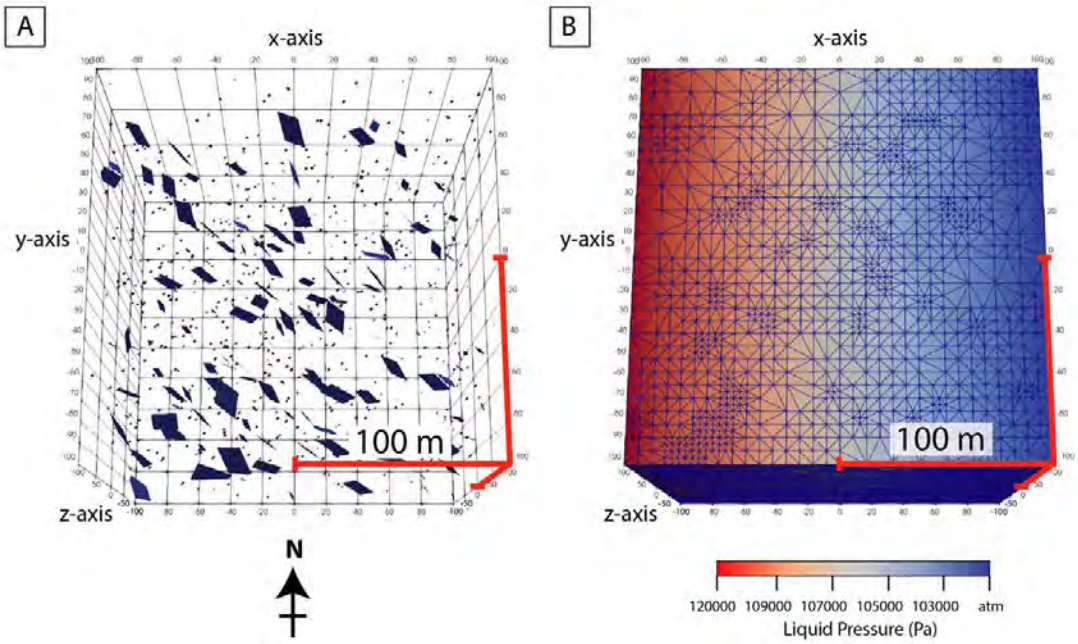

Figure 1. dfnWorks models of distal zone lavas. Diagrams are orientated top to the north, with depth (z axis) into the page. (A) DFN model; (B) Meshed block model. Liquid pressure gradient (colours) during flow from W to E, with meshed volumes shown as polygons. Largest mesh volume is 25 m diameter. Detail of meshing increases where fractures intersect block surfaces. Liquid pressure varies from the inflow at the western face to outflow at the eastern face by the equivalent of 1 m hydraulic head or 0.000981 MPa.

REFERENCES

Hyman, J.D., Karra, S., Makedonska, N., Gable, C.W., Painter, S.L., Viswanathan, H.S., 2015: dfnWorks: A discrete fracture network framework for modeling subsurface flow and transport. Comput. Geosci. 84, 10–19. https://doi.org/10.1016/j.cageo.2015.08.001.

Sweeney, M.R., Gable, C.W., Karra, S., Stauffer, P.H., Pawar, R.J., Hyman, J.D., 2019: Upscaled discrete fracture matrix model (UDFM): An octree-refined continuum representation of fractured porous media. Comput. Geosci. 24, 293–310. https://doi.org/10.1007/s10596-019-09921-9.

14.3
Reconciling the extreme precipitation-flood paradox in a warming climate

Manuela I. Brunner[1,5], Daniel L. Swain[1,3,4], Raul R. Wood[2], Florian Willkofer[2], James M. Done[1], Eric Gilleland[1], and Ralf Ludwig[2]

[1] *National Center for Atmospheric Research, Boulder CO, USA.*
[2] *Department of Geography, Ludwig-Maximilians University Munich, Munich, Germany*
[3] *Institute of the Environment and Sustainability, University of California, Los Angeles, CA, USA*
[4] *The Nature Conservancy of California, San Francisco, CA, USA*
[5] *Institute of Earth and Environmental Sciences, University of Freiburg, Freiburg, Germany*

There is clear evidence that precipitation extremes will increase in a warming climate. However, the hydrologic response to this increase in heavy precipitation is more uncertain - and there is little historical evidence for systematic increases in flood magnitude despite observed increases in precipitation extremes. These dual realities yield a paradox with considerable practical relevance: will the divergence between extreme precipitation increases and flood severity persist, or are land-surface processes at work? Here, we investigate how flood magnitudes in hydrological Bavaria change in response to warming using a single model initial condition large climate ensemble coupled to a hydrological model (hydro-SMILE). We find that there exists an extremeness threshold, i.e. a return interval threshold, above which precipitation increases clearly yield increased flood magnitudes, and below which flood magnitude is modulated by land surface processes. Our findings help reconcile climatological and hydrological perspectives on changing flood risk in a warming climate, and highlight the importance of large ensembles.

14.4
Development of a Forecasting Tool for Groundwater Levels in Valais Using Artificial Intelligence

Romane Collin[1], Corinna Frank[1], Pascal Ornstein[2], Javier Fluixa[2], Devis Tuia[3]

[1] Environmental Sciences and Engineering, EPFL Ecole Polytechnique Fédérale de Lausanne, Station 2, CH-1015 Lausanne (romane.collin@epfl.ch)
[2] CREALP Centre de recherche sur l'environnement alpin, Rue de l'Industrie 45, CH-1950 Sion
[3] Environmental Computational Science and Earth Observation Laboratory, EPFL Valais Ecole Polytechnique Fédérale de Lausanne, Rue de l'Industrie 17, CH-1951 Sion

The reliable monitoring of groundwater is vital for sustainable and safe water management in Switzerland. Groundwater in the Rhône's valley is of particular interest since its levels undergo rapid changes due to the Rhône river dynamics and the seasonal recharge from meltwater and rainfall. Early detection of groundwater level rises is thereby an important measure to anticipate flooding, as well as contamination by the rise of water bodies underneath polluted sites (Spreafico 2005). A key component for a robust monitoring is the forecasting of future groundwater levels to enable early protection measures.

Groundwater forecasting has been studied using empirical relationships between groundwater level time series and environmental predictor variables (Mackay 2015). Algorithms for spatialised prediction were proposed in Sharafati et al. (2020). This project aims to explore the potential of Machine Learning (ML) methods for predicting the groundwater level at a discrete set of locations, namely the measurement stations of the cantonal observation network of Valais. Two major steps were considered: first, an exploratory data analysis to identify drivers of groundwater levels and to quantify the reaction time of the water body to these elements. The above information was used to cluster the measurement stations according to their reaction to the drivers (Figure 1). Secondly, a Random Forest Regressor (Breiman, 2001) was trained with environmental predictors (e.g. air temperature, precipitation and discharge) to predict groundwater levels one, two and three weeks in the future.

Figure 2 presents two examples of predictions. The model is able to predict groundwater levels better than a baseline (the average level over the previous week) and reaches an overall R^2 score of 0.80 against 0.72 with the baseline. The Root Mean Squared Error of the predictions is 0.11 m, 0.16 m and 0.18 m for the one, two and three weeks forecast, respectively. The prediction accuracy is of variable quality among the measurement stations and among the clusters of stations identified in the exploratory data analysis. The model has shown the ability of forecasting at stations unseen during training with the same precision, but extrapolates badly on extreme events as major floods. Further, it is favourable to build a specified model for each behavioural cluster.

Current improvements are based on exploring the potential of additional features and on the reduction of the variability of prediction quality between the stations.

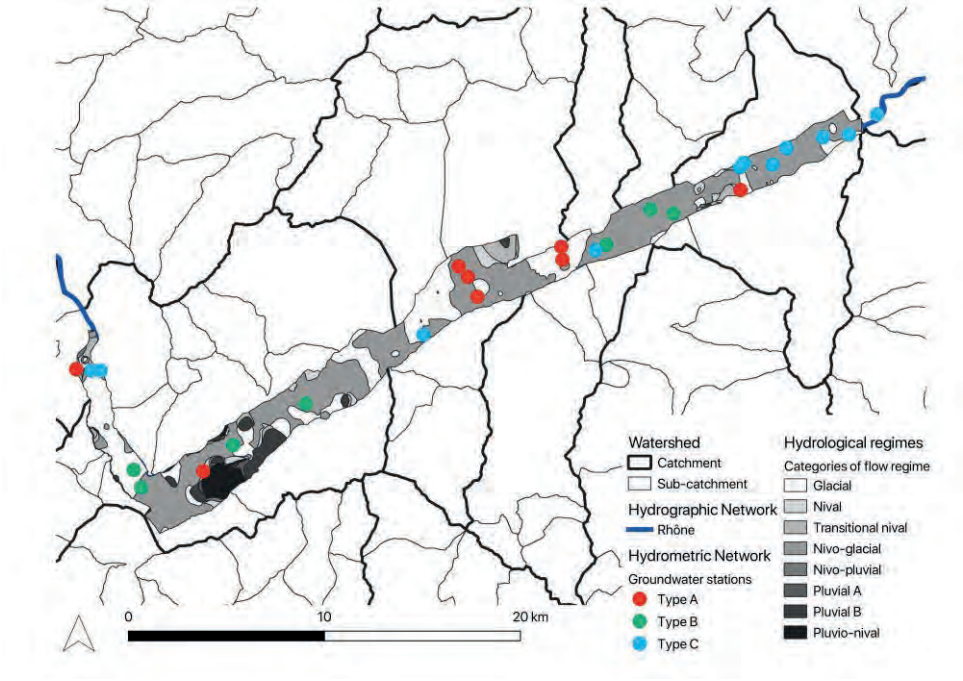

Figure 1. Studied hydrometric stations lying in the region of Valais Central clustered into three types according to their identified drivers.

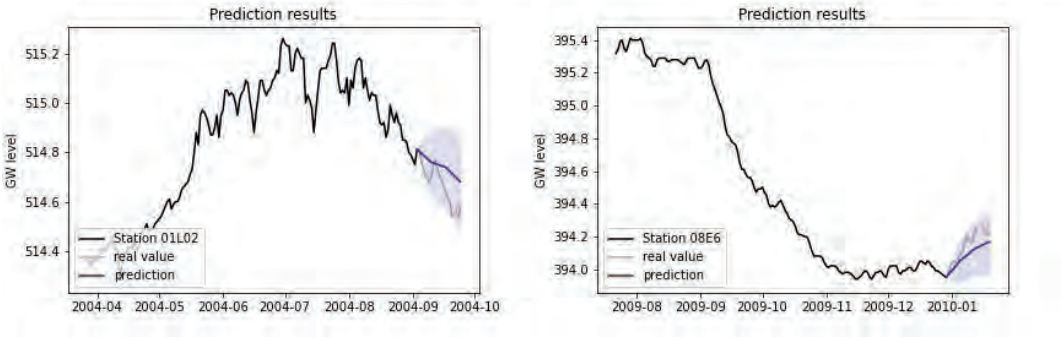

Figure 2. Examples of groundwater level predictions. The black line corresponds to the history used for the forecasting task, the blue lines are the predicted levels (the blue shading is the confidence interval). The grey lines are the actual onservations for comparison.

REFERENCES

Breiman L. 2001: Random Forests, Machine Learning, 45, 5-32.

Mackay, J. D., Jackson, C. R., Brookshaw, A., Scaife, A. A., Cook, J., & Ward, R. S. 2015: Seasonal forecasting of groundwater levels in principal aquifers of the United Kingdom, Journal of Hydrology, 530, 815–828.

Sharafati, A., Asadollah, S. B. H. S., & Neshat, A. 2020: A new artificial intelligence strategy for predicting the groundwater level over the Rafsanjan aquifer in Iran, Journal of Hydrology, 591, 125468.

Spreafico, M. & Weingartner, R. 2005: The Hydrology of Switzerland, Reports of the FOWG (Federal Office for Water and Geology), Water Series No. 7

14.5
Managed Aquifer Recharge (MAR) by karst groundwater on the Swiss plateau

Pierre-Yves Jeannin[1], Michael Sinreich[2]

[1] Swiss Institute for Speleology and Karst-Studies, SISKA (pierre-yves.jeannin@isska.ch)
[2] Swiss Federal Office for the Environment (FOEV)

The amount of persistent pollutants in groundwater is an increasing problem worldwide, especially where agriculture, industry and urban development are the most intensive. Therefore, in many regions the stress on groundwater resources is growing, with a significant number of wells showing contaminant concentrations close or beyond recommended/limit values. The problem may be strengthened in some areas by temporary groundwater shortage due climate change. Alternative resources have thus to be found and Managed Aquifer Recharge (MAR) could be an appropriate approach for solving problems in groundwater quantity and quality. In this context, karst aquifers may represent a supplemental resource or a storage body for water injection and recovery.

In Switzerland, the major part of drinking water is taken from unconsolidated porous aquifers in alluvial lowland settings, where anthropogenic pressure is focused. Besides, karst environment represents about 20% of the Swiss territory with more than 50% of the total groundwater potential resources. A large portion of karst is situated in the Jura Mountains, directly north-west of the Swiss lowland. Up to now, karst water was not extensively used given the frequently high bacterial and turbidity load, mainly related to recharge events. However, as karst regions are less exposed to agricultural land-use the level of persistent pollutants is relatively low in related groundwater.

Considering this situation, a project is being develop to assess the potential of using karst water at the foothill of the Jura Mountains as a source for MAR. This comprises the mixing with impacted groundwater in alluvial porous aquifers in order to improve their quality. On the other hand, deeper carbonate aquifers can serve themselves as storage reservoir. So far, MAR approaches were implemented in Switzerland only in highly populated regions (Basel, Zurich, Geneva), where surface water derived from local streams artificially recharges alluvial aquifers. The actual project on karst groundwater is therefore novel for Switzerland and may be pathbreaking for many other regions with karst-adjacent lowland aquifers.

For this project, a regional assessment of all water resources related to karst was carried out, including deep groundwater in carbonate rocks (down to a depth of 500 meters below ground). The well-established KARSYS approach, including the 3D modelling of carbonate aquifers, was systematically applied in order to characterize the aquifer structure, roughly quantify the respective resources, as well as identifying potential access-points for withdrawal and artificial recharge.

More than 1000 km^2 of land surface were modelled and evaluated. About 50 potential targets, which could potentially be used for MAR, were defined. The assessed water amount is larger than $3*10^7$ Mm^3/an, i.e. a water supply for ~500'000 inhabitants. The further objective is to develop specific MAR scenarios according to local hydrogeological settings and demands. This includes improving groundwater quality of contaminated alluvial aquifers by dilution, as well as injection and recovery in deep carbonate rocks. These findings highlight that even in countries with significant natural groundwater recharge, such as Switzerland, MAR can be an innovative and promising solution, especially in the case of groundwater quality problems.

14.6
Hybrid Hydrological Modeling for Sub-seasonal Droughts Forecasts - A Combination of Traditional Models and Machine Learning Techniques for Streamflow and Lake Level Predictions For the Alpine Aare Basin

Simone Jola[1], Annie Y.-Y. Chang[1,2], Konrad Bogner[2], Daniela I.V. Domeisen[1], Massimiliano Zappa[2]

[1] *Institute for Atmospheric and Climate Science, ETH Zürich, Universitätstrasse 16, CH-8006 Zürich (sijola@student.ethz.ch)*
[2] *Swiss Federal Institute for Forest, Snow and Landscape Research, WSL, Zürcherstrasse 111, CH-8903 Birmensdorf*

Droughts can occur on a wide spatial and temporal range and are a normal phenomenon in the mid-latitude seasonal climate. However, extreme events, such as that of summer 2003 and 2018, have severe impacts on water resources, water supply, agriculture, energy production and natural ecosystems (Brunner et al. 2019). To mitigate and reduce such harmful effects, warning systems aiming to the early recognition of droughts are a fundamental tool for public and private water managers. In an integrated risk management perspective, sub-seasonal streamflow and lake levels ensemble forecasts provide useful information for medium-long term. Recently, approaches from machine learning (ML) have shown to outperform traditional hydrometeorological modeling approaches, mainly due to their hyper-flexibility (Kratzert et al. 2018). Nevertheless, purely ML-based modeling depends on large data availability, ignores general knowledge about system functioning, and it does not easily extrapolate to unseen conditions. Combining general knowledge and learning-from-data in hybrid models is therefore currently seen as a promising paradigm for hydrological and earth science modelling (Kraft et al. 2021).

The purpose of this study was to investigate the power of ML as a routing scheme for PREVAH medium-sized discharge output to provide ensemble sub-seasonal streamflow and lake level forecast for the alpine Aare basin at the outlet of both lake Brienz (Aare - Ringgenberg, Goldswil) and lake Biel (Aare - Brügg, Aegerten). We addressed droughts occurrence to the complex and non-linear combination of multiple controls: (a) hydrological control (runoff), (b) catchment control (initial conditions), (c) meteorological control (weather regimes) and (d) human control (hydropower operations). Three research questions were formulated for this study:

1. How much can machine learning improve the accuracy on the current sub-seasonal streamflow and lake level forecasts in a normal and low-flow perspective.
2. How much can added information, such as catchments, meteorological and human controls provide any benefit to machine learning performance and further improve the forecast performance.
3. Are pre-processed meteorological forecasts a better input to machine learning compared to raw meteorological forecasts.

We demonstrate that hybrid hydrological modeling outperforms traditional approaches to forecast sub-seasonal streamflow and lake level for both Brienz and Biel basin. In Figure 1 we summarize results for the second research question. For the Brienz basin we show that for both, streamflow and lake level, giving additional information to the ML algorithms significantly increase the model performance. For larger basins, the use of ML algorithms remains justified even if, in the case of streamflow forecasts, a rapid decrease in the performance is noted after seven days lead time. Finally, we also show that raw meteorological forecasts give better results compared to ones obtained using the pre-processed meteorological forecasts.

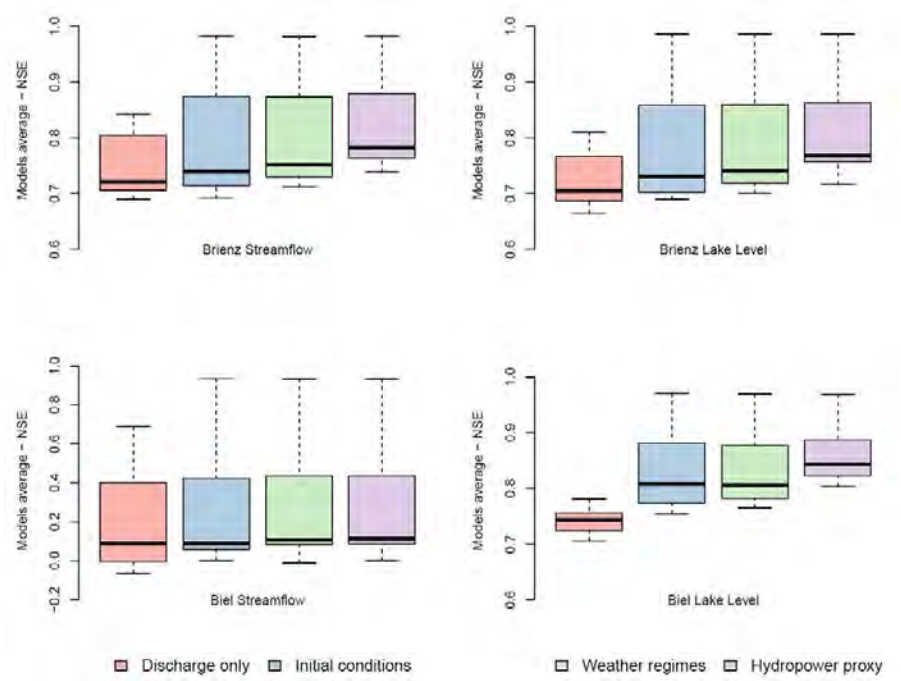

Figure 1. Temporally averaged ML model performance for the different controls for Brienz streamflow (top left), Brienz lake level (top right), Biel streamflow (bottom left) and Biel Lake Level (bottom, right). Boxplots are obtained by applying the average to the different ML algorithms and seeds.

REFERENCES

Brunner, M. I., Liechti, K., & Zappa, M. (2019). Extremeness of recent drought events in Switzerland: Dependence on variable and return period choice. Natural Hazards and Earth System Sciences, 19(10), 2311–2323.

Kraft, B., Jung, M., Körner, M., Koirala, S., & Reichstein, M. (2021). Towards hybrid modeling of the global hydrological cycle. Hydrology and Earth System Sciences Discussions, 1–40.

Kratzert, F., Klotz, D., Brenner, C., Schulz, K., & Herrnegger, M. (2018). Rainfall–runoff modelling using Long Short-Term Memory (LSTM) networks. Hydrology and Earth System Sciences, 22(11), 6005–6022.

14.7
Laser-induced fluorescence study of solute mixing in 3D-printed fractured porous media

Xiang-Zhao Kong[1,+], Mehrdad Ahkami[2], Isamu Naets[1], Martin O. Saar[1,3]

[1] Geothermal Energy and Geofluids (GEG) Group, Department of Earth Sciences, ETH Zurich, Sonneggstrasse 5, CH-8092 Zurich, Switzerland ([+]xkong@ethz.ch)
[2] Department of Engineering Geology and Hydrogeology, RWTH Aachen University, Aachen, Germany
[3] Department of Earth and Environmental Sciences, University of Minnesota, Minneapolis, USA

Solute transport in fractured porous media is of significant importance for various applications, such as subsurface contaminant migration, geological CO_2 sequestration, and geothermal energy utilization. It is well-known that the presence of geometry heterogeneity in porous media enhances the solute mass mixing due to the fluid velocity heterogeneity. However, laboratory measurements are still sparse on solute mixing in heterogeneous, particular fractured, porous media.

In this study, transport of solute is quantified after a pulse-like injection of fluorescent dye into a 3D-printed fractured porous media with distinct heterogeneity. Here, the 3D-printed medium consists of two low- and high-permeability matrices, each with one flow-through and one dead-end fracture. We have conducted Particle Image Velocimetry measurements in this 3D-printed medium (Ahkami et al., 2019) to determine the pore-scale fluid velocity field.

In this study, the dye concentration is determined using laser-induced fluorescence techniques. The migration of solute is characterized with a progression and a depletion process, assisted with descriptions of the evolution of concentration field, spatial moment analyses, and mixing metric evaluations in different regions of the medium. The asymmetry between the progression and depletion processes suggests a non-Fickian transport behavior. Our study provides insights into solute mass distribution and interplay (Ahkami et al., 2020) between fractures and their surrounding matrix, which is crucial to characterize the associated reactive transport processes.

REFERENCES

Ahkami, M., Roesgen, T., Saar, M. O., Kong, X.-Z. 2019: High-Resolution Temporo-Ensemble PIV to Resolve Pore-Scale Flow in 3D-Printed Fractured Porous Media. Transp. Porous Media 129, 467–483.

Ahkami, M., Parmigiani, A., Palma, P. R., Saar, M. O., Kong, X.-Z. 2020: A lattice-boltzmann study of permeability-porosity relationships and mineral precipitation patterns in fractured porous media. Computational Geosciences, 24, 1865–1882.

14.8
Joint use of $^3H/^3He$ apparent age and on-site helium analysis to identify groundwater flow dynamics and transport of PCE

Christian Moeck[1], Andrea Popp[1,2], Matthias S. Brennwald[1], Mario Schirmer[1,3], Rolf Kipfer[1,2,4]

[1] Department of Water Resources and Drinking Water, Eawag, Swiss Federal Institute of Aquatic Science and Technology, Dübendorf, Switzerland
[2] Department of Environmental Systems Science, ETH Zurich, Zurich, Switzerland
[3] Centre of Hydrogeology and Geothermics (CHYN), University of Neuchâtel, Neuchâtel, Switzerland
[4] Department of Earth Sciences, ETH Zurich, Zurich, Switzerland

$^3H/^3He$ apparent water ages have been shown to provide essential insights on groundwater-related processes. However, their analysis is expensive as well as labor- and time-intensive. Recent developments of a portable field-operated gas equilibrium membrane inlet mass spectrometer (GE-MIMS) system (Brennwald et al., 2016) provide a unique opportunity to measure dissolved gas concentrations, such as helium-4 (^4He), in groundwater systems with a high resolution at relatively low costs.

By establishing an inter-relationship between $^3H/^3He$ apparent groundwater ages (analysed in the laboratory) and helium-4 concentrations (analysed in-situ with the GE-MIMS system; Popp et al., 2019) we demonstrate that the ^4He concentrations derived from the GE-MIMS system serve as a suitable proxy for the sophisticated laboratory based analyses. The combined use of $^3H/^3He$ lab-based ages and predicted ages from the $^3H/^3He$ – ^4He age relationship opens new opportunities for more detailed site characterization due to the high-resolution measurements facilitated by the GE-MIMS.

For an urban study site, we combined groundwater ages with hydrochemical data, water isotopes ($\delta^{18}O$ and δ^2H), and perchloroethylene (PCE) concentrations (1) to identify spatial inter-aquifer mixing between artificially infiltrated groundwater and water originating from regional flow paths and (2) to explain the spatial differences in PCE contamination within the investigated groundwater system. The results obtained from the age distribution analysis are strongly supported by the information gained from the isotopic and hydrochemical data (Moeck et al., 2021). Moreover, for some wells, we identify fault-induced aquifer connectivity as a preferential flow path for the transport of older groundwater, leading to elevated PCE concentrations.

REFERENCES

Brennwald, M. S., Schmidt, M., Oser, J., & Kipfer, R. 2016: A portable and autonomous mass spectrometric system for on-site environmental gas analysis. Environmental science & technology, 50(24), 13455-13463.

Moeck, C., Popp, A. L., Brennwald, M. S., Kipfer, R., & Schirmer, M. 2021: Combined method of 3H/3He apparent age and on-site helium analysis to identify groundwater flow processes and transport of perchloroethylene (PCE) in an urban area. Journal of contaminant hydrology, 238, 103773.

Popp, A.L., Scheidegger, A., Moeck, C., Brennwald, M.S., Kipfer, R. 2019: Integrating Bayesian groundwater mixing modeling with on-site helium analysis to identify unknown water sources, Water Resour. Res., 55 (12), 10602-10615

14.9
HYDROGEOMORPHOLOGICAL ASSESSMENT OF FUTURE WATER AVAILABILITY FOR ECOSYSTEM DEVELOPMENT IN PROGLACIAL CATCHMENTS

Tom Müller[1,2], Matteo Roncoroni[1], Stuart N. Lane[1], Bettina Schaefli[2]

[1]*Institute of Earth Surface Dynamics, University of Lausanne, Quartier UNIL-Mouline, CH-1015 Lausanne (tom.muller.1@unil.ch)*
[2]*Institute of Geography, University of Bern, Hallerstrasse 12, CH-3012 Bern*

Rapid glacier retreat leads to the emergence of barren landscapes. The common assumption of the presence of bare bedrock underlying glaciers is quickly challenged by the rapid accumulation of sediments leading to the formation of diverse geomorphological landforms in proglacial zones, both on the slopes and at the previous glacier bed. The combined effect of important sediment release and strong hydrological variations makes the emergence of life difficult. Combined with future glacier decline and earlier snowmelt, the role of these structures to retain water and to provide suitable environments for the development of life is still unclear.

Based on a thorough field monitoring of the hydrological functioning of the proglacial area of the Otemma glacier in Switzerland, combined with hydrological modelling, we show how different landforms are connected to different water sources such as snow or ice melt, at which time scale they retain water and how they may provide water in the future both for vegetation development and stream ecosystems. Vegetation onset mainly appears on the talus slopes or on the sides of alluvial aquifer where sufficient water is provided and where disturbances are limited. Such moisture is mainly maintained by surface water from surface tributaries or water leakages at the base of the hillslopes supplied by snow melt in higher part of the hillslopes. These landforms are however rapidly draining and may stop to provide water if early snow melt is combined with droughts in summer. Based on isotopic and geochemical observations, we show however, that bedrock leakages may still provide enough moisture in focused zones. On the other hand, we show that the flatter outwash plain provide limited moisture for surface vegetation development as their water table is not sufficiently shallow, but may play a significant role to store and release water to maintain baseflow during drought in future summers. Due to their location at the base of the catchment, they are connected both to recharge from the hillslopes but especially by the upstream river system and due to their shape and sedimentological structure, they release water at time scales of months, allowing them to maintain high water storage throughout the summer and to provide more baseflow for aquatic ecosystems. While their role may appear marginal at present times, they may become increasingly important with potentially new outwash plains forming with glacier retreat and for secondary vegetation reaching deeper aquifers.

In this work, we focus on the hydrogeological response of the proglacial zone of the Otemma glacier. We provide field observations and modelling of the outwash plain as well as geochemical observations of the water origins, flowpaths and recharge of the various landforms and propose a conceptual model of water availability for both surface and stream habitats.

14.10
Mapping piezometric fluctuations in the Rhone valley: results of over 40 year of monitoring

Romain Sonney[1], Marie Arnoux[1], Pascal Ornstein[1], Pierre Christe[2], Romaine Perraudin Kalbermatter[3], Frédéric Zuber[4], Laurent Maret[5]

[1]Centre de recherche sur l'environnement alpin (CREALP) (romain.sonney@crealp.vs.ch)
[2] Département de la mobilité, du territoire et de l'environnement (DMTE), Service de l'environnement (SEN), Canton du Valais
[3] Département de la mobilité, du territoire et de l'environnement (DMTE), Service de la protection contre les crues du Rhône (SPCR), Canton du Valais
[4] Département des finances et de l'énergie (DFE), Service de l'énergie et des forces hydrauliques (SEFH), Canton du Valais
[5] Département de l'économie et de la formation (DEF), Service de l'agriculture (SCA), Office des améliorations structurelles, Service de l'agriculture (SCA), Canton du Valais

Groundwater levels in the Rhône valley upstream of Lake Geneva are continuously monitored for more than 40 years. The number and the distribution of measuring stations have evolved according to the studies and needs of the services/offices of the Canton of Valais. The interpolation of these data by external drift kriging has allowed the production of average monthly piezometric maps for the period 1976-2017 between Lake Geneva and Sierre. The method used is dependent on hydrogeological characteristics, point density, data quality and anthropogenic impacts. The reference maps obtained improve the hydrogeological knowledge of the groundwater dynamics in the valley and are particularly useful for the management, exploitation and protection of groundwater resources.

14.11
Application of soil water potential threshold in Swiss landslide early warning systems

Sabrina Walder[1,2], Adrian Wicki[1], Peter Lehmann[2], Manfred Stähli[1]

[1] Swiss Federal Research Institute WSL, Mountain Hydrology and Mass Movements, Zürcherstrasse 111, 8903 Birmensdorf (waldersa@wsl.ch)
[2] ETH Zurich, Institute of Biogeochemistry and Pollutant Dynamics, Universitätstrasse 16, 8092 Zürich

Landslides triggered by rainfall pose a major risk to people and infrastructure.
To forewarn of possible landslide danger, regional landslide early warning systems (LEWS) are developed. LEWS are typically based on rainfall exceedance thresholds only, whereas antecedent water conditions and the prewetting of the slope are commonly neglected (or only indirectly considered by antecedent cumulative rainfall). The performance of landslide forecasts may be improved significantly by including more information about the current and antecedent hydrological state in the soil (Ciavolella et al. 2016, Greco et al. 2016).

Recently, Wicki et al. (2020, 2021) analysed soil water content data to quantify the temporally variable landslide probability in Switzerland. Complementary to soil water content, the soil water potential describes the hydrologic state of the soil. Soil water potential has a direct effect on soil stability with negative potential values (soil suction) increasing soil strength and positive pressure values indicating the formation of a destabilizing water table. Due to this direct link between water potential and soil strength, we hypothesize that direct measurement of pore pressure can be used to predict conditions prone to landslide release.

Soil water potential is monitored in Switzerland for many years to provide thresholds for construction work and agricultural activities (to prevent mechanical damage of the soil). To assess whether there is a relation between the temporal variability of soil water potential and landslide occurrence, the following procedure was conducted: first, soil water potential measurement data over several years from 73 sites in whole Switzerland was collected, homogenized and normalized. In the next step, depth-averaged means of potential values were calculated. From these means, infiltration events were detected and described by different infiltration event characteristics (antecedent conditions, event dynamics and saturation conditions). Using the Swiss flood and landslide damage database (WSL) these infiltration events were characterized as landslide triggering or landslide non-triggering. This is conducted for eight specific forecast distances. Next, a logistic regression model is applied to predict whether these infiltration event characteristics correspond to landslide triggering or not. To evaluate the appropriate thresholds to distinguish landslide triggering from non-landslide triggering infiltration events, receiver operating characteristic (ROC) analysis is performed. The logistical regression model is further evaluated with a cross-validation scheme.

Results show that the soil water potential can successfully be used to differentiate between triggering and non-triggering conditions. In general, the shorter the prediction distances between soil water potential measuring station and landslide occurrence location, the better the forecast quality. Furthermore, the forecast quality of the model is better for long-lasting rainfalls than for rainfalls of short durations (thunderstorms).
By adding infiltration event properties that characterize the occurrence of saturated conditions, the forecast quality increases significantly. These findings demonstrate that soil water potential data may be used in a hydrological-based landslide threshold model to complement other data such as soil moisture or rainfall measurements.

REFERENCES

Greco, R., & Bogaard, T. 2016: The influence of non-linear hydraulic behavior of slope soil covers on rainfall intensity-duration thresholds. In S. Aversa, L. Cascini, L. Picarelli, & C. Scavia (Eds.), Landslides and Engineered Slopes: Experience, Theory and Practice: Proceedings of the 12th International Symposium on Landslides (Napoli, Italy, 12-19 June 2016) (pp. 1021-1025). CRC Press. https://doi.org/10.1201/b21520-12

Ciavolella, M., Bogaard, T., Gargano, R., & Greco, R. 2016: Is there predictive power in hydrological catchment information for regional landslide hazard assessment?. Procedia Earth and Planetary Science, 16, 195-203.

Wicki, A., Lehmann, P., Hauck, C., Seneviratne, S. I., Waldner, P., and Stähli, M. 2020: Assessing the potential of soil moisture measurements for regional landslide early warning. Landslides, 17(8), 1881-1896.

Wicki, A., Jansson, P.-E., Lehmann, P., Hauck, C., and Stähli, M. 2021: Simulated or measured soil moisture: which one is adding more value to regional landslide early warning?, Hydrol. Earth Syst. Sci., 25, 4585–4610, https://doi.org/10.5194/hess-25-4585-2021, 2021.

14.12
Implementing lake regulations into a hydrological model to disentagle climatic and regulatory impacts

Tobias Wechsler[1,3,4], Andreas Inderwildi[2], Bettina Schaefli[3,4], Massimiliano Zappa[1]

[1] *Swiss Federal Institute for Forest, Snow and Landscape Research WSL, Zürcherstrasse 111, 8903 Birmensdorf (tobias.wechsler@wsl.ch)*
[2] *Swiss Federal Office for the Environment FOEN, Papiermühlestrasse 172, 3063 Ittigen*
[3] *Institute of Geography GIUB, University of Bern, Hallerstrasse 12, 3012 Bern*
[4] *Oeschger Centre for Climate Change Research OCCR, University of Bern, Falkenplatz 16, 3012 Bern*

Alpine regions are particularly sensitive to climate warming, due to its pronounced effect on snow and glacier melt. Past water resources studies therefore had a strong focus on the role of the cryosphere in modulating how climate change might modify the water supply and accentuate the pressure from competing water uses. However, large Alpine lakes also play a key role for water resource and natural hazard management, but surprisingly, are often only roughly modelled in available climate change impact studies on hydrology. Indeed, regulation of lake water levels and underlying regulation rules are the key to bringing together diverse interests, such as fishery, shipping, energy production, nature conservation and the mitigation of high and low extremes.

In Switzerland, the focus of this study, most of the large lakes located on the Plateau are regulated according to a specific regulation diagrams that define a target outflow for every day of the year and every water level. Such diagrams can be completed by a set of exceptions, e.g. to preventively lower lake levels in case of forecasted large scale flooding. Ideally, this regulation diagrams (and exceptions) should be agreed upon such that the annual pattern that both corresponds to natural fluctuations and respects the different needs of the lake ecosystem, its immediate environment and upstream and downstream interests. A key question that remains open to date is how to incorporate these regulatory effects into a hydrological model?
To anticipate climate change impacts, we simulated daily streamflow with the hydrological model PREVAH, using 39 climate model chains and 3 emission scenarios in transient simulation from the new Swiss Climate Change Scenarios CH2018. The simulations span from 1981 to 2099. PREVAH consists of several model components covering the hydrological cycle: interception, evapotranspiration, snow, glacier, soil- and groundwater, runoff formation and transfer. To implement the anthropogenic effect of lake regulations, we created an interface with the hydrodynamic model MIKE11. In this study, we present a unregulated and a regulated lake, that are hydraulically connected. The catchment area of these lakes was already affected by water scarcity in isolated years.
The hydrological projections at the end of the century show minor changes in mean annual lake levels and outflow for both lakes, but there is a pronounced seasonal redistribution of both lake level and outflow. The changes intensify over time and missing climate protection measures. In the winter, mean lake levels rise and outflow increases; in the summer, mean lake levels fall and outflow decreases. The lake level change of the unregulated lake is significantly higher, with a difference of up to half a metre, than of the regulated lake, which only changes around 5 cm; the changes in outflow are of the same order of magnitude in both lakes. The extremes show an increased frequency of reaching the drawdown limit, but no clear change in frequency of reaching the flood limit.

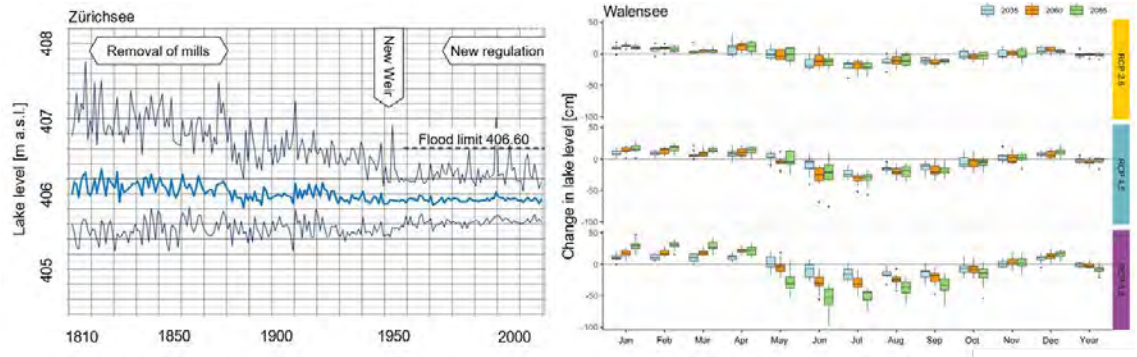

Figure 1. Left: a historical record of the mean (light blue, bold), minimum and maximum annual lake levels (dark blue) of Lake Zurich (regulated) and the effects of increasing regulation. The dashed line represents the flood limit at 406.6 m a.s.l. Right: CH2018 projections of mean monthly changes in lake levels [cm] of Lake Walensee (unregulated) and the annual mean (far right), divided into three future scenarios (2035, 2060, 2085) and three emission scenarios (RCP2.6, RCP4.5, RCP8.5).

REFERENCES

BAFU (Hrsg.) (2021): Auswirkungen des Klimawandels auf die Schweizer Gewässer. Hydrologie, Gewässerökologie und Wasserwirtschaft. Bundesamt für Umwelt BAFU, Bern. Umwelt-Wissen Nr. 2101: 134 S.

Brunner, M.I., Björnsen Gurung, A., Zappa M., Zekollari H., Farinotti D., Stähli, M. (2019): Present and future water scarcity in Switzerland: Potential for alleviation through reservoirs and lakes. Science of the Total Environment: 1033–1047.

CH2018 (2018): CH2018 – Climate Scenarios for Switzerland, Technical Report, National Centre for Climate Services. Zürich: 271 pp.

DHI (2004): River Network Editor. In MIKE 11 - River Modelling Unlimited DHI.

Speich, M.J.R., Bernhard, L., Teuling, A.J., Zappa, M. (2015): Application of bivariate mapping for hydrological classification and analysis of temporal change and scale effects in Switzerland. Journal of Hydrology 523: 804–821.

Viviroli, D., Zappa, M., Gurtz, J., Weingartner, R. (2009): An introduction to the hydrological modelling system PREVAH and its pre- and post-processing-tools. Environmental Modelling & Software 24 (10): 1209–1222.

P 14.1
Initial investigations into microbial dynamics and biogeochemical cycling in the Bedretto Tunnel

Andrew Acciardo[1], Moira Arnet[1], Bernard Brixel[1], Nima Gholizadeh[1] , Quinn Wenning[1] , Marian Hertrich[1], Cara Magnabosco[1]

[1] *Department of Earth Sciences, ETH Zurich, Sonneggstrasse 5, CH-8092 Zurich*

Over 70% of Earth's bacteria and archaea live in the subsurface. These rock-dwelling microorganisms are capable of exerting considerable influence on their environment by altering and recycling nutrients, as well as inducing changes to fluid flow paths through bioclogging. Subsurface life, therefore, has considerable implications for both natural and engineered subsurface environments. The Bedretto tunnel, located within the Swiss Alps, is 5,218 meters long and is host to the Bedretto Underground Laboratory for Geosciences and Geoenergies (BULGG), which was built to study the feasibility of large-scale geothermal energy storage and extraction. The tunnel, with a maximum overburden of approximately 1,650m, is embedded within both gneiss and Rotondo granite and offers an ideal location to investigate the biogeochemical feedbacks associated with natural fluids. For these reasons, a multi-year, monthly survey of fracture fluids at over 20 locations across the entire length of the tunnel has been carried out since August 2020 with the goal of performing 16S rRNA sequencing of cells captured by 0.22µm Millipore Sterivex filters and cell and virus enumeration by epifluorescence microscopy of samples fixed with formaldehyde. Initial 16S rRNA sequencing results indicate that there are diverse taxa found at the different sites, with some sites hosting microbes capable of sulfur or methane cycling. Furthermore, preliminary microscopy observations reveal high virus to cell ratios. With continued monitoring through 2021, we will determine whether there is significant variability of microbes at different locations within the tunnel and the relationship between the hydrochemical properties of the fluids and the microbial communities. Alongside the profiling survey, whole genome sequencing will be used to learn more about the genetic diversity and metabolic capacity of the microbial communities. These results will be compared to other subsurface environments around the globe to gain a more holistic understanding of microbial dynamics in the terrestrial subsurface.

P 14.2
Geostatitical piezometric products in the Rhone valley: tools for groundwater management and protection

Marie Arnoux[1], Romain Sonney[1], Pascal Ornstein[1], Pierre Christe[2], Romaine Perraudin Kalbermatter[3], Frédéric Zuber[4], Laurent Maret[5]

[1]*Centre de recherche sur l'environnement alpin (CREALP) (marie.arnoux@crealp.vs.ch)*
[2] *Département de la mobilité, du territoire et de l'environnement (DMTE), Service de l'environnement (SEN), Canton du Valais*
[3] *Département de la mobilité, du territoire et de l'environnement (DMTE), Service de la protection contre les crues du Rhône (SPCR), Canton du Valais*
[4] *Département des finances et de l'énergie (DFE), Service de l'énergie et des forces hydrauliques (SEFH), Canton du Valais*
[5] *Département de l'économie et de la formation (DEF), Service de l'agriculture (SCA), Office des améliorations structurelles, Service de l'agriculture (SCA), Canton du Valais*

The production of monthly reference piezometric maps for the period 1976-2017 between Lake Geneva and Sierre has enabled the development of a number of cartographic products that provide particularly useful information on the dynamics of the water table of the Rhône aquifer. The absolute natural amplitude of the water table fluctuations, the seasonal differences as well as regions where water levels are particularly influenced by rivers or mountainside contributions have been highlighted. In addition, since 2018 with a smaller dataset and thanks to the reference maps, it has been possible to produce monthly piezometric maps which provide the month-by-month status of the water table. Finally, the impacts of specific localized situations on water levels, such as the spring frost episode in April 2017 during which significant pumping was carried out, the intense precipitations in January 2018, or the important melt in July 2019, were highlighted. All of these maps serve to improve hydrogeological knowledge and management, but also to assess danger situations linked to excessive rises in the water table.

P 14.3
Exploratory study on the application of time series models to simulate groundwater levels and estimate recharge in Switzerland

Raoul Collenteur[1,2], Christian Moeck[2], Mario Schirmer[2,3], Steffen Birk[1]

[1] *Institute of Earth Sciences, NAWI Graz Geocenter, University of Graz, Heinrichstr. 26, A-8010 Graz, Austria (raoul.collenteur@uni-graz.at)*
[2] *Eawag, Department Water Resources and Drinking Water (W+T), Ueberlandstr. 133, CH-8600 Dübendorf, Switzerland*
[3] *University of Neuchâtel, Centre of Hydrogeology and Geothermics (CHYN), Rue Emile-Argand 11, CH-2000 Neuchâtel, Switzerland*

A prerequisite for sustainable water resource management is a good understanding of groundwater systems and their behavior over time. Time series modeling (TSM) has been shown to be a suitable tool to improve our understanding. TSM using predefined impulse response functions (von Asmuth et al., 2002) has become an increasingly popular method to model groundwater level fluctuations and gain a better understanding of the subsurface system. The method requires limited time and effort from the modeler, and only few assumptions are made about the system under study. This makes the method applicable for a wide range of environmental locations. Recently, it has been shown that these models may also be applied to obtain estimates of groundwater recharge (Collenteur et al., 2021). However, most studies applied the method to monitoring wells located in climate regions where precipitation primarily occurs as rainfall. In cold-temperature regions, where part of the precipitation falls as snowfall, applications of the aforementioned TSM have been limited. In this exploratory study, we test the use of TSM for selected groundwater monitoring wells in Switzerland. A simple degree-day snow model is added to the TSM to account for snowfall and make the method applicable to cold-temperature regions. Preliminary results show that the use of a snow model routine improves the simulation of groundwater recharge in the winter period, leading to a better prediction of the groundwater levels. We further compare estimated recharge flux from TSM to independent seepage measurements from a lysimeter located in the Rietholzbach catchments, which shows similar rates and behavior. The preliminary results from this study can be used to further explore the use of TSM to better understand groundwater systems in cold-temperature regions.

REFERENCES

von Asmuth, J. R., Bierkens, M. F., & Maas, K. 2002: Transfer function-noise modeling in continuous time using predefined impulse response functions. Water Resources Research, 38 (12), 23-1.

Collenteur, R. A., Bakker, M., Klammler, G., and Birk, S. 2021: Estimation of groundwater recharge from groundwater levels using nonlinear transfer function noise models and comparison to lysimeter data, Hydrol. Earth Syst. Sci., 25, 2931–2949.

P 14.4
Impacts of climate change-influenced hydrology on dam failure risks

Javier Fluixa-Sanmartin[1], Ignacio Escuder-Bueno[2,3], Adrian Morales-Torres[3]

[1] Centre de Recherche sur l'Environnement Alpin, Rue de l'Industrie 45, CH-1951 Sion (javier.fluixa@crealp.vs.ch)
[2] Instituto Universitario de Investigación de Ingeniería del Agua y Medio Ambiente, Universitat Politècnica de València (UPV), 46022 Valencia, Spain
[3] iPresas Risk Analysis, 46023 Valencia, Spain

Large dams as well as protective dikes are critical infrastructures whose associated risk must be properly managed in a continuous and updated process. Usually, dam safety management is carried out assuming stationary hydrological conditions, including the persistence of historical patterns of natural variability and the likelihood of extreme events (IPCC, 2012). However, evidence shows that climate change is likely to modify hydrological factors in the mid and long term. Thus, the assumptions of past stationary climatic baselines are no longer appropriate for long-term dam safety management (USACE, 2016).

Hydrometeorological analyses are useful tools that help characterizing the magnitude and the frequency of the floods generated within the basin, that represent the main loads to which the dam is subjected. By analysing the climatic effects on the hydrology of river basins, we can assess the evolution of the dam risks according to different scenarios and models.

The authors (Fluixa-Sanmartin et al., 2019) have performed a comprehensive quantitative analysis of the climate-influenced hydrology of the Santa Teresa dam (Spain) and the resulting effects on the dam's failure risk, using different models and data sources. The following multi-model scheme is proposed to quantify risk at present situation and for different time horizons in the future until the end of the 21st century: (i) Extraction and correction of climate projections; (ii) Hydrological modelling; (iii) Risk modelling; and (iv) Adjustment of resulting risks.

Results (Figure 1) show that in most future scenarios higher hydrological loads are expected over time, thus increasing the social and economic risks of the dam. Indeed, the risk tends to increase in comparison to the present risk level but a certain dispersion of the risk appears with time, thus enlarging the uncertainty of the results.

This study provides valuable new information with respect to previous dam risk studies and makes it possible to improve the efficiency of risk-based decisions on the long term by incorporating the effects of climate change. Moreover, further analyses on how to tackle risk evolution with time and climate uncertainty were carried out in the author's PhD thesis (Fluixa-Sanmartin, 2020).

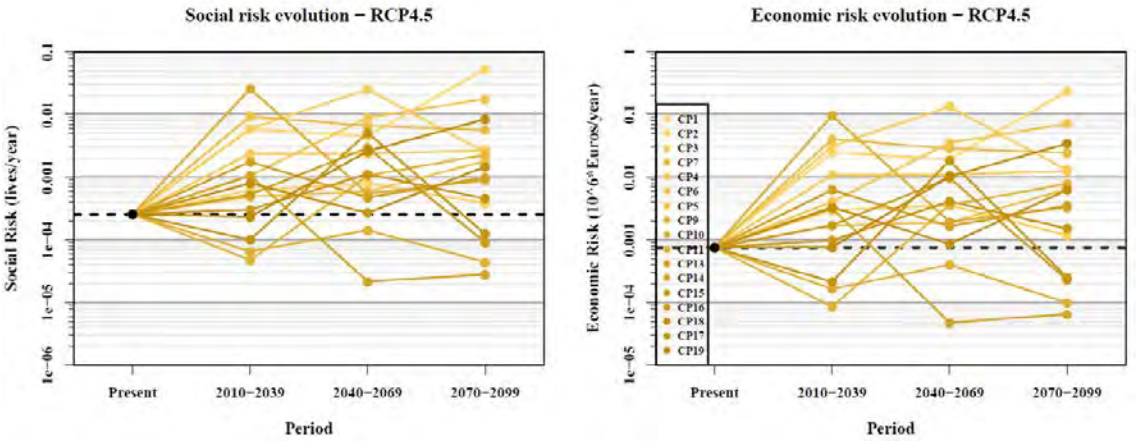

Figure 1. Example of social and economic risks affected by climate-influenced hydrology, for RCP4.5 scenario. The base case situation is highlighted with a black point and a horizontal dashed line (source: Fluixa-Sanmartin et al., 2019).

REFERENCES

Fluixa-Sanmartin, J., 2020: Adaptation strategies of dam safety management to new climate change scenarios informed by risk indicators. PhD thesis, Universitat Politècnica de València, Valencia (Spain).

Fluixa-Sanmartin, J., Morales-Torres, A., Escuder-Bueno, I., and Paredes-Arquiola, J., 2019: Quantification of climate change impact on dam failure risk under hydrological scenarios: a case study from a Spanish dam. Natural Hazards and Earth System Sciences, 19(10), 2117–2139.

IPCC, 2012: Managing the Risks of Extreme Events and Disasters to Advance Climate Change Adaptation. A Special Report of Working Groups I and II of the Intergovernmental Panel on Climate Change. Cambridge University Press, Cambridge, UK, and New York, NY, USA, 582 pp.

USACE, 2016. Guidance for Incorporating Climate Change Impacts to Inland Hydrology in Civil Works Studies, Designs, and Projects.

P 14.5
CH-GNet – Swiss Groundwater Network

Christian Moeck[1,2]

[1] *Department of Water Resources and Drinking Water, Eawag, Swiss Federal Institute of Aquatic Science and Technology, Dübendorf (Christian.moeck@eawag.ch)*
[2] *CH-GNet, Ueberlandstrasse 133, CH-8600 Dübendorf*

About 80% of Swiss drinking water is obtained from groundwater and therefore groundwater is a very valuable resource that must be protected. Contamination from various sources, anthropogenic influences on the hydrogeological system and climate change have a major impact on groundwater quality and quantity. Thus, there is a need for continuous competence building, expert support and a facilitated exchange between research and stakeholders in Switzerland to assess hydrogeological issues and challenges under the pressure of new developments, to come up with solutions and measures and to implement these. For this purpose, the CH-GNet was created.

The aims of the CH-GNet are to coordinate and promote practice-oriented research. Scientific facts are to be compiled and strongly practice-oriented research is to be achieved by notice groundwater-relevant problems as well as possible solutions. Through the work of the CH-GNet, current but also future research-central questions and, above all, voluntary solutions and approaches are to be made “explicit”. Together with the advisory board (FOEN, CHYN, SVGW, Eawag, Canton Baselland, and SGH), the CH-GNet is setting concrete thematic priorities and is determining fundamental strategic directions.

The CH-GNet sees itself as a “think tank”, whereby one of the most important functions of the CH-GNet is the presentation of research results and the setting of concrete thematic priorities. Purely scientific facts are to be worked out for the respective main topics and political statements are to be avoided. The promotion of a public and scientific debate and the provision of advice to practitioners are central to this. Through this, a strengthening of research advice has to take place. Among other things, this should increase the visibility of groundwater research and exchange with practice in Switzerland in the long term. By bundling practice-relevant research results and making them visible, through organized workshops and the development of documents, help promoting continuous competence building, expert guidance and a smooth exchange of information, the CH-GNet wants to support the cooperation of various interest groups and represent a source of information.

P 14.6
Mobilization of toxic elements in high-alpine streams of the Eastern Alps: monitoring strategy and first results

Hoda Moradi[1], Gerhard Furrer[2] , Michael Margreth[3], Christoph Wanner[1]

[1] *Rock-Water Interaction Group, Institute of Geological Sciences, University of Bern, Baltzerstrasse 3, CH-3012 Bern, Switzerland (hoda.moradi@geo.unibe.ch)*
[2] *Institute of Biogeochemistry and Pollutant Dynamics (IBP), Department of Environmental Systems Science, ETH Zurich, CH-8092 Zurich, Switzerland*
[3] *Swiss Federal Institute for Forest, Snow and Landscape Research WSL, Mountain Hydrology and Mass Movements, Zürcherstrasse 111, CH-8903 Birmensdorf*

In the Eastern Alps, there are several high-alpine streams with distinctively white colored streambeds (Fig. 1). The white color originates from the precipitation of nanocrystalline basaluminite [$Al_4OH_{10}(SO_4)\cdot(H_2O)_3$] sticking to the bedload of the streams. The phenomenon is triggered at the origin of the streams where the oxidation of pyrite occurs in rock glacier bodies (i.e. permafrost). This leads to the production of sulfuric acid and the subsequent dissolution of aluminum from the host rock. Owing to its pH-dependent solubility, precipitation of basaluminite eventually occurs when the acidic and aluminum-rich streams are neutralized along their flow paths (Wanner et al., 2018).

Acidic conditions in the affected streams are accompanied by elevated concentrations of mildly toxic elements such as Ni, Mn and F also mobilized from the host rock and strongly exceeding the drinking water limits. Based on a long-term monitoring study performed in a similar setting in the Rocky Mountains (Todd et al., 2012), it is very likely that these concentrations will be increased in the future. A likely scenario is that the ongoing permafrost retreat will expose more pyrite-bearing bedrock to aerobic waters and that the production of sulfuric acid and mobilization of toxic elements will increase in the future. Therefore, a detailed monitoring of such catchments is needed to better understand this recent phenomenon and to assess the accompanied hazard for the water quality on a regional scale.

For this contribution we present the monitoring concept for the affected Aua da Prasüra stream located in Val Costainas, Val Müstair, Eastern Switzerland. To track the mobilization of toxic elements occurring in the rock glacier body at the origin of the stream, we have initiated a detailed investigation in late spring of 2021. The monitoring includes the determination of the mobilized element fluxes at two distinct locations along the stream. At the outlet of the rock glacier, we collect water samples and perform discharge measurements using the salt dilution method on a monthly basis between June and October. In addition, we have installed a combined pressure and conductivity probe at a distance of roughly 5 km from the origin of the stream. Selected discharge measurements at this location allow to relate the recorded pressure date to discharge values. Similarly, we collect water samples on a bi-weekly basis to relate the conductivity data to element concentrations. By integrating the two datasets we aim at automatically determine toxic element fluxes on a high time-resolved basis. A long-term operation of the probe should then track the evolution of annual element fluxes over time and assess whether they will increase in the future.

First results for 2021 demonstrate that all toxic element fluxes show strong seasonal variations. While they were low in spring when the source area (i.e. rock glacier) was still covered by snow, they strongly increased during the snowmelt and reached maximum values of 125 kg/day of Al, 33 kg/day of Mn, 17 kg/day of Ni, and 127 kg/day of F in July 2021. These values demonstrate that the mobilization of toxic elements is highly significant and thus justify the continuation of our monitoring effort in the upcoming years.

Figure 1. Photographs of white streambeds in the Eastern Alps.

REFERENCES

Todd, A.S., Manning A.H., Verplanck P.L., Crouch C., McKnight D.M. & Dunham, R. 2012: Climate-change-driven deterioration of water quality in a mineralized watershed. Environmental Science & Technology. 46, 9324-9332.

Wanner, C., Pöthig, R., Carrero, S., Fernandez-Martinez, A., Jäger, C. & Furrer, G. 2018: Natural occurrence of nanocrystalline Al-hydroxysulfates: Insights on formation, Al solubility control and As retention, Geochimica et Cosmochimica Acta, 238, 252-269.

P 14.7
Understanding sources of isotopic mismatch of tree water and soil water of a sub-alpine coniferous forest

Ankit Shekhar, Nina Buchmann, Mana Gharun

Department of Environmental Systems Science, ETH Zürich, 8092 Switzerland

Stable water isotopologues of soil water and tree xylem water is widely used to understand tree water uptake. In most used approach, the soil water, bound and/or mobile water, from different depths acts as source, whereas the xylem water, twigs and/or stem cores, act as target, which are then evaluated using a source-target Bayesian mixing model to estimate the TWU depth. However, isotopic mismatch between tree xylem water (δxw) and soil water (δsw), possibly due to non-inclusion of all water sources (fog, dew, stream, rocks) and tree physiological processes complicates the estimation of TWU depth from these source-target Bayesian mixing models. Here, we evaluate the isotopic offset between δxw (from tree twigs) and δsw (bulk soil), sampled on nine dates and 15 trees over the 2020 growing season (May – September) at a sub-alpine coniferous forest to estimate tree water uptake depth. Additionally, we also measured latent heat flux (LE - indication of evaporation/condensation), sapflux (indication of transpiration), air temperature, vapor pressure deficit, and soil water content to explain the possible variation of relation between δxw and δsw throughout the growing season. To detect the offset of the soil and xylem samples from the local meteoric water line (LMWL), we calculated line-conditioned excess: LC-excess (‰) = δ2H - aδ18O – b, where a and b are slope and intercept of LMWL. Finally, we conducted principal component analysis with all the additional measurement to explain the lc-excess of xylem samples. Our results show a considerable isotopic offset between δxw and δsw earlier during growing season (May-July). The soil samples (δsw) consistently indicated negative lc-excess (signs of evaporated precipitation) throughout the measurement. Xylem samples, however showed an interesting pattern of positive lc-excess (4.1‰ to 7.3‰) in the early growing season (five dates from May-July) and negative lc-excess (-5‰ to -15‰) in the late growing season (four dates from August-September). Principal component analysis showed that the first principal component (PC1) comprising of early morning LE, transpiration, temperature and VPD explained 70% variation in lc-excess of xylem samples. The five dates with positive lc-excess, showed higher early morning water vapor condensation (possible signs of fog), lower transpiration rate, and lower air temperature and VPD, than the four dates with negative lc-excess. Our results suggest a possible influence of dew water on tree water update that needs to be tested.

P 14.8
The Value of Synthetic High-resolution Daily Snow Cover Maps for Long-term Hydrological Modeling

Pau Wiersma[1], Fatemeh Zakeri[1], Grégoire Mariéthoz[1]

[1] *Institute of Earth Surface Dynamics, University of Lausanne, Lausanne (pau.wiersma@unil.ch)*

To understand the long-term changes in the hydrology of snow-fed catchments, there is a need for long-term time series of snow cover data. Satellite imagery and climate reanalysis can both be used to quantify past snow cover, but they lack in baseline period length and spatial resolution respectively. In this preliminary study, we apply statistical methods to generate synthetic high-resolution daily snow cover maps, and consequently use these maps as forcing in long-term hydrological modeling. The results are benchmarked against a case without synthetic snow cover forcing. Multiple hydrological models are used to reduce the uncertainty related to the model choice. The study is performed on the Thur catchment in Eastern Switzerland, a meso-scale catchment covering a wide elevation range and experiencing multiple periods of intermittent snow cover annually. We expect the synthetic snow cover maps to provide added value through the high-resolution spatial information on snow appearance and disappearance, leading to better estimates of snow melt runoff. However, we also expect them to show some physical inconsistencies, particularly after periods of high snow accumulation. Should it prove promising, this approach can be used to study both past and future hydrological changes in any snow-fed catchment using ERA5 and CMIP6 climate data, potentially spanning the entire period 1950-2100. Additionally, this framework of synthetic satellite data generation could be expanded to other hydrological variables or to environmental image time series in other fields than hydrology.

P 14.9
Groundwater Drainage-Induced Rock Mass Deformation during the Gotthard Base Tunnel Excavation in the Swiss Alps: 3D Modelling and Comparison to Field Measurements

Chenxi Zhao[1,2], Qinghua Lei[1,*], Zixin Zhang[2], Simon Loew[1]

[1] *Chair of Engineering Geology, Department of Earth Science, ETH Zurich, Clausiusstrasse 2-30, CH-8006 Zurich (*qinghua.lei@erdw.ethz.ch)*
[2] *Department of Geotechnical Engineering, College of Civil Engineering, Tongji University, Siping Road 1239, PRC-200092 Shanghai*

The Gotthard Base Tunnel (GBT) is a deep tunnel located in the Central Alps of Switzerland. During its construction, significant ground deformations up to about 10 centimetres occured in the surrounding hard crystalline rocks, which may be attributed to the drainage of groundwater into the excavated tunnel (Loew et al., 2015). To investigate the physical mechanism driving the observed ground deformation, a coupled hydro-mechanical model is developed to simulate the perturbation of the groundwater pressure field and the poroelastic response of faulted rock masses over both space and time domains during the advance of tunnel excavation faces. First, a realistic 3D geological model (16 km × 10 km × 6 km) including complex topographical features, multiple lithological units and reconstructed fault zones is built. Material properties of faults and rocks masses are defined based on laboratory testing results and site investigation data. We also consider the important depth-dependency of some of the hydro-mechanical properties (e.g. modulus, stiffness, permeability, and storativity) of faults and rock masses. The model is mechanically preconditioned by a relevant in-situ stress state and then constrained by roller conditions for the bottom and four lateral boundaries during the simulation of tunnel excavations. We define a spatially variable field of surface hydraulic heads which are constrained by available information of surface water systems (e.g. streams, rivers, and lakes). We solve the coupled system of multiphysics governing equations to simulate the hydro-mechanical behaviour and elastic response of the faulted rock mass in response to the Gotthard Base Tunnel excavation. Here, transient advancement of tunnel faces is simulated by setting the pressure along excavated sections of the tunnel trajectory to be zero and updating such a constraint in a time marching fashion. Figure 1 shows some simulation results of ground settlements by our 3D numerical model with a further comparison to some of the field measurement data in both space and time domains. The good match between our simulation results and field measurements justifies the validity and accuracy of our numerical model. As is shown in Figure 2, based on this 3D numerical simulation, we observe that faults play a critical role in the drainage process by serving as high-permeability flow pathways that transmit water quickly into the tunnel. Faults also serve as drainage surfaces such that low-permeability rock mass compartments (dissected and bounded by these faults) drain progressively, resulting in phenomena of depressurisation and consolidation as well as ground surface displacements (including both vertical settlements and horizontal displacements). Furthermore, significant stress perturbation occurs in both near- and far-field as a result of pore pressure variations and poroelastic effects. However, no conspicuous slippage along the faults is observed, suggesting that fault reactivation may play a minor role in the ground deformation.Insights gained from our simulation have important implications for many excavation-related geoengineering activities such as deep excavations in alpine mountains and fluid withdrawal in subsurface aquifers.

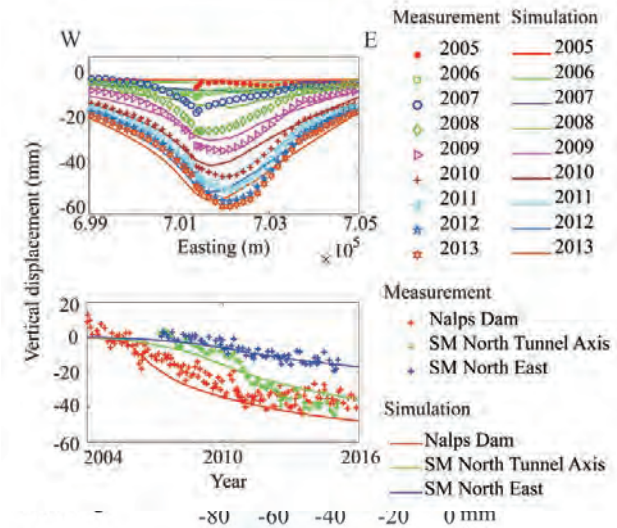

Figure 1. Drainage-induced ground settlement during the excavation of the Gotthard Base Tunnel.

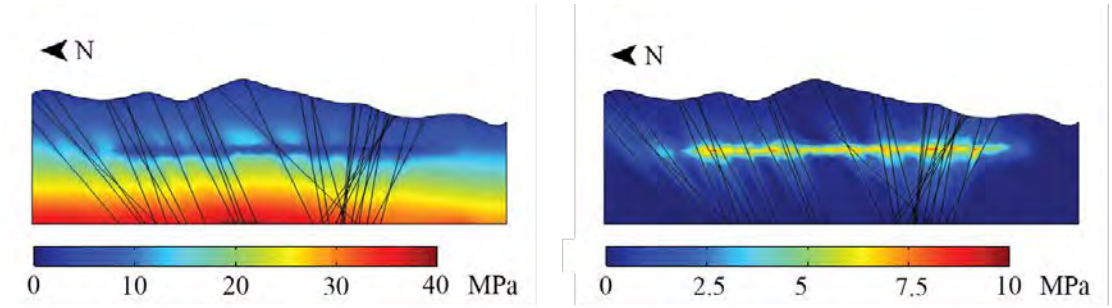

Figure 2. Pore pressure distribution and maximum principal stress variation after tunnel excavation.

REFERENCES

Loew, S., Lützenkirchen, V., Hansmann, J., Ryf, A., & Guntli, P. 2015. Transient surface deformations caused by the Gotthard Base Tunnel. International Journal of Rock Mechanics and Mining Sciences, 75, 82–101.

15. Limnology in Switzerland

Damien Bouffard, Michael Döring, Dorothea Hug Peter, Natacha Tofield-Pasche

Swiss Society for Hydrology and Limnology SGHL

TALKS:

15.1 Ajallooeian et al.: Seasonal temperature variability on freshwater branched glycerol dialkyl glycerol tetraethers: a mesocosm approach

15.2 Carratalà et al.: Spatiotemporal dynamics of bacteria communities in Lake Geneva.

15.3 Escoffier et al.: Fine scale dynamics of calcite precipitation in a large hardwater lake unveiled from high-frequency sensor data

15.4 Forrest et al.: Submersible Probe with In-line Calibration and Symmetrical Reference Element for Long-term Continuous Measurements

15.5 Lepori et al.: Trophic propagation of production loss in a deep lake

15.6 Mettra et al.: Detailed hydrodynamics of cold density currents generated by differential cooling along the sloping bed of Lake Geneva

15.7 Perolo et al.: Is gross primary production carbon-limited in Lake Geneva?

15.8 Piccolroaz et al.: Near-surface convection under the combined effect of cooling and radiative heating: the case of Lake Geneva

15.9 Piton et al.: Suspended sediments in Lake Geneva: Observations, settling behaviour and mechanisms in the Rhône River plume

15.10 Strigaro et al.: An open and cost-effective monitoring system for the protection and management of lake ecosystems

15.11 Van Grinsven et al.: The role of oxygen and substrate origin in shaping methane producing communities in lakes

15.12 Von Fumetti: Long-term research on springs and headwaters in the Engiadina Val Müstair UNESCO biosphere reserve

POSTERS:

P 15.1 Bandli et al.: Life at the extreme – high alpine springs and glacial outflows in the Lauterbrunnen valley (BE)

P 15.2 Bärenbold et al.: Towards a Swiss lake temperature monitoring network

P 15.3 Doda et al.: Cross-shore transport induced by differential cooling in lakes

P 15.4 Dürrenberger: Hydrogeochemistry of Black Forest springs from Germany: Insights from physical and hydrogeochemical parameters, stable isotopes and Macroinverterbrates

P 15.5 Frey et al.: Influence of preservatives on stable isotopes of nitrous oxide in aquatic environments

P 15.6 Ibelings et al.: Variation in Lake Geneva seston C:P as a function of phytoplankton species identity and P-levels

P 15.7 Maner et al.: RAINBOWflow CHIPonline: An impedance-based biosensor for water quality monitoring using permanent fish cell lines

P 15.8 Many et al.: Predicting CO_2 Dynamics In Lake Geneva Using A Deep Learning Approach (LSTM RNN)

P 15.9 Pasche et al.: Temporal and spatial variations in the composition and fluxes of settling particles in Lake Geneva

P 15.10 Rotta et al.: Microplastics in Lake Lugano: vertical distribution and colonization by microorganisms

15.1
Seasonal temperature variability on freshwater branched glycerol dialkyl glycerol tetraethers: a mesocosm approach

F. Ajallooeian [1], M. A. Lever [2], C. De Jonge [1]

[1] *Institute of Geology, Swiss Federal Institute of Technology Zurich (ETHZ), Switzerland*
[2] *Institute of Biogeochemistry and Pollutant Dynamics, Swiss Federal Institute of Technology Zurich (ETHZ), Switzerland*

Branched Glycerol Dialkyl Glycerol Tetraethers (brGDGTs) are ubiquitous bacterial membrane spanning lipids, containing 4 to 6 methyl branches that can form cyclopentane moieties following internal cyclization. BrGDGTs have been encountered in soils, marine and lake sediments, and the lake water column. On a global scale, the degree of methylation of 5- methyl brGDGTs (calculated as MBT'5ME ratio) correlates with temperature. Similarly, the cyclization index of tetraethers (CBT' ratio), as well as the abundance of 6-methyl brGDGTs (IR) correlate with soil pH.

Although proposed MBT'5ME and CBT' proxies have successfully been applied to many paleoclimate studies, the mechanisms that cause the dependency on temperature and pH are still not fully understood. Specifically, it is not clear whether the composition of the brGDGT membrane lipid is changed in direct response to changes in temperature, or if temperature causes the composition of the bacterial community to change. Although some bacterial taxa have been proposed as producers of brGDGT lipids, the main producers of brGDGTs in the environment are not well known.
To investigate the response of brGDGTs and their producing bacteria to changing temperatures, our experiment uses local lake/river freshwater mesocosms that are subjected to three different growth temperatures (10°C, 17.5°C and 25°C), and sampled at several timepoints (24h, 1, 2, 3 and 5 weeks). Water is collected in Lake Rot (47°21'05.8"N 8°31'12.7"E) and Sihl River (47°21'05.8"N 8°31'12.7"E), both with midrange pH (6.8-7.4). Here, oxic surface water is collected seasonally. With these experiments, we aim to understand i) which brGDGTs are produced in different temperature conditions and ii) how this production depends on the composition of the bacterial community based on 16S rRNA genes. Other inorganic parameters that will be measured and evaluated as drivers of brGDGTs distribution include alkalinity, concentration of cation and anions, dissolved oxygen, pH and conductivity.

Initial results presented reflect the spring season. Here, MBT'_{5ME} values do not increase with temperature (25 °C> 17.5°C> 10°C) as previously assumed. However, changes in the brGDGT distribution with time are observed between different growing temperatures. Specifically, 6-methyl compounds. Our mesocosm experiments thus enable us to study season- and temperature-dependent production of brGDGTs. Insights into the temperature-dependent production of brGDGTs will improve the accuracy of current paleoclimate proxies.

15.2
Spatiotemporal dynamics of bacteria communities in Lake Geneva

Anna Carratalà[1], Coralie Chappelier[1], Annie Guillaume[2], Elia Vajana[2], Tamar Kohn[1], Stéphane Joost[2].

[1] *Environmental Chemistry Laboratory, ENAC. École Polytechnique Fédérale de Lausanne (EPFL), Switzerland.*
[2] *Geographic Information Systems Laboratory, ENAC. École Polytechnique Fédérale de Lausanne (EPFL), Switzerland.*

Bacteria communities play major roles in freshwater ecosystems such as contributing to the primary production of lakes and to the biogeochemical cycles of many key elements. Because of their fast life cycles, bacteria are readily responsive to environmental variations. However, predicting how prokaryotic communities may adapt to climate change and how their response may influence ecosystem functioning is currently difficult, partly because the ecology of many bacteria groups is largely unknown. Since August 2019, we are conducting a monitoring project in the experimental floating platform Léxplore, in Lake Geneva, in which to date we have collected more than 200 water samples at different depths, from the lake's surface to 100 meters deep, and analyzed them by 16S amplicon high throughput sequencing. Simultaneously, we have compiled a dataset of the environmental conditions using CTD sensors, and measured the concentration of nutrients in the water column. This project has allowed us to obtain about 25 million bacteria sequences, classified in more than 17,000 different species. Our results show interesting spatio-temporal patterns in the bacteria communities of Lake Geneva and their predicted functions, and allow us to characterize cyanobacteria blooms caused by *Planktothrix rubescens,* a toxic cyanobacteria that is favored by global warming. In addition, combined with our environmental dataset our taxonomic data represent a unique opportunity to use ecological distribution modelling to predict community assemblage under future climate change scenarios.

15.3
Fine scale dynamics of calcite precipitation in a large hardwater lake unveiled from high-frequency sensor data

Nicolas Escoffier[1], Pascal Perolo[1], Gaël Many[1], Natacha Tofield Pasche[2,3], Marie-Elodie Perga[1]

[1] Institute of Earth Surface Dynamics, University of Lausanne, Switzerland (nicolas.escoffier@unil.ch)
[2] Limnology Center, ENAC, Ecole Polytechnique Fédérale de Lausanne, Switzerland
[3] Physics of Aquatic Systems Laboratory, Margaretha Kamprad Chair, ENAC, Ecole Polytechnique Fédérale de Lausanne, Switzerland

In hardwater lakes fueled by carbonate weathering from surrounding catchments, calcium carbonate (calcite) precipitation represents a pivotal biogeochemical process coupling carbon and nutrient cycling with autotrophic microbial activity. Though the drivers of calcite precipitation are well described theoretically, their relative contributions in shaping its dynamics at distinct spatial and temporal scales remain less understood. Such limitation holds especially true in large lakes, as Lake Geneva, as our comprehension of precipitation mechanisms reflected in bottom sediments is confounded by complex morphometry and hydrological mixing regimes. In this study, we aim at quantifying the magnitude of epilimnetic calcite precipitation in the deeper basin of Lake Geneva and identifying the environmental conditions that constrain its temporal and vertical occurrence. Using depth-resolved continuous measurements of specific conductance to trace calcium concentrations, we evidence that seasonal calcium stock depletion during stratification (130 – 180 g Ca m^{-2}) scales with the epilimnetic heat content but that higher daily depletion rates are localized within water layers of maximum stability. Moreover, continuous pH data coupled with discrete sample analyses yield complementary insights on the geochemical conditions supporting a preferential precipitation at specific depth levels. Altogether, our results provide a refined mechanistic understanding of the calcite precipitation process and confirm its major contribution to carbon cycling in Lake Geneva.

15.4
Submersible Probe with In-line Calibration and Symmetrical Reference Element for Long-term Continuous Measurements

Tara Forrest[1], Thomas Cherubini[1], Stéphane Jeanneret[1], Elena Zdrachek[1], Polyxeni Damala[1], Eric Bakker[1]

[1] *Department of Inorganic and Analytical Chemistry, University of Geneva, Quai Ernest-Ansermet 30, CH-1221 Genève (tara.forrest@unige.ch)*

Nitrogen is an essential nutriment in a healthy lake ecosystem, mainly promoting the growth of aquatic plants and algae. The balance of it is crucial as nitrogen excess will lead to extreme algae growth, which will result in oxygen depletion and eutrophication of the lake. Nitrate is the main aquatic source of nitrogen and comes from the conversion of nitrite by bacteria. Excessive nitrate levels are often found in streams crossing rural areas, where nitrate-based fertilisers are still routinely used for agricultural purposes. Recent trends show an increase of the general water quality and a decrease of nitrate levels, but the global monitoring process is tedious and not uniform.

Water quality is currently being monitored at fixed sampling stations or when punctual sampling is performed at strategic sites. Performing these measurements often requires an expensive infrastructure and significant manpower, which makes it impossible to ensure a constant monitoring of nitrate levels. Submersible potentiometric probes provide a good alternative to conventional measurement techniques and have already been used in environmental studies. As of now, these probes were relying on a pump to drive the sample to the measuring electrode, which makes them unsuitable for continuous measurement due to power consumption issues.

We present here a new nitrate-selective submersible probe that can perform independent and continuous measurements over an extended period of time. In this case the sensing head is located directly in contact with the sample allowing for constant monitoring without any additional power. An in-built miniature low consumption peristaltic pump can be pre-programmed to perform a one-step calibration at a predetermined time interval to correct for underlying drifts that would bias the results. To reduce the temperature dependency on the sensor signal, a new reference element based on the principle of electrochemical symmetry has been tested and implemented into the probe. This probe has been successfully deployed in Lake Geneva during a field campaign and the nitrate levels that were measured on-site were comparable with those of traditional measurements methods. Due to its low power consumption and drift correction, it is estimated that this system can run maintenance-free for several months.

REFERENCES

Pankratova N., Crespo G. A., Afshar M. G., Crespi M. C., Jeanneret S., Cherubini T., Tercier-Waeber M., Pomati F. & Bakker E. 2015: Potentiometric sensing array for monitoring aquatic systems, Environmental Science: Processes & Impacts, 17 (5), 906-914

15.5
Trophic propagation of production loss in a deep lake

Fabio Lepori[1], Camilla Capelli[1], Camille Minaudo[2], Federica Rotta[1], Massimilano Cannata[1]

[1] Institute of Earth Sciences, University of Applied Sciences and Arts of Southern Switzerland, Via Flora Ruchat-Roncati 15, CH-6850 Mendrisio (fabio.lepori@supsi.ch)
[2] Physics of Aquatic Systems Laboratory, EPFL, CH-1015 Lausanne

Pelagic ecosystems contribute the majority of primary production in oceans, seas and large lakes (Vadeboncoeur et al., 2008). Part of this production accumulates as phytoplankton biomass, while the rest flows up the food chain, serving as a major energy source for the production of zooplankton and fish. In these systems, both primary production and the flow of production between trophic levels are potentially sensitive to external pressures such as climate and nutrient inputs. For example, studies in pelagic marine systems have shown that climate change can reduce primary production and that the impact can amplify at higher trophic levels (Stock et al., 2014). In lakes, however, the effects of climate change and other pressures on pelagic primary production, and the propagation of these effects up the food chain, remain poorly known.

We used monitoring data (1989-2018) to examine the effects of climatic variation (Lepori and Roberts, 2015) and nutrient reduction (Lepori and Roberts, 2017) on the pelagic production of Lake Lugano, Switzerland and Italy. Our main goals were to examine [1] whether these pressures influenced primary production (hereafter PP), [2] to what extent the effects on primary production were propagated to secondary production of zooplankton (hereafter SZP), and [3] what factors influenced the transfer between PP and SZP (quantified as the ratio SZP:PP). Climate was quantified using air temperature and nutrient status using total phosphorus concentration.

Preliminary results indicate that phosphorus concentration had positive effects on PP, SZP and the SZP:PP ratio (Fig. 1). In other words, phosphorus reduction caused a loss of PP and a proportionally greater loss of SZP, indicating trophic amplification. Air temperature had no effects on any response variables as a single predictor, but had a joint (negative) effect with phosphorus on SZP:PP, indicating that warming and phosphorus reduction acted additively to reduce transfer between PP and SZP. Explorations of the causes of this apparent amplification, which are still underway, point to a change in phytoplankton composition, wich may be causing a shift toward greater grazing resistance (Anneville et al., 2019).

Studies in deep lakes worldwide indicate that warming is reducing turnovers and, as a result, the replenishment of nutrients in the upper, productive waters (Pilla et al., 2020). Moreover, in lakes undergoing restoration, phosphorus is decreasing owing to improved nutrient management. Reduced phosphorus replenishment is predicted to reduce pelagic PP (Schwefel et al., 2019). This effect is welcome in culturally-eutrophied lakes. However, amplified losses of zooplankton would cause undesirable effects in both eutrophic and unpolluted lakes, including losses of grazing and, potentially, fishery yields (one of the most important ecosystem services provided by lakes). Future studies will help elucidate how PP losses propagate to the rest of the food chain (e.g. fish), how widespread trophic propagation is in lakes, and what are the specific mechanisms involved.

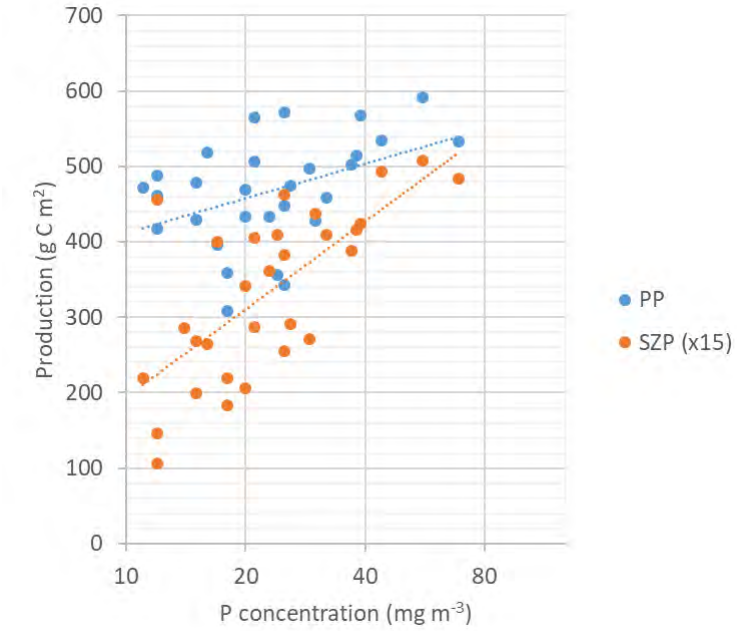

Figure 1. Relationship between total phosphorus concentration (yearly average in the 0-20 m layer, P) and production (cumulative annual primary production, PP, and secondary zooplankton production, SZP) in Lake Lugano (data from 1989 to 2018). Values of SZP were multiplied by 15 to scale with PP.

REFERENCES

Anneville, O., Chang, C.W., Dur, G., Souissi, S., Rimet, F. and Hsieh, C.H., 2019: The paradox of re□oligotrophication: the role of bottom–up versus top–down controls on the phytoplankton community. Oikos, 128, 1666-1677.

Lepori, F. and Roberts, J.J., 2015: Past and future warming of a deep European lake (Lake Lugano): What are the climatic drivers?. Journal of Great Lakes Research, 41, 973-981.

Lepori, F. and Roberts, J.J., 2017: Effects of internal phosphorus loadings and food-web structure on the recovery of a deep lake from eutrophication. Journal of Great Lakes Research, 43, 255-264.

Pilla, R.M., Williamson, C.E., Adamovich, B.V. et al. 2020: Deeper waters are changing less consistently than surface waters in a global analysis of 102 lakes. Scientific Reports, 10, 20514.

Schwefel, R., Müller, B., Boisgontier, H. and Wüest, A., 2019: Global warming affects nutrient upwelling in deep lakes. Aquatic Sciences, 81, 1-11.

Stock, C.A., Dunne, J.P. and John, J.G., 2014: Drivers of trophic amplification of ocean productivity trends in a changing climate. Biogeosciences, 11, 7125-7135.

Vadeboncoeur, Y., Peterson, G., Vander Zanden, M.J. and Kalff, J., 2008: Benthic algal production across lake size gradients: interactions among morphometry, nutrients, and light. Ecology, 89, 2542-2552.

15.6
Detailed hydrodynamics of cold density currents generated by differential cooling along the sloping bed of Lake Geneva

François Mettra, Rafael Sebastian Reiss, Ulrich Lemmin, David Andrew Barry

Ecological Engineering Laboratory (ECOL), Institute of Environmental Engineering (IIE), Faculty of Architecture, Civil and Environmental Engineering (ENAC), Ecole Polytechnique Fédérale de Lausanne (EPFL), CH-1015 Lausanne
Corresponding author: francois.mettra@epfl.ch

Deep water ventilation and mixing are of great importance for large lake ecosystems. Relevant processes include cold density currents due to differential cooling, inter-basin exchange and upwelling. At present, a good understanding of these processes in large lakes under realistic external forcing is still missing, which prevents, for example, to assess their relative contribution to and their evolution with climate change. Cold density currents bring cold surface water with oxygen and potential pollutants from coastal regions to the deep layers of the lake along the sloping boundaries. Earlier hydrodynamic studies allowed determination of the general behavior of those currents in Lake Geneva (Fer et al., 2001, 2002). With the recent advances in instrument capabilities, we were able to collect more detailed field data in the bottom boundary layer. In this study, we present preliminary results on the hydrodynamics of cold density currents generated by differential cooling using a unique high spatial and temporal resolution dataset.

Acoustic Doppler Current Profilers (ADCPs) and vertical thermistor lines were deployed during the winter season on the northern shore of Lake Geneva on the shallow shelf and along the sloping lakebed. In addition, CTD (Conductivity-Temperature-Depth) profiles were taken during periods of strong cooling in order to obtain a broader view of the temperature field along a cross-shore transect. After a cold, calm night, strong differential cooling forms between the shallow shelf and the open lake, initiating cold dense water from the shelf that flows as pulses along the sloping lakebed. Analysis of the velocity profile shows that the maximum velocity is relatively close to the bed, as would be expected for a density current. However, the height above the lakebed of this maximum velocity fluctuates depending on the stage of the flow (accelerating or decelerating). During the accelerating stage, i.e., at the beginning of a new pulse, the flow is thick enough to elucidate details of the velocity profiles close to the boundary – the measured profiles are logarithmic, as expected for a boundary flow (e.g., Kneller et al., 1999). Moreover, this new dataset enables us to determine the stability of the flow and the entrainment of the ambient water into the density current.

REFERENCES

Fer, I., Lemmin, U., & Thorpe, S. A. 2001: Cascading of water down the sloping sides of a deep lake in winter. Geophysical Research Letters, 28(10), 2093-2096.

Fer, I., Lemmin, U., & Thorpe, S. A. 2002: Winter cascading of cold water in Lake Geneva. Journal of Geophysical Research: Oceans, 107(C6), 13-1.

Kneller, B. C., Bennett, S. J., & McCaffrey, W. D. 1999: Velocity structure, turbulence and fluid stresses in experimental gravity currents. Journal of Geophysical Research: Oceans, 104(C3), 5381-5391.

15.7
Is gross primary production carbon-limited in Lake Geneva?

Pascal Perolo[1], Hannah Chmiel[2], Nicolas Escoffier[1], Gael Many[1], Damien Bouffard[3] and Marie-Elodie Perga[1]

[1] *Institute of Earth Surface Dynamics, University of Lausanne, Quartier Mouline, CH-1015 Lausanne (*pascal.perolo@unil.ch*)*
[2] *Physics of Aquatic Systems Laboratory, Margareth Kamprad Chair, Swiss Federal Institute of Technology Lausanne, Station 2, CH-1015 Lausanne*
[3] *Eawag, Swiss Federal Institute of Aquatic Science and Technology, Surface Waters – Research Management, Seestrasse 79, CH-6047 Kastanienbaum*

For 6 months in Lake Geneva, carbon dioxide (CO_2) concentrations in the euphotic zone are highly undersaturated, suggesting that gross primary production (GPP) could carbon-limited. Fundamentally, surface gas dynamics between dissolved oxygen (O_2) and CO_2 should covary inversely in aquatic ecosystems following the metabolic stoichiometry in a ratio of ~1.2. During the establishment of the pelagic stratification, GPP at the water surface should be limited as a result of the rapid consumption of the CO_2 stock and its physical isolation from the deep layer rich in CO_2. On the other hand, the littoral zone could maintain a higher GPP due to its proximity to sediment and macrophytes. In addition, the physical processes (e.g., wind, convection, and internal motion) that can have different intensities between the two areas could significantly affect these dynamics. Therefore, differences in shaping ecosystem processes should be observed considering the temporal and spatial scale in a large hardwater lake such as Lake Geneva.

Here, we extracted and compared high frequency data (CO_2, O_2 and alkalinity) of sunny days and calm days (wind < 3.7 m s^{-1}) from an annual cycle in littoral and pelagic areas (Fig. 1; Buchillon antenna and LéXPLORE platform, respectively) to avoid strong impacts of physical processes on the daily pattern (Fernández Castro et al., 2021). Our analysis was based on the paired O_2–CO_2 departure from atmospheric equilibrium (Vachon et al., 2020). The first results revealed levels of GPP that were 1 to 4 times higher in the littoral than in the pelagic area, depending on the season. Nevertheless, both environments highlighted a GPP maintained despite CO_2 depletion as recently showed in Connecticut River (Aho et al., 2021). This can be attributed to a direct and indirect consumption of bicarbonates (HCO_3^-) through assimilation by specific enzymes or calcite precipitation, demonstrated by the hourly variations of alkalinity. Thus, we show that in Lake Geneva, inorganic geochemical processes deliver continuously inorganic carbon to primary producers, hampering carbon-limitation of primary production. Furthermore, with a longer and stronger stratification of large lakes under climate warming, we expect that phytoplankton species whose metabolism allows bicarbonate use shall get predominant.

Figure 1. Two study sites: Buchillon antenna for the littoral zone (4 m depth; left side) and LéXPLORE platform for the pelagic zone (110 m depth; right side).

REFERENCES

Aho, K. S., Hosen, J. D., Logozzo, L. A., McGillis, W. R., & Raymond, P. A. 2021: Highest rates of gross primary productivity maintained despite CO2 depletion in a temperate river network, Limnology and Oceanography Letters, lol2.10195.

Fernández Castro, B., Chmiel, H. E., Minaudo, C., Krishna, S., Perolo, P., Rasconi, S., & Wüest, A. 2021: Primary and net ecosystem production in a large lake diagnosed from high-resolution oxygen measurements. Water Resources Research, 57(5).

Vachon, D., Sadro, S., Bogard, M. J., Lapierre, J., Baulch, H. M., Rusak, J. A., Denfeld, B. A., Laas, A., Klaus, M., Karlsson, J., Weyhenmeyer, G. A., & Giorgio, P. A. 2020: Paired O_2–CO_2 measurements provide emergent insights into aquatic ecosystem function, Limnology and Oceanography Letters, 5 (4), 287–294.

15.8
Near-surface convection under the combined effect of cooling and radiative heating: the case of Lake Geneva

Sebastiano Piccolroaz[1,2 †], Hugo Cruz[1], Alfred Wüest[1,3], Hugo N. Ulloa[1,4 †]

[1] *Physics of Aquatic Systems Laboratory, École Polytechnique Fédérale de Lausanne, Station 2, CH-1015, Lausanne*
[2] *Department of Civil, Environmental and Mechanical Engineering, University of Trento, via Mesiano 77, I-38122 Trento (s.piccolroaz@unitn.it)*
[3] *Eawag, Swiss Federal Institute of Aquatic Science and Technology, Surface Waters - Research and Management, Seestrasse 79, CH-6047 Kastanienbaum*
[4] *Department of Earth and Environmental Sciences, University of Pennsylvania, 240 South 33rd Street, PA 19104-6316 Philadelphia (ulloa@upenn.edu)*
[†] *These authors contributed equally to this work.*

When a lake's surface cools, the very surface fluid parcels become denser than their neighbours below, leading to a gravitational unstable density distribution which may trigger `free convection'. This phenomenon typically occurs when the atmosphere cools below the temperature of the surface waters, i.e. usually at night time but more persistently during the cooling period from fall to winter. In the latter case, it is not rare to observe convection occurring during day time. Hence it may happen that some lakes constantly lose heat at the surface while gaining heat in their bulk due to the action of short-wave radiation penetrating into the water column. The above joint action can lead to near-surface temperature distributions in which an unstable layer lays on a stably stratified layer. Depending on the relative intensity of surface cooling () and surface short-wave radiation (), the surface convective layer undergoes different formative processes. To the best of our knowledge, the ubiquity and extent to which the above gravitationally unstable density distribution can lead to convective driven mixing are unknown.

Since June 2020, a focus study within the upper water column of Lake Geneva has taken place to investigate near-surface vertical fluxes. For this, upward-looking turbulence microstructure profiles of the upper ~30 m of the water column (Fig. 1a) have been acquired at the LéXPLORE platform (https://lexplore.info/) about weekly, at a 10-minute frequency from early morning to late afternoon. The analysis of these profiles (Fig. 1b) and of the concurrent meteorological data measured at the LéXPLORE provided direct observation of the near-surface temperature resulting from the concurrent action of surface cooling and volumetric radiative heating. The acquired observations have been intepreted in light of a steady-state analytical expression for the water temperature profile where the wind action is neglected (Fig. 2). The solution allowed classifying different convective regimes depending on the relative importance of surface cooling and surface solar radiation flux (). For the regimes in which the near-surface temperature distribution is gravitationally unstable, we derived an analytical solution for the compensation depth (, here defined as the depth at which the loss of surface heat flux balances the injected radiative heat flux), and a nonlinear algebraic equation to determine the length scale of the expected convective mixing layer (), both as a function of the water transparency (light extinction length scale,). Additionally, the analysis of the heat flux data available for Lake Geneva allowed to examine the statistical occurrence of the three different convective regimes identified by the analytical solution at daily and seasonal scales.

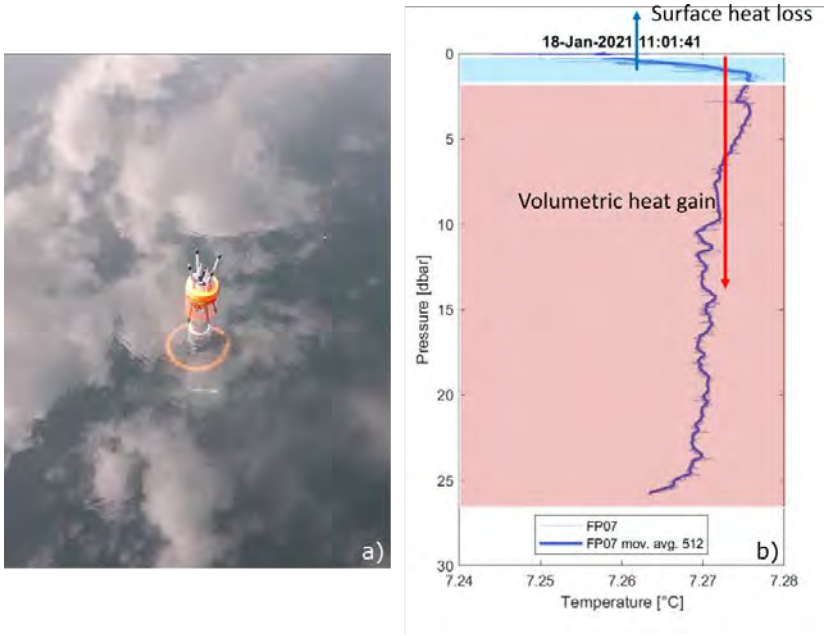

Figure 1. a) MicroCTD (Rockland Scientific International) reaching the calm lake surface of Lake Geneva after an upward profile; b) Temperature microstructure profile measured by one of the two high-resolution FP07 thermistors showing the contributions of surface cooling and volumetric heating.

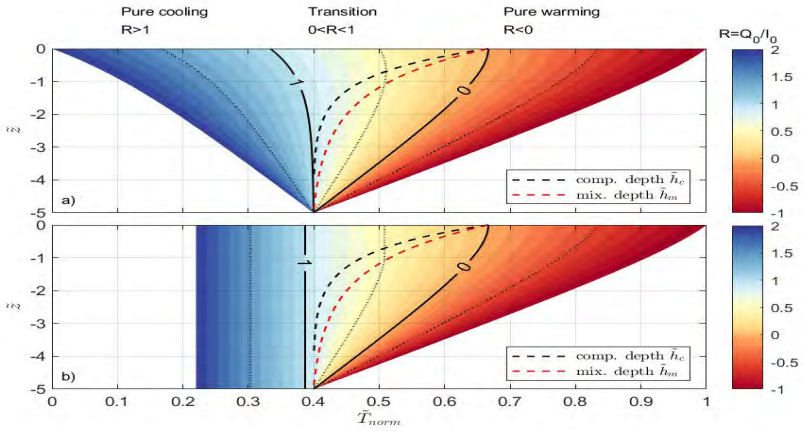

Figure 2. Dimensionless temperature profiles, compensation and mixing depths as a function of the ratio as provided by the steady-state analytical solution developed here. a) Analytical temperature profiles and b) analytical temperature profiles after top-to-bottom mixing of the gravitationally unstable layer . The dimensionless depth is defined as and is an opportunely normalized dimensionless temperature.

Acknowledgements: We thank the team from the LéXPLORE platform for their admistrative and technical support. This work has been supported by SNF Grant 200021_179113 Primary Production. In particular, we thank the fruitful discussions with Bieito Fernández-Castro and Tomy Doda.

15.9
Suspended sediments in Lake Geneva: Observations, settling behaviour and mechanisms in the Rhône River plume

Violaine Piton, Ulrich Lemmin, Htet Kyi Wynn, Valentin Kindschi, David Andrew Barry

Ecological Engineering Laboratory (ECOL), Institute of Environmental Engineering (IIE), Faculty of Architecture, Civil and Environmental Engineering (ENAC), Ecole Polytechnique Fédérale de Lausanne (EPFL), Station 2, CH-1015 Lausanne

In estuaries and marine environments, primary particles are frequently transported as large flocculated particles. This study provides, for the first time, evidence of in situ flocculation in Lake Geneva, a glacier-fed freshwater lake on the Swiss/French border. Measurements were focused in the nearfield of the Rhône River plume as it flows as an interflow into the stratified lake. Direct observations of flocculated particles in the whole water column with a digital holographic camera (LISST-HOLO 20-2000 µm), permitted estimation of the variability of sediment floc properties (size, nature and shape) with depth. Combined with full depth in situ laser particle sizing (LISST-100X), the measurements revealed that primary particles (< 4 µm) and microflocs (4-100 µm) are dominant in the Rhône River interflow, which exhibited the highest suspended sediment loads in the water column. Macroflocs (100-450 µm) dominate. In the hypolimnion below the interflow, where the sediment loads were the lowest, macroflocs (100-450 µm) were most frequent. The estimated fractal dimension (DF_{3D}) of the flocs in the hypolimnion range between 2.0 and 2.6, highlighting a large variability in the floc shape. Estimates of the settling velocities (W_s) showed an increase from 0.05 to 3 mm s^{-1} when floc sizes increased from 30 to 500 µm. This emphasizes the important influence of flocculation of fine sediments on the increase of W_s. These estimates are similar to previous estimates of W_s for fluvial flocs (Thonon et al., 2005). However, they are slightly faster (up to 2 times) than W_s estimated for flocs in the vicinity of the Rhône River plume as it flows into the Mediterranean Sea (Many et al., 2019). This difference in W_s between the two Rhône River plume environments is explained by the shapes of the flocs, which overall are less complex and therefore flocs settle faster in Lake Geneva compared to the Mediterranean Sea. Furthermore, the influence of instantaneous turbulent kinetic energy as a factor limiting the maximum floc size within the Rhône River interflow was investigated. The observed turbulence level in the interflow corresponded to an estimated Kolmogorov microscale of less than ~200 µm. This results in the potential breakup of flocs larger than 200 µm into smaller primary particles and microflocs and thus can explain the smaller floc size in the interflow compared to that in the hypolimnion.

REFERENCES

Many, G., Durrieu de Madron X., Verney R., Bourrin F., Renosh P. R., Jourdin F., Gangloff A. 2019: Geometry, fractal dimension and settling velocitiy of flocs during flooding conditions in the Rhône ROFI, Estuarine, Coastal and Shelf Science, 219, 1-13. https://doi.org/10.1016/j.ecss.2019.01.017

Thonon, I., Roberti J. R., Middelkoop H., van der Perk M., Burrough P. A. 2005: In situ measurements of sediment settling characteristics in floodplains using a LISST-ST, Earth Surface Processes and Landforms, 30, 1327-1343, doi: 10.1002/esp.1239

15.10
An open and cost-effective monitoring system for the protection and management of lake eco-system

Daniele Strigaro[1,2], Massimiliano Cannata[2], Fabio Lepori[2], Camilla Capelli[2], Michela Rogora[3], Dario Manca[3], Andrea Lami[3]

[1] *Dipartimento di Scienze della Terra e dell'Ambiente, Università di Pavia, Via Ferrata 9, 27100 Pavia, Italy*
[2] *Institute for Earth Sciences, SUPSI, Via Flora Ruchat-Roncati 15 CH-6850 Mendrisio*
[3] *CNR - Istituto di Ricerca Sulle Acque, sede di Verbania, Viale Tonolli 50, 28922 Verbania, Italy*

New technologies and solutions (Internet of Things , Big Data analysis, Edge Computing, etc.) are increasingly adopted to improve the temporal and spatial resolution of monitoring data. However, as regards lake ecosystems, monitoring activities are still largely dependent by manual sampling using e.g. multi-parameters probes and laboratory analyses performed with low temporal resolution (i.e. monthly, Mantzouki et al., 2018). While in some cases this approach cannot be replaced by automatic techniques, several parameters could be observed taking advantage of the new technologies. A promising option is the application of Automatic High Frequency Monitoring (AHFM) systems which, unfortunately, are still hampered by several difficulties in deployment, maintenance and data quality control (Marcé et al., 2016). Additionally, the initial investment could be conspiquous, as the costs of a platform or buoy and hardware components could represent a barrier for the adoption of AHFM at large scales.

Therefore, our research aims at designing and validating a digital, cost-effective, open and interoperable AHFM system that addresses the above-mentioned challenges. Once all the necessary steps will be completed, this system could be freely replicated (open license) with the result of increasing interoperability and offering data management and analyses tools to ultimately foster an advanced lake ecosystem management. Used in assistance with traditional monitoring, the AHFM approach may prove especially valuable in tackling the local effects of climate change on lake ecosystems and identify short-term phenomenon (e.g. algal bloom). Moreover, due to cost-effectiveness, this approach could be used, not only in developed societies but also in low-income and developing countries. To test the potential benefits, an experimental AHFM system, developed within the EU INTERREG project SIMILE, has been installed on Lake Lugano to monitor dissolved oxygen, water temperature, photosynthetic pigments (to be developed), and weather parameters (air pressure, air temperature, air humidity, solar radiation, wind speed and direction). Data are pre-processed at the edge, transmitted, archived, quality controlled, processed and distributed with interoperable services (OGC SOS) for further processing. For example, the data collected are quality controlled and then elaborated to calculate the metabolism of the lake (i.e. gross production, net production and respiration). We will present the preliminary results of this pilot study and share the architecture design, either at the monitoring node and at the server side, to the outputs produced during the data analysis. Finally, we will discuss possible future improvements, regarding e.g. additional sensors, new processing capabilities and other technical features (e.g. the adoption of a new data transmission).

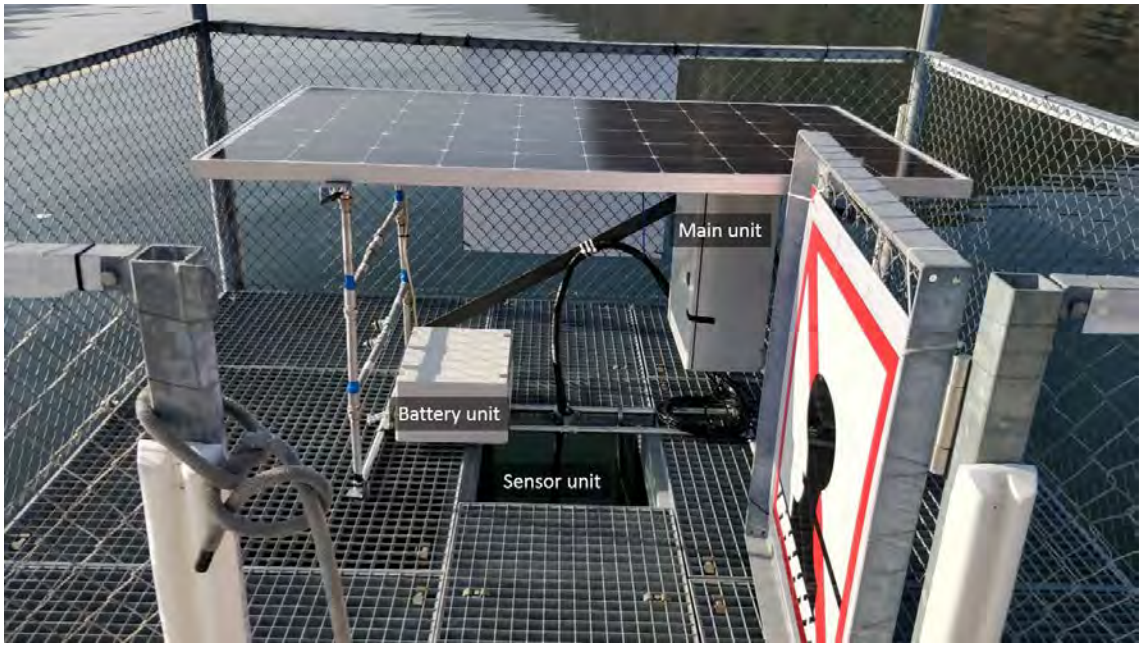

Figure 1. AHFM system installation.

REFERENCES

Mantzouki, E., Beklio□lu, M., Brookes, J. D., de Senerpont Domis, L. N., Dugan, H. A., Doubek, J. P., Grossart, H.-P., Nejstgaard, J. C., Pollard, A. I., Ptacnik, R., Rose, K. C., Sadro, S., Seelen, L., Skaff, N. K., Teubner, K., Weyhenmeyer, G. A., & Ibelings, B. W. (2018). Snapshot Surveys for Lake Monitoring, More Than a Shot in the Dark. Front. Ecol. Evol. 6:201. doi: 10.3389/fevo.2018.00201

Marcé, R., George, G., Buscarinu, P., Deidda, M., Dunalska, J., de Eyto, E., Flaim, G., Grossart, H.-P., Istvanovics, V., Lenhardt, M., Moreno-Ostos, E., Obrador, B., Ostrovsky, I., Pierson, D. C., Potužák, J., Poikane, S., Rinke, K., Rodríguez-Mozaz, S., Staehr, P. A., … Jennings, E. (2016). Automatic High Frequency Monitoring for Improved Lake and Reservoir Management. Environmental Science & Technology, 50(20), 10780–10794. doi: 10.1021/acs.est.6b01604

15.11
The role of oxygen and substrate origin in shaping methane producing communities in lakes

Sigrid van Grinsven[1], Mark A. Lever[2], Clemens Glombitza[2], Natsumi Maeda[1], Carsten J. Schubert[1,2]

[1]*Department of Surface Waters – Research and Management, Swiss Federal Institute of Aquatic Science and Technology (EAWAG), Seestrasse 79, Kastanienbaum, 6047, Switzerland.*
[2]*Institute of Biogeochemistry and Pollutant Dynamics, Swiss Federal Institute of Technology, Zurich (ETH Zurich), Universitätstrasse 16, Zurich, 8092, Switzerland.*

Lacustrine methane production predominantly occurs in lake sediments, in the absence of oxygen. The archaeal methane producers, called methanogens, depend on a diverse microbial community to break down incoming organic matter (OM) to methanogenic substrates (H_2, acetate, methanol). Despite the methanogens themself being strict anaerobes, the degradation of OM by the microbial community occurs under either oxic or anoxic conditions. Ongoing eutrophication of lakes worldwide both enhances algal growth, und thus the quantity of organic matter that is coming in and can be converted to methane, as well as water column anoxia. It is therefore essential to understand the role of the OM origin and of oxic/anoxic conditions on the sedimentary methanogenesis rates, methanogens, and wider microbial community. We performed incubation experiments with both oligotrophic and eutrophic lake sediments, in which we manipulated the incoming biomass origin as well as the temperature and oxygen conditions under which degradation proceeded. Not only natural substrates were analyzed, but also biodegradable and non-biodegradable plastic foils, commonly used on agricultural fields. CO_2 and methane concentration analysis confirmed that much more methane was produced under permanently anoxic conditions, whereas an initial oxic period of 3 weeks decreased the methane emissions drastically. The effect of the oxic period on the wider microbial community composition, as well as on methanogens and methanotrophs, was explored by 16S, mcrA and pmoA sequencing. Our results suggest that oxic bottom water conditions are essential in mediating methane emissions following algal blooms, and that artificial aeration directly after the occurrence of an algal bloom may partly compensate for the enhanced greenhouse gas emissions following eutrophication.

15.12
Long-term research on springs and headwaters in the Engiadina Val Müstair UNESCO biosphere reserve

Stefanie von Fumetti[1]

[1] Geoecology Research Group, University of Basel, Klingelbergstr. 27, CH-4056 Basel (stefanie.vonfumetti@unibas.ch)

Springs and headwaters worldwide face severe environmental changes caused by Global Climate Change. These changes will be more drastic in alpine regions. Rising water temperatures and a shifting discharge regime will impact springs and spring-fed headwaters as well as glacier-fed headwaters. It is, however, still unknown what the consequences will be for species composition and ecosystem functioning. Overall, biodiversity loss and a homogenization of species assemblages are expected. For venturing future predictions on how species composition in springs could change two prerequisites are necessary: We need to know the status quo and we need to conduct a sophisticated long-term monitoring. In 2019 a long-term research project started in the Engiadina Val Müstair UNESCO biosphere reserve including the Swiss National Park on 40 selected springs and headwaters. The goal is to understand how these aquatic systems will react to predicted hydrogeological changes caused by climatic changes. First results show relatively stable hydrogeological conditions and slight annual variation of water temperature and ion concentrations. Species assemblages are dominated by Limnephilid-species (Trichoptera), Protonemura lateralis and Chironomids. Species richness is highest within Hydrachnidia, Plecoptera and Trichoptera. Significant differences between springs and their brooks were not found, but slight changes in species composition are obvious. After a third field campaign in 2021 and a thorough data analysis 15-20 springs and headwaters will be selected for long-term research in the following decades.

P 15.1
Life at the extreme - high alpine springs and glacial outflows in the Lauterbrunnen valley (BE)

Andri Bandli* & Stefanie von Fumetti**

* *Geoecology Research Group, University of Basel, Klingelbergstr. 27, CH-4056 Basel (andri.bandli@stud.unibas.ch)*
** *Geoecology Research Group, University of Basel, Klingelbergstr. 27, CH-4056 Basel (stefanie.vonfumetti@unibas.ch)*

Ongoing climatic changes will alter the discharge and temperature regime of high alpine headwaters considerably. In this study we investigate groundwater- fed springs and headwaters and glacial outflows in the uppermost Lauterbrunnen valley in the Bernese alps. In total ten sites - two springs, three groundwater fed streams and five glacial outflows – are considered. All sites are situated on an altitude level between 1800 and 2100 meters above sea level. In July 2021 aquatic macroinvertebrates were collected qualitatively using a hand net. Abiotic parameters such as electrical conductivity and turbidity are measured in monthly intervals, while water temperature is continuously monitored using temperature loggers. First preliminary results reveal reduced discharge in glacially fed outflows during summer and a strong difference in turbidity between groundwater-fed sites and glacial outflows. Species richness is considerably higher in groundwater-fed sites. The aim of the study is to discover differences in the macroinvertebrate community between springs/ groundwater fed streams and glacial outflows. I want to investigate if it is possible to make predictions on how the biodiversity in high alpine streams, groundwater fed as well as glacially influenced, will evolve with further climatic changes and glacial recession.

P 15.2
Towards a Swiss lake temperature monitoring network

Fabian Bärenbold[1], Thilo Herold[2], Damien Bouffard[1], Martin Schmid[1]

[1] Dept. of Surface Waters – Research and Management, Eawag, Seestrasse 79, CH-6047 Kastanienbaum (fabian.baerenbold@eawag.ch)
[2] Hydrology Division, Federal Office for the Environment, Papiermühlestrasse 172, CH-3063 Ittigen

Lakes and reservoirs are experiencing major changes world-wide as a result of climate warming. Swiss lakes are expected to experience a reduction in ice cover, an increase of the duration of summer stratification and a shift of dimictic to monomictic mixing regime for mid-altitude lakes (Vinnå et al., 2021). Such changes can have large impacts on lakes as ecosystems. Most larger lakes in Switzerland are already monitored by cantonal agencies. However, the time resolution of this monitoring was shown to be not sufficient to accurately detecting changes in the thermal stratification (Bouffard et al., 2019).

Therefore, the Swiss Federal Agency for the Environment (FOEN) decided to establish a monitoring network of lake temperature across Switzerland. It has mandated Eawag to deploy pilote measurement stations in several lakes and ponds (see Figure 1) and to give recommendation on how to couple observations with numerical modelling.

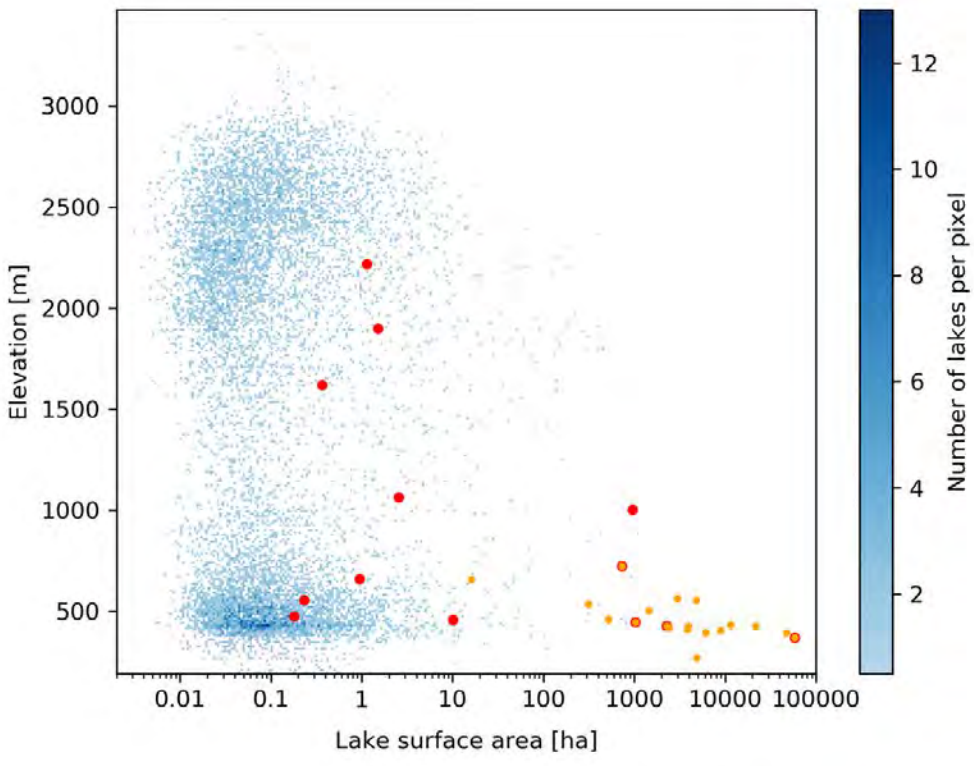

Figure 1. Distribution of the > 11'000 Swiss water bodies larger than 30 m^2 as a function of area and elevation (taken from the Swiss landscape model Vector25). Red dots indicate water bodies with pilot stations within this project; orange dots indicate lakes with at least 3 profiles per year by cantonal agencies.

Thus, within this project we investigate the following research questions:

- How can small and remote water bodies be monitored in a cost and time effective way?
- Which minimum sensor accuracy is needed to gather insight on mixing dynamics in small water bodies?
- Should temperature sensors be sheltered from sunlight and if yes, how?
- For larger lakes, is it more useful to have a temperature mooring (i.e. sensors at fixed depths) or a profiling system (i.e. one probe going up and down)?
- How, when and in which lakes should we monitor to achieve a representative monitoring system across Switzerland?
- How can numerical modelling be used to infer temperature dynamics of unobserved (i.e. without temperature measurements) lakes?

Here, we will present first measurement results from pilote monitoring stations, along with numerical simulations with the one-dimensional model Simstrat (Gaudard et al., 2019), to get insight about mixing dynamics in small water bodies during summer. In addition, we show how water temperature sensors react to direct sunlight and discuss whether this is an issue for water temperature monitoring.

REFERENCES

Bouffard, D., Dami, J., & Schmid, M. (2019). Swiss lake temperature monitoring program. Report Commissioned by the Federal Office for the Environment (FOEN).

Gaudard, A., Råman Vinnå, L., Bärenbold, F., Schmid, M., & Bouffard, D. (2019). Toward an open access to high-frequency lake modeling and statistics data for scientists and practitioners–the case of Swiss lakes using Simstrat v2.1. Geoscientific Model Development, 12(9), 3955-3974.

Vinnå, L. R., Medhaug, I., Schmid, M., & Bouffard, D. (2021). The vulnerability of lakes to climate change along an altitudinal gradient. Communications Earth & Environment, 2(1), 1-10.

P 15.3
Cross-shore transport induced by differential cooling in lakes

Tomy Doda[1,2], Cintia L. Ramón[1,3], Hugo N. Ulloa[2,4], Damien Bouffard[1]

[1] *Eawag, Swiss Federal Institute of Aquatic Science and Technology, Department of Surface Waters - Research and Management, Seestrasse 79, CH-6047 Kastanienbaum (tomy.doda@eawag.ch)*
[2] *Physics of Aquatic Systems Laboratory, École Polytechnique Fédérale de Lausanne, Station 2, CH-1015 Lausanne*
[3] *Water Research Institute and Department of Civil Engineering, University of Granada, Spain. Edificio Fray Luis, C/ Ramón y Cajal, 4, ES-18003 Granada*
[4] *Department of Earth and Environmental Science, University of Pennsylvania, 251 Hayden Hall, 240 South 33rd Street, US-PA 19104-6316 Philadelphia*

Differential cooling occurs in lakes when their sloping topography is subject to surface cooling. The shallow littoral region cools faster than the deep pelagic region, which produces a horizontal convective circulation formed by a downslope density current and a surface return flow (Fig. 1). This phenomenon, called “thermal siphon”, increases lateral water exchange, with implications for the transport of dissolved constituents. There is a need for a comprehensive understanding of the conditions required to form thermal siphons, with the objective of better predicting their occurrence and intensity in lakes.

By combining a one-year long monitoring of thermal siphons in a small wind-sheltered lake (Rotsee, LU) with large eddy simulations (LES) and Reynolds-averaged Navier-Stokes simulations (RANS), we relate the forcing conditions to the formation and dynamics of the convective circulation. We find that thermal siphons are more frequent in autumn and flush the littoral region daily. Their seasonal occurrence and intensity can be predicted from the bathymetry, stratification and meteorological forcing.

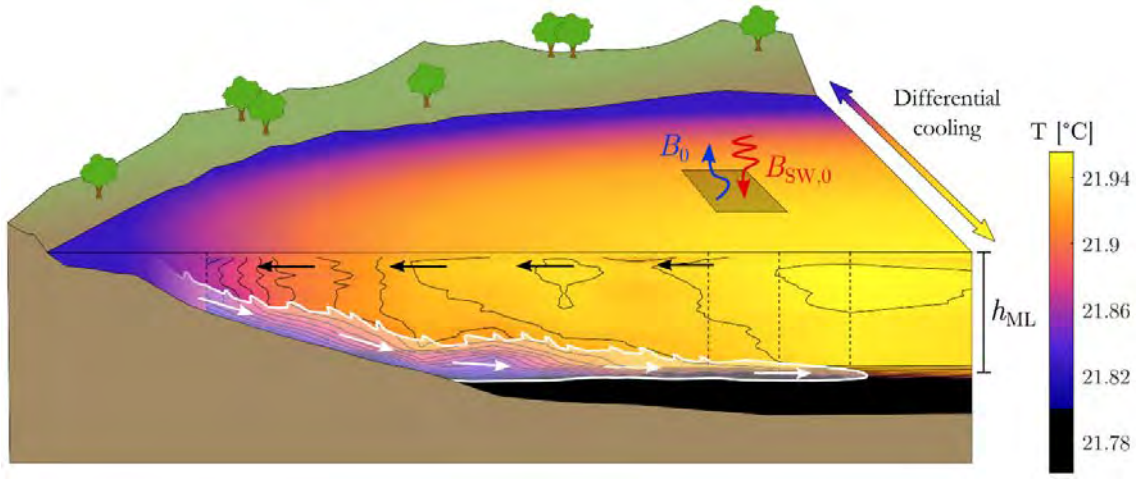

Figure 1. Schematic of the thermal siphon induced by differential cooling. The density current and the surface return flow are depicted by white and black arrows, respectively. B_0 is the surface buoyancy flux (cooling), $B_{sw,0}$ is the radiative buoyancy flux (heating) and h_{ML} is the mixed layer depth.

P 15.4
Hydrogeochemistry of Black Forest springs from Germany: Insights from physical and hydrogeochemical parameters, stable isotopes and Macroinverterbrates

Thomas Dürrenberger* & Stefanie von Fumetti**

** Geoecology Research Group, University of Basel, Klingelbergstr. 27, CH-4056 Basel (t.duerrenberger@.unibas.ch)*
*** Geoecology Research Group, University of Basel, Klingelbergstr. 27, CH-4056 Basel (stefanie.vonfumetti@unibas.ch)*

Hydrogeochemical studies of springs can provide critical information regarding sources and timing of groundwater recharge, water-rock interaction, mixing of distinct groundwater bodies and their influence on the inhabiting invertebrates. The Southern Black Forest, bordering on Switzerland, has a great diversity of geological units and springs. Macroinvertebrates, water-bulk quantity, pH, temperature, discharge, stable isotopes ($\delta^{18}O$, $\delta^{2}H$, $\delta^{13}DIC$) and 24 chemical variables will be monitored in a one-year period in 24 springs in a southeast longitudinal profile of the Black Forest. The investigated springs in the Black Forest represent waters influenced by chemical weathering of Paleozoic, Mesozoic and Cenozoic rock beds consisting of shell limestone, breccia, mudstone, granite, gneiss, shale, porphyry and acid pyroclasts. The study approach involved field sampling and in-situ measurements of physicochemical parameters followed by laboratory hydrochemical and stable isotope analyses of the spring water samples. Canonical Correspondence Analysis (CCA) will be used to assess relationships between rock layers, invertebrates and environmental conditions. First preliminary results show the spring outflows differed in hydrological conditions like water-bulk quantity as well as in the concentrations of dissolved oxygen, dissolved cations and heavy metals. The aim of the study is to understand how the hydrogeochemical processes and recharge source are critical to the sustainability and the hydrochemical evolution of springs. Further, it should be possible to link spring types to individual aquatic invertebrate groups and better understand the habitat requirements of spring species. Given the high productivity and biodiversity of springs and their highly threatened status, identifying geomorphological similarities between spring types may be important for the conservation of these important ecosystems.

P 15.5
Influence of preservatives on stable isotopes of nitrous oxide in aquatic environments

Claudia Frey [1], Weiyi Tang[2], Bess Ward[2], Moritz Lehmann[1]

[1] *Department of Environmental Science, University of Basel, Basel, Switzerland*
[2] *Department of Geosciences, Princeton University, Princeton, NJ, 08544, USA*

Nitrous oxide (N_2O) is an ozone-depleting substance and a greenhouse gas, with increasing atmospheric mixing ratios being of major concern. Aquatic environments can represent significant hotspots of N_2O but with great spatial and temporal variability. The stable isotopes of oxygen and nitrogen in N_2O provide a powerful tool to disentangle its sources and sinks in a given depth in the water column of a lake or coatsal region. In aquatic studies, the most extensively used preservation method for N_2O concentration and isotope measurements has been the usage of mercury chloride ($HgCl_2$). However, $HgCl_2$ is environmentally hazardous and the commission of the European union has agreed to reduce the usage of $HgCl_2$ in the Minamata convention in 2017. Currently, we are lacking a systematic comparison of the effect of different preservation methods on the isotopic composition of nitrogen and oxygen in N_2O.

The current study tested the influence of 4 different fixatives ($HgCl_2$, zinc chloride ($ZnCl_2$), sodium hydroxide (NaOH) and a mix of hydrochloric acid (HCl) with Sulfamic Acid) and their interaction with NO_2^- on the nitrogen and oxygen isotope composition of N_2O in surface lake and coastal water. The influence of storage length on bulk N_2O isotopes was tested for up to 6 months. Results indicate that the presence of high levels of NO_2^- alters the isotopic composition of N_2O despite the fixative. When fixed with $ZnCl_2$, storage length and low NO_2^- concentrations strongly impacted the composition of N_2O isotopes. Therefore, $ZnCl_2$ should not be used. However, NaOH had little effect on nitrogen and oxygen isotopes in N_2O providing a good alternative for $HgCl_2$.

P 15.6
Variation in Lake Geneva seston C:P as a function of phytoplankton species identity and P-levels

Geraldine Panetti[1], Fabio Correia[1], Roxane Fillion[1], Patrick Kathriner[2], Beat Muller[2], Mridul Thomas[1], Bas Ibelings[1]

[1] Department F.-A. Forel for Environmental and Aquatic Sciences, University of Geneva; [2]Department of Surface Waters, EAWAG

A team of scientists of EAWAG and UNIGE is interested to (i) verify the existence and strength of potential stoichiometric bottlenecks in the foodweb of Lake Geneva, whose occurrence might be a consequence of successful lake re-oligotrophication, and (ii) to assess to what extent a long-term increase in seston C:N.P affects zooplankton growth, restricting trophic transfer in the Lake Geneva food web. Here, we address the question to what extend the variability in C:P at seasonal time scales can be explained by dynamics in the community composition of the lake`s phytoplankton. We performed weekly sampling from LeXPLORE to obtain insight in the short term variation in C:P, which is then matched to dynamics in the phytoplankton composition. In complementary, lab-based experiments a range of species from Lake Geneva phytoplankton were grown in controlled fed-batch cultures under a large range of P-concentrations. For each of the species the C:P was measured across the full range of P-concentration, giving novel insights into the extend to which C:P varies as a function of species identity and higher order phytoplankton groups. By combining results from the LeXPLORE sampling of C:P and phytoplankton with the batch culture experiments we aim to dig deeper into the question of how phytoplankton community composition determines variation in C:P of the seston, ultimately allowing us to better understand the long term rise in C:P of the lake.

P 15.7
$RAINBOW_{FLOW}$ $CHIP_{ONLINE}$: An impedance-based biosensor for water quality monitoring using permanent fish cell lines

Jenny Maner[1,2], Carolin Drieschner[3], Christian Ebi[4], René Schönenberger[1], Levin Angst[4], Simon Bloem[4], Miguel Solsona[5], Philippe Renaud[5], Kristin Schirmer[1,2,6]

[1] *Department Environmental Toxicology, Swiss Federal Institute of Aquatic Science and Technology (Eawag), Überlandstrasse 133, CH-8600 Dübendorf (jenny.maner@eawag.ch)*
[2] *Laboratory of Environmental Toxicology, Environmental Engineering Institute, School of Architecture, Civil and Environmental Engineering, Swiss Federal Institute of Technology Lausanne, EPFL ENAC IIE TOX, Station 2, CH-1015 Lausanne*
[3] *Department of Systems Engineering, HSE·AG, Garstligweg 6, CH-8634 Hombrechtikon*
[4] *Department Urban Water Management, Swiss Federal Institute of Aquatic Science and Technology (Eawag), Überlandstrasse 133, CH-8600 Dübendorf*
[5] *Microsystems Laboratory 4, Electrical and Micro Engineering, School of Engineering, Swiss Federal Institute of Technology Lausanne, EPFL STI IMT LMIS4, Station 17, CH-1015 Lausanne*
[6] *Institute of Biogeochemistry and Pollutant Dynamics, Department of Environmental Systems Science, Swiss Federal Institute of Technology Zurich, ETHZ D-USYS IBP, Universitätstrasse 16, CH-8092 Zürich*

The aquatic environment is subject to contamination by a multitude of chemicals from a range of point and diffuse sources (Schwarzenbach et al. 2006). Fish form an integral part of the aquatic environment and are important indicators for the health of their ecosystem. As a consequence, chemical toxicity to fish is a critical component in prospective chemical risk assessment. Once present in the environment, however, chemicals occur in mixtures of regionally and temporally varying composition and concentration, making the effects on fish hard to predict. To know whether fish toxicity occurs, flexible biological monitoring sensors are therefore necessary.

The $RAINBOW_{FLOW}$ $CHIP_{ONLINE}$ is an impedance-based biosensor using live cells: an intestinal cell line from the rainbow trout (*Oncorhynchus mykiss*), RTgutGC, forms the core of this sensor. This and other fish cells have been shown to be able to predict toxic effects on whole fish (Tanneberger et al. 2013; Schug et al. 2019). The biosensor is integrated into a portable field instrument, programmed for automatic and continuous sampling, so that the cells can be exposed to surface water continually at a location of interest. Impedance sensing allows the measuring of cell viability non-invasively in real time (Tan & Schirmer 2017). Inclusion of an LTE router makes it possible to access the data remotely, allowing the observation of water quality online. The first application will be carried out on the LéXPLORE platform on Lake Geneva in September 2021 and the results will be presented here.

REFERENCES

Schug, H., Maner, J., Hülskamp, M., Begnaud, F., Debonneville, C., Berthaud, F., Gimeno, S. & Schirmer, K. 2019: Extending the concept of predicting fish acute toxicity in vitro to the intestinal cell line RTgutGC. ALTEX 37, 37-46.

Schwarzenbach, R.P., Escher, B.I., Fenner, K., Hofstetter, T.B., Johnson, C.A., Von Gunten, U. & Wehrli, B. 2006: The challenge of micropollutants in aquatic systems. Science 313, 1072-1077.

Tan, L. & Schirmer, K. 2017: Cell culture-based biosensing techniques for detecting toxicity in water. Curr. Opin. Biotechnol. 45, 59–68.

Tanneberger, K., Knöbel, M., Busser, F.J.M., Sinnige, T.L., Hermens, J.L.M. & Schirmer, K. 2013: Predicting Fish Acute Toxicity Using a Fish Gill Cell Line-Based Toxicity Assay. Environ. Sci. Technol. 47, 1110–1119.

P 15.8
PREDICTING CO_2 DYNAMICS IN LAKE GENEVA USING A DEEP LEARNING APPROACH (LSTM RNN)

Gaël Many[1], Pascal Perolo[1], Philippe Jacquet[2], Nicolas Escoffier[1], Marie-Elodie Perga[1]

[1] *IDYST, University of Lausanne, 1015, Lausanne*
[2] *DCSR, University of Lausanne, 1015, Lausanne*

Accurate predictions of CO_2 outgassing in hardwater lakes are crucial to understand whole ecosystem carbon budgets as well as to figure out the main drivers of CO_2 and the impact of their future evolution. Deep learning neural networks are now more and more used in biogeochemical applications due to the variety of their architecture that can be applied to any given problem. In this work, we used a LSTM RNN (long-short term memory recurrent neural network) deep learning approach to figure out the main drivers of CO_2 and reconstruct the CO_2 concentrations in Lake Geneva based on monthly observations from 1980 to 2020. The dataset encompasses observations from physical and biogeochemical behavior of the Lake Leman (SLH2 long-term observations), rivers input, and measurements from a local weather station. The LSTM RNN is built using the Matlab software and the deep learning toolbox. Main parameters as number of hidden layers, number of epochs, sequence length and initial learning rate are found using the Bayesian optimization (i.e. multi-parameters optimization). To avoid using covariate variables in the LSTM RNN, we use a correlation matrix to estimate the correlation between each time series. The training dataset is then divided into 5 folds. Every fold appears in the training dataset (4 times) and is used as a validation parameter (RMSE between pCO_2 predicted and observed). Ongoing results show that the LSTM RNN appears well-suited to predict CO_2 dynamics in the Lake Geneva based on multivariate time series analysis.

P 15.9
Temporal and spatial variations in the composition and fluxes of settling particles in Lake Geneva

Natacha Pasche[1], Hannah Chmiel[1], Beat Müller[2], Nathalie Dubois[2], Pierre Véron[1], Guillaume Cunillera[1]

[1] Limnology Center, EPFL, Station 2, CH-1015 Lausanne (natacha.tofield-pasche@epfl.ch)
[2] Surface waters – Research and Management, Eawag, Seestrasse 79, CH-6047 Kastanienbaum

Particulate matter in the lake water column can originate from the atmosphere, the catchment area or can be produced directly in-situ. During the settling process, this matter is exported to the deep water, and depending on its composition can be degraded. This degradation is important for the recycling of organic matter within a lake and leads to oxygen consumption. The determination of the composition of this matter and its settling rates are therefore essential to determine the fate of the different types of particles. In this study, we assessed the spatial and temporal variations of the settling matter in the water column of Lake Geneva.

In this study, we collected monthly samples of settling matter using sediment traps at two locations in Lake Geneva: in the middle of the lake (point SHL2) in 2017 at 110, 200, 290, and 306 m depth; and at the LéXPLORE platform in 2020 and 2021 at 10, 30, 50 and 100 m depth. These samples were analysed for organic and inorganic carbon, total phosphorus, total nitrogen, and biogenic silica. The collected material was composed of ~30 to 50% organic matter and carbon precipitates. The total sedimentation rates indicated a peak from June to September, which corresponds to elevated discharge of the Rhône River during the melting season. The spatial comparison showed that the pelagic location had lower settling rates than the location nearer to the shores, similar to previous observations (Graham et al. 2016). In conclusion, the sedimentation rates and composition of the settling particles in Lake Geneva varied seasonally and between years. These variabilities reflect the fluctuations from the Rhône River, the primary production and carbonate precipitation.

REFERENCES

Neil D. Graham, N. D., Bouffard, D., & Loizeau, J.-L. 2016: The influence of bottom boundary layer hydrodynamics on sediment focusing in a contaminated bay, Environ Sci Pollut Res, 23, 25412-25426.

P 15.10
Microplastics in Lake Lugano: vertical distribution and colonization by microorganisms

Federica Rotta[1], Federica Mauri[1], Livia Guerini[1], Giulia Donnarumma[1], Fabio Lepori[1], Camilla Capelli[1]

[1] Department of Environment Constructions and Design, University of Applied Sciences and Arts of Southern Switzerland, Via Flora Ruchat-Roncati 15, CH-6850 Mendrisio (federica.rotta@supsi.ch)

Microplastics are ubiquitous pollutants in aquatic environments across the globe. Compared with marine environments, data on the sources, distribution and fate of microplastics in fresh water ecosystems are still scarce. For example, the majority of microplastic research in lakes has focused only on water's surface, which may underestimate microplastics contamination across the water column. This lack of information needs to be addressed, since recent research suggests that microplastic contamination in fresh waters can be as severe as in marine systems (Li et al., 2018*).*

The potential persistence of microplastics in aquatic environment has also raised concerns because of the potential threats to biological communities and humans. When released in waters, plastic debris provide a durable substrate that can support the growth of different microorganisms, including potential pathogens (Amaral-Zettler *et al.* 2020). New evidence suggests that microbial communities may also influence the environmental fate of microplastics by modifing particles physical properties including their density, buoyancy and sinking rate. A better understanding of these interactions is therefore needed to gain insigths into the persitence, fate and potential pathogenecity of microplastics.

We present preliminary results from ongoing microplastic research in Lake Lugano (Switzerland and Italy). In this lake, microplastics are one of the major emerging environmental concerns. For example, monitoring data from 2020 indicated that the mean surface microplastic concentration (0.27 # m^{-2}) was approximately twice as high as that of other Swiss lakes. The main objectives of our research are *i)* to measure the abundance and distribution of microplastics in the water column and *ii)* to evaluate microbe-microplastics interactions.

Preliminary results suggest that microplastics occured throughout the water column (0 – 90 m depht), with concentrations decreasing with increasing depth. The analysis of environmental samples and an *in situ* experiment showed that the microplastics were colonised by a complex biological community, consisting of bacteria and algae. The effect of this biofilm on the fate and distribution of microplastics will be analysed in the next step.

The results of our project will provide a comprehensive basis for understanding and managing the environmental impact of microplastics in lakes.

REFERENCES

Amaral-Zettler, L. A., Zettler, E. R. & Mincer, T. J. (2020): Ecology of the Plastisphere. Nature Reviews Microbiology 18, 139-151.

Li, J., Liu, H., Chen, J. P. (2018): Microplastics in freshwater systems: a review on occurrence, environmental effects, and methods for microplastics detection. Water research 137, 362-374.

16. Cryospheric Sciences

Matthias Huss, Theo Jenk, Kathrin Naegeli, Nadine Salzmann, Andreas Vieli

Swiss Snow, Ice and Permafrost Society

TALKS:

16.1 Balasubramanian S., Hoelzle M., Lehning M., Bolibar J., Wangchuk S., Oerlemans J., Keller F.: Influence of meteorological conditions on artificial ice reservoir (Icestupa) evolution

16.2 Chen T.Y.: Navigating Various Machine Learning Techniques for Sea Ice Drift Forecasting in the Arctic Circle

16.3 Dall'Alba V., Neven A., Juda P., Straubhaar J., Renard P.: Basal topography simulation and ice volume estimation using advanced geostatistical methods: Application on the Tsanfleuron Glacier (Swiss Alps).

16.4 Egli P.E., Belotti B., Ouvry B., Irving J., Lane S.N.: Increasing frequency of subglacial channel collapse features at alpine glaciers

16.5 Evers L., Smets P., Assink J., Shani-Kadmiel S.: The sound of glaciers: remote and passive infrasound monitoring of glacier dynamics

16.6 Häusler M., Moser R., Fäh D.: Passive Seismic Investigations at Gemstock: Mapping and Monitoring of Permafrost

16.7 Jones N., Strozzi T.: Slope instability mapping in glacier fore-field environments of the High Valais Alps using advanced DInSAR techniques

16.8 Michel A., Gubler S., Kotlarski S., Aschauer J.,Jonas T., Lehning M., Marty C.: SPASS – A Spatial Snow Climatology for Switzerland

16.9 Naegeli K., Rietze N., Franke J., Premier V., Stengel M., Wu X., Wunderle S.: Drivers and dynamics of four decades seasonal snow cover: West, Central and East Himalaya tell different stories

16.10 Paitz P., Lindner N., Edme P., Sovilla B., Fichtner A., Walter F., Huguenin P., Hohl M.: Towards avalanche monitoring with distributed acoustic sensing

16.11 Reinthaler J., Paul F.: New Little Ice Age glacier extents for three Arctic regions

16.12 Rietze N., Wunderle S., Naegeli K., Huss M.: Seasonal Glacier Mass Balance Estimation Using AVHRR Imagery

16.13 Studemann G., Steiner L., Grimm D., Fierz Ch., Marty Ch.: Low-Cost GNSS Measurement Setup for the Determination of Water Equivalent of Snow Cover by GNSS-RTK in the Field

16.14 Tedstone A., Machguth H.: Greenland meltwaters run off from far into the percolation zone

16.15 Tollenaar V., Zekollari H., Tuia D., Lhermitte S., Tax D., Debaille V., Goderis S., Claeys P., Pattyn F.: A data-driven approach to quantifying Antarctic blue ice areas and the presence of meteorites

POSTERS:

P 16.1 Buri P., Fatichi S., Shaw T., Miles E., McCarthy M., Fyffe C., Fugger S., Ren S., Kneib M., Pellicciotti F.: Application of a high-resolution Earth surface model to simulate blue green water interactions in a glacierized Himalayan catchment

P 16.2 Fees A., van Herwijnen A., Lombardo M., Schweizer J.J.: On dynamics of glide-snow avalanche release as inferred from time-lapse photography

P 16.3 Gentizon J., Magnin F., Ravanel L., Lambiel C.: The Cryosphere of High Alpine Rock Walls: Insights From The Pointes Du Mourti (3563 M A.S.L., Switzerland)

P 16.4 Grimmer M., Baggenstos D., Schmitt J., Fischer H.: Mean Ocean Temperature (MOT) during MIS5-6 based on noble gas ratios in the EDC ice core

P 16.5 Gugerli, R., Desilets, D. and Salzmann, N.: Application of a muonic cosmic ray snow gauge to monitor the snow water equivalent on an alpine glacier

P 16.6 Guidicelli M., Huss M., Gabella M., Salzmann N.: Machine learning techniques to downscale solid precipitation from climate reanalyses generating SWE estimates over high-mountain glaciers of the world

P 16.7 Jouberton A., Shaw T.E., Miles E., Ren S., Yang W., McCarthy M., Fugger S., Dehecq A., Pellicciotti F.: Precipitation Phase Change Accelerates Glacier Mass Loss In The Southeastern Tibetan Plateau

P 16.8 Jullien N, Tedstone A., Machguth H.: Development of ice slabs in the high percolation zone of the Greenland Ice Sheet

P 16.9 Krauss F., Mächler L., Baggenstos D., Walther R., Bereiter B., Tuzson B., Emmenegger L., Schmitt J., Fischer H.: Development and application of a noble continuous laser-sublimation extraction technique coupled to a Quantum Cascade laser Spectrometer for greenhouse gas measurements (CO_2, $\delta^{13}C$, CH_4, N_2O) in ice cores

P 16.10 Machguth H., Tedstone A., Clerx N., Jullien N.: Accelerating mass loss of Greenland: Firn and the shifting runoff limit

P 16.11 Mathys T., Hilbich C., Pohl E., Hauck C., Hoelzle M.: Assessing permafrost distribution and ground ice volumes in Central Asia (Kyrgyzstan): results from a first geophysical field campaign

P 16.12 Nalivaika P., Jenk T., Schwikowski M., Eichler A.: Ice-core based modern heavy metal pollution records for the territory of the FSU

P 16.13 Simon V., Kraft T.: High-resolution analysis of the recent onset of seasonal microseismicity in the Mt. Blanc Massif

P 16.14 Singer T., Jenk T.M., Schwikowski M.: Towards a near-source reconstruction of pre-industrial to industrial changes in carbonaceous aerosols from ice core archives

P 16.15 Søndergaard A.S., Egholm D.L., Larsen N.K.: Million year Greenland wide ice sheet cover from $^{26}Al/^{10}Be$ ratios in bedrock and inverse modelling

P 16.16 Wicky J., Hauck C.: Ground ice can be formed and maintained by air convection in low elevation talus slopes

16.1
Influence of meteorological conditions on artificial ice reservoir (Icestupa) evolution

Suryanarayanan Balasubramanian[1,3], Martin Hoelzle[1], Michael Lehning[2], Jordi Bolibar[4], Sonam Wangchuk[3], Johannes Oerlemans[4] and Felix Keller[5,6]

[1] *University of Fribourg, Fribourg, Switzerland (suryanarayanan.balasubramanian@unifr.ch)*
[2] *WSL Institute for Snow and Avalanche Research, Davos, Switzerland*
[3] *Himalayan Institute of Alternatives Ladakh, Leh, India*
[4] *Institute for Marine and Atmospheric Research, Utrecht University, Utrecht, The Netherlands*
[5] *Academia Engiadina, Samedan, Switzerland*
[6] *ETH, Zürich, Switzerland*

Mountain communities in Ladakh, India have been using Artificial Ice Reservoirs (AIRs) for additional irrigation water supply. However, there is a large variability associated with this water supply due to the local weather influences of the construction location chosen. This study compares the evolution of AIRs built in Ladakh, India (IN21) and Guttannen, Switzerland (CH20, CH21) based on the influence of different surface processes responsible for their spatial and temporal ice volume variance using a surface energy balance model. Model input consisted of meteorological data in conjunction with fountain discharge rate (mass input of an AIR). Model calibration and validation were performed through ice volume and area measurements taken from several Uncrewed Aerial Vehicle (UAV) flights. The model achieved a root mean squared error (RMSE) within 11 % of the maximum ice volume with the UAV ice volume observations for all the three AIRs. The location in Ladakh, with a maximum ice volume around six times larger, was more favourable compared to the Guttannen site. However, the corresponding water losses for all the AIRs were > 75 % of the total fountain discharge due to high fountain water runoff. Drier and colder locations in relatively cloud free regions are expected to produce AIRs with a faster freezing rate and slower melting rate respectively. This is a promising result for dry mountain regions, where AIR technology could provide a relatively cheap and sustainable strategy to alleviate climate change induced water stress.

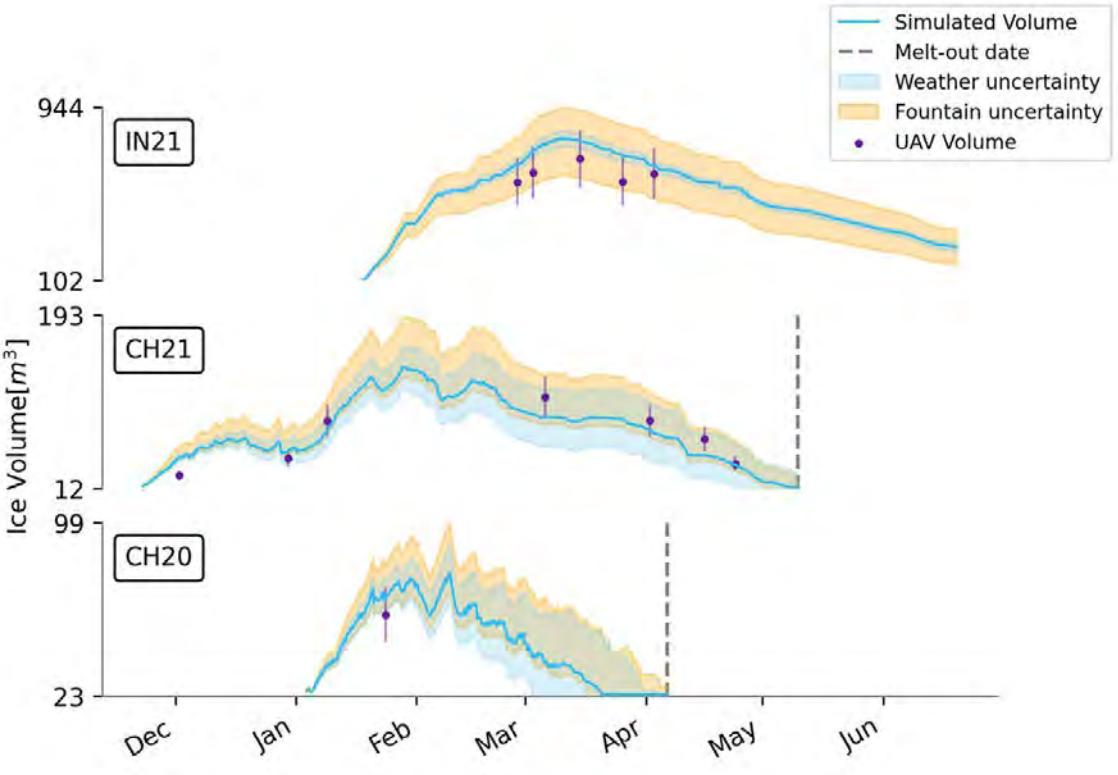

Figure 1. Simulated ice volume during the lifetime of the AIRs (blue curve). The shaded regions (light blue and orange) represent the 90 % prediction interval of the AIR ice volume caused by the variation in weather and the fountain parameters. The lower bounds of the y-axis represents AIR dome volume. Violet points indicate the UAV ice volume observations. The grey dashed line represents the observed melt-out date for each AIR.

16.2
Navigating Various Machine Learning Techniques for Sea Ice Drift Forecasting in the Arctic Circle

Thomas Y. Chen[1]

[1] *Academy for Mathematics, Science, and Engineering, 520 W Main Street, Rockaway, NJ 07866, USA*

The movement of sea ice is influenced by a number of factors, from winds to ocean currents. As climate change continues to occur rapidly, understanding sea ice drift in the Arctic is a key parameter to understanding the effects of rising temperatures in the region. Recent literature has shown that the Arctic and the Antarctic are most affected by global warming, which raises questions regarding climate justice, as most of the carbon emissions causing anthropogenic climate change are produced in other regions. To analyze this impact, we employ artificial intelligence to predict sea ice drift velocity based on external features. Machine learning is the process of computers gaining insights by seeing and correlating large quantities of data. Using external parameters, including wind speed, and drift velocity ground truth as the inputs of the model, we train multiple different architectures and compare the results. In particular, we experiment with a convolutional neural network (CNN), a random forest (RF), and a support vector machine (SVM). We also experiment with various model specifications. This research leads to a greater understanding of the Arctic's response to climate change.

16.3
Basal topography simulation and ice volume estimation using advanced geostatistical methods: Application on the Tsanfleuron Glacier (Swiss Alps).

Valentin Dall'Alba[1], Alexis Neven[1], Przemysław Juda[1], Julien Straubhaar[1] and Philippe Renard[1,2]

[1] *Center of Hydrogeology and Geothermics, University of Neuchâtel, Neuchâtel Switzerland (valentin.dallalba-arnau@unine.ch)*
[2] *Department of Geosciences, University of Oslo, Oslo Norway*

In Alpine environments, changes in precipitation and temperature due to global climatic changes have modified the glaciers' mass balance equilibrium, resulting in the most likely disappearance of the majority of them in the next decades. With the disappearance of these ice sheets, monitoring of glacier thickness and their associated ice volume are essential for future water resources management, sediment production, and slope stabilization assessment. Moreover, the estimation of the basal topography can play an essential role in the sub-hydrogeological flow and sediment transport.

In 2019, Ground Penetrating Radar (GPR) lines were acquired on the Tsanfleuron Glacier (Switzerland). GPR measurements provide thickness data along the acquisition lines. An interpolation step is then required to produce a spatially continuous basal map of the glacier. The Tsanfleuron Glacier lays on homogeneous limestone bedrock, with complex karstic geomorphological features, which can be tedious to model using simple interpolation approaches.

This study investigates the applicability and advantages of Multiple Point Statistics (MPS) simulations to interpolate the complex glacier basal topography using GPR lines as conditioning data and the uncovered bedrock as training image. Variogram-based methods such as Sequential Gaussian Simulation (SGS) and Kriging estimation are also compared to the MPS approach, on both synthetic - with known topography - and real cases. These methods are compared using both pixel-based quality indicators and global volume estimation.

Depending on the chosen interpolation strategy, the calculated ice volumes and the basal topography can differ significantly. This study shows the benefits of using advanced geostatistical algorithms for the reproduction of complex sub-glacial structures. Moreover, the use of a stochastic approach allows us to quantify the uncertainty relative to the geostatistical model. Using the modeled MPS basal topography and a high-resolution DEM acquired from a UAV in 2019, the ice volume for the Tsanfleuron Glacier was estimated to be 113.9 ± 1.6 Mio m3 in 2019. All the details of the methodology and results are given in Neven et al. (2021).

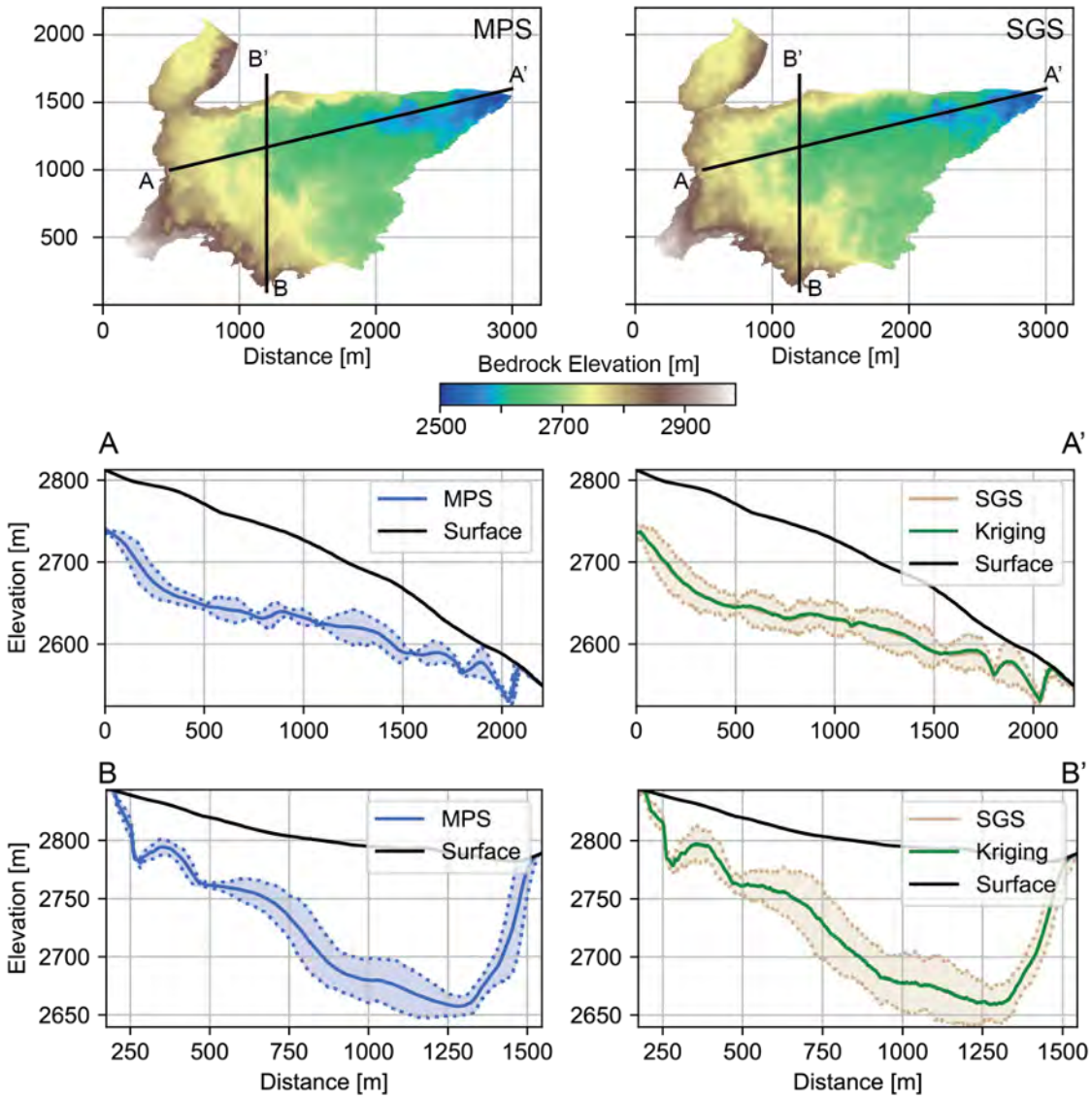

Figure 1. Simulated basal topography of the Tsanfleuron Glacier with the MPS method (in blue) and with the SGS method (in brown). The kriging estimated topography is displayed alongside the SGS simulation in green.

REFERENCES

Neven, A., Dall›Alba, V., Juda, P., Straubhaar, J., & Renard, P. (2021). Ice volume and basal topography estimation using geostatistical methods and GPR measurements: Application on the Tsanfleuron and Scex Rouge glacier, Swiss Alps. The Cryosphere Discussions, 1-27.

16.4
Increasing frequency of subglacial channel collapse features at alpine glaciers

Pascal E. Egli[1], Bruno Belotti[2], Boris Ouvry[3], James Irving[4], Stuart N. Lane[1]

[1] *Institute of Earth Surface Dynamics, University of Lausanne, Switzerland (pascal.egli@unil.ch)*
[2] *Department of Geological Sciences, University of Idaho, Idaho, USA*
[3] *Institute of Geography, University of Zurich, Switzerland*
[4] *Institute of Earth Sciences, University of Lausanne, Switzerland*

The retreat of temperate Alpine glaciers has increased markedly since the late 1980s, and is commonly linked to the effects of rising temperature on surface melt. Much less considered are processes associated with glacier surface collapse. A detailed survey of 22 retreating Swiss glaciers suggests that snout marginal collapse events have increased in frequency since the late 1980s, driven by ice thinning and reductions in glacier-longitudinal ice flux. Detailed measurement of a collapse event at one glacier with Uncrewed Aerial Vehicles and ablation stakes showed high rates of vertical ice deformation at the main subglacial channel, the position of which was derived via Ground Penetrating Radar.
With low rates of longitudinal ice flux and vertical creep closure, deformation was insufficient to counteract the melt-out of this channel in the snout marginal zone and avoid channel collapse due to melt and block caving. We hypothesize that such channels maintain contact between subglacial ice and the atmosphere, allowing greater incursion of warm air up-glacier, thus enhancing melt from below. The associated enlargement of subglacial channels at glacier snouts leads to surface collapse and the removal of ice via fluvial processes.

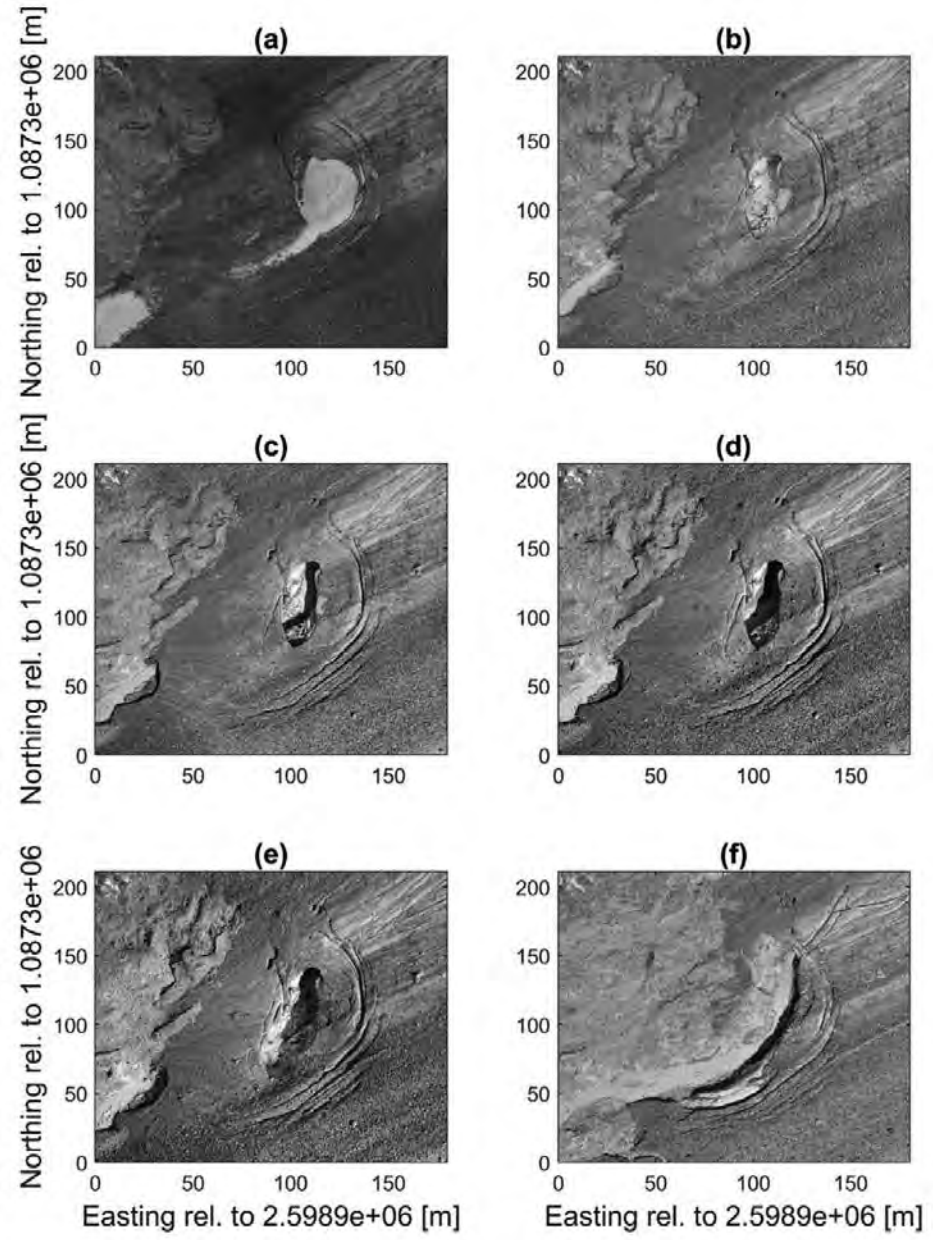

Figure 1. Orthophotos of the ice marginal area of Glacier d'Otemma showing the evolution of a subglacial channel collapse feature. The imagery extends from 3rd July 2018 to 31st July 2019. Images were acquired on (a) 3.7.2018, (b) 7.8.2018, (c) 12.8.2018, (d) 20.8.2018, (e) 23.8.2018, (f) 31.7.2019.

16.5
The sound of glaciers: remote and passive infrasound monitoring of glacier dynamics

Läslo Evers[1,2], Pieter Smets[2], Jelle Assink[1], Shahar Shani-Kadmiel[1]

[1] Royal Netherlands Meteorological Institute (KNMI), De Bilt, the Netherlands (evers@knmi.nl)
[2] Delft University of Technology, Delft, the Netherlands

The International Monitoring System (IMS) is a global sensor network to verify the Comprehensive Nuclear-Test-Ban Treaty. The infrasound component of the IMS is not only capable of detecting nuclear-test explosions, a wide variety of natural and anthropogenic sources are continuously measured by the network.

A rich infrasonic wavefield is recorded by station I18DK, located in Northwest Greenland. I18DK is located in an unique environment far above the polar circle. Operations started in 2004, enabling long-term monitoring of its surroundings and building a statistically reliable soundscape. The infrasonic recordings reveal lots of infrasonic activity during summer, while the surroundings are infrasonically quiet in winter. Array processing is applied to the recordings of I18DK to identify different sources of infrasound and to suppress noise by enhancing the signal-to-noise ratio. The sounds appear associated to glaciers around I18DK, active during the melting season. Different mechanisms like run-off and calving generate the detected infrasound. It is found that sea and land-terminating glaciers leave a distinctly different infrasonic signature.

The simultaneous observation of sounds from different glaciers over a long time period paves the way for studying the melting behavior in the Arctic cryosphere under a changing climate. Between and within the years a large variability is found in infrasonic activity of the glaciers. Such activity is quantified in terms glacier dynamics by comparing it to both modeled and locally measured run-off.

16.6
Passive Seismic Investigations at Gemsstock: Mapping and Monitoring of Permafrost

Mauro Häusler[1], Raphael Moser[1,2], Donat Fäh[1]

[1] *Swiss Seismologial Service, Institute of Geophysics, ETH Zurich, Sonneggstrasse 5, CH-8092 Zürich (mauro.haeusler@sed.ethz.ch)*
[2] *Laboratory of Hydraulics, Hydrology and Glaciology, ETH Zurich, Hönggerbergring 26, CH-8093 Zürich*

Degrading alpine permafrost is a major driver for the destabilization of rock slopes and threatens infrastructure in high alpine areas. Therefore, mapping and monitoring the presence of permafrost is a prerequisite for sound rockfall and landslide hazard assessment. Recordings of ambient vibrations were observed to be sensitive to thermal conditions and potentially to the presence of pore ice and permafrost. For instance, the seismic wavefield amplification increases during thawing periods, while at the same time the resonant frequency of unstable rock volumes is lowered (Weber et al., 2019).

Here, we analyze ambient vibrations recorded by a temporary seismic array deployed at the Gemsstock cable car top station in Switzerland (2960 m a.s.l.). We show that seismic amplifications are increased on the southern slope of the ridge, where the permafrost and ground ice map (Kenner et al., 2019) indicates ground temperatures betweeen 0 and +1°C with possible patchy permafrost. In contrast, no distinct amplifications are visible in the northern slope, where permafrost is present (Figure 1). Therefore, measuring ambient vibrations might support local mapping of permafrost-rich areas.

In addition, we installed a permanent seimic station on the northeastern ridge of Gemsstock in fall 2018 and monitor the dynamic respone of a small (300 to 400 m^3) rock pillar in near real-time by using normal mode monitoring (Häusler et al., 2021). We observe strong annual variations of resonant frequencies with lowest values reached in fall just before deaily mean temperatures drop below 0°C. Here, we present preliminary results of ongoing slope monitoring and provide first interpretations with respect to the influence of permafrost.

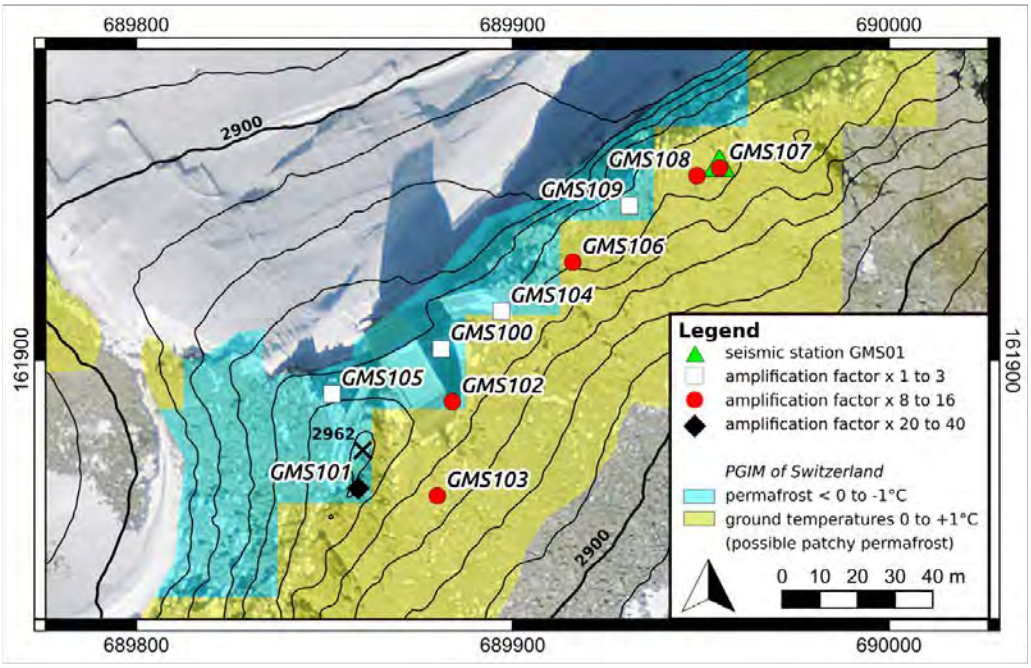

Figure 1. Orthoimage of Gemsstock with the Permafrost and Ground Ice Map (PGIM) by Kenner et al. (2019) and sensor locations of the temporary seismic array. The symbols represent clusters of similar seismic amplification characteristics. Note the higher amplification at the southside of the ridge, where no continuous permafrost is present. Geodata source: Federal Office of Topography, figure modified from Häusler (2021).

REFERENCES

Häusler, M. 2021: On the dynamic response of unstable rock slopes: characterization, monitoring and numerical modeling based on ambient vibrations, ETH dissertation 27855 (submitted).

Häusler, M., Clotaire, M., Burjánek, J., & Fäh, D. 2021: Monitoring the Preonzo rock slope instability using resonance mode analysis, Journal of Geophysical Research: Earth Surface, 126, e2020JF005709.

Kenner, R., Noetzli, J., Hoelzle, M., Raetzo, H., & Phillips, M. 2019: Distinguishing ice-rich and ice-poor permafrost to map ground temperatures and ground ice occurrence in the Swiss Alps, The Cryosphere, 1925-1941.

Phillips, M., Haberkorn, A., Draebing, D., Krautblatter, M., Rhyner, H., & Kenner, R. 2016: Seasonally intermittent water flow through deep fractures in an Alpine rock ridge: Gemsstock, central Swiss Alps, Cold Regions Science and Technology, 125, 117-127.

Weber, S., Fäh, D., Beutel, J., Faillettaz, J., Gruber, S., & Vieli, A. 2018: Ambient seismic vibrations in steep bedrock permafrost used to infer variations of ice-fill in fractures, Earth and Planetary Science Letters, 501, 119-127.

16.7
Slope instability mapping in glacier fore-field environments of the High Valais Alps using advanced DInSAR techniques

Nina Jones[1], Tazio Strozzi[1]

[1] *Gamma Remote Sensing AG, Worbstrasse 225, CH-3074 Gümligen (jones@gamma-rs.ch; strozzi@gamma-rs.ch)*

Slope instabilities increasingly develop in glacier fore-field environments due to the observed atmospheric warming and associated deglaciation effects. De-buttressing effects due to retreating glaciers as well as degrading permafrost and destabilising rock glaciers can induce slope failures in the generally steep and rough terrain typically found in high mountain glacial regions. As part of ESA's research project *Glacier Science in the Alps (AlpGlacier, https://eo4society.esa.int/projects/alpglacier)*, we detect and map slope instabilities in the High Valais Alps region in order to assess associated geohazards. Popular and efficient methods to undertake such mapping of regional, inaccessible areas are related to satellite differential synthetic aperture radar interferometry (DInSAR) (Wasowski & Bovenga 2014).

In our contribution, we will present results from standard and advanced DInSAR analyses of the Valais High Alps region. In particular, we applied differential interferometry, multi-looked temporal interferometry (MTI) and persistent scatterer interferometry (PSI) using ESA's Sentinel-1 satellite constellation. Sentinel-1 ensures systematic data coverage of the High Valais Alps since 2015, acquiring SAR images with a revisit time of 6 to 12 days at C-band wavelength. This allows the detection of slope instabilities and generation of displacement maps to show the spatial distribution of surface movement in glacier fore-field environments. In addition, we will present time series results of particular features of interest to highlight their temporal evolution and understand associated geohazards. In light of these results, we will outline the practical considerations associated with the use of DInSAR techniques in mountainous regions and discuss the advantages and disadvantages of each method.

Standard DInSAR involves the generation of differential interferograms of a certain time frame defined by the selected temporal baselines, and gives a first indication of slope movement through the depiction of coloured fringes (Strozzi et al. 2010). In mountainous areas, however, DInSAR is strongly affected by decorrelation effects related to snow and vegetation cover, atmospheric artifacts and geometric distortions. In order to retrieve a more precise displacement map, advanced DInSAR techniques are applied. MTI stacks differential interferograms according to selected baselines to reduce phase noise and increase the signal to noise ratio (SNR), thus more clearly highlighting surface movement. PSI retrieves deformation rates based on selected persistent targets that retain a high coherence and scattering behaviour in multiple SAR images and thus also ensures relatively high coherence and SNR (Berardino et al. 2002, Ferretti et al. 2001, Wasowski & Bovenga 2014). Both these techniques generate one-dimensional displacement maps in the satellite's line of sight (LOS) direction that allow the extraction of time series over the period of available input data at specific locations, enabling an evaluation of the progressive spatial and temporal evolution of certain slope instabilities. Due to their application in mountainous areas, however, they are still subjected to data loss due to geometric distortions and some decorrelation effects. These limitations can partly be overcome by using other remote sensing methods, for example digital image correlation (DIC) (Manconi et al. 2018), which combines two images of different dates, either SAR or optical, and tracks their offset between pixels to determine surface displacement. Contrary to DInSAR techniques, DIC allows extraction of movement in two dimensions, i.e., in horizontal ground range and azimuth direction when based on SAR data and East-West and North-South directions for optical data. DIC thus constitutes a valuable and complementary technique to advanced DInSAR methods and is frequently applied in comprehensive remote sensing slope instability analyses.

REFERENCES

Berardino P, Fornaro G, Lanari R, Sansosti E (2002) A new algorithm for surface deformation monitoring based on small baseline differential SAR interferograms. IEEE Trans Geosc Remote Sens 40, 2375-2383.

Ferretti A, Prati C, Rocca F (2001) Permanent scatterers in SAR interferometry. IEEE Trans Geosc Remote Sens 39, 8-20.

Manconi A, Kourkouli P, Caduff R, et al (2018) Monitoring Surface Deformation over a Failing Rock Slope with the ESA Sentinels: Insights from Moosfluh Instability, Swiss Alps. Remote Sens 10, 672.

Strozzi T, Delaloye R, Kääb A, et al (2010) Combined observations of rock mass movements using satellite SAR interferometry, differential GPS, airborne digital photogrammetry, and airborne photography interpretation. J Geophys Res, 115, F01014.

Wasowski J and Bovenga F (2014) Investigating landslides and unstable slopes with satellite Multi Temporal Interferometry: Current issues and future perspectives. Eng Geol 174,103–138.

16.8
SPASS – A Spatial Snow Climatology for Switzerland

Adrien Michel[1,2], Stefanie Gubler[3], Sven Kotlarski[3], Johannes Aschauer[1], Tobias Jonas[1], Michael Lehning[1,2], Christoph Marty[1]

[1] SLF, WSL-Institut für Schnee- und Lawinenforschung, 7260 Davos, (adrien.michel@wsl.ch)
[2] CRYOS, École Polytechnique Fédérale de Lausanne, 1001 Lausanne
[3] Federal Office of Meteorology and Climatology MeteoSwiss, 8058 Zürich-Flughafen

The SPASS research project between SLF and MeteoSwiss aims at developing a daily gridded snow dataset for Switzerland on a climatological scale (i.e., since 1961) based on the model system currently employed by the operational snow-hydrological service model (OSHD) of SLF.

Snow water equivalent (SWE) is modelled using the OSHD model framework. Usually, the OSHD system (referred to as OSHD-EKF) uses sequential data assimilation methods to incorporate available snow measurements into their models (Magnusson et al., 2014). However, over longer time scales, the use of data assimilation creates spatiotemporal inconsistencies, as the availability of snow observations constantly changes over time. For this reason, the present project uses a “climatological” version of OSHD (referred to as OSHD-CL), driven by daily gridded temperature and precipitation datasets developed by MeteoSwiss (TabsD and RhiresD) and thus available since 1961, that runs without the assimilation of snow observations. Instead, we use spatially-explicit homogenization procedures to correct for biases in these offline simulations.

In order to enhance the output of OSHD-CL, the simulated OSHD-CL SWE fields are corrected using OSHD-EKF data as a training dataset. For this purpose, OSHD-EKF is run over a 22-year period (1998-2020) assimilating data from a fixed set of 320 snow stations, and OSHD-CL is then mapped to OSHD-EKF through quantile mapping. The quantile mapping method applied is similar to the one used for the CH2018 dataset, but adapted for snow. We present here the first results of this research project.

REFERENCES

Magnusson, J., Gustafsson, D., Hüsler, F., and Jonas, T. 2014: Assimilation of point SWE data into a distributed snow cover model comparing two contrasting methods, Water Resour. Res., 50, 7816–7835, doi:10.1002/2014WR015302.

CH2018. 2018: CH2018 – Climate Scenarios for Switzerland, Technical Report, National Centre for Climate Services, Zurich, 271 pp. ISBN: 978-3-9525031-4-0

16.9
Drivers and dynamics of four decades seasonal snow cover: West, Central and East Himalaya tell different stories

Kathrin Naegeli[1,2], Nils Rietze[1,2], Jörg Franke[1,2], Valentina Premier[3], Martin Stengel[4], Xiaodan Wu[1,5], Stefan Wunderle[1,2]

[1] *Department of Geography, University of Bern, Hallerstrasse 12, CH-3012 Bern, (kathrin.naegeli@giub.unibe.ch)*
[2] *Oeschger Centre for Climate Change Research, University of Bern, Hochschulstrasse 4, CH-3012 Bern*
[3] *Eurac Institute for Earth Observation, Viale Druso 1, IT-39100 Bolzano*
[4] *Deutscher Wetterdienst, Frankfurter Str. 135, DE-63067 Offenbach am Main*
[5] *College of Earth and Environmental Sciences, Lanzhou University, Gansu Province Tianshui South Road No. 222, Lanzhou City*

The Hindu Kush Himalaya (HKH), the worlds 'water tower', contains the largest volume of snow and ice outside of the polar ice sheets. Due to the complex topography and great spatial extent the HKH is characterised by variable temperature and precipitation pattern and thus exhibits large heterogeneity in the presence of seasonal snow cover (SSC). In this study, we provide a comprehensive assessment of the SSC dynamics in the HKH. For the first time, thanks to the unique spatio-temporally resolved data basis over multiple climate periods, the high variability of SSC emphasising a complex interplay between regional climate, continental warming trends, and influence of circulation pattern for precipitation events is unravelled.

Our results are based on Advanced Very High Resolution (AVHRR) data, providing daily, global imagery at a spatial resolution of 5 km from 1982 up to today. This unique dataset is exceptionally valuable to derive pixel-based SSC information at great spatial and long temporal scale (Naegeli et al. 2021). Calibrated and geocoded reflectance data and a consistent cloud mask, derived in the ESA CCI cloud project, are used (Stengel et al. 2020). A temporal gap-filling was applied to mitigate the influence of clouds. Reference snow maps from high-resolution optical satellite data as well as in-situ station data were used to validate the time series (Wu et al. 2021).

We investigate SSC phenology, which is directly linked to climate change and thus of high relevance for seasonal water storage and mountain streamflow. Our assessment reveals strong SSC dynamics at all time scales. Large difference in the amount and long-term trends of SSC across the Himalaya from west to east are observed. Linking our satellite-based snow cover with temperature and precipitation data we shed light on the nonuniform behaviour of SSC in times of global atmospheric warming. We find a significant decline in snow cover area percentage during summer months and a decreasing tendency from mid-spring to mid-fall indicating a shift in seasonality. Thanks to the uniquely spatio-temporally resolved dataset, we can highlight the complex behaviour of SSC and emphasise that recently observed extreme events can be expected to reoccur.

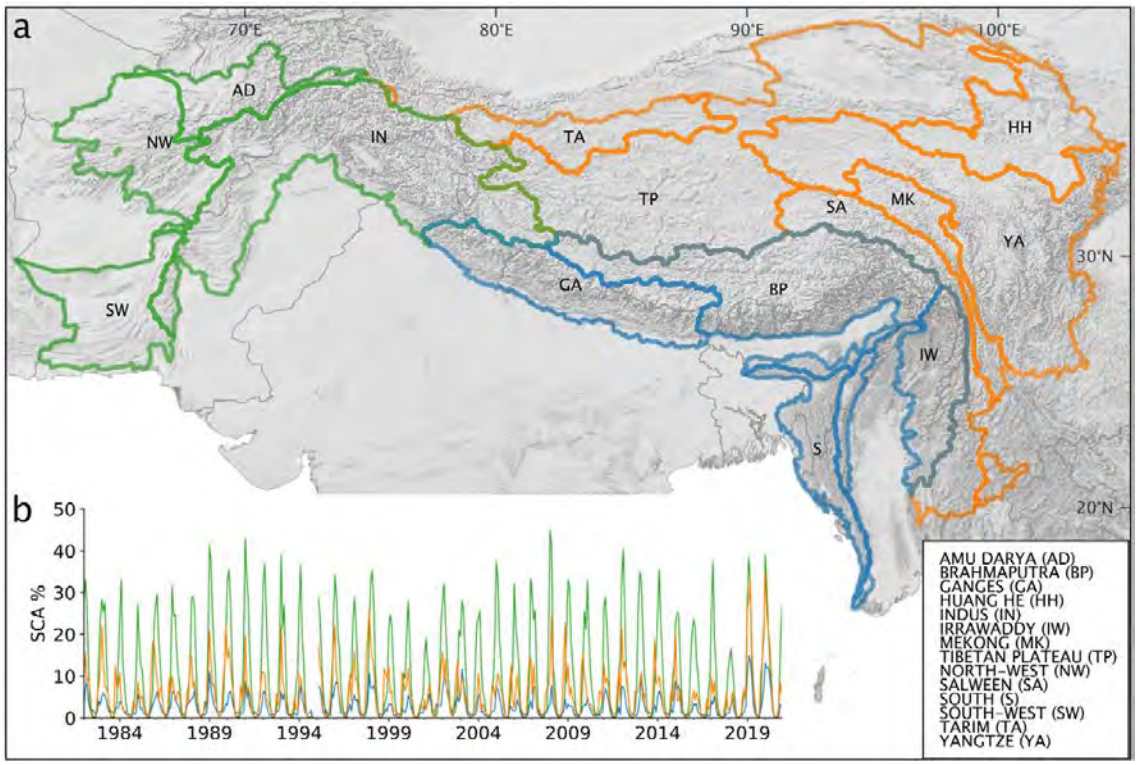

Figure 1. (a) The Hindu Kush Himalaya and the greater regions West (green), Central (blue) and East (orange). (b) Regional monthly mean snow cover area percentage time series over the study period 1982-2020.

REFERENCES

Naegeli, K., C. Neuhaus, A.-B. Salberg, G. Schwaizer, A. Wiesmann, S. Wunderle, and T. Nagler. 2021: ESA Snow Climate Change Initiative (Snow_cci): Daily Global Snow Cover Fraction - Snow on Ground (SCFG) from AVHRR (1982 - 2019), Version1.0, https://doi.org/10.5285/5484dc1392bc43c1ace73ba38a22ac56.

Stengel, Martin, Stefan Stapelberg, Oliver Sus, Stephan Finkensieper, Benjamin Würzler, Daniel Philipp, Rainer Hollmann, Caroline Poulsen, Matthew Christensen, and Gregory McGarragh. 2020: Cloud_cci Advanced Very High Resolution Radiometer Post Meridiem (AVHRR-PM) Dataset Version 3: 35-Year Climatology of Global Cloud and Radiation Properties. *Earth System Science Data* 12: 41–60, https://doi.org/10.5194/essd-12-41-2020.

Wu, X, K Naegeli, C Marin, and S Wunderle. 2021: Evaluation of snow extent time series derived from AVHRR GAC data (1982-2018) in the Himalaya-Hindukush. *The Cryosphere*, 1–38, https://doi.org/10.5194/tc-2021-46.

16.10
Towards avalanche monitoring with distributed acoustic sensing

Patrick Paitz[1], Nadja Lindner[1], Pascal Edme[1], Betty Sovilla[2], Andreas Fichtner[1], Fabian Walter[2], Pierre Huguenin[2] and Michael Hohl[2]

[1] *Seismology and Wave Physics, Institute of Geophysics, D-ERDW, ETH Zürich, Sonneggstrasse 5, CH-8092 Zürich (patrick.paitz@erdw.ethz.ch)*
[2] *WSL Institute for Snow and Avalanche Research SLF, Birmensdorf / Sion / Davos Dorf, Switzerland*

Since alpine mass movements such as avalanches and debris-flows are hard to predict, they pose a significant hazard to both the population as well as critical infrastructure - especially in alpine areas.

Existing monitoring solutions of snow avalanches include cameras, radar and infrasound sensors. Such measurements are limited to observations above or on the surface, which is why seismic sensors have gained an increase in popularity for mass-movement monitoring since they have the capability to also capture sub-surface processes. Sparse seismic networks are successfully used to detect and characterize avalanches locally, but they lack in spatial resolution and extent. Furthermore, their deployment in difficult terrain is not straightforward.

To increase the resolution and extent, we propose the use of Distributed Acoustic Sensing (DAS) to measure and monitor avalanche-induced ground motion. DAS is a technology to measure strain or it's spatial derivative utilizing backscattered light along a fiber-optic cable. This technology therefore allows a conventional fiber-optic cable to be turned into a distributed "seismic antenna", with unprecedented spatial (sub-meter) and temporal (up to kHz) resolution and great spatial extent (up to tens of kilometers of range).

During winter 2020/2021 we have recorded avalanches at the avalanche test site in the Vallée de la Sionne (CH) operated by the Swiss Federal Institute for Forest, Snow and Landscape Research (WSL) with such a DAS system. We have been passively monitoring a 700 m long stretch of fiber-optic cable and were able to record a wide range of different avalanches signals.

In this initial analysis, we discuss and analyze different avalanche types and compare our DAS measurements to conventional radar observations. We highlight the capabilities of DAS for avalanche monitoring, avalanche detection, surge propagation speed estimation and shallow subsurface tomography. Based on our results, we believe that DAS has the potential to revolutionize the field of alpine mass-movement monitoring and event detection due to its unprecedented resolution and detection capabilities.

16.11
New Little Ice Age glacier extents for three Arctic regions

Johannes Reinthaler[1] and Frank Paul[1]

[1] *Department of Geography, University of Zurich, Winterthurerstr. 190, CH-8057 Zurich (johannes.reinthaler@geo.uzh.ch)*

Most glaciers in the world reached their Holocene maximum extent during the so-called Little Ice Age (LIA). A comparison to modern glacier extents reveal insights into the climatic changes that were responsible for the observed glacier changes. Such analysis have already been performed and published for several regions in the world, but the digital outlines were often not forwarded to a data repository and many regions are not covered at all. For this study we have compiled an overview on already existing (i.e. digitally available) and only published LIA glacier extent datasets and identified remaining data gaps. In the framework of the Horizon2020 project PROTECT we have collected digital outlines from published studies and created new LIA glacier outlines for several selected regions that were still sparsely covered. The new dataset will provide a more comprehensive overview on glacier changes since the LIA and provided to the GLIMS glacier database for long-term storage and easy access.

In this study, we present what has been collected so far and the new datasets we created for Alaska, Baffin Island and Novaya Zemlya. The main data sources for the manual digitizing were the very high-resolution ArcGIS imagery base layer, supplemented by Sentinel-2 images, the ArcticDEM and a selection of historic maps. Geomorphological indicators (trimlines, moraines, vegetation free zones) and glaciological considerations were applied to guide the digitizing. Geolocation uncertainties were determined against independent data sources. The possible timing of the former maximum extents was obtained from the literature to the extent possible, but here large uncertainties remain.

In total, LIA outlines for 371 glaciers were digitized which now broke apart into 710 entities due to successive glacier shrinkage and split. The related relative area change was -20%, -15% and -26% for Alaska, Baffin Island and Novaya Zemlya, respectively. Further LIA maximum extents will be digitized to have at least one dataset available in each of the 19 first order regions of the Randolph Glacier Inventory (RGI).

16.12
Seasonal Glacier Mass Balance Estimation Using AVHRR Imagery

Nils Rietze[1,2], Stefan Wunderle[1,2], Kathrin Naegeli[1,2], Matthias Huss[3,4,5]

[1] Institute of Geography, Remote Sensing Research Group, University of Bern, Hallerstrasse 12, CH-3012 Bern (nils.rietze@giub.unibe.ch)
[2]Oeschger Centre for Climate Change Research, University of Bern, Hochschulstrasse 4, CH-3012 Bern
[3]Department of Geosciences, University of Fribourg, Ch. du Musée 4, CH-1700 Fribourg
[4]Laboratory of Hydraulics, Hydrology and Glaciology, ETH Zurich, Hönggerbergring 26, CH-8093 Zurich
[5] Swiss Federal Institute for Forest Snow and Landscape Research WSL, Zürcherstrasse 111, CH-8903 Birmensdorf

Understanding the seasonal glacier mass balance is crucial to decompose the drivers of glacier mass loss in mountain ranges worldwide. Resolving mass changes at seasonal level demands for repetitive and sustained observations on glaciers both in winter and summer. Performing seasonal field measurements on a regional level is logistically impractical and often limited by the accessibility of glaciers. Recent developments in remotely sensed mass balances (MB) offer a new technique to derive spatially comprehensive and temporally resolved estimates of annual and in some regions seasonal MB. This work presents an extensive collection of seasonal and annual MB derived from a 38-year long snow cover archive of 1 km and 4 km spatial resolution from the Advanced Very High Resolution Radiometer instrument. The linear relation between “regional mean snowline elevations” from AVHRR snow maps and observed MB is of excellent quality and can therefore be exploited to model mass balances from 1982 to 2019. This study was then able to extrapolate *in situ* MB to 92 % of the glacierized surface in the European Alps and a selection of 149 glaciers in the Gangotri range in the Himalaya. A thorough validation of the resulting mass balances was conducted and revealed that the extrapolation schemes can accurately mimic the long-term mass balance behaviour. The coarser snow cover maps of the Himalaya were capable of reproducing the incomplete observed mass changes on the five monitored glaciers. The wealth of data produced in this study calls for further MB assessments using the global AVHRR snow maps in mountain ranges across the world.

REFERENCES

Drolon, V., Maisongrande, P., Berthier, E., Swinnen, E. & Huss, M. Monitoring of seasonal glacier mass balance over the European Alps using low-resolution optical satellite images. J. Glaciol. 62, 912–927 (2016).

16.13
Low-Cost GNSS Measurement Setup for the Determination of Water Equivalent of Snow Cover by GNSS-RTK in the Field

Géraldine Studemann[1], Ladina Steiner[2], David Grimm[1], Charles Fierz[3], and Christoph Marty[3]

[1] Institue of Geomatics, University of Sciences and Arts of Northwestern Switzerland (FHNW), Hofackerstrasse 30, CH-4132 Muttenz (geraldine.studemann@students.fhnw.ch)
[2] Alfred Wegener Institute, Helmholtz Centre for Polar and Marine Research, Am Alten Hafen 26, D-27568 Bremerhaven
[3] WSL Insitute for Snow and Avalanche Research SLF, Flüelastrasse 11, CH-7260 Davos Dorf

The quantity of snow and the amount of water stored inside the snow cover is strongly influencing the flood development during the season of snow melt. By assessing early on the water equivalent of snow cover (SWE) in the mountain regions, the risks of high floods can be reduced due to appropriate safety measurements. Lately, sub-snow GNSS techniques – often using high-end systems – are proposed to evaluate liquid water content or/and SWE. This technique is affordable, flexible, and provides accurate and continuous observations independent on weather conditions.

The potential benefit of phase-based differential GNSS processing is evaluated by temporaly placing one GNSS antenna underneath the snowpack, instead of installing the low-cost GNSS antenna during the snow-free season and keeping it there for the whole snow season. Therefore, the low-cost antenna is placed below the snow cover through a borehole only when being in the field for a planned measurement campaign. To investigate this concept, a feasibility study has taken place at the WSL/SLF test site “Versuchsfeld Weissfluhjoch”.

The feasibilty study used a measurement setup assembled by light and small low-cost components. The two GNSS antennas are attached to an avalanche probe at the lower and upper end which ensures a stable and known baseline between two GNSS antennas. Additionally, the length of the avalanche probe is used to overcome the snow depth. This setup also ensures that the second antenna is above the snow layer.

The installation of the measurement setup in the field is done by drilling a hole through the snow cover. After lowering the lower antenna inside the borehole, SWE can be assessed. By observing fixed GNSS baselines between the two antennas of the setup, SWE measured in the field are inside a 10 percent interval of the reference observation for SWE at that location.

Figure 1. The measurement setup is installed in a borehole and stabilized by three ropes. The visible antenna is attached at the top of an avalanche probe to ensure that it is above the snow. The second antenna is underneath the snow cover.

16.14
Greenland meltwaters run off from far into the percolation zone

Andrew Tedstone[1], Horst Machguth[1]

[1] *Department of Geosciences, University of Fribourg, Switzerland (andrew.tedstone@unifr.ch)*

Greenland Ice Sheet melting and runoff has accelerated in recent decades, contributing ~6 mm to global sea level since 1992. However, not all meltwater which is produced runs off. Higher elevations of the ice sheet are underlain by porous snow and firn, into which meltwater can percolate and refreeze within the pore spaces, so the fate of meltwater in these areas is poorly constrained. Here we identify the annual visible runoff limits of the ice sheet, by mapping surface hydrological features in 25,000 images from the Landsat satellite archive. Between 1985-1992 and 2013-2020, the runoff limits along the west and north margins rose by 51-334 metres depending on the region, expanding the runoff area by 29%. The largest increases in area occurred along the western margin. During the last decade the runoff limit has reached high elevations in most melt seasons, even in summers of relatively little melt. The expanded runoff area has likely contributed 529-601 Gt of runoff to the oceans since 1985. The expanded runoff area coincides with regions where relatively impermeable ice slabs have been identified, revealing that firn densification has enabled widespread surface runoff from high elevations to commence. As firn densification continues, the ice sheet's runoff limits are likely to rise further during this century.

16.15
A data-driven approach to quantifying Antarctic blue ice areas and the presence of meteorites

Veronica J.W. Tollenaar[1], Harry Zekollari[1,2], Devis Tuia[3], Stef Lhermitte[2], David M.J. Tax[4], Vinciane Debaille[5], Steven Goderis[6], Philippe Claeys[6], Frank Pattyn[1]

[1] Laboratoire de Glaciologie, Université libre de Bruxelles, Brussels, Belgium (Veronica.Tollenaar@ulb.be)
[2] Department of Geoscience and Remote Sensing, Delft University of Technology, Delft, The Netherlands
[3] Environmental Computational Science and Earth Observation Laboratory, École polytechnique fédérale de Lausanne Valais, Sion, Switzerland
[4] Pattern Recognition Laboratory, Delft University of Technology, Delft, The Netherlands
[5] Laboratoire G-Time, Université libre de Bruxelles, Brussels, Belgium
[6] Analytical-, Environmental-, and Geo-Chemistry, Vrije Universiteit Brussel, Brussels, Belgium

Most of the surface of Antarctica is covered by snow. However, in certain areas, blue-coloured glacial ice is directly exposed at the surface. These blue ice areas, scattered over the continent, account for ca. 1.5% of the total surface (e.g., Hui et al. 2014). Blue ice areas are of great scientific interest, as they contain (very) old ice that is easily accessible for paleoclimatic studies. Moreover, some blue ice areas bear high concentrations of meteorites, which provide an unparalleled view on the origin and evolution of the Solar System. In this contribution, we use data-driven approaches to (i) explain why we find blue ice at the surface at certain locations and (ii) distinguish meteorite-rich blue ice areas from those absent from meteorites.

(i) The presence of blue ice strongly relates to the local surface topography: the subsurface topography is expressed at the surface (e.g., Leong & Horgan 2020)we present DeepBedMap - a novel machine learning method that can produce Antarctic bed topography with adequate surface roughness from multiple remote sensing data inputs. The super-resolution deep convolutional neural network model is trained on scattered regions in Antarctica where high-resolution (250 m, the ice flow velocity relates to surface slope, and topographic features govern katabatic wind patterns that prevent snow accumulation in blue ice areas. However, the exact configuration of the features that lead to the exposure of blue ice has never been quantified on a continental scale. Here, we aim to predict the presence of blue ice over the whole of Antarctica by relying on a digital elevation model and machine learning. As contextual patterns are leading in the prediction, we use a convolutional neural network. Labelled data exists (Hui et al. 2014), but suffers from considerable uncertainties introduced by the areas' sensitivity to temporal aspects such as temporary snow covers. Initial results show that with surface elevation alone, we can predict the presence of blue ice relatively well. However, errors in the prediction persist, especially when applying the trained neural network to independent test data. To reduce these errors, we explore how other data can be used (e.g., visual data), and involve the temporal aspect of blue ice areas (such as seasonal variations and temporary snow cover).

(ii) To predict which blue ice areas are meteorite-rich, we use indirect properties of the ice sheet, as meteorites are too small (on average 2.5 cm) to directly detect from remote sensing imagery. After an exhaustive feature selection, four properties arise: the surface temperature, the ice flow velocity, the intensity of radar backscatter, and the surface slope. By comparing data from meteorite-free areas (documented in the literature after unsuccessful search campaigns) to a random sample of locations, it appears that the former two properties (surface temperature and ice flow velocity) allow to distinguish meteorite-rich areas from areas that were unsuccessfully visited. The latter two properties (radar backscatter and surface slope) separate meteorite-rich areas from randomly selected ones, which include snow-covered and rock-exposed areas. Through our data-driven approach, we provide the first continent-wide estimates of the probability to find meteorites at any given location. The resulting set of meteorite-rich blue ice areas, with an estimated accuracy of over 80%, reveals the existence of unexplored zones, some of which are located close to research stations.

REFERENCES

Hui, F., Ci, T., Cheng, X., Scambos, T. A., Liu, Y., Zhang, Y., Chi, Z., Huang, H., Wang, X., Wang, F., Zhao, C., Jin, Z., & Wang, K. 2014: Mapping Blue-Ice Areas in Antarctica Using ETM+ and MODIS Data, Annals of Glaciology, 55(66), 129–37.

Leong, W. J., & Horgan, H. J. 2020: DeepBedMap: A Deep Neural Network for Resolving the Bed Topography of Antarctica, Cryosphere, 14(11), 3687–3705.

P 16.1
Application of a high-resolution Earth surface model to simulate blue green water interactions in a glacierized Himalayan catchment

Pascal Buri[1], Simone Fatichi[2], Thomas Shaw[1], Evan Miles[1], Michael McCarthy[1], Catriona Fyffe[3], Stefan Fugger[1], Shaoting Ren[4], Marin Kneib[1], Francesca Pellicciotti[1,3]

[1] Swiss Federal Research Institute WSL, Zürcherstrasse 111, 8903 Birmensdorf, Switzerland (pascal.buri@wsl.ch)
[2] Department of Civil and Environmental Engineering, National University of Singapore, 1 Engineering Drive 2, Singapore 117576, Singapore
[3] Department of Geography and Environmental Sciences, Northumbria University, City Campus, Newcastle upon Tyne NE1 8ST, UK
[4] State Key Laboratory of Remote Sensing Science, Aerospace Information Research Institute, Chinese Academy of Sciences, Beijing, China

The snow and glacier reservoirs of High Mountain Asia play a key role in sustaining water resources supply to mountain communities and downstream ecosystems, populations and economic activities, but little is known about the response of rain, snow- and ice melt to climate and how vegetation amplifies or suppresses runoff deficit.

We generate simulations of catchment response to climate using an Earth surface model that includes a physical representation of both cryosphere- and biosphere processes at high detail and resolution. We use the model to study how different processes affect the hydrological cycle and how vegetation can change water yield from the high mountains of a glacierized Himalayan catchment downstream. This bridges the modelling gap between snow- and glacier dynamics, which generate the runoff, and vegetation processes, which might mediate runoff production at lower elevations.

We use as a case study the upper Langtang catchment (~4000-7000 m a.s.l.) in the Nepalese Himalayas, and simulate for two years (2017-2019) catchment runoff and track the relative contribution of precipitation, snow- and ice melt, avalanching and the interaction with soil and vegetation to the hydrological cycle. We calibrate a minimal set of variables (physical properties of supraglacial debris) and use integrative variables such as catchment runoff or glacier mass balance only for validation of the model output. The availability of a rich dataset of field- and remote sensing observations in the catchment allows validation of numerous physical processes simulated by the model and helps to drastically reduce the probability of internal error compensation.

The results provide the first quantification of the importance of vegetation feedback on water yields and local water availability in a glacierized Himalayan catchment. We show precipitation to be the major source of uncertainty in our simulations and that vegetation is crucial in determining the amount of runoff transferred further downstream even for high elevation, extensively glacierized Himalayan catchments.

P 16.2
On dynamics of glide-snow avalanche release as inferred from time-lapse photography

Amelie Fees, Alec van Herwijnen, Michael Lombardo, Jürg Schweizer

WSL Institute for Snow and Avalanche Research SLF, Flüelastrasse 11, 7260 Davos Dorf (amelie.fees@slf.ch)

Glide-snow avalanches release due to a loss of friction at the interface between the snowpack and the ground. As a result, these avalanches can involve large snow volumes and have a high damage potential. Glide-snow avalanches, which are sometimes preceded by the formation and expansion of glide cracks, are still relatively poorly understood and difficult to forecast. This is in part because the underlying glide process is not well documented. A relatively easy and intuitive method to monitor glide-cracks and glide-snow avalanches is with time-lapse photography. To track changes in glide-crack geometry, we developed a pixel-detection algorithm based on Otsu's threshold. It allows for the automatic identification of all pixels within a glide crack, even under changing illumination and shadow conditions. Georeferencing the images further allowed us to extract glide rates. We used this algorithm on images of more than 600 glide-snow avalanches over a period of 10 years at the Dorfberg field site above Davos, Switzerland. These data allowed us to investigate seasonal glide-snow avalanche activity, as well as the influence of glide rates, glide crack geometry and local topography. Overall, glide-snow avalanche activity varied greatly from year to year, and the majority of glide-snow avalanches released without the appearance of a glide-crack. Most glide-snow avalanches that released after a visible glide-crack opened, released within two days. Our results further suggest that glide rate dynamics and crack geometries were somewhat different if a glide-crack resulted in an avalanche or not. More specifically, increases in glide rates were generally more pronounced when a glide-snow avalanche released, and larger glide-cracks were less likely to result in an avalanche. Finally, at our field site, slope angle and small-scale terrain roughness were the best indicators of potential glide-snow avalanche slopes. Overall, our results provide the first comprehensive investigation of typical time scales involved in glide-snow avalanching and provide valuable insight into snow gliding dynamics. In the future, we will investigate the influence of meteorological parameters and perform detailed soil measurements to better understand the processes driving snow gliding, and ultimately improve glide-snow avalanche forecasting

P 16.3
THE CRYOSPHERE OF HIGH ALPINE ROCK WALLS: INSIGHTS FROM THE POINTES DU MOURTI (3563 M A.S.L., SWITZERLAND)

Jérémie Gentizon[1], Florence Magnin[2], Ludovic Ravanel[3], Christophe Lambiel[4]

[1] Institute of Earth Surface Dynamics, University of Lausanne, Géopolis Building, Unil Mouline, CH-1015 Lausanne (jeremie.gentizon@unil.ch)
[2] Laboratoire edytem – UMR5204, Morphodynamics team, University of Savoie Mont Blanc, Pôle Montagne Building, 5, bd de la mer Caspienne, F-73376 Le Bourget du lac cedex (florence.magnin@univ-smb.fr)
[3] Laboratoire edytem – , University of Savoie Mont Blanc, Pôle Montagne Building, 5, bd de la mer Caspienne, F-73376 Le Bourget du lac cedex (ludo.ravanel@cegetel.net)
[4] Institute of Earth Surface Dynamics, University of Lausanne, Géopolis Building, Unil Mouline, CH-1015 Lausanne (christophe.lambiel@unil.ch)

The accelerated warming of atmospheric temperatures since the early 1990s has had major impacts on mountain environments. While accelerated glacier retreat is the most visible manifestation, changes in permafrost areas are also very significant. However, available data on permafrost bedrock and hanging glaciers at highest elevations are limited even in the European Alps. In particular, knowledge about the temperature distribution in steep Alpine rock slopes is still limited and practically unknown in hanging glaciers mainly due to the complicated and costly logistics in such extreme and remote terrain. Our project aims thus at improving the knowledge on the distribution and structure of permafrost in a partially glaciated alpine summit, the Pointes de Mourti in the Valais Alps (Val d›Anniviers), culminating at 3653 m a.s.l.

The objectives of our study are to:

i.) characterize the thermal state of the permafrost in the different rock faces of the summit, by surveying the surface temperatures (10 cm deep) of the rock in 8 different locations;
ii.) document the permafrost distribution at depth using geophysics in the different rock faces; two electrical resistivity tomography profiles (ERT) composed of 48 or 24 electrodes with a 5 m spacing were carried out on the east and west faces from the main summit and on the north face from a secondary summit;
iii.) investigate the thermal regime of the north-facing hanging glacier by the recording of temperatures in two 13 m - deep boreholes drilled through the entire thickness of the glacier;
iv.) model the distribution of the permafrost in the mountain from the different data collected;

Preliminary results indicate a strong heterogeneity in the permafrost distribution. The east and west faces present surface temperatures above 0°C, while ERT data suggest unfrozen conditions at depth. The north face is unfrozen in the first top 50 m, due to thermal fluxes from the south face, while it is frozen at lower elevations. Finally, the temperatures of the hanging glacier are comprised between 0°C and -3°C. In addition, the drillings through the hanging glacier showed the presence of a large cavity between the base of the glacier and the underlying bedrock.

P 16.4
Mean Ocean Temperature (MOT) during MIS5-6 based on noble gas ratios in the EDC ice core

Markus Grimmer[1,2], Daniel Baggenstos[1,2], Jochen Schmitt[1,2], Hubertus Fischer[1,2]

[1] Climate and Environmental Physics, Physics Institute, University of Bern, Sidlerstrasse 5, CH-3012 Bern (markus.grimmer@unibe.ch)
[2] Oeschger Center for Climate Change Research, University of Bern, Hochschulstrasse 4, CH-3012 Bern

The ocean plays a key role in the climate system. Its high heat capacity, paired with its efficient heat transport, makes it Earth's dominant energy reservoir on a glacial-interglacial time scale, only rivalled by the latent heat changes connected to the waxing and waning of ice sheets. Thus, global ocean heat content can serve as a proxy for Earth's energy imbalance (Baggenstos et al. 2019). However, quantifying this heat content throughout past glacial-interglacial variations proofs to be a major challenge. While marine sediment cores can be used to deduce the sea surface temperature or deep ocean temperature in many (but not all) ocean areas, the representativeness of their proxy information is limited to the coring site. Stacks of data from multiple sea sediment cores can partially resolve this issue, but are highly labour-intensive and require stringent cross-dating constraints. Furthermore, the proxy information gained from these sediments may be affected by complex biogeochemical processes and sea level changes. Also, they may be limited in precision, in particular for the cold deep ocean.

A different approach for the reconstruction of past ocean heat content, that is fully independent of marine sediments, is to use ratios of noble gases and molecular nitrogen trapped in polar ice cores. Since noble gases are inert, their past atmospheric abundances on glacial-interglacial time scale are solely dependent on their well understood temperature-dependent physical solubilities in ocean water. As the atmosphere is well-mixed, a single ice core sample is sufficient to obtain a snapshot of the global ocean's noble gas content, and, thus, through the temperature-dependent solubilities, its heat content. To this end, several systematic effects induced by the gas archive in polar ice cores have to be corrected for. However, thanks to high precision mass spectrometry measurements of the noble gas ratios and their isotopic composition, the 1σ uncertainty of such a MOT estimate is still only about 0.4°C (Häberli et al. 2021).

Here, we present a detailed description of the noble gas based MOT methodology, as well as some preliminary MOT data for the MIS 5-6 period. Previous studies found a glacial-interglacial MOT difference of 2.6-3.2°C for Termination II (Häberli et al. 2021; Shackleton et al. 2020). In their Last Interglacial MOT record, Shackleton et al. 2020 also identified an overshoot that is characteristic to many other Termination II climate records. However, no highly resolved MOT dataset for the entire MIS 5-6 period exists to date. By extending the MOT record well into MIS 6, we aim to obtain a more complete picture of Termination II MOT variations, and to learn whether glacial millennial-scale oscillations are also found in MOT, as suggested by recent modelling studies (Galbraith et al. 2016, Pedro et al. 2018).

REFERENCES

Baggenstos, D., Häberli, M., Schmitt, J., Shackleton, S. A., Birner, B., Fischer, H., Severinghaus, J., and Kellerhals, T. 2019: The Earth's radiative imbalance from the Last Glacial Maximum to the present, P. Natl. Acad. Sci. USA, 110, 14881–14886, https://doi.org/10.1073/pnas.1905447116.

Galbraith, E. D., Merlis, T. M., and Palter, J. B. 2016: Destabilization of glacial climate by the radiative impact of Atlantic Meridional Overturning Circulation disruptions, Geophysical Research Letters, 43, 8214–8221, https://doi.org/10.1002/2016GL069846.

Haeberli, M., Baggenstos, D., Schmitt, J., Grimmer, M., Michel, A., Kellerhals, T., and Fischer, H. 2021: Snapshots of mean ocean temperature over the last 700 000 years using noble gases in the EPICA Dome C ice core, Clim. Past, 17, 843–867, https://doi.org/10.5194/cp-17-843-2021.

Pedro, J. B., Jochum, M., Buizert, C., He, F., Barker, S., and Rasmussen, S. O. 2018: Beyond the bipolar seesaw: Toward a process understanding of interhemispheric coupling, Quaternary Science Reviews, 192, 27-46, https://doi.org/10.1016/j.quascirev.2018.05.005, http://www.sciencedirect.com/science/article/pii/S0277379117310351.

Shackleton, S., Baggenstos, D., Menking, J. A., Dyonisius, M. N., Bereiter, B., Bauska, T. K., Rhodes, R. H., Brook, E. J., Petrenko, V. V., McConnell, J. R., Kellerhals, T., Häberli, M., Schmitt, J., Fischer, H., and Severinghaus, J. P. 2020: Global ocean heat content in the Last Interglacial, Nat. Geosci., 13, 77–81, https://doi.org/10.1038/s41561-019-0498-0.

P 16.5
Application of a muonic cosmic ray snow gauge to monitor the snow water equivalent on an alpine glacier

Rebecca Gugerli [1], Darin Desilets[2] and Nadine Salzmann[1]

[1] *Departement of Geosciences, University of Fribourg, Chemin du Musée 4, CH-1700 Fribourg, Switzerland (rebecca.gugerli@unifr.ch)*
[2] *Hydroinnova LLC, Albuquerque, NM 87106, USA*

Temporally continuous snow water equivalent (SWE) measurements are a key variable in many hydrological, meteorological and glaciological studies, especially for high mountain regions. Obtaining accurate and reliable SWE measurements in the harsh environments of high mountain regions, however, remains a challenge. In this study, we explore the use of muons from secondary cosmic rays to infer SWE on an alpine glacier. To this end, we deployed two muonic cosmic ray snow gauge (μ-CRSG), one below and one above the snowpack, on the Glacier de la Plaine Morte in Switzerland. Over the snow rich winter season 2020/21, almost up to 2000 mm w.e. were observed. To infer SWE from muon counts, we derive a first-cut conversion function based on manual SWE observations by means of snow pits and snow cores. To evaluate the measurements by the μ-CRSG, we also compare the inferred SWE with SWE estimates by a neutronic cosmic ray snow gauge. The n-CRSG was previously validated with 22 manual measurements over five winter seasons (2016/17-2020/21) and showed an underestimation of -1% ±12% (one standard deviation) for this site. Overall, the μ-CRSG agrees well with the n-CRSG on the evolution of the snowpack at a daily resolution and thus demonstrates its great potential. Also, the inferred SWE measurements lie within the uncertainty of manual observations. Furthermore, the μ-CRSG has several additional advantages over the n-CRSG. It is cheaper, lighter and has a higher measurement precision due to the improved counting statistics of the muon count rates. We conclude that the μ-CRSG is a highly promising method to monitor SWE in remote high mountain environments.

REFERENCES

Gugerli, R., Desilets, D., and Salzmann, N.: Brief communication: Application of a muonic cosmic ray snow gauge to monitor the snow water equivalent on alpine glaciers, The Cryosphere Discuss. [preprint], https://doi.org/10.5194/tc-2021-277, in review, 2021.

P 16.6
Machine learning techniques to downscale solid precipitation from climate reanalyses generating SWE estimates over high-mountain glaciers of the world

Matteo Guidicelli[1], Matthias Huss[1,2,3], Marco Gabella[4], Nadine Salzmann[5]

[1] Departement of Geosciences, University of Fribourg, Fribourg, Switzerland
(matteo.guidicelli@unifr.ch)
[2] Swiss Federal Institute for Forest, Snow and Landscape Research (WSL), Birmensdorf, Switzerland
[3] Laboratory of Hydraulics, Hydrology and Glaciology (VAW), ETH Zurich, Zurich, Switzerland
[4] Federal Office of Meteorology and Climatology MeteoSwiss, Locarno-Monti, Switzerland
[5] WSL-Institut für Schnee- und Lawinenforschung SLF, Davos, Switzerland

The scarcity and limited accuracy of precipitation observation and estimation in high-mountain regions are a major drawback for enhancing our understanding of climatic-cryospheric processes and reduces uncertainties in related climate impact studies. We are tackling this research need by combining data and methods from atmospheric and cryospheric sciences to derive improved data products. In our study, the seasonal cumulative precipitation data from ERA-5 and MERRA-2 reanalysis products are compared with the winter mass balance observations of 99 high-altitude glaciers distributed over the Alps, Canada, Central Asia and Scandinavia. We propose a machine learning model to downscale the gridded precipitation of the reanalysis products to the altitude of interest. The model is a gradient boosting regressor (GBR), which combines several meteorological variables (gridded and downscaled) and topographical parameters. These GBR-derived estimates are evaluated against the winter mass balance observations by means of a leave-one-glacier-out cross-validation (site-independent). We furthermore compare them with results obtained by pre-existing statistical downscaling methods (c.f. Liston and Elder (2006)). The GBR estimates show lower biases and higher correlations with the winter mass balance observations than pre-existing methods. Among the most important variables selected by our model, are downscaled relative humidity and downscaled air temperature. As a next step, the precipitation estimates of the different reanalysis and downscaling models will be also compared at higher temporal resolution with automated snow water equivalent observations obtained on two alpine Swiss glaciers using a cosmic ray sensor, and manual monthly observations on the Abramov glacier (Pamir Alai, Central Asia).

REFERENCES

Liston, G. E., and Elder, K. (2006), A Meteorological Distribution System for High-Resolution Terrestrial Modeling (MicroMet), *Journal of Hydrometeorology*, 7, 217-234.

P 16.7
Precipitation Phase Change Accelerates Glacier Mass Loss In The Southeastern Tibetan Plateau

Achille Pierre Jouberton[1], Thomas Edward Francis Shaw[1], Evan Miles[1], Shaoting Ren[1,2], Wei Yang[3,4], Michael McCarthy[1,5], Stefan Fugger[1,6], Amaury Dehecq[7], Francesca Pellicciotti[1,8]

[1] *Swiss Federal Institute for Forest, Snow and Landscape Research (WSL), France (achille.jouberton@wsl.ch)*
[2] *State Key Laboratory of Remote Sensing Science, Aerospace Information Research Institute, Chinese Academy of Sciences, Beijing 100101, China*
[3] *Institute of Tibetan Plateau Research, Chinese Academy of Sciences, Beijing, China*
[4] *Ministry of Education Key Laboratory for Earth System Modeling, Department of Earth System Science, Tsinghua University, Beijing, China*
[5] *British Antarctic Survey,Natural Environment Research Council,Cambridge,UK* [6] *Institute of Environmental Engineering, ETH Zurich, 8093 Zurich, Switzerland* [7] *Laboratory of Hydraulics, Hydrology and Glaciology (VAW), ETH Zurich, 8093, Zurich, Switzerland*
[8] *Department of Geography, Northumbria University, Newcastle, UK*

Glaciers are key components of the mountain water towers of Asia and are vital for downstream domestic, agricultural and industrial uses. The highest rate of glacier mass loss in this region occurs in the Southeastern Tibetan Plateau, where it has accelerated in the past four decades. This acceleration has been attributed to increased warming, but the mechanisms behind these glaciers' high sensitivity to warming remaing unclear, while the influence of changes in precipitation over the past decades is poorly quantified. Here, we reconstruct catchment runoff and glacier mass changes since 1975 at Parlung No. 4 glacier, using a fully distributed glacio-hydrological model (TOKPAPI-ETH), to shed light on the drivers of mass losses for the monsoonal, spring-accumulation glaciers of this region. Parlung No.4 Glacier is considered as a benchmark glacier in this region, since its meteorology, surface energy fluxes and mass-balance have been examined since 2006. Our modelling demonstrates how a temperature increase (mean of 0.39°C dec^{-1} since 1990) has accelerated mass loss rates by altering both the ablation and accumulation regimes in a complex manner. The majority of the post-2000 annual mass loss occurred during the monsoon months, caused by simultaneous decreases in the solid to total precipitation ratio (from 70% to 56%) and precipitation amount (-10%), leading to reduced monsoon accumulation (-26%). Higher solid precipitation in spring (+18%) during the last two decades was increasingly important in mitigating glacier mass loss by providing mass to the glacier and protecting it from melting in the early monsoon. With bare ice exposed to warmer temperatures for longer periods, icemelt and catchment discharge have unsustainably intensified since the start of the 21st century, raising concerns for long-term water supply and hazard occurrence in the region.

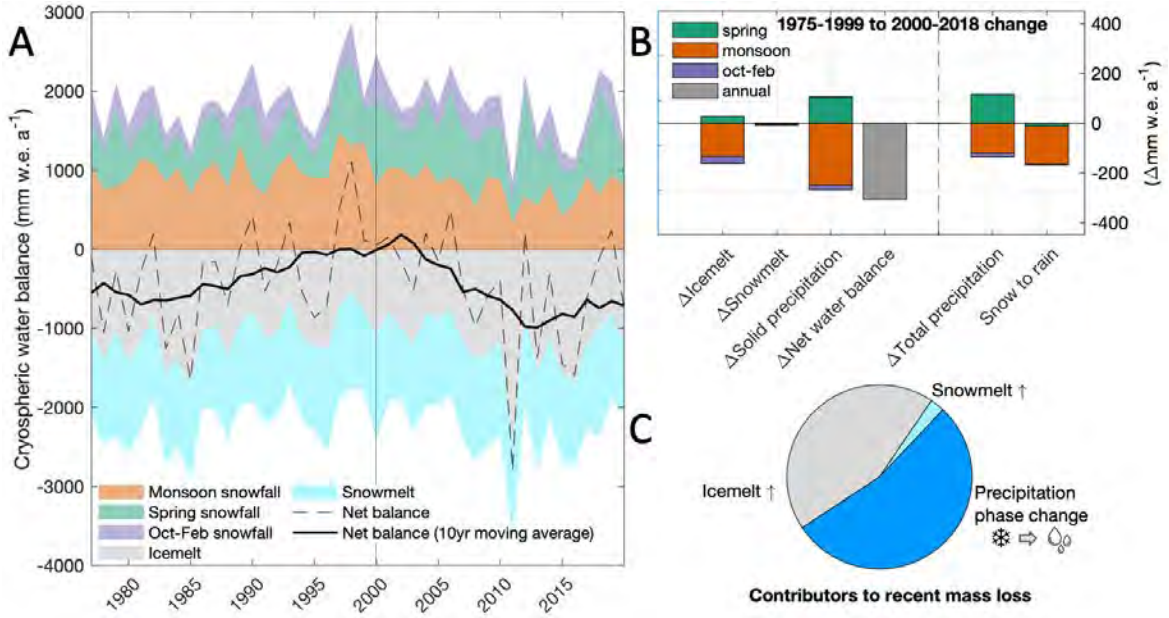

Figure 1. Cryospheric water balance and contributors to recent mass loss. The net water balance is calculated as : Solid precipitation - (Icemelt + Snowmelt). A) Annual cryospheric water balance. B) Changes in the cryospheric water balance between the early and the recent periods, a negative sign indicates less (more) water entering (leaving) the cryospheric storage. C) Relative contribution of each component to the net annual mass loss over the glacier area. The change in solid precipitation was separately attributed to a change in precipitation phase and to a change in precipitation amounts.

REFERENCES

Brun, F, et al. 2017: A spatially resolved estimate of High Mountain Asia glacier mass balances from 2000 to 2016. Nat. Geosci.10, 668–673.

Zhu, M, et al. 2018: Differences in mass balance behaviorfor three glaciers from different climatic regions on the Tibetan Plateau .Clim. Dyn.50, 3457–3484.

Yang, Y, et al. 2013: Mass balance of a maritime glacier on the southeast Tibetan Plateau and its climatic sensitivity. J. Geophys. Res. Atmospheres118, 9579–9594.

Ragettli, S, et al. 2015: Unravelingthe hydrology of a Himalayan catchment through integration of high resolution in situ data and remote sensing with an advanced simulation model. Adv.WaterResour.78, 94–111.

Sakai, A & Fujita, K. 2017: Contrasting glacier responses to recent climate change in high-mountain Asia.Sci. Reports.

P 16.8
Development of ice slabs in the high percolation zone of the Greenland Ice Sheet

Nicolas Jullien, Andrew Tedstone, Horst Machguth

Department of Geosciences, University of Fribourg, Fribourg, Switzerland

At high elevations of the Greenland Ice Sheet, percolating meltwater which refreezes in the pore space of firn can buffer the contribution of meltwater to sea level rise. However, in the past two decades, there have been several seasons of strong melting and refreezing, dramatically increasing the ice content of the near-subsurface firn. Relatively impermeable ice slabs, several metres thick, have formed and which have been identified by firn cores and in airborne radar surveys undertaken during 2010-14. These ice slabs have made it harder for the meltwater to percolate and subsequently refreeze deep in the firn column. Meltwater now increasingly runs off over the surface of the percolation zone instead. Here examine the timescales of ice slab formation by analysing pan-Greenland airborne radar surveys made in 2002-2003, 2010-2014 and 2017-2018. Where flight survey tracks were repeated over several years we were able to track the transition from porous firn to ice slabs. We show that new ice slabs began to develop at least early as 2002 in south-west Greenland, leading a transition to a firn runoff regime in several new areas of the ice sheet. Finally, we use simulations from regional climate models to calculate the amount of excess melting that is required to generate ice slabs.

P 16.9
Development and application of a noble continuous laser-sublimation extraction technique coupled to a Quantum Cascade laser Spectrometer for greenhouse gas measurements (CO_2, $\delta^{13}C$, CH_4, N_2O) in ice cores

Florian Krauss[1], Lars Mächler[1], Daniel Baggenstos[1], Remo Walther[1], Bernhard Bereiter, Béla Tuzson[2], Lukas Emmenegger[2], Jochen Schmitt[1], Hubertus Fischer[1]

[1] Climate and Environmental Physics Institute and Oeschger Centre for Climate Change Research, University of Bern, Bern, Switzerland.
[2] Empa, Laboratory for Air Pollution / Environmental Technology, Überlandstrasse 129, 8600 Dübendorf, Switzerland.

Ice cores are natural archives that preserve valuable information of past atmospheric greenhouse gas concentrations (CO_2, CH_4 and N_2O) and changing climate systems.

To understand how these complex changes of biochemical cycles will respond in the future, we need to decipher the role of changing greenhouse gas concentration and the rearrangement within the major carbon reservoirs (sediment, terrestrial biosphere, ocean and atmosphere) in the past (Bauska et al. 2018; Schmitt et al. 2012).

For this purpose, $\delta^{13}C$ measurements (ratio of the stable isotopes ^{13}C:^{12}C) are a useful tool to identify variations of CO_2 (the most important greenhouse gas after water vapour) driven by biogeochemical processes and to disentangle short- and long-term carbon cycle changes (Schmitt et al. 2012).

The main goal of this PhD project will be to enable high-resolution and high-precision isotopic studies of $\delta^{13}C$ in ice core samples via a noble continuous laser-sublimation extraction technique (Bereiter et al. 2020). A quantitative statement of the most common greenhouse gases (CO_2, CH_4 and N_2O) is to be made to reconstruct quantitative environmental processes controlling past greenhouse gas concentration changes.

REFERENCES:

Bauska, T.K., Brook, E.J., Marcott, S.A., Baggenstos, D., Shackleton, S., Severinghaus, J.P., Petrenko, V.V., 2018. Controls on Millennial-Scale Atmospheric CO_2 Variability During the Last Glacial Period. Geophys. Res. Lett. 45, 7731–7740. https://doi.org/10.1029/2018GL077881

Bereiter, B., Tuzson, B., Scheidegger, P., Kupferschmid, A., Looser, H., Mächler, L., Baggenstos, D., Schmitt, J., Fischer, H., Emmenegger, L., 2020. High-precision laser spectrometer for multiple greenhouse gas analysis in 1 mL air from ice core samples. Atmos. Meas. Tech. 13, 6391–6406. https://doi.org/10.5194/amt-13-6391-2020

Schmitt, J., Schneider, R., Elsig, J., Leuenberger, D., Lourantou, A., Chappellaz, J., Kohler, P., Joos, F., Stocker, T.F., Leuenberger, M., Fischer, H., 2012. Carbon Isotope Constraints on the Deglacial CO2 Rise from Ice Cores. Science 336, 711–714. https://doi.org/10.1126/science.1217161

P 16.10
Accelerating mass loss of Greenland: Firn and the shifting runoff limit

Horst Machguth[1], Andrew Tedstone[1], Nicole Clerx[1], Nicolas Jullien[1]

[1] *Department of Geosciences, University of Fribourg, Chemin du Musée 4, CH-1700 Fribourg (horst.machguth@unifr.ch)*

Meltwater running off the flanks of the Greenland ice sheet accounts for roughly 60% of its mass loss, the rest being due to calving. Only meltwater originating from below the elevation of the runoff limit leaves the ice sheet, contributing to mass loss; melt above this limit refreezes in the porous firn and does not drive mass loss. Shifts in the runoff limit therefore affect the rate of mass loss and sea level rise. Recent evidence shows surface runoff at increasingly high elevations, but the processes which define the position of the runoff limit remain enigmatic.

CASSANDRA is a European Research Council (ERC) research project running from 2019 to 2024. We focus on the runoff limit as a powerful yet poorly understood modulator of Greenland mass balance. The project uses a combination of remotely-sensed, modelling and field approaches. We are using three of the largest and oldest remote sensing archives, Landsat, MODIS and AVHRR, to identify the mechanisms driving fluctuations in the runoff limit.

Our field campaigns began in 2020 and will last around three years. We are making firn hydrological measurements along the K-Transect on the west of the ice sheet. We have installed 10 automated measuring stations which operate year-round and record observations of meltwater production, percolation, refreezing and ice motion. Additional in-situ experiments to constrain firn hydrology and meltwater runoff are being carried out during field campaigns each spring and summer.

We are applying our process understanding gained from our remotely-sensed and field observations to develop firn hydrology models. These models will be capable of simulating runoff and the associated runoff limit over time. The ultimate aim is to estimate how changing firn hydrology will impact Greenland's future mass balance.

P 16.11
Assessing permafrost distribution and ground ice volumes in Central Asia (Kyrgyzstan): results from a first geophysical field campaign

Tamara Mathys[1], Christin Hilbich[1], Eric Pohl[1], Christian Hauck[1], Martin Hoelzle[1]

[1] Department of Geosciences, University of Fribourg, Chemin du Musée 4, CH-1700 Fribourg (tamara.mathys@unifr.ch)

With ongoing climate change, there is a pressing need to better understand how much water is stored as near surface ground ice in regions with extensive permafrost occurrences. This is especially important in arid regions, such as Central Asia (CA), where water security is threatened as a result of rapid glacier recession (Barandun et al., 2020). The Central Asian region contains one of the largest areas of mountain permafrost in the world (Marchenko et al., 2007). Nevertheless, very little is known about the permafrost distribution, current thermal ground conditions, and ground ice contents in CA. This is mostly due to the lack of (in-situ) geothermal and geophysical baseline datasets in the region, which would be important tools to improve water management strategies, as well as aiding the development of sound model estimates that quantify future changes on CA's permafrost under climate change.

To contribute to reducing the data scarcity regarding permafrost distribution and ground ice content in Central Asia, we conducted extensive ERT (Electrical Resistivity Tomography) surveys in the Tien Shan and Pamir Alay of Kyrgyzstan. The field sites of the ERT surveys carried out in summer 2021 comprise a variety of landforms including amongst others rock glaciers, talus slopes, moraines, and vegetated planes. Our results indicate widespread permafrost occurrences at all study sites and point to potentially substantial ground ice volumes that are not limited to rock glaciers alone. This clearly reveals the importance of permafrost research in the region, particularly with regard to its hydrological significance.

These measurements represent the first surveys in the framework of a planned Central Asian permafrost monitoring network in Kyrgyzstan, Tajikistan, and Kazakhstan that will include (i) the annual repetition of selected ERT profiles to detect potential resistivity changes with climate change that can indicate changes in the content of ground ice and liquid water (ii) distributed ground surface temperature (GST) measurements, and (iii) drilling of new boreholes to monitor the thermal state of permafrost in Central Asia.

REFERENCES

Barandun, M., Fiddes, J., Scherler, M., Mathys, T., Saks, T., Petrakov, D., & Hoelzle, M. 2020: The state and future of the cryosphere in Central Asia. Water Security, 11, 100072.

Marchenko, S. S., Gorbunov, A. P., & Romanovsky, V. E. 2007: Permafrost warming in the Tien Shan Mountains, Central Asia. Global and Planetary Change, 56(3–4), 311–327.

P 16.12
Ice-core based modern heavy metal pollution records for the territory of the FSU

Petr Nalivaika[1,2,3], Theo Jenk[1,3], Margit Schwikowski[1,2,3], Anja Eichler[1,3]

[1] *The Laboratory of Environmental Chemistry, Paul Scherrer Institute, Forschungsstrasse 111, CH-5232 Villigen, (petr.nalivaika@psi.ch)*
[2] *Department of Chemistry, Biochemistry and Pharmaceutical Sciences, University of Bern, Freiestrasse 3, CH-3012 Bern*
[3] *Oeschger Centre for Climate Change Research, University of Bern, CH-3012 Bern*

Atmospheric pollution by heavy metals presents a significant issue because of its hazardous effect on human health. Anthropogenic heavy metal pollution sources include mining, metal smelting, waste incineration and fossil fuel combustion. Heavy metal records can be obtained from natural archives, such as ice cores, which are unique recorders of past pollution levels. Whereas recent heavy metal pollution is well documented in natural archives for many regions worldwide, existing ice core records and expert emission estimates for the territory of the former Soviet Union (FSU) reveal an opposing trend in the recent ~30 years. Evaluation of modern heavy metal pollution for that region is complicated by the scarce data monitoring and, in addition to that, very few emission data are available.

Here we present a record of post-Soviet Union anthropogenic heavy metal (Cd, Cu, Pb, Sb) emissions and its significance compared to the Soviet Union times based on the three available ice cores from the Mongolian Altai (Tsambagarav ice core, period 1710-2009 AD) and Siberian Altai (Belukha ice cores, period 1680-2018 AD). Heavy metal concentrations in the studied cores were measured using inductively coupled plasma sector-field mass spectrometry that allows quantification of trace elements at low ppt levels. In contrast to updated expert heavy metal emission estimates we found an increase in heavy metal concentrations between the 1990s and the beginning of the 20th century. We relate that to emissions from the reemerging metal production in the FSU countries after the SU breakdown, not considered in the expert emission estimates yet.

P 16.13
High-resolution analysis of the recent onset of seasonal microseismicity in the Mt. Blanc Massif

Verena Simon[1], Toni Kraft[1]

[1] *Swiss Seismological Service, ETH Zürich, Sonneggstrasse 5, CH-8092 Zürich (verena.simon@sed.ethz.ch)*

Seasonal variations in seismic activity have been reported for several mountain regions. Often the seismicity is correlated with seasonal variation in the hydrological recharge with a delay time of several weeks to months. This observation has been interpreted as being the result of external forcing from meteorological parameters. In particular, groundwater recharge from precipitation, and glacier or snow melt, is thought to trigger seismicity on pre-stressed faults at various time scales.

Here we investigate the ongoing earthquake swarm in the Grandes Jorasses of the Mt. Blanc Massif (France/Italy) that is showing a strong annual periodicity of the seismicity starting in fall 2015 with several thousands of shallow microearthquakes of magnitudes M_L<3. To improve the understanding of the ongoing seismicity, three temporary stations were installed from summer 2019 to fall 2020.

We enhance the routine catalog of the Swiss Seismological Service of the swarm sequence with a matched-filter analysis technique that ensures a uniform detection sensitivity and a consistent magnitude estimation over decade-long time spans. To better resolve the spatio-temporal occurrence patterns of the seismicity, we perform a high-precision relative relocation and a high-resolution statistical analysis.

Based on the enhanced catalog and long-term records of high-resolution gridded rainfall data and glacier elevation and mass change time series, we test if the occurrence of the sequence is driven by hydrological factors. The abrupt onset of the seasonality in 2015 may allow us to reliably estimate the delay in the seismic response to the imposed hydraulic forcing. Finally, we aim to compare our estimates to existing measurements of residence times of surface water infiltrating in the summit regions of the Massif and the Mt. Blanc Tunnel obtained from tracer tests.

P 16.14
Towards a near-source reconstruction of pre-industrial to industrial changes in carbonaceous aerosols from ice core archives

Thomas Singer[1,2,3], Theo M. Jenk[1,2], Margit Schwikowski[1,2,3]

[1] *Paul Scherrer Institute, CH-5232 Villigen*
[2] *Oeschger Centre for Climate Change Research, University of Bern, CH-3012 Bern*
[3] *Department of Chemistry, Biochemistry and Pharmaceutical Sciences, University of Bern, CH-3012 Bern*

Atmospheric aerosols are an issue with growing interest because they affect the climate system by changing cloud characteristics, and have profound impacts on the thermodynamic and radiative energy budgets of the Earth by scattering and absorbing radiation. This is noticeable in a wide range of geophysical and environmental problems, ranging from local issues (e.g. air pollution) to the global scale (e.g. climate change). However, the impact of aerosols on climate remains poorly constrained, leading to considerable uncertainties in predicting the climate sensitivity to greenhouse gases. A large fraction of these uncertainties is due to our deficient knowledge of the composition and magnitude of natural emissions before 1750 (Carslaw et al., 2013), especially for organic aerosols, forming 20-70% of today's fine particulate matter (Murphy et al., 2006).

Ice sheets and glaciers are valuable natural archives that contain information about the history of the Earth's atmosphere. In comparison to polar ice cores, high-alpine ice cores from high altitude and lower-latitude glaciers provide information necessary to study processes where human activities (e.g. aerosol from combustion of fossil fuels) are concentrated, due to their geographical location. Radiocarbon analysis (14C) of water insoluble organic carbon (WIO^{14}C) and elemental carbon (E^{14}C) is a powerful tool for dating non-polar ice cores, but also allows a reconstruction and distinction of natural (biogenic) and anthropogenic (fossil) sources in the past (Jenk et al., 2006; Jenk et al., 2009). However, WIOC and EC represent only two fractions of the carbonaceous aerosol, but a major part of which consists of water soluble organic carbon (WSOC). The aim of this study is to gain in-depth knowledge of long-term trends in the mass concentration of organic aerosols from the pre-industrial to the industrial period by analysing two well-documented ice cores, and to identify emission sources using radiocarbon data in order to quantify the influence of humans ever since.

REFERENCES

Carslaw, K. S., et al 2013: Large contribution of natural aerosols to uncertainty in indirect forcing, Nature, 503 (7474), 67–71.

Jenk, T. M., et al., 2006: Radiocarbon Analysis in an Alpine Ice Core: Record of Anthropogenic and Biogenic Contributions to Carbonaceous Aerosols in the Past (1650-1940), Atmospheric Chemistry and Physics Discussions, vol. 6, no. 4, pp. 5905–31.

Jenk, T. M., et al., 2009: A Novel Radiocarbon Dating Technique Applied to an Ice Core from the Alps Indicating Late Pleistocene Ages, Journal of Geophysical Research Atmospheres, vol. 114, no. 14, pp. 1–8.

Murphy, D. M., et al., 2006: Single-particle mass spectrometry of tropospheric aerosol particles, J. Geophys. Res., 111.

P 16.15
Million year Greenland wide ice sheet cover from $^{26}Al/^{10}Be$ ratios in bedrock and inverse modelling

Anne Sofie Søndergaard[1], David Lundbek Egholm[2], Nicolaj Krog Larsen[2,3]

[1] Institute for Particle Physics and Astrophysics, Department for Physics, ETH Zürich, Otto-Stern-Weg 5, 8093 Zürich, Switzerland
[2] Department of Geoscience, Aarhus University, Høegh Guldbergs Gade 2, 8000 Aarhus C, Denmark
[3] Centre for GeoGenetics, GLOBE institute, University of Copenhagen, Øster Voldgade 5-7, 1350 Copenhagen K, Denmark

The Greenland Ice Sheet (GrIS) has waxed and waned over the past million years, and ice has continously covered some parts of Greenland for long, while other parts of Greenland were nearly ice free for extensive periods (Bierman et al., 2016; Schaefer et al., 2016). The Late Glacial and Holocene evolution of the GrIS is relativeley well constrained, but our understanding of the long-term ice sheet evolution and its extent during the past million years, is still poor. Only fragmentary traces of past long-term ice sheet cover are present on land and offshore, as these are mostly buried beneath the present day GrIS or overridden during one of the most recent glacials (Bierman et al., 2016; Schaefer et al., 2016; Knutz et al., 2019). However, recent studies, using mainly paired cosmogenic nuclides form bedrock onshore and in sediment cores offshore, expose possible scenarios for the initiation and long-term evolution of the GrIS in particularly West, East and Central Greenland (Bierman et al., 2016; Schaefer et al., 2016; Knutz et al., 2019; Christ et al., 2020).

In this study we explore new cosmogenic $^{26}Al/^{10}Be$ ratios from two bedrock samples collected in Inglefield Land, western North Greenland in relation to the long term ice sheet history of this remote area. We use an inverse modelling approach and constrain various ice sheet restricted parameters, including a first ice approximation and constraints on the $\delta^{18}O$ threshold. We combine the new $^{26}Al/^{10}Be$ ratios from bedrock samples in Inglefield Land with already existing data from West, East and Central Greenland. Using the inverse modelling approach on all available data, we explore possible ice sheet histories for each study site and evaluate these in the context of a million year Greenland wide ice sheet history and its implications for the buildup and melting patterns of the GrIS.

REFERENCES

Bierman, P. R.,Shakun, J. D.,Corbett, L. B.,Zimmerman, S. R. & Rood, D. H. 2016. A persistent and dynamic East Greenland Ice Sheet over the past 7.5 million years. Nature, 540, 256-260.

Christ, A. J.,Bierman, P. R.,Knutz, P. C.,Corbett, L. B.,Fosdick, J. C.,Thomas, E. K.,Cowling, O. C.,Hidy, A. J. & Caffee, M. W. 2020. The Northwestern Greenland Ice Sheet During The Early Pleistocene Was Similar To Today. Geophysical Research Letters, 47.

Knutz, P. C.,Newton, A. M. W.,Hopper, J. R.,Huuse, M.,Gregersen, U.,Sheldon, E. & Dybkjær, K. 2019. Eleven phases of Greenland Ice Sheet shelf-edge advance over the past 2.7 million years. Nature Geoscience, 12, 361-368.

Schaefer, J. M.,Finkel, R. C.,Balco, G.,Alley, R. B.,Caffee, M. W.,Briner, J. P.,Young, N. E.,Gow, A. J. & Schwartz, R. 2016. Greenland was nearly ice-free for extended periods during the Pleistocene. Nature, 540, 252-255.

P 16.16
Ground ice can be formed and maintained by air convection in low elevation talus slopes

Jonas Wicky[1], Christian Hauck[1]

[1] *Department of Geosciences, University of Freiburg, Chemin du Musée 4, CH-1700 Freiburg (jonas.wicky@unifr.ch)*

We developed and applied a numerical modelling approach to simulate heat transfer in periglacial landforms with a focus on ground air convection (Wicky & Hauck, 2017; 2020). Our model solves for heat conduction and accounts explicitly for air convection adopting a Darcy term with a Boussinesq approximation for air circulation in the porous ground. Numerical experiments with forcing data from the low altitude talus slope Dreveneuse in the Valais Pre-Alps, a former PERMOS site, which showed permafrost conditions in the past, suggest that air convection is the key to form and maintain ground ice. In a model setup where the porous talus slope is underlain by a layer of water-bearing morainic material, ground ice forms due to air convection in years where the gradient between air temperature and talus temperature is high enough to launch an efficient ground cooling. If the model accounts only for conduction or permeability of the porous talus is low, ground ice is not formed. These findings are insofar important as ground ice can be formed in landforms with a MAAT > 0°C because of ground air convection combined with the presence of water and does not need to be of glacial or snow origin.

REFERENCES

Wicky, J. and Hauck, C. (2020). Air Convection in the Active Layer of Rock Glaciers. Frontiers in Earth Science 8: 335.

Wicky, J. and Hauck, C. (2017). Numerical modelling of convective heat transport by air flow in permafrost talus slopes. The Cryosphere 11(3): 1311-1325.

17. Atmospheric Composition and Biosphere-Atmosphere Interactions

Martin Steinbacher, Christof Ammann, Stefan Brönnimann, Mana Gharun, Ulrich Krieger, Werner Eugster

ACP – Commission on Atmospheric Chemistry and Physics
ProClim (SCNAT)

TALKS:

17.1 Alpert P.A., Dou J., Corral Arroyo P., Schneider F., Xto J., Luo B., Peter T., Huthwelker T., Borca C.N., Henzler K.D., Schaefer T., Herrmann H., Raabe J., Watts B., Krieger U.K., Ammann M.: Radical Production Mapped in Single Aerosol Particles

17.2 Baffelli S., Brunner D., Hüglin C., Emmenegger L.: Assimilation of atmospherisc CO_2 measurements from the CarboSense network using the COSMO-GHG model

17.3 Barczyk L., Kuntu-Blankson K., Calanca P., Six J., Ammann C.: N_2O emissions from grazed pastures – Influence of urine patch characteristics

17.4 Bruggisser M., Gharun M., Shekhar A., Hörtnagl L., Feigenwinter I., Damm A., Buchmann N.: Detecting changes in the contributions of abiotic vs. biotic factors to regular and extreme carbon dioxide and water vapor flux events

17.5 dos Reis Martins M., Keel S.G.: Can soil nitrous oxide emissions of complex cropland management be captured by a process-based model?

17.6 Kilchhofer K., Alpert P.A., Bell D., Surdu M., El Haddad I., Cheung K.Y., Torrent L., Ammann M.: Radical Cycling Induced by Transition Metal Complex Photochemistry in Viscous Organic Aerosol Particles

17.7 Kleinheins J., Marcolli C., Peter T., Lohmann U.: Thermodynamic modelling of the co-condensation of organic compounds on atmospheric aerosol particles

17.8 Mahrt F., Newman E., Huang Y., Zaks J., Devi A., Qin Y., Ohno P.E., Martin S.T., Ammann M., Bertram A.K.: Phase behaviour of mixtures of primary and secondary organic aerosol material

17.9 Pieber S.M., Tuzson B., Henne S., Karstens U., Gerbig C., Koch T., Brunner D., Steinbacher M., Emmenegger L.: Towards understanding the regional CO_2 contributions at the high Alpine observatory Jungfraujoch

17.10 Rust D., Katharopoulos I., Vollmer M.K., Henne S., Hill M., Emmenegger L., Zenobi R., Reimann S.: Assessing Swiss halocarbon emissions from regional atmospheric measurements

17.11 Stagakis S., Feigenwinter C., Vogt R., Pitacco A., Kalberer M.: An observation-based approach for monitoring urban CO_2 fluxes at high spatial and temporal resolution

17.12 Valach A., Jocher M., Bretscher D., Ammann C.: Nitrous oxide emissions from different fertiliser and crop combinations using time integrated measurements

POSTERS:

P 17.1 Arosio T., Ziehmer M., Nicolussi K., Sigl M., Schlüchter C., Leuenberger M.: Tree-ring stable isotopes variations after major tropical and north hemispheric volcanic eruptions

P 17.2 Krochin W., Murk A., Stober G.: Studying Atmospheric Waves in the middle atmosphere from ground-based temperature measurements

P 17.3 Kuntu-Blankson K., Barczyk L., Ammann C., Six J., Mezbahuddin S., Grant F.R., Calanca P.: Arriving at an optimum setup for simulating N_2O emissions from cattle urine patches in ecosys- a comprehensive ecosystem model

P 17.4 Sauvageat E., Maillard Barras E., Hocke K., Haefele A., Murk A.: Harmonized retrieval of middle atmospheric ozone from two microwave radiometers in Switzerland

P 17.5 Wenyue W., Klemens H., Christian M.: Physical Retrieval of Rain Rate from Ground-Based Microwave Radiometry

P 17.6 Zeppenfeld C., Erhardt T., Jensen C.M., Fischer H.: Quantifying past changes in dielectric and absorbing particles in ice cores from East Greenland during the early Holocene and Termination 1

17.1
Radical Production Mapped in Single Aerosol Particles

Peter A. Alpert[1], Jing Dou[2], Pablo Corral Arroyo[1,6], Frederic Schneider[1], Jacinta Xto[3], Beiping Luo[2], Thomas Peter[2], Thomas Huthwelker[3], Camelia N. Borca[3], Katja D. Henzler[3], Thomas Schaefer[4], Hartmut Herrmann[4], Jörg Raabe[5], Benjamin Watts[5], Ulrich K. Krieger[2], Markus Ammann[1]

[1] Laboratory of Environmental Chemistry, Paul Scherrer Institute, Villigen, Switzerland (peter.alpert@psi.ch)
[2] Institute for Atmospheric and Climate Science, ETH Zurich, Zurich, Switzerland
[3] Laboratory for Synchrotron Radiation and Femtochemistry, Paul Scherrer Institute, Villigen, Switzerland
[4] Atmospheric Chemistry Department, Leibniz Institute for Tropospheric Research, Leipzig, Germany
[5] Laboratory for Synchrotron Radiation-Condensed Matter, Paul Scherrer Institute, Villigen, Switzerland.
[6] Laboratory for Physical Chemistry, ETH Zurich, Zurich, Switzerland

Aerosol particles suspended in the atmosphere can cause oxidative stress when inhaled affecting respiratory health. Atmospheric aerosol components that generate radicals and reactive oxygen species (ROS) in lungs are linked to toxicity, inflammation, lung disease, and thus, loss of human life. All aerosol particles contain organic matter, such as organic acids, that can form complexes with transition metal ions commonly present in the atmosphere (Tapparo et al. 2020). We have found that these organic-metal particles can be viscous, and sunlight may induce anoxic conditions that stabilize reactive oxygen species (ROS) and carbon-centered radicals (CCRs) (Alpert et al. 2021). Using in situ scanning transmission X-ray microscopy coupled to near edge X-ray absorption fine stucture (STXM/NEXAFS) spectroscopy, we tracked the photochemical reduction of iron and reoxidation with ROS inside individual aerosol particles. Figure 1 shows an example image of particles composed of iron(III)-citrate and citric acid exposed to oxygen after UV irradiation where the iron was photochemically reduced in the interor of particles, but reoxidized only near the surface. The first photochemical reaction step produces CCRs, however their reaction with oxygen could only have been limited to these surface layers to be involved in ROS formation leaving an abundance of CCR in their core. In addition, we performed measurements using 2 other laboratory experiments that reveal the mass loss and radical formation and release from photoactive organic particles containing iron. All these data were used to constrain a newly developed photochemical reaction and diffusion model (Dou et al. 2021), which we used to define the range of temperature and relative humidity, including ambient conditions, that control ROS build up and CCR persistence in photochemically active, viscous organic particles. We find that radicals can attain high concentrations, altering aerosol chemistry and exacerbating health hazards of aerosol exposure. In addition, ambient concentrations of radicals could be reproduced by our model under the assumption that particles were in a viscous state (Arangio et al. 2016). We could also reproduce previous work that a burst of ROS compounds was observed immediately after UV exposure (Paulson et al. 2019). Our physicochemical kinetic model confirmed these results, implying that oxygen does not penetrate such particles due to the combined effects of fast reaction and slow diffusion near the particle surface, allowing photochemically-produced radicals to be effectively trapped in an anoxic organic matrix.

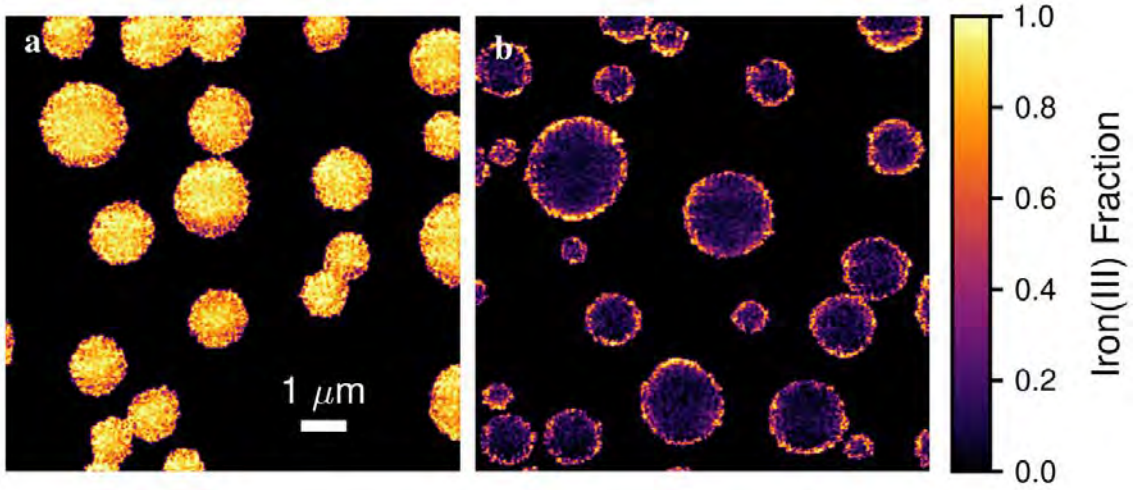

Figure 1. A STXM/NEXAFS images of the iron(III) fraction in particles **a** before and **b** after UV irradiation revealing reoxidation only near the surface of particles. The images were smoothed by increasing the pixel resolution and interpolating. The scale bar applies to both images.

REFERENCES

Alpert P. A. et al. Photolytic radical persistence due to anoxia in viscous aerosol particles. Nat. Comm. 12, 1769 (2021).

Arangio, A. M. et al. Quantification of environmentally persistent free radicals and reactive oxygen species in atmospheric aerosol particles. Atmos. Chem. Phys. 16, 13105-13119 (2016).

Dou, J. et al. Photochemical degradation of iron(III) citrate/citric acid aerosol quantified with the combination of three complementary experimental techniques and a kinetic process model. Atmos. Chem. Phys. 21, 315-338 (2021).

Paulson, S. E. et al. A light-driven burst of hydroxyl radicals dominates oxidation chemistry in newly activated cloud droplets. Sci. Adv. 5, eaav7689 (2019).

Tapparo, A. et al. Formation of metal-organic ligand complexes affects solubility of metals in airborne particles at an urban site in the Po valley. Chemosphere 241, 125025 (2020).

17.2
Assimilation of atmospheric CO_2 measurements from the CarboSense network using the COSMO-GHG model

Simone Baffelli[1], Dominik Brunner[1], Christoph Hüglin[1], Lukas Emmenegger[1]

[1] Air Pollution / Environmental Technology, Empa, Überlandstrasse 129, 8600 Dübendorf (simone.baffelli@empa.ch)

During the CarboSense project we deployed an unique swiss-wide CO_2 observation network consisting of 240 sensors(Müller et al., 2020). This observation system was designed to study carbon sinks and sources at high temporal and spatial resolution. The network consists of more than 200 low-cost SenseAir LP8 nondispersive IR (NDIR) sensors, 20 mid-cost SenseAir HPP NDIR instruments, and 7 high-precision Picarro cavity ringdown spectrometers (CRDS) employed as reference instruments. The sensors relay their observations at 10 minute intervals through the LoraWAN low power network to a database, where it is subject to calibration and data control. As a complement to the observation network, the COSMO-GHG atmospheric transport model was set up for the domain of Switzerland and used for simulation of the emissions, biospheric exchange fluxes and transport of CO_2 at the kilometer scale(Jähn et al., 2020) (Liu et al., 2017).

Both the model and the observations from the network suffer from limitations. The low-cost sensors are subject to long-term drift and may be sensitive to local emissions sources at a spatial scale unmodeled by COSMO-GHG. We correct the drifts by comparison with observations from the high-precision sensors during periods of well-mixed atmosphere. Similarly, the model COSMO-GHG shows a bias induced by the boundary coditions taken from CAMS and it assumes too much vertical mixing of the atmosphere during night, which leads to an underestimation of the predicted CO_2 concentrations.

Data assimilation can help in this context by combining observations and models in a statistically consistent manner and thereby identifying and correcting biases in both model and observations. We have set up a data assimilation system that combines the observations with COSMO-GHG to produce accurate hourly CO_2 maps at 2 Km resolution over Switzerland using a reduced-rank Kalman filter. The state vector consists of the corrected CO_2 field, the model bias field, and one measurement bias per sensor. We assume model error and model bias to have different correlation lengths and to follow an isotropic, squared exponential covariance structure. Thanks to these assumptions, the assimilation is computed in a subspace defined by the first 50 discrete cosine transform (DCT) basis vectors, as the covariance matrix in this basis is diagonal and most of the energy is concentrated in the low-frequency basis vectors(Rasmussen & Williams, 2006). This rank-reducing transformation greatly reduces the computation time and storage requirements, allowing to assimilate observations from all sensors in the network in less than 10 seconds.

We validate the system using leave-one-out cross validation by removing measurements from one high-precision sensor, assimilating the observations from the remaining sensors and repeating the procedure for all high-precision sensors. The assimilation reduces the bias and increases the correlation coefficent, showing that the Kalman filter can improve the data quality and correct both model and sensor biases.

In summary, because of the efficient implementation of the algorithm, the high resolution transport model and the dense observation network, our assimilation system produces CO_2 maps at the Swiss country scale with high quality while running on a regular desktop PC, provided that the COSMO-GHG model outputs are available. Furthermore, because of the flexible nature of the Kalman filter, the assimilation process is also valuable to detect, address and overcome limitations in both models and measurements.

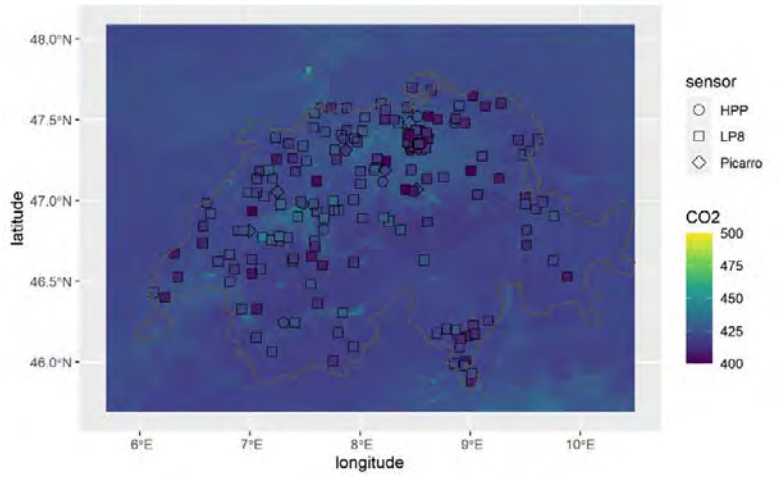

Figure 1 Example of an assimilated CO_2 field obtained using the assimilation system.

REFERENCES

Jähn, M., Kuhlmann, G., Mu, Q., Haussaire, J.-M., Ochsner, D., Osterried, K., Clément, V., & Brunner, D. (2020). An online emission module for atmospheric chemistry transport models: Implementation in COSMO-GHG v5.6a and COSMO-ART v5.1-3.1. Geoscientific Model Development, 13(5), 2379–2392. https://doi.org/10.5194/gmd-13-2379-2020

Liu, Y., Gruber, N., & Brunner, D. (2017). Spatiotemporal patterns of the fossil-fuel CO_2 signal in central Europe: Results from a high-resolution atmospheric transport model. Atmospheric Chemistry and Physics, 17(22), 14145–14169. https://doi.org/10.5194/acp-17-14145-2017

Müller, M., Graf, P., Meyer, J., Pentina, A., Brunner, D., Perez-Cruz, F., Hüglin, C., & Emmenegger, L. (2020). Integration and calibration of non-dispersive infrared (NDIR) CO_2 low-cost sensors and their operation in a sensor network covering Switzerland. Atmospheric Measurement Techniques, 13(7), 3815–3834. https://doi.org/10.5194/amt-13-3815-2020

Rasmussen, C. E., & Williams, C. K. I. (2006). Gaussian processes for machine learning. MIT Press.

17.3
N_2O emissions from grazed pastures - Influence of urine patch characteristics

Lena Barczyk[1,2], Kate Kuntu-Blankson[1,2], Pierlugi Calanca[1], Johan Six[2], Christof Ammann[1]

[1] Climate and Agriculture group, Agroscope Research Station, Reckenholzstrasse 191, CH-8046 Zürich (lena.barczyk@agroscope.admin.ch)
[2] Sustainable Agroecosystem group, Institute of Agricultural Sciences, ETH Zürich, Universitätstrasse 2, CH-8092 Zürich,

In pasture systems, nitrogen (N) inputs are mainly attributed to fertilizer applications and to the excreta of grazing animals. Especially urine patches of grazing animals form hotspots of N supply and are prone to N losses like nitrate leaching and emission of the important greenhouse gas nitrous oxide (N_2O). The default emission factor (EF) of 2 % for grazing based N inputs is used to quantify national N_2O emissions in Switzerland. However, some countries established country-specific EFs showing considerable differences. To better understand urine patch N dynamics and to link N_2O fluxes to influencing factors, we examine N_2O fluxes and resulting EF values of artificially applied urine patches in relation to possible drivers like urine N concentration, urination volume and urine patch area. Eight urine application experiments were performed in the grazing seasons of the years 2020 and 2021 on a pasture field located in Aadorf/Thurgau. N_2O fluxes are measured by a manually operated chamber connected to an online gas analyzer. It is the first study in Switzerland investigating patch-scale N_2O fluxes by controlled application of synthetic and real urine. We present and discuss results of these measurements.

17.4
Detecting changes in the contributions of abiotic vs. biotic factors to regular and extreme carbon dioxide and water vapor flux events

Moritz Bruggisser[1], Mana Gharun[1], Ankit Shekhar[1], Lukas Hörtnagl[1], Iris Feigenwinter[1], Alexander Damm[2,3], Nina Buchmann[1]

[1] Institute of Agricultural Sciences, ETH Zurich, Universitätstrasse 2, CH-8092 Zurich (moritz.bruggisser@usys.ethz.ch)
[2] Department of Geography, University of Zurich, Winterthurerstrasse 190, CH-8057 Zurich
[3] Eawag, Swiss Federal Institute of Aquatic Science & Technology, Surface Waters – Research and Management, Überlandstrasse 133, CH-8600 Dübendorf

Extreme weather events such as droughts and heat waves are expected to occur more frequently due to climate change. A changing climate and weather extremes affect ecosystem functioning through altered dynamics of temperature, precipitation and, thus, water availability. At the same time, biotic vegetation characteristics such as biochemistry and canopy structure influence vegetation functioning. Abiotic and biotic drivers thereby have an interacting contribution on the functioning of ecosystems, while acting on different time-scales from short to medium time ranges, and even cause shifts in the phenology.

In order to unravel these interacting impacts of abiotic vs. biotic drivers on the carbon dioxide (CO_2) and water vapor exchange fluxes between the vegetation and the atmosphere, we used measurements of abiotic drivers including soil conditions and meteorology alongside with remotely sensed measurements of biotic drivers.

Compound events of meteorological drivers such as high temperature co-occurring with low water availability, however, complicate the identification of ecosystem responses to extreme weather events. We thus approached the extreme conditions from the impact's perspective and identified extreme conditions via anomalous ecosystem responses. We particularly analysed CO_2 and water vapor fluxes measured by means of the eddy covariance (EC) method. Flux measurements from three test sites in Switzerland were used, namely from an arable field (Oensingen), a mixed temperate forest (Lägeren) and an alpine coniferous forest (Davos). The respective time series cover a minimum of 15 years, i.e. the years 2004-2018 (Oensingen), 2004-2020 (Lägeren) and 1997-2019 (Davos). At each site, potential abiotic drivers (i.e. air temperature, soil temperature, relative humidity, precipitation, soil water content, incoming shortwave radiation) were recorded simultaneously to the fluxes. Remote sensing data from airborne and spaceborne missions were available for the characterization of the biotic conditions including canopy structure, biochemistry and phenology.

Half-hourly EC CO_2 and water vapor flux measurements were aggregated to mean daily fluxes. Daily aggregated fluxes, thus, formed the basis for the detection of extreme flux events. In order to detect days with anomalous fluxes, we compared daily fluxes to long-term weekly average fluxes. Days with fluxes falling below the 5th or above the 95th percentile of the long-term weekly mean fluxes were marked as days with extreme fluxes. Finally, we defined extreme events as periods with a minimum of three consecutive extreme daily fluxes. These extreme events with a minimum duration of three days formed the basis for the further analysis. Applying such a definition, we identified 95, 64 and 171 extreme CO_2 flux events for Oensingen, Lägeren and Davos during the 15+ years, respectively. During 46, 38 and 89 of these identified extreme events at the three respective sites, the daily fluxes fell below the 5th percentile of weekly reference fluxes and, thus, are events with anomalous CO_2 uptakes. Contrary, daily fluxes during 49, 26 and 82 events were above the 95th percentile compared to the reference periods, corresponding to anomalous CO_2 releases. Likewise, we detected 97, 61 and 183 extreme water vapor flux events at the three sites. 49, 24 and 88 of these events at the respective sites correspond to periods with extremely low water vapor fluxes, i.e. fluxes falling below the 5th percentile during the reference periods. Fluxes during 48, 37 and 95 events at the three respective sites, in contrast, exceeded the 95th flux percentile. Extreme events for both fluxes at any given site coincided in 17, 4 and 34 cases, respectively.

Generalized additive mixed models (GAM) were subsequently used to quantify the contribution of the abiotic vs. biotic drivers to the observed extreme fluxes. The comparison of their contribution during regular, i.e. non-extreme events, versus extreme flux events allowed us to identify modifications in the ecosystem responses under extreme events. Particularly, short to mid-term weather conditions and phenological patterns which lead to extreme flux events could be revealed. On the one hand, these could be weather phenomena, e.g. heat waves, preceding an extreme flux event on short-terms which trigger extreme fluxes. On the other hand, the experimental setup allowed to investigate whether the productivity of the ecosystem at an earlier time during the phenological cycle impacts the occurrence of extreme flux events later during the growing season, which is possibly dominated by changed meteorological conditions.

17.5
Can soil nitrous oxide emissions of complex cropland management be captured by a process-based model?

Marcio dos Reis Martins, Sonja G. Keel

Climate and Agriculture Group, Research Division Agroecology and Environment, Agroscope, Zurich, Switzerland (marcio.dosreismartins@agroscope.admin.ch)

For national greenhouse gas reporting, N_2O emissions from agricultural soils are currently estimated using a rather simple emission factor approach that does not account for temporal and spatial variability (FOEN 2021). Furthermore, it does not allow estimating mitigation potentials of specific practices. Here we evaluate the process-based model DayCent for prediction of N_2O emissions in six different cropland sites.

Calibration was incrementally performed for parameters controlling (i) plant growth, (ii) management effects on different soil N pools, and (iii) N transformation on soil by nitrification and denitrification (N-cycle parameters). A leave-one-out cross-evaluation was performed to test DayCent's ability to predict N_2O emissions for new, independent sites. Prediction of crop yields was also evaluated as a quality control of the overall model performance.

The site-specific calibration of parameters improved DayCent's ability to predict daily fluxes and cumulative emissions of N_2O. This improvement increased the model's ability to detect treatment-induced differences in N_2O emissions. Compared to the use of default parameterization, average values of the calibrated parameters, derived from the leave-one-out evaluation, increased Daycent's ability to predict crop yields and the mean N_2O fluxes for independent sites. We further suggest that some additional improvement of the model's predictive ability for N_2O emissions could be achieved by using specific values for N-cycle parameters for different conditions (e.g., soil and climate).

To perform a comparison with the IPCC emission factor (EF) approach, we estimated mean cumulated N_2O emissions simulated for twenty-three cropping cycles with reasonable coverage of flux measurements. Compared to mean observed emissions per crop cycle (3.0 kg N ha^{-1}), DayCent clearly provided a more accurate estimate (2.8 kg N ha^{1}) than the EF approach (1.3-1.5 kg N ha^{1}). Overall, our results indicate that DayCent can be a useful tool for reporting N_2O emissions in Swiss croplands and for evaluating potential mitigation scenarios.

REFERENCES

FOEN 2021: Switzerland's greenhouse gas inventory 1990–2019. National inventory report of Switzerland 2021, Federal Office for the Environment, Bern.

17.6
Radical Cycling Induced by Transition Metal Complex Photochemistry in Viscous Organic Aerosol Particles

Kevin Kilchhofer[1,2], Peter Aaron Alpert[1], David Bell[3], Mihnea Surdu[3], Imad El Haddad[3], Ka Yuen Cheung[3], Laura Torrent[4] and Markus Ammann[1]

[1] *Laboratory of Environmental Chemistry, Paul Scherrer Institute, Villigen, 5232 (kevin.kilchhofer@psi.ch)*
[2] *Department of Environmental System Science, Institute for Atmospheric and Climate Science, ETH Zürich, Zürich*
[3] *Laboratory of Atmospheric Chemistry, Paul Scherrer Institute, Villigen, 5232*
[4] *Bioenergy and Catalysis Laboratory, Paul Scherrer Institute, Villigen, 5232*

Radical chemistry in atmospheric aerosol particles can affect human health, climate and aerosol lifetime. Photolysis of iron-carboxylate complexes in aerosol particles produces carbon-centered free radicals (CCFR) and reactive oxygen species (ROS). This is important for depletion of organic aerosol (OA) (Weller et al., 2013) and the total aerosol burden (Dou et al., 2021). Here, we use particles composed of citric acid, iron(III)-citrate and copper(II)-citrate as model surrogate for atmospheric aerosol composed of organic and transition metal ions (TMIs). Iron(III)-citrate is a complex that photolyzes to make radicals, however the impact of copper in the TMI redox cycling in photochemical processes in organic aerosols is highly uncertain. Furthermore, in aerosols with high viscosity oxygen can be depleted, leading to anoxic conditions in the interior of the particles (Alpert et al., 2021) potentially giving rise to unique organic products.

In this study, we observe the iron and copper oxidation state in particles using X-ray spectro-microscopy in an in situ photochemical environment reaction cell. Additionally, organic products at high mass resolution are observed using a unique setup, which consists of coupling an aerosol flow tube (AFT) experiment to an online extractive electrospray ionisation mass spectrometer (EESI-TOF-MS, Lopez-Hilfiker et al., 2019).

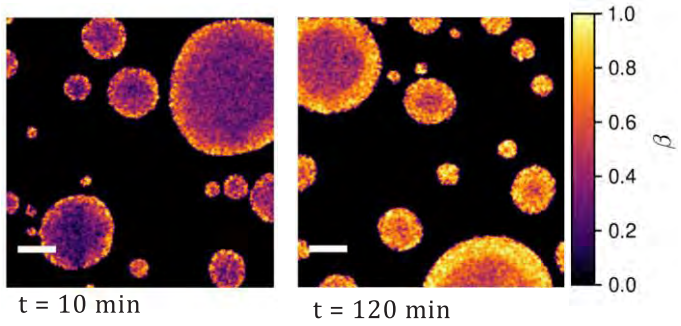

Figure 1. X-ray images of the iron(III) fraction, β, in particles with a Fe:Cu mole ratio of 5:1 directly showing the reduction of iron(III) to iron(II) by photolysis in the presence of O_2 and at *RH* = 45%. The white scale bar is 0.5 µm.

X-ray images of particles were obtained before and after UV irradiation as a function of relative humidity, *RH*, at the PolLux beamline of the Swiss Light Source. Figure 1 shows the iron(III) fraction, β, of particles with an iron : copper : citric acid mole ratio of 5:1:5 at *RH* = 45%. Reoxidation occurred near the surface of the particles only and remained constrained to within about 0.5 µm. This shows that molecular oxygen transport through the particle and its involvement in reoxidizing iron must have been limited. Having this in mind, we use the AFT-EESI-TOF-MS setup in order to determine the fate of organic species in anoxic and oxic conditions and at different *RH* conditions. We have detected a major first generation fragmentation product, a ketodicarboxylic acid, and also accretion products during irradiation. The corresponding O:C ratio indicates that it might result from the recombination of CCFRs. The photochemical production is more apparent at high *RH* and different between samples with and without copper as additional TMI. This implies higher turnover of free radicals or ROS.

The results will help to assess photochemical reaction schemes in organic aerosols, which we will also apply in larger scale atmospheric modelling.

REFERENCES

Alpert, P. A. … Ammann, M. (2021). Photolytic radical persistence due to anoxia in viscous aerosol particles. *Nature Communications 2021 12:1*, *12*(1), 1–8. https://doi.org/10.1038/s41467-021-21913-x

Dou, J. … Krieger, U. K. (2021). Photochemical degradation of iron(III) citrate/citric acid aerosol quantified with the combination of three complementary experimental techniques and a kinetic process model. *Atmospheric Chemistry and*

Physics, *21*(1), 315–338. https://doi.org/10.5194/ACP-21-315-2021

Lopez-Hilfiker, F. D. … Slowik, J. G. (2019). An extractive electrospray ionization time-of-flight mass spectrometer (EESI-TOF) for online measurement of atmospheric aerosol particles. *Atmospheric Measurement Techniques*. https://doi.org/10.5194/amt-12-4867-2019

Weller, C. … Herrmann, H. (2013). Photolysis of fe(iii) carboxylato complexes: Fe(ii) quantum yields and reaction mechanisms. *Journal of Photochemistry and Photobiology A: Chemistry*. https://doi.org/10.1016/j.jphotochem.2013.06.022

17.7
Thermodynamic modelling of the co-condensation of organic compounds on atmospheric aerosol particles

Judith Kleinheins[1], Claudia Marcolli[1], Thomas Peter[1], Ulrike Lohmann[1]

[1] *Institute for Atmospheric and Climate Science, ETH Zurich, Universitätsstrasse 16, CH-8092 Zurich (judith.kleinheins@env.ethz.ch)*

In the atmosphere, tiny liquid or solid particles with diameters from nanometers to micrometers—so-called aerosol particles—can interact with solar radiation and thereby influence the global climate (Lohmann et al. 2016). The aerosol particle size is a crucial parameter determining the final radiative forcing. Therefore, measuring and modelling the accurate particle size of atmospheric aerosol particles is key to obtain more accurate climate projections that allow us to timely prepare for further climate change.

To date, the hygroscopic growth of aerosol particles typically has been measured with hygroscopic tandem differential mobility analyzers (HTDMAs) (Lopez-Yglesias et al. 2014). When relative humidities (RH) reach a critical value above 100 %, particles ultimately undergo cloud droplet activation, which is traditionally modelled by Köhler theory (Köhler 1936). Both, the measurement principle and the modelling of aerosol particle growth are based on the assumption that the gas phase contains air and water vapour only and the particles consist of non-volatile substances. However, neither of these assumptions is strictly fulfilled. Rather, the atmosphere contains a substantial amount of semi-volatile organic substances (SVOCs) (Cappa & Jimenez 2010). SVOCs can be found both in the gas and in the particle phase, whereas classical Köhler theory assumes this to be the case only for water. SVOCs often condense hardly on their own on a dry aerosol particle. However, at higher relative humidity and consequently higher water content of the particle, the SVOCs can partly condense along with the water vapor, a process called co-condensation. Similarly, the SVOCs can co-evaporate when drying an atmospheric aerosol sample, which is typically done in aerosol measuring devices.

Here, we report on the new project ORACLE (aerOsol-cloud interactions: the Role of orgAnic compounds on CLoud droplEt activation), in which we investigate to what extent aerosol particle size and activation properties are biased by co-condensation or co-evaporation processes in HTDMAs and Köhler theory modelling.

To illustrate the influence of co-condensation on aerosol hygroscopic growth, we present calculations of particle size at prescribed RH and SVOCs using the thermodynamic model AIOMFAC (Zuend et al. 2011). In a first test, the particles consist of ammonium sulfate—a common inorganic non-volatile substance in atmospheric aerosols—and sugar (e.g. glucose) to represent low-volatile organic substances. Then, water and an organic model compound representing the semi-volatile organic compounds, such as alcohols with different numbers of OH-groups, are allowed to equilibrate at varying humidity levels. We show to what extent co-condensation influences the hygroscopic growth and how state-of-the-art measurement techniques can produce misleading results.

REFERENCES

Cappa, C. D., Jimenez, J. L. 2010: Quantitative estimates of the volatility of ambient organic aerosol. Atmospheric Chemistry and Physics, Vol. 10, No. 12, p. 5409-5424.

Köhler, H. 1936: The nucleus in and the growth of hygroscopic droplets. Trans. Faraday Soc. 32, 1152–1161.

Lohmann, U., F. Lüönd, and F. Mahrt 2016: An Introduction to Clouds: From the Microscale to Climate. Cambridge University Press, Chapter 12.

Lopez-Yglesias, X., Yeung, M., Dey, S., Brechtel, F., Chan, C. 2014: Performance Evaluation of the Brechtel Mfg. Humidified Tandem Differential Mobility Analyzer (BMI HTDMA) for Studying Hygroscopic Properties of Aerosol Particles. Aerosol Science and Technology , Vol. 48, No. 9 Taylor & Francis, p. 969-980.

Zuend, A., Marcolli, C., Booth, A. M., Lienhard, D. M., Soonsin, V., Krieger, U. K., Topping, D. O., McFiggans, G., Peter, T., and Seinfeld, J. H. 2011: New and extended parameterization of the thermodynamic model AIOMFAC: calculation of activity coefficients for organic-inorganic mixtures containing carboxyl, hydroxyl, carbonyl, ether, ester, alkenyl, alkyl, and aromatic functional groups. Atmos. Chem. Phys. 11, 9155–9206.

17.8
Phase behaviour of mixtures of primary and secondary organic aerosol material

Fabian Mahrt[1,2], Elli Newman[1], Yuanzhou Huang[1], Julia Zaks[1], Annesha Devi[1], Yi Ming Qin[3], Paul E. Ohno[3,4], Scot T. Martin[3,5], Markus Ammann[2], and Allan K. Bertram[1]

[1] Department of Chemistry, University of British Columbia, 2036 Main Mall, Vancouver, BC, V6T 1Z1, Canada
2 Laboratory of Environmental Chemistry, Paul Scherrer Institute, 5232 Villigen, Switzerland
3 John A. Paulson School of Engineering and Applied Sciences, Harvard University, Cambridge, MA 02138, USA
4 Center for the Environment, Harvard University, Cambridge, MA 02138, USA
5 Department of Earth and Planetary Sciences, Harvard University, Cambridge, MA 02138,USA

Aerosol particles play an important role for air quality and climate. Primary organic aerosol (POA) and secondary organic aerosol (SOA) make up a significant mass fraction of submicron atmospheric particles. POA denotes aerosols that are directly emitted into the atmosphere as particles, while SOA is mainly formed from oxidation of precursor gases, followed by gas-to-particle conversion of the low-volatility oxidation products. In order to describe SOA formation in atmospheric models, and predict their impact on air quality and climate, knowledge on the phase behaviour, i.e., the number and types of phases, in mixtures of POA and SOA material is essential. For example, models often assume that SOA formation is enhanced in the presence of POA seed particles due to a lowering of the activities in the liquid organic aerosol phase in case of single-phase POA+SOA particles. The presence of POA will have a smaller effect on the formation of SOA mass in case of phase-separated particles.

Here, using optical and fluorescence microscopy, we observed the phase behaviour of individual particles containing mixtures of proxies of POA and SOA as a function of relative humidity (RH) between 90% to 0% RH. Commercially available organic molecules were used as proxies for POA and SOA material, covering a range of oxygen-to-carbon ratio between 0 and 1.0. For most of the mixtures investigated, phase-separated particles dominated. Our results suggest that the phase behaviour strongly depends on the oxygen-to-carbon ratio of the two mixed proxies. Results using more complex SOA material generated in environmental chambers and mixed with the same POA proxies confirm the dominance of phase separated POA+SOA particles. Our results have important implications for air pollution policies being considered to limit SOA formation in urban environments.

17.9
Towards understanding the regional CO_2 contributions at the high Alpine observatory Jungfraujoch

Simone M. Pieber[1], Bela Tuzson[1], Stephan Henne[1], Ute Karstens[2], Christoph Gerbig[3], Thomas Koch[3], Dominik Brunner[1], Martin Steinbacher[1], Lukas Emmenegger[1]

[1] *Laboratory for Air Pollution and Environmental Technology, Empa, Switzerland (simone.pieber@empa.ch)*
[2] *ICOS Carbon Portal, Lund University, Sweden*
[3] *Max Planck Institute (MPI) for Biogeochemistry (BGC), Jena, Germany*

Reliable regional quantification of greenhouse gas (GHG) emissions into the atmosphere is a prerequisite to determine the effectiveness of mitigation strategies to limit global warming. In this study, we challenged our understanding of the regional contributions of carbon dioxide (CO_2) at the location of the high altitude research station Jungfraujoch ("JFJ", Switzerland, 3580 m above sea level).

To this purpose, we combined receptor-oriented atmospheric transport simulations for CO_2 concentration in the period of 2009–2017 with stable carbon isotope ($\delta^{13}C\text{-}CO_2$) information. We applied two Lagrangian particle dispersion models driven by output from two different numerical weather prediction sys-tems (FLEXPART-COSMO and STILT-ECMWF). Both models were used to simulate CO_2 concentration at JFJ based on regional CO_2 fluxes, to estimate atmospheric $\delta^{13}C\text{-}CO_2$, and to derive mixed source signatures ($\delta^{13}C_m$). Anthropogenic fluxes were taken from a fuel type-specific version of the EDGAR v4.3 inventory and ecosystem fluxes were based on the Vegetation Photosynthesis and Respiration Model (VPRM). The simulated CO_2 and $\delta^{13}C\text{-}CO_2$ data and forward estimated $\delta^{13}C_m$ were compared to observations performed by quantum cascade laser absorption spectroscopy.

The comparison indicates that around 40 % of the regional CO_2 variability above or below the large-scale background can be captured by the models, and up to 35 % of the regional variability in $\delta^{13}C\text{-}CO_2$. Best agreement between simulations and observations in terms of short-term variability and intensity of the signals for CO_2 and $\delta^{13}C\text{-}CO_2$ was found between late autumn and early spring. For the summer, however, the CO_2 simulations poorly reproduced the regional CO_2, and a quantitative discrepancy remained in the early autumn periods. This may be associated with the atmospheric transport representation in the models, as we found that the signal intensity in summer differed between the models. In addition, the net eco-system exchange fluxes are a possible source of error, either through inaccuracies in their representation in VPRM for the (Alpine) vegetation or through a day (uptake) vs. night (respiration) transport discrimination to JFJ. Furthermore, the simulations suggest that JFJ's remote location, combined with limited planetary boundary layer-influence during winter, exposes the station predominantly to rather local (within 100 km) ecosystem CO_2, which appear to outweigh the regional anthropogenic influence. Even during the winter months, simulated gross ecosystem respiration accounted for approximately 50 % of all regional contributions to the CO_2 concentrations.

17.10
Assessing Swiss halocarbon emissions from regional atmospheric measurements

Dominique Rust[1,2], Ioannis Katharopoulos[1], Martin K. Vollmer[1], Stephan Henne[1], Matthias Hill[1], Lukas Emmenegger[1], Renato Zenobi[2], Stefan Reimann[1]

[1] Laboratory for Air Pollution and Environmental Technology, Empa, Überlandstrasse 129, CH-8600 Dübendorf (dominique.rust@empa.ch)
[2] Department of Chemistry and Applied Biosciences, ETH Zurich, Vladimir-Prelog Weg 1-5/10, CH-8093 Zurich

Human-made halocarbons contribute approximately 10% to the anthopogenically caused radiative forcing from long-lived greenhouse gases (GHGs). In addition, chlorinated or brominated halocarbons cause stratospheric ozone depletion. To curb these environmental impacts, the production and consumption of halocarbons is prohibited or regulated by international treaties, such as the Montreal and Kyoto Protocols. To assess human halocarbon emissions directly from the observed atmospheric abundances of these gases, so called “top-down” inverse modelling approaches have been developed. These methods rely on atmospheric measurements at sites that capture global or continental atmospheric background concentrations of halocarbons. Additional regional-scale measurements allow the calculation of local or national halocarbon emissions.

We present 18 months of continuous, high-frequency, high-precision halocarbon measurements from the Beromünster and Sottens tall towers, located on the Swiss Plateau. Together, the two sites are sensitive to the most densely populated part of Switzerland. Every hour, a two-liter air sample was drawn from the top of each tower and pre-concentrated at low temperatures. The analytes were separated by gas chromatography and detected by quadrupole mass spectrometry (GC-MS).

Based on the measured concentration records at Beromünster, we assessed the Swiss emissions and source regions of 28 halocarbons by applying two top-down calculation methods: a tracer ratio method, with carbon monoxide (CO) as the independent tracer, and a Bayesian inversion based on atmospheric transport modelling. Our results show ongoing outgassing from existing foams and refrigeration units for the banned chlorofluorocarbons (CFCs) and the regulated hydrochlorofluorocarbons (HCFCs), indicating their extensive use in the past. For the major hydrofluorocarbons (HFCs), our top-down emission results agree well with the Swiss bottom-up inventory values, as annually reported to the United Nations Framework Convention on Climate Change (UNFCCC). An exception is HFC-134a, for which our top-down emissions of 300 Mg yr^{-1} are 30% lower than the Swiss national inventory, hinting at a possible overestimation of the latter. Finally, we report the first national emission values for three recently phased-in hydrofluoroolefins (HFOs), totalling to 50 Mg yr^{-1}. These results will be complemented with the data from the on-going Sottens measurement campaign, based on which we can additionally investigate emissions from the southeastern part of France.

17.11
An observation-based approach for monitoring urban CO_2 fluxes at high spatial and temporal resolution

Stavros Stagakis[1], Christian Feigenwinter[1], Roland Vogt[1], Andrea Pitacco[2], Markus Kalberer[1]

[1] *Department of Environmental Sciences, University of Basel, Klingelbergstrasse 27, 4056, Basel, Switzerland (stavros.stagakis@unibas.ch)*
[2] *Department of Agronomy, Food, Natural resources, Animals and Environment, University of Padova, Viale dell'Università 16, Legnaro, PD I-35020, Italy*

Climate change mitigation actions will be critical to keep global warming below the threshold of 2 °C in the coming decades. Cities emit almost three quarters of the total anthropogenic CO_2 and therefore have an increasingly important role towards achieving climate neutrality. So far, many cities around the globe have shown clear ambition in taking action against climate change and have committed to ambitious climate action plans in accordance to the goals and directives of the Paris Agreement in 2015. To assess the progress towards these emission reduction targets, cities often develop their own greenhouse gas (GHG) inventories and methodologies of emission reporting. However, the consistency, quality and accuracy of these methods are not systematically assessed and often their spatial and temporal resolution are not adequate to inform urban planning decisions.

This study introduces an observation-based method to monitor urban CO_2 fluxes (F_C) at 20 m resolution and hourly intervals, which can be used as an independent reference to urban inventories and as a tool for sustainable urban planning. The approach is divided at two discrete steps. At the first step, the main urban F_C components (i.e. building emissions, traffic emissions, human metabolism, photosynthetic uptake, plant respiration, soil respiration) are modelled independently based on high resolution geospatial, meteorological, population and traffic activity datasets. At the second step, the modelled F_C components (priors) are combined with observed total F_C from tower-based Eddy Covariance systems using a probabilistic inversion method (Bayesian inference) to derive optimized flux estimates of each component (posteriors) and their uncertainties. The combination between the gridded flux priors and the Eddy Covariance F_C measurements is accomplished through turbulent flux footprint modelling, parameterized anisotropically according to the directional urban morphology around each tower.

The method is applied on the city centre of Basel, Switzerland, covering an area of 9 km^2. The study area includes two permanent Eddy Covariance towers, providing continuous flux measurements from areas with different CO_2 source/sink characteristics. The study reveals the spatial and temporal complexity of the urban CO_2 flux dynamics both diurnally and seasonally. It is demonstrated that Eddy Covariance observations can be efficiently explained by the modeled F_C for both tower sites and different wind directions, leading to successful inversion modelling and optimization results. Building emissions are the most important F_C component in the study area of Basel, showing intense seasonal and spatial variability that is challenging to estimate. Moreover, the spatial representation of building emissions and the combination with Eddy Covariance measurements is another challenging part of the methodology that is accounted for in the model through flux footprint extent normalization factors.

17.12
Nitrous oxide emissions from different fertiliser and crop combinations using time integrated measurements

Alex Valach[1], Markus Jocher[1], Daniel Bretscher[1], Christof Ammann[1]

[1] Climate and Agriculture Group, Agroscope, Reckenholzstrasse 191, Zürich, Switzerland
(alex.valach@agroscope.admin.ch)

Nitrous oxide (N_2O) is a potent greenhouse gas with 80 % of emissions stemming from agricultural activities. Switzerland currently reports contributions of N_2O in its greenhouse gas emission inventory using Tier 1 methods, i.e. multiplying the N inputs in agricultural fields with default global emission factors. Recent refinements suggest to differentiate between different N input types, as well as to apply country-specific emission factors derived from local field measurements of representative agricultural systems. Since climate, soil properties, N input types (e.g. different fertilisers), as well as land management practices all affect N_2O emissions, it is important to quantify fluxes from representative Swiss conditions to improve our inventory reporting.

N_2O emissions display considerable pulsing behaviour in both space (hot spots) and time (hot moments). Due to this pulsing behaviour, spatial and temporal heterogeneities of the conditions driving N_2O emissions can result in measurements from different sites or timeframes not being comparable. Emissions from hot moments can lead to biases in annual emission budgets when relying on data from short or infrequent measurement methods, such as manual chambers, while sufficient replicates are needed to capture the spatial variations. Therefore comparing the emissions from different crops and fertiliser combinations requires a concurrent experimental setup with an appropriate control. We measured N_2O emissions at a long-term field experiment at Reckenholz consisting of multiple concurrent crops in a typical rotation receiving different fertiliser treatments, which allows a direct comparison of the fertiliser and crop combinations. Here we present the ongoing measurements of fluxes from a complete growing season and discuss potential implications for Swiss emission inventory reporting.

P 17.1
Tree-ring stable isotopes variations after major tropical and north hemispheric volcanic eruptions

Tito Arosio[1,2], Malin M. Ziehmer[1,2,5], Kurt Nicolussi[3], Michael Sigl[1,2,] Christian Schlüchter[4], and Markus Leuenberger[1,]

[1] *Climate and Environmental Physics, Physics Institute, University of Bern, 3012 Bern, Switzerland*
[2] *Oeschger Centre for Climate Change Research, University of Bern, 3012 Bern, Switzerland*
[3] *Department of Geography, Universität Innsbruck, 6020 Innsbruck, Austria*
[4] *Institute of Geological Sciences, University of Bern, 3012 Bern, Switzerland*
[5] *Swiss Tropical and Public Health Institute, Socinstrasse 57, 4051 Basel, Switzerland*

Tree-ring widths (TRW) have already been widely used for climate investigations and dating of major volcanic eruptions in the last millennia due to its annual resolution. The stable isotopes of tree rings are known to be climatic proxies complementary to TRW. However, only few studies are available using stable tree-ring isotopes to track climate variability after volcanic eruptions. To investigate which of the three stable cellulose isotopes carry information of the climate changes driven by eruptions, we analyzed the isotope values of cellulose from trees living in the periods around the eruption of the tropical Tambora volcano eruption of 1815 CE and of the Icelandic Katla volcano eruptions of 720-780 CE. The year-resolved $\delta^{18}O$ data overlapped those of 5-year resolution available in the *Alpine Holocene Tree Ring Isotope Records*. The $\delta^{18}O$ values show a climatic variation after the Tambora event, but not after the Katla eruption. A significant correlation was found between the cellulose $\delta^{18}O$ and the summer temperature records of HISTALP database (period 1800-2010). The analysis was extended to several tropical and Icelandic volcano eruptions using the *Alpine Holocene Tree Ring Isotope Records,* with 5-year resolutions. This confirmed that $\delta^{18}O$ values, but not δD and $\delta^{13}C$ values, were partially sensitive to the climatic impact of eruptions. In conclusion, our data indicate that cellulose $\delta^{18}O$ values can provide significant information on the climatic variations following strong volcanic eruptions providing additional information to the TRW

P 17.2
Studying Atmospheric Waves in the middle atmosphere from ground-based temperature measurements

Witali Krochin[1,2], Axel Murk[1,2], Gunter Stober[1,2]

[1] *Institute of Applied Physics, University of Bern, Sidlerstrasse 5, CH-3012 Bern (witali.krochin@iap.unibe.ch)*
[2] *Oeschger Centre for Cliamte Change Research, University of Bern, Hochschulstrasse 4, CH-3012 Bern*

Atmospheric temperatures and their vertical variability play a key role for the understanding of atmospheric processes and dynamics. Temperature observations at the middle atmosphere, which consist of the stratosphere and mesosphere, are rare. However, these altitudes are crucial to investigate the energy and momentum transport by atmospheric waves and impacts the global energy budget. Furthermore, the vertical propagation of atmospheric waves results in coupling between different atmospheric layers altering the energy budget far away from their source regions.

A better understanding of the global energy transport and vertical coupling driven by atmospheric waves is essential to improve the performance of climate models, which are still only partially capable to obtain a realistic circulation at the mesosphere and to resolve the wave-driven processes. This improvement would not only lead to a more fundamental understanding of atmospheric dynamics but also would improve long term weather forecast.

Atmospheric waves can be observed by measuring the atmospheric temperature profile. However, the temporal resolution often is limited and, thus, provides an observational filter for certain atmospheric waves. In particular, satellites sample a certain geographic location only once or twice per day. Ground-based remote sensing permits to overcome this limitation and become an established to study atmospheric wave dynamics at a much higher temporal resolution. Moreover this measurement technique covers altitudes (20-55 km) which are difficult to observe with other methods because it is too high for balloon soundings and too low for satellites in-situ probing.

In 2013, the University of Bern has developed a ground-based temperature radiometer (TEMPERA) observing microwave radiation from atmospheric oxygen in a frequency range between 52-53 GHz (see Figure 1). After the latest improvements of the measurement technique and data processing TEMPERA measurements provides temperature profiles with an altitude range from 20 - 55 km and a current time resolution of one profile per 3h (see Figure 2), which appears to be sufficient to investigate atmospheric tides, which typically have a period of an integer fraction of a day. Here we present first results and a validation of the measurements with two atmospheric reanalysis models.

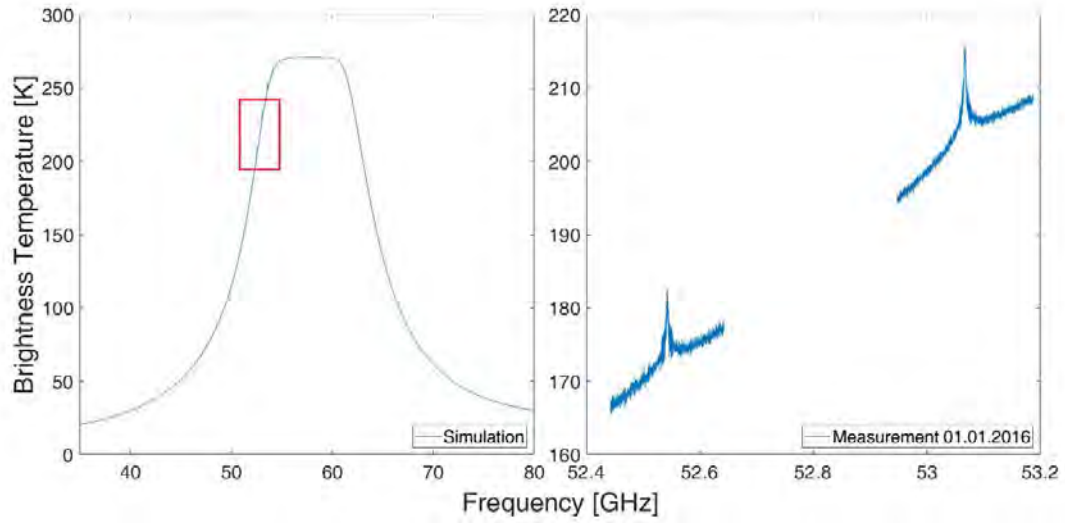

Figure 1. Simulation of the atmospheric radiation in a frequency range between 40-80 GHz. The red box indicates the measurement range of TEMPERA (left). Calibrated spectrum measured by TEMPERA (right).

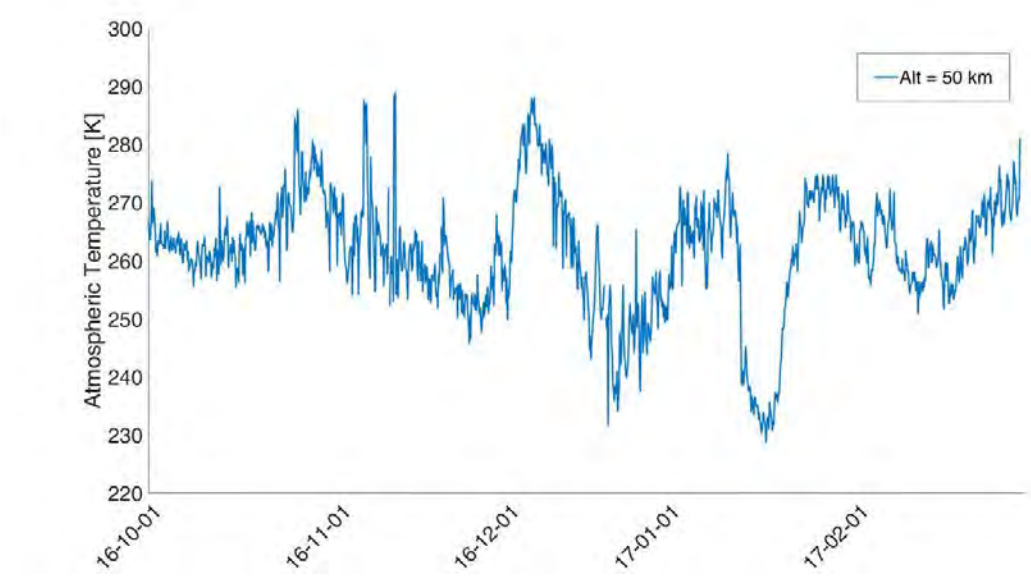

Figure 2. Continuous temperature measurements at an altitude of 50 km. Oscillating structures with periods of about a few weeks are so-called planetary waves, which are very typical during winter.

P 17.3
Arriving at an optimum setup for simulating N_2O emissions from cattle urine patches in ecosys- a comprehensive ecosystem model

Kate Kuntu-Blankson[1,2], Lena Barczyk[1,2], Christof Ammann[1] , Johan Six[2], Symon Mezbahuddin[(3)], Robert F. Grant[(3)] and Pierlugi Calanca[1]

[1] Climate and Agriculture group, Agroscope Research Station, Reckenholzstrasse 191, CH-8046 Zürich (kate.kuntu-blankson@agroscope.admin.ch)
[2] Sustainable Agroecosystem group, Institute of Agricultural Sciences, ETH Zürich, Universitätstrasse 2, CH-8092 Zürich
[3]Department of Renewable Resources, University of Alberta, Edmonton, AB T6G 2E3, Canada

The livestock sector is a major contributor to agricultural greenhouse gas (GHG) emissions, including nitrous oxide (N_2O) emissions. In grasslands, cattle excreta, in particular urine patches, represent hotspots for N_2O emissions as well as other nitrogen (N) losses. The IPCC Tier 1 guidelines assume a default emission factor (EF) of 2% for grazing related (livestock excreta N return) N_2O emissions. Recent studies from several countries, however, suggest that N_2O EF are highly influenced by local climatic, soil and management circumstances. Hence, there is a large bias when this default 2% value is used in estimating N_2O emissions for national GHG inventories across different ecological zones. For this reason, the IPCC guidelines recommend the use of more sophisticated methods such as the use of process-based models in quantifying country-specific grazing related N_2O EF. We contribute to this undertaking in the framework of the SNF project REFGRASS (Towards Representative N_2O Emission Factors for Grazing Systems in Switzerland) by conducting numerical experiments with *ecosys*, a comprehensive, process-based ecosystem model. Our efforts are currently focused on defining an optimum model setup for simulating the behaviour of cattle urine-N return to grasslands in terms of N_2O production, consumption and diffusion processes as well as N loss to other pathways. We represent urine as urea fertilizer with fast hydrolysis rate and examine how this N is cycled in the model's world. We compare the output with data from field experiments to assess the credibility of the model output. In this contribution, we present and discuss the results of preliminary simulations made so far.

P 17.4
Harmonized retrieval of middle atmospheric ozone from two microwave radiometers in Switzerland

Eric Sauvageat[1,2], Eliane Maillard Barras[3], Klemens Hocke[1,2], Alexander Haefele[3], Axel Murk[1,2]

[1] *Institute of Applied Physics, University of Bern, Sidlerstrasse 5, CH-3012 Bern (eric.sauvageat@iap.unibe.ch)*
[2] *Oeschger Centre for Climate Change Research, University of Bern, Hochschulstrasse 4, CH-3012 Bern*
[3] *Office Fédéral de Météorologie et de Climatologie MétéoSuisse, Chemin de l'Aérologie 1, CH-1530 Payerne*

Ozone profiles derived from ground-based microwave radiometers are important for detecting and estimating ozone trends in the middle-atmosphere. These instruments are capable of providing long-term, continuous measurements of strato-mesospheric ozone mixing ratio profiles with a high temporal resolution. Unlike many other techniques, they can measure during day and night under a large range of atmospheric conditions and possess almost unbiased sampling capabilities. The main drawbacks of passive microwave radiometry are its low vertical resolution and the technical challenges related to the instrument operation and stability.

In Switzerland, two ground-based ozone radiometers are operated since more than 20 years in Payerne (MeteoSwiss) and in Berne (University of Bern). Both devices are part of the Network for the Detection of Atmospheric Composition Change (NDACC) and are regularly used to assess ozone trends or perform cross validation of satellite observations over Central Europe. In addition, their geographic proximity offers a unique opportunity to compare their observations and to assess measurement uncertainties, possible instrumental failures, calibration and retrieval errors.

Discrepancies were found in the time series and trends derived from these two radiometers calling for further investigations. Given the lack of satisfactory explanation for these discrepancies, it was decided to perform a complete harmonization of the data processing, with the aim of obtaining two improved and independent datasets. The harmonization includes the calibration of the raw data, the retrievals of ozone profiles, and all required additional data. It also introduces new features to identify and flag spurious data at all levels of the processing.

In this contribution, we present the first results and comparisons of the new harmonized data series from both instruments since 2010 (an example for the period 2017-2018 is shown in Figure 1). We show a first validation of the new ozone data series against satellite observations and highlight the improvements in the ozone retrievals compared to the old data processing. We also identify and document spurious time periods for both instruments, which should help to update the NDACC database and to compute new, harmonized ozone trends over Switzerland.

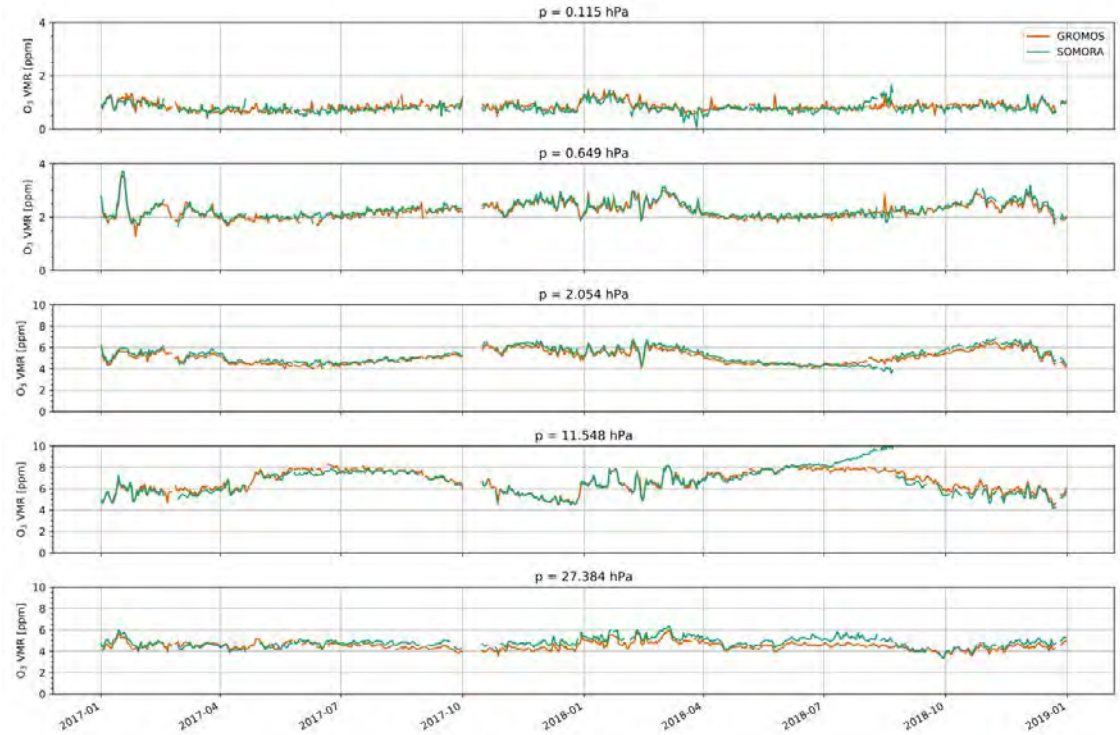

Figure 1. Harmonized time series of ozone volume mixing ratios (VMR) at different pressure levels from GROMOS (Bern) and SOMORA (Payerne). The two upper panels show ozone measurements in the lower mesosphere (≈ 50-60 km) whereas the three lower panels are observations from the stratosphere, the so-called "ozone layer" (≈ 20-40 km).

P 17.5
Physical Retrieval of Rain Rate from Ground-Based Microwave Radiometry

Wenyue Wang[1,2], Klemens Hocke[1,2], Christian Mätzler[1,2]

[1] *Institute of Applied Physics, University of Bern, CH-3012 Bern, Switzerland; (wenyue.wang@iap.unibe.ch)*
[2] *Oeschger Centre for Climate Change Research, University of Bern, CH-3012 Bern*

Because of its clear physical meaning, physical methods are more often used for space-borne microwave radiometers to retrieve the rain rate, but they are rarely used for ground-based microwave radiometers that are very sensitive to rainfall. In this article, an opacity physical retrieval method is implemented to retrieve the rain rate (denoted as Opa-RR) using ground-based microwave radiometer data (21.4 and 31.5 GHz) of the tropospheric water radiometer (TROWARA) at Bern, Switzerland from 2005 to 2019. The Opa-RR firstly establishes a direct connection between the rain rate and the enhanced atmospheric opacity during rain, then iteratively adjusts the rain effective temperature to determine the rain opacity, based on the radiative transfer equation, and finally estimates the rain rate. These estimations are compared with the available simultaneous rain rate derived from rain gauge data and reanalysis data (ERA5). The results and the intercomparison demonstrate that during moderate rains and at the 31 GHz channel, the Opa-RR method was close to the actual situation and capable of the rain rate estimation. In addition, the Opa-RR method can well derive the changes in cumulative rain over time (day, month, and year), and the monthly rain rate estimation is superior, with the rain gauge validated R^2 and the root-mean-square error value of 0.77 and 22.46 mm/month, respectively. Compared with ERA5, Opa-RR at 31GHz achieves a competitive performance.

P 17.6
Quantifying past changes in dielectric and absorbing particles in ice cores from East Greenland during the early Holocene and Termination 1

Chantal Zeppenfeld[1], Tobias Erhardt[1,2], Camilla M. Jensen[1], Hubertus Fischer[1]

[1] *Climate and Environmental Physics and Oeschger Centre for Climate Change Research, University of Bern, Sidlerstrasse 5, 3012 Bern, Switzerland (chantal.zeppenfeld@climate.unibe.ch)*
[2] *Alfred Wegener Institute, Helmholtz-Zentrum für Polar und Meeresforschung, Bremerhaven, Germany*

Ice cores represent archives that contain information about past climatic conditions such as the composition of the atmosphere. By melting the ice and analysing the enclosed impurities, climatic variations can be reconstructed. Of these impurities, insoluble particles are of interest due to their influence on the ocean biogeochemistry and the Erath's radiative balance. Changes in their concentration, size distribution or mineralogy reflect alterations in the source regions, transport, or deposition mechanisms.

To investigate the particles and to quantify the past changes in their concentration and properties, the Classizer One instrument, which is based on the novel Single Particle Extinction and Scattering (SPES) method, has been incorporated into the continuous flow analysis set-up in Bern. The method allows for high-resolution continuous and simultaneous measurements of particle number, size, and refractive index in the size range of 0.2 to 2 μm. This size range covers the maximum of the particle number distribution expected in polar ice cores, which was inaccessible by previously available particle sizing methods with typical lower detection limits of around 1 μm. Furthermore, the new method allows for a distinction between absorbing and dielectric particles for periods of low dust concentration.

Here we will present the SPES data from the East Greenland ice core for the period 8000 to 15000 years before 2000 (b2k). The transition from the Younger Dryas (YD) to the Holocene coincides with a decrease in mean particle diameter by approximately 45 nm from 740 to 785 nm. Besides the changes in size distribution, we find approximately 10 times higher particle concentrations during the YD. We will also show results for the absorbing particle numbers for the early Holocene up to the year 8000 b2k and the last millennial based on the data from shallow ice cores drilled at the EGRIP site.

REFERENCES

Harrison, S. P., Kohfeld, K. E., Roelandt, C., and Claquin, T. 2001: The role of dust in climate changes today, at the last glacial maximum and in the future, Earth-Science Reviews, 54 (1-3), 43–80

Legrand, M., & Mayewski, P. 1997: Glaciochemistry of polar ice cores: A review, Review of Geophysics, 35 (3), 219-243

Potenza, M. A., Sanvito, T., and Pullia, A. 2015: Measuring the complex field scattered by single submicron particles, AIP Advances, 5 (11)

18. Tackling the Climate Crisis: Interdisciplinary Perspectives on Climate Change Education and Communication

Moritz Gubler, Viktoria Cologna, Stephanie Moser, Matthias Probst, Andreas Linsbauer

TALKS:

18.1 Hellmann L., Gugerli R., Habermann M., Mathys T., Kronenberg M., Mollaret C., Schaub Y., Schwikowski M., Vögeli N., Wee J., Wenner M., Naegeli K.: From glacier to classroom: peer-to-peer communication to foster curiosity in science

18.2 Nesur K., Salim E., Girault C. & Ravanel L.: Glacier interpretation centre in climate change education : objectives of local stake holders and strategy of scientific mediation

18.3 Poelsma F., Wymann S., Moser S.: How to gain public engagement for climate action? Challenges and opportunities for energy transitions in mountainous and rural areas

18.4 Salim E., Ravanel L.: The role of endangered destinations in climate change education: exploratory perspectives in the glacier tourism context

POSTERS:

P 18.1 Hernández-Almeida I., Saavedra-Pellitero M.: Comics as a narrative to engage teens with science: an example from the PAGES Horizons experience

P 18.2 Imanalieva P., Weber H., Mathys T., Sarsebekova Z., Djololova D., Koenig C., Kronenberg M., Barandun M.: Science communication across borders – “Adventure of science: Women and glaciers in Central Asia”

18.1
From glacier to classroom: peer-to-peer communication to foster curiosity in science

Lena Hellmann[1,2,3], Rebecca Gugerli[1,4], Marijke Habermann[1], Tamara Mathys[1,4], Marlene Kronenberg[1,4], Coline Mollaret[1,4], Yvonne Schaub[1], Margit Schwikowski[1,3,5], Natalie Vögeli[1], Julie Wee[1,4], Michaela Wenner[1,6], Kathrin Naegeli[1,2,3] and the Girls on Ice Switzerland Team[7]

[1] *Girls on Ice Switzerland, Mühleweg 14, CH-8136 Gattikon, (lena@girlsonice.org)*
[2] *Department of Geography, University of Bern, Hallerstrasse 12, CH-3012 Bern*
[3] *Oeschger Centre for Climate Change Research, University of Bern, Hochschulstrasse 4, CH-3012 Bern*
[4] *Department of Geosciences, Chemin du Musée 4, CH-1700 Fribourg*
[5] *Paul Scherrer Institute, Forschungsstrasse 111, CH-5232 Villigen PSI*
[6] *Laboratories of Hydraulics, Hydrology and Glaciology (VAW), Hönggerbergring 26, CH-8093 Zürich*
[7] *www.inspiringgirls.org/switzerland*

The active involvement of the Swiss youth in regional and national climate strikes and related actions indicates an increasing interest of young people in global climate change. Many young students are well informed, want to be part of political changes and to be heard in scientific debates. However, participation and active involvement comes along with background knowledge, support from the surrounding environment and last but not least self-confidence. Some young people - in particular young women - lack this support, interactions, and access to information, or miss self-confidence to take action and adapt themselves to coming changes. We strongly believe that discussions about climate change and its impact on society have to take place in all socio-demographic groups and school levels.

Hence, we offer tuition-free glacier expeditions for teenage girls in combination with school workshops and daily excursions, both led by participant-scientist tandems. With that, we enhance the dialogue about the scientific process and related scientific facts about climate change impacts on the alpine environment and Swiss glaciers, in particular. At the same time, immersion during the glacier expedition provides the personal experience that is crucial for effective subsequent communication. The expedition participants become science ambassadors for their peers and at the same time strongly increase their self-confidence. The great strength of our communication method is the mix of personal expedition-experience of a female peer and work-experience of a scientist in a setting that allows for actual questions and conversations. The close support of a scientist ensures a reliable frame of scientific facts, but also positions the female scientist as a role model for the younger generation. The peer-to-peer communication as well as the interactive structure of our workshops and excursions open the floor for honest, scientific-based and diverse discussions among young students, supported by science-ambassadors.

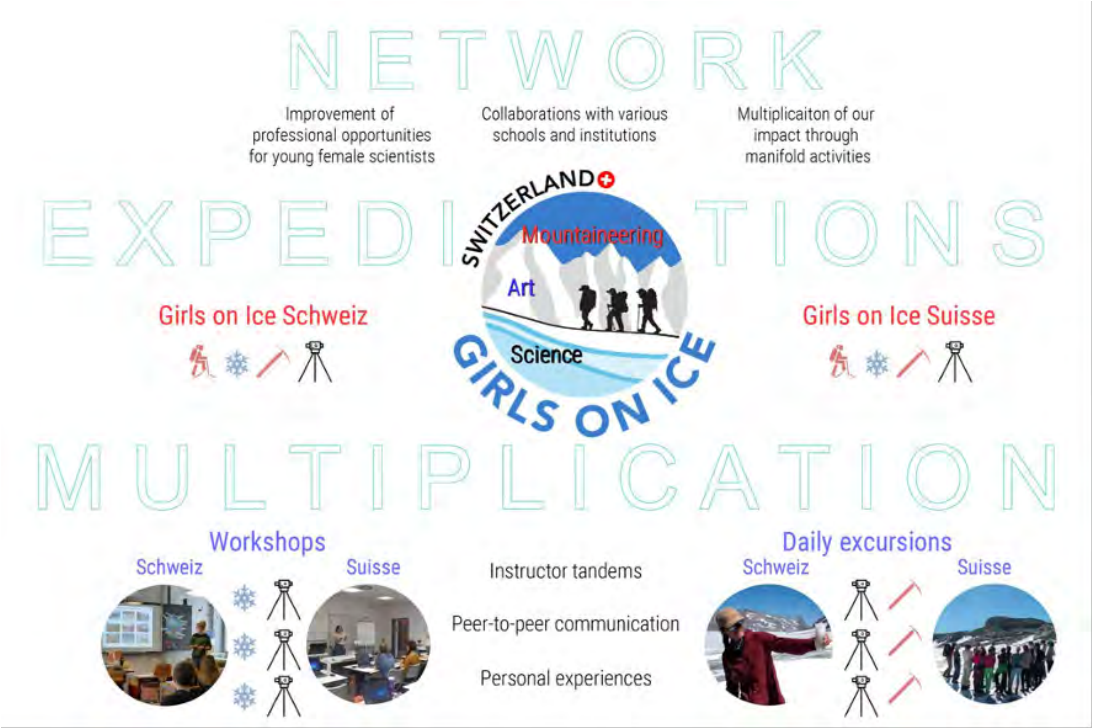

Figure 1. Organisational structure of the peer-to-peer science communication of *Girls on Ice Switzerland* based on our activities ranging from glacier expeditions to school workshops and daily excursions led by female student-scientist tandems.

18.2
Glacier interpretation centre in climate change education : objectives of local stake holders and strategy of scientific mediation

Kalpana Nesur[1], Emmanuel Salim[1], Camille Girault[1], Ludovic Ravanel[1,2]

[1] EDYTEM, University Savoie-Mont-Blanc, CNRS, Le Bourget-du-Lac, France
[2] University of Lausanne, Interdisciplinary Centre for Mountain Research (CIRM), Ch. de l'Institut 18, CH-1967 Bramois, Switzerland

Climate change (CC) is a current and global phenomenon that clearly affects mountain areas, where almost all of the world's glaciers are retreating synchronously, since the 1950s (IPCC, 2021). In this context, tourist activities related to glaciers are particularly impacted; this is the case, for example, of the Fox and Franz Josef glaciers in New Zealand (Stewart et al., 2016), of the Mer de Glace in France (Salim & Ravanel, 2020) or of the Athabasca Glacier in Canada (Weber et al., 2019). Relative to this evolution, during these last two decades, we observe a new form of tourism, related to the scientific value of glaciers (Salim et al., 2021). One of these forms of tourism consists in developing glacier interpretation centres (GICs), tools for scientific mediation, dealing with glacier dynamics and glaciers as sensitive natural heritage (Clivaz & Savioz, 2020). However, very few studies have been conducted in this field and even less in terms of origin of these projects, their objectives, local stake holders, etc.

Glacier retreat is one of the tangible and visible witnesses of CC (Gardent et al., 2014). Nevertheless, how local stake holders have mobilised for the creation of these GICs? How GICs can become a tool for raising awareness on CC with the present glacier retreat as a marker ? What are the initial objectives of their creation ? How the message is presented ? In order to answer these questions, 3 GICs have been studied according to their caracteristics, their accessibility and proximity of sites : Espace Glacialis (Champagny en Vanoise, France), Glaciorium (Montenvers - Mer de Glace, France) and World Nature Forum (Naters, Switzerland) . The study is based on qualitative data: 15 interviews with local stakeholders (semi-structured interviews) to better understand the origin of the GIC projects and synergy between local actors.

The study shows that the concerned GICs aims to demonstrate present dynamics of their local glaciers (natural heritage) through proper scientific mediation (didactic panels, videos, interactive objects, games…). Climate change is a complex phenomenon, permanent exhibitions in GICs, based on vulgarised scientific findings and evidence can help visitors to better understand local environment (landscape, evolution of glaciers...), and to get aware on challenges related to high-mountain regions as well as on CC.

REFERENCES

Clivaz, C. & Savioz, A., 2020 : Recul des glaciers et appréhension des changements climatiques par les acteurs touristiques locaux. Le cas de Chamonix-Mont-Blanc dans les Alpes françaises, Via Tourism Review, n°18, P. 22. https://doi.org/10.4000/viatourism.6066.

Einhorn, B., Eckert, N., Chaix, C., Ravanel, L., Deline, P., Gardent, M., Boudières, V., Richard, D., Vengeon, J.-M., Giraud, G., & Schoeneich, P., 2015: Changements climatiques et risques naturels dans les Alpes. Impacts observés et potentiels sur les systèmes physiques et socio-économiques. Journal of Alpine Research, Revue de géographie alpine, 1032.

Gardent, M., Rabatel, A., Dedieu, J.-P., & Deline, P., 2014 : Multitemporal glacier inventory of the French Alps from the late 1960s to the late 2000s. Global and Planetary Change, 120, 2437.

IPCC, 2021: Summary for Policymakers. In: Climate Change 2021: The Physical Science Basis. Contribution of Working Group I to the Sixth Assessment Report of the Intergovernmental Panel on Climate Change [Masson-Delmotte, V., Zhai, P., Pirani, A., Connors, S. L., Péan, C., Berger, S., Caud, N., Chen, Y., Goldfarb, L., Gomis, M. I., Huang, M., Leitzell, K., Lonnoy, E., Matthews, J.B.R., Maycock, T. K., Waterfield, T., Yelekçi, O., Yu, R. & Zhou, B., (eds.)]. Cambridge University Press. In Press.

Salim, E. & Ravanel, L., 2020 : Last chance to see the ice: visitor motivation at Montenvers-Mer-de-Glace, French Alps, Tourism Geographies, p. 1-23.

Salim, E., Gauchon, C. & Ravanel, L., 2021 : Voir la glace. Tour d'horizon des sites touristiques glaciaires alpins, entre post- et hyper-modernités , Journal of Alpine Research, Revue de géographie alpine, Varia, URL : http://journals.openedition.org/rga/8358.

Stewart, E. J., Wilson, J., Espiner, S., Purdie, H., Lemieux, C., & Dawson, J. 2016 : Implications of climate change for glacier tourism, Tourism Geographies, 18(4), 377398. https://doi.org/10.1080/14616688.2016.1198416.

Weber, M., Groulx, M., Lemieux, C. J., Scott, D. & Dawson, J., 2019: Balancing the dual mandate of conservation and visitor use at a Canadian world heritage site in an era of rapid climate change, Journal of Sustainable Tourism, vol. 27, n°9, p. 1318-1337.

18.3
How to gain public engagement for climate action? Challenges and opportunities for energy transitions in mountainous and rural areas

Felix Poelsma[1], Susanne Wymann[1], Stephanie Moser[1],

[1]Centre for Development and Environment, University of Bern, Mittelstrasse 43, CH-3012 Bern (felix.poelsma@unibe.ch)

A shift towards more sustainable and cleaner energy systems is vital to limit adverse effects of climate change, but also to ensure economic development and reliable energy infrastructures throughout the world. Current energy systems are interwoven with other societal systems, such as transportation, housing and industries, but also with current values and lifestyles, which implies that to achieve these targets, radical systemic changes based on public engagement with climate change are necessary.

Policies supporting sustainable energy transitions are often contested and without support of local inhabitants, projects might not be implemented (Naumann & Rudolph, 2020). The recent rejection of the CO2-Act by the Swiss population underlines that social acceptance is key for implementing polices in regard to transitions towards sustainability. But how can such broader social acceptance in regard with the radical systemic changes needed be achieved?

An approach, with goes beyond previous education and communication strategies is 'transition management'. Over the last decade, research on sustainability transition management has grown rapidly (Köhler et al., 2019). This caused the development of various multi-actor initiatives which aim to support sustainability transitions (Hyysalo et al., 2019). Such initiatives typically involve societal as well and academic actors who jointly develop 'experiments' which contribute towards sustainability transitions (Luederitz et al. 2017). These initiatives allow actors from different sectors of society to participate in shaping/co-designing and jointly implementing policies. On the one hand, inclusion and providing opportunities for public participation can enhance societal acceptance and behaviour change and thus contribute to the shift to more sustainable and cleaner energy systems (Langer et al., 2017). However, it also provides several communication challenges, such as developing a joint understanding of the situation at hand, a shared vision and agenda to act.

The research project, which will be presented in this contribution aims to gain insights into such participation processes in energy transitions in mountainous and rural areas. In the Global North, energy transitions have predominantly focused on urban energy transitions (Naumann & Rudolph, 2020). However, the boundaries of energy systems are usually not limited to urban or rural settings, since they are linked. Energy production sites are for instance often located in rural areas (Naumann & Rudolph, 2020). This is especially relevant for renewable energy production sites, as renewables often require a greater surface area compared to fossil fuel based energy production. We therefore focus on mountainous and rural areas, where the potential renewable energy production is high.

The presented research project is based on a case study in a Swiss Alpine Region, the administrative district Interlaken-Oberhasli, located in the Bernese Oberland. In this region a particiative transistion management process is implemented between 2021 and 2023 under the project name: '**L**ocal **E**nergy **T**ransition **E**xperiments' (LETE) for a low-carbon society transformation – Piloting a transition management process in the Bernese Alps, under the lead of the authors of this contribution. A systemicatic overview of the research project is presented in Figure 1. This project will serve as a case study for public participation in energy transitions in rural and mountainous areas.

The LETE research project consist of several workshops with local actors. At the symposia on the SGM, experiences of the first workshop (joint problem framing) will be presented. This research contributes to finding inclusive ways to design more successful energy policies and support actors throughout society to engage in more sustainable projects and behaviours for fighting climate change. Furthermore, it expands the insight of transitions management to communities living in mountainous and rural areas.

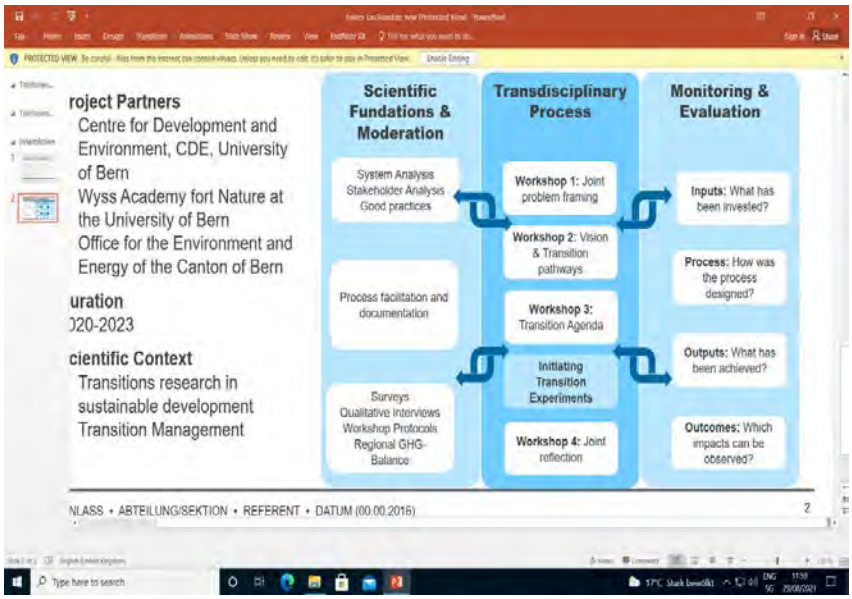

Figure 1. Overview of the LETE-research project.

REFERENCES

Hyysalo, S., Lukkarinen, J., Kivimaa, P., Lovio, R., Temmes, A., Hildén, M., ... & Pantsar, M. 2019: Developing policy pathways: redesigning transition arenas for mid-range planning, Sustainability, 11, 603.

Köhler, J., Geels, F. W., Kern, F., Markard, J., Onsongo, E., Wieczorek, A., ... & Wells, P. 2019: An agenda for sustainability transitions research: State of the art and future directions, Environmental innovation and societal transitions, 31, 1-32.

Langer, K., Decker, T., & Menrad, K. 2017: Public participation in wind energy projects located in Germany: Which form of participation is the key to acceptance?, Renewable Energy, 112, 63–73.

Luederitz, C., Schäpke, N., Wiek, A., Lang, D. J., Bergmann, M., Bos, J. J., ... & Westley, F. R. 2017: Learning through evaluation–A tentative evaluative scheme for sustainability transition experiments, Journal of Cleaner Production, 169, 61-76.

Naumann, M., & Rudolph, D. 2020: Conceptualizing rural energy transitions: Energizing rural studies, ruralizing energy research, Journal of Rural Studies, 73, 97-104.

18.4
The role of endangered destinations in climate change education: exploratory perspectives in the glacier tourism context

Emmanuel Salim[1] & Ludovic Ravanel[1,2]

[1] EDYTEM, University Savoie-Mont-Blanc, CNRS, Le Bourget-du-Lac, France (emmanuel.salim@univ-smb.fr)
[2] University of Lausanne, Interdisciplinary Centre for Mountain Research (CIRM), Ch. de l'Institut 18, CH-1967 Bramois, Switzerland

Human-induced climate change threatens societies and livelyhood (IPCC, 2021). Tourism is an industry that is highly impacted worldwide (Mora et al., 2018) and, at the same time, responsible for more than 8% of the global greenhouse gaz emissions (Lenzen et al., 2018). However, despite the general awarness of the effects of climate change in the population, tourism is a sector where behaviour remains unsustainable and intention to act is relatively low (Juvan et al., 2016). The example of the 'Last Chance Tourism' (LCT), i.e. when tourists travel to see endangered features before they disappear (Lemelin et al., 2010), is a representative example. LCT visitors are often well aware of the human origin of climate change and its impacts but travel over long distances to see LCT places without really taking into account the implication of their travels on greenhouse gas (GHG) emissions (D'Souza et al., 2021). This phenomenom is considered as a form of cognitive dissonance as beliefs and acts are contradictory (Salim & Ravanel, 2020). Nonetheless, could evidences of climate change help to solve this paradox? Moreover, how can scientific culture in tourism help to achieve this goal?

To move forward in this direction, we conducted an exploratory study at the Montenvers-Mer-de-Glace, a so-called glacier-related LCT destination. First, the study includes a quantitative survey whose objective is to test different constructs (place attachment, landscape perception, emotions, motivations, and environmental worldview) on intentions to adopt pro-environmental behaviour (based on Halpenny›s 2010 scale). Then, semi-structured interviews were conducted with visitors on the field with the aim to identify the consonnance strategies they developped to sustain their behaviours.

Succinctly, the quantitative survey shows that perceiving glacial landscape as the reflection of climate change effects as well as emotion felt increase the intention to adopt pro-environmental behaviours. Moreover, the qualitative interviews show that justifications (consonnance strategies) for not acting come from a lack of knowledge and understanding of scientific data, or from a lack of knowledge concerning the existing alternatives (e.g. mobility). These results allow stakeholders to reconsider the communication on the glacier sites by focusing on the so identified lack of knowledge and by proposing and presenting possible alternatives and actions to be taken to reduce the GHG emissions.

As a conclusion, we argue that tourism – and espacially tourism related to endengered places – can be an interesting lever to promote sustainable behaviours and to raise willingness to act for mitigating climate change.

REFERENCES

D'Souza, J., Dawson, J., & Groulx, M. (2021). Last chance tourism: A decade review of a case study on Churchill, Manitoba's polar bear viewing industry. Journal of Sustainable Tourism, 0(0), 1–19. https://doi.org/10.1080/09669582.2021.1910828

Halpenny, E. A. (2010). Pro-environmental behaviours and park visitors: The effect of place attachment. Journal of Environmental Psychology, 30(4), 409–421. https://doi.org/10.1016/j.jenvp.2010.04.006

IPCC. (2021). Climate Change 2021: The Physical Science Basis. Contribution of Working Group I to the Sixth Assessment Report of the Intergovernmental Panel on Climate Change (Masson-Delmotte, V., P. Zhai, A. Pirani, S. L. Connors, C. Péan, S. Berger, N. Caud, Y. Chen, L. Goldfarb, M. I. Gomis, M. Huang, K. Leitzell, E. Lonnoy, J. B. R. Matthews, T. K. Maycock, T. Waterfield, O. Yelekçi, R. Yu and B. Zhou (eds.)). Cambridge University Press.

Juvan, E., Ring, A., Leisch, F., & Dolnicar, S. (2016). Tourist segments' justifications for behaving in an environmentally unsustainable way. Journal of Sustainable Tourism, 24(11), 1506–1522. https://doi.org/10.1080/09669582.2015.1136635

Lemelin, H., Dawson, J., Stewart, E. J., Maher, P., & Lueck, M. (2010). Last-chance tourism: The boom, doom, and gloom of visiting vanishing destinations. Current Issues in Tourism, 13(5), 477–493. https://doi.org/10.1080/13683500903406367

Lenzen, M., Sun, Y.-Y., Faturay, F., Ting, Y.-P., Geschke, A., & Malik, A. (2018). The carbon footprint of global tourism. Nature Climate Change, 8(6), 522–528. https://doi.org/10.1038/s41558-018-0141-x

Mora, C., Spirandelli, D., Franklin, E. C., Lynham, J., Kantar, M. B., Miles, W., Smith, C. Z., Freel, K., Moy, J., Louis, L. V., Barba, E. W., Bettinger, K., Frazier, A. G., Colburn Ix, J. F., Hanasaki, N., Hawkins, E., Hirabayashi, Y., Knorr, W., Little, C. M., … Hunter, C. L. (2018). Broad threat to humanity from cumulative climate hazards intensified by greenhouse gas emissions. Nature Climate Change, 8(12), 1062–1071. https://doi.org/10.1038/s41558-018-0315-6

Salim, E., & Ravanel, L. (2020). Last chance to see the ice: Visitor motivation at Montenvers-Mer-de-Glace, French Alps. Tourism Geographies, 1–23. https://doi.org/10.1080/14616688.2020.1833971

P 18.1
Comics as a narrative to engage teens with science: an example from the PAGES Horizons experience.

Iván Hernández-Almeida[1], Mariem Saavedra-Pellitero[2]

[1] Geological Institute, Department of Earth Science, ETH, 8092, Zürich, Switzerland (ivan.hernandez@erdw.ethz.ch)
[2] University of Birmingham, School of Geography, Earth and Environmental Sciences, Birmingham B15 2TT, UK

Raising awareness and thereby understanding the effects of global changes to modern societies will facilitate both behavioural change and support for the actions that future societies will have to face in the next decades. Paleoscience studies enable to get a unique temporal perspective on the long history of climate and evolution of systems, and provides information about prior states. Technical language or some concepts used in paleoscience, such as the temporal perspective, are additional barriers when communicating science. Moreover, narratives used to communicate sometimes do not have a specific age target, or they are biased towards a more general 'adult audience'. Science communication efforts aimed at young people need to be have narratives, questions or topics adapted what that group of population finds interesting or appealing. Visual narratives, such as comics and animations, are becoming increasingly popular as a tool for science education and communication. In 2021, the project Past Global Changes International Project Office (PAGES) published the first issue of their 'Horizons' magazine (Vannière et al., 2021). The goal of this initiative was to present topics of interest for the next generation using easy alternative narratives, related to the environment and the Earth system and from a paleo perspective. The issue was mainly aimed at older high-school students and undergraduate. In the comic 'How green were the oceans in the past?' showed that issue, we presented the concept of ocean primary productivity, tools to reconstruct it in the past, and projection into the future of the primary productivity evolution due to global warming. We use our creative experience and feedback as an example to illustrate the importance of alternative narratives and adapted language to reach younger readers.

REFERENCES

Vannière, B., Gil-Romera, G. and Eggleston, S. (2021). Past Global Changes Horizons 1. https://10.22498/pages.horiz.1

P 18.2
Science communication across borders – "Adventure of science: Women and glaciers in Central Asia"

Perizat Imanalieva*, Helga Weber**, Tamara Mathys***, Zamira Sarsebekova****, Dilorom Djololova*****, Cassandra Koenig***, Marlene Kronenberg***, Martina Barandun*******

*Central Asian *Institute for Applied Geosciences, KG-720027 Bishkek, (centralasia@girlsonice.org)*
***Oeschger Centre for Climate Change Research and Institute of Geography, University of Bern, CH-3012 Bern*
****Departement of Geosciences, University of Fribourg, Chemin de Musée 4, CH-1700 Fribourg, Switzerland*
***** SE "KazMudflowProtection", Kazakhstan*
****** Glaciology Centre, Academy of Sciences, Tajikistan,*
******** Institute of Earth Observation, EURAC research, Bolzano, Italy*

Increasing the participation and diversity of women in field sciences, art, and outdoor recreation stimulates the local communities and fosters regional development. "Adventure of science: Women and glaciers in Central Asia" is a program that fosters science communication by inspiring young women in science, nature, and art. It takes young Central Asian women from diverse backgrounds on an expedition in an alpine environment (Imanalieva et al., 2021). The instructor team consists of local and international female scientists and a female mountain guide. During the program, the participants (i) get an introduction into cryospheric sciences and environmental change; (ii) acquire mountaineering and wilderness camping skills; (iii) cultivate observational and critical thinking competencies; and (iv) take part in tailored activities introducing them to scientific methods. The expedition includes pre- and post-course events, where participants are given the opportunity to discuss their experiences and present scientific findings to a public audience. A further aim of the project is to build a regional network of female scientists and professionals working in domains affected by climate change.

The program curriculum is based on the "Girls on Ice" (i.e. "Girls on Ice Switzerland") programs coordinated by "Inspiring Girls Expeditions" (IGE 2019). The program employs inquiry-based teaching and experimental learning methods within science, art and mountaineering subjects. A central course element are scientific projects, which are planned and implemented by participant teams and supervised by program instructors. "Adventure of Science: Women and glaciers in Central Asia" includes capacity building components designed to empower young women and encourage them to pursue a career in traditionally male-dominated domains, while also growing a network of young women across national borders.

Under the ongoing pandemic an in-person expedition to an alpine environment was difficult to organise in Central Asia and a new (online) program "Adventure of Science at home" was developed to create a virtual expedition for young women in the region. "Adventure of science: Women and glaciers in Central Asia" and "Adventure of science at home", is led by an international, female-only team of professional scientists who seek to increase young women's self-confidence in their physical, intellectual, and leadership abilities through the application of art and science. The program includes four distinct learning modules developed and delivered by the instructor team through a series of virtual lectures, breakout discussions and interactive exercises with participants. The program aims to create lifelong advocates for Earth science and wilderness stewardship, and support a network for early-career scientists, artists, and guides. The project also has institutional impact by encouraging local institutions to involve young female scientists and students in academic activities and research.

REFERENCES

Imanalieva, P., Serzhankyzy, Z., Kronenberg, M., Mathys, T., Tovmasyan, K., Barandun, M. (2021), A new scientific communications program "Adventure of science: Women and glaciers in Central Asia", Conference proceedings IWRM - «Женщины и ледники». Central Asian Journal of Water Research

IGE 2019, www.inspiringgirls.org.

Tashtemkhanova, R., Medeubayeva, Z. , Serikbayeva, A. & Igimbayeva, M., 2015. Territorial and Border Issues in Central Asia: Analysis of the Reasons, Current State and Perspectives. Anthropologist 22(3), 518–25.

19. Geoscience and Geoinformation, Earth Observation and Remote Sensing – Combined Symposium

For Geoscience and Geoinformation:
Nils Oesterling, Massimiliano Cannata, Michael Sinreich, Elmar Brockmann

For Earth Observation and Remote Sensing:
Stefan Wunderle, Alex Damm, Dominik Brunner, Othmar Frey

Swiss Geological Survey
Swiss Geodetic Commission
Swiss Geophysical Commission
Swiss Hydrogeological Society
Swiss Commission for Remote Sensing

TALKS:

19.1 Aichinger-Rosenberger M., Moeller G., Shehaj E., Limpach P., Rothacher M.: 3D modelling and analysis of temporal variations of atmospheric water vapor in the Valais area: Initial results from a small-scale GNSS network in the Matter Valley

19.2 Araya D., Podgorski J., Kumi M., Amankwah Mainoo P., Berg M.: Geospatial modelling of fluoride contamination in Ghana, considerations on spatial cross-validation and uncertainty assessment.

19.3 Carreaud A., Gressin A., Lis K.: Fast image labelling using 3D reconstruction

19.4 Doerffel G.: 3D Processing of Drone & Aerial Survey data in ArcGIS

19.5 Hadjipetrou S., Mariethoz G.: Geostatistical Simulation of Satellite-derived Offshore Wind Speed Patterns

19.6 Iosifescu Enescu I., Plattner G.-K., Haas-Artho D., Kurup Buchholz R., de Espona L., Hägeli M.: Cloud-native Access Patterns as Foundation for an Efficient Implementation of Geospatial Functionalities in EnviDat

19.7 Kenner R., Gischig V., Gojcic Z., Quéau V., Kienholz C., Figi D., Thöny R., Bonanomi Y.: Brinzauls, Pizzo Cengalo, Spitze Stei: Analysing detailed rock kinematical processes using point cloud models

19.8 Malard A., Jeannin P.-Y., Doerfliger N., Laube S., Béon O., Zein A., Vogel M.: A webtool for the 3D conceptualization and animation of groundwater flow systems

19.9 Miville F., Fandel C., Renard P.: pyKasso: a stochastic karst network generator

19.10 Neven A., Christiansen A.V., Renard P.: Automatic valley-scale clay models from TEM and boreholes data : Application on the upper Aare Valley

19.11 Oesterling N., Baumberger R., Leu E.: swissgeol.ch – Web-based 3D subsurface visualisation

19.12 Perozzi L.; Guglielmetti L.; Moscariello A.: GECOS: A webapp to explore geothermal chance of success

19.13 Shakas A., Wenning Q., Hertrich M., Maurer H., Giardini D.: Probabilistic geological model using multi-scale geophysical data: An example from the Bedretto Lab

19.14 Shehaj E., Geiger A., Miotti L., Soja B., Moeller G., D'Aronco S., Wegner J.D., Rothacher M.: Modeling tropospheric effects in space geodetic signals by machine learning and collocation

POSTERS:

P 19.1 Salehipour Milani A.R., Sabzaliyan M.: Mapping recent pyroclastic flow using Sentinel-2 image in De Fuego volcano, Guatemala

P 19.2 Zakeri F., Mariethoz G.: Snow Cover Mapping: Generating Long-Term Landsat Imagery Consistent with Climate Data

P 19.3 Doerffel G.: Cloud-based Imagery storage and analysis in ArcGIS

P 19.4 Doerffel G.: Multidimensional Imagery /TimeSeries in ArcGIS

19.1
3D modelling and analysis of temporal variations of atmospheric water vapor in the Valais area: Initial results from a small-scale GNSS network in the Matter Valley

Matthias Aichinger-Rosenberger[1], Gregor Moeller[1], Endrit Shehaj[1], Phillipe Limpach[1], Markus Rothacher[1]

[1]*Institute of Geodesy and Photogrammetry, ETH Zürich, Robert-Gnehm-Weg 15, CH-8093 Zürich (maichinger@ethz.ch)*

Troposheric parameters derived from GNSS observations, such as Zenith Total Delay (ZTD), are nowadays extensively used in meteorological and climatological applications. However, 3D modelling of water vapor utilizing GNSS observations still denotes a major challenge, especially in mountainous regions. In the course of a BAFU project, aiming for the build-up of an alpine labortory for defomation modelling merging various techniques, the group of Mathematical and Physical Geodesy at ETH Zürich built up a dense local network of GNSS stations in the Matter Valley. As the specific area is very prone to natural hazards (especially rockfall, rock slides and mudflows), the main goal of the network is the provision of accurate 3D tropospheric corrections for Interferometric Synthetic Aperture Radar (InSAR) deformation analyses. Furthermore, the emerging dataset can also be used to study small-scale deviations of water vapor content, related to specific meteorological phenomena encountered in the study area.

This talk presents detailed information on the network and its build-up as well as an initial evaluation and data analysis of GNSS-derived ZTD and its temporal variations at different stations. Moreover, we evaluate the performance of 3D modelling of ZTD and related parameters using the collocation software COMEDIE, that was developed in-house, in the respective area. Therefore, 3D fields as well as station-wise ZTD estimations are compared to gridded data from the Numerical Weather Predicition (NWP) model COSMO-1.

REFERENCES

Aichinger-Rosenberger, M. & Wolf, A. & Limpach, P. & Moeller, G. 2021: Development of the next-generation GNSS-Meteo stations, E-Poster, IAG Scientific Assembly 2021, Beijing.

Wilgan, K. & Geiger, A. 2019: High-resolution models of tropospheric delays and refractivity based on GNSS and numerical weather prediction data for alpine regions in Switzerland. J Geod 93, 819–835. https://doi.org/10.1007/s00190-018-1203-6

Shehaj, E. & Wilgan, K. & Frey, O. & Geiger, A. 2020: A collocation framework to retrieve tropospheric delays from a combination of GNSS and InSAR. NAVIGATION. 67: 823– 842. https://doi.org/10.1002/navi.398.

19.2
Geospatial modelling of fluoride contamination in Ghana, considerations on spatial cross-validation and uncertainty assessment.

Dahyann Araya[1,*], Joel Podgorski[1], Michael Kumi[2], Patrick Amankwah Mainoo[2], Michael Berg[1]

[1)] *Eawag, Swiss Federal Institute of Aquatic Science and Technology, Department of Water Resources and Drinking Water, 8600 Dübendorf, Switzerland.*
[2)] *CSIR-Water Research Institute, P. O. Box AH 38, Achimota-Accra, Ghana.*

About 25% of Ghana's population lacks access to essential drinking water services, and 73% do not have access to reliable and clean water sources. The population therefore relies on groundwater for drinking, especially in rural areas, though the fluoride contamination of groundwater leads to dental fluorosis (Alfredo, Lawler, & Katz, 2014). Children, especially in the first two years of life, are particularly susceptible to the adverse effects of fluoride and can retain 80–90% of a fluoride dose, compared to 60% in adults (WHO, 2004)..

Despite numerous local studies, there is no spatially continuous picture of the fluoride contamination across Ghana, nor is there an estimate of how much of the population is potentially exposed to unsafe levels. Here, we spatially model the probability of fluoride concentrations exceeding a threshold of 1.0 mg/L in groundwater across Ghana to identify risk areas and estimate the number of children and adults exposed to unsafe fluoride levels in drinking water. We use a set of geospatial predictor variables with random forest, evaluate model performance using state-of-the-art spatial cross-validation and assess model uncertainties. We found that ~15% of the country has a high probability of fluoride contamination, with about 924,000 (3% of the population) and about 250,000 children (0–9 years) exposed in at-risk areas. Geology and high evapotranspiration are the main drivers of contamination, which means the problem is expected to worsen with climate change. Our maps should raise awareness and understanding of fluoride contamination in Ghana and can advise local-level actions to avoid or mitigate fluoride-related risks.

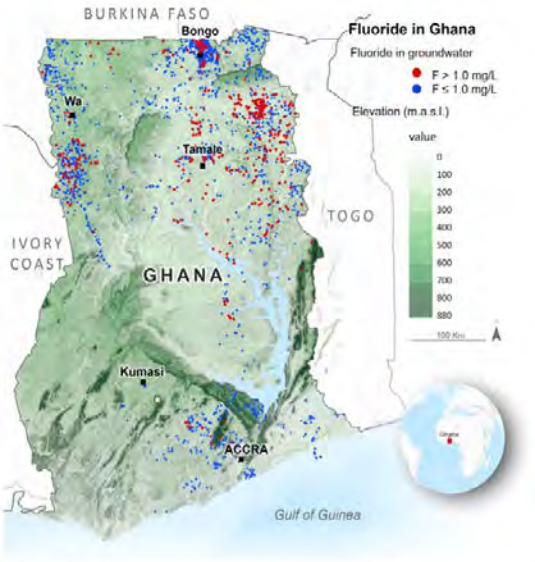

Figure 1. Fluoride concentrations in groundwater and topography. Red points represent fluoride concentration >1.0 mg/L. This image was created using ArcGIS Pro v.2.7.2.

REFERENCES

Alfredo, K. A., Lawler, D. F., & Katz, L. E. (2014). Fluoride contamination in the Bongo District of Ghana, West Africa: Geogenic contamination and cultural complexities. *Water International*, *39*(4), 486–503. https://doi.org/10.1080/02508060.2014.926234

WHO (2004). Fluoride in Drinking-water Background document for development of WHO Guidelines for Drinking-water Quality. In *Fluoride* (Vol. 51).

19.3
FAST IMAGE LABELLING USING 3D RECONSTRUCTION

A. Carreaud[a], K. Lis[b], A. Gressin[a]

[a] *University of Applied Sciences Western Switzerland (HES-SO / HEIG-VD), Insit Institute - (antoine.carreaud, adrien.gressin)@heig-vd.ch*
[b] *Computer Vision Laboratory (CVLAB), Swiss Federal Institute of Technology (EPFL), krzysztof.lis@epfl.ch*

1. INTRODUCTION

Deep learning can solve many problems in computer vision such as image classification, objects detection and segmentation, image enhancement (colorization, super-resolution), but it requires large training dataset with high quality labels, which is a timeconsuming and expensive task. When training a neural network for objects detection, it is common to acquire the same object from numerous points of view. In this specific case, structure from motion algorithms can be used to obtain 3D representation of such objects (as seen in Figure 1) that are sometimes used when depth maps are needed, for example to train new neural networks which try to create a depth map from a single image. In this paper, we propose an innovative semi-automatic method to take advantage of such 3D reconstruction from multiple points of view in order to speed up manual labelling for object or instance segmentation, by labelling 3D data and project it on each image. Finally, our method is applied on a real project, for pipeline segmentation.

Figure 1: 3D reconstruction of pipelines objects from multiple points of view images.

2. STATE OF THE ART OF LABELLING

2.1 Image labelling

Image labelling is a laborious work consisting in manually drawing the shape of all the objects of interest visible on an image, this stage requires a lot of time in order to obtain accurate ground truth, which is a mandatory step before training a deep learning algorithm. Several papers propose methods to optimise/ accelerate this step, for example by working on improving the human-machine interface or by using image segmentation algorithms to automatically extract object envelopes (Wada, 2016, Chen et al., 2014, Gao et al., 2001). Otherwise, (Braun and Borrmann, 2019) propose to fuse photogrammetry 3D data and a BIM model to automatically label images. However, the use of the convex hull to group 3D point in image geometry does not allow to correctly deal with complex objects (like ”U” shape). The other limitation of their method is the fact that they do not separate objects instances.

2.2 Point cloud labelling

Research in various fields, for example autonomous cars, requires labelled 3D data, thus several labelled point cloud datasets have been created (SEMANTIC3D.NET, Stanford Large-Scale 3D Indoor Spaces Data Set, Paris-Lille-3D, etc.). This requires the optimisation of the time-consuming labelling step and various methods have appeared in recent years. Several softwares allow to manually label a point cloud with more or less sophisticated tools. One of the most efficient is Terrascan module from Terrasolid, but as licences are very expensive, open source solutions, such as CloudCompare, are a good alternative. Other automatic or semi-automatic methods exist, for example using labelled images or using active learning solutions. We decided here to use a simple manual solution by labelling the point clouds with Cloud- Compare.

3. METHOD

Our method is composed of three main steps. Firstly, a 3D reconstruction by photogrammetric processing provides localized and oriented images with a dense point cloud (3D data). This process have been fully automated using the Agisoft

Metashape Python API. Then, the point cloud is manually labelled by an operator in CloudCompare software. In order to save time, no instance separation is made manually on the 3D data. Instances will be computed automatically in the last step. Finally, 3D labelled data is cleverly projected on each image to obtain labelled images (in COCO format). This last stage is the core of our method (see Figure 2): (1) point cloud is sorted by classes; (2) DBSCAN algorithm is employed on each classes to create object instances; (3) depthmap (from the 3D reconstruction) are used to project only visible points on the image; (4) alpha-shape algorithm allows to create the hull around the objects; (5) finally labelled images and annotation files in COCO format are computed and exported. All processing have been automated in a Python script.

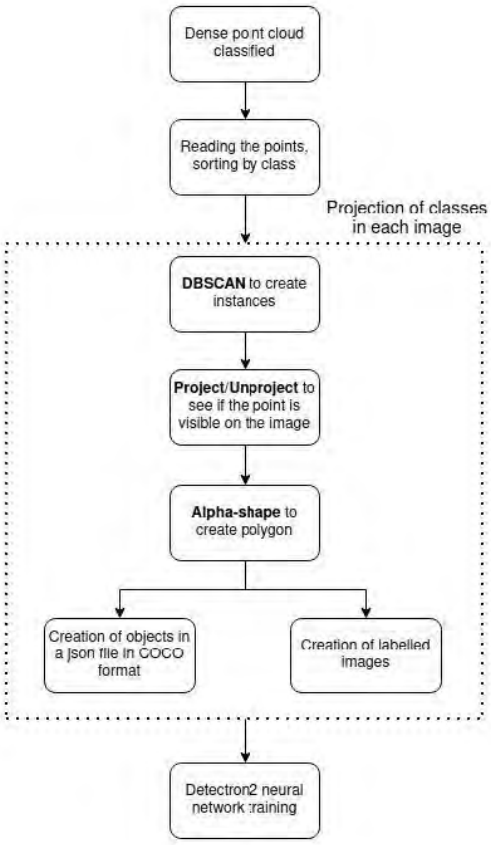

Figure 2: Processing chain of the projection step.

4. RESULTS AND DISCUSSIONS

The proposed labelling method have been compared to a fully manual method on a typical excavation site composed of 30 images with 20 objects, both in term of accuracy and time saving. The labelling accuracy is linked to the processing method but also to the accuracy of the operator who labels the point cloud. As a manual ground truth is needed to calculate an accuracy, evaluation of operator labelling is tedious, thus only the automatic process has been evaluated in this paper. The method used to estimate the labelling accuracy is Intersection over Union (IOU) which is widely used in machine learning (Hui, 2018). We found that there are unlabelled points on the images after our processing that would have been labelled by hand. When passing from the point cloud to the image, some areas that are not reconstructed in 3D (therefore non-existent in the point cloud) are not projected on the image. On the other hand objects can be very tedious to label by hand on 2D images, humans can easily take shortcuts where the machine will remain strict. As can be seen in Figure 3, the labelling of the 3D object is done by clicking 4 times in two different views (images 1 and 2), resulting on a precise labelling (image 3). Whereas in the 2D image the user should be careful to draw the envelope of the complex object. In this case, the accuracy of the proposed method will be better than that of the human.

Moreover, on this dataset, processing time has been reduced by a factor of 3 as seen in Table 1, allowing to save almost one hour with an acceptable loss of accuracy. As explained above the accuracy depends on the point cloud, if the point cloud is complete, the IOU value is close to 100 %, if there are missing areas in the point cloud, the lowest IOU was 95 %.

Figure 3: Manual 3D labelling process in only two steps (1+2) and result after projecting 3D labels on one image with our method (3).

Time per step	Manual	Semi-automated
Time for 3D reconstruction	X	5 min.
Time for point cloud labelling	X	25 min.
Time for reprojection process	X	5 min.
Time for labelling per image	5 min.	X
Total time (30 images)	90 min.	35 min.
Accuracy (IoU)	≈100 %	95-100 %

Table 1: Comparison of time and accuracy of the manual labelling method and our semi-automated method.

5. APPLICATION TO REAL PROJECT

The industrial services of Geneva (SIG) have approached the HEIG-VD to study the future of survey methods for updating the underground cadastre of the canton of Geneva. This concerns the possibilities of automation (in order to speed up fieldwork) as well as their impact on the profession of surveyor. This connection has given rise to a broader project: the ”Automatic Network Survey” project in partnership with the city of Lausanne and the EPFL. In particular, it seeks to find out whether it is possible to automatically recognise the objects making up the underground cadastre (water and gas networks, etc.) during excavation work, using automatic learning techniques (deep learning or artificial intelligence). After the acquisition phase, we have created an attribute table of 43 codes to identify the elements of the water network (valve, pipe, etc.). In order to train the automatic recognition algorithm we have chosen (Detectron2 (Wu et al., 2019)), we used the method presented above to label our images (20 excavation sites, 700 images), resulting on more than 5000 objects instances on 2D image. Manual labelling have been estimated to 50 hours (5 minutes per image, which is optimistic in many cases), when we successfully labelled all this dataset in less than 20 hours thanks to our method, saving about 60% of time.

REFERENCES

Braun, A. and Borrmann, A., 2019. Combining inverse photogrammetry and BIM for automated labeling of construction site images for machine learning. Automation in Construction.

Chen, L. C., Fidler, S., Yuille, A. L. and Urtasun, R., 2014. Beat the MTurkers: Automatic image labeling from weak 3D supervision. Proceedings of the IEEE Computer Society Conference on Computer Vision and Pattern Recognition pp. 3198–3205.

Gao, H., Siu, W. C. and Hou, C. H., 2001. Improved techniques for automatic image segmentation. IEEE Transactions on Circuits and Systems for Video Technology 11(12), pp. 1273–1280.

Hui, J., 2018. mAP (mean Average Precision) for Object Detection.

Wada, K., 2016. labelme: Image Polygonal Annotation with Python. https://github.com/wkentaro/labelme.

Wu, Y., Kirillov, A., Massa, F., Lo, W.-Y. and Girshick, R., 2019. Detectron2. https://github.com/facebookresearch/detectron2.

19.4
3D Processing of Drone & Aerial Survey data in ArcGIS

Guenter Doerffel

Esri Inc., Stationsplein 45, NL-3013 AK Rotterdam, (gdoerffel@esri.com)

This is not a scientific presentation but a relevant product capabilities overview for GeoScience Users of ArcGIS to increase methodological competence for integrated analytical approaches.

Drones, or for larger areas and higher accuracy traditional frame camera technology, are used to capture “Reality”. The reason might be a single event (archeological site, historic building, landslide, avalanche, flood) or recurring monitoring (roads, train-tracks, construction site, built-up area, ..), with outputs in 2D (high-resolution image) 2.5D (DTM, DSM) or real 3D (point-cloud, 3D Mesh). This presentation will explain different options, decision criteria, workflows and the expected results as well as the usecases for those results.

The presented solutions will range from on-premise desktop-like processing to Cloud solutions and large-scale high-resolution solutions. Sharing/Publishing of results will be covered as well.

The session is potentially most productive if most time is used for discussion / questions, which would be the approach taken.

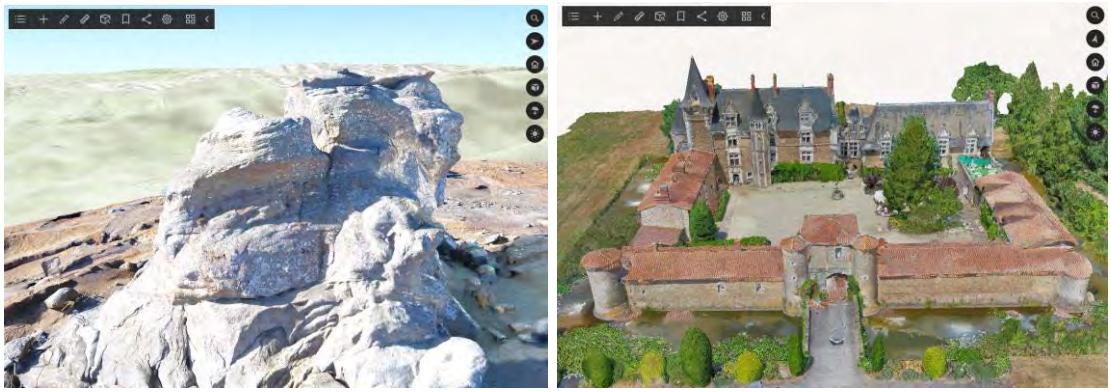

2 Examples illustrating potential use cases: A geological formation in Romania and a historic building complex in France.

19.5
Geostatistical Simulation of Satellite-derived Offshore Wind Speed Patterns

Stylianos Hadjipetrou[1,2], Gregoire Mariethoz[2]

[1] *Department of Civil Engineering and Geomatics, Cyprus University of Technology, 2-8 Saripolou, 3036 Limassol, Cyprus (sk.hadjipetrou@edu.cut.ac.cy)*
[2] *Institute of Earth Surface Dynamics (IDYST), University of Lausanne, UNIL-Mouline, Geopolis, 1015 Lausanne, Switzerland*

Offshore wind energy capacity has been increasingly connected to the grid, paving the way for a more sustainable energy production. However, the lack of consinstent data regarding spatial and temporal variability of offshore wind makes it challenging to assess the energy potential of this ressource. Synthetic Aperture Radars (SAR) have been typically used to retrieve the spatial distribution of wind fields along the sea surface at a fine spatial resolution. SAR-derived wind speed estimates are retrieved via the backscattered normalized radar cross section of the sea surface by utilizing a geophysical model function. Sentinel 1A & 1B satellites, in particular, record scenes in the broader offshore Cyprus area, albeit with a low repeat frequency.

In this work, we employ a geostatistical framework, namely Multiple-point Statistics (MPS), to realistically simulate wind speed patterns at time instances where satellite information is absent. Synthetic fine-resolution wind speed images are generated conditioned to available Uncertainties in Ensembles of Regional ReAnalysis (UERRA) information at coarser scale. Available co-registered spatiotemporal information between the two data sources is used as a training dataset. Synthetic image time-series are evaluated via cross-validation as well as by statistical comparison against raw Sentinel 1 data. Multiple realizations were also generated to assess the uncertainty associated with the simulation outputs. Results show that the proposed methodology can realistically reproduce wind speed patterns at the fine scale leading thus to a detailed offshore wind speed assessment. Furthermore, it paves the way for other applications where incomplete image time-series require homogeneization while preserving realistic spatial patterns.

19.6
Cloud-native Access Patterns as Foundation for an Efficient Implementation of Geospatial Functionalities in EnviDat

Ionut Iosifescu Enescu[1], Gian-Kasper Plattner[1], Dominik Haas-Artho[1], Rebecca Kurup Buchholz[1], Lucia de Espona[1], Martin Hägeli[1]

[1] *Swiss Federal Research Institute WSL, Zürcherstrasse 111, CH-8093 Birmensdorf (ionut.iosifescu@wsl.ch)*

EnviDat is the FAIR (Findable, Accessible, Interoperable and Reusable) environmental data portal and repository of the Swiss Federal Research Institute WSL [Iosifescu et al. 2018]. Driven by requirements of WSL researchers, EnviDat has embarked on integrating comprehensive geospatial visualization functionalities in a new geospatial module.

A major challenge of implementing Geospatial Information Systems (GIS) functionalities in EnviDat is the managing and serving of very large raster time series. Those data cannot be efficiently configured and interactively delivered by traditional Spatial Data Infrastructures (SDIs) and conventional Web Map Services (WMS) as explained in [Iosifescu et al. 2020]. Furthermore, extracting, visualizing and processing large areas of interest from global datasets would require a substantial amount of computation time with SDI geoprocessing services. Therefore, efficient parallel interactions with a multitude of concurrent users, as usual for interactive portals such as EnviDat, would only be possible with significant additional investments in the computing infrastructure.

One of the guiding principles at WSL is the careful and sustainable use of available resources. Consequently, the proficient display of large raster time series in EnviDat is enabled by the use of modern and capable formats and not by adding additional server infrastructure. Cloud Optimized GeoTIFF (COG) files enable web-optimized access to single raster images. A COG has a specific internal organization of tiles and pixels that enables clients to request portions of the file by issuing HTTP-range requests. The same principles are also applied to raster time series saved in Cloud Optimized Raster Encoding (CORE). CORE enables an efficient storage and management of gridded data by applying video encoding algorithms. CORE is a web-native streamable format that can compactly contain raster imagery as a data cube [Iosifescu et al. 2021]. The CORE encode data is available in MP4 or WebM containers, that can be directly streamed to the web browser.

In conclusion, with the use of COG and CORE, we are overcoming the Web-GIS challenges for the visualization of large environmental datasets in EnviDat by (1) the use of modern cloud-native access patterns, (2) the use of efficient compression, including video encoding, and (3) the participation of the user's web browser in geospatial processing and visualization. Geospatial information has the potential to become a central element for any specialized environmental data portal. Enhanced Web-GIS and geoportal capabilities in EnviDat will facilitate the presentation, documentation and efficient exchange of scientific geoinformation to a wide range of users from academia, practice and the public.

REFERENCES

Iosifescu Enescu, I., Plattner, G.-K., Espona Pernas, L., Haas-Artho, D., Bischof, S., Lehning, M., & Steffen K. 2018: The EnviDat Concept for an Institutional Environmental Data Portal, Data Science Journal, 17, p.28, DOI: https://doi.org/10.5334/dsj-2018-028

Iosifescu Enescu, I., Hanimann, D., Karger, D. N., Plattner, G.-K., Haas-Artho, D., Kurup Buchholz, R., Espona Pernas, L., Zimmermann, N. E., Pellissier, L. & Hägeli M. 2020: Challenges for Integrating Web-EGIS Functionalities in the Environmental Research Data Portal EnviDat, In Proceedings of the 18th Swiss Geoscience Meeting, Zurich, Switzerland.

Iosifescu Enescu, I., de Espona, L., Haas-Artho, D., Kurup Buchholz, R., Hanimann, D., Rüetschi, M., Karger, D.N., Plattner, G.-K., Hägeli, M., Ginzler, C., Zimmermann, N.E. & Pellissier L. 2021: Cloud Optimized Raster Encoding (CORE): A Web-Native Streamable Format for Large Environmental Time Series, Geomatics, 1, 369-382, DOI: https://doi.org/10.3390/geomatics1030021

19.7
Brinzauls, Pizzo Cengalo, Spitze Stei: Analysing detailed rock kinematical processes using point cloud models

Robert Kenner[1], Valentin Gischig[2], Zan Gojcic[3], Yvain Quéau[4], Christian Kienholz[5], Daniel Figi[6], Reto Thöny[6], Yves Bonanomi[7]

[1] *WSL Institute for Snow and Avalanche Research, Davos, Switzerland*
[2] *CSD Ingenieure AG, Liebefeld, Switzerland*
[3] *Institute of Geodesy and Photogrammetry, ETH Zürich, Zurich, Switzerland*
[4] *Normandie Univ, UNICAEN, ENSICAEN, CNRS, GREYC, Caen, France*
[5] *GEOTEST AG, Zollikofen, Switzerland*
[6] *BTG Büro für Technische Geologie AG, Sargans, Switzerland*
[7] *Bonanomi-Gübeli AG, Igis, Switzerland*

The rock slope instabilities Brienz/Brinzauls (GR), Spitze Stei - Kandersteg (BE) and Pizzo Cengalo (GR) are amongst the largest currently observed in Switzerland and have significant hazard potential. Multiannual LiDAR point clouds were used to analyse the kinematical processes of these slope deformations. While the information content of point-clouds from UAV or LiDAR is commonly not exhaustively exploited, we show how they can be used to (1) highlight active shear planes within the moving rock mass, even if the shearing movement is more than one magnitude smaller than the main slope displacements, (2) identify differences in kinematical behaviour of individual rock compartments, (3) define the kinematic process behind the slope displacements, (4) model basal sliding planes based on the 3D surface movements of rock slides, (5) calculate exact displacement angles and (6) give estimations of destabilised rock volumes. The results are discussed in a geological context.

19.8
A webtool for the 3D conceptualization and animation of groundwater flow systems

Arnauld Malard[1], Pierre-Yves Jeannin[1], Nathalie Doerfliger[2], Silvan Laube[3], Olivier Béon[2], Alfredo Zein[2], Manfred Vogel[3]

[1] Swiss Institute for Speleology and Karst-Studies, SISKA (pierre-yves.jeannin@isska.ch)
[2] Danone Waters, 74503 Evian les Bains, France
[3] I4DS, Institute for Data Science, Fachhochschule Nordwestschweiz, CH 5210 Windisch

It is often difficult to communicate groundwater-related aspects (fast vs. slow groundwater circulation, mineralization processes, contamination paths, etc.) to people without a basic hydrogeological knowledge. The description of groundwater flow systems is particularly difficult in complex geological environments, and this may lead to differences in interpretation and understanding. Either, conceptual models are highly schematized and static, or dynamic models are too sophisticated, and request hydrogeological skills to understand processes. In order to better explain the various hydrogeological processes in a given aquifer system to stakeholders, a webtool (interactive 3D-animation) to visualize conceptual models of groundwater flow-systems in 3D has been developed as an extension to visualkarsys.com within the frame of a joint-project between Danone Waters, SISKA and I4DS. This is designed for all types of hydrogeological settings, and can address different timescales (few days event, seasonal regimes, long term trends) and spatial scales. The aim of this webtool is to explicitly show how groundwater flows (infiltration to unsaturated zone, flowpaths in the saturated zone) through complex heterogeneous aquifer systems (high-contrasted permeabilities, thick unsaturated zones, cascading aquifers, multi-layers aquifers, etc.).

Input rainfall is generated as falling 3D drops which may be spatialized at a certain location or extrapolated over the whole project area. When touching the ground surface, 3D drops are converted into particles which may runoff and/or infiltrate depending on the hydraulic conductivity of the geological layer. Particles infiltrate vertically through the unsaturated zone until penetrating the saturated zone or until reaching the basement of the aquifer. In that case, particles follow the topography of the aquifer basement before penetrating the saturated zone. In this zone, particles organize as a flow-field and converge toward the main outlets (springs or tapped/artesian drillholes). Tools for representing residence time and mineralization processes are also available.

Users may parameterize the timescale, the precipitation rate as well as a series of more global parameters (ET and P versus elevation, etc.). Animation scenarios may be saved and later retrieved by all users having the permissions to access the project.

From a technical point of view, the webtool is built on a per-project basis which can be shared between users. Frontend functionalities are based on the Angular 7 web framework (TypeScript) and 3D animations run with threeJS.

19.9
pyKasso: a stochastic karst network generator

François Miville[1], Chloé Fandel[2], Philippe Renard[1]

[1] *Centre for Hydrogeology and Geothermics (CHYN), University of Neuchâtel, Rue Emile-Argand 11, CH-2000 Neuchâtel, Switzerland (francois.miville@unine.ch)*
[2] *Hydrology and Atmospheric Sciences, University of Arizona, 1133 E. James E. Rogers Way, Tucson, USA (cfandel@email.arizona.edu)*

In Switzerland, karst environment covers around 20% of the total surface and contributes just as much to drinking water supply. Yet, karst system are extremely sensitive to surface pollution because of their high hydraulic conductivity. Then karst network simulation can help us in protection of water quality, but are currently time-consuming and complex to operate.

Here we present pyKasso, a python3 open-source package intended to easily and quickly simulate karst network using a geological model, hydrogeological, and structural data. It relies on a pseudo-genetic methodology where stochastic data and fast-marching methods are combined to perform thousands of simulation rapidly. The method is based on the stochastic karst simulator developped by Borghi et al (2012). It is extended to account for anisotropy allowing to simplify the algorithm while accounting better for the geological structure following the method presented in Fandel et al. (2021). Geometricals indicators of computed karst network are then statistically compared with real karst network indicators in order to evaluate their plausibility. The application of the method is illustrated with a few examples.

REFERENCES

Fandel, C., Miville, F., Ferré, T., Goldscheider, N., Renard, P. 2021: The stochastic simulation of karst conduit network geometries using anisotropic fast marching, and its application to a geologically complex alpine karst system. Submitted to Hydrogeology Journal

Borghi, A., Renard, P., Jenni, S. 2012: A pseudo-genetic stochastic model to generate karstic networks, Journal of Hydrology, 414–415, https://doi.org/10.1016/j.jhydrol.2011.11.032.

19.10
Automatic valley-scale clay models from TEM and boreholes data : Application on the upper Aare Valley

Alexis Neven[1], Anders Vest Christiansen[2], Philippe Renard[1,3]

[1] *Centre of Hydrogeology and Geothermics, University of Neuchâtel, Neuchâtel, Switzerland (alexis.neven@unine.ch)*
[2] *Department of Earth Sciences, Aarhus University, Aarhus C, Denmark*
[3] *Department of Geosciences, University of Oslo, Oslo, Norway*

In most urbanized and agricultural areas of central Europe, the shallow underground is constituted of Quaternary deposits. The thickness can vary from a few meters to hundreds of meters, and are often the most extensively used layers (Water pumping, shallow geothermic, material excavation). However, all these deposits are often intertwined (a lake deposit can be partially eroded by a glacier, and refilled with river sediments). This leads to a high spatial variability in such sediments and is one of the main causes of the high complexity of Quaternary geological and hydrological modelling. Geophysical data can be a fast and reliable source of information, but integration of such data is time consuming and does not account for uncertainty. Furthermore, linking geophysical data to permeability or lithology is always tricky.
Therefore, there is a need for an automatic approach that would be able to integrate multiple data types of various scales and produce geological models with parametric fields for flow models, with a robust uncertainty quantification from the data to the model. In this study, we propose a methodology to combine multiple data types such as boreholes, geophysical and hydrological data with uncertainty in an automatic framework. This framework is based on stochastic methods such as MPS algorithms and Gaussian Random Function. We applied this methodology to estimate various lithological, and hydrological parameters using a towed Time-domain Electromagnetic (tTEM) geophysical dataset acquired in the Quaternary filled upper Aare valley, Switzerland and covering more than 1500 hectares of land with a resolution in the order of 10m. The depth of investigation varies from 50m to 100m. Combined with thousands of boreholes and hydrological estimation as control point, we were capable to automatically generate realistic underground lithological and parametrical models at a valley scale, with a high spatial resolution and with an uncertainty carried down the workflow.

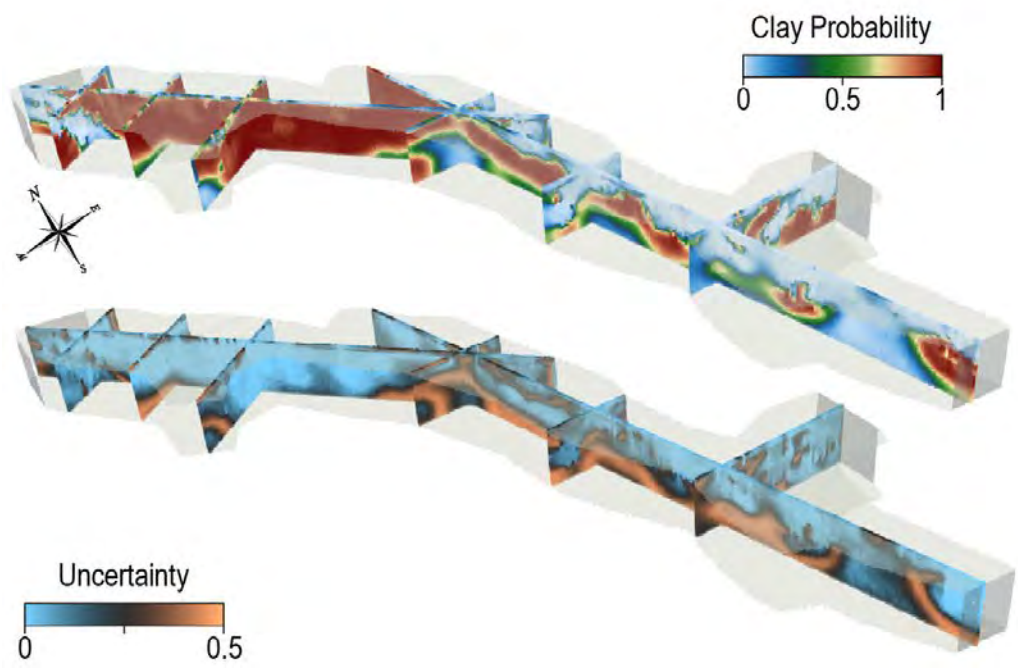

Figure 1. Exemple of a few cross-sections through the automatically generated model. The top sub-figure shows the probability of having a Clay facies. The lower sub-figure shows the assocaited uncertainty.

19.11
swissgeol.ch – Web-based 3D subsurface visualisation

Nils Oesterling[1], Roland Baumberger[1], Elisabeth Leu[2]

[1] Federal Office of Topography swisstopo, Swiss Geological Survey, Seftigenstrasse 264, CH-3084 Wabern (nils.oesterling@swisstopo.ch)
[2] Camptocamp SA, EPFL Innovation Park, Bldg. A, CH-1015 Lausanne

GIS and 2 / 2.5 dimensional data is common in geosciences. Also 3D data such as city-models is getting increasingly available, especially in web-based applications like Google Maps or GoogleEarth etc. All of this data is located on or above the earth surface. Fly tracks are even located somewhere in the atmosphere.

Subsurface data, such as drill holes, geometries of geological strata, infrastructure objects, e.g. tunnels, is usually not shown in its correct position in the underground, but is projected to a 2D map view. For other purposed 3D data (e.g. geological cross sections or even entire 3D models) is usually represented in a model-centred manner, disconnected from its geographic context.

To embed 3D subsurface data into a geographic context and to represent it in its correct spatial position in the underground, the web-based 3D viewer swissgeol.ch was developed.

This new approach for 3D visualization is available at https://swissgeol.ch, containing various geographic and geoscientific data as well as diverse functionality for viewing and investigating spatial data - above and below the surface. Some selected data and tools are:

- Geological vector data (GeoCover) and cross sections
- 3D model of the Swiss Molasse Basin (GeoMol)
- Recent (< 90 days) and historical earthquakes (magnitude > 3)
- Parameter models (voxel) in selected areas
- Bore holes (selection)
- Railroad, water and highway tunnel (swissTLM3D) and swissBuildungs3D

- Download of selected data
- Slicing of 3D scences (line- / block-slicing)
- Uploading of own data in kml or gpx format for combining it with data provided by swissgeol.ch
- Creating and downloading of geometries such as Points of intrest, reogion of interest

Data content and functionality is continously extended.

This presentation gives a brief overview of swissgeol.ch and its functionality. The technical basis and future developments are shown.

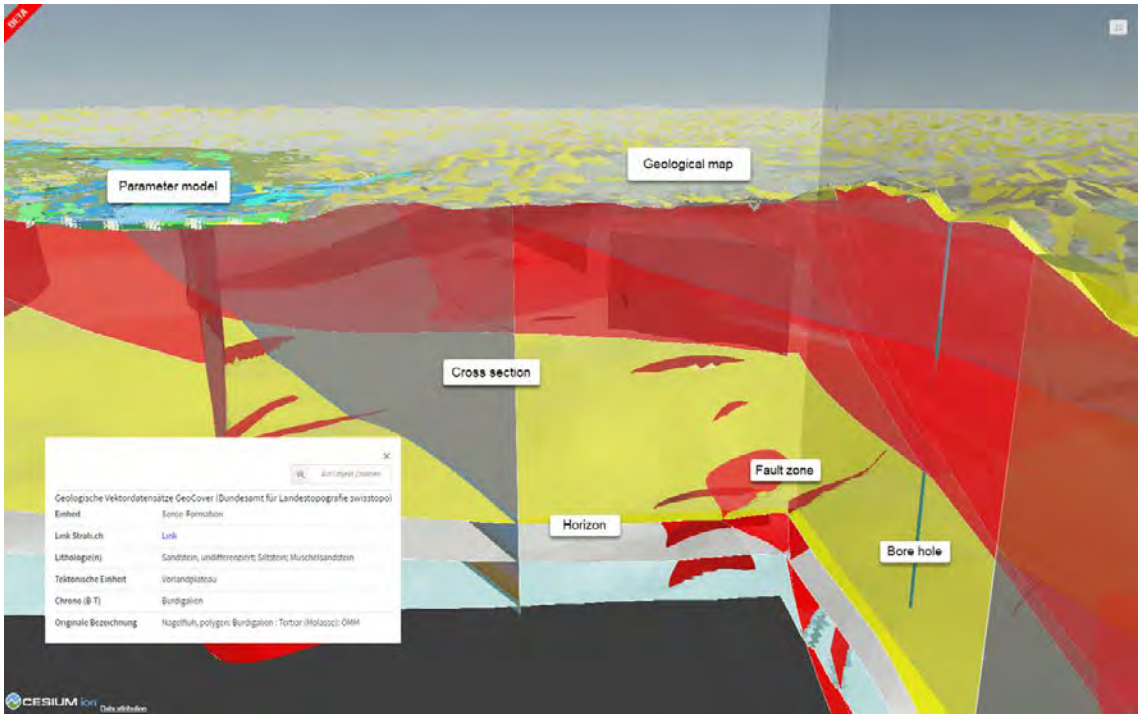

Figure 1. Sliced 3D scene in swissgeol.ch. Inverse box-slicing aplied for illustrating subsurface structures in the Thun region. Geologic horizons, faults together with a bore hole and a lithological parameter (voxel) model are shown. Attribute information is displayed in tool-tip window.

19.12
GECOS: A webapp to explore geothermal chance of success

Lorenzo Perozzi[1], Luca Guglielmetti[1], Andrea Moscariello[1]

[1]*GE-RGBA Group, of Earth Science, University of Geneva, 13 rues des Maraichers 1205 Geneva, Switzerland (lorenzo.perozzi@unige.ch)*

The Chance of Success (COS) is defined as the possibility for an event to occur. COS is associated with the concepts of probability and risk and, therefore, their associated uncertainty.

Quantification of the COS of a geo-energy project is part of the overall evaluation process and commonly used in the industry as a decision-making tool. For instance, the assessment of projets COS also known as POS (probability of success) is used in hydrocarbon industry in prospect appraisal to define the success ratio in extracting a minimum volume of resource. The overall idea of the Geothermal Energy Chance of Success (GECOS) project is to support industrial investors with a tool able to provide the required subsurface information for geothermal developments. The GECOS project focused on the Canton of Geneva where the Mesozoic carbonates of the Lower Cretaceous and Upper Jurassic are, at present, the main subsurface geothermal target for the *Geothermies* program aiming at implementing geothermal projects for heating & cooling applications.

To assist these exploration activities, the GECOS decision-making tool allows the identification of the most favorable sectors of a prospect where to direct further investigations to identify drilling targets. In the framework of the GECOS project, a Play Fairway Analysis (PFA) approach has been used, which allowed to produce a COS index according to the reservoir geothermal potential and the geophysical data investigation potential for the entire Canton of Geneva.

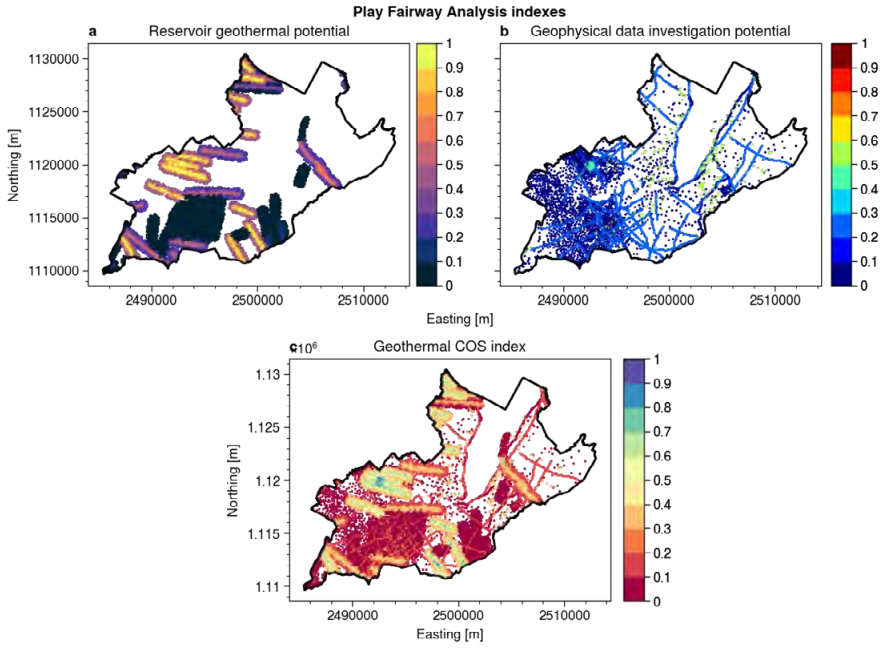

Figure 1: a) Reservoir geothermal potential index, normalized between 0 and 1, b) Geophysical data investigation potential, normalized between 0 and 1; c) Geothermal chance of success index resulting from the summation of a) and b).

The former gives the thermal power that can be potentially extracted at a certain location based on a set of subsurface information available, whereas the latter has the goal to inform about the reliability of the geophysical data collected over an area. The sum of these two elements is computed and the COS of the Canton of Geneva map was produced, as shown in Figure 1.
However, to be efficient, the decision-making tool should be easily accessible to the final user who should have the possibility to interact with it, by, for example, selecting/filtering some data, investigating the COS at different depths, etc. Classical Geographic Information System (GIS) software allows interacting with the data but have two main limitations: 1) the user needs to have an installed version of the software to open and interact with the project, and 2) the learning curve of this software can be steep depending on the user experience.

With this in mind, we opted for the creation of a web application, built with Dash, an open-source library, released under the permissive MIT license. Dash is a productive Python framework for building web analytic applications. Written on top of

Flask, Plotly.js, and *React.js*, Dash is ideal for building data visualization applications with highly custom user interfaces in pure Python. We applied the hexagon binning technique that is a form of bivariate histogram useful for aggregating and visualizing the structure in datasets with large data points (Carr et al., 1987). Figure 2 shows a screenshot of the webapp, deployed on Heroku, a container-based cloud platform.

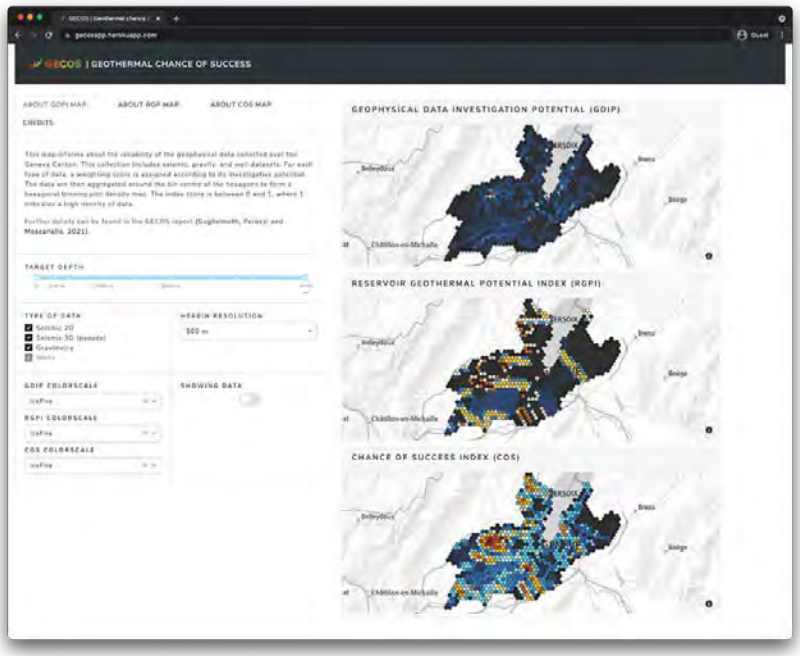

Figure 2: GECOS webapp

REFERENCES

Carr, D. B., Littlefield, R. J., Nicholson, W. L., & Littlefield, J. S. (1987). Scatterplot Matrix Techniques for Large N. Journal of the American Statistical Association, 82(398). https://doi.org/10.2307/2289444

19.13
Probabilistic geological model using multi-scale geophysical data: An example from the Bedretto Lab

Alexis Shakas[1], Quinn Wenning[2], Marian Hertrich[2], Hansruedi Maurer[1], Domenico Giardini[3]

[1] Exploration and Environmental Geophysics, ETH Zurich, Sonnegstrasse 27, CH-8092 Zurich (alexis.shakas@erdw.ethz.ch)
[2] BULGG - Bedretto Underground Lab
[3] Seismology and Geodynamics, ETH Zurich, Sonnegstrasse 27, CH-8092 Zurich

Deep geothermal energy in Switzerland is considered as one of the resources that will ease the transition to nuclear-free energy and provides a sustainable and emission-free alternative to fossil fuels. To fully utilize the potential of the natural geothermal heat gradient, boreholes must be drilled to several km depth. At such depths, the basement rock is often impermeable and must be “engineered” in order to create fluid pathways. These pathways are then used to extract heat that is used for electricity production. Evidently, characterizing the existing (natural) fluid pathways, such as faults and fractures, as well as the engineered structures is of major importance. Borehole geophysics plays a central role in this respect, as it provides the tools and techniques to probe close and away from boreholes, in a cheap and non-destructive manner. Still, the uncertainties away from boreholes remain large. Foremost, the uncertainty on borehole trajectories must be taken into account, as well as uncertainties in parameter estimates that are used to obtain a geological model (for example the topology of a fault) from geophysical data.

The Bedretto Lab is a recently established underground laboratory situated in the valley of Bedretto, Ticino. The lab has been engineered from an old audit tunnel that has a total length of 5 km. At 2 km, the main laboratory exists and offers an overburden of ~1 km of granite. A total of 8 long boreholes were drilled in the Bedretto lab and borehole logging (acoustic and optical televiewer) as well as single-hole ground penetrating radar (GPR) data is available from all boreholes, each with its own sources of uncertainty. From these datasets we created a framework that accounts for the respective uncertainties and allows constructing a probabilistic geological model of a major fault zone. This fault zone is the first structure intersected in our rock volume of interest, and governs much of the hydro-mechanical response we observe in the upper volume. From the final probabilistic model we can assess its extension, topology and intersection with the tunnel, and extend the methodology to further structures imaged from borehole geophysics.

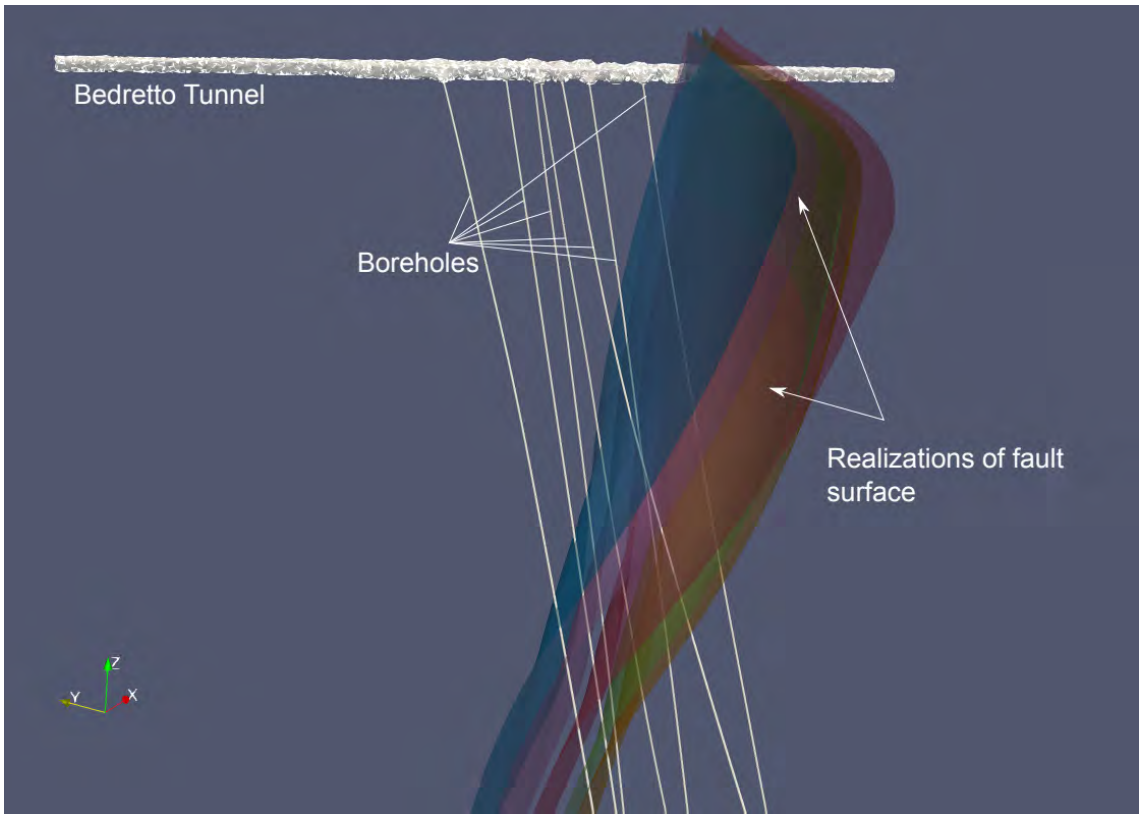

Figure 1. A view of the Bedretto Tunnel, the 8 drilled boreholes and 5 realizations of the fault surface, based on prior uncertainties extracted from borehole logging and GPR datasets.

19.14
Modeling tropospheric effects in space geodetic signals by machine learning and collocation

Endrit Shehaj*, Alain Geiger*, Luca Miotti*, Benedikt Soja*, Gregor Moeller*, Stefano D'Aronco*, Jan Dirk Wegner*,**, Markus Rothacher*

** Institute of Geodesy and Photogrammetry, ETH Zürich, Robert-Gnehm-Weg 15, 8093 Zürich, Switzerland (eshehaj@ethz.ch)*
*** Institute for Computational Science, University of Zurich*

Atmospheric water vapor is directly connected to Earth's greenhouse effect, as well as natural disasters and global warming. Furthermore, its high spatio-temporal variations are considered a nuisance in space geodetic techniques, such as Global Navigation Satellite Signals (GNSS), causing delays that are very difficult to model or predict.

In the last years, at the Institute of Geodesy and Photogrammetry (IGP), we have deployed machine learning methods for the prediction of tropospheric delay time series. We have obtained satisfying results (cm level accuracy) for the prediction of delays at locations used in the training phase. However, difficulties arise when we try to predict tropospheric delays at new sites. To resolve this issue, we combine the machine learning results with other methods that already proved successful for spatial interpolation. Indeed, for decades, our group at IGP has been using collocation methods for modelling and interpolation of tropospheric delays, obtained for instance through GNSS processing or numerical weather prediction (NWP) models. Therefore, we can obtain tropospheric delay fields for the area of investigation (such as entire Switzerland) without processing any additional GNSS data but using only meteorological parameters that are publicly available. These data can benefit any receiver in the territory, as well as be used for cross-validation of tropospheric delays obtained through other methods.

For this work, we use time series of 11 years, from the GNSS networks AGNES (provided by swisstopo) and COGEAR in Switzerland as well as meteorological data from the SwissMetNet (provided by MeteoSwiss). The first 10 years (2008-2017) are used to train the machine learning models, while the last year (2018) is used for validation of our results.

P 19.1
Mapping recent pyroclastic flow using Sentinel-2 image in De Fuego volcano, Guatemala

Alireza Salehipour Milani [1] and Mahdiyeh Sabzaliyan [1]

[1]*Department of Physical Geography, Faculty of Earth Science, Shahid Beheshti University, Tehran, Iran.*

De Fuego is one of the most active volcanoes in the world, with a history of 60 eruptions over 500 years, most of which occurred in or near February and September. The De Fuego volcano erupted on the morning of June 2018, killing at least 72 people when volcanic lava hit the ground, buildings and residential areas around the volcano. Thus, identification and monitoring of this volcano are essential. Monitoring changes in lava and pyroclastic flow and their direction during the time can help scientists and planner to save the lives of many people. In this research sentinel2 satellite image and maximum likelihood classification used to detect the direction of lava and pyroclastic during the De Fuego volcano eruption in June 2018. The result indicates The highest range of Pyroclastic was flowing in the western and eastern part of volcano vent, which has moved to the lower part due to the topographic slope.

Introduction

The eruption of volcanic lava is one of the dangers that can affect many human communities (Pedrazzi et al., 2008; Cappello et al., 2015a, b; Del Negro et al, 2015). therefore, the study and development of volcanic lava flow paths can be a very valuable resource for researchers and earth science planners (Pedersen et al., 2017). In addition, the possibility of estimating the future path of lavas in the possibility of acceptance. In the past, volcanoes have been studied through field studies, but today remote sensing techniques have provid researchers with a very powerful tool to study this phenomenon and have accepted the possibility of a more comprehensive study (Abrams, 1991; Blackett, 2013). Using multispectral data and covering it at different time intervals is one of the objectives of this technique (Bonaccorso et al., 2011.)

Study area

At the southern edge of De Fuego Volcano is a belt of Tertiary volcanic rocks consisting of lava flows and the Lahar units that make up the Guatemalan highlands, and to the south is another young volcano called Akatenango. Together, these two volcanoes form twin volcanoes. However, their lavas are structurally different, such as the Akatenango Andesite lavas and the De Fuego basaltic lavas. De Fuego is also one of three large stratospheric volcanoes adjacent to the city. Antigua Guatemala, the former capital of Guatemala, is located. (Venzke, 2013).

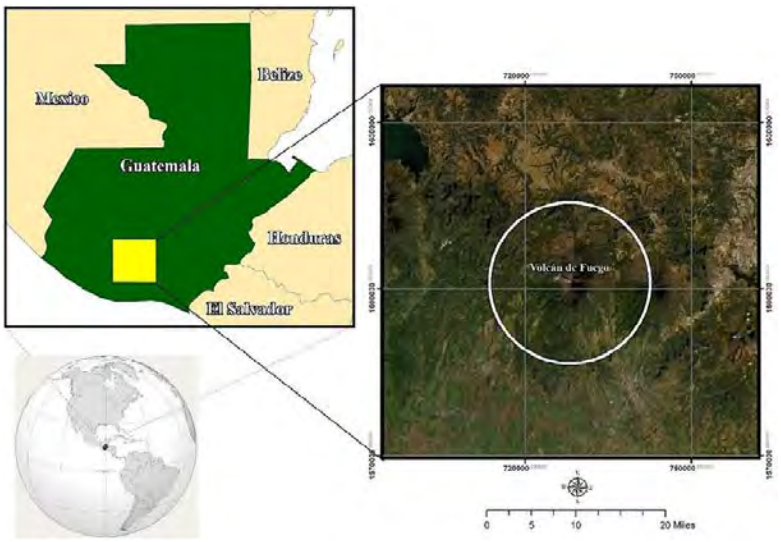

Figure 1.Geographical position of the De Fuego volcano

Eruption of The De Fuego volcano in 2018

The De Fuego volcano erupted before noon on June 3, hitting the ground, buildings and residents of several residential areas around the volcano, killing at least 72 people and injuring about 300, leaving 192 missing. Many buildings were destroyed, and the international airport La Guerra City, Guatemala City, was closed, and the volcanic eruption reached the Guatemalan capital due to a change in the direction of the ash wind. According to the Guatemalan Disaster Management Authority, rapid flow called «pyroclastic», a mixture of very hot gas and volcanic material, covered the residential areas of El San Miguel Los Lotus, destroying homes and burning a number of residents. He was killed and due to the lava covering of this village, the access of rescue forces has become very difficult. On June 6, the volcano erupted again and molten material flowed from its southern side. At the same time as the volcano erupted again, rescue and relief workers were on

the scene rescuing the injured, who later fled the area. Officials say the eruptions and volcanic eruptions have affected the lives of 1.7 million people, leaving 3,000 homeless and living in shelters. On November 19, the De Fuego volcano erupted for the fifth time this year, and nearly 4,000 residents around the volcano were evacuated to shelters due to the risk of lava and ash from the eruption.

Methodology

In this study, in order to determine the areas affected by the volcanic eruption, Sentinel 2 satellite images related to the volcanic activity of history were used. Radiometric and atmospheric corrections of satellite images were performed in SNAP software. In order to prepare the land use map of Fogo volcano, the first educational sampling of city units, settlements, gardens, agricultural lands, barren lands and also lava was carried out. In the next step, the maximum probability was used to classify the satellite images using the classification technique. This type of classification uses the formula of normal multidimensional distribution to form decision surfaces in a quadratic form, as a result of which these surfaces will have a parabolic, elliptical and circular shape. The classification algorithm evaluates the maximum probability of variance and covariance of the classes. To do this, it is assumed that all educational areas have a normal distribution. To make changes in many spectral properties in this continuous range. Finally, volcanic lava zones in the study area were determined.

Discussion

In order to classify satellite imagery, 250 training samples were taken from the study area and in different land use units, according to the color, morphology, landscape difference in the satellite imagery. Agriculture, garden, forest, lava and pyroclastic were classified in satellite images using amaximum likelihood algorithm. The highest range of Pyroclastic flow is in the western and eastern part of volcano vent, which has moved to the lower part due to the topographic slope. The movement of these materials has caused a part of the study area to be destroyed compared to before the eruption. Studies show that the predominant path of lava and pyroclastic has not changed much and has continued the same trend of previous eruptions. However, in some parts, such as the southern and northwestern parts, several new and small routes have been formed and some of the materials from these routes have spread to the lower elevation parts.

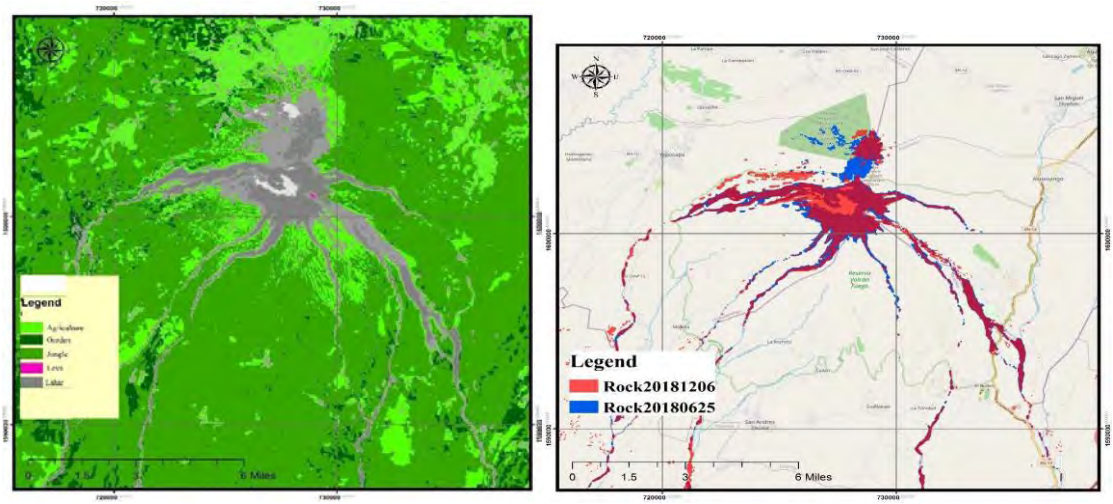

Figure 2. pyroclastic flow in 2018 volcano eruption

Conclusion

Overall, both classifiers were able to accurately distinguish pyroclastic material such as lahar, volcanic rock, and sand. Because spatial resolution affects LC accuracy, high-resolution images provided better LC accuracy results. Information provided by LC maps can be used in the generation of maps on disaster-prone regions, particularly pyroclastic material debris area. Therefore, the results of the current study may be useful for predicting the susceptibility of volcanic regions to pyroclastic debris damage.

REFERENCES

Abrams, M., Abbott, E., & Kahle, A. 1991: Combined use of visible, reflected infrared, and thermal infrared images for mapping Hawaiian lava flows, Journal of Geophysical Research: Solid Earth, 96(B1), 475-484.

Bonaccorso, A., Caltabiano, T., Currenti, G., Del Negro, C., Gambino, S., Ganci, G., & Boschi, E. 2011: Dynamics of a lava fountain revealed by geophysical, geochemical and thermal satellite measurements: The case of the 10 April 2011 Mt Etna eruption, Geophysical Research Letters, 38(24).

Cappello, A., Geshi, N., Neri, M., & Del Negro, C. 2015: Lava flow hazards—An impending threat at Miyakejima volcano, Japan. Journal of Volcanology and Geothermal Research, 308, 1-9.

Cappello, A., Zanon, V., Del Negro, C., Ferreira, T. J., & Queiroz, M. G. 2015: Exploring lava-flow hazards at Pico Island, Azores Archipelago (Portugal), Terra Nova, 27(2), 156-161.

Del Negro, C., Cappello, A., Neri, M., Bilotta, G., Hérault, A., & Ganci, G. 2013: Etna flank lava flows between 1610 and 2008, PANGAEA

Del Negro, C et al. 2013: Lava flow hazards at Mount Etna: constraints imposed by eruptive history and numerical simulations, Scientific Reports, 3, 3493,

Pedersen, G. B. M., Höskuldsson, A., Dürig, T., Thordarson, T., Jonsdottir, I., Riishuus, M. S., ... & Schmith, J. 2017: Lava field evolution and emplacement dynamics of the 2014–2015 basaltic fissure eruption at Holuhraun, Iceland, Journal of Volcanology and Geothermal Research, 340, 155-169.

Pedrazzi, D., Cappello, A., Zanon, V., & Del Negro, C. 2015: Impact of effusive eruptions from the Eguas–Carvão fissure system, São Miguel Island, Azores archipelago (Portugal), Journal of volcanology and geothermal research, 291, 1-13.

P 19.2
Snow Cover Mapping: Generating Long-Term Landsat Imagery Consistent with Climate Data

Fatemeh Zakeri[1], Gregoire Mariethoz[1]

[1] *University of Lausanne, Institute of Earth Surface Dynamics, Switzerland (fatemeh.zakeri@unil.ch)*

Remote sensing is a valuable tool for observing snow cover changes. Having a complete snow cover daily time series provides an opportunity for studying the timing and duration of the melting season, snowmelt, and run-off. However, satellite data are limited due to clouds, clouds, shadows, and revisiting time. Moreover, accessing high temporal and spatial resolutions snow cover observation is still a challenge due to the trade-offs among these resolutions.

When there is a resemblance between two states of the atmosphere, the meteorological phenomena associated with them should also bear a resemblance to each other (Gibergans-Báguena and Llasat 2007). Accordingly, we postulate that snow patterns from previous years could be repeatable in many regions between years with similar meteorological characteristics (Pflug et al. 2021). Using Landsat, climate, and in situ datasets, we synthesize Landsat images focusing on snow cover for dates where no observations are available. The principle of the proposed method is based on a K-nearest-neighbour approach. For a given target day where no Landsat observations are available, two steps are applied: 1) selection of a set of days (analogue days) where Landsat imagery is available, and which are similar to the target day in terms of meteorological conditions, and 2) estimation of snow pattern for the target day based on the analogue days.

Synthetic snow cover maps for the western Swiss Alps are generated from 2000 till 2017 to evaluate the effectiveness of the proposed method. The results are analyzed using visual comparison and a leave-one-out cross-validation by removing each image at random for each year. Then, the synthetic image is compared with the actual image. Both accuracy procedures demonstrate that the combination of Landsat and climate data results in a good performance in predicting Landsat-based daily snow cover maps.

REFERENCES

Gibergans-Báguena, J., & Llasat, M. (2007). Improvement of the analog forecasting method by using local thermodynamic data. Application to autumn precipitation in Catalonia. *Atmospheric Research, 86*, 173-193

Pflug, J., Hughes, M., & Lundquist, J. (2021). Downscaling snow deposition using historic snow depth patterns: Diagnosing limitations from snowfall biases, winter snow losses, and interannual snow pattern repeatability. *Water Resources Research*

P 19.3
Cloud-based Imagery storage and analysis in ArcGIS

Guenter Doerffel

Esri Inc., Stationsplein 45, NL-3013 AK Rotterdam, (gdoerffel@esri.com)

This is not a scientific presentation but a relevant product capabilities overview for GeoScience Users of ArcGIS to increase methodological competence for integrated analytical approaches.

Up till recently, creating Imagery services required running on-premise or cloud-based self-managed infrastructure. This is still ONE of three modes of operation supported. Key topics for this mode is an optimized cloud storage strategy – which will be part of this presentation.

Recently the offerings have been extended and now offer 2 alternatives: Storing Imagery and offering Image Services via any ArcGIS Online account and signing up for a cloud hosted, Esri managed dedicated Server that can be integrated into any infrastructure.

The presentation will discuss pro's and con's of all three models, explain the respective publishing and analytical processes and discuss decision criteria for common operative scenarios ranging from "project" and "strictly private" to "multi-year archive" to "public high volume access".

P 19.4
Multidimensional Imagery /TimeSeries in ArcGIS

Guenter Doerffel

Esri Inc., Stationsplein 45, NL-3013 AK Rotterdam, (gdoerffel@esri.com)

This is not a scientific presentation but a relevant product capabilities overview for GeoScience users of ArcGIS to increase methodological competence for integrated analytical approaches.

TimeSeries Analysis, like Change Detection, has become a de-facto standard for many scientific questions. Increasing spatial and temporal resolution of data support and at the same time require this methodology. Atmospheric and aquatic sciences are typical examples for multidimensional sensor technology and consequently analysis in the wake of this. With formats like GRIB or NetCDF, common standards to distribute self-descriptive multidimensional raster (and vector) data are available.

This presentation will give an overview of how to use existing multidimensional data or define new multidimensional datasets, visualize, analyze and process them and share them back out as datasets or services. As to the very different reqiurements in (interdisciplinary and cooperative) Science today, the approaches using UI Tools, Python and Jupyter notebooks will be adressed. Analytical capabilities like “on-the-fly” process chains, capturing of training data for Classification/AI and Charting/Graphs are mentioned.

Cloud data sources and cloud specific processes are relevant today, especially with very dynamic high-volume data like Copernicus or archives of commercial vendors today.A Sentinel-2 sample will illustrate such a workflow and the results.

Some Web-client examples illustrate how to offer multidimensional data to end-users from dynamic, frequently updated sources.

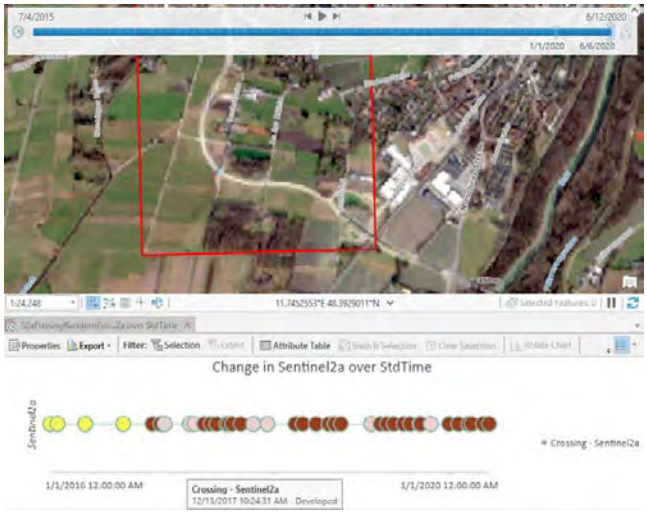

Example of a self-defined land-use classification and the query of a single location over a range of time from a Multidimensional Sentinel-2 dataset

20. Scalability, transferability and transformative potential of global change research in mountains

Carolina Adler, Jörg Balsiger, Raffaella Balzarini, Philippe Bourdeau, Iago Otero, Emmanuel Reynard

TALKS:

20.1 Chakraborty R., Sherpa P.Y: From Climate Change to Climate Justice: Critical reflections on the IPCC and Himalayan climate knowledges

20.2 Reynard E., Bonnemains A., Clivaz M., Dubath C., Gros-Balthazard M., Lambiel C., Neumann M., Metzger A., Randin C., Trouilloud S.: Val d'Hérens 1950/2050 – A citizen science project for transformation towards sustainability in a mountain valley

20.3 Vijayan D., Sam A.S., Kaechele H., Girindran R.: Forest conversion in mountains and changes of socio-ecological systems: Perception of indigenous communities

20.1
From Climate Change to Climate Justice: Critical reflections on the IPCC and Himalayan climate knowledges

Ritodhi Chakraborty, Pasang Y Sherpa

Climate knowledge production in the Himalayan region reflects different organizational and functional biases which include a geographical bias favoring experts from the global north, a gender bias in favor of men, a disciplinary bias in favor of the natural sciences over the social sciences and humanities, and finally, a cosmological bias favoring western science over indigenous knowledges. This reflects the broader culture of climate knowledge production as espoused by the IPCC. In recent years, scholars have noted changes in these processes, pointing at the inclusion of social science/humanities perspectives and a growing engagement with plural worldviews. Despite such forays, all aspects of climate knowledge production, within the IPCC still echo the aspirations of nation states and quantitative models of attribution and detection. In this talk, we focus on our personal experiences with local communities from the Himalayas and bring it in dialogue with our experiences with the IPCC knowledge production process. In doing so, we have two objectives: first, to highlight marginalized stories of climate-society relationships that challenge normative climate science/policy and second, in light of these stories, suggest some salient considerations required to foreground justice and equity in future engagements with the IPCC, which explores the production of democratic knowledge and how such knowledge can be wielded to achieve regional climate justice.

20.2
Val d'Hérens 1950/2050 – A citizen science project for transformation towards sustainability in a mountain valley

Emmanuel Reynard[1,2], Anouk Bonnemains[1,2], Mélanie Clivaz[1,2], Candice Dubath[1,2], Marjolaine Gros-Balthazard[1,2,3], Christophe Lambiel[1,4], Marie Neumann[5], Alexis Metzger[1,2,6], Christophe Randin[1,7,8], Séverine Trouilloud[1,5]

[1] Interdisciplinary Centre for Mountain Research (CIRM), University of Lausanne, Chemin de l'Institut 18, CH-1967 Bramois (emmanuel.reynard@unil.ch)
[2] Institute of Geography and Sustainability (IGD), University of Lausanne, Géopolis, CH-1015 Lausanne
[3] PACTE Laboratory, University Grenoble Alpes, 14 Avenue Marie Reynoard, F-38100 Grenoble
[4] Institute of Earth Surface Dynamics (IDYST), University of Lausanne, Géopolis, CH-1015 Lausanne
[5] Culture and Science Communication Department, University of Lausanne, Amphipôle, CH-1015 Lausanne
[6] Ecole de la nature et du paysage, 9 rue de la chocolaterie, F-41000 Blois
[7] Department of Ecology and Evolution (DEE), University of Lausanne, Biophore, CH-1015 Lausanne
[8] Alpine Centre for Phytogeography (CAP), and Flore-Alpe Alpine Botanical Garden, Route de l'Adray 27, CH-1938 Champex-Lac

Sustainable development seeks on the one hand to balance the environmental, economic and social dynamics of a territory and on the other hand to preserve good livelihood conditions for future generations. Citizen science can both contribute to the sustainability and transformation of society by involving the inhabitants in the co-production of knowledge (Pettibone et al., 2018; Fraisl et al., 2020; Sauermann et al., 2020; Moczek et al., 2021) and as a tool to promote the public understanding of science in general (Strasser et al., 2019) and drivers and impacts of ongoing global changes in particular.

To address these two dimensions of sustainability – the balance between economic development and environmental protection, involving society, and the intergenerational dimension – the citizen science project "Val d'Hérens 1950/2050 – Lives, images and practices of a changing territory" was set up by the University of Lausanne in the Hérens valley (Valais, Switzerland).

The project – carried out jointly by the Interdisciplinary Centre for Mountain Research (CIRM) and the Culture and Science Communication Department (SCMS) of the University of Lausanne – combines participatory research, scientific outreach activities and artistic approaches. It is currently taking place over two years (2021 and 2022) and involves several research teams as well as inhabitants of the valley. The general objective is to answer the question: what are the challenges of living in the mountains in a context of global changes?

The research teams, involved in the project following an internal CIRM call, are working on nine thematics: the evolution and perception of landscapes, soundscapes, socio-economic development, the impacts of climate change on mountaineering, on the forest boundaries or on heritage plants, climatic perceptions, as well as hunting and dog-sledding practices. Regarding the timescale, the project is structured around three periods: (i) Past – collecting and sharing the living history of the valley; (ii) Present – establishing shared diagnoses (with the population) and (iii) Future – imagining and projecting possible futures.

This poster presents the first results of four thematic axes. It focuses on the contributions and difficulties of participatory approaches to research on sustainability in the mountains and on serendipity (i.e. the ability to exploit the unexpected), as a mean of stimulating creative and transforming citizen science (Otero et al., 2020).

REFERENCES

Fraisl, D., Campbell, J., See, L. et al. 2020: Mapping citizen science contributions to the UN sustainable development goals. Sustainability Science, 15, 1735-1751.

Moczek, N., Voigt-Heucke, S.L., Mortega, K.G. et al. 2021: Self-assessment of European citizen science projects on their contribution to the UN Sustainable Development Goals (SDGs), Sustainability, 13, 1774.

Otero, I., Darbellay, F., Reynard E. et al. 2020: Designing inter- and transdisciplinary research on mountains: What place for the unexpected?, Mountain Research and Development 40(4), D10-D20,

Pettibone, L., Blättel-Mink, B., Balázs, B. et al. 2018: Transdisciplinary sustainability research and citizen science: Options for mutual learning, GAIA, 27(2), 222-225.

Sauermann, H., Vohland, K., Antoniou, V. et al. 2020: Citizen science and sustainability transitions, Research Policy, 49(5), 103978.

Strasser, B.J., Baudry, J., Mahr, D. et al. 2019: "Citizen Science"? Rethinking Science and Public Participation, Science & Technology Studies, 32(2), 52-76.

20.3
Forest conversion in mountains and changes of socio-ecological systems: Perception of indigenous communities

Dhanya Vijayan[1], Anu Susan Sam[2], Harald Kaechele[1,3], Renoy Girindran[4]

[1] *Sustainable Land Use in Developing Countries, Leibniz Centre for Agricultural Landscape Research (ZALF), 15374-Müncheberg, Germany (Dhanya.Vijayan@Zalf.de)*
[2] *Kerala Agricultural University, Regional Agricultural Research Station, Kumarakom, Kerala, India*
[3] *University of Applied Science Eberswalde, 16225-Eberswalde, Germany*
[4] *School of Geography, University of Nottingham, Nottingham NG7 2RD, United Kingdom*

Large scale conversion of natural forests to forest plantations is a global challenge. Forest conversions have much larger implications on the interactions between forests and forest dependent populations. Many communities depend on natural forests for their life and livelihoods. For these communities, natural forests are not just a mere source of income, but these forest resource systems also shape their lives (Vijayan et al. 2021). In order to balance the ecological functions of forests and requirements of indigenous communities, it is essential to understand the complex interaction between the natural habitats and forest dependent communities and how this interaction changes with forest conversions. The long-standing relationships of indigenous communities with their surrounding environments and the holistic knowledge accumulated by them for centuries to govern social-ecological systems (SES) can help to better understand the changes occurred to SES in relation to forest conversions. In case of reserved and protected forests managed by the government, most of the rights and ownership of the forests lies with the government. The government policies determine how the forest land is being managed that includes the rights of indigenous communities. Understanding of changes in SES within government managed forest lands are important for improving the forest management practices as well as in ensuring the cultural and livelihood securities of forest dependent populations.

Based on two case studies from Western Ghats in India, we demonstrate how indigenous knowledge can be used to identify the changes in SES in relation to forest conversions. Our case studies constituted two indigenous settlements from *'Malapandaram'* communities located within the government managed reserved forest. The SES framework developed by Ostrom (2009) is used to identify the SES variables within the government managed forest ecosystem. This framework permits the integration of data from disciplines, and thus provides a clear understanding about the dynamics and inferences of social-ecological interactions (Leslie et al. 2015). Our results show that indigenous communities are able to identify the SES and the changes happened to them. Furthermore, our study also shows that indigenous communities who live within the forests largely follow their own informal rules and norms regarding their access and use of forest resources. Due to this they possess distinct and unique knowledge in identifying SES variables. However, currently these knowledge systems are affected by forest changes and government policies. Though it is evident that their knowledge can be utilised for sustainable forest management, it is also important to understand that the loss of indigenous knowledge may restrict the usage of the same. Thereby, this issue is not just of managing forest systems in a sustainable way, but it also points towards the significance of protecting the forest systems to preserve indigenous socio-ecological knowledge. Hence, our study highlights the importance of incorporating the local indigenous socio-ecological knowledge in government-led forest management programmes and the challenges associated with the same.

REFERENCES

Leslie, H. M., X. Basurto, M. Nenadovic, L. Sievanen, K. C. Cavanaugh, J. J. Cota-Nieto, B. E. Erismang, E. Finkbeiner, G. Hinojosa-Arango, M. Moreno-Báez, S. Nagavarapu, S. M. W. Reddy, A. Sánchez-Rodríguez, K. Siegel, J. J. UlibarriaValenzuela, A. H. Weaver, and O. burto-Oropeza. 2015. Operationalizing the social-ecological systems framework to assess sustainability. Proceedings of the National Academy of Sciences 112(19):5979–5984. http://dx.doi.org/10.1073/pnas.1414640112

Ostrom, E. 2009. A general framework for analysing sustainability of social-ecological systems. Science 325 (5939):419–422. http://dx.doi.org/10.1126/science.1172133

Vijayan, D, Kaechele, H., Girindran, R., Chattopadhyay, S., Lukas, M. C., Arshad, M. 2021.Tropical forest conversion and its impact on indigenous communities Mapping forest loss and shrinking gathering grounds in the Western Ghats, India, Land Use Policy, 102, 105133, https://doi.org/10.1016/j.landusepol.2020.105133.

21. Human Geographies: Materials, Natures, Politics

Rony Emmenegger

Swiss Association for Geography (ASG)

TALKS:

21.1 Rony Emmenegger: The geo/politics of public controversies about geoscience projects in the geological underground. Towards an interdisciplinary research agenda. (abstract)

21.2 Jean Chamel: Ethnographying the Rearrangements of Sensitive, Ritualized and Aesthetic Relationships with the High Alpine Mountains. (abstract)

21.3 Rémi Willemin: Inferring watercourse assessment categories, detrimental practices and ecosystem services from Swiss Jura farmers' perceptions of waterscape quality with photo-response. (abstract)

21.4 Sandro Loi: Actualism, denial of coevalness and geographical living fossils: social and spatial issues of geology. (abstract)

21.5 Marina Cracco: How do Swiss residents value nature's contributions to people? Preliminary results. (abstract)

21.6 Ian Florin: Programming rural partners to implement sustainability in Europe: what benefits communities are expected to draw from a large-scale conservation and development initiative and how they deal with it. (abstract)

21.7 Timo Oliveri, Annina Michel: Assessing perceptions and societal values of landscapes with go-along interviews. (abstract)

21.8 Armelle Choplin: CONCRETE CITY: Material flows and urban making in Africa. (abstract)

21.9 Roland Cochard: Land cover changes (~forest transition) over fifty years (1968-2019) in Thua Thien Hue Province, Vietnam: Illustrations and insights on aspects of 'sustainability'. (abstract)

21.10 Nguyen Thi Hai Van: New Forests, New People in the 'landscape of transition'? Environmental Subject and Identity in the contemporary Uplands of Vietnam. (abstract)

21.11 Christian Kull: In what sense may a 'forest transition' be a 'transition to sustainability', or rather not? Reflections with reference to socio-ecological changes in Central Vietnam. (abstract)

21.12 Alexander Vorbrugg: Russia's New Forests. Envisioning Sustainable Development through Forest Transitions? (abstract)

21.13 Stephan Rist, Susan Thieme, Alexander Vorbrugg: CRITICAL SUSTAINABILITY STUDIES IN (RESEARCH) PRACTICE (abstract)

21.1

The geo/politics of public controversies about geoscience projects in the geological underground. Towards an interdisciplinary research agenda.

By Rony Emmenegger

Public controversies about geoscience projects in the geological underground are shaped by a fundamental dilemma: The geological underground is literally “underground” and therefore shielded off from human observation and experience. In such a context, the public inevitably has to rely on geoscience and geoscience knowledge for “knowing” about what lies beyond the surface. Despite the ever more sophisticated scientific techniques to represent and model dynamics in the underground at ever greater depth, geoscience projects have been object of intense public contestations. In this paper, I argue, that public controversies accompanying geoscience projects need to be understood in a broad context of the shifting relation between “the social” and “the geos”. To substantiate this argument, I build on an emerging body of literature in political geology and the “geological turn” in order to outline different ways of how the relation between the social and the geological can be conceptually captured. I do so by outlining different constellations in which the geos can comes to “matter” in political processes and governance at the surface, with the geos (1) conditioning political actions, thought and authority, (2) being enacted in onto/political negotiations, or (3) engaging actively in geo/politics as an agent or power. Taking seriously such constellations is thus of key significance for the social science analysis of public controversies about geoscience projects. It requires essentially, as I suggest, an an interdisciplinary proceeding.

21.2

Ethnographying the Rearrangements of Sensitive, Ritualized and Aesthetic Relationships with the High Alpine Mountains

Jean Chamel

Rachel Carson Center for Environment and Society, LMU, Munich &
Institut de Géographie et Durabilité, Université de Lausanne, CH-1015 Lausanne (jean.chamel@unil.ch)

As a result of global warming, glaciers retreat is accelerating and rocks collapses are multiplying in the high mountains (Sommer et al. 2020; Adler et al. 2019). This geological collapse is disrupting the Alpine landscape and leading to another collapse, that of the perception of these mountains (Reichler 2020a; 2020b). At the same time, other forms of relationship to them, such as the recent funeral ceremonies for vanishing glaciers, are emerging.

The overall objective of the research project I am just starting is to study these socio-cultural transformations, which are still little known and which concern the imaginary, emotions, aesthetics, and sensitive and ritualised practices in the face of these collapses. It aims to ethnograph situations of "concrete collapsology" and interactions with "Earth Beings" (Cadena 2015) of the people who share a sensitive and affective relationship with the mountains of the Mont Blanc range and the Valais Alps: guides, crystal diggers, glaciologists, mountaineers, huts keepers, photographers, artists, etc.
The project pursues the following three specific goals:

1 Mapping these mountain practitioners' networks and collecting and analysing their discourses around their relationships to the high mountains, with a particular attention to the expressions of feelings of loss, sadness, but also to the ways of overcoming this "mourning" by developing new forms of interrelationships with the mountain, with specific places/beings.
2 Observing concrete situations of interactions with specific entities such as glaciers and documenting the processes of ritual innovation related to them, through a sensitive ethnography of interactions and rituals, as well as eco-therapeutic practices.
3 Documenting the transformations of the aesthetic perceptions of a mountain which is disintegrating within the same milieu, from the construction of their judgement of beauty to the feelings experienced (a new form of sublime?) in the face of the changes observed (see for instance Figure 1).

Preliminary outcomes show that perceptions and reactions are not uniform: while some persons are touched by what is lost, draw direct links with a perspective of societal collapse and emphasize the negative consequences of climate and landscape changes, others tend to focus more on adaptation, in terms of practice but also of perception and relationship. The modernist divide between the humans and their environment can then give place to other entanglements with the mountains, with for instance more direct relationships that can be related to animism.
Time scales is also a crucial issue, with huge differences of perspectives when timeframes are considered at geological, humanity or individual levels.

REFERENCES

Adler, Carolina, Christian Huggel, Ben Orlove, and Anne Nolin. 2019. « Climate Change in the Mountain Cryosphere: Impacts and Responses ». Regional Environmental Change 19 (5): 1225-28. https://doi.org/10.1007/s10113-019-01507-6.

Cadena, Marisol de la. 2015. Earth Beings: Ecologies of Practice across Andean Worlds. Durham: Duke University Press Books.

Reichler, Claude. 2020a. « Glaciers fantômes. Les glaciers valaisans dans trois ensembles de photographies artistiques ». Édité par Emmanuel Reynard, Alain Dubois, et Muriel Borgeat-Theler. Le Rhône. Territoire, ressource et culture, Cahiers de Vallesia, , no 33: 327-40.

———. 2020b. « Le paysage des Alpes, de la splendeur à la finitude ». In Effondrement des Alpes - Premier journal, Mabe Bethônico, Camille Garnier, Stéphane Sauzedde, and Emilie-Cerise Pelloux (eds.), 27-30. Annecy: ESAAA éditions.

Sommer, Christian, Philipp Malz, Thorsten C. Seehaus, Stefan Lippl, Michael Zemp, and Matthias H. Braun. 2020. « Rapid Glacier Retreat and Downwasting throughout the European Alps in the Early 21st Century ». Nature Communications 11 (1): 3209. https://doi.org/10.1038/s41467-020-16818-0.

Figure 1. © Laurence Piaget-Dubuis (2014). Le couple (Agonie d'un glacier). Glacier of Rhône. www.matterofchange.org.

21.3
Inferring watercourse assessment categories, detrimental practices and ecosystem services from Swiss Jura farmers' perceptions of waterscape quality with Photo-response

Rémi Willemin

Department of Geography, University of Zurich, Winterthurerstrasse 190, 8057 Zürich (remi.willemin@geo.uzh.ch)

Inspired by the Manifesto for Practice of the materiality/visuality approach (Rose and Tolia-Kelly 2012), our photo-response project (Alam, McGregor, and Houston 2018) looks at and co-developed perceptions of practices impacting the water quality in the Swiss Jura. Farmers and beekeepers captured waterscapes that best depict their relationships to water. On the basis of their photography, we explore how water, detrimental practices and social activities interact and co-create waterscapes. We code our discussions on water according to four categories of watercourse assessment: ecomorphology, biology, chemistry and hydrology. Likewise, we assume that our discussions on practices that can affect water and ecosystems reflect concerns over detrimental practices. Finally, our discussions on social activities can be interpreted in a broad sense as ecosystems services (Berbés-Blázquez 2011). By conceptualizing our object of research, waterscape, as hydro, chemo and social components, we address both positive aspects of waterscapes and concerns and threats upon them. This alternative approach of assessing social values of 'landscapes' and 'nature' triggers methodological questioning: *how and what can we learn from perceptions of social values of waterscape (unseen) quality through visual methods?*

REFERENCES

Alam, A., McGregor, A. & Houston, D. 2018. Photo-Response: Approaching Participatory Photography as a More-than-Human Research Method. Area. 50(2), 256–265. https://doi.org/10.1111/area.12368.

Berbés-Blázquez, M. 2011. A Participatory Assessment of Ecosystem Services and Human Wellbeing in Rural Costa Rica Using Photo-Voice. Env. Manag., 49(4), 862–875. https://doi.org/10.1007/s00267-012-9822-9.

Rose, G. & Tolia-Kelly, D. P. 2012. Visuality/Materiality: Images, Objects and Practices. Farnham: Asghate Publishing Limited.

21.4
Actualism, denial of coevalness and geographical living fossils: social and spatial issues of geology

Sandro Loi

Département de géographie et environnement, University of Geneva, Boulevard Carl-Vogt 66, CH-1205 Geneva (sandro.loi@unige.ch)

Like any other sciences, geology is not neutral. But we usually think about it like an activity of scholars, simply studying the deep time of Earth's history, and analysing rock formations. However, history of the geological discipline itself shows us that this neutrality needs to be examined. In fact, in the past centuries, geology was not alien to colonial enterprise led by european imperialism : some rocks, but also some spaces and bodies – black, autochtonous – were exploited and appropriated. They had some properties, and became commodities and properties, like any other mineral ressources. This history, where geology meets slavery and colonialism, remains little discussed, even at a time when environmental issues and debates on the Anthropocene have confronted social sciences with geological narratives (Yusoff 2018).

Nevertheless, following the work of Elizabeth Povinelli, social sciences began focusing on the inert, on the geological world. To really understand the different forms that power could take nowadays, the australian anthropologist invites us to go beyond biopolitics. She tells us how these forms of power can also play on the distinction between life and non life. As a complement to biopower, this *geotopower* was and is crucial in some epistemic and colonial violences indigenous people have suffered and are still suffering (Povinelli 2016). Their universe, their ontologies and their humanity have been denied, relegated to the realm of the non-existent (Santos 2016). They were lifeless and appropriable entities with exploitable properties (Yusoff 2018).

However, if geology, as an activity of knowledge, has shaped our western ways of seeing the world around us, we should be able to deconstruct this *geological gaze*, here in Europe and in Switzerland. My intention is to focus on a very important principle in geology, often implicit in representations of the Earth's history to the public: actualism. This principle makes it possible to explain the geological past from phenomena that we observe today. A very powerful and useful tool in earth sciences, its use is not without posing some epistemological issues (Von Engelhardt & Zimmermann 1988). I think that these issues are not restricted to geology alone, but can also have social and spatial consequences.

Basically, my hypothesis is that the comparison between the present and the past that we wish to explain can, in some cases, freeze spaces and (non-) human populations in a particular space-time, different from that of Western modernity. In doing so, we reproduce a negation of contemporaneity between their spaces, these populations, and our western point of view (Santos 2016, 178). Because a landscape resembles Earth's past, it becomes a kind of geographical living fossil. Therefore, we reproduce a (colonial) spatialization of time, justified by geological knowledge itself (Yusoff 2018).
In recent years, issues of knowledge's and institution's decolonization have reached Switzerland, in human sciences but also in public and politic arenas. Specifically, these issues raised questions about, for example, the conditions in which we acquired some "exotic" objects, in a country without any colonies, or what this could have meant in the construction of the otherness in Switzerland (Étienne 2020). Although these debates are very important, they seem to relate mainly to institutions or museums of ethnography, art, human history and, to a lesser extent, natural history; basically, we are especially interested in everything that resonates with the life – cultural artefacts, human or animal remains, etc. –, while the realm of the non-life – rocks, minerals, fossils – does not appear in the debates. But with the geontological distinction between life and non-life, geology also took part in the construction of otherness (Povinelli 2016; Yusoff 2018). Therefore, through a study of actualism and its temporal and spatial mobilizations, it would be worthwhile to include geological narratives and there representations in these discussions.

REFERENCES

Étienne, N. 2020: Introduction. In: Une Suisse exotique? Regarder l›ailleurs en Suisse au siècle des Lumières (Ed. by Étienne, N. et al.). 7-25. Zurich, Paris, Diaphanes

Povinelli, E. 2016: Geontologies. A Requiem to Late Liberalism. Durham, London, Duke University Press

Santos, B. D. S. 2016: Épistémologies du Sud. Mouvements citoyens et polémique sur la science. Paris, Desclée de Brouwer

Von Engelhardt, W & Zimmermann, J. 1988: Theory of Earth Science. Cambridge, New York, New Rochelle, Melbourne, Sidney, Cambridge University Press

Yusoff, K. 2018: A Billion Black Anthropocenes of None. Minneapolis, University of Minnesota Press

21.5
How do Swiss residents value nature's contributions to people? Preliminary results

Marina Cracco (UNIL), Gretchen Walters (UNIL)

Understanding how different people perceive and value nature is critical for biodiversity conservation and to improve human well-being and good quality of life (GQoL). Because perceptions can influence people's behavior, the analysis of perceptions can shed light on elements that guide conservation action and decision. As part of the "Valuing the ecological infrastructure in Swiss parks" transdisciplinary research project, one of the three sub measures of the Action Plan for the Swiss Biodiversity Strategy, we examine the perceptions of the Swiss population living inside and outside of selected Swiss parks on the value of nature, nature's contributions to people (NCP) and GQoL. We aim to provide inputs on the social benefits and added value of the ecological infrastructure (EI) in Swiss parks of national importance and to contribute to the knowledge base on park research, and EI in Switzerland and internationally. We use a mixed method approach to understand such perceptions and values, with a software (SenseMaker®) that allows the collection of large amounts of data and the analysis of narratives from the study regions. We developed a questionnaire based on literature review and stakeholder workshops. We implemented an online and paper-based survey in French and German from February to April 2021, sent to a representative sample of the population living in the study area. In the questionnaire, we asked respondents a prompting question to encourage them to share an experience they have had with nature in Switzerland. The respondents were then asked questions about their experience, linked to specific NCP and GQoL indicators, placing part of the data interpretation in the hands of the respondent, rather than the researcher, and so reducing bias. Analysis of results reveals trends of what values are present or absent and which NCP are more frequently connected with which experiences. Because the software offers a visually supported analysis, it facilitates the presentation of results to the public and decision makers. Preliminary study results are expected to contribute to the understanding of public opinion and perceptions to inform park management and initiatives for the conservation of the EI.

21.6
Programming rural partners to implement sustainability in Europe: what benefits communities are expected to draw from a large-scale conservation and development initiative and how they deal with it

Ian Florin*

**Institut des Sciences de l'Environnement – Pôle de Gouvernance de l'Environnement et Développement Territorial, Université de Genève, Boulevard Carl Vogt 66, CH-1205 Genève*

Following the recent call of the European commission to widen the union's protected area network in order to contribute to "the good of [the] environment and [the] economy", initiatives simultaneously promoting rural livelihoods and ecological connectivity are set to become important components of policy within the next few years. Using regional working groups of a protected area network from northern Europe as a case studies, this paper investigates the ways in which large-scale conservation frames conservation and development efforts in European rural areas in relation to the benefits that local people can draw from nature.

First, I describe how the promise of a win-win-win scenario for nature, economic growth and local livelihoods – notably via the development of nature-based tourism – is mainstreamed within the initiative. Second, I demonstrate how the local is depicted as *the* level of intervention where organizations and individuals are presented as essential stakeholders, as they are supposedly familiar with project management, regional singularities and European cross-border cooperation funding instruments. Third, I show that the responsibility put on local stakeholders can promote modes of collective action that undermine agency at the grassroots level by by constraining them to take on roles of apolitical service providers or project managers.

These findings provide material for questioning how a seemingly consensual and participatory approach to rural sustainable development built on a *Nature's Contribution to People* type of framework can constrain local actors' agency and decrease the chance of generating collective and durable outcomes.

21.7
Assessing perceptions and societal values of landscapes with go-along interviews

Timo Oliveri (timo.oliveri@geo.uzh.ch) [1]
Annina Michel (annina.michel@geo.uzh.ch) [1, 2]

[1] *Geograifsches Institut, Universität Zürich, Winterthurerstrasse 190, 8057 Zürich*
[2] *University Research Priority Program "Global Change and Biodiversity", University of Zurich, Winterthurerstrasse 190, 8057 Zürich*

This paper reflects on the values and challenges of go-along interviews to assess everyday perceptions and meanings of near-natural landscapes in Switzerland.

A go-along interview is a valuable method to identify environmental and landscape values (see Bergeron et al. 2014). By avoiding an "artificial" or "traditional" interview setting using, for example, decontextualised material such as photographs, the go-along interview is fully emmersed in the landscape and uses mobility to establish in-situ contact with nature and the environment (Evans and Jones 2011).

This study is part of the research project "ValPar.CH – Values of the ecological infrastructure (EI) in Swiss parks", which aims to analyze ecological, economic, and social values of EI using the Nature's Contributions to People (NCP) framework (Reynard, Grêt-Regamey & Keller 2021). In this particular study, go-along interviews are used to assess how stakeholders perceive and evaluate certain NCPs. Interviewees are asked to guide the interviewer to everyday, meaningful places in the (near-natural) landscape. This shifts power relations between interviewer and interviewee, which facilitates in-depth conversations and opens up pathways to engage with emotions and perceptions beyond the visual.This paper therefore shares practical experience gained with data collection on social values of NCPs and discusses the advantages and disadvantages of the method.

Figure 1. GPS-Tracking of a go-aglong interview in Park Beverin, Timo Oliveri

REFERENCES

Bergeron, J., Paquette, S. & Poullaouec-Gonidec, P. 2014: Uncovering landscape values and microgeographies of meanings with the go-along method, Landscape and Urban Planning, 122, 108–121.

Evans, J. & Jones, Ph. 2011: The walking interview: Methodology, mobility and place, Applied Geography 31, 849-858.

Reynard, E., Grêt-Regamey, A. & Keller, R. 2021: The ValPar.CH project – Assessing the added value of ecological infrastructure in Swiss Parks, Management & Policy Issues, 13(2), 65-68.

21.8
Concrete City: Material flows and Urban making in Africa

Armelle Choplin

[1] *Associate Professor, University of Geneva, Departement of Geography and Environment & Global Studies Institute, (armelle.choplin@unige.ch)*

Africa is experiencing rapid urban growth resulting in a spread of `concrete cities'. Concrete has become the symbol of the frenetic urbanization, construction boom and capitalistic emergence of the continent. Drawing from my book *Matière Grise de l'Urbain, La vie du ciment en Afrique* (2020, MétisPresses), forthcoming in English, *Concrete City, Material flows and urban making in Africa* (2021, Wiley), this presentation offers a contribution to understanding African cities through their materiality and the lens of concrete, a global commodity with local impacts. Concrete is both a material and a conceptual "binder" for analyzing city-making across political, economic, social and environmental perspectives.

In combining an ethnography of building practices with a politico-economic analysis of the concrete chain, my presentation aims to decipher the politics of concrete which accompany the 'Rising Africa' discourses. It analyses the construction boom and its actors shaping African cities. It deciphers the social values and imaginaries linked to the building cultures and dwelling practices. It finally addresses debates and controversies on concrete and its environmental impact, and explores sustainable alternatives for rethinking cities.

By following material flows, primarily bags of cement, from the quarry to the plot of land, from the cement tycoons to the dwellers and builders, I propose an exploration of the West African urban corridor linking Abidjan, Accra, Lomé, Cotonou and Lagos. Drawing on long-term fieldwork, it examines Africa's largest mega-city under construction: over 40 million people live, travel, consume and build… with concrete.

This exploration of the life of concrete in Africa reveals that it is not an inert but an active material, at the heart of urban metabolism and experiences. By drawing parallels between African and European (Swiss) situation regarding the construction sector and built environment, this presentation invites to rethink the links between materiality, (non)human and urban futures.

21.9
Land cover changes (~forest transition) over fifty years (1968-2019) in Thua Thien Hue Province, Vietnam: Illustrations and insights on aspects of 'sustainability'

Roland Cochard[1]

[1]*Institute of Geography and Sustainability (IGD), Université de Lausanne, 1015 Lausanne*

Vietnam has been noted as the first country in Southeast Asia which has gone through a 'forest transition' (FT), with allusions of an associated 'successful transition' towards 'sustainable forest management'. In this presentation we take a close look at the forest cover (and other land cover) changes in the Central Vietnamese province of Thua Thien Hue (TTH). Based on this case study we query some of the inherent assumptions in general FT theorizing, such as 1.) a 'conventional' pattern of pre-industrial forest degradation, 2.) pure economic drivers of 'modernization', and 3.) verifiable 'forest regrowth' as an actual 'event'. With respect to point 1: Many open spaces of 'forestlands' (i.e. open/destroyed/degraded forest *alias* 'wasteland') already existed in TTH before 1968, were further created through massive war effects until 1975 (e.g. air strikes and arboricides such as Agent Orange), and were consolidated through resource extraction (mainly intensive logging and local land clearing) during the immediate post-war era (~1975-1990). With regard to point 2: Indigenous communities which had lived in the forest valleys of upland TTH within – historically – relatively stable land use systems were severely affected by the war as well as by post-war political restructuring, state-defined re-territorialization, and economic development. Since the 1990s many communities were resettled from remote areas, i.e. areas which were subsequently 'developed' for hydro-electricity production and for 'nature conservation' (~tourism). As for point 3: What is actually a 'forest' or 'reforestation'? Since the 1990s so-called 'forest regrowth' mainly happened via the widespread development of acacia plantations in various forms (i.e. 'production forests' and 'protection forests'). The tropical natural forest can hardly be said to 'regrow' in ways as is usually implied in somewhat 'euro-centric' FT theorizing. We conclude the presentation with an overview of land cover changes and some considerations on various aspects of 'sustainability' (cf. companion presentation).

Keywords: deforestation and forest degradation, Agent Orange, swidden systems, acacia plantations, afforestation, social-encological resilience

21.10
New Forests, New People in the 'landscape of transition'? Environmental Subject and Identity in the contemporary Uplands of Vietnam

Nguyen Thi Hai Van[1]

[1]*Institute of Geography and Sustainability (IGD), Université de Lausanne, 1015 Lausanne*

Vietnam's Upland Forests are in transition. Underneath the superficial smooth curve of forest cover statistics, complex transitions have been taking place. These are a longer-term outcome of state policies and interventions to transform upland forests into ideal subjects. I ask how do uplanders, whose culture was traditionally based on shifting cultivation and hunting, deal with these changes? On the basis of ethnographic fieldwork in the uplands of Central Vietnam, I show that successive state interventions have established a system of strict rules on protecting forests, banned and transformed local forest practices, but also provided lucrative opportunities from both commercial tree plantations and forest protection for local villagers. The villagers have been enrolled actively in the state-making processes and adopted new forest management attitudes and behaviors. However, beyond 'finding a way to live', individual aspirations towards modernity, and the pride of the ethnic identity have inspired local villagers to form new forest livelihood patterns and gradually become the 'new forest people'. By bringing the aspect of culture and identity into the debate of 'environmentality' (Agrawal, 2005), this paper discovers how the new 'environmental subjects' with their own environmental subjectivities have emerged. It also investigates the vulnerabilities and resilience capacities of local people in the face of dynamic changes. This piece, therefore, hopes to contribute to a fuller picture of the making of a forest transition in practice.

Keywords: environmentality, environmental rule, agrarian change, livelihood strategies, Uplands, Vietnam.

21.11
In what sense may a ‘forest transition’ be a ‘transition to sustainability’, or rather not? Reflections with reference to socio-ecological changes in Central Vietnam

Roland Cochard[1], Nguyen Thi Hai Van[1], Christian Kull[1]

[1]*Institute of Geography and Sustainability (IGD), Université de Lausanne, 1015 Lausanne*

A ‘forest transition’ (FT, *sensu* Mather 1992) is an incisive turn-over from deforestation to forest regrowth within a specific territory, as captured in graphs by a U-shaped curve. FTs have initially been described mainly from historic case studies of European or other northern countries, with literature often equating FTs with a ‘transition to sustainability’. The situation (ecological, social, political, historic) in southern countries differs in various respects. Both, ‘concepts’ of FT and sustainability, take multiple forms and flavours, i.e. forms which may be more convenient for ‘green marketing’ rather than genuine/tangible assessment of environmental changes. Referring to the case of Thua Thien Hue province (TTH) in Central Vietnam, we present several observations and discuss their meaning/relevance with regard to cornerstones of ‘sustainable development’ (as specified in the UN Sustainable Development Goals). 1.) In TTH so-called ‘reforestation’ largely comes in the form of acacia plantation mono-cultures (plus some spontaneous woody regrowth). The acacia boom currently significantly contributes to economic growth, thereby supporting a wood industry that provides jobs and incomes for many people. Will this industry be stable or follow a boom-and-bust pattern? 2.) An FT such as in TTH also implies some sort of ‘transition’ of livelihoods and cultures of so-called ‘forest people’. How does this transition take place; who profits who loses in terms of land assets, stable/resilient livelihoods, and job opportunities? What does the transition imply in terms of cultural adaptation and traditional knowledge? What does it imply in terms of spaces/impetus for local farm-based innovation and economic/sustainable creativity, including adaptiveness. 3.) A ‘bifurcation of forest spaces’ (quasi-agricultural tree plantations as one branch, and remaining ‘natural forestlands’ as another) implies new landscape dynamics with associated sustainability-relevant questions. How have the parameters of ecosystem services shifted under a binary FT? Will forest biodiversity remain stable or further decline? Will the forest cover be stable and maintain critical functions of soil protection, water provisioning (during droughts), and disaster mitigation (e.g. floods, landslides during storms, forest pathogen and pest species outbreaks, etc.)?

Keywords: reforestation, Sustainable Development Goals, land use change, livelihoods, cultural transformation, social-ecological resilience

REFERENCE:

Mather AS (1992). The forest transition. *Area* 24(4): 367-379.

21.12
Russia's New Forests. Envisioning Sustainable Development through Forest Transitions?

Alexander Vorbrugg, University of Bern

Trees have regrown on dozens of million hectares of abandoned farmland in Russia over the past decades. So far, their status has remained largely informal which has limited their commercial use but also forced rural dwellers to burn succession vegetation to avoid being fined. Recent propositions to formalize forests and forestry on abandoned farmland spurred legislatorial processes and political controversies. Thus, besides a large scale but unplanned and unstable forest transition over the past decades, there now are plans and propositions to actively develop "new forests" on abandoned farmland.

After introducing some characteristics and implications of the 'informal' forest transition to date, I will discuss how far and how "new forests" have become vehicles and projects to envision new 'sustainable' future pathways in Russia. Firstly, I show how certain "new forest" models go along with a reframing of abandoned farmland, long associated with loss and degradation, as part of a future-oriented vision with ecological, social and economic benefits. Secondly, I introduce some of the concrete plans and steps to realize "new forests" as well as controversies about them. Thirdly, I discuss some of their (potentially) problematic implications such as the bracketing of local perceptions and needs, or companies' rising interest in reforestation as a means to 'offset' or rather 'greenwash' their emission-intensive businesses. Taken together, this makes graspable different transition options for forests on abandoned farmland that differ substantially in terms of their sustainability.

21.13
Exchange: Critical Sustainability Studies in (research) practice

Stephan Rist, Susan Thieme, Alexander Vorbrugg (Bern)

Sustainability has become a buzzword across many societal domains including academia. Different positions and approaches are assembled under this umbrella, which is perceived both as a strength and a problem: It bears the promise to step outside of thematic and disciplinary silos to collectively address planetary challenges but also the risk of losing the "critical edge" necessary to envision and fight for the substantive transformations needed to reach sustainability. We invite colleagues to join a conversation about the possibilities and risks that go along with the continuing institutionalisation and mainstreaming of sustainability studies in academia, and your suggestions for putting critical sustainability principles into practice in collaborative (research) projects, and politics within and outside of the academy.

Brief panel inputs will be followed by an open discussion. Questions for discussion may include:

- Is sustainability's "critical edge" equivalent to the integration of established critical theories (political economy/ ecology, feminist and postcolonial theories etc.) or are there further important standards for critical sustainability studies?
- How do and can we translate visions for sustainability into everyday practices including research and activism? How do your projects provide grounds for crucial collaborations within academia and beyond?
- How do you bring together broad and sometimes vague sustainability frameworks, specific research topics and concrete strategies of radical societal transformation?
- What are the possibilities and risks that go along with the institutionalization and mainstreaming of sustainability studies? How to deal with the concurrent mainstreaming of sustainability studies on the one hand, and increasing attacks on many other critical and radical traditions on the other?

Panelists:
Deniz Ay (Bern)
Basil Bornemann, Marius Christen, Rony Emmenegger (Basel)
Christian Kull (Lausanne)

22. Human Geographies: Bodies, Cultures, Societies

Karine Duplan, Irène Hirt

Swiss Association for Geography (ASG)

TALKS:

22.1 Morgane Rudaz (University of Geneva): “You cut us off, we paste it!” Exploring the militant strategy employed by the Collages Féministes in public spaces. (abstract)

22.2 Claske Dijkema (Swisspeace & University of Basel): Urban violence in France as body politics. (abstract)

22.3 Raghad Saqfalhait (independant resesarcher, Ramallah) & Clémence Vendryes (IREMAM & IFPO): How can a dead body claim ownership over a land ? (abstract)

22.4 Armelle Choplin: CONCRETE CITY: Material flows and urban making in Africa. (abstract)

22.5 Christine Bichsel (University of Fribourg): Split Spaces and Warped Borders: The Geometry of Power in China Miéville’s The City & The City (2009). (abstract)

22.6 Robert A Saunders (State University of New York),: (Be)longing to/for the Past: Negotiations of Time, Space, and Identity in Beforeigners (2019-). (abstract)

22.7 Jueling Hu (University of Fribourg): Between mechanical and human bodies: Producing Erica in glitches. (abstract)

22.8 Lorenzo Andolfatto (University of Fribourg): Waste Tides and Capital Flows in Chen Qiufan’s The Waste Tide and Wu Ming-yi’s The Man with Compound Eyes. (abstract)

22.1
"You cut us off, we paste it!" Exploring the militant strategy employed by the *Collages Féministes* in public spaces

Morgane Rudaz[1]

[1] *Institute of Gender Studies, Institute of Environmental Governance and Territorial Development, University of Geneva, Boulevard du Pont-d'Arve 40, CH-1205 Geneva*

Drawing on the geographical literature on public spaces and feminist activism, this research provides a critical spatial analysis of the particular form of feminist activism associated with the movement of the *Collages Féministes*, also known as the *Collages Féminicides*. Started in Marseille and Paris in early 2019 as a way to raise awareness about femicides, the movement soon expanded to other Francophone cities and progressively addressed other feminist issues.

This research seeks to investigate the multiple ways in which feminist activists use the visual militant tactic of pasting slogans on street walls, buildings, and monuments in order to denounce gender-based violence and provide support to gender minorities. While focusing specifically on the activists' perspectives in regard to their militant practices, this research aims to explore how the activists engage with, relate to, and use their activism in public spaces.

Through the visual analysis of two Instagram accounts dedicated to the *Collages Féministes* in Geneva, and a textual analysis of four semi-structured interviews conducted with feminist activists pasting in Geneva, this research examines how the activists perform their activism, what their motivations for their activism are, and what this particular form of activism allow them to achieve. It is argued that putting centre stage the activists' perspectives on their activism is critical to the development of a complex understanding of any form of militant practices. Finally, a few areas for further research on the spatial militant phenomenon of the *Collages Féministes* are proposed.

22.2
Urban violence in France as body politics

Claske Dijkema[1]

swisspeace, University of Basel, Steinengraben 22, CH-4051 Basel (claske.dijkema@unibas.ch)

This contribution approaches urban violence, which in this context mainly means setting objects on fire and thereby provoking police intervention and altercation, as a form of self-defense by the subaltern that uses the body rather than words to make a statement. I draw on Dorlin (2017) to explain that if the subalterns are not considered worth defending by those in power, physical violence is one of the few tools they have left to defend their dignity. Youth turn the hypervisibilisation of urban violence by mainstream media into a means to publicize their anger. They choose fire as a means of public address, not because of their incapacity to speak but because of their refusal of interlocution. If one has the feeling that one is not heard, violence -in this case setting objects on fire- can become a viable option. While the established may well require that post-colonial immigrants and inhabitants of marginalised neighbourhoods ask for their rights politely and patiently wait for their demands to be taken into account, eruptions of violence are only to be expected if the established are perceived to be unwilling to listen and refuse to recognize the subaltern as legitimate political adversaries. The riots that took place in Grenoble in 2010 serve as empirical grounding of this argument.

REFERENCES

Dorlin, E. 2017: *Se Défendre: Une Philosophie de La Violence*. Paris: Zones.

22.3
How can a dead body claim ownership over a land ?

Raghad Saqfalhait[1], Clémence Vendryes[2]

[1] *Architect and researcher based in Ramallah, Palestine (saqfalheit.raghad@gmail.com)*
[2] *IREMAM, Université d'Aix-Marseille and IFPO, based in Jerusalem (clemence@vendryes.fr)*

In a context like Palestine, where an apartheid system is ethnically cleansing indigenous people, evicting them from their homes, and confiscating their lands, the act of existing by itself becomes an act of protest (Mbembe, 2003, Butler, 2004). Is dying the opposite of existing? In this paper we argue that it isn't; it gives birth to new models of protest beyond the conventional. Palestinian bodies laying in the ground are examples of a tenacious collective meaning and value (Bayart and Warnier, 2004); an epitaph is like an identity card (Turnbull, 2002) and the grave produces a sense of belonging.
As the West Bank has been administratively divided in three different areas of A, B, and C since Oslo accords in 1993, graveyards have been acting as tools for Palestinians to assert sovereignty in area A but also to claim land in area C where the land is frozen until new Israeli settlements are built. Graves are structures that expand slowly but steadily (Ard, 2008), outpacing the battle against time, and grounding their roots deep down where they stand; all of which are active agents against a colonial regime. At the crossroads of architecture and human geography, we wish to analyse these structures through bodily relationship between Palestinians and their land :

1. Sovereignty of the body : zone A (Beit Sahour)
2. Claiming palestinian land : building a cemetery in zone C (Al-Bireh, Kufr Aqab)
3. Towards the future cemetery «A project: Scales of Integration: The Body, the Cemetery, and the Terrain».

REFERENCES

Ard K. J., (2008), The Reconstructed Cemetery: An Architectural Seam, p. 17-24
Bayart J.-F. Et Warnier J.-P. (dir.), (2004), Matière à politique. Le pouvoir, les corps et les choses, Paris, Karthala, 256 p.
Butler J., (2004), Precarious Life: The Powers of Mourning and Violence, Verso Books, 168 p.
Mbembe A., (2003), « Necropolitics », Public Culture 15 (1), Duke University Press, p. 11-40
Leshem N., (2015), « Over our dead bodies », (2015), Political Geography, n°45, Elsevier, p. 34-44
Turnbull P., (2002), « Indigenous Australian people, their defence of the dead and native title » in C. Fforde C., Hubert J., & Turnbull P. (dir.), The dead and their possessions : Repatriation in principle, policy, and practice, New York, USA, Routledge, p. 63-86

22.4
Concrete City: Material flows and Urban making in Africa

Armelle Choplin

[1] *Associate Professor, University of Geneva, Departement of Geography and Environment & Global Studies Institute, (armelle.choplin@unige.ch)*

Africa is experiencing rapid urban growth resulting in a spread of `concrete cities'. Concrete has become the symbol of the frenetic urbanization, construction boom and capitalistic emergence of the continent. Drawing from my book *Matière Grise de l'Urbain, La vie du ciment en Afrique* (2020, MétisPresses), forthcoming in English, *Concrete City, Material flows and urban making in Africa* (2021, Wiley), this presentation offers a contribution to understanding African cities through their materiality and the lens of concrete, a global commodity with local impacts. Concrete is both a material and a conceptual "binder" for analyzing city-making across political, economic, social and environmental perspectives.

In combining an ethnography of building practices with a politico-economic analysis of the concrete chain, my presentation aims to decipher the politics of concrete which accompany the 'Rising Africa' discourses. It analyses the construction boom and its actors shaping African cities. It deciphers the social values and imaginaries linked to the building cultures and dwelling practices. It finally addresses debates and controversies on concrete and its environmental impact, and explores sustainable alternatives for rethinking cities.

By following material flows, primarily bags of cement, from the quarry to the plot of land, from the cement tycoons to the dwellers and builders, I propose an exploration of the West African urban corridor linking Abidjan, Accra, Lomé, Cotonou and Lagos. Drawing on long-term fieldwork, it examines Africa's largest mega-city under construction: over 40 million people live, travel, consume and build… with concrete.

This exploration of the life of concrete in Africa reveals that it is not an inert but an active material, at the heart of urban metabolism and experiences. By drawing parallels between African and European (Swiss) situation regarding the construction sector and built environment, this presentation invites to rethink the links between materiality, (non)human and urban futures.

22.5
Split Spaces and Warped Borders: The Geometry of Power in China Miéville's *The City & The City* (2009)

Christine Bichsel[1]

[1] *Department of Geosciences, Geography Unit, Chemin du Musé 4, 1700 Fribourg (christine.bichsel@unifr.ch)*

China Miéville's weird crime fiction *The City & The City* (2009) tells the story of a murder and its pursuit by a detective across two cities. Beszel and Ul-Qoma are twin cities unlike others; they are not coterminous, but fully overlap in their spatial extension. In other words, they occupy exactly the same geographical space. However, political discourses and everyday practices continuously reproduce the separation of this space into two co-existing urban entities, and even two different states. *The City & The City* challenges a basic assumption in international relations and political geography: the mutual exclusivity of state territory. In Westphalian tradition, state territory can be exchanged, grow or shrink due to environmental processes, or be contested, but it cannot be shared. In this paper, I examine Miéville's literary universe for the conditions and operations that enable the sovereignty of Besźel and Ul-Qoma despite their overlapping spatial extent of state power. To this aim, I draw on Michel Foucault's concept of disciplinary power with a focus on regimes of visuality and subjectivity. I argue that Miéville's novel is timely and relevant for contemporary geopolitics. Currently, we are witnessing spectacular border reinforcements through the building of walls and fences supported by drones, cameras and "sound cannons". Miéville's novel refocuses our attention to the subtler mechanisms of bordering at play. Such mechanisms provide the foundations for this spectacular politics, both preceding and reinforcing it.

22.6
(Be)longing to/for the Past: Negotiations of Time, Space, and Identity in *Beforeigners* (2019-)

Robert A Saunders

State University of New York (SUNY), 2350 Broadhollow Road, Farmingdale, New York 11735 USA (robert.saunders@farmingdale.edu)

While geographers have examined the ways in which films, documentaries, and social media engage with the so-called 'migrant crisis' in Europe, there has been little work on fictional TV series as a force in world-building and place-making against the chimera of 'unchecked migration'. Building on recent research on televisual interventions into the issues of migration, (b)orders, and securitisation, this article interrogates HBO Europe's Norwegian-language sf series *Beforeigners*. With a focus on fantastical constructions of spatiality against temporality, the primary focus of this article is on the ways in which near-future science fiction engages with ontological insecurities around integration, xenophobia, and territorial belonging. This is accomplished by applying analytical tools drawn from the 'temporal turn' in cultural geography which are then applied to a time-travel drama that denies agency to those 'migrants' it screens (while also removing the issue of 'race' from the debate). Recognising television series' contributions to cultural, social, and political transformations that are of geographical significance, this essay seeks to expand and complicate scholarship on the suasive power of migrant representation on the small screen.

REFERENCES

Anderson, Ben. 2019. "Cultural Geography II: The Force of Representations." Progress in Human Geography 43 (6):1120-1132.

May, Vanessa. 2017. "Belonging from Afar: Nostalgia, Time and Memory." Sociological Review 65 (2):401-415.

Žižek, Slavoj. 2015. «The Non-Existence of Norway (On the Refugee Crisis).» London Review of Books 37 (17):no pp.

22.7
Between mechanical and human bodies: Producing Erica in glitches

Jueling Hu[1]

[1] *Department of Geosciences, Geography Unit, Chemin du Musé 4, 1700 Fribourg (jueling.hu@unifr.ch)*

The YouTube channel *Erica Channel* (“エリカちゃんねる” in Japanese) documents a series of “first contacts” between humanoid robot Erica, a new employee in Tokyo Broadcasting System (TBS), and a group of her human colleagues. These audio-visual records capture bodily and sensory experience when the human staffs *feel* intimate with their special colleague Erica. Counterintuitively, while the announcers fascinate how humanoid Erica can be, their feelings of robot anthropomorphization are generated from experiencing Erica’s material features, which identify Erica as a robot – her silicon body, synthesized responses, electronic wires... Namely, humanoid features make the robot *look* like humans; yet it is the gap between humans and the robot that enables Erica to be *perceived* as an alternative intimate subject. In this paper, from a new materialistic perspective, I investigate the technological and material conditions when robot Erica is perceived and acknowledged as a unique subject. I argue that the records from *Erica Channel* challenge the existing theory of robot anthropomorphization, calling for wider understandings of body and subjectivity that transcend the dualist division of subject/object, human/nonhuman. Here, Erica is neither a human substitute nor a machine; rather, she is a mechanically-assembled human-like subject, with whom humans are able to establish intimacy. Erica’s case sheds light on the potential positioning of nonhuman subjects in society: the ways that humans can perceive the physical, cognitive, and emotional closeness of social robots situate in glitches – the subtle but absolute gap between humans and robots.

Keywords: body, subjectivity, social robot, speculative intimacy

22.8
Waste Tides and Capital Flows in Chen Qiufan's *The Waste Tide* and Wu Ming-yi´s *The Man with Compound Eyes*

By Lorenzo Andolfatto (University of Fribourg)

This paper advances a comparative reading of Chen Qiufan's *The Waste Tide* (2013) and Wu Ming-yi's *The Man with Compound Eyes* (2012) as examples of "climate realism" (Kornbluh) in opposition to the genres—respectively science fiction and eco-fantasy parable—to which these texts are conventionally ascribed. In the epilogue of *The Waste Tide*, the protagonist Chen Kaizong sets out to sea to explore a trash island in the Pacific Ocean, where "strange things are happening . . . and perhaps people are living there"; in the opening pages of *The Man with Compound Eyes*, the character of Atile'i fulfills his duty as a second son by sailing away from his tribe's ancestral island, but instead of dying at sea he lands on a similar garbage patch, which becomes his provisional home before it disastrously crashes against the Eastern coast of Taiwan. The former a dystopic, cyberpunk tale about the logistics of e-waste disposal written by a former Google engineer from Guangdong, the latter an "eco-fantasy" novel by a Taiwanese environmental activist and artist, these two novels "explore," as Anna Tsing would have it, "the ruins that have become our collective home." Such ruins engender a shared living space that is defined less by national borders than by maritime (thalassic and pelagic) flows which function as continuous conduits for "the lethal solubilization of capital flow" (Kornbluh) and its trails of debris, ecological destruction, and diasporic existences that mark global late capitalism today. Exploring in fictional terms the webs of life entangling these ruins, these two novels engage with the material aspects of what Lukacs described as the "transcendental homelessness" of our modern condition, updating it to our era of global precarity and dispersion.

23. Human Geographies: Cities, Regions, Economies

Julio Paulos, Sven Daniel Wolfe

Swiss Association for Geography (ASG)

TALKS:

23.1 Dennis Pauschinger *Policing the City: State Violence in the Age of Far-Right Populism and Digitalisation*

23.2 Sven Daniel Wolfe *Imprisoned for a Retweet: More-or-less digital contestation and repression in increasingly authoritarian Russia*

23.3 Mark Maguire and David A. Westbrook *Counterterrorism in the Airport City*

23.4 Alexa Agoropoulos, Ben Hundertmark, Jasper Janssen and Tabea Louis *The Thick Blue Line: The Hashtag thinblueline and the Digital Community Policing by the Lower Saxony State Police on Instagram*

23.5 Sébastien Lambelet *Le plan de quartier : dispositif phare d'exploitation des ressources urbaines latentes*

23.6 Markus Hesse and Charlotte Schaeben *A global knowledge-enclave situated on cross-border territory: tracing the CERN as a dispositif of multi-scalar, relational urbanisation*

23.7 Armelle Choplin *CONCRETE CITY: Material flows and urban making in Africa*

23.8 Fabien Reix and Adrien Gonzalez *La métropole coopérative et ses ressources*

23.9 Bárbara Polo-Martin *COVID19: the urban model´s change of Spanish cities through cartography*

23.10 Raphaël Languillon *Faster & higher Tokyo: between urban renaissance and spacial fix, speeding up the urban making of a mature city*

23.11 Stephan Rist, Susan Thieme, Alexander Vorbrugg *blabla*

23.1
Policing the City:State Violence in the Age of Far-Right Populism and Digitalisation

Dennis Pauschinger

University of Neuchâtel

Increasingly, Big Data, algorithms and new technologies are integrated in everyday public security and policing routines. Promising greater efficiency, effectiveness and a reduction in violent conflict, smart, resilient and predictive urban securtiy strategies, however, co-exist and intermingle with repressive and lethal forms of state violence. Recently, this association has become amplified by a global league of far-right populists who radicalise the political discourse, encourage state forces to use violence, undermine democratic norms and downplay racist institutional structures. From the killing of George Floyd in Trump's America to Rio de Janeiro's deadly police forces in Bolsonaro's Brazil, the implementation of digital security technologies, the use of state violence, and the rise of far-right populism, have traditionally been studied separately from each other. Much less attention has been paid to how these phenomena coalesce, influence each other and are essentially lived, negotiated and contested by police officers themselves and how they consequently transform contemporary societies.

This session aims to come closer to an understanding of this global phenomenon by placing central emphasis upon *how governmental far-right populist discourse and the digitalisation of urban security politics transform state violence.* The session puts forth the hypothesis that, despite the magnified mobilisation of digital security technologies, state violence increases with the security politics of globally ascending far-right populists. The session is therefore guided by three main interrelated objectives: 1) to critically examine how practices of state violence and digital security technologies are discursively proliferated, authorised and spatially distributed by radical political discourse, 2) to investigate how state violence and digital security technologies are used and experienced by police officers and political actors themselves, and 3) to advance an innovative research agenda to comprehend state violence in times of digitalisation and far-right populism. In an introductory presentation the session starts with theoretically weaving together and developing further conceptions from the technopolitical – the agency of materiality in the composition of the social – state sovereignty – here broadly understood as the state's monopoly of violence or the right to kill exercised by the police and – far-right populism – as a renewed phenomenon that globally threatens the way of life of so many, furnished with empirical examples of long-standing research into Rio de Janeiro's digital security infrastructures and specialised police forces that recently participated in the most lethal police intervention in the city's history.

To initiate a fruitful discussion and dialogue about the ways in which state violence in its manifold forms proliferates in the age of increasing far-right populism and digitalisation, the session welcomes contributions in, but not limited to, the following set of areas of interest:

- Far-right populism and authoritarian tendencies as a global phenomenon
- Social protest and repression in the digital age and under authoritarian politics
- Digital security technologies and its spatial proliferation in violent cities
- The spatial logics of police work in the digital age and authoritarian politics
- Global perspectives upon state violence and its manifold forms
- The spatial power of (political) discourse in times of increasing far-right politics
- Social media, state propaganda, election manipulation and state violence
- The role of geography and social scientific research in these times of unrest

23.2
Imprisoned for a retweet: More-or-less digital contestation and repression in increasingly authoritarian Russia

Sven Daniel Wolfe

University of Lausanne (SvenDaniel.Wolfe@unil.ch)

In May 2021, Evgeny Roizman, the former mayor of Ekaterinburg – a major industrial city in Russia's Ural mountain region – was jailed for nine days (Mediazona 2021). Ekaterinburg is well-known in Russia as an oppositional capital, and the former mayor has positioned himself as an outspoken critic of Russia's increasing authoritarianism. Roizman was imprisoned for his support of opposition politician Alexey Navalny, who had been poisoned by state security services, airlifted to Germany for medical treatment, and arrested upon his voluntary return to Russia. The official legitimation for Roizman's imprisonment was one tweet and one retweet in support of the public protests for Navalny's freedom (Roizman 2021).

Roizman's attempts to express political freedom and subsequent imprisonment are emblematic of a new wave of state repression in Russia's increasingly authoritarian turn. This crackdown is taking place across both online and offline geographies, in what can be understood as the more-or-less digital (Merrill et al. 2020). Roizman is far from the only Russian who has suffered physically for his online behavior: in recent months Russian virtual spaces have been overflowing with stories of people who have been arrested by the security services for their oppositional politics, and most of them lack the fame and visibility of Ekaterinburg's former mayor.

This paper investigates the geographies of this latest wave of more-or-less digital repression in Russia. In highlighting everyday stories of increasing state repression, it illustrates how actors in the Russian state apparatus use online spaces to further a far-right isolationist agenda, and how everyday citizens continue to adapt their behavior in order to stay safe and resist. The paper builds on previous work on Russian digital contestation (Wolfe 2021) but pushes further to reveal the increasing speed and severity of political closures in contemporary Russia.

LITERATURE

Mediazona. 2021. "Byvshy mer Ekaterinburga Roizman poluchil devyat sutok aresta za tvity ov aktsii 31 yanvarya [Former Mayor of Ekaterinburg Roizman gets nine days in jail for tweets about the January 31 action]." Mediazona. May 12, 2021. https://zona.media/news/2021/05/12/roizman.

Merrill, Samuel, Shanti Sumartojo, Angharad Closs Stephens, and Martin Coward. 2020. "Togetherness after Terror: The More or Less Digital Commemorative Public Atmospheres of the Manchester Arena Bombing's First Anniversary." *Environment and Planning D: Society and Space* 38 (3): 546–66. https://doi.org/10.1177/0263775819901146.

Roizman, Evgeny. 2021. "@roizmangbn Tri Protokola. 31-Go Yanv. Organizatsiya. 21-Go Apr. Organizatsiya i Uchastiye. Organizatsiya - Eto Tvit i Odin Retvit. Eto Zhe i Priziv. Dazhe Ne Mogu Vspomnit Vsye. Ni Ot Chego Ne Otkazivayus. [Three Infractions. Jan 31, Organization. Apr 21, Organization and Participation. Organization Is One Tweet and One Retweet. That's Calling for Protests. I Can't Even Remember Everything. I Deny Nothing.]." Instagram. May 12, 2021. https://twitter.com/roizmangbn/status/1392352032426762240?s=20.

Wolfe, Sven Daniel. 2021. "Blogging the Virtual: New Geographies of Domination and Resistance In and Beyond Russia." *Antipode* 53 (4): 1251–69. https://doi.org/10.1111/anti.12709.

23.3
Counterterrorism in the Airport-City

Mark Maguire*, David A. Westbrook**

** Maynooth University Faculty of Social Sciences*
*** University at Buffalo School of Law, and New York City Programme in Finance & Law*

There has been much comment recently on the rise of security technoscience, the nesting of various “solutions” in urban space and in societal institutions, and the legitimation of violence as counterterrorism. These elements seem to coalesce in international airport-cities. International airports are frequently the target of terrorism, but they are notoriously difficult to police, with their massive urban footprints, multiple bureaucratic dominions, and vast crowds in motion. Recent technoscientific interventions in airports include second-generation biometrics, ambient environments, and augmented-reality policing. But, for all the techno-scientific solutionism, rather old bureaucratic questions endure: who makes the rules, who gets to enforce them, and by what means? This paper draws from our recent ethnography Getting Through Security: Counterterrorism, Bureaucracy, and a Sense of the Modern (2020), a study of the secret world of counterterror operators, and a reflection on the scholarly discussions that often fail to understand security. Here, empirically, we explore several terror attacks on airports, describing the bureaucratic response (which includes the search for technoscience solutions), but also revealing counterterrorism’s “secret colleges”, the high-level network spaces where bureaucratic order yields to something else. Our ethnography with senior level bureaucrats and counterterror combat operators shows precisely how kinetic force, new technology, and old, intractable bureaucratic problems meet and mingle in the contemporary airport-city. Finally, we turn back to Max Weber before reflecting on what remains—the public.

23.4
The Thick Blue Net: The Hashtag *thinblueline* and the *Digital Community Policing* by the Lower Saxony State Police on Instagram.

Alexa Agoropoulos, Ben Hundertmark, Jasper Janssen and Tabea Louis

Department of Social Sciences, University of Hamburg

Using the Hashtag *#instacops*, German police officers from Lower Saxony State Police report on official Instagram-accounts on their everyday lives. This new personalized communication strategy is based on the concept of *Digital Community Policing*, which aims to increase citizens "openness, sensitivity and trust" (Lower Saxony State Police 2020) towards the police and to expand the institutional presence into the digital space.

Within this context, so-called *Instacops* regularly tag their posts with the *#thinblueline* and furthermore produce visual and intertextual references to the authoritarian and right-wing narrative of the *Thin Blue Line* (TBL), which stylizes the police as the only defender of a society under constant threat from regressing into anomy and chaos. The TBL narrative articulates the police as the primary force which secures humanity and aims to claim a license for the police to an endless war in the name of humanity (Wall 2020, p. 391). But it also imagines police officers in a vulnerable position on the thin frontier to the abyss of human barbarism, thus shaping the self-conceptions of men and women in uniform as a devoted and self-sacrificial service for the good cause.

By sharing observations from the digital widths of Instagram, we aim to shed light on the subtle incorporation of the TBL narrative into official police communications on social media. We argue that Instagram provides a fruitful environment for the police to place the TBL narrative due to the platforms specific algorithmic and social logics. Moreover, a virtual journey along the *#thinblueline* on Instagram offers the opportunity to gain insights into imaginations of society by police institutions as well as it allows to demonstrate contemporary mechanisms of *copaganda* (Wood and McGovern 2020) on social media.

REFERENCES

Lower Saxony State Police. 2020. *Digitales Community Policing*. https://www.polizei-nds.de/wir_ueber_uns/polni_socialmedia/digital.community.policing/digital.community.policing-112171.html. Author's translation.

Wall, Tyler. 2020. 'The Police Invention of Humanity: Notes on the "Thin Blue Line"'. *Crime, Media, Culture: An International Journal* 16 (3): 319–36. https://doi.org/10.1177%2F1741659019873757

Wood, Mark A, and Alyce McGovern. 2020. 'Memetic Copaganda: Understanding the Humorous Turn in Police Image Work'. *Crime, Media, Culture: An International Journal*, Online First: https://doi.org/10.1177%2F1741659020953452

23.5
Le plan de quartier : dispositif phare d'exploitation des ressources urbaines latentes

Sébastien Lambelet [1,2]

[1] *Département de science politique et relations internationales (SPERI), Université de Genève, Uni-Mail, 40, Bd. du Pont-d'Arve, CH-1205 Genève*
[2] *Pôle de Gouvernance de l'Environnement et Développement Territorial (GEDT), Université de Genève, 66, Bd. Carl-Vogt, 1205 Genève.(sebastien.lambelet@unige.ch)*

Depuis les années 1990, la Suisse est entrée, comme bon nombre de pays européens, dans une phase de métropolisation de son territoire (Bassand 2004). En perte de vitesse des années 1960 aux années 1990, les grands centres urbains suscitent à nouveau les convoitises et redeviennent des lieux de concentration de multiples ressources urbaines latentes (D'Arienzo *et al*. 2016 ; Michel & Ribardière 2017). Néanmoins, ce processus s'accompagne d'une injonction, tant économique (concurrence interurbaine accrue) que politique (nouvelle LAT), à renouveler la ville. Les autorités locales ambitionnent dès lors de transformer substantiellement le tissu urbain existant, alors que cette démarche s'inscrit le plus souvent en porte-à-faux avec les intérêts des citoyens-habitants qui les élisent.

La présente communication cherchera à démontrer que les autorités locales tentent de résoudre ce dilemme en transformant le plan de quartier (PQ) en un nouveau dispositif foucaldien leur permettant d'obtenir, au moins tacitement, l'aval d'une majorité d'électeurs pour ces grands projets. Jadis cantonné à la simple délimitation de zones d'affectation (Gaudin 1985), le processus d'élaboration du PQ contemporain cumule, en sus, les trois archétypes de dispositif foucaldien – légal, disciplinaire et sécuritaire – identifiés par Raffnsøe (2008).

Sur le plan empirique, cette communication se penchera sur le renouvellement urbain de trois villes suisses (Zurich, Berne et Genève) à l'aune de grands projets emblématiques ayant marqué une rupture dans leur trajectoire de développement (*Europaallee*, *Wankdorf-City* et les cités CEVA). Cette comparaison permettra d'illustrer des variations importantes relatives *a)* au processus d'élaboration des PQs ou *b)* à la manière de traiter les oppositions émanant des citoyens-habitants. Finalement, nous conclurons en nous interrogeant sur les effets à moyen-long terme de ces nouveaux quartiers monofonctionnels, accueillant essentiellement des bureaux. Ce manque de diversité des usages ne va-t-il pas déprécier les ressources urbaines de ces villes à l'avenir ?

REFERENCES

Bassand, M. 2004: *La métropolisation de la Suisse*, Lausanne, PPUR.

D'Arienzo, R., Younès, C., Lapenna, A., Rollot, M., & Groupe d'études et de recherches Philosophie. 2016: *Ressources urbaines latentes : Pour un renouveau écologique des territoires*, Genève, MétisPresses.

Gaudin, J.-P. 1985: *L'avenir en plan : technique et politique dans la prévision urbaine*, Seyssel, Editions Champ Vallon.

Michel, A. & Ribardière, A. 2017: "Identifier les ressources urbaines pour lire les inégalités socio-spatiales. Introduction", *EchoGéo*, no. 39, https://doi.org/10.4000/echogeo.14925.

Raffnsøe, S. 2008: "Qu'est-ce qu'un dispositif ?: L'analytique sociale de Michel Foucault", *Symposium*, 12 (1), 44–66, https://doi.org/symposium20081214.

23.6
A global knowledge-enclave situated on cross-border territory: tracing the CERN as a dispositif of multi-scalar, relational urbanisation

Markus Hesse[1], Charlotte Schaeben[2]

[1] Department of Geography & Spatial Planning, University of Luxembourg, 11, Porte des Sciences, L-4366 Esch-sur-Alzette (markus.hesse@uni.lu)
[2] NEWROPE Chair of Architecture & Urban Transformation, ETH Zurich, Neunbrunnenstr. 50, ONA.J25, CH-8093 Zurich (schaeben@arch.ethz.ch)

This paper aims to contribute to the emerging debate of relational urbanisation processes, that is, processes within which small places have gained a strong position in the systems of global finance, corporate services, or knowledge creation. This pattern of urbanisation is considered highly selective and usually unfolds only on the grounds of a particular combination of enabling factors, such as flows, scale, historical trajectories and peculiar governance conditions. As a case in point, we explore the supra-national institute of nuclear research CERN, operated by meanwhile 23 European countries and situated on cross-border territory belonging to France and Switzerland. The CERN is known as one of the top European research clusters, its scientific merits are recognised even by a wider public, as it happened there in 1989/90 when Tim Berners Lee invented an early version of the standard that would later become the Internet. However, little is known about the material appearance of this institution, how its infrastructure and built environment are manifested in peri-urban, cross-border territory. This applies also to the life-worlds and social composition of the small municipalities in the Geneva periphery where CERN-staff (permanent, temporary, international) is localised. Based on field exploration on site and a systematic assessment of secondary sources, we approach the CERN as a dispositif of a research policy that represents an ideal type of relational space: one that has emerged on the grounds of rather particular multi-scalar dynamics at global, regional and local levels. It brought about a built space whose future growth trajectory challenges the local and regional setting in specific ways. These challenges will be pertinent in the upcoming process of the extension of the particle accelerator. The case exemplifies the tensions that are associated with knowledge-based urbanisation, calling for a better adjustment of contradicting interests and competing powers.

REFERENCES

Hesse, M. & Wong, C. M.-L. 2020: Cities seen through a relational lens. Niche economic strategies and related urban development trajectories in Geneva (Switzerland), Luxembourg (Luxembourg) and Singapore. Geographische Zeitschrift, 108(2), 74-98.

Schaeben, C. 2018: Zone Franche du Pays de Gex, Jardins metropolitains (Master Thesis, Architecture). Chair of Architecture of Territory, Prof. Topalovic. Zurich: ETH.

23.7
Concrete City: Material flows and Urban making in Africa

Armelle Choplin

[1] *Associate Professor, University of Geneva, Departement of Geography and Environment & Global Studies Institute, (armelle.choplin@unige.ch)*

Africa is experiencing rapid urban growth resulting in a spread of `concrete cities'. Concrete has become the symbol of the frenetic urbanization, construction boom and capitalistic emergence of the continent. Drawing from my book *Matière Grise de l'Urbain, La vie du ciment en Afrique* (2020, MétisPresses), forthcoming in English, *Concrete City, Material flows and urban making in Africa* (2021, Wiley), this presentation offers a contribution to understanding African cities through their materiality and the lens of concrete, a global commodity with local impacts. Concrete is both a material and a conceptual "binder" for analyzing city-making across political, economic, social and environmental perspectives.

In combining an ethnography of building practices with a politico-economic analysis of the concrete chain, my presentation aims to decipher the politics of concrete which accompany the 'Rising Africa' discourses. It analyses the construction boom and its actors shaping African cities. It deciphers the social values and imaginaries linked to the building cultures and dwelling practices. It finally addresses debates and controversies on concrete and its environmental impact, and explores sustainable alternatives for rethinking cities.

By following material flows, primarily bags of cement, from the quarry to the plot of land, from the cement tycoons to the dwellers and builders, I propose an exploration of the West African urban corridor linking Abidjan, Accra, Lomé, Cotonou and Lagos. Drawing on long-term fieldwork, it examines Africa's largest mega-city under construction: over 40 million people live, travel, consume and build… with concrete.

This exploration of the life of concrete in Africa reveals that it is not an inert but an active material, at the heart of urban metabolism and experiences. By drawing parallels between African and European (Swiss) situation regarding the construction sector and built environment, this presentation invites to rethink the links between materiality, (non)human and urban futures.

23.8
La métropole coopérative et ses ressources

F. Reix [1], A. Gonzalez [2]

[1] *ENSAP Bordeaux, & PAVE/Centre Emile Durkheim (fabien.reix@bordeaux.archi.fr)*
[2] *Laboratoire PAVE adrien.gonzalezsarochar@gmail.com*

Comment coopérer sans être sur un pied d'égalité (Jousseaume, 2017) ? Alors que le découpage entre ville et campagne reste un marqueur des représentations en matière d'inégalités dans le développement territorial, les territoires riches en ressources semblent tirer leur épingle du jeu face à des métropoles souvent perçues comme « vampirisantes » (Vanier, 2015). Notre étude porte plus précisément sur la gestion des ressources en eau et en alimentation entre Bordeaux Métropole (Département de la Gironde, Région Nouvelle Aquitaine, France) et ses territoires voisins. Menée dans le cadre du programme de recherche français « POPSU[1] (Plateforme d'observation des projets et stratégies urbaines) Métropoles », notre enquête témoigne de la mise en place de projets de coopération entre territoires qui tentent de s'organiser autour de biens et d'intérêts communs. Territoire connu pour sa viticulture, ses côtes sauvages et ses lacs, le département de la Gironde est l'une des communes les plus attractives du pays, et sa métropole bordelaise organise sa stratégie de peuplement et son développement économique en s'ouvrant vers ses voisins. L'étude de la gestion de ressources vitales et à fort enjeu comme l'eau et l'alimentation a donné l'occasion de révéler ce qui se trame dans les coulisses, entre les acteurs métropolitains et leurs voisins, et de mettre en récits leurs représentations croisées. Nous avons ainsi étudié la façon dont les coopérations autour de ces ressources ont été médiatisées dans la presse quotidienne régionale. Puis, nous avons directement interrogé les acteurs territoriaux engagés dans ces transactions sur les manières dont ils perçoivent ces logiques coopératives à travers une série d'entretiens menés sous forme d'auditions. Loin d'être unanimement partagée, cette image d'une métropole coopérative est mise à l'épreuve du polycentrisme girondin (Godier et al., 2018). L'analyse des jeux d'acteurs à l'œuvre en matière de relocalisation du système alimentaire et de mutualisation des ressources en eau potable entre Bordeaux métropole et ses territoires voisins éclairent les conditions d'émergence et les enjeux de récits coopératifs de nature interterritoriale (Pasquier, 2012). En s'intéressant à ces scènes transactionnelles émergentes, il s'agit aussi de mettre en lumière les dimensions formelle et informelle (Rémy, Foucart, 2013) que prend l'interterritorialité à travers l'identification des outils et des instruments politiques à disposition des acteurs locaux d'une part, et des représentations des relations de dépendance, de solidarité et/ou de concurrences entre territoires d'autre part.

BIBLIOGRAPHIE

Godier P. et *al*., (2018) *L'éveil Métropolitain, l'exemple de Bordeaux*, Le Moniteur, Collection Popsu.
Jousseaume V. (2017). « La métropole peut-elle s'allier sans dominer ? », *Pouvoirs Locaux : les cahiers* de la décentralisation / Institut de la décentralisation, Institut de la décentralisation, inPress, L'alliance des territoires.
Pasquier R. (2012), *Le pouvoir régional. Mobilisation, décentralisation et gouvernance en France*, Presses de Sciences Po.
Rémy J. & Foucart, J. (2013). « La transaction : une manière de faire de la sociologie », *Pensée plurielle*, 33-34, pp. 35-51.
Vanier, M. (2015), « Réforme territoriale et espace rural », *Pour*, 228, pp. 147-153.

1 https://popsu.archi.fr/

23.9
COVID19: the urban model´s change of Spanish cities through cartography

Bárbara Polo-Martin

Universidad Internacional de Valencia, Barcelona-Spain

During centuries, the pandemics were something very natural to the human being, but as result of the industrialisation during the 19th century, they became a problem. The arrival of population to big cities provoked the development of irregular and overpopulated quarters with any measures of safety, and facilitated the expansion of tiny diseases. The problem resided in the sanitation's problems. As for example happened in London and Paris. As solution, in different cities, and as starter point Paris with the Haussman´s proposals, different inner reforms and extension plans. Humanity believed that these extension plans would give us a healthy density and an ordered expansion. But nothing further from reality. At the beginning of 21th century, the history repeats. A new pandemic crisis has raised and has shown that cities have, again, a crisis of congestion. But in this time, in comparison with 19th century, governments have acted very quickly in order to enhance the welfare of citizens. Governs have known how to recover the previous state of the city and to promote spaces of quality. It is proposed that within 10 to 20 years cities are clean, green and car-free. The COVID's crisis has allowed to pedestrianize centres, to create cycle lanes, to increase the use of public transport, and all this, using few resources. Governments have used unique situations like this in which the city is transforming to achieve sustainable development. The question that arises is whether the temporary experiment becomes permanent in the centre. Crises make tangible changes, they invite governments and citizens to dream, a crisis to evolve, but the citizen has to be the main defender of these new changes, and not governments as on previous occasions.

This paper provides Spanish models, such as Barcelona and Madrid, of improving urban environments that facilitate the population's access to the healthiest options. However, despite the clear solution of sustainability, the main problem of urbanism is how to make it possible. For that, Spanish experts in different fields like cartography, geography, urbanism or architecture, look for the ideal model of city, in which has a relevant role an autonomous city and not the smart city, as it was thought lately. It will be necessary to divide large cities into more or less autonomous pieces that are capable of responding individually to the new requirements of an overpopulated and globalized planet. All of this only could be possible together with citizens agreement, something that consistories are taking into account through different surveys.

REFERENCES

Arnould, J. (1902), Nouveaux éléments d'hygiene. París: Libr. J.B. Baillière et Fils, pp. 1.003. Retrieved from: https://archive.org/stream/BIUSante_90141x1903x49/BIUSante_90141x1903x49_djvu.txt

Besson, R. (2016). Madrid's citizen laboratories – a response to the Spanish economic crisis and the invention of "tactical urbanism" or "precarious urbanism"?. Bulletin des professionnels de Adp-Villes en developpement, pp.2-3.

Capel, H, & Tatjer, M. (1991). Reforma social, serveis assistencials i higienisme a la Barcelona de final del segle XIX (1876-1900). In A. Roca Rosell (ed.), Cent anys de Salut Pública a Barcelona (pp. 31-73). Barcelona, ES: Ajuntament de Barcelona.

Coronas Vida, L. J. (2008). El abastecimiento de agua potable a las capitales de Castilla y León: entre la concesión y la municipalización (1886-1959). In IX Congreso Asociación Española de Historia Económica. doi 10.14295/rbhc. v9i18.448

Geneviève, M.G. (2007). Pour une histoire environnementale de l'urbain. Histoire urbaine, 18, 5-21. doi: 10.3917/rhu.018.0005

Halliday, S. (2013). The Great Stink of London: Sir Joseph Bazalgette and the Cleansing of the Victorian Metropolis. Stroud, UK: The History Press.

Hamlin, C. (1991). The Sanitarian Becomes an Authority. 1859. In International Conference on the History of Public Health and Prevention. Stockholm.

Hamlin, C. (1992). Predisposing causes and public health in early nineteenth century medical thought. Soc. Hist. Med., 5, 43-70. doi: 10.1093/shm/5.1.43

Hartley, L ; Lydon, M; Budahazy, M; Monisse, N; Yee, M ; Mengel, A and Wallace, K. (2014) Tactical Urbanism: Volume 4. CoDesign Studio, The Street Plans Collaborative.

Hauser, P. (1979). Madrid bajo el punto de vista médico-social. Madrid, ES: Ed. del Moral y C. Editora nacional.

Hauser, P. (1913). Geografía médica de la Península Ibérica (pp. 235-236). Madrid, ES: Eduardo Arias.

Hildreth, M.L. (1987). Doctors, Bureucrats and Public Health in France, 1888-1902. New York-London: Garland publishing Inc.

Lydon, M, and Garcia, A. (2015). Tactical Urbanism: Short-term Action for Long-term Change. Island Press.

New York City Regional Heat Island Initiative (October 2006). «Mitigating New York City›s Heat Island With Urban Forestry, Living Roofs, and Light Surfaces». New York State Energy Research and Development Authority. p. II.

Pogliano, C. (1984). L`utopia igienista (1870-1920). In F. Della Peruta, (ed.), Storia d`Italia. Annali 7. Malattia e Medicina (pp.

589-631). Torino, IT: G. Einaudi editori.
Pulido Fernandez, A. (1902). Sanidad pública en España y ministerio social de las clases médicas. Madrid, ES: Est. Tip. Enrique Teodoro.
Real Consejo de Sanidad. (1901). Cuestiones fundamentales de Higiene Pública en España. Madrid, ES: E. Teodoro.
Rodger, R. (1996). A Consolidated Bibliography of Urban History. Aldershot, UK: Scholar Press.
Rodríguez Ocaña, E. (1994). La salud pública en España en el contexto europeo, 1890-1925. Revista de Sanidad e Higiene Pública, 68(0), 11-27.
Rodríguez Santillana, J.C. (2002). Saneamiento y espacio urbano (Burgos 1870-1920). Burgos, ES: Dosoles
Sgobbo, A. (2017). Eco-social innovation for efficient urban metabolisms. TECHNE Journal of Technology for Archi-tecture and Environment, 14, 337-344. doi: 10.13128/Techne-20812
Smith, F. B. (1979). The people´s health 1830-1910. Canberra, AU: Australian National University Press.
Solecki, William D.; Rosenzweig, C.; Parshall, L.; Pope, G.; Clark, M.; Cox, J.; Wiencke, M. (2005). «Mitigation of the heat island effect in urban New Jersey». Global Environmental Change Part B: Environmental Hazards. 6 (1): 39–49.
Sussman, G.D. (1977). Enlightened Health Reform, Profesional Medicine and Traditional Socety: The Cantonal Physicians of the Bas-Rhin, 1810-1870, Bull. Hist. Med, 51, 565-584. doi: 10.1017/CBO9781139381185.011
United States Environmental Protection Agency (2008). Reducing urban heat islands: Compendium of strategies (Report). pp. 7–12
Virgili Blanquet, Maria Antònia (1979). Desarrollo urbanístico y arquitectónico de Valladolid: 1851-1936. Valladolid, ES: Ayuntamiento de Valladolid.
Villanova, J. L. (2011). Dionisimo Casañal y Zapatero: Del catastro a la topografía (1864-1878). In C. Montaner; F. Nadal and L. Urteaga (eds.), Cartografía i agrimensura a Catalunya i Balears al segle XIX. 2011 (pp. 209-223). Barcelona, ES: Institut Cartogràfic de Catalunya.
Wohl, Anthony S. (1983). Endangered Lives: Public health in Victorian Britain. London, UK: Dent.

23.10
Faster & higher Tokyo: speeding up the urban making of a renascent city through spatial fix dispositives

Raphaël Languillon-Aussel[1]

[1] *Institut Français de Recherches sur le Japon, Maison Franco-japonaise, 3-9-25 Ebisu Shibuya-ku, Tokyo 150-0013 (languillon@mfj.gr.jp)*

After one decade of urban crisis, following the burst of the financial bubble in 1991, the Japanese central government issued in 2002 a new urban policy, called *Urban Renaissance Special Measure Law* – lately reinforced in 2011. Its aim was to remobilize toxic land assets generated by the financial bubble burst, that led to the multiplying of unused or underused lands in Japanese main city centers, especially in central Tokyo. This law allowed to create a new special zoning, called *Urban Regeneration Urgent Redevelopment Area* (URUDA), where private developers could derogate to the urban planning common law, and also benefit from new rights (public aid, loans at preferential rates, simplified and accelerated administrative procedures…).

As a new spatial dispositive, URUDAs played the role of urban regeneration accelerator and facilitator, or even instigator. But what is the nature of the resources invested in URUDAs' redevelopment projects, and where did they come from? In this presentation, we make the hypothesis that the highly selective, centrally concentrated nature of urban renaissance has created a two-tier city, provoking debate over what David Harvey calls the spatial fix, i.e. the temporary spatial solutions adopted by capitalists to save their assets from a downward spiral in values. In a context of urban resource scarcity, URUDAs have led to an over concentration of resources in few areas, at the detriment of the rest of the city, redeveloping the whole metropolis in hot and cold spots.

This unequal use of resources through special zoning dispositives has been reinforced in the 2010s by the coming of the Tokyo Olympic Games. From a spatial fix perspective, the Olympic Games have generated an additional fix effect through the setting up of a temporal horizon to investments and political actions envolved in Tokyo urban making. A second hypothesis postulates the idea that Olympic Games have generated a shift from spatial to temporal incentive, speeding up the spatial concentration of an unequal capitalistic accumulation in few areas of central Tokyo.

This presentation will examine the assumed continuity between the 2000s (urban renaissance) and the 2010s (Olympic development) and discuss the pertinence of spatial fix concept over the past two decades of intense urban generatoon in Tokyo.

REFERENCES

ARRIGHI Giovanni, 2006, Spatial and Other "Fixes" of Historical Capitalism, in Chase-Dunn C. & Babones S. J., *Global Social Change. Historical and Comparative Perspective*, Baltimore, The John Hopkins University, Press, pp. 201-212.

BOURDIER Marc & PELLETIER Philippe (dir.), 2000, L'Archipel accaparé. La question foncière au Japon, Paris, Éditions de l'École des Hautes Études en Sciences Sociales, 310 p.

FUJII Sayaka, ARITA Tomokazu & OMURA Kenjiro, 2006, The Impact of the "Urban Renaissance" Policy in Japan: the Analysis of Deregulation in the Building Standard Law of Japan, *Proceedings of International Symposium on Urban Planning*, pp. 451-461.

HARVEY David, 2001, Globalization and the "Spatial Fix", *Geographishe Revue*, 2, pp. 23-30.

JESSOP Bob, 2008, Spatial Fixes, Temporal Fixes, and

Spatio-Temporal Fixes, in Castree N. et Gregory D., *David Harvey: A Critical Reader*, Londres, Blackwell Publishing, pp. 142-166.

KUBO Tomoko, 2014, Super High-Rise Condominium Development in the Tokyo Bay Area and their Residents' Lives , *Chiri*, 59-4, pp.23-31.

LANGUILLON-AUSSEL Raphaël, De la renaissance urbaine des années 2000 aux Jeux olympiques de 2020 : retour sur vingt ans d'intense spatial fix à Tokyo, *Ebisu*, 55. URL : http://journals.openedition.org/ebisu/2324

MOLOTCH Harvey, 1976, The City as a Growth Machine: Toward a Political Economy of Place, *American Journal of Sociology*, 82-2, pp. 309-332.

SAITO Asato, 2003, World City Formation in Capitalist Developmental State: Tokyo and the Waterfront Sub-centre Project, *Urban Studies*, 40-2, pp. 283–308.

23.11
Exchange: Critical Sustainability Studies in (research) practice

Stephan Rist, Susan Thieme, Alexander Vorbrugg (Bern)

Sustainability has become a buzzword across many societal domains including academia. Different positions and approaches are assembled under this umbrella, which is perceived both as a strength and a problem: It bears the promise to step outside of thematic and disciplinary silos to collectively address planetary challenges but also the risk of losing the "critical edge" necessary to envision and fight for the substantive transformations needed to reach sustainability. We invite colleagues to join a conversation about the possibilities and risks that go along with the continuing institutionalisation and mainstreaming of sustainability studies in academia, and your suggestions for putting critical sustainability principles into practice in collaborative (research) projects, and politics within and outside of the academy.

Brief panel inputs will be followed by an open discussion. Questions for discussion may include:

- Is sustainability's "critical edge" equivalent to the integration of established critical theories (political economy/ ecology, feminist and postcolonial theories etc.) or are there further important standards for critical sustainability studies?
- How do and can we translate visions for sustainability into everyday practices including research and activism? How do your projects provide grounds for crucial collaborations within academia and beyond?
- How do you bring together broad and sometimes vague sustainability frameworks, specific research topics and concrete strategies of radical societal transformation?
- What are the possibilities and risks that go along with the institutionalization and mainstreaming of sustainability studies? How to deal with the concurrent mainstreaming of sustainability studies on the one hand, and increasing attacks on many other critical and radical traditions on the other?

Panelists:
Deniz Ay (Bern)
Basil Bornemann, Marius Christen, Rony Emmenegger (Basel)
Christian Kull (Lausanne)